where P/S is the friction power per unit transfer surface area. Assuming operation at the same temperature conditions, the heat transfer performance of equal surface areas may be compared at the same friction power expenditure. The method of Colburn was modified by London and Ferguson[3] by evaluating the fluid properties at a standard temperature and pressure, and plotting h_{std} versus $(P/S)_{std}$. Kays and London[4] extended the usefulness of this method by multiplying the h_{std} and $(P/S)_{std}$ parameters by a compactness parameter, i.e. the ft^2 of surface area per ft^3 core volume. This allowed comparisons to be made on an equal volume basis. Expressions for the ratio of power consumption to heat transfer were derived by Eckert and Irvine[5] and plotted versus a velocity parameter, a volume parameter, and a weight parameter. Their analysis included terms which took into account fin efficiency and entrance and exit friction losses. In an early paper by Stacey and Ashley[6] the heat transfer coefficient at standard conditions, h_{std}, was plotted against a coil rating parameter which, it will be shown, is proportional to $(P/S)_{std}/h_{std}$. None of the aforesaid methods of comparing or optimizing heat exchanger geometries had attempted to include the effects of both fluid streams.

The object of this paper is to describe the significance and advantages of the method of Stacey and Ashley, extend it to include the influence of the metal and secondary fluid thermal resistances, and illustrate its application to the comparison of surface area, weight, volume, and face area requirements for three practical heat exchanger geometries.

COIL RATING FACTOR DEFINED

Although any fluid may be considered, let it be assumed that the primary fluid, i.e. the fluid whose heat transfer and friction performance is of primary interest, is air. The secondary fluid will be referred to as the tube side fluid, although it is not necessary that this method be restricted to tubular heat exchangers. Also, it will be assumed that only sensible heat transfer occurs on the air side. The coil rating factor, Z, is defined as the pressure drop times the mean temperature difference between the air and the tube side fluid divided by the temperature rise or fall of the air.

$$Z = \frac{\Delta p\, \theta_m}{\theta_a} \qquad (1)$$

The ratio θ_a/θ_m, however, is equal to the ratio US/wc_p, sometimes referred to as the NTU, where the overall heat transfer coefficient, U, is based on the air side surface area, S. Substituting in Equation (1) gives:

$$Z = \frac{\Delta p\, wc_p}{US} = \frac{\Delta p}{L} R_o G \left(\frac{LA}{S}\right) c_p \qquad (2)$$

where R_o is the overall thermal resistance based on air side surface area, G is the mass velocity, A is the coil frontal area, and L is the coil depth in the air flow direction. The expression for Z can be further

expanded by introducing the individual resistances:

$$Z = \frac{\Delta p}{L}\left(R_a + R_m + \frac{R_a}{h_i} \right) G \left(\frac{LA}{S} \right) \frac{(3)}{c_p}$$

where R_a is the air thermal resistance, R_m is the metal resistance, h_i is the tube side heat transfer coefficient, and R_a is the ratio of the effective air side surface area to the effective tube side surface area. Finally, it is possible to arbitrarily select a standard temperature and pressure upon which to base the air properties, as was done in Refs. 3 and 4. Values of 70 F and 1 atmosphere have been chosen as standards.

$$Z_{70} = \frac{\Delta p_{70}}{L}\left(R_{a70} + R_m + \frac{R_a}{h_i} \right) G \frac{c_{p70}}{s_v} \quad (4)$$

where s_v is the compactness parameter — ft² surface area per ft³ core volume.

LIMITATIONS

An inspection of Equation (4) reveals that each term is relatively independent of the overall dimensions of the heat exchanger, being a function only of the geometry and the mass velocity.

1. The assumption that $\Delta p_{70}/L$ is a function of the mass velocity for a given geometry implies that the entrance and exit losses are small in relation to the core loss. Furthermore, it implies that the core friction factor is not strongly dependent on the L/r_h ratio.
2. The assumption that R_{a70} is a function only of the mass velocity for a given geometry implies that the heat transfer factor, $N_{St}(N_{Pr})^{2/3}$, is not influenced by the depth of the core in the air flow direction. This is not generally true, especially for prime surface heat exchangers where a considerable row to row variation in the heat transfer coefficient has been measured, Refs. 7 and 8. However, if comparisons are restricted to applications where the coil depths do not vary appreciably from those upon which the heat transfer data are based, then the effect of this assumption upon the comparison will not be great.
3. The metal resistance, R_m, is a function of the fin efficiency, which in turn is a function of the air side heat transfer coefficient. However, as demonstrated by Carrier and Ander-

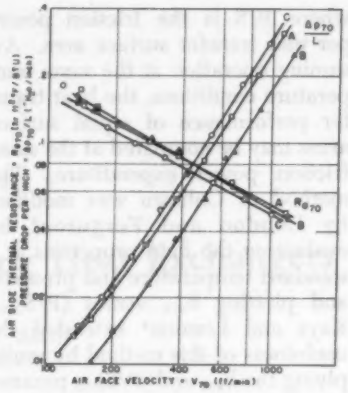

Fig. 1 Heat transfer and pressure-drop for three spiral fin heat exchanger geometries

son,[9] the metal resistance varies slightly for given materials and geometry, over a wide range of heat transfer coefficients.

4. The tube side heat transfer coefficient, h_i, depends on a great number of variables, especially the fluid, the process it undergoes (two phase or single phase) and the method of circuiting. Rather than assume an infinite coefficient, it is possible to assume a constant but finite value. For an air cooled Refrigerant 12 condenser, for example, a value of 400 Btu/hr/ft²/F would be reasonable.[10] The effect of tube side heat transfer coefficient may have a substantial effect upon the relative ranking of heat exchangers, so it is better to assume a value than to neglect it entirely.

BASIS OF COMPARISON

Fig. 1 illustrates heat transfer and pressure drop data for three smooth spiral fin heat exchanger geometries obtained in the Carrier Corporation heat transfer laboratory.[11] A tabulation of the physical characteristics of these heat exchangers appears in Table I. Each heat exchanger was tested using air on the finned side and water inside the tubes. Air side resistance was obtained by subtracting the computed water side and metal resistances from the measured overall resistance. Water side resistances were obtained using the method of Wilson.[12] The abscissa in Fig. 1 is the mass velocity, expressed as a linear velocity of standard air. The ordinates, air thermal resistance and pressure drop per in. of coil depth, have been corrected to a standard air temperature of 70 F by assuming correlations of the form:

$$R_a = C_1 \frac{(N_{Re})^n (N_{Pr})^{1/3}}{Gc_p} \qquad (5)$$

$$\frac{\Delta p}{L} = C_2 (N_{Re})^{-m} \frac{G^2}{2\rho} \frac{1}{r_h} \qquad (6)$$

where the constants are, in general, different for each coil geometry.

Since the coil rating factor and

TABLE I

Coil	—	A	B	C
Fins per in.	in.$^{-1}$	13.9	9.39	13.7
Fin height	in.	13/32	13/32	5/16
Fin base thickness	in.	0.008	0.008	0.008
Fin material	—	Copper	Copper	Copper
Tube outside diameter	in.	⅝	⅝	⅝
Tube wall thickness	in.	0.025	0.025	0.025
Tube material	—	Copper	Copper	Copper
Surface ratio	—	21.0	14.4	14.9
Tube face spacing	in.	1-25/64	1-25/64	1-7/32
Tube row spacing	in.	1-13/64	1-13/64	1-1/16
Arrangement	—	Staggered	Staggered	Staggered
Compactness	ft²/ft³	275	188	252
Weight factor	ft³/lb	5.05	4.06	3.90
Metal resistance	hr/ft²/F/Btu	0.0075	0.0074	0.0040

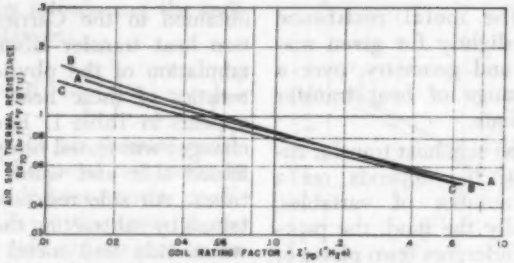

Fig. 2 Air side surface area comparison — Air thermal resistance dominating

the air side thermal resistance are both functions only of the mass velocity it is possible to plot the thermal resistance versus the rating factor as shown in Fig. 2. The coil rating factor, Z'_{TO}, was computed from Equation (4) with the metal and tube side thermal resistances neglected. Likewise, by assuming a value for the tube side heat transfer coefficient, it is possible to compute the overall thermal resistance and plot this against a coil rating factor based on this overall thermal resistance, as shown in Fig. 3. In this case, the tube side resistance was calculated using an assumed tube side coefficient of 400 Btu/hr/ft²/F; metal resistance values are tabulated in Table I. The tubing is assumed to have no internal finning. Fig. 3 represents a comparison based on overall performance whereas Fig. 2 represents a comparison based on air side performance only.

In order to understand clearly the significance of the coil rating factor as a basis for comparing heat exchangers, assume that two heat exchangers are sized so that they cool or heat the same air weight flow (cfm of std. air) the same number of deg at the same pressure drop. Furthermore, assume that their entering air temperature, tube side fluid temperature, and tube side fluid temperature drop are identical. Then the overall mean temperature difference, θ_m, will be the same and, from Equation (1), the Z factor will be the same. Consequently, by comparing heat exchangers at the same value of the coil rating factor, one may consider that the performance aspects are identical, with the physical characteristics: size, shape, surface area, weight, and volume — left as dependent variables. Fig. 4 shows block diagrams of two heat exchangers compared on this basis. Coil I would, in general, be a geometry having a higher pressure drop than Coil II at the same velocity and, consequently, must have a larger face area in order to operate at a lower velocity and the same pressure drop.

SURFACE AREA COMPARISON

Turning back to Fig. 3, at a Z factor

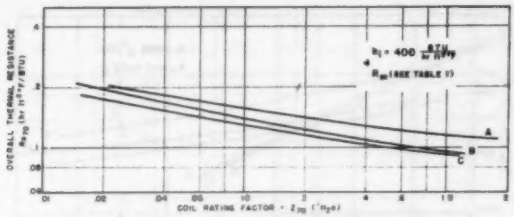

Fig. 3 Air side surface area comparison —Values of the ordinate are directly proportional to air side surface area

of 0.2 in. H_2O coils A, B, and C have overall thermal resistances of 0.134, 0.123 and 0.115 hr/ft²/F/Btu respectively. The overall resistance, however, can be written as

$$R_o = \frac{S\theta_m}{q} \qquad (7)$$

and, since the coils are being compared at the same total heat transfer, q, and mean temperature difference, θ_m, the surface area requirements will be in direct proportion to the overall thermal resistances. Consequently, it can be stated that Coil A requires about 9% more surface area than Coil B and 16.5% more surface area than Coil C under identical performance conditions. Fig. 2 may be interpreted in the same manner for the case where the tube side and metal resistances are negligible.

It is important to note the influence of both tube side heat transfer coefficient and operational velocity on the relative ranking of the heat exchanger geometries. Whereas at Z = 0.2 in. H_2O Coil A required 9% more surface area than Coil B when operating with a tube side coefficient of 400 Btu/hr/ft²/F, Fig. 3, Coils A and B require about the same surface area in an application where the tube side and metal resistances are negligible, Fig. 2. Note also from Fig. 2 the effect of Z on the relative ranking of heat exchangers A and B. At low velocity (small Z value) Coil A is superior (from a surface area consideration) whereas at high velocities Coil A is better. Coil C, on the other hand, requires less surface area than the others over the entire velocity range for all tube side coefficients.

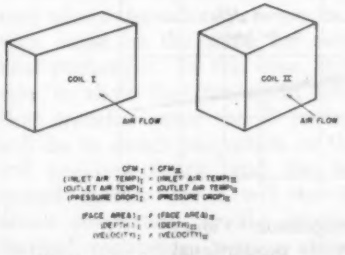

Fig. 4 Basis of comparison

VOLUME AND WEIGHT COMPARISONS

Fig. 5 illustrates a volume com-

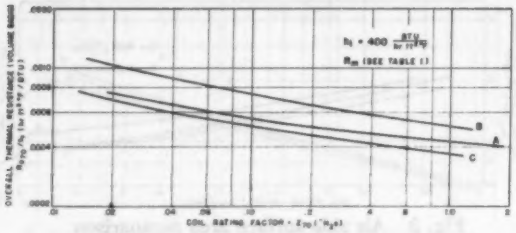

Fig. 5 Core volume comparison—Values of the ordinate are directly proportional to the core volume

parison between the three heat exchangers which is obtained by plotting the thermal resistance divided by the compactness versus the coil rating factor. This gives an ordinate which is equal to the volume divided by the total heat transfer rate per unit mean temperature difference. Since comparisons are being made at equal values of q and θ_m, then the ratio of the ordinates, at fixed Z, is equal to the ratio of the core volumes at equal performance conditions. A weight comparison may be made in the same manner by dividing the thermal resistance by the weight parameter, s_m, ft² of surface area per lb core weight, as shown in Fig. 6. Any number of parameters, or even weighted groups of parameters, may be optimized in this way provided they are directly proportional to the heat exchanger surface area.

CONSOLIDATED COMPARISON

One of the advantages of the coil rating factor parameter is that it remains the same regardless of what is being optimized. Consequently, several comparisons may be made on the same graph as demonstrated in Fig. 7. Also, shown at the top of Fig. 7, are curves which allow de-

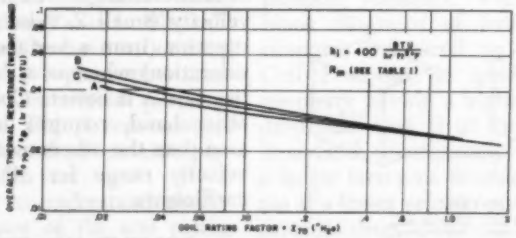

Fig. 6 Core weight comparison—Values of the ordinate are directly proportional to the core weight

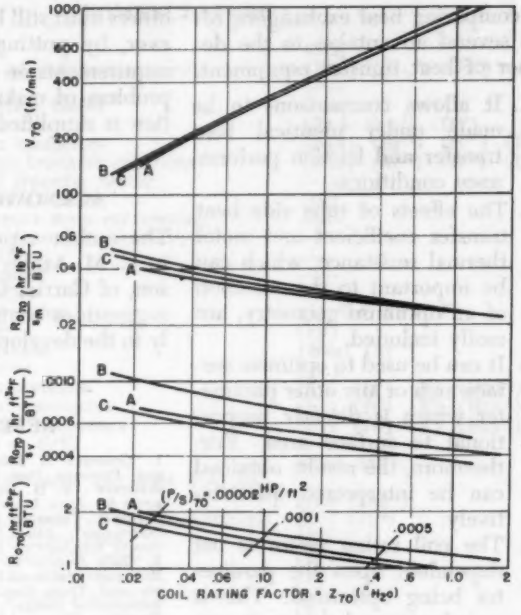

Fig. 7 Consolidated comparison chart

termination of the face velocities corresponding to each coil rating factor. Since the heat exchangers are assumed to be operating at the same cfm, then the ratio of the velocities will be inversely as the ratio of the face areas at the same Z factor. Another way in which the velocity lines may be used is in the case where the velocity, hence face area, must be the same for each heat exchanger. In this case, it is easy to show that for equal total heat transfer rates the Z factors will be in direct proportion to the coil pressure drops, and the required surface areas will be in direct proportion to the overall thermal resistances corresponding to these Z factors.

The coil rating factor is related to the friction power per unit surface area, $(P/S)_{std}$, as used in Ref. 3. Rearranging Equation (2) gives:

$$Z = \frac{\Delta p}{L} R_o G \left(\frac{LA}{S}\right) c_p = (P/S)\, R_o \rho\, c_p \qquad (8)$$

At standard conditions, therefore, the coil rating factor is directly proportional to the product of the friction power per unit surface area and the overall thermal resistance, so that lines of constant P/S will be 45 deg straight lines on a log-log plot of R_o versus Z. These are shown dotted on Fig. 7.

CONCLUSIONS

The coil rating factor, as a basis

for comparing heat exchangers, offers several advantages to the designer of heat transfer equipment.

1. It allows comparisons to be made under identical heat transfer and friction performance conditions.
2. The effects of tube side heat transfer coefficient and metal thermal resistance, which can be important to the selection of an optimum geometry, are easily included.
3. It can be used to optimize surface area or any other parameter which is directly proportional to surface area. Furthermore, the results obtained can be interpreted quantitatively.
4. The coil rating factor is not dependent upon the parameter being optimized. This is an advantage because it permits graphical comparisons of surface areas, weights, volumes, etc., using a single abscissa.
5. An additional curve for each heat exchanger provides both a face velocity and face area comparison. These curves are also useful if comparisons at fixed face area but variable pressure drop are desired.
6. Lines of constant friction power per unit surface area are easily included.

Obviously, considerable judgment must still accompany final selection of a heat exchanger. Factors such as casing and header costs, labor costs, dehumidification performance, noise, fouling, and many others must still be evaluated. However, by putting the performance requirements on an equal basis, the problem of making the final selection is simplified greatly.

ACKNOWLEDGMENT

The author expresses appreciation to C. M. Ashley and S. W. Anderson, of Carrier Corporation, whose suggestions contributed significantly to the development of this paper.

REFERENCES

1. "Concepts of Efficiency of Heat Transfer and Pressure Drop Relations in Heat Exchangers", R. H. Norris, Proc. 5th Int. Congress for Appl. Mech., Cambridge, Mass., 1939.
2. "Heat Transfer by Natural and Forced Convection", Allan P. Colburn, Purdue University Engineering Bulletin 26, January 1942.
3. "Test Results of High Performance Heat Exchanger Surfaces Used in Aircraft Intercoolers and Their Significance for Gas Turbine Regenerator Design", A. L. London and C. K. Ferguson, Trans. ASME, Vol. 71, 1949.
4. "Heat Transfer and Flow Friction Characteristics of Some Compact Heat Exchanger Surfaces", W. M. Kays and A. L. London, Trans. ASME, Vol. 72, 1950.
5. "Selection of Optimum Configurations for a Heat Exchanger with One Dominating Film Resistance", E. R. G. Eckert and T. F. Irvine, ASME paper No. 56-S-20, August 1955.
6. "A Proposed Method for Comparison of Effectiveness of Indirect Heating Surfaces", A. E. Stacey, Jr. and C. M. Ashley, Trans. ASHVE, Vol. 31, 1925.
7. "Experimental Investigation of the Influence of Tube Arrangement on Convection Heat Transfer and Flow Resistance in Cross Flow of Gases Over Tube Banks", O. L. Pierson, Trans. ASME, Vol. 59, 1937.
8. "Basic Heat Transfer and Flow Friction Design Data for Gas Flow Normal to Banks of Staggered Tubes—Use of a Transient Technique", W. M. Kays and R. K. Lo, Tech. Rept. 15, NR-035-104, Dept. of Mech. Engineering, Stanford University, California, August 1952.
9. "The Resistance to Heat Flow Through Finned Tubing", W. H. Carrier and S. W. Anderson, Heating Piping and Air Conditioning, May 1944.
10. "Condensation of Freon-12 in a Horizontal Tube", R. C. Potter and S. P. Patel, Refrigerating Engineering, May 1956.
11. "Heat Transfer—Friction Performance of Smooth Spiral Fin Surfaces", S. W. Anderson, Carrier Corp., Engineering Report RD1006-S9, Report #1, October 1958.
12. "Basis for Rational Design of Heat Transfer Apparatus", E. E. Wilson, Trans. ASME, Vol. 37, 1915.

NOMENCLATURE

A	face area	(ft^2)
c_p	specific heat at constant pressure	(Btu) (lb_m^{-1}) (F^{-1})
C	coefficient	——
f	Fanning friction factor	——
G	mass velocity	(lb_m) (hr^{-1}) (ft^{-2})
h	heat transfer coefficient	(Btu) (hr^{-1}) (ft^{-2}) (F^{-1})
h_i	tube side heat transfer coefficient	(Btu) (hr^{-1}) (ft^{-2}) (F^{-1})
j	Colburn heat transfer factor	——
L	length in flow direction	(in)
m	slope in pressure drop correlation	——
n	slope in heat transfer correlation	——
N_{Pr}	Prandtl Number	——
N_{Re}	Reynolds Number	——
N_{St}	Stanton Number	——
Δp	static pressure drop	(in. H_2O at 60 F)
P	friction power	(hp)
q	heat transfer rate	(Btu) (hr^{-1})
r_h	hydraulic radius	(in.)
R_a	air thermal resistance	(hr) (ft^2) (F) (Btu^{-1})
R_m	metal thermal resistance	(hr) (ft^2) (F) (Btu^{-1})
R_o	overall thermal resistance	(hr) (ft^2) (F) (Btu^{-1})
R_s	surface ratio $= S/S_i$	——
ρ	density	(lb_m) (ft^{-3})
s_m	air side surface area per unit core material mass	(ft^2) (lb_m^{-1})
s_v	air side surface area per unit core volume	(ft^2) (ft^{-3})
S	total air side surface area	(ft^2)
S_i	total tube side surface area	(ft^2)
θ_a	air temperature difference	(F)
θ_m	overall mean temperature difference	(F)
t	temperature	(F)
U	overall heat transfer coefficient	(Btu) (hr^{-1}) (ft^{-2}) (F^{-1})
V	mean value frontal velocity	(ft) (min^{-1})
w	mass rate of flow	(lb_m) (hr^{-1})
Z	coil rating factor based on overall thermal resistance	(in. H_2O at 60 F)
Z'	coil rating factor based on air side thermal resistance	(in. H_2O at 60 F)

DISCUSSION

J. B. CHADDOCK, Lafayette, Ind.: This is an interesting variation on the method of comparing heat exchangers, which has been used by Kays and London and others. It would appear to have considerable merit for our industry. One question which I would like to ask is, why the change in metal resistance with operating conditions was not allowed for in the analysis? As is well known, the fin efficiency will change considerably with changes in air velocity and temperature difference, and this is directly related to the metal resistance. What were your reasons for treating the metal resistance as a constant?

CLOSURE BY AUTHOR RICH: The thermal resistance of the tube wall is generally small and therefore was not considered.

It was shown by Messrs. Carrier and Anderson years ago that the metal resistance of a heat exchanger can be determined from the fin efficiency, and the metal resistance will be relatively constant over a wide range of heat transfer coefficients. Therefore, it is convenient to use the concept of metal thermal resistance. This has but one value and the fact that the fin efficiency varies with the heat transfer coefficient is not important.

If the heat transfer rates are changed in the equation, the fin efficiency changes; but the metal resistance only changes a few per cent. The ASHRAE DATA BOOK covers this point. The metal resistance is approximately one minus the fin efficiency divided by the heat transfer coefficient times the fin efficiency. Substituting different air sides coefficients in this equation makes the fin efficiency vary over a wide range, but not the metal resistance.

J. LEITERSDORF, Hamilton, Ont.: One variation has not been considered, namely, the fluid side pressure drop of the coils. Further, how can equal power consumption for different flow rates be considered if the same face velocities are not used for different tubes?

AUTHOR RICH: In this method of comparison the airside face velocity was allowed to vary in order to make the pressure drop equal for each coil. This is the only reasonable way to make a comparison between the heat exchangers. Tube side pressure drop must be considered, but I know of no way to consider this factor in this type of comparison.

W. L. MCGRATH, Syracuse, N. Y.: The tube side pressure drop can be fixed since it can be controlled by circuiting. In air to water heat exchangers, proper tube curcuiting will allow fixing the pressure drop at the value desired, and the heat transfer coefficients then obtained will be within a reasonable range for purposes of comparison.

C. M. ASHLEY, Syracuse, N. Y.: The effect of the power used in the exchanger by the second fluid can be taken into account by substituting for the pressure drop function the sum of the powers used by the two fluids, divided by the weight flow of the fluid of primary interest (air). Separate curves should be made for each of several velocities of the second fluid for each type of service. The overall optimum is then determined from the most favorable value of this family.

1702

No. 1702

Frost Formation on Refrigeration Coils

W. F. STOECKER
Member ASHRAE

This paper is a report on the continuation of studies of frost formation on refrigeration coils. A previous paper[1] presented the results of the accumulation of frost on a finned coil which cools air by forced convection. This paper reports the effects of frost on heat transfer by natural convection to a horizontal pipe coil.

The objectives of this study were two-fold: (1) to investigate the physical properties of frost under conditions that are representative of commercial practice, and (2) to measure the overall effect of frost accumulation on the rate of heat transfer by natural convection. Unfinned pipe was selected rather than finned pipe in order not to introduce further complications in attempting to achieve the first objective. The studies on bare pipe may also serve as a basis on which to extend research to finned surface, the type that is most popular in industrial practice.

Most of the information that is available on the effect of frost on natural-convection heat transfer comes as a result of qualitative observations of operating refrigeration plants. Piening[2] conducted studies similar to the ones reported in this paper, although in his method of operation water condensed first as a liquid and then froze rather than transforming directly from vapor into solid. The deposit was therefore solid ice rather than porous frost. The investigations reported in this paper were at temperatures typical of a large segment of industrial refrigeration applications.

Equipment. Fig. 1 is a schematic diagram of the test equipment. The test coil consists of a horizontal coil of eight 6-ft lengths of 1¼-in. steel pipe spaced on 3½-in. centers. The coil was fed with chilled ethylene glycol antifreeze through flexible connections and was sus-

W. F. Stoecker is Associate Professor of Mechanical Engineering, University of Illinois.
This paper was presented at the ASHRAE Semiannual Meeting in Dallas, Texas, February 1-4, 1960.

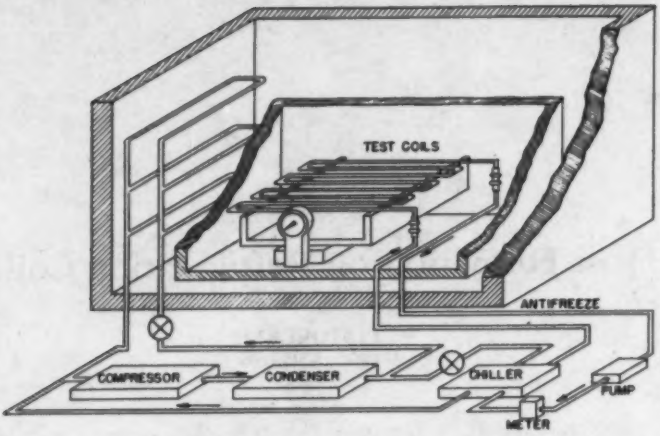

Fig.1—Schematic diagram of equipment

pended on a scale. An inner room housed the coil, and this room was maintained at approximately 7 F by supplementary evaporator coils and at 80% relative humidity by adding moisture in the form of steam.

Instrumentation. The flow rate of antifreeze and the temperature of the antifreeze in and out of the test coil provided the data from which the rate of heat transfer was calculated. In addition to the temperature of the antifreeze, temperatures of the pipe surface and of the room air were measured with thermocouples, while the relative humidity was determined with the aid of dry- and ice-bulb psychrometer.

The frost thickness was measured by a depth gauge consisting of a needle that could be pushed through the frost to the pipe surface and on which was a micrometer head that could be screwed down until it touched the surface of the frost. Thickness of the frost was measured at the top, sides, and bottom of both ends of the eight pipes that composed the test coil.

Procedure. One test continued for a period of several months during which daily readings were taken. To set the test into operation, the supplementary coils pulled down the temperature in the room to the operating temperature. Next, the antifreeze at approximately −16 F was circulated through the test coil, and, after conditions stabilized, the temperature and flows were measured to determine the heat transfer of the unfrosted pipe. To begin frosting, steam was admitted into the room at a controlled rate to maintain the

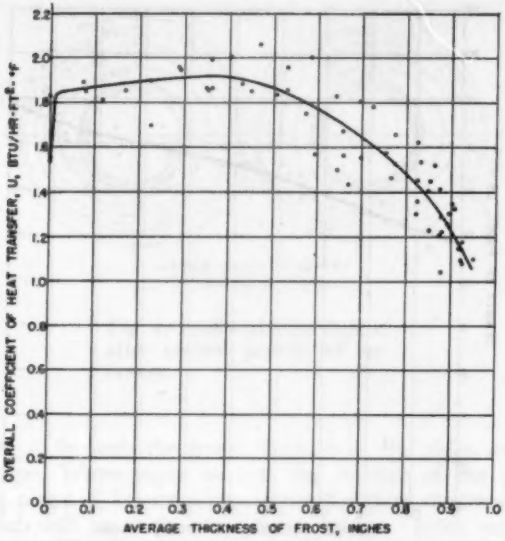

Fig. 2 Effect of frost thickness on the overall coefficient of heat transfer between air and antifreeze

relative humidity at 80%.

Daily thereafter, temperatures, the frost thickness and weight, and the antifreeze flow were measured.

TEST RESULTS

Overall coefficient of heat transfer. The overall coefficient of heat transfer is defined as the rate of heat transfer in Btu/hr per sq ft of heat transfer area per deg difference in temperature between the air and the antifreeze. The process under frosting conditions is actually a combined transfer of heat and mass, but since the latent heat transfer was always less than 5% of the total, all of the heat transfer was considered as sensible heat. This overall coefficient of heat transfer, U, is plotted in Fig. 2 as a function of the average thickness of frost. The U-value is based on the inside or anti-freeze side area which remained constant throughout the test. From a U-value in the neighborhood of 1.55 to 1.60 Btu/hr-ft^2-F for a frost-free coil, the value jumps by about 20% with the first appearance of frost.

This sudden increase is due to the roughening of the air-side heat transfer surface and the increase in air-side heat transfer area. This phenomenon of initial increase in the U-value was observed also in the studies of forced-convection coils. Instead of the U-value de-

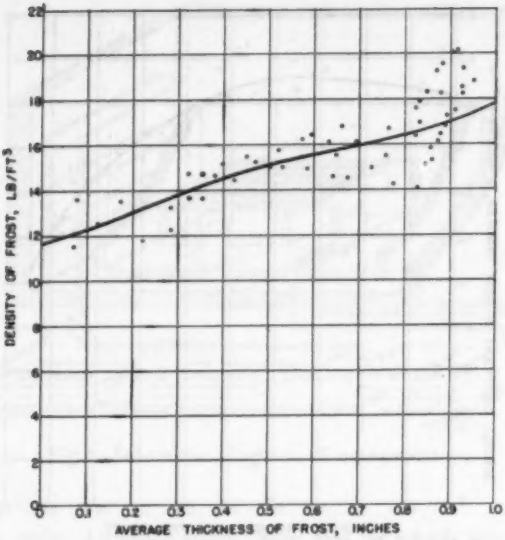

Fig. 3 Change in frost density during the course of the test

creasing progressively as the frost becomes thicker after this initial deposit of frost, the U-value remains somewhat constant until the frost becomes about ½ in. thick whereupon the U-value drops off continuously.

Three reasons seem likely to explain the reluctance of the U-value to diminish. First, the accumulation of frost also increases the air-side heat transfer area which reduces the resistance to heat transfer on the air-side. Also, as the frost ages, the density increases which also increases the conductivity of the frost. Again, as the air passage between the frosted pipes becomes narrow, the velocity of air flowing by natural convection is increased due to the reinforcement provided by the opposing cold surfaces.

The realization that the overall coefficient of heat transfer does not immediately diminish confirms the recommendations[3,4] that some frost on the coil is not necessarily undesirable. Reference 3 states that the rate of heat transfer to pipe coils under natural convection is unaffected until the frost buildup exceeds ½ in. thickness.

Density of the frost. The average density of the frost increased steadily throughout the test from about 12 lb/ft³ to 20 lb/ft³ as is shown in Fig. 3. The reason for this trend lies in the diffusion of

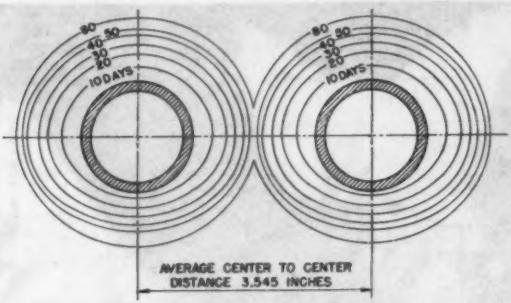

Fig. 4—Profile of frost deposit after various periods of operation

the water vapor through the frost toward the pipe. Water vapor migrates to the point of lowest temperature which will be at the surface of the pipe. The first frost to form at the surface of the pipe was granular and somewhat fluffy, but after 80 days of operation, cutting into the frost showed this layer at the surface of the pipe almost to have assumed the character of ice.

Some water vapor molecules diffuse continuously through the frost toward the pipe which increases progressively the density of the frost. One of the effects of the high-density frost is to increase its conductivity, which is desirable. Older frost is likely to be more dense and thus have a higher conductivity.

Pattern of frost deposit. The frost did not form as a perfect circle about the refrigerated pipe. The character and grain size of the frost differed on the top, sides and bottom of the pipe. Fig. 4 shows that in the early stages, the frost is thickest at the sides and thinnest at the bottom of the pipes. This general pattern continues until the frost bridges from one pipe to another at which condition the top and bottom portions of the pipes are the only places where the thickness can continue to increase.

Fig. 5 shows some of the irregularities in the deposit of the frost. The character of the frost is different at the bottom of the pipe compared to the top. At the bottom the crystals are longer and less dense than at the top. Although it is not clear from the illustration, a visual examination indicated that the frost is more dense closer to the pipe surface. Another observation is that the bridge of frost between the two coils occurred at a plane above the plane of the centerlines of the pipes. The maximum rate of deposit occurred, therefore, at about 2 o'clock and 10 o'clock on the pipe circumference.

Rate of frost deposit. The rate at which frost precipitated on the

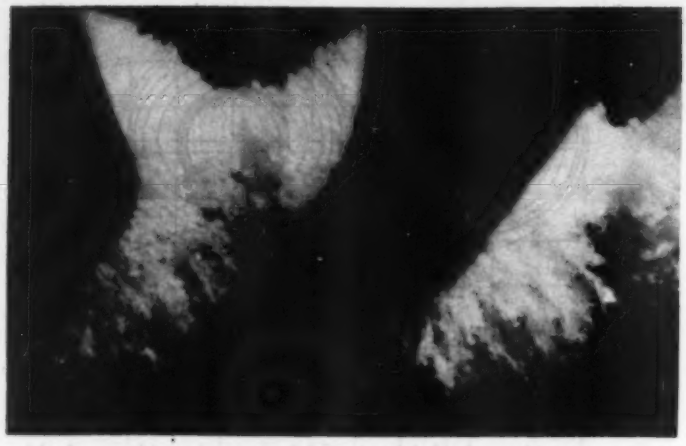

Fig. 5 Irregularities of frost deposit around pipes

coil decreased steadily throughout the test as is shown in Fig. 5. In the early stages of the test, frost accumulated at a rate of 0.017 lb/day-ft of pipe, while at the latter stage the rate diminished to 0.011 lb/day-ft. The rate of deposit decreased even during the period when the rate of heat transfer was nearly constant. This trend is explained because the surface temperature of the frost-air interface increased due to the shift in the heat transfer resistance from the outside air film to the layer of frost. This trend is similar to the principle used in the selection of heat transfer surface where by selecting a large area and operating with a reduced temperature difference the rate of dehumidification can be decreased.

ANALYSIS

This part of the report seeks to explain by means of the principles of heat transfer and fluid flow the trends in (1) the combined resistance of the frost and air film, and (2) the pattern of the frost deposit on the tubes.

Combined Resistance of Frost and Air Film. The expression for the overall resistance to sensible heat transfer from the air to the refrigerant neglecting the resistance of the pipe is:

$$\frac{1}{A_i U_i} = \frac{1}{A_i h_i} + \frac{1n \frac{A_f}{A_o}}{2\pi Lk} + \frac{1}{A_f h_o} \quad (1)$$

where $\frac{1}{A_i U_i}$ is the total resistance based on the inside or refrigerant side surface, hr/F/Btu.

U_i is the overall coefficient of heat transfer based on the inside surface, Btu/hr/ft²/F.

A_i is the inside surface area, ft².

h_i is the inside convection coefficient, Btu/hr/ft²/F.

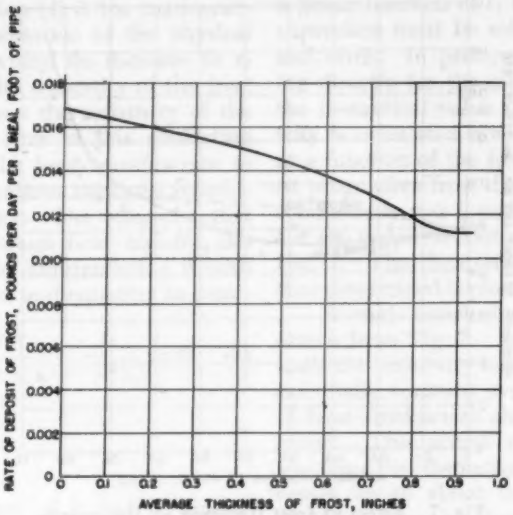

Fig. 6—Rate of frost deposit

A_o is the area of the outside of the pipe, ft².
A_f is the surface area of the frost, ft².
L is the length of pipe, ft.
k is the conductivity of the frost, Btu/hr/ft/F.
and h_a is the air-side convection coefficient, Btu/hr/ft²/F.

Equation (1) is based on the idealizations of an annular cross-section of the frost and uniform values of k and h_a. Equation (1) can be expressed in terms of resistivities by multiplying each term by A_1, giving:

$$\frac{1}{U_1} = \frac{1}{h_1} + A_1 \frac{1n \dfrac{A_f}{A_o}}{2\pi Lk} + \frac{A_1}{A_f h_a} \qquad (2)$$

The ratio of areas can be expressed as the ratio of radii:

$$\frac{1}{U_1} = \frac{1}{h_1} + \frac{r_1 \, 1n \dfrac{r_f}{r_o}}{k} + \frac{r_1}{r_f h_a} \qquad (3)$$

The antifreeze side coefficient remained essentially constant throughout the test at 19.5 Btu/hr/ft²/F so the reciprocal of 19.5 is the resistivity of the inside film. This resistivity can be subtracted from the total resistivity $1/U_1$ to give the combined resistivity of the frost and air film, R, where

$$R = \frac{r_1 \, 1n \dfrac{r_f}{r_o}}{k} + \frac{r_1}{r_f h_a} \qquad (4)$$

The total resistivity, $1/U_1$ is the reciprocal of the value shown in Fig. 2.

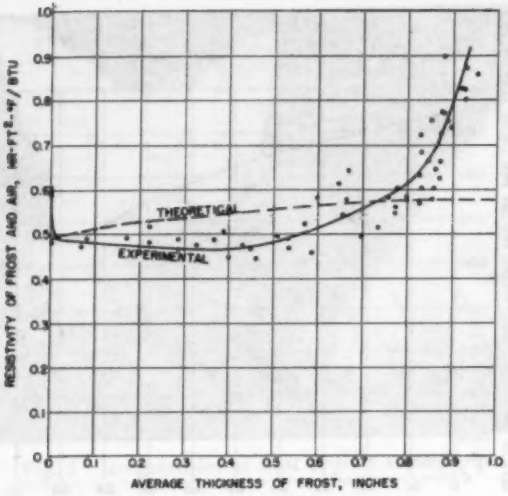

Fig. 7 Effect of frost thickness on the experimental and theoretical resistivity of frost and air

The experimental value of R is shown in Fig. 7 as the solid line as it varies with the frost thickness. What is the theoretical prediction of R? To make such a prediction the values of the air-side convection coefficient h_a and the conductivity of the frost must be determined. The value of h_a is found from Fig. 7 at the point just after the bare pipe surface has been roughened by the first trace of frost. The same roughened surface is assumed to prevail during the entire period of frosting. This condition was selected also, because at this state all of the resistivity is due to the air film on the roughened surface and the first term on the right side of Equation (4) is zero. The value of h_a thus determined was 1.70 Btu/hr/ft²/F.

The conductivity of frost has been determined experimentally by several observers,[5, 6, 7, 8] and in every instance the conductivity was found to increase with an increase in density. Values from Schropp[8] approximately represent the mean values of the other observers and are used for the calculations in this report. Table I shows such values as a function of the frost density.

TABLE I.
CONDUCTIVITY OF FROST[8]

Density, lb/ft³	Conductivity, Btu/hr/ft/F
10	0.075
12	0.084
14	0.098
16	0.114
18	0.135
20	0.168

Equation (4) is the mathematical representation of the physical situation where an increase in r_f increases the resistivity of the frost but decreases the resistivity of the air film. Due to this conflicting influence the heat transfer rate in certain situations increases by adding insulation. The value of r_f that gives maximum heat transfer can be found by differentiating R with respect to r_f and equating to zero.

$$\frac{dR}{dr_f} = \frac{r_i r_o}{r_o r_f k} - \frac{r_i}{r_f^2 h_a} = 0 \quad (5)$$

critical

$$r_f = \frac{k}{h_a}$$

If the values of k and h_a give a magnitude of the critical r_f that is less than the inside diameter of the frost layer r_o, any addition of frost should increase the resistivity and decrease the overall coefficient of heat transfer.

A critical r_f less than the inside diameter of the frost was apparently the situation in the recent tests of Chung and Algren[9] where the heat transfer coefficient decreased continuously with an increase in thickness of frost. The high value of h_a in the forced convection tests of Chung and Algren contribute to a low value of critical r_f as is shown by Equation (5).

Equation (5) is not satisfactory for the case where the frost density and conductivity change progressively throughout the test, but a variable value of k must be used. A mathematical expression for the critical radius is not practical because even if k can be expressed as a linear function of r_f the resulting expression must be solved by trial and error. In preference to solving directly for the critical radius, the theoretical value of the resistivity is calculated from Equation 4 as a function of the frost thickness. At progressive frost thicknesses the conductivity was found from Table I at the density as determined from Fig. 3. The theoretical resistivity thus determined is plotted in Fig. 7.

Several conclusions may be drawn from Fig. 7. Even theoretically the resistivity tends to remain essentially constant over the range of frost thicknesses shown on the graph. The actual resistivity is less than the theoretical for thicknesses up to about 0.7 in. This deviation may be due to the increased value of the air-side coefficient h_a brought about by reinforced air flow of the adjacent frost surfaces. The apparent increase in h_a caused by the neighboring pipes is discussed further in the next section of this paper. At frost thickness beyond 0.7 in. the actual resistivity exceeds the theoretical because of the closing of the air passages and the consequent reduction in h_a.

Pattern of Frost Deposit and Local Convection Coefficient. The distribution of the frost thickness over the circumference of the pipe gives an indication of the magnitude of the local heat transfer coefficient because of the analogy of heat and mass transfer. Hermann[10] developed an expression for the local Nusselt number as a function of the position on a single tube

TABLE II.
VALUES OF F(Θ)

θ (deg)	0	30	60	90	120	150	165	180
f(θ)	0.760	0.752	0.718	0.664	0.581	0.458	0.360	0

undergoing heat transfer by natural convection:

$$Nu = 0.604\ (Gr)^{1/4}\ f(\Theta) \qquad (6)$$

where Nu is the Nusselt number, Gr is the Grashof number and f(Θ) is a function of the angle Θ measured from the top vertical position which is given in Table II. The angles used by Hermann for a hot pipe are reversed for the situation in this report where the pipe is cold.

The equation of Hermann shows that the local coefficient of heat transfer is greatest at the top of the pipe and decreases progressively toward the bottom. The thickness of frost deposit should be at least roughly proportional to the local convection coefficient and Nusselt number, which means that the thickness should be roughly proportional to the values of f(Θ) in Table II. The distribution of frost thickness reported by Piening[2] corresponds fairly well to the expected pattern, but the distribution in the studies reported in this paper did not. The principal deviation is that the frost was thickest at a sector between 60 deg and 90 deg measured from the top vertical and not at the top as would be expected.

The explanation for the greater thicknesses at the sides lies probably in the effect of the presence of neighboring tubes on both convection and radiation. The investigations of Hermann and Piening were for single tubes while the studies of this paper were for pipes in a horizontal row. The presence of neighboring pipes probably increases the local coefficient of heat transfer by reinforcing the air velocity between the tubes. A test of the plausibility of this explanation requires some information on how far from the tube the air is set into motion. Jodelbauer[11] in a test with a tube 1.96 in. O.D. and 90 F temperature difference between the tube and the remote air reported that the air was in motion more than 0.4 in. from the tube and had a maximum velocity about 0.07 in. from the tube. Under those conditions, the velocity of air between the tubes would be increased if the surface-to-surface distance is less than 0.8 in. In the tests reported in this paper, the surface-to-surface distance was 1.8 in. initially but decreased as frost accumulated.

With the relatively low values of heat transfer coefficients experienced in natural convection, the proportion of heat transferred by radiation is often significant and is so considered in these tests.

The heat transfer by radiation also offers a further explanation for the pattern of frost deposit. The frost surfaces at the top of the pipes

"see" principally the slightly warmer surfaces of the ceiling while the surfaces of the frost on the side of the pipe see principally the neighboring cold surface. Due to radiation, therefore, the surface at the sides of the pipes will be colder and accumulate more frost than those surfaces at the tops of the pipes.

The combined effect of the increased convection coefficient due to neighboring pipes and due to radiation may be illustrated by comparing the experimental value of the heat transfer coefficient with one of the commonly used equations for the coefficient of a single tube. Using the equation[12] for air

$$h = 0.27\left(\frac{\Delta t}{D_o}\right)^{1/4} = 0.27\left(\frac{21}{0.14}\right)^{1/4} =$$

0.95 Btu/(hr) (ft²) (F)

The actual value of h with the frost-free coil determined from Fig. 2 by deducting the resistance to heat transfer of the antifreeze and the metal of the pipe is 1.41 Btu/hr/ft²/F. The reinforcing of air flow caused by the neighboring pipe is probably one of the factors which increases the actual value over that of the single pipe.

SUMMARY

When frost is accumulating on pipe coils that are cooling air by natural convection, the first deposit of frost, strangely, increases the coefficient of heat transfer. This increase in the coefficient is due to the roughening of the surfaces which gives a greater area for heat transfer in the same manner as the addition of fins will increase the rate of heat transfer. As the frost deposit thickens, the coefficient of heat transfer remains somewhat constant instead of decreasing as might be expected. This maintenance of a nearly constant coefficient of heat transfer is attributable to two causes: one is the increase in external surface area, and the other is the increase in conductivity of the frost as the frost becomes more dense due to aging. These two effects compensate for the increased resistance to heat transfer brought about by the thickening of the frost deposit. The coefficient of heat transfer begins to diminish when the thickness exceeds 0.5 to 0.6 in. and drops off rapidly when the passages for air flow become blocked. As a rough rule of thumb, the recommended point at which to defrost appears to be when the frost bridges over from pipe to pipe and blocks the air flow.

The presence of neighboring pipes in the coil and radiation from the pipes increase the coefficient of heat transfer over that of a single tube and also cause accelerated rate of deposit of frost on the side of the tubes.

ACKNOWLEDGMENTS

This research was conducted with the aid of grants from the Refrigeration Research Foundation and the American Society of Refrigerating Engineers, one of the two predecessor societies to American Society of Heating, Refrigerating and Air-Conditioning Engineers.

A number of investigators worked on the project during the installation and testing including Fred Turk, John K. Young, and Herbert Siewert.

BIBLIOGRAPHY

1. Stoecker, W. F., "How Frost Formation on Coils Affects Refrigeration Systems", *Refrigerating Engineering*, vol. 65, no. 2, p. 42, Feb. 1957.

2. Piening, W., "Der Warmuebergang an Rohren bei freier Stromung unter Beruchsichtigung der Bildung von Schwitzwasser und Reif", *Gesundheits-Ingenieur*, vol. 56, p. 493, October 21, 1933.

3. Berns, N., "Defrosting Coils—Requirements and Methods", *TREF Commodity Storage Manual*, 1956.

4. Equipment Manual, York Div of Borg-Warner Corporation, Section A-6, p. 5.

5. Prins, L., "Warme-und Stoffubertragung in einem querangestromten bereifenden Luftkuhler", *Kaltetechnik*, vol. 8, no. 5, p. 160, May 1956.

6. Schmidt, Th. E., "Der Warmeubergang in Luftkuhlern mit Rippenrohren", Feih, Za. ges. Kalteind., Reithe 2, no. 6, 1933.

7. Coles, Willard D., "Experimental Determination of Thermal Conductivity of Low-Density Ice", NACA, Tech. Note 3141, March 1954.

8. Schropp, K., "Untersuchungen uber Tau- und Reifbildungen an Kuhlrohren in ruhender Luft und ihr Einfluss auf die Kalteubertragung", Za. ges. Kalteind, 42 (1935) pp 81-85, 126-131, 151-154.

9. Chung, P. M. and A. B. Algren, "Frost Formation and Heat Transfer on a Cylinder Surface in Humid Air Cross Flow", *Heating, Piping, and Air Conditioning*, Part I, vol. 30, no. 9, p. 171, Sept., 1958, and Part II, vol. 30, no. 10, p. 115, October 1958.

10. Hermann, R., "Wärmeubergang bie freier Strömung am waagerechten Zylinder in zweiatomigen Gasen", VDI Forschungsheft, vol. 7, no. 379, p. 1-24, July-August 1936.

11. Jodelbauer, K., "Das Temperatur- und Geschwindigkeitsfeld um ein geheiztes Rohr bei freier Konvection", Forschung a. d. Gebeite des Ingenieurwesens, vol. 4, no. 4, p. 157, July-August 1933.

12. McAdams, W. H., "Heat Transmission", 3rd ed., McGraw-Hill Book Company, New York, 1954.

DISCUSSION

UNIDENTIFIED SPEAKER: I think you would be interested in knowing that some of your basic findings have been confirmed in commercial installations using a finned coil with a fixed fan behind it. In tests to determine the economic point of defrost, the initial build-up of frost did not decrease the heat transfer but tended to increase it slightly until it reached the critical point, following closely the results of the paper. It was also found that the use of a finned coil with wide fin spacing and the accumulation of a heavy frost to cut down the frequency of defrosting caused a reduction in the coefficient because the critical point was passed and the heat transfer fell off sharply after that point. In designing equipment, the fin spacing was not as critical as the timing of the defrost.

CLOSURE BY AUTHOR STOECKER: I am glad that similar results have been observed. No mention of fin coils was made since the work was confined to bare coils. Bare coils were selected (although fin coils have more commercial application) because the process was complex enough, even with the cylindrical surface. People in industry have said that fin coils are often somewhat more sensitive to frost than bare pipes.

F. GOVAN, Washington, D. C.: In the bridgement of the frost between coils, was there an increase in the density of the frost in the bridge?

AUTHOR STOECKER: The frost grew progressively outward from each of the pipes, and after bridging, the whole coil tended to merge into one big rectangular mass, making it difficult to tell if the density of the bridge increased or not.

C. M. ASHLEY, Syracuse, N. Y.: The trend of the points in Fig. 3 is not to follow the curve which is drawn through them; the points seem to have a consistent pattern. Should the curve follow the points? Is this a problem of measurement of the average density which involves determining the thickness?

In respect to the sharp drop in the heat transfer coefficient between 0.8 and 0.9 in. thickness, at that point the rate of accumulation has decreased, particularly considering the larger envelope. Therefore, the opportunity for diffusion with respect to the thickness becomes considerably greater and an increase should be expected.

Theoretically, if the room temperature is close to 0 F and the surface temperature is about −20 F, this general range will produce snow providing the entering air was virtually saturated. If you started from less than saturation you shouldn't get snow. Have any such tests been made, and if so, do they confirm this?

AUTHOR STOECKER: The curve in Fig. 3, concerning the average density where the points would indicate a sharp increase at the heavy thickness, shows that the measurements of thickness become inaccurate after bridging of the frost occurs. With the cross-section of the

frost becoming progressively less circular, the method of calculating the volume of the frost becomes less accurate; therefore, the curve was extended rather than made to follow the points at heavy thickness.

Concerning the question of degree of saturation and possibility of snow, about 80% humidity was maintained with which there was no snow. In one exploratory test, the humidity was very high and no snow resulted, but on every surface in the room there were long crystals of frost 1 to 2 in. long.

WARREN VIESSMAN, Baltimore, Md.: As an amateur photographer, I think the crystals showed up quite well in the slides.

What is the definition of the critical pipe diameter?

Are the results in this paper for pipes comparable to separate flat plates under natural convection?

AUTHOR STOECKER: There is a brief discussion in the paper on calculations of the critical radius. The critical radius is the convection heat transfer coefficient divided by the conductivity of the frost.

It would not be advisable to apply the results of this paper to flat plates. Certain phenomena such as the increase of density, would be applicable, but the increase in area due to the progressive increase of frost would probably not occur in the flat plate as it would in a cylindrical section.

W. L. HOLLADAY, Los Angeles, Calif.: Commenting further, some years ago I ran some tests on flat plates in household evaporators and found that the increase of insulating effect with small amounts of frost was compensated for by the increased roughness of the surface, just as in the pipe used in your test.

It was stated that the increased accumulation of frost slightly above the mid-point at 10 a.m. and 2 p.m. probably was due to the reinforcing of air streams. Was such a condition found at one of the outside pipes that did not have an adjacent pipe?

AUTHOR STOECKER: That is a good question, and the answer is that no such increase was observed.

1703

No. 1703

Frost Formation upon a Thin Aluminum Tank Containing Liquid Oxygen

J. L. LOPER

Cooling of a gas-vapor mixture or a mixture of several vapors results in condensation of one or more of the vapors when their respective dew-points are reached. A mass transfer of the vapor to the cooling surface occurs, accompanied by energy transfer as the vapor gives up its latent heat of vaporization to the surface and becomes a liquid. The condensation of a vapor onto a cool surface causes a liquid build-up to a certain steady state thickness which flows off by gravity action if the surface is sloped enough to allow this to happen. This liquid accumulation adds resistance to the further transfer of mass and energy.

A mixture of water vapor and air at atmospheric pressure, coming into contact with a surface whose temperature is below the freezing point of water, results in a build-up of frost or snow, which varies with time, adding resistance against the flow of mass and heat. It is unlike condensation in that the frost layer is continually increasing, though at a much slower rate after time intervals exceeding an hour. The frost builds up in crystal form and has the ability to adhere to a smooth surface until the sheer force becomes too great and portions of the formation slide off.

The results of a transient heat transfer analysis are presented for the determination of the heat transfer rate and corresponding liquid boil-off rate of liquid oxygen from a thin aluminum tank.

The effects of dry bulb temperature, relative humidity, wind, thermal radiation, and increasing frost thickness were considered in the analysis.

This subject is of interest in liquid rocket missile work in being

J. L. Loper is a Senior Research Engineer, The Western Company. This paper was presented at the ASHRAE Semiannual Meeting in Dallas, Texas, February 1-4, 1960.

able to predict the magnitude of liquid oxygen losses which result from exposure to widely varying atmospheric conditions.

This is essentially a transient heat flow problem involving an accumulating thickness of frost on a cylindrical aluminum tank exposed to the atmospheric elements. The total heat transfer rate from the outside to the cold interior of the tank is composed of convection, radiation, and mass diffusion heat transfer. Convection heat transfer is influenced by the wind velocity across the tank and the dry bulb temperature. Thermal radiation exchange is controlled by the temperature of the frost surface and temperature level of the surroundings as well as the emissivity of the frost surface layer on the outside wall. Mass diffusion heat transfer is a function of the quantity of water vapor in the atmosphere, the wind velocity across the tank, the temperature of the cold wall, and the diffusing ability of the water vapor through the boundary layer to the cold wall.

Analysis is based upon a quasi-steady state method whereby small time intervals were selected and the heat transfer rate, outside temperature of frost layer (air-frost interface temperature) and increments of frost thickness were determined.

The following assumptions were made:

1. Heat flow is one dimensional.
2. Liquid oxygen boiling film offers negligible resistance to the flow of heat.
3. Aluminum tank wall offers negligible resistance to the flow of heat.
4. Aluminum wall is at a uniform and constant temperature of −297 F.
5. Cylindrical tank is of sufficient length that convection end effects are negligible.
6. Thermal conductivity of frost varies with temperature exactly as the thermal conductivity of air varies. The basis for this assumption is that frost, being porous, is a composite material of frost crystals and air.
7. Radiation effects are the result of thermal (long wave length) radiation. The tank wall is shielded from direct solar radiation.
8. Wind velocity remains uniform and steady across the tank wall.
9. Time interval for initial cooling of the aluminum tanks is negligible due to the high thermal diffusivity of this material.
10. Steady state conditions exist for small time intervals (quasi-steady state conditions) so that frost thickness, vapor pressure at the frost-air interface and frost temperature at the interface are essentially constant during the time interval.

The mass flow rate per unit area is defined by an equation involving the vapor pressure gradient across the boundary layer existing at the tank wall.[1, p. 250]

$$W_v = \frac{144 h_m}{R_v T_1} (P_{v2} - P_{v1}) \frac{LB_m}{hr\text{-}ft^2} \quad (1)$$

The Lewis equation [1, p. 252]

$$h_m = \frac{h_c}{\rho_a C_{pa}} \frac{ft}{hr} \quad (2)$$

can be employed in order to obtain a relationship between the mass transfer coefficient, h_m, and the heat transfer convection coefficient, h_c.

The heat flux due to mass diffusion of water vapor through air can be expressed as the product of the enthalpy change of the water and the mass flow rate of equation (1):

$$\left(\frac{Q}{A}\right)_m = l_w w_v = \frac{144 l_w h_m}{R_v T_1} (P_{v2} - P_{v1}) \frac{Btu}{hr\text{-}ft^2} \quad (3)$$

For the heat transfer convection coefficient, a correlation was selected giving the average film coefficient around a cylinder in a flow normal to the axis [1, p. 163]

$$h_c = C_1 \frac{K}{D} (R_e)^m \left(\frac{T_f}{T_a}\right)^{-n} \frac{Btu}{hr\text{-}ft^2\text{-}F} \quad (4)$$

The constant, C_1, and the exponent, m, are functions of Reynold's Number.

The heat flux due to forced convection is:

$$\left(\frac{Q}{A}\right)_c = h_c (t_a - t_1) \frac{Btu}{hr\text{-}ft^2} \quad (5)$$

where $(t_a\text{-}t_1)$ is the temperature gradient across the boundary layer from the ambient air temperature, t_a, to the temperature at the outside of the frost layer, t_1.

The heat flux equation for radiation is:

$$\left(\frac{Q}{A}\right)_R = .173 F \epsilon F_A \left[\left(\frac{T_A}{100}\right)^4 - \left(\frac{T_1}{100}\right)^4\right] \frac{Btu}{hr\text{-}ft^2} \quad (6)$$

where, for a small body surrounded by a large body, the emissivity factor is equal to ϵ (ϵ being the emissivity of the frost on the tank surface).

The total heat flux $\left(\frac{Q}{A}\right)_t$ is a summation of the diffusion, convection, and radiation effects:

$$\left(\frac{Q}{A}\right)_t = \left(\frac{Q}{A}\right)_m + \left(\frac{Q}{A}\right)_c + \left(\frac{Q}{A}\right)_R \frac{Btu}{hr\text{-}ft^2} \quad (7)$$

Introducing a conduction equation for the transfer across the frost thickness, aluminum wall and boiling film:

$$\left(\frac{Q}{A}\right)_t = \frac{\Delta T_{TOTAL}}{R_{FROST} + R_{WALL} + R_{BOILING}} \frac{Btu}{hr\text{-}ft^2} \quad (8)$$

By assumptions 2 and 3, the resistances R_{wall} and $R_{boiling}$ are negligible, therefore, the temperature drops across the aluminum wall and the boiling region along the inside wall are extremely small. Thus, the total conduction from the air film to liquid oxygen can be handled by the equation:

$$\left(\frac{Q}{A}\right)_t = \frac{(t_1 - t_a)}{\frac{X_f}{K_f}} \frac{Btu}{hr\text{-}ft^2} \quad (9)$$

In this steady state equation, x_f is a function of the variables K_f, h_c, p_v, ρ_a, Cp_a and t_1; however,

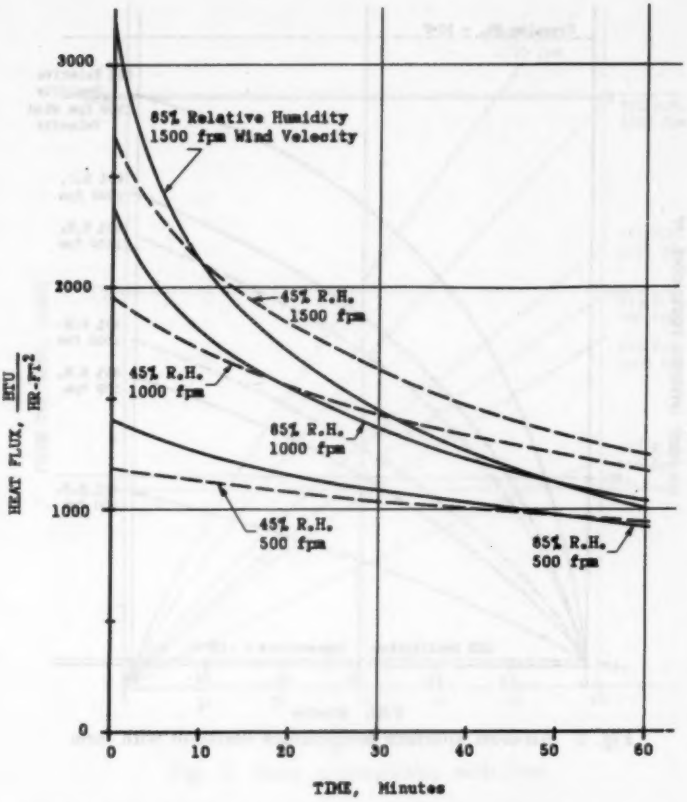

Fig. 1 Heat flux variation with time for 45 and 85% relative humidities and wind velocities of 500, 1000 and 1500 fpm

each of these is, in turn, a function of t_1, for a fixed wind velocity and ambient temperature. Therefore, the steady state equation can be expressed as:

$$X_f = f(t_1)$$

After the tank is initially filled, frost will commence to build up on the wall at a rate controlled by the variables listed above. The frost thickness is also a function of time, θ, and can be expressed by the following relationship:

$$X_f = \frac{144\, h_c (P_{v_a} - P_{v_1})}{60\, \rho_f R_v T_1 \rho_a Cp_a} \theta \text{ ft} \quad (10)$$

From equation (10) it is observed that the frost thickness is a function both of t_1 and time, θ, for

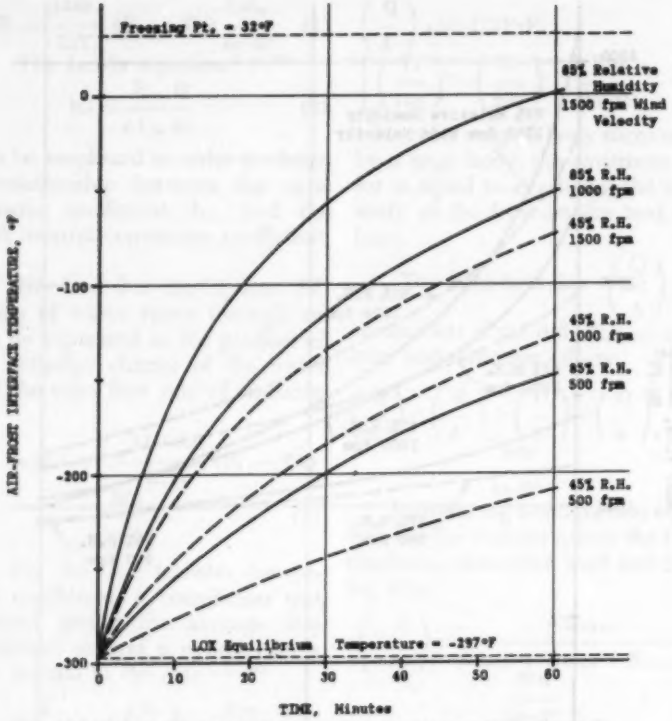

Fig. 2 Air-frost interface temperature variation with time

a fixed wind velocity and ambient temperature:

$$X_f = f(t_a, \theta)$$

The total frost build-up after θ_t minutes have elapsed is:

$$X_{ft} = \Delta X_{f1} + \Delta X_{f2} + \cdots + \Delta X_{fn} \text{ ft}$$

where each increment of frost thickness ΔX_{fn} corresponds to an increment of time, $\Delta\theta_n$. Steady state conditions exist by assumption No. 10. The selection of short time intervals initially (on the order of one and two minutes) during which time conditions are most rapidly changing, and longer time intervals later (five to ten minutes) when the rate of change has decreased, will approximate the true transient condition.

Tests conducted by Paul[4] indicate that the frost build-up on aluminum walls containing liquid oxygen has a density range from 15 to 20 lb cu ft. For calculation purposes a value of 17.0 lb/cu ft was selected.

The thermal conductivity value of frost used in calculations was

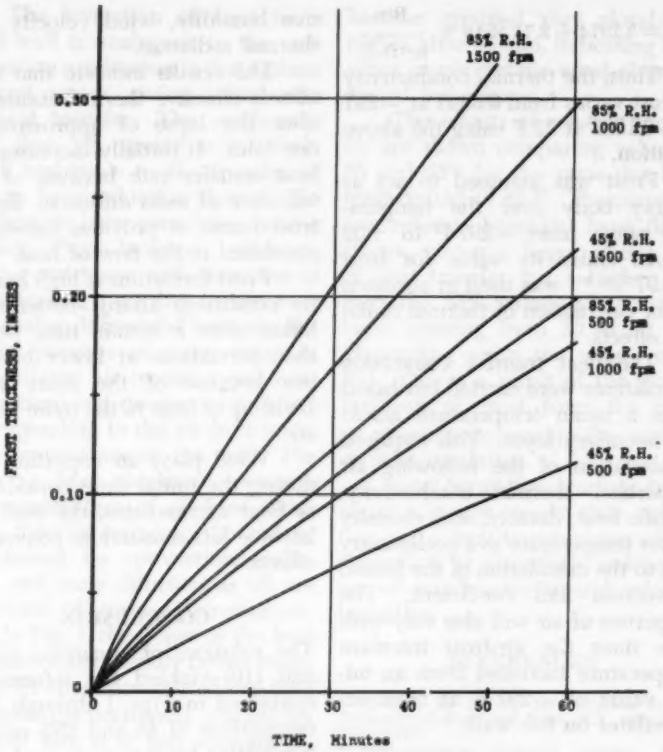

Fig. 3 Frost accumulation with time

$$0.1083 \frac{\text{Btu}}{\text{hr-ft-F}} \text{ at } 32\text{ F}$$

corresponding to a density of 15.7 lb/cu ft.[2, p. 213] Since the frost temperatures occurring here would, in most cases, be far below freezing, it was thought necessary to correct for variations of K with temperature by using an extrapolation process. Direct data were lacking for this change with temperature.

The correction of K with temperature was determined in the following manner: the average slope of K for air [3, Table 1510.11a] was calculated over the range of temperatures from −316 F to +32 F. Frost is a porous material consisting of ice crystals and air; therefore, it was assumed that frost would have a K variation with temperature which follows closely that for air. Based upon this assumption, the equation for frost is:

$$K_f = 0.1074 + 2.74 \times 10^{-4} t \quad \frac{\text{Btu}}{\text{hr-ft-F}}$$

Thus, the thermal conductivity of frost varies from 0.0993 at −297 F to 0.1083 at 32 F using the above equation.

Frost was assumed to act as a gray body over the temperature range from −297 F to +32 F. An emissivity value for frost of 0.97 [1, p. 277] was used in equation (6) for calculation of thermal radiation effects.

The heat transfer convection calculations were carried out based upon a mean temperature across the boundary layer. This required a tabulation of the following air properties: thermal conductivity, specific heat, density, and viscosity versus temperature as a preliminary step to the calculation of the forced convection film coefficient. The properties of air will also vary with time since the air-frost interface temperature increases from an initial value of −297 F as frost accumulates on the wall.

SUMMARY

Equations have been developed making it possible to predict the following characteristics of frost formation: the heat transfer rate, frost thickness, and air-frost interface temperature as functions of time. The heat transfer mechanisms of water-vapor diffusion, convection, conduction, and radiation were utilized.

Certain atmospheric effects, influencing the formation of frost, were included in the analysis. They were dry bulb temperature, relative humidity, wind velocity and thermal radiation.

The results indicate that frost affords effective thermal insulation after the lapse of approximately one hour. It initially increases the heat transfer rate because of the influence of mass diffusion. But as frost forms, it provides increasing resistance to the flow of heat.

Frost formation at high humidity conditions affords better insulation after a certain time period than formations at lower humidities because of the more rapid build-up of frost in the more humid air.

Wind plays an important role during the initial time periods but as frost accumulates, the wall will become less sensitive to convection effects.

CONCLUSION

The solutions of equations (7), (9) and (10) yielded the information contained in Figs. 1 through 3. A comparison of 45 and 85% relative humidities for parameters of wind velocities from 1500 fpm to 500 fpm are shown in these graphs.

The mass diffusion of water vapor through air plays an important role in the transfer of heat to surfaces maintained at extremely low temperatures. Frost is an effective thermal insulator. The mass transfer of water vapor to a cold wall at first increases the rate of heat transfer to the wall, but after a certain time period has elapsed, the resulting frost formation decreases the heat transfer rate as compared to the constant rate obtained in dry air.

The formation of frost on a cold wall is analogous to the condensation mechanism in that a phase change occurs, giving a high rate of heat transfer. The condensate will flow off, giving a relatively small resistance to the transfer of energy by conduction through the condensate layer remaining on the surface. Frost, however, builds up, adding resistance with time, but at a decreasing rate due to the ever decreasing differential between the partial pressure of water vapor in the ambient air (water vapor concentration) and the partial pressure corresponding to the air-frost interface temperature on the wall. The growing frost thickness increases the temperature of air-frost interface, thereby reducing the energy transferred by convection, radiation, and mass diffusion as all are functions of surface temperature.

In Fig. 1, the slopes of the heat flux curves are initially rather steep, but after approximately 45 min they approach the horizontal. The energy transfer rate is at first strongly influenced by the wind velocity and relative humidity of the ambient air. The initial values of heat flux are rather widely dispersed but become grouped very closely together after 45 min, indicating little effect caused by the wind after this period has elapsed.

The effects of relative humidity are shown comparing values at 85 and 45% for the same dry bulb temperature of 82 F. The curves of low relative humidity have flatter slopes, giving a lower initial rate of heat transfer but a higher rate than the 85% values after a time lapse running from 10 to 50 min (depending upon the wind velocity). This is a result of the slower build-up of frost from the drier air, thereby decreasing the benefits of frost insulation.

Frost formation tends to bring about a nearly steady state condition and a heat transfer rate whose magnitude is essentially independent of wind velocity and relative humidity.

REFERENCES

1. Eckert, E. R. G., *Introduction to the Transfer of Heat and Mass*, N.Y., McGraw-Hill, 1950.

2. International Critical Tables, N.Y., McGraw-Hill, 1929, Vol. 2.

3. Navy Ordnance Report 1488, Handbook of Supersonic Aerodynamics, Vol. 5, August 1953.

4. Paul, H. G., Unpublished Data, Huntsville, Alabama, June, 1955.

NOMENCLATURE

C_{p_a}	Specific heat of air	$\frac{\text{Btu}}{\text{lb}_m\ \text{R}}$
D	Diameter of cylinder	ft
h_c	Convection coefficient	$\frac{\text{Btu}}{\text{hr-ft}^2\text{-F}}$
K_f	Frost thermal conductivity	$\frac{\text{Btu}}{\text{hr-ft-F}}$

h_m	Mass transfer coefficient for turbulent boundary layer	$\frac{ft}{hr}$
l_w	Enthalpy change for water in transforming from vapor to frost	$\frac{Btu}{lb_m}$
P_{v_2}	Water vapor pressure at temperature, T_2	$\frac{lb_f}{ft^2}$
P_{v_1}	Water vapor pressure at temperature, T_1	$\frac{lb_f}{ft^2}$
$\left(\frac{Q}{A}\right)_c$	Heat flux due to air convection along wall	$\frac{Btu}{hr\text{-}ft^2}$
$\left(\frac{Q}{A}\right)_m$	Heat flux due to enthalpy change of water vapor transferred to wall by diffusion	$\frac{Btu}{hr\text{-}ft^2}$
$\left(\frac{Q}{A}\right)_R$	Heat flux due to radiation to wall	$\frac{Btu}{hr\text{-}ft^2}$
R_e	Reynold's number	Dimensionless
R_v	Gas constant for water vapor	$\frac{lb_f\ ft}{lb_m\ R}$
$R_{boiling}$	Heat transfer resistance across boiling film	$\frac{hr\text{-}ft^2\text{-}R}{Btu}$
R_{frost}	Heat transfer resistance across frost layer	$\frac{hr\text{-}ft^2\text{-}R}{Btu}$
R_{wall}	Heat transfer resistance across wall	$\frac{hr\text{-}ft^2\text{-}R}{Btu}$
T_a, t_a	Ambient dry bulb temperature	R, F
T_1, t_1	Air-frost interface temperature	R, F
T_3, t_3	Outside wall temperature	R, F
T_2, t_2	Liquid oxygen equilibrium temperature	R, F
W_v	Water vapor mass diffusion rate	$\frac{lb_m}{hr\text{-}ft^2}$
X_f	Total frost accumulated thickness after time Θ	in.
ΔX_f	Frost build-up during an increment of time, $\Delta\Theta$	in.
ϵ	Emissivity of frost layer on wall	Dimensionless
Θ	Time	Minutes
ρ_a	Density of air	$\frac{lb_m}{ft^3}$
ρ_f	Density of frost	$\frac{lb_m}{ft^3}$
σ	Stefan-Boltzmann Constant	$\frac{Btu}{hr\text{-}ft^2\text{-}R^4}$

DISCUSSION

V. J. JOHNSON, Boulder, Colo.: Mr. Loper is to be complimented on his fine handling of this analytical paper.

In the equation, what was the average density and factor used? What was the uniform frost build-up rate? Can it be used for the entire circumference in actual practice? Often it will build up in different thicknesses. Were there sides from the wind, sun, etc. where there might be different build-up rates if other conditions were used?

If there is any breeze at all, or artificially created wind of 5 mph or more, it will cause the frost to be removed, beginning on the surface in the direction of the wind. Was any frost removed during the first five or 10 minutes of the test?

CLOSURE BY AUTHOR LOPER: The analysis of the density was based on 17 lb per cu ft, which was prompted by a lack of precise information. Perhaps the analysis should have been based on variable densities. The data used were from a 1954 test. This was the condition of a medium value between 15-20 lb per cu ft, the density obtained for frost accumulation upon a tank containing liquid nitrogen. The densities vary greatly and are difficult to measure.

To cope with the variations in coefficients and frost build-up along the surface, an average coefficient was used. The analysis was based on an ideal situation. The equations were based on a flat plate, which gives better results than a cylinder. The coefficient used in the test was an average for the complete tank circumference. If the tank is exposed to solar radiation, the intensity and incident angle must be considered.

On the cylinder, frost removal occurs after an hour and after a large amount has accumulated. If the frost does tear off at the beginning, the wall reverts to an earlier time period and the frost starts to build up rapidly again in the regions where it came off. Since the interface temperature is lower in that region, frost will build up rapidly.

No. 1704

Noise Reduction Characteristics of Package Attenuators for Air-Conditioning Systems

NORMAN DOELLING

ASHRAE publications and its technical committees give recognition to the need for noise control. As noted in chapter 40 of the Guide, certain noise control problems involving air-conditioning systems are most economically solved by the use of prefabricated, package attenuators. However, the lack of a uniform method for testing the acoustical characteristics of such attenuators and a scarcity of quantitative acoustical data of any nature have combined to keep such units from being widely used. This paper provides some of the needed information and approaches the following aspects of noise reduction:

1. Definition of noise reduction and an experimental test technique for describing the noise reduction of package attenuators.
2. Description of the physical mechanisms by which noise reduction is obtained.
3. Comparison of the noise reduction vs. frequency characteristics of about 20 commercially available prefabricated units.
4. Some guides for quickly selecting package attenuators to solve a specific noise problem.

An exploratory committee of the American Standards Association and one of ASHRAE's technical committees are undertaking currently to establish standards to define noise reduction and to measure the noise reduction characteristics of package attenuators and other mufflers. The need for standards is obvious. Discussions with manufacturers and other consultants reveal that many different types of

Norman Doelling is a Consulting Engineer, Bolt, Beranek and Newman, Inc. This paper was presented at the ASHRAE Semiannual Meeting in Dallas, Texas February 1-4, 1960.

testing methods are being used now to establish acoustical characteristics of attenuators. Frequently, the test results are all indiscriminately given the same name (attenuation is a popular term) even though the test procedures are radically different. Further, one may find that two manufacturers use the same test technique, but give different names to the results (noise reduction and insertion loss, for example). It is therefore virtually impossible to select a package attenuator by comparison of available technical data.

It is hoped that the technical results of our measurement program will be useful in establishing a firm basis for comparing of the acoustical performance of some of the currently available package attenuators.

NOISE REDUCTION

Our criterion for defining noise reduction was that the term should be easily related to measurable physical quantities. Our criteria for establishing a measurement technique were: First, the measurements should be repeatable by others, and, second, they should yield results which would aid in prediction, that is, the results should accurately describe the acoustical performance of the units in heating and ventilating systems. In addition, the experimental system should be as simple as possible.

Fig. 1 illustrates the experimental test set-up that was used in this program for measuring noise reduction. The dimensions shown vary somewhat. For example, the distance from the unit under test to the anechoic wedges will be longer for shorter units. Similarly, the duct width becomes smaller for a smaller test unit.

The average sound pressure level (SPL) in each measurement plane is determined from a number of measurements at different positions in the plane. We prefer to use at least three positions for small (6 x 12 in.) ducts and at least five for larger ducts (12 x 24 in. and greater). The number of positions depends also on the symmetry of the unit under test. The noise reduction of the attenuator is defined as the differenoe in the average SPL measured at the input and output planes which were located as shown in Fig. 1.

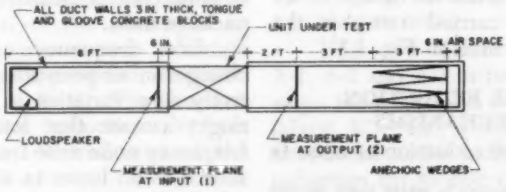
ALL DUCT WALLS 3 IN. THICK, TONGUE AND GLOOVE CONCRETE BLOCKS
UNIT UNDER TEST
6 FT
6 IN.
2 FT
3 FT
3 FT
6 IN. AIR SPACE
LOUDSPEAKER
MEASUREMENT PLANE AT INPUT (1)
MEASUREMENT PLANE AT OUTPUT (2)
ANECHOIC WEDGES
NOISE REDUCTION = AVERAGE SPL AT PLANE (1) − AVERAGE SPL AT PLANE (2)

Fig. 1 Experimental test set-up

1704

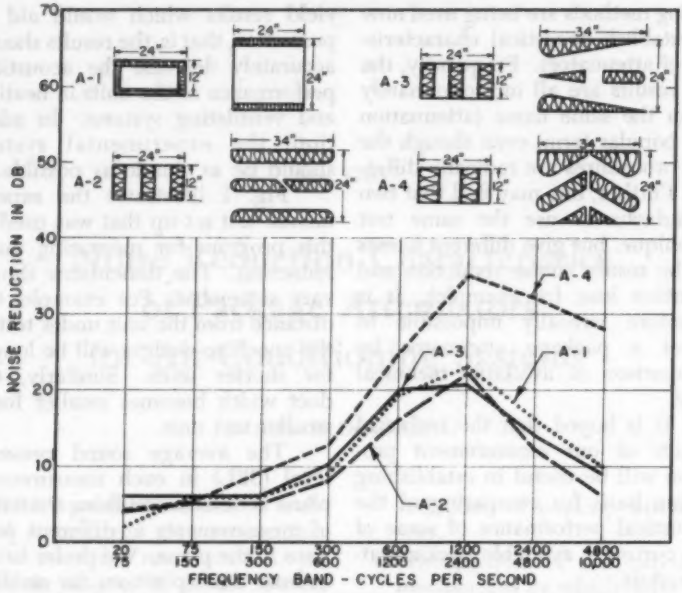

Fig. 2 Characteristics of four different package attenuators

Details of the measurement equipment, the relative merits of the measurement technique, the reproducibility of test results and the relative merits of this definition of noise reduction (and others) are described elsewhere.[1,2] Throughout this paper, the noise reduction of a unit represents the result of an experiment carried out by the method indicated in Fig. 1.*

NOISE REDUCTION MECHANISMS

Theory of the reduction of noise in ducts is discussed in many excellent works[3,4] and we shall not go into details here. However, by being familiar with a few of the physical principles involved, one can avoid being misled by over-zealous advertising, and one can also avoid some common errors in the design of noise control measures involving package units.

Low frequency noise yields changes in air pressure with a relatively slow variation in time. One might assume that losses in low frequency noise arise from the same source as do losses in air pressures which do not vary in time at all. For example, a good way to lose static pressure or to reduce low

* The Noise Reduction in octave bands depends somewhat on the slope of the noise spectrum at the input. The data here apply for a white noise input with slope equal to +3 db/octave. The data will also apply for spectra having slopes as great as ±10 db/octave.

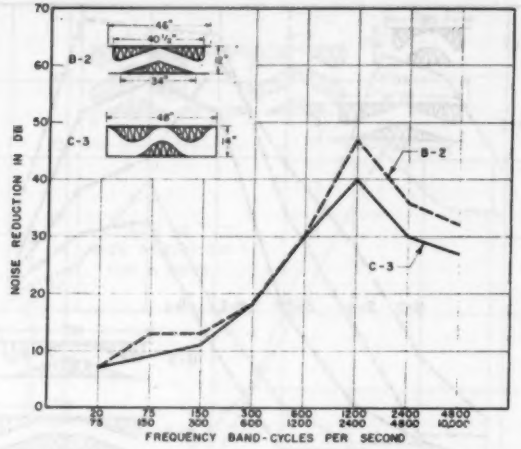

Fig. 3 Characteristics of two, 4-ft package attenuators

frequency noise in an air duct is to expand and contract the duct abruptly. To minimize pressure drop, the duct is made uniform in cross-section by lining the sides of the expanded section with a glass fiber blanket. The glass fiber lining, of course, provides some low frequency noise reduction and even higher mid-frequency noise reduction.

Roughly, the noise reduction at low frequencies depends almost entirely on the ratio of the total cross-section of the attenuator to the open cross-section through which air flows, provided, of course, the length is fixed. The low frequency noise reduction depends but little on other factors of the geometry.

Fig. 2 helps clarify this point. Unit A-1 is a simple lined duct which has an open area of about 55% Unit A-2 is another version of the lined duct (called parallel baffles or splitters), longer than A-1 but having an open area of about 67%. Note that the noise reduction is somewhat smaller than that of Unit A-1, even though Unit A-2 is somewhat longer than A-1. A similar unit, A-3, is of comparable average cross-section to A-2 and the noise reduction is comparable. Generally, the noise reduction of units of comparable size will be inversely proportional to the percentage of open area.

Unit A-4 differs from units A-1, A-2 and A-3 in two significant ways. First, the open area is smaller (about 46%) and a bend has been introduced in the baffles; the noise reduction up to 600 cps increases slightly because of the decrease in open area. Second, a significant increase in noise reduction (above

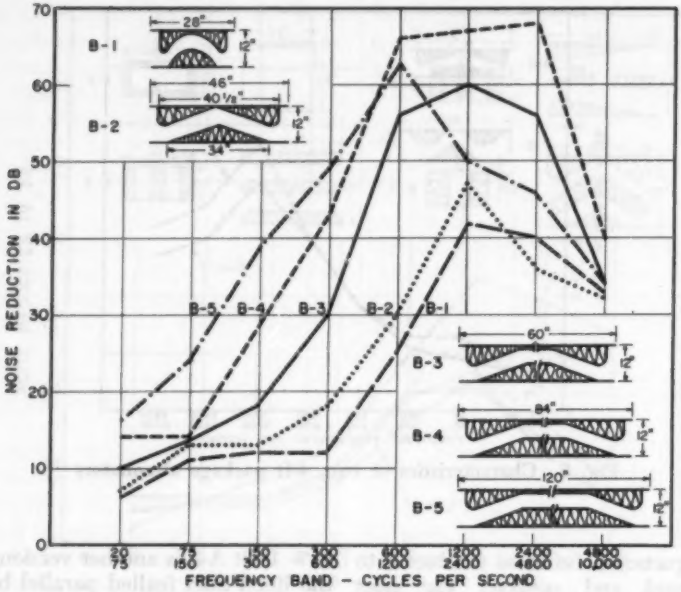

Fig. 4 Characteristics of five similar units which differ in length

600 cps.) results from the addition of a bend in the unit.

At high frequencies, sound waves behave much like a beam of light. If line-of-sight through the muffler is prohibited, the noise reduction will generally be quite large. High frequency noise reduction depends much more on the bends than on the lining of the duct walls.

Fig. 3 illustrates the noise reduction characteristics of two mufflers which appear to be of different geometries. However, both have bends and both have roughly the same percentage of open area. As a result the noise reduction characteristics are similar in spite of the different geometries (actually C-3 has a slightly larger average open area and hence a lower noise reduction).

DEPENDENCE ON LENGTH

So far we have looked at mufflers of approximately the same length and dimensions and have found that noise reduction depends primarily on the percentage of open area at the lower frequencies and on geometry at the higher frequencies. Let us consider how noise reduction varies with length if we hold the cross section, open area, and geometry constant.

An illustration is given in Fig. 4 which shows the noise reduction

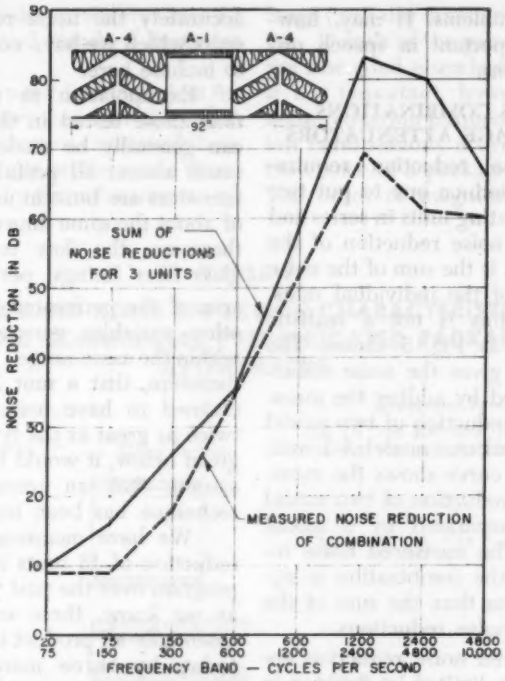

Fig. 5 Series combinations of package attenuators

characteristics of five similar units. Units B-3, B-4 and B-5 incorporate essentially the same construction as B-2, but the length is increased by adding a lined duct section. The noise reduction generally increases with increasing length, but it is definitely not directly proportional to length. For example, the noise reduction of Unit B-4 is not twice as great as Unit B-2 although B-4 is about twice as long as B-2. Note that the percentage of high frequency noise reduction varies little as a function of length. The noise reduction at high frequencies is accomplished almost entirely by the bends, the duct between the bends adding little noise reduction.

Unit B-5 has a noise reduction spectrum which is different from that of the other units. In this unit the glass fiber behind the perforated metal duct wall was found to be encased in a flexible plastics sheet. This plastics sheet causes a degradation of the high frequency performance; but, as we shall see later, the loss of high frequency is not generally important in fan

silencing problems. It may, however, be important in speech privacy problems.

SERIES COMBINATIONS OF PACKAGE ATTENUATORS

Severe noise reduction requirements may induce one to put two noise attenuating units in series and assume the noise reduction of the combination is the sum of the noise reductions of the individual units. Generally, this is not a realistic assumption as Fig. 5 shows. The solid curve gives the noise reduction obtained by adding the measured noise reduction of two model A-4 units and one model A-1 unit. The dotted curve shows the measured noise reduction of two model A-4 units separated by a model A-1 unit. The measured noise reduction of the combination is significantly less than the sum of the individual noise reductions.

Measured noise reduction appeared to be limited by flanking in the 1200-2400 cps band even though these data were obtained in a duct system which was carefully designed and tested to minimize flanking paths. Extreme care must be taken to avoid flanking paths in the field if noise reductions over 60 db are to be obtained.

We have over-simplified the dependence of noise reduction on several parameters and neglected some important parameters such as flow resistance of the glass fiber and percent open area of the perforated facing. However, the considerations above and the data presented below will enable the architect-engineer to estimate quite accurately the noise reduction of units which we have not been able to include here.

Extrapolation to units other than those tested in this program can generally be made easily because almost all prefabricated attenuators are built in module units of about the same dimensions. Furthermore, the flow resistance of glass fiber linings, per cent open area of the perforated facings and other variables generally all fall within the same range. If one finds, therefore, that a unit 3 ft long is claimed to have noise reductions twice as great as the typical values given below, it would be logical to assume that an unusual testing technique has been used.

We have measured the noise reduction of 18 units in our study program over the past year. So far as we know, these units include essentially all product types offered today by three manufacturers. Three tables summarize these data.

Data were obtained from modular units of one particular cross section. We had an opportunity to check the same modular unit made with a different cross section. Specifically, unit C-3 had a cross section of 14 x 12 in. A similar unit with a 14 x 24 in. cross section was measured at a later date. The average difference (over frequency) between the two measured noise reductions was less than 1 db. The standard deviation was about 2 db. Actually, flanking problems in the peak noise reduction band existed because the 24 x 14 in. unit did not fit our 12 x 24 in. test duct which was set up at the time. Actual dif-

ference would probably be 0.5 db or less and standard deviation about 1 db.

We have not included data for the last octave band in the table. The noise reductions achieved there depend strongly on the mode structure excited by the noise source and large (± 5 db) fluctuations may occur. Details of the general problem are discussed elsewhere.[5] The loss is not important, however, as the noise reduction requirements in the last band seldom, if ever, influence the choice of a package attenuator. The order of magnitude of noise

TABLE I

OCTAVE BAND NOISE REDUCTION CHARACTERISTICS OF SOME COMMERCIAL PREFABRICATED PACKAGE ATTENUATORS

Unit	Length In.	Cross Section	Frequency Bands 20–75	75–150	150–300	300–600	600–1200	1200–2400	2400–4800
A-1	24		2	6	6	9	19	23	16
A-2	34	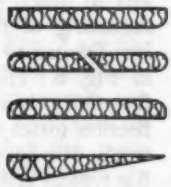	4	5	5	8	16	22	12
A-3	34	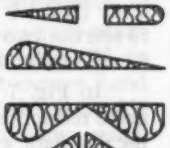	6	6	6	10	20	21	14
A-4	34	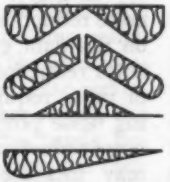	4	5	9	13	25	35	32
A-5	34		7	7	9	12	24	29	22

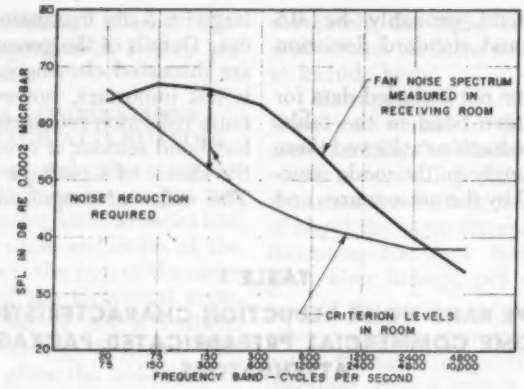

Fig 6 Typical criterion sound pressure level

reduction in the last band may be obtained from the previous figures.

As noted earlier, the test procedure minimizes flanking paths. Noise reductions above 50 to 60 db may not be obtained in the field if flanking paths are not controlled.

APPLICATION OF DATA

Considering the vast array of data resulting from only three product lines, selection of a package attenuator to satisfy specific noise reduction requirements might at first appear difficult. Let us review briefly the approach presented in the GUIDE to find typical noise reduction requirements for a package attenuator. A power spectrum of a centrifugal fan has a slope of about 5 db/octave. However, the spectrum shape is generally changed by end reflection losses and by reflection losses at bends.

Devotees of high fidelity are aware of the difficulty of radiating low frequency sound from a small area. Similarly, it is difficult to radiate low frequency sound from a small outlet grille. This phenomenon, which causes "hi-fi" enthusiasts so much trouble, results in a flattening of the spectrum in the low frequency region as indicated in Fig. 6. The drop in the high-frequency levels is caused by reflection losses at bends in the duct work. We have also plotted in Fig. 6 a typical criterion sound pressure level (NC-40). The difference between the two curves shown in Fig. 6 is the reduction of noise required.

In Fig. 7 we have plotted the noise reduction requirements based on the data given in Fig. 6. This noise reduction spectrum is typical of those required in air-conditioning noise problems. Values of the noise reduction in each octave band may increase or decrease by a fixed amount, but the shape of the spectrum does not vary greatly. If there are several bends in the air

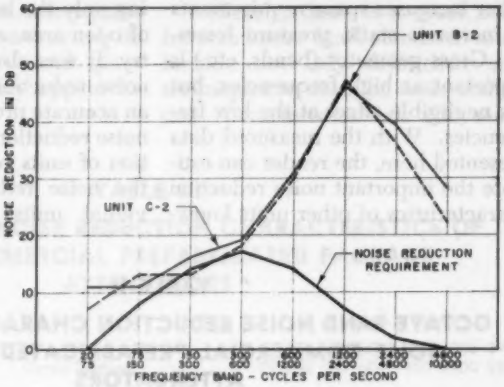

Fig. 7 Noise reduction requirements for the example given in Fig. 6

path, the high frequency requirements will drop. If the duct sizes are large, then the low frequency noise reduction requirements will be greater than those given here. (For this example we have considered an outlet grille with an open area of about 1 sq ft.)

Also plotted in Fig. 7 are the noise reduction spectra of two package attenuators which would satisfy this set of noise reduction requirements. Note that the noise reduction spectra for the units approximately match the spectrum of the noise reduction requirements in the frequency range from 75 to 600 cps. In the first octave band and in the octave bands above 600 cps, one generally obtains much more noise reduction than is necessary to meet a typical noise reduction spectrum. In other words, the noise reduction in the bands between 75 and 600 cps are the only numbers of any real interest. In fact, a preliminary selection of a package attenuator can be made accurately on the basis of the 75-150 cps or 150-300 cps band alone.

If package attenuators were to be rated by a single number, it would seem logical to recommend an arithmetic average of the noise reduction in the frequency bands from 75-600 cps, at least insofar as fans (centrifugal or vane axial) are concerned.

For speech transmission problems, however, the engineer must also consider the noise reduction in the frequency range from 600-4800 cps. Again, a check in one band (for example the 600-1200 cps band) will provide enough information for a preliminary selection of units.

SUMMARY

We have seen that a few gross variables can be used to estimate the approximate noise reduction of package attenuators. Percentage of open area and length are the significant variables at the important low frequencies. Thus increasing low-frequency noise reduction

either increases space requirements or increases static pressure losses.

Gross geometry (bends, etc.) is important at high frequencies, but has negligible effect at the low frequencies. With the measured data presented here, the reader can estimate the important noise reduction characteristics of other units knowing only the length, the percentage of open area, and the gross geometry. It was also shown that scaling noise reduction with length is not an accurate procedure. Nor can the noise reduction of a series combination of units be simply found from the noise reductions of the individual units. (These conclusions

TABLE II

OCTAVE BAND NOISE REDUCTION CHARACTERISTICS OF SOME COMMERCIAL PREFABRICATED PACKAGE ATTENUATORS

Unit	Length In.	Cross Section	Frequency Bands 20–75	75–150	150–300	300–600	600–1200	1200–2400	2400–4800
B-1	28		6	11	12	12	25	42	40
B-2	46		7	13	13	18	30	47	36
B-3	60		10	13	18	30	56	60	56
B-4	84		14	14	28	43	66	67	68
B-5	120		16	24	39	49	63	50	46

were reached on the assumption that the units are constructed of perforated sheet metal and glass fibers, as all units today appear to be.)

Clearly, there is a great need for standards. Such standards must include not only definitions and techniques to describe noise reduction characteristics but also must

TABLE III

OCTAVE BAND NOISE REDUCTION CHARACTERISTICS OF SOME COMMERCIAL PREFABRICATED PACKAGE ATTENUATORS

Unit	Length Ft.	Cross Section	Frequency Bands 20–75	75–150	150–300	300–600	600–1200	1200–2400	2400–4800
C-1	2		9	9	11	15	25	37	28
C-2	3	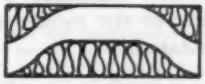	11	11	16	19	30	44	38
C-3	4	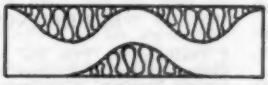	7	9	11	19	29	40	28
C-4	5		11	12	20	26	45	55	49
C-5	6		10	10	17	25	45	55	44
C-6	8		11	14	25	33	56	62	52
C-7	8		13	15	25	34	59	63	62

consider ways of dealing with noise generation characteristics of package attenuators and the effects of high speed air flow on noise reduction. The latter characteristics are not important in low pressure systems, but they may become important in high pressure, high velocity systems.

The definition and measurement technique presented here can undoubtedly be refined. However, lacking standards, it would seem that measurements of this type have some merit. First, the results of the measurements are almost independent of the noise source used. Thus, the noise reduction measured will be essentially the same for a fan as for a loudspeaker. This is not true for an "Insertion Loss" measurement. Second, the results of a measurement reflect an acoustical characteristic of the unit under test and do not include end reflection losses of an arbitrary duct as a typical "two-room" method does. Finally, the results are stable or repeatable. One unit, C-1, was measured four times during the course of our tests. Each time the experimenters were different people; distance-to-source and distance-to-termination were different; loudspeakers, microphones and cross-section of the duct varied. However, the noise reduction data remained constant within a decibel or two. Data taken by this method have been applied successfully to noise control problems for several years. Thus the criterion of predictability has been well tested.

ACKNOWLEDGMENTS

It is a pleasure to acknowledge the assistance of Dr. F. M. Wiener, J. H. Ball and C. M. Gogos of Bolt, Beranek and Newman, Inc. who participated in this program. The assistance and guidance of Dr. Leo L. Beranek and Samuel Labate who initiated the program is acknowledged gratefully. The cooperation of J. Gildard of the Koppers Company, Inc. and E. Bishop of Elof Hansson Company who observed many of the measurements is appreciated.

REFERENCES

1. Doelling, N., "On the Noise Attenuation Characteristics of Package Mufflers for Ventilating Systems," paper presented at the 58th Meetings of the Acoustical Society of America, Cleveland, October 1959.
2. Doelling, N., "Dissipative Mufflers," Chapter 17 of Noise Reduction, Edited by L. L. Beranek, McGraw-Hill Book Company, Inc., New York, New York (To be published in 1960).
3. Morse, P. M., "The Transmission of Sound Inside Pipes," Journal of the Acoustical Society of America, Volume 11 (1939) p. 205.
4. Lukasik, S. J. and Nolle, A. W., "Handbook of Acoustic Noise Control," Vol. I, Supplement I, WADC TR 52-204 (April 1955) pages 217-261.
5. Dyer, I., "Measurement of Noise Sources in Ducts," Journal of the Acoustical Society of America, Vol. 30, No. 9, pages 833-841, September 1958.

DISCUSSION

S. P. SOLING and W. E. BLAZIER, JR., York, Pa. (Written): Mr. Doelling's paper fills a need for additional data on package attenuators as long as the scope is adhered to, although certain additional information is necessary. When the paper deals with test methods, it departs from the scope and fails to describe other methods of testing.

Fig. 1 in Chapter 25 of the 1959 ASHAE GUIDE describes the procedure for attacking a

noise control problem. What is needed is a method of measurement yielding a numerical value that can be inserted into Step 10 of the GUIDE procedure. This should result in a lower and predictable sound pressure level in the room. The logical way to do this is to measure the "Before" and "After" sound pressure levels in the room for the package attenuator, which is the insertion loss method. The paper describes an "In-Duct" method, the validity of which needs to be proven.

The method of the paper is questionable when compared to actual usage. The input (1) reading is in a reverberant duct, and due to the acoustic impedance of the attenuator gives a reading higher than would be obtained without the attenuator in place. In turn, the output plane of measurement is also in a duct in which the anechoic wedges will reduce the readings below what would be obtained in an actual duct system (unlined) with the same attenuator in place. Thus, the method described could result in a difference in readings higher than would be expected, and higher than on an actual installation.

There are other questions that ought to be answered to enhance the value of the paper. The paragraph which refers to Fig. 1 states that the "dimensions shown vary somewhat." How do the dimensions vary, and why? How should the dimensions be described if the tests were to be repeated?

Where the number of measurements are described, how was the measurement plane arrived at? Was the one upstream from the attenuator found by obtaining the maximum sound pressure level? The implication of what this would do to measured noise is apparent.

The footnote states that the noise reduction depends "somewhat" on the slope of the noise spectrum at the input. The data apply to a white noise with a positive slope, whereas the attenuators will be used with fans with a negative slope. It is also stated that the data will apply for slopes as great as ± 10 db per octave. How can the data apply if the noise reduction depends upon the slope?

Under the section, Series Combinations, is a statement concerning over-simplification of the dependence of noise reduction on several parameters and the neglect of some important parameters, coupled with the statement that quite accurate estimates of noise reduction can be made. Something must be missing because if important parameters are neglected, an accurate estimate cannot be made; conversely, if accurate estimates can be made, then the omissions are unimportant.

In the reference to a unit claimed to have noise reduction twice as great as typical values, does the author mean noise reduction numerically twice as great, or 3 db more?

Under the section, Applications of Data, mention is made of the possibility of a single number rating of a package attenuator in the range from 75 — 600 cps, but in the very next paragraph, the engineer is cautioned to consider the noise reduction in the frequency range from 600 — 4800 cps. How could this be done if a single number rating had been obtained?

As noted in the Summary, there is a need for standards, and such standards will be the result of ASHRAE Standards Committee activity. Full consideration will be given to a testing method in which the unit will be tested under actual operation conditions with air flow through the unit, not in an artificial set-up under static conditions, unless the correlation has been proven. A discussion of the pros and cons of test methods could be a separate paper and valuable background material for future Standards Committee work.

MR. DOELLING: As I have pointed out this morning, insertion loss, especially of the duct-to-room type, is a quantity which will vary over a wide range in the field. A muffler does not have an insertion loss. It has insertion losses. For a number of physical reasons which I have considered elsewhere[1], one finds that noise reduction as I have defined and measured it here provides a better approximation to the average (overall field situations) insertion loss than any duct-to-room method. A unique, real number for describing the behavior of a muffler in all field environments simply does not exist.

You state that my "input reading—gives a higher reading than would be obtained without the muffler in place." There is no physical ground for such a generalization. The input reading may be higher, lower or equal to that obtained without the muffler in place depending on the input impedance[2, 3] of the specific muffler under test. The same comments apply to the same measured levels "downstream" of the muffler.

The dependence of noise reduction on the slope of the input spectrum is negligible until one encounters very great slopes. The exact dependence is given in a chart which I prepared for NOISE CONTROL[4].

I have over-simplified the dependence of noise reduction by omission of the effects of certain important parameters. However, so long as manufacturers of mufflers for ventilating systems all use essentially the same materials (perforated metal and glass or mineral wool fibers), the generalizations I have made are valid. I do not recommend that you apply those generalizations to other mufflers, such as those used for automobiles.

In reference to single number ratings, I have noted that this can be done for fan noise problems, by considering only the low frequency noise reduction. However, for speech privacy problems one cannot neglect the noise reduction characteristics in the higher frequencies.

References

[1] Doelling, N. "On the Noise Attenuation Characteristics of Package Mufflers" Paper presented at 58th Acoustical Society of America meeting, October, 1959.

[2] Harris, C. Ed. *"Handbook of Noise Control"* Chapter 21- McGraw-Hill, N. Y., 1959.

[3] Beranek, L. L., Ed. *Noise Reduction* Chapters 16 and 17-McGraw-Hill, N. Y., 1960.

[4] Doelling, N. *"Noise Control"* Vol 5, No. 2, p. 45, March, 1959.

C. M. ASHLEY, Syracuse, N. Y.: It has been stated that it is important to recognize the difference in the methods of measurement which can be used, and the differences in the results. I would prefer a different method of measurement which approaches more closely the normal conditions found in the duct. The effect of this will be to make some reduction in the measured amount of noise reduction. However, the magnitude is limited and, theoretically, it cannot be more than 3 db.

Another point to be emphasized is that a considerable variation exists in the amount of regenerative noise caused by the flow of air through the sound absorber, depending upon whether the passages are straight or not. In curved passage flow there may be a substantial noise generation, whereas, in straight flow it will be negligible. The placement of the sound absorber in the duct system will influence the importance of the generation; if placed near the fan, it is of very little importance. If it is placed near the room, it can be quite significant.

AUTHOR DOELLING: Again I must state that the noise reduction defined here may be greater or less than other measures, depending on the input impedance. I agree that the effects of flow and regenerative noise are worthy of considerations. I hope we shall see more work in this important field.

C. N. RINK, New York, N. Y. (Written): Our company has been engaged in a long research program and we also find that the noise reduction of package attenuators at lower frequencies (75-600 cps) depends mainly on the real free area and the high frequency problem does not exist in most fan systems as far as fan-generated noise is concerned.

We wish to supplement one of the statements in Mr. Doelling's paper concerning the two-reverberant room method of rating, which when used can eliminate the end reflection effect by subtracting "empty tunnel" noise reduction. Our previous tests confirm Mr. Doelling's tests as well as the tests by the Armour Research Foundation. However, it is to be noted that our new catalog depicts a product that is considerably different from the units of our manufacture tested by Mr. Doelling which form a part of the data for this paper. Our design now has less than 25% real free area and has straight passages. By minimizing free area we have improved low frequency performance without an increase in pressure loss.

AUTHOR DOELLING: I have seen data comparing the method described in my paper with the room-to-room, insertion loss method that Mr. Rink described above. There is good correlation between the two methods for the data which he has shown me. In principle, however, there is no reason to anticipate that the correlation would be as good for different mufflers or for slightly different test geometries. Indeed, an analysis by R. Wells of General Electric has shown that in certain instances there should be very poor correlation. I hope that Mr. Wells will one day publish the results of his analysis which, insofar as I know, are at present only in draft form.

1705

No. 1705

Attenuation and Generation of Sound in Elbows with Turning Vanes

W. F. KERKA
Member ASHRAE

Should it happen that a customer finds his air conditioning system to be "not as quiet" as the contractor and designer had predicted, the designer may demonstrate that the customer's claims are not well-founded by placing a speaker sound source at one end of the duct system. The sound may be barely audible at the other end, but when the system fans are turned on the noise problem still exists.

What then is the cause of the problem? Although the fan is the primary source of noise, some of this sound will be attenuated by the elbows, filters, and coils of the system. As the high-velocity air passes through these components (and for that matter over any projection into the air stream, each in turn serves as an individual noise generator, due primarily to air turbulence and vortex shedding. As a result, a condition in the duct system may be reached where the noise-generation level of the components begins to exceed the attenuated sound level from the fan. To date, most published data on the acoustic performance of elbows, commercial sound traps, and terminal devices are based on their sound-attenuation performance only, and probably were determined with speaker sound sources. With high-velocity systems becoming more prevalent, however, information on the noise-generation of the components must be known to predict accurately the expected levels within the duct, and ultimately within the occupied space.

The purpose of this study, therefore, was to determine as a function of frequency, both the noise generation and sound attenuation in elbows with turning vanes. Although the elbows and connecting duct were of standard Navy design, the information presented

W. F. Kerka is a Research Engineer, ASHRAE Research Laboratory. This paper, the result of research conducted at the laboratory under a grant furnished by the Bureau of Ships, U. S. Navy, was presented at the ASHRAE Semiannual Meeting in Dallas, Texas, February 1-4, 1960.

is applicable to commercial duct systems.

Performance of elbows in series — In this study, four basic sound levels were considered:

1. Input sound pressure level to an elbow, SPL_i.
2. Output sound pressure level from an elbow, SPL_o.
3. No-flow attenuation of the elbow, ΔSPL_a (as determined with a speaker sound source with no air flow in the duct system).
4. Noise-generation level of the elbow, SPL_g, at a specific air velocity.

The net attenuation across a duct component (elbow in this case) is then equal to the following:

$$\text{Net Atten.} = SPL_i - SPL_o \qquad (1)$$

The output level, SPL_o, is equal to $SPL_i - \Delta SPL_a$ only when the factor SPL_g is negligible; that is, much lower in level than SPL_i. This could occur at low air velocities. At higher air velocities where SPL_g is significant, the output level is, therefore, equal to the following relationship:

$$SPL_o = 10 \log_{10} \left[\frac{SPL_i - \Delta SPL_a}{10} + \frac{SPL_g}{10} \right] \qquad (2)$$

This was derived from the known method of adding power levels. When $SPL_g \rightarrow 0$, then Equation 2 approaches the restricted relationship previously noted.

When analyzing the acoustic performance of a number of elbows in series, the output level from the first elbow can be considered as the input level to the next elbow, etc. (excluding for the time being any effect caused by the connecting duct). As an example, arbitrary values of SPL_i, SPL_g and ΔSPL_a were chosen, and the net attenuation (as indicated by Equation 1) versus number of elbows in series was plotted as shown in Fig. 1. The family of curves represents different values of $SPL_i - SPL_g$ and the slope of the line to which the curves are asymptotic is determined by ΔSPL_a. By comparing these curves with some experimental results obtained from Ref. 1, certain observations may be made. The results from Table II of Ref. 1 (determined from measurements made on one elbow and from room levels on shipboard where the duct system contained a known number of elbows in series) plot close to the line, $\theta = 10$, as was found for other octave-band values of net attenuation (not shown). From this it could be concluded that in the duct systems tested, the input level from the fan, SPL_i, was only about 10 decibels above the noise-generation level,

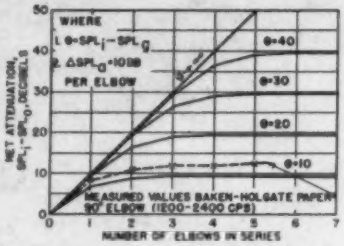

Fig. 1 Net attenuation for a number of elbows in series

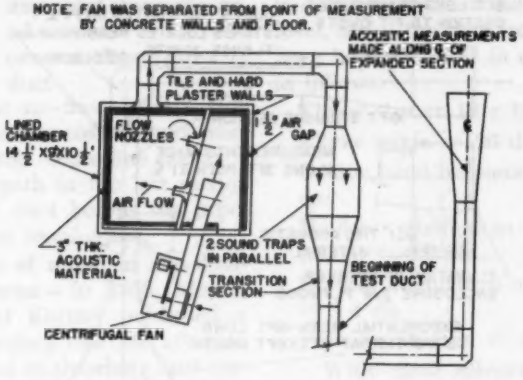
NOTE: FAN WAS SEPARATED FROM POINT OF MEASUREMENT BY CONCRETE WALLS AND FLOOR.
ACOUSTIC MEASUREMENTS MADE ALONG ℄ OF EXPANDED SECTION
TILE AND HARD PLASTER WALLS
LINED CHAMBER
FLOW NOZZLES
AIR GAP
AIR FLOW
3" THK. ACOUSTIC MATERIAL.
2 SOUND TRAPS IN PARALLEL
TRANSITION SECTION
BEGINNING OF TEST DUCT
CENTRIFUGAL FAN

Fig. 2 Layout of the quiet source of air system

SPL_g produced by the elbow components.

TEST APPARATUS

To measure noise generation, a system was needed to furnish sufficient quantities of air for producing desired velocities through the duct component being studied; while at the same time, the sound from the fan supplying the air quantities had to be attenuated below the level of the noise generated by the test device. Such a system is called a "quiet source of air." Fig. 2 illustrates the test system used in this study. Basically the noise generated by the fan was first attenuated in a large chamber lined with acoustic material, and secondly by two commercial sound traps mounted in parallel. The units were mounted in this way so that air velocities through them would be minimized, thus reducing the possibility of noise generation at this point in the system. Air flow was regulated by covering or opening flow nozzles (mounted on a partition in the chamber) and by adjusting a bleed-off port.

The system for measuring the no-flow attenuation in the various elbows and in the straight duct is shown in Fig. 3. A loud-speaker was used as a sound source, and the duct system terminated in an exponential horn (to acoustically couple the duct to the surroundings) having a 6 x 6-ft mouth dimension and a designed cut-off frequency of 32 cps. The speaker was mounted in the enclosure so as not to "see" down the length of duct. A random-noise generator coupled through an amplifier drove the speaker.

Acoustic measurements were made with a General Radio Type 1551-A sound-level meter coupled to a Scott Type 420-A Frequency Analyzer used for both octave and one-half octave band analysis. The General Radio Type 1551-P1 condenser microphone system was also

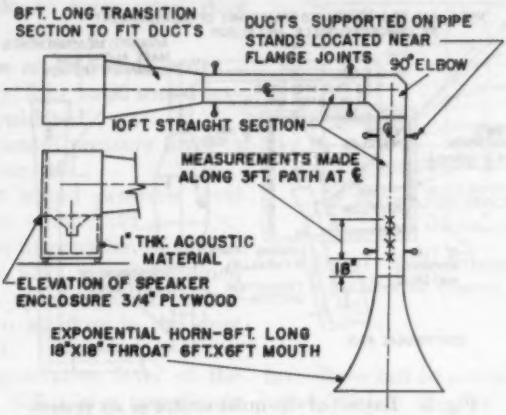
8FT. LONG TRANSITION SECTION TO FIT DUCTS
DUCTS SUPPORTED ON PIPE STANDS LOCATED NEAR FLANGE JOINTS
90° ELBOW
10FT STRAIGHT SECTION
MEASUREMENTS MADE ALONG 3FT. PATH AT ℄
1" THK. ACOUSTIC MATERIAL
18"
ELEVATION OF SPEAKER ENCLOSURE 3/4" PLYWOOD
EXPONENTIAL HORN-8FT. LONG 18"X18" THROAT 6FT.X6FT MOUTH

Fig. 3 Speaker system for determining no-flow attenuation

used. Actually, two frequency analyzers were coupled in series to give sharper cutoff slopes in each band, thus reducing the influence of noise in adjacent bands.

TEST PROCEDURE

The insertion-loss method of testing was employed; that is, a series of measurements were made before and then after a component was mounted in place; and the difference in readings was attributed to the effect of the component. In studying both the noise generation and the sound attenuation of a number of elbows in series, the input-sound pressure levels, SPL_1, were first determined for a section of straight duct only. An elbow and another 10-ft straight section was then added, and sound-level readings were again taken. The output level from the first elbow and straight section was used as the input level to the second elbow. The second elbow and straight section was now added and the procedure repeated until the desired number of elbows was tested.

In the noise-generation studies, sound measurements were made along the centerline of an expanded section coupled to the end of the duct system. The decrease in air velocity in the section reduced the self-noise generated by the microphone screen sufficiently below that of the level being measured, even though this level decreased due to the expanding area of the section. The expanded section (having a 28½ x 28½ in. mouth dimension) also acted as a conical horn termination. The levels in the duct were determined by adding 10 $\log_{10} S_2/S_1$ to the levels in the expanded section.

Where

S_2 = cross sectional area at

any point along expanded section

S_1 = cross sectional area of duct

In the no-flow attenuation studies, sound measurements were made at the centerline along a three-foot path in the last section of straight duct before the exponential horn termination.

Attenuation of sound in non-dissipating systems – In 1958, Meyer, Mechel and Kurtze[2] published a paper indicating that the attenuation of sound in absorbing duct systems (dissipating) was affected by the velocity of air in the system, especially above 3500 fpm. They found, however, that in non-dissipating systems, the attenuation was unaffected by air movement. This fact was later substantiated more fully by the work of Chaddock, Moore, Bell, and Nunnely.[3] Since the systems studied in this paper were of the latter type, the attenuation values determined with a speaker sound source were concluded to be valid under conditions with air flow. The analysis of the test data was, therefore, based upon this fact.

Noise-generation levels were determined with the "quiet source of air." In actuality the attenuation component, ΔSPL_a, was also included in the measurements; and this factor had to be accounted for before the value, SPL_g could be determined. Attenuation of sound in the connecting sections of straight duct between the elbows also had to be included in the analysis.

METHOD OF ANALYSIS

To best illustrate the method used in determining the noise-generation level, SPL_g, the data from one run have been included in an example as follows:

Elbow size = 18 x 18 in.

Elbow angle = 90 deg

Octave band frequency, 600-1200 cps

No-flow attenuation of elbow, ΔSPL_a = 2.6 db

No-flow attenuation in 10 ft duct = 1.4 db

Velocity in duct = 4000 fpm

With three elbows in series, the schematic drawing of the setup is as follows:

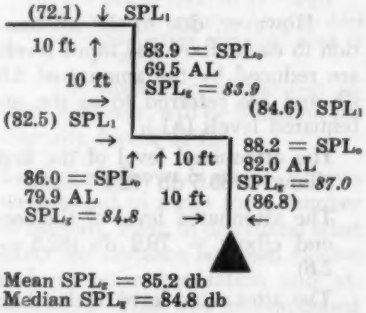

Mean SPL_g = 85.2 db
Median SPL_g = 84.8 db

Although the tenths of a decibel were carried through all calculations, the accuracy of results is reported later.

Numbers in parenthesis represent the levels within the duct as determined from measurements taken along the centerline in the expanded section, and are the mean of four readings.

Input level to the first elbow, SPL_1 = 72.1 db. – Measured

Input level to the second elbow, SPL_1 = 82.5 db. – Measured

Input level to the third elbow, SPL_i = 84.6 db. — Measured

Measured output level from the third elbow and 10 ft length of duct = 86.8 db. (This would have been the input level to a fourth elbow had another been added.)

To find the output level of each elbow, 1.4 db must be added (the no-flow attenuation in the duct) to the input levels as follows:

Output level from first elbow, SPL_o = 83.9 db (82.5 + 1.4)

Output level from second elbow, SPL_o = 86.0 db (84.6 + 1.4)

Output level from third elbow, SPL_o = 88.2 db (86.8 + 1.4)

However, due to the attenuation in each elbow the input levels are reduced by the amount of 2.6 db and are referred to as the attenuated levels (AL):

The attenuated level of the first elbow = 69.5 db (72.1 — 2.6)

The attenuated level of the second elbow = 79.9 db (82.5 — 2.6)

The attenuated level of the third elbow = 82.0 db (84.6 — 2.6)

By using Equation 2, the generated level of each elbow can now be determined. Taking the third elbow for example:

The output level, SPL_o = 88.2 db

The attenuated level =

$$SPL_i - \Delta SPL_a = 84.6 - 2.6 = 82.0 \text{ db}$$

Therefore, $SPL_o = 10 \log_{10}$

$$\left[\frac{SPL_i - \Delta SPL_a}{10} + \frac{SPL_g}{10} \right] \quad (2)$$

$$8.82 = \log_{10} \left[10^{8.3} + 10^{\frac{SPL_g}{10}} \right]$$

taking the antilog of both sides of the equation,

$$\text{antilog}_{10}\, 8.82 = 10^{8.3} + 10^{\frac{SPL_g}{10}}$$

$$10^{8.82} - 10^{8.3} = 10^{\frac{SPL_g}{10}}$$

Therefore, SPL_g = 87 db

However, the generated level, SPL_g, can be found much more readily by using a background-noise correction chart as on p. 47 of Reference 4. This same procedure was followed in determining the noise-generation levels in the remaining octave bands and in all of the other elbows tested. The limiting condition in this method of analysis occurs when the attenuated level equals the output level SPL_o. In this case, the generated level,

$$SPL_g \leqq SPL_o - 10 \text{ db}$$

This can happen when the input level from the "quiet source of air" cannot be reduced adequately below the generated level of the elbow under study. This problem exists in the lower frequencies.

Although reference has been made to the "noise generation of an elbow," in reality, the levels, so determined, represent the noise generation due to the elbow and its connecting duct, since the elbow is both acoustically and physically coupled to it. In other words, it would not be correct to simply hold a turning-vane section in an airstream and say that its noise generation was equal to the increased sound level produced in the environment. The component must be analyzed under the acoustical

conditions in which it will ultimately be used.

The levels SPL_i and SPL_o represent the energy flux, or intensity, within the duct before and after a component, and are indicative of the flow of acoustic energy away from the source and in the direction of air flow through the duct and ultimately to the terminating space. Admittedly, these are hypothetical values. An analysis of the preceding example by considering the reflection and generation of sound at each elbow component, its absorption in the duct and re-reflection of the next elbow, and then superimposing upon this the reflections of sound from adjacent elbows gives a theoretical output from the second and third elbows of 2 and 2.6 db respectively above the output level of one elbow (assuming that each elbow generates the same amount of sound). Experimentally the output level from the third elbow was somewhat higher (88.2 db compared to 83.9 + 2.6 or 86.5 db) than predicted. Based on this analysis, the experimental generated levels would be 83.9, 84, and 85.6 db for the first, second and third elbows respectively, or a mean of 84.5 db. For the method of analysis used in the paper, the mean generated level was 85.2 db, or an error +0.7 db. This is well within the limits of experimental error discussed later.

Although the method of analysis used in this paper may involve a small error, its use is rather straightforward, and hence could well be applied with reasonable accuracy to the solution of duct problems where the noise generation of the system components is considered along with attenuation expected in the ducts, elbows, etc. Sample problems using this method have been included in the appendix.

The noise-generation level, SPL_g, also represents the acoustic energy flux generated by a section in the direction of air flow. For conversion to a power-level basis for solving duct problems, it is only a matter of taking the cross sectional area of the duct into account:

Thus by definition:

$$PWL = SPL + 10 \log_{10} S \qquad (3)$$

where

PWL = power level re 10^{-13} watt
SPL = sound-pressure level in duct
S = duct cross sectional area in sq ft

The discussion of the test results, however, will be based on the intensity levels, SPL_g.

Testing of elbows in series—Elbows were tested in series for a number of reasons. First, to determine what effect the distance between elbows had on noise generation and attenuation. This was accomplished by comparing the test results for the elbows separated by the 10-ft sections with the results for the elbows bolted directly together. It was found that within the expected experimental accuracy, there was no evidence to show that the noise generation caused by the elbows differed significantly under these conditions. This would be likely since the turning vanes in the elbows guided the air stream uniformly through the section so that the entrance flow conditions to each elbow were not altered when

the distance between them was changed. However, where a section would be mounted directly to the outlet of a fan and subjected to erratic flow conditions, its noise-generation characteristics could be altered. For elbows without turning vanes, increased noise generation due to turbulence and uneven flow distribution might occur when the elbows were mounted directly together, especially in an "S" shaped arrangement. Testing a number of elbows rather than only one also resulted in a more accurate average value of noise generation per section.

For the elbows in series and separated by the 10-ft sections of duct, the attenuation over the frequency range was about the same as when they were bolted directly together, taking into account, of course, the attenuation in the connecting duct. Hence, the mean values reported in the paper are based on the test results of both setups. It was noticed, however, that the attenuation in the first elbow was consistently greater, especially in the mid-frequencies, than it was in the second and third elbows when they were added to the duct system. This was not due to any change in the speaker output as elbows were added, since a microphone survey along the centerline of a straight section of duct before and then after several elbows were added showed that the levels increased in accordance with what was expected with the reflection of sound from the elbows back to the source. A survey in the duct between elbows showed also that the attenuation in the second elbow was less than that in the first, and for that matter was nearly the same in all frequency bands as the mean values found for a number of elbows in series by the insertion-loss technique. For the tests where only one elbow was available (as noted later) corrections were made to the results based on the attenuation in one elbow compared to the expected mean of three in series.

Determining sound attenuation in straight ducts – In determining the no-flow attenuation in the straight-ducts, the method of adding sections to get the effect of increased lengths was employed so as to comply with the procedure used in the study of elbows. In other words, acoustic measurements were first made along the 3-ft path (shown in Fig. 3) near the end of one 10-ft straight section; another section was then added and the process repeated until four sections (5 in the case of the 12 x 12 in. duct) were bolted in place. A 3-ft path was used since the distance was short enough to obtain a reasonably average level. The increments between the mean levels at the end of each section were then added together to obtain the attenuation for the entire length of the duct. Since this method of testing differed from that used by Chaddock[3] and other experimentators in the past, it was necessary to check its validity.

This was done by making an extensive microphone probe along the centerline of the assembled 12 x 12 in. duct. Measurements in each frequency band were made at 2-ft intervals for a distance of 30 ft. A line then drawn through plotted

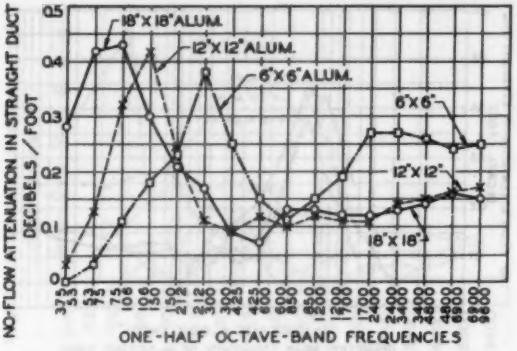

Fig. 4 No-flow attenuation vs. half-octave band frequencies for three duct sizes

levels for each band (the slope of which was determined by the method of least squares) represented the attenuation over the entire length. A comparison of these results with those found by the addition of sections showed excellent agreement. It was concluded, therefore, that the test method was valid. The method of least squares was also used in comparing the slope of the line through the plotted levels at the end of each 10-ft section with the attenuation found by the addition of the increments between mean levels. Again the agreement was good; hence, the determination of the attenuation in the straight duct by the method employed was concluded to be sufficiently accurate.

It has been found from previous work, Refs. 3, 5, 6, that at some frequencies there exist strong transverse wave patterns in the duct, measurements were made along the centerline only, in all the ducts studied because only the differences in levels (and not absolute levels) were being considered. In the 24 x 6 in. duct, however, because of the high aspect ratio, measurements were made along the centerline and at two other positions 6 in. on either side.

RESULTS

Attenuation of sound in straight ducts—Attenuation per ft of length by half-octave bands for three duct sizes, 6 x 6 in., 12 x 12 in., and 18 x 18 in. is plotted in Fig. 4. The work of Chaddock[3] has shown that the attenuation in unlined ducts is independent of the mass of the duct walls above 500 cps, but reaches a maximum at lower frequencies, depending upon the resonance frequency of the duct surfaces. This dependence upon mass appears evident as the peak attenuation shifts to a lower frequency with increased duct size. Although the wall thickness (standard wall thickness and description of ducts are listed in Table Ia of the Appendix) increases

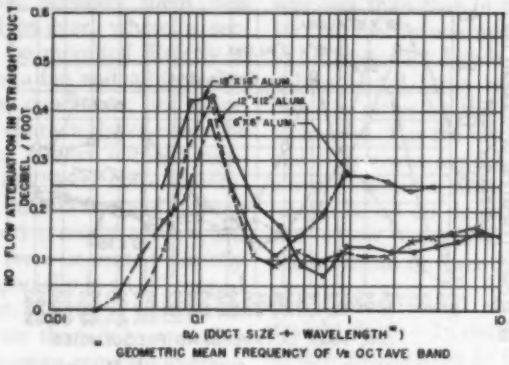

Fig. 5 No-flow attenuation vs. duct size/ wavelength

with duct size, the added mass of the metal and especially the increased length of the undamped surface from edge to edge, causes the resonance frequency to decrease.

The independence of attenuation above 500 cps is evident in the 12 x 12 in. and 18 x 18 in. ducts where the relative magnitude of the decibel drop per ft is about the same as the results obtained by Chaddock[3] for steel ducting. The attenuation in the 6 x 6 in. duct above 500 cps is somewhat higher than expected, however. Because of the small duct size, the microphone had to be positioned to 0-degree orientation.

Although the sensitivity to high frequencies is greater for this microphone position, this should not have been a factor in giving higher values since the attenuation results are based on the differences of absolute levels. It is possible, however, that the transverse modal effect that is quite pronounced at wave lengths equal to the duct dimension may have contributed to this. In Fig. 5, the attenuation values have been plotted on a dimensionless basis, with the abscissa as the duct dimension divided by the wave length of the geometric mean frequency for each half octave band. Although each of the curves peak at about 0.1 wave length, it would appear that this is fortuitous. The higher attenuation in the 6 x 6 in. duct at $D/\lambda = 1$ is evident.

Effect of aspect ratio on duct attenuation is illustrated in Fig. 6. Instead of only one peak attenuation value, as occurred in square ducts, two such points now appear as the aspect ratio is increased. The peak in the lower frequencies is evidently due to the resonance frequency of the two longer duct surfaces, while the other peak is caused by the resonant vibration of the shorter sides. In the 24 x 6

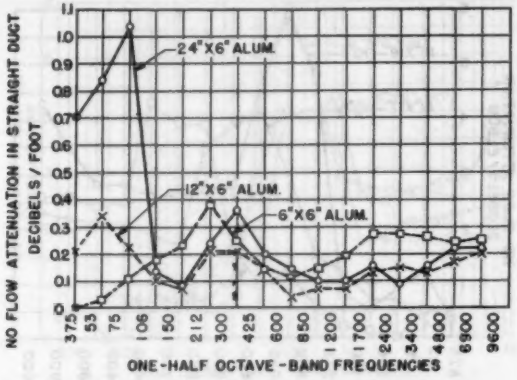

Fig. 6 No-flow attenuation vs. half-octave band frequencies for ducts of different aspect ratio

in. duct, stiffer angles had been riveted around the outer surfaces of each 10-ft section at the one-third points. This was in accordance with standard Navy practice. If the duct had not been stiffened, the lower attenuation peak would probably have shifted to the left. The heavier gauge metal in the duct walls has an added effect in stiffening the 6-in. side, hence the second peak occurs at a higher frequency than in the 6 x 6 in. duct. The independence of the attenuation from duct wall mass above 500 cps is again evident in the 24 x 6 in. and the 12 x 6 in. sizes. Under some conditions, Navy practice would call for a splitter septum in the 24 x 6 in. duct. In this case, the attenuation should be about the same as in the 12 x 6 in. duct. Attenuation of sound by octave bands is tabulated in Table Ia of the Appendix for all of the ducts.

Attenuation of sound in 90-deg. elbows with turning vanes for three different sizes is shown in Fig. 7.

In Fig. 8, the attenuation values have been plotted against the elbow size divided by the wavelength of the geometric mean frequency for each half-octave band. The peaks of attenuation at about ½ λ are evident. This also appears to be true for elbows without turning vanes.[7] The attenuation in the higher frequencies is also less than that expected from elbows without vanes.[7]

In Fig. 9, the decrease in sound attenuation with a decrease in elbow angle is obvious. While the vane widths of the 45, 60, and 90 deg elbows are the same, there is less chance for the sound to be reflected as the vane decreases in curvature. The sudden rise in attenuation for the 30-deg. elbow in the lower frequencies is unexplain-

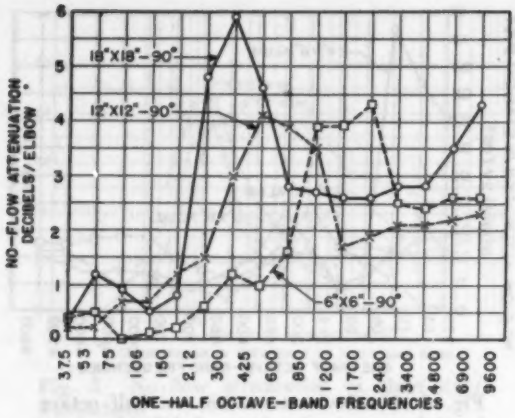

Fig. 7 No-flow attenuation vs. half-octave band frequencies for three 90-deg elbow sizes

able. The difficulty of accurately measuring in the lower frequencies may have contributed to this apparent discrepancy. Although the results are for 12 x 12 in. elbows, it is expected that this same trend in the attenuation would exist for elbows of other sizes.

Trends in the sound attenuation over the half-octave band frequency range for the elbows of higher aspect ratio are not so evident as shown in Fig. 10. In this case, two different types of elbows are involved for each ratio. In the 24 x 6 in. and 12 x 6 in. elbows, the turning vanes are of the same configuration, size and spacing as in the 6 x 6 in., 90-deg. elbows. Those in the 6 x 12 in. elbow are identical to the vanes in the 12 x 12 in., 90-deg. section, and the vanes in the 6 x 24 in. elbow are like those in the 18 x 18 in., 90-deg. section. As in the case of high-aspect-ratio ducts, several peaks appear in the attenuation curve over the frequency spectrum. Since only one each of these elbows was available, the results in Fig. 10 have been corrected to represent the mean attenuation of a number of elbows in series.

The sound attenuation by octave bands is tabulated in Table IIa of the Appendix for all of the elbows.

NOISE

Noise-generation levels, SPL_E, for each octave band versus the logarithm of the air velocity for three of the vaned elbows studied are shown in Figs. 11-13. In general, the spectrums appear to be broadband in nature (except for some pure-tone components which will be discussed later) and fall off in intensity in the higher frequencies.[8] The slope of the lines drawn

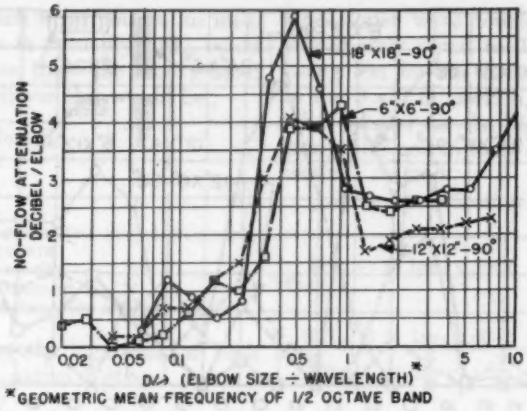

Fig. 8 No-flow attenuation vs. elbow size/wavelength

through the plotted points for the 6 x 6 in., 90-deg. elbow increases as the frequency increases. This would indicate that noise generation in the higher frequencies increases more rapidly as the velocity increases, and appears to be in accordance with the results obtained by Marvet[9] in his study of grille noise. This trend is less evident in the 18 x 18 in. elbow. Except for the difference in the slope of the line representing the 2400-4800 cps band of the 12 x 12 in.

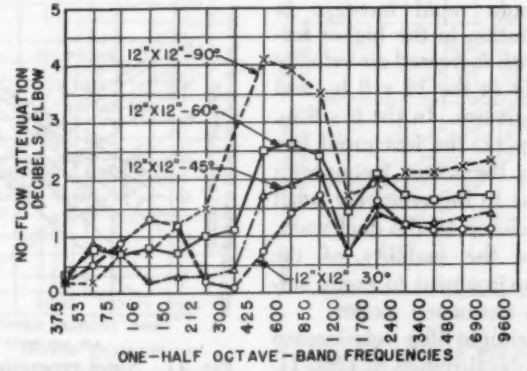

Fig. 9 No-flow attenuation vs. half-octave band frequencies for different elbow angles

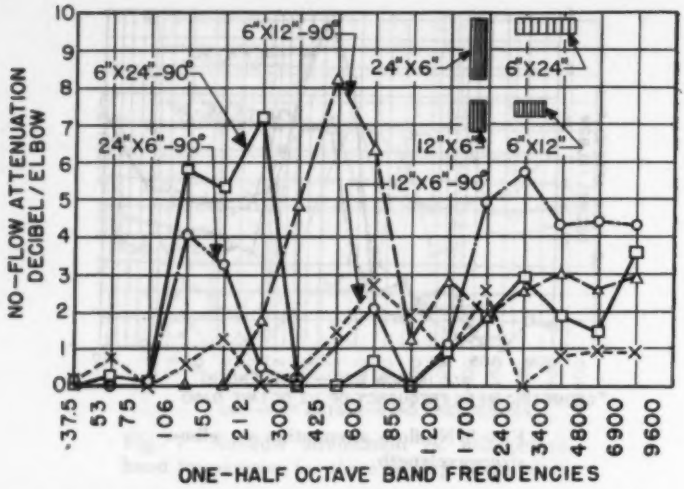

Fig. 10 No-flow attenuation vs. half-octave band frequencies for 90-deg. elbows of different aspect ratio

elbow, the increase in generated level with velocity over the frequency range for this section appears to be fairly uniform.

In the rest of the vaned elbow studies (see Table IIa of Appendix A), the more rapid increase in noise generation in the higher frequencies with increased air velocity was evident in the 12 x 6 in. and 6 x 12 in. elbows. In the 6 x 6 in. elbow, Fig. 11, the less rapid rise in level in the lower frequencies may be due to the relatively small volume enclosed by the duct walls, and hence the inability of the acoustic environment to excite sufficient low-frequency modes.

The straight-line relationship of the graphical results in Figs. 11, 12, and 13 indicates that the generated sound pressure varies exponentially with the air velocity. The limiting condition for no air velocity is zero sound pressure. (Under this condition, $SPL_g \rightarrow$

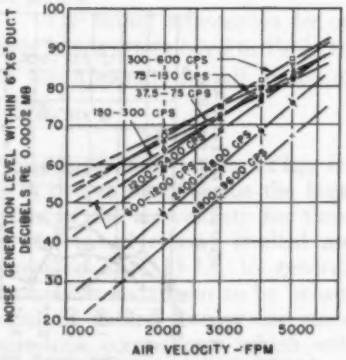

Fig. 11 Noise generation level by octave bands vs. air velocity for 90-deg., 6 x 6 in. elbow

— ∞ which is, of course, an ideal case since in actuality SPL_g could be no less than the background noise, whatever this would be.)

Therefore if
$P = f(V)$
Then
$$P = CV^n \quad (4)$$
Where
P = the generated sound pressure, microbars
V = air velocity
n = an exponent
C = a constant for a given elbow

Taking the logarithm of both sides of equation 3 gives:

$$\text{Log } P = \log C + n \log V \quad (5)$$

which is a straight line when plotted on log-log paper with n as the slope.

To establish an order of magnitude for the exponent, n, the generated levels in each octave band were converted to sound pressure and plotted against air velocity. The slopes were found to be approximately equal to 3, this value being less for the low frequencies in the 6 x 6 in. section, and somewhat greater for the high frequencies in this and in some of the other sections studied.

Since by definition:

$$SPL = 20 \log_{10} \frac{P}{0.0002}$$

then

$$SPL_g = 21 \log_{10} \frac{CV^3}{0.0002} \quad (6)$$

and

$$SPL_g = 60 \log V + 20 \log C + 74 \quad (7)$$

Equation 7 could be used to estimate the noise-generation levels in each octave band over a range of air velocities provided that the level at a specific velocity can be measured. Where Equation 7 is applied to small sections, the coefficient, 60, would have to be reduced

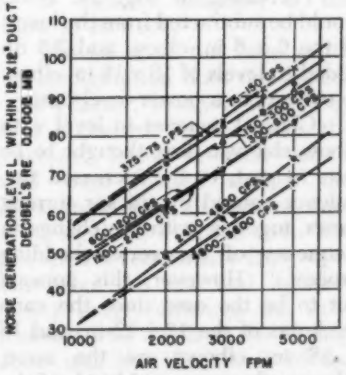

Fig. 12 Noise generation level by octave bands vs. air velocity for 90-deg., 12 x 12 in. elbow

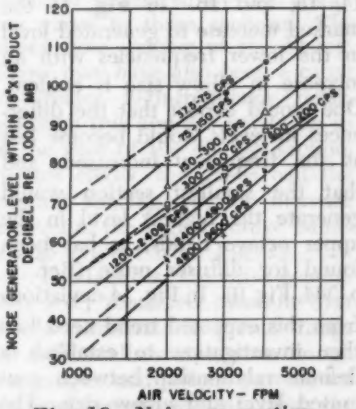

Fig. 13 Noise generation level by octave bands vs. air velocity for 90-deg., 18 x 18 in. elbow

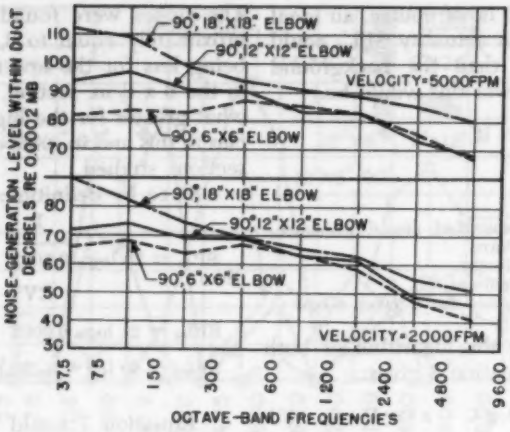

Fig. 14 Noise generation level by octave bands for three elbow sizes

to about 50 for the lower frequencies.

Effect on noise-generation level with respect to elbow size, angle, and aspect ratio is shown in Figs. 14, 15, and 16. In Fig. 14 the marked increase in generated level in the lower frequencies with an increase in elbow size is evident. One would expect that the differences in levels would become less as the frequency increased, and that the smallest section would generate the highest level in the upper octave bands, as has been found for diffuser noise (Ref. 7, p. 344, Fig. 9). In Fig. 14 deviations from this expected trend need further investigation to establish a definite relationship between generated level and elbow size. The comparison of these levels is relative, however, as the elbows are not geometrically similar in regard to the dimensions of the turning vanes. If a comparison were made on a power-level basis, a correction for the duct cross sectional area would have to be included as noted by Equation 3.

Therefore, in Fig. 14, 6 db would be subtracted from the levels of the 6 x 6 in. elbow and 3.5 db added to levels of 18 x 18 in. elbow to convert to a power-level basis.

General increase in level with elbow size was first thought to be due, in part, to the increased turbulence caused by thicker turning vanes, together with the change in frequency of the vortex-shedding process.[10] However, this appears not to be the case since the vane thickness of the 12 x 12 in. and 18 x 18 in. elbows are the same, whereas the generated levels of the latter are generally greater for a given flow rate. The other factors that could affect the level are the

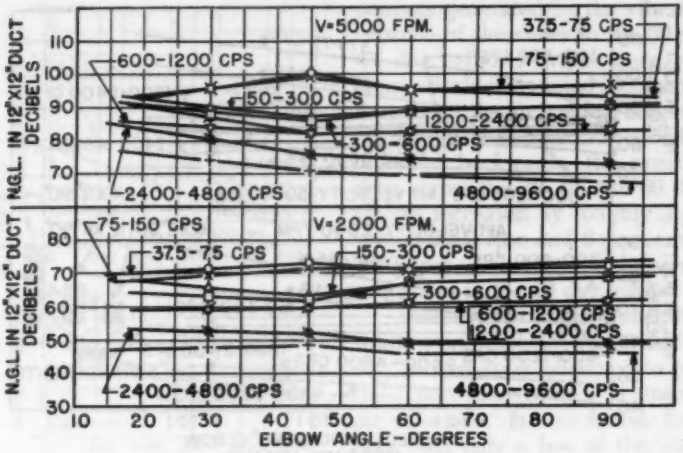

Fig. 15 Noise generation level vs. elbow angle

vane width and configuration and the dimensions and volume of the acoustic environment bounded by the surfaces of the elbow and the connecting duct (now referred to as the acoustic coupling of the elbow to its duct).

The effect of the vane width and configuration does not appear to be a factor, however, when Fig. 15 is examined. In this case, the generated levels in each octave band were plotted against the elbow angle since all sections were of the same (12 x 12 in.) size. The generated levels remain fairly constant over the low and mid-frequency range, although the vane thickness and width of the 30-deg. elbow was less than those of the 45, 60, and 90-deg. sections. The vane configuration (shape) and spacing of each section also differed.

The general increase in level in the higher frequencies for the 30 and 45-deg. elbows may have been due in part to harmonic frequencies generated by the vibrating vanes in these sections. The closer vane spacing of the 30-deg. elbow may have also been a cause of greater high-frequency noise, although this appears not to be so in the case of the 45-deg. section. In this elbow, the vanes had the greatest spacing, yet the increase in level in the higher octave bands is also evident from Fig. 15.

The fact that the noise-generation level remained constant over the low and mid-frequency range for a given elbow size, even though the angle and other parameters changed, would indicate that the dimensions of the elbow and its acoustic coupling with the adjacent duct are influencing factors.

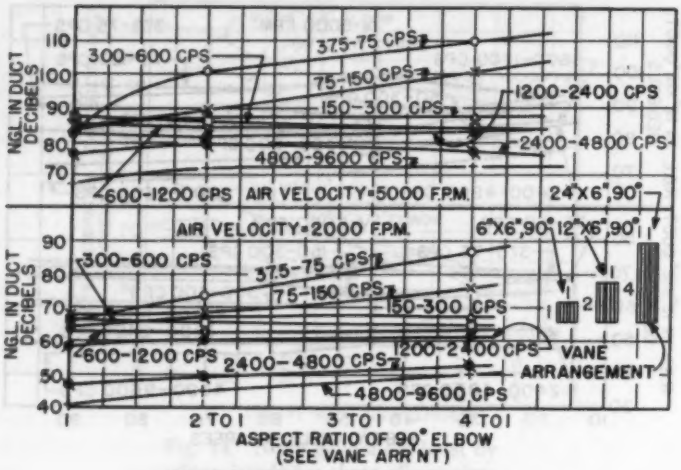

Fig. 16 Noise generation level vs. aspect ratio, 1 to 1, 2 to 1, 4 to 1

Effect of aspect ratio on noise generation is illustrated in Fig. 16, with the vane arrangement as noted. In each section the vane configuration, size, and spacing were identical to those of the 90-deg., 6 x 6 in. elbow; only the vane length differed. Essentially the same experimental results were obtained for the elbows that were of the same aspect ratio, but opposite in the plane of turning. In this case the vanes (all were 6 in. long in each of these three sections) in the 2 to 1, aspect-ratio elbow were identical to those in 90-deg. 12 x 12 in. elbow, and those in the 4 to 1 section were identical to those in the 90-deg., 18 x 18 in. section. Therefore, the increase in the generated level in the lower frequencies as the aspect ratio increases appears to be influenced more by the dimensions of the elbow and connecting duct than by the turning vanes themselves. Again the larger volume bounded by the duct walls for the 24 x 6 in. (4 to 1) section would promote the excitation of more low-frequency modes. The relatively constant level in the mid-frequency range with change in aspect ratio is evident. The slight rise in generated level in the higher frequency bands with increased aspect ratio was noted for both types of elbows, and hence could not be attributed to a specific vane characteristic.

Because only one each of each type of 2 to 1 and 4 to 1 aspect-ratio elbows were available for testing, the accuracy of the no-flow attenuation values and hence the determined generated levels are considered with somewhat less ac-

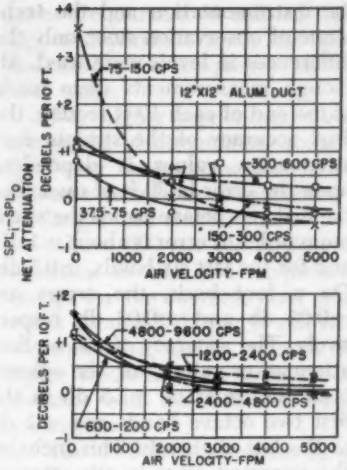

Fig. 17 Net attenuation in straight ducts vs. air velocity

curacy than the results for the average of three sections. The conclusions drawn from Fig. 16 should therefore consider this fact.

EFFECT ON NOISE

In some cases, the turning vane assembly could be mistakenly riveted to the elbow shell in a backward position. To ascertain how this would affect noise generation, the 30, 45, 60, and 90 deg. elbows were each mounted counter to the normal flow of air and the generated levels were determined. No significant differences in the generated levels were observed between the two different positions, although a slight rise in level was noted in the last four octave bands of the 30 deg. elbow. This was due more to experimental error than to any other factor. The pure-tone components generated by the vibration of some of the vanes in the 30 and 45 deg. elbows were more pronounced when mounted incorrectly. Because of the less perfect flow conditions through the vanes when mounted backwards, the pressure drop across the 30, 45, and 60 deg. elbows increased by roughly 3 per cent at 2000 fpm and 6 per cent at 5000 fpm. A negligible difference was noted in the 90 deg. elbow.

During the noise-generation studies, one each of the 30 and 45 deg. elbows were observed to produce pure-tone sounds at specific air velocities. It was found, however, that only a few of the vanes were responsible for this due to excessive vibration. The problem could easily be rectified by tack-welding a rod across the leading edge of the vanes at the midpoint.

Noise generation in straight ducts—Although Chaddock[3] and others[3] have found that the attenuation in unlined (non-dissipating) ducts is not affected by air flow, it appears that there is some generated noise even in straight ducting. This is brought out by Fig. 17 in which the net attenuation in a straight section of 12 x 12 in. duct was determined for a range of air velocities. The attenuation values at 0 air velocities are the ones determined with a speaker sound source; and the net attenuation values over the range of air velocities were again found by the addition of 10-ft sections. Although above velocities of 2000 fpm the net attenuation is nearly equal to zero for all frequency bands, it must be remembered that these curves are based

on a relatively low value of SPL_i, the input level from the quiet source of air. Because of this, it was not possible to make a survey within a long section of duct, since the generated noise of the microphone would have overshadowed the levels being measured. Had noise directly from the fan, or additional speaker noise, been transmitted down the ducts thus increasing the value of SPL_i, the net attenuation values with air flow would have been more nearly equal to the no-flow attenuation.

Accounting for the relative effects of SPL_i, SPL_g, and ΔSPL_s in straight ducting introduces more complexities into the analysis of the system. For this reason the generated levels of the elbows with vanes, as reported, include any additional effect that is contributed by the connecting straight duct. Even if the sections are bolted together, as long as reasonable lengths of straight duct precede and follow the sections, the noise-generation levels as determined are valid and applicable.

FLANKING NOISE

Since the mouth of horn termination was exposed to noise that could flank directly around from the noise source to the point of measurement, the background level produced by this effect was constantly checked. Only in some of the lower frequency bands were slight corrections necessary to the measured levels of a section under test.

In the no-flow attenuation studies, the accuracy of results depended mainly upon the stability of the instrumentation and the technique of observation since only the differences in levels were used. Although measurements were made at the end of each 10-ft section, the final accuracy of the straight-duct attenuation values is dependent upon the error in 30 ft of duct. For the first two octave bands the maximum order of error is about ± 1 db, and for the last six bands, ± 0.5 db. On a foot basis, the errors are ± 0.05 db and ± 0.02 db respectively. The accuracy of the no-flow attenuation values for the elbows is of the order of ± 1.5 db in the first two octave bands and ± 1 db in the last six bands. This includes the expected error in the attenuation of the connecting straight duct. Where only one elbow was available for testing, the accuracy would be less.

In the noise-generation studies where the order of accuracy was basically dependent upon absolute levels, the accuracy was observed to be about ± 4 db in the first octave, ± 3 db in the second band, and ± 2 db in the last six octave bands. The errors also include any factor contributed by the performance of the expanded section (at the end of the duct system) in not acting as an ideal horn termination in the lower frequency bands.

CONCLUSIONS

In air-conditioning and especially high-velocity duct systems, the noise-generation level of the system components should be considered to predict accurately the levels in the occupied spaces.

The no-flow attenuation in the

lower frequencies of unlined ducting is dependent upon the mass and resonance frequency of the duct walls.

For higher aspect-ratio ducts, two peaks of attenuation occur in the lower frequencies due to the different resonance frequencies of the longer and shorter sides.

Above 500 cps the no-flow attenuation in the mid frequencies (except for the smallest duct studied) is about 0.1 db per ft and rises to a somewhat higher value in the higher frequencies. This is in accordance with the results of other investigators.

The no-flow attenuation in elbows with turning vanes is dependent upon the elbow size and angle.

The noise-generation levels of vaned elbows are significant, and in general may be only about 10 db less than the level of the fan in the system.

For vaned elbows of the same size but of different angle, the noise-generation level in the low and mid-frequency range is about the same for a given air velocity.

The noise-generation level in the low frequencies of vaned elbows of the same angle increases markedly as the size increases.

The noise-generation level of vaned elbows of different aspect ratios (with opposite sides remaining constant in size) is nearly the same in the mid frequencies but increases in the lower frequencies and to a lesser extent in high frequencies as the aspect ratio increases.

REFERENCES

1. A Method for Estimating Octave Band Levels of Noise Generated by Air Conditioning Systems—F. B. Holgate and S. Baken, April, 1957.
2. Experiments on the Influence of Flow on Sound Attenuation in Absorbing Ducts —E. Meyer, F. Mechel, and G. Kurtze, *JASA*, Vol. 30, No. 3, March, 1958, p. 165.
3. Sound Attenuation in Straight Ventilation Ducting—J. B. Chaddock, T. L. Moore, H. H. Bell, and J. K. Nunnely, *Refrigerating Engineering*, Vol. 67, No. 1, Jan., 1959, p. 37.
4. Handbook of Noise Measurement, General Radio Company, Cambridge, Massachusetts.
5. Evaluation of Four Methods for Determining Sound-Power Output of a Fan—W. F. Kerka, ASHAE Journal Section, *Heating, Piping and Air Conditioning*, Vol. 29, No. 4, April, 1957, p. 139.
6. Measurement of Noise Sources in Ducts —Ira Dyer, *JASA*, Vol. 30, No. 9, September, 1958, p. 833.
7. Heating, Ventilating, Air Conditioning GUIDE, 1959, Chapter 25, p. 345 and Fig. 10. (Published by the American Society of Heating Refrigerating and Air-Conditioning Engineers).
8. On the Spectrum of Noise from Turbulence—Osman K. Mawardi *JASA*, Vol. 27, No. 3, May, 1955, p. 442.
9. Experimental Study of Grille Noise—B. H. Marvet, *ASHRAE Journal*, July 1959, p. 63.
10. On the Production of Sound by Jets—Nigel Thomas, *JASA*, Vol. 27, No. 3, May, 1955, p. 446.

APPENDIX

TABLE IA NO-FLOW ATTENUATION* IN STRAIGHT UNLINED AND UNINSULATED ALUMINUM DUCT BY OCTAVE-BAND ANALYSIS

Duct Dimensions Inches	37.5 75	75 150	150 300	300 600	600 1200	1200 2400	2400 4800	4800 9600	Wall Thickness Inches
6 x 6	0.03	0.11	0.29	0.21	0.13	0.25	0.26	0.25	0.032
12 x 12	0.08	0.36	0.13	0.11	0.11	0.12	0.16	0.16	0.051
18 x 18	0.39	0.37	0.18	0.07	0.14	0.10	0.14	0.17	0.064
6 x 12[a]	0.29	0.18	0.14	0.18	0.06	0.08	0.12	0.18	0.051
6 x 24[b]	0.83	0.70	0.14	0.26	0.08	0.12	0.12	0.16	0.064

* All values in decibels per foot

a. Also applies to 12 in x 6 in duct
b. Also applies to 24 in x 6 in duct

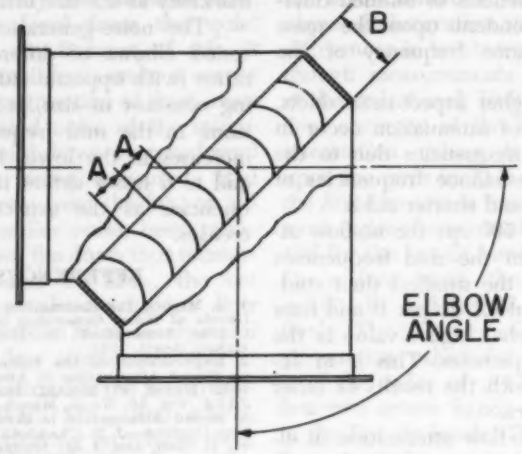

Examples for determining the acoustical performance of duct systems—Although the data for only one frequency band will be considered, the following procedure would also apply to other bands.

The following system will be analyzed:

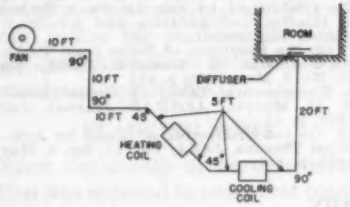

Given:

300-600 cps band
PWL of fan re 10^{-13} watt, 91 db
Duct size, 12 x 12 in.
Air velocity in duct, 4000 fpm

Component	SPL$_s$†	No-Flow Atten.
Duct		0.11 db per ft
90° elbow	86 db	3.5 db
45° elbow	81 db	1 db
Heating coil	69 db*	1.5 db
Cooling coil	69 db*	3 db
Diffuser	70 db*	10 db

Estimated levels only for the purpose of illustrating the example.

† Based on 1 sq ft area.

* Assuming that the free area of the coils and diffuser is greater than the duct, and hence the velocity much less.

Find: The sound level in the room. Starting with the fan, the power-level input to the first section of duct would be 91 db. Since the analysis will be made on a power-level basis, the sound-pressure levels are converted by the equation, $PWL = SPL + 10 \log_{10} S$. However, since $S = 1$ in this example, the power levels by choice are numerically equal to the sound-pressure levels. The following tabulation shows the procedure.

The output power level, PWL_o, from the diffuser equals 76 db (rounded off). Assuming a room constant of 200, the sound level 5 ft from the diffuser would be $76 - 16 = 60$ db.

If only the attenuation values, as determined under no-flow conditions, had been considered, the room level would have been estimated at 40.5 db, which is low. Any attempt to reduce the final level in the room by adding lining in the duct preceding the diffuser section would be limited by the noise-generation level of the diffuser, whatever this would be in actual practice.

Duct Component	Attenuated PWL_1	ΔSPL_a	Level	PWL_2	PWL_o	Remarks
Fan					91	
Duct	91	1.1	89.9	—	89.9	Atten. in 10 ft
90° Elbow	89.9	3.5	86.4	86	89.2	SPL_o = logarithmic Addition of 86 & 86.4
Duct	89.2	1.1	88.1	—	88.1	Atten. in 10 ft
90° Elbow	88.1	3.5	84.6	86	88.4	
Duct	88.4	1.1	87.3	—	87.3	Atten. in 10 ft
45° Elbow	87.3	1	86.3	81	87.4	
Duct	87.4	0.5	86.9	—	86.9	Atten. in 5 ft
Htg. Coil	86.9	1.5	85.4	69	85.4	
Duct	85.4	0.5	84.9	—	84.9	Atten. in 5 ft
45° Elbow	84.9	1	83.9	81	85.7	
Duct	85.7	0.5	85.2	—	85.2	Atten. in 5 ft
Cooling Coil	85.2	3	82.2	69	82.2	
Duct	82.2	0.5	81.7	—	81.7	Atten. in 5 ft
90° Elbow	81.7	3.5	78.2	86	86.7	
Duct	86.7	2.2	84.5	—	84.5	Atten. in 20 ft
Diffuser	84.5	10	74.5	70	75.9	

TABLE IIA NO-FLOW ATTENUATION* IN ELBOWS WITH TURNING VANES BY OCTAVE-BAND ANALYSIS

Elbow Size		Octave-Band Frequencies							
Inches	Elbow Angle	37.5	75	150	300	600	1200	2400	4800
		75	150	300	600	1200	2400	4800	9600
6 x 6	90	0	0	0.5	1	2	4	2	2.5
12 x 12	90	0	0.5	1.5	3.5	3.5	2	2	2.5
18 x 18	90	1	0.5	2	5	2.5	2.5	3	3
6 x 12	90	0.5	0	0	6	1.5	1	3.5	3.5
6 x 24	90	0	2.5	7	0	0	0.5	3	3
12 x 6	90	0	0	0.5	1	2	3.5	1	1
24 x 6	90	0	0	2	1	1.5	4	5.5	5
12 x 12	60	0.5	1	1	1.5	2.5	2	1.5	1.5
12 x 12	45	0	0.5	0	1	2	1	1	1.5
12 x 12	30	0	1	0.5	0.5	1.5	1	1	1

* All values in decibels rounded off to nearest ½ decibel.

TABLE IIIA PHYSICAL DIMENSIONS OF STANDARD NAVY ALUMINUM ELBOWS WITH TURNING VANES

Elbow Size Inches	Elbow Angle Degrees	Number of Vanes	A Vane Spacing Inches	B Vane Width Inches	W* Inches	Standard Thickness of Vane Inches	Shell Wall Thickness Inches
6 x 6	90	10	3/4	1 1/2	1 3/4	0.0808	0.032
12 x 12	90	10	1 1/2	3	3 5/8	0.1019	0.051
18 x 18	90	8	2 7/8	6	7 1/4	0.1019	0.064
6 x 12	90	10	1 1/2	3	3 5/8	0.1019	0.051
6 x 24	90	11	2 7/8	6	7 1/4	0.1019	0.064
12 x 6	90	10	3/4	1 1/2	1 3/4	0.0808	0.051
24 x 6	90	10	3/4	1 1/2	1 3/4	0.0808	0.064
12 x 12	60	10	1 1/4	3	3 1/4	0.1019	0.051
12 x 12	45	7	1 9/16	3	3 1/16	0.1019	0.051
12 x 12	30	11	1	1 1/2	1 1/2	0.0808	0.051

* W = actual vane width when flattened out.

Note: Aluminum vanes are welded to frame assembly which is riveted to inside of the elbow shell.
Shell is constructed from 52S-H32 temper, aluminum alloy. Flanges are riveted to outside of shell.

DISCUSSION

UNIDENTIFIED SPEAKER: A great deal of work and much information is given in Mr. Kerka's paper. I was particularly interested in the fact that in the attenuation characteristics of the vaned elbows, a peak value was reached where the elbow size was about one-half wavelength, and then at higher frequencies the attenuation fell off. The GUIDE Chapter on sound shows some results for elbows without vanes and the attenuation increases in the higher frequencies. I should like to inquire if Mr. Kerka has made some studies on elbows without vanes for comparison.

CLOSURE BY AUTHOR KERKA: I have not made studies on elbows without vanes; however, I have tested a 90-deg, 12 in. x 12 in. commercial elbow with two radius splitters and have found that its attenuation characteristics are about the same as the standard Navy vaned elbow of the same size. It is probable that the vanes, or splitters, beam the high-frequency sound through the elbow, and hence the attenuation is less than that obtained when the sound is reflected back to the source from the surface of a right-angle bend. It is my understanding that the GUIDE data were obtained from concrete ducts and bends, thus I have wondered at their validity as applied to standard metal fittings.

UNIDENTIFIED SPEAKER, Houston, Texas: I would like to ask the author how far he thinks the data in his paper can be extended. For example, can the attenuation characteristics for the 6 to 18 in. duct sizes be extrapolated to apply to a 120 x 120 in. duct size under any condition, or would more data be needed to answer this?

AUTHOR KERKA: The information presented covers a range of duct sizes of 3 to 1, and it might be reasonable to assume that the data could be extended by another factor of 3, that is up to a 54-in. duct size. In Fig. 5, where the attenuation has been plotted on a dimensionless basis, the peak value occurs at the same point for the three duct sizes. However, this is probably by chance since the same duct material was used in each and the wall thickness increased proportionally as the size increased. Since this peak depends to a great extent on the resonant frequency of the duct walls, the size of the duct, the wall thickness, the material used, and additional wall stiffening, all would have to be considered. More research would certainly be needed to show what trend each of these factors has up to duct sizes as large as 120 in.

C. M. ASHLEY, Syracuse, N. Y.: There are questions which arise from the interpretation of the results and their application. The data are acceptable for other sizes of elbows but not for the effect of duct attenuation and other effects.

If the location of the noise-generating source in the system is close to the beginning of the system (that is, the sound source or fan), then the duct noise generation is of little importance. But if it is near the end of the system, the noise generation problem is acute.

The attenuation of the elbow is reflective in nature and must be treated accordingly when there are a number of elbows in series. For this reason, the results of an analysis obtained by considering attenuation by dissipative means only are not entirely satisfactory.

AUTHOR KERKA: Size and attenuation and generation of sound in elbows are considered in the paper under the section Method of Analysis, and are based on C. M. Ashley's comments to me during the preparation of the paper.

1706

No. 1706

Draft Performance of Chimneys

W. G. BROWN C. WACHMANN

Recently published information on the draft performance of domestic chimneys,[1,2,3] although obtained for specific chimney shapes and sizes, has been useful in estimating performance for many actual conditions. Occasionally, however, information is required which does not fall within the limits covered by these test records, for example in chimneys of unusual shape or size, and some suitable design procedure is required.

In this connection, many solely mathematical approaches to the prediction of chimney performance have been made[4] and are still being made[5] without the benefit of experimental comparison. More recently, Schmitt and Engdahl[3] have shown indirectly that these mathematical calculations compare quite poorly with experiment. They proposed an empirical design method for masonry chimneys 10 to 25 ft in height and with cross-sectional areas of 35 to 55 sq in., which has been included in the ASHAE Guide. This design method has been criticized for accuracy, because some other records[1] disagreed considerably for chimney heights slightly greater than 25 ft.

The effect of wind on chimney draft performance has not been studied in detail in actual chimney installations although Schmitt and Engdahl have made a laboratory study which showed wind could either improve or retard the ability of a chimney to exhaust its gases, depending on the direction of the wind. Model studies by Wannenburg and Van Straaten[6] to determine the pressures over the walls and roofs of buildings indicated that the performance of a chimney in wind would probably depend on the shape and orientation of the building.

Calm conditions, under which the available performance records have been obtained, are not frequent. In Ottawa, Canada, for example, calm periods occur on a yearly basis only 1 to 2 per cent

W. G. Brown is a Research Officer, and C. Wachmann a former Research Officer, Div of Building Research, National Research Council, Canada. This paper is a contribution of the Div of Building Research of the National Research Council of Canada and is published with the approval of the Director of the Division; it was presented at the ASHRAE Semiannual Meeting in Dallas, Texas, February 1-4, 1960.

of the time and wind speeds of 6 to 8 mph occur during 30 per cent of the year.[7] Although these wind effects are likely to be of considerable importance in some chimney installations, there is every indication that they can be treated separately from the performance under conditions of no wind.[6,8] Hence before attempting to analyze these effects the steady no-wind performance should be established as completely as possible.

In a previous paper[8] the general theory of steady-state chimney performance was developed and appeared to compare well with the experimental records for one of the fourteen chimneys tested by Achenbach and Cole.[2] Friction losses for the chimney were determined by isothermal tests on a model, the assumption being that the losses were essentially the same for non-isothermal flow of the chimney gases. To study further the usefulness of the design method indicated by the theory, tests were suggested to determine the friction losses for other shapes and sizes of chimneys. This work has now been extended and results of both model friction-loss tests and draft tests on a masonry chimney are reported in this paper.

THEORY

As reported previously,[8] the draft available in a chimney could be determined with reasonable accuracy from the equations*:

$$\frac{D}{\Delta\rho_T\, gH} = Y\left(1 - K \cdot \frac{\rho_m}{\Delta\rho_m} \cdot \frac{V_m^2}{2gH}\right) \quad (1)$$

$$Y = \frac{\Delta\rho_m}{\Delta\rho_T} = \left(\frac{T_m - T_o}{T_i - T_o}\right) \cdot \frac{T_i}{T_m} \quad (2)$$

and

$$T_m = \frac{T_i + \left(\frac{F}{R}\right)\left(\frac{H\,T_R}{C_p\,W}\right)}{1 + \left(\frac{F}{R}\right)\left(\frac{H}{C_p\,W}\right)} \quad (3)$$

where:

- D = chimney draft (ambient air pressure minus pressure at chimney inlet)
- $\Delta\rho_T$ = difference in density between ambient air and chimney gas at the chimney inlet
- g = acceleration due to gravity
- H = chimney height above chimney inlet
- $\Delta\rho_m$ = mean difference in density between ambient air and chimney gas within the chimney
- ρ_m = mean chimney gas density
- V_m = mean chimney gas velocity
- T_m = temp corresponding to the mean chimney gas density (absolute)
- T_o = ambient air temp (absolute)
- T_i = chimney inlet temp (absolute)
- T_R = room air temp (absolute) for inside chimneys (equal to T_o for outside chimneys)
- F = a constant depending only on the geometry of the chimney
- R = thermal resistance of the chimney walls
- C_p = specific heat of the chimney gases
- W = mass flow rate of the chimney gases
- K = the chimney friction factor (for isothermal flow at least, dependent only on the Reynolds number $\frac{V_m d}{\nu_m}$ where d is a characteristic chimney size parameter, usually diam, and ν_m is the kinematic viscosity).

Equation (1) is the basic equation for chimney draft relating

* These equations are given in slightly different form from that used previously.

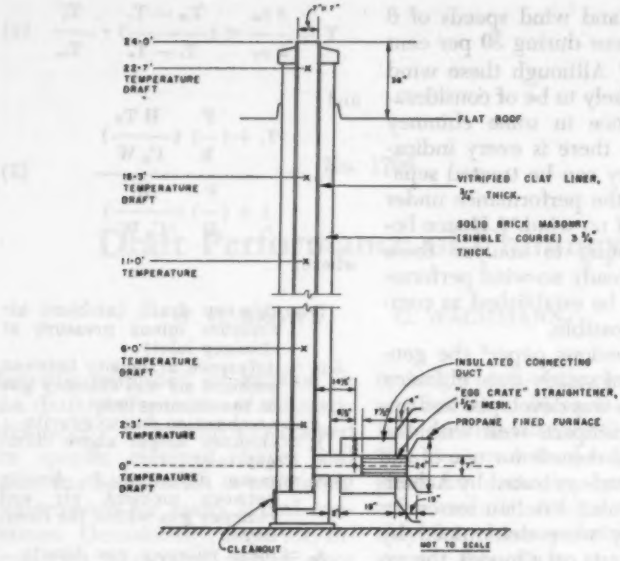

Fig. 1 Layout of the NRC test chimney

chimney efficiency, $\frac{D}{\Delta\rho_T g H}$, to friction pressure loss, $K\rho_m \frac{V_m^2}{2}$ and to heat exchange through the chimney walls as manifest in the term Y. Equation (3), giving the temperature T_m corresponding to the mean chimney gas density is derived by eliminating the chimney exit temperature T_2 from the two following equations:

$$T_m = T_1 - F(T_1 - T_2) \quad (4)$$

and

$$W C_p(T_1 - T_2) = \frac{H}{R}(T_m - T_2) \quad (5)$$

Equations (4) and (5) presume that the temperature drop occurring throughout the chimney is approximately linear and that the temperature corresponding to the mean density of the chimney gases is the same as the mean temperature. Equation (5) equates the heat loss by the chimney gases to the heat flow across the chimney walls.

EQUIPMENT AND TEST PROCEDURE

NRC masonry chimney – The test chimney (to be referred to as the NRC chimney), (Fig. 1), was constructed of standard clay brick with a vitrified clay liner firmly grouted into place. Flue dimensions were 7 x 7 in. The chimney thimble, a 7-in. inside diam steel tube, entered

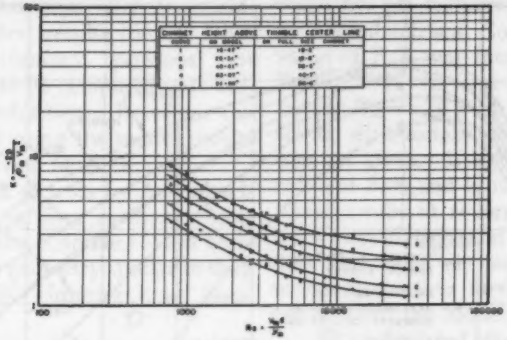

Fig. 2 Isothermal friction losses in a model of a chimney with a 7 x 7 in. sq flue and a 7 in. diam thimble

the chimney at right angles 3.3 ft above the floor. Overall chimney height above the thimble center-line was 24.0 ft, of which 38 in. extended above the top of the containing building. Draft probes were installed in the connecting duct 1.2 ft from the inside face of the chimney liner and at flue center-line 6.0, 16.3, and 22.7 ft above the thimble center-line. During tests differential drafts between the thimble and various points along the vertical chimney were measured by connecting the draft probes to a micromanometer. Bare chromel-alumel thermocouples were installed at connecting duct center-line, at the position of the draft probe and at flue center-line at heights above thimble of 2.3, 6.0, 11.0, 16.3 and 22.7 ft. In addition, an aspirating thermocouple was used to check thermocouple readings.

Flue gas for the tests was supplied by a propane furnace. An egg-crate type air straightener fitted in the connecting duct between the furnace and chimney ensured uniform temperature and velocity at the chimney inlet. Combustion air was supplied by a blower. Air flow to the furnace was measured with calibrated orifices and propane gas flow was measured with a wet-test meter.

Models—Several models of conventional chimney shapes, including that of the NRC chimney, were constructed of round and rectangular tubing about 1/5 to 1/7 scale. Friction-loss tests on these models were conducted using the method previously outlined.[8]

Scope of tests—The NRC masonry chimney was tested at flue gas flow rates of 25, 50, 75 and 100 cfm, (standard air, 70 F and 29.92 in Hg), and at chimney inlet temperatures of 350 F and 750 F. All tests were made in summer and early fall, so room temperature T_R was essen-

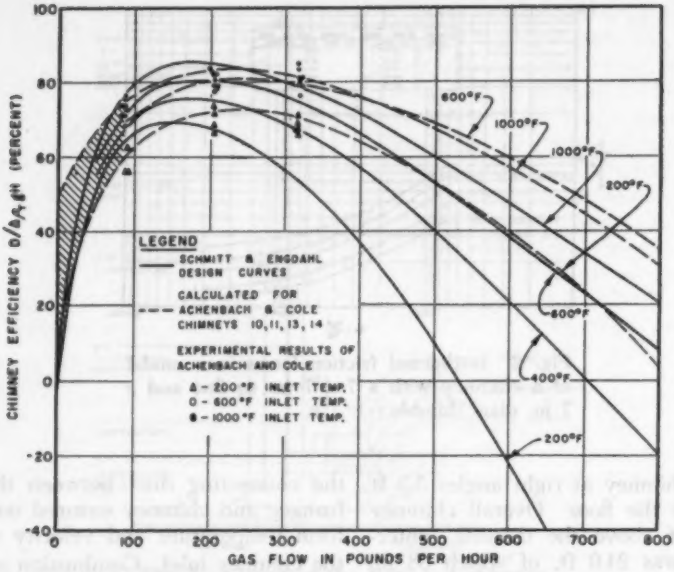

Fig. 3 Comparison of ASHAE design curves (Schmitt and Engdahl) with data of Achenbach and Cole and calculated performance

tially the same as the outside air temperature T_0.

The model chimneys were tested at room temperature at various flow rates corresponding to the range of Reynolds numbers observed in full-size chimneys.

RESULTS AND OBSERVATIONS

Isothermal friction tests with models — Results of tests to determine the friction factor on a model of the NRC masonry chimney (Fig. 2) showed the manner in which K varied with Reynolds number for isothermal flow. (Both $K = \frac{-2D}{\rho_m V_m^2}$ and $Re = \frac{V_m d}{\nu}$ were computed on the basis of the mean chimney thimble velocity and thimble diam.) Results obtained with the other models were similar although values differed depending on the geometry. Results were also similar to those observed previously[8] for models with round chimneys and thimbles of the same size.

Comparison of observed and calculated results for previously tested

masonry chimneys—Before considering the test results for the NRC masonry chimney, previous test records shall be compared with calculated performance based on the theory and using the model results for the friction factor K.

Results of tests by Achenbach and Cole[2] on four masonry chimneys of cinder concrete 15½ ft high and having geometry similar to that of the NRC chimney have been plotted in Fig. 3 as $\frac{D}{\Delta\rho_T gH}$ against flow rate as suggested by Schmitt and Engdahl.[3] The recommended design curves of the latter authors are included for comparison. The experimental results agree moderately well with the design curves in the range of flow rates tested, but there is an indication that at high rates (above 300 lb/hr) agreement will be increasingly poor. This is especially noticeable at a gas temperature of 200 F. Similarly, the shape of the design curves appears to be considerably different from that of the experimental curves.

With the assumption that friction losses in non-isothermal flow remain essentially the same as in isothermal flow it is now possible to use Equations (1) to (3) to calculate the performance of the brick chimneys. The factors F and R (both assumed constant) in Equation (3) are difficult to calculate accurately, however, hence the actual experimental temperature data for the four chimneys were used to determine average values.

Using Equation (3) and the mean flue gas temperature as given by Achenbach and Cole, the mean value of F/R was found to be 1.2 Btu/hr/F/ft. (It was necessary to assume $T_R = 70$ F for these calculations since indoor air temperature was not given.) Using this average value of F/R and Equation (3), the temperatures at several flow rates were calculated and substituted into Equations (1) and (2) along with the friction factor K determined from the model tests.

The calculated efficiency–flow-rate curves are superimposed on the experimental results (Fig. 3). The theoretical curves agree well with the experimental results but do not agree with the design curves, especially at low chimney inlet temperatures and high gas flow rates.

Remaining records for all fourteen chimneys tested by Achenbach and Cole were analyzed as above using the model results for the different chimney shapes. This study showed similar agreement between calculated and observed performance. All these chimneys were tested in the range 85 to 320 lb/hr and showed efficiencies in the same range as those of Fig. 3. Each type of chimney construction, however, had its own specific efficiency – flow-rate relationship.

Draft performance of the NRC chimney – Although the above analysis appeared to confirm that Equations (1) to (3) could be used for chimney design purposes, some doubt remained as to the validity of the assumption that friction pressure-loss would be the same

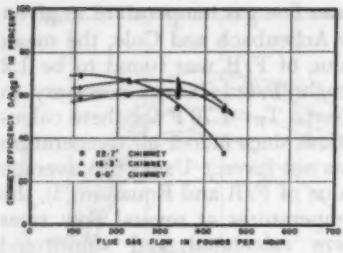

Fig. 4 Efficiencies of the NRC test chimney. (Inlet temp 350 F)

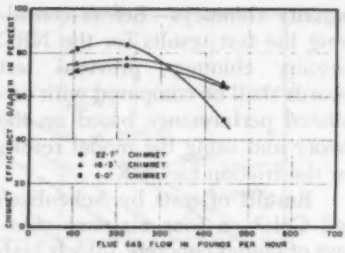

Fig. 5 Efficiencies of the NRC test chimney. (Inlet temp 750 F)

under isothermal and nonisothermal conditions. The NRC masonry chimney was operated therefore to obtain further records of draft for different chimney heights. This information can be compared with that given by Achenbach and Cole.

As pointed out, the draft in the NRC chimney was measured differentially between a point in the connecting duct near the thimble and the chimney. This method of measurement was necessary because even notably low winds over the chimney top were found to contribute significantly to the draft when measured in the usual way (i.e. between the ambient air and a point in the thimble). This effect was verified by simple wind tests on a model, which also offer support for the previously proposed method[8] of using models to study wind effects. (Results are given in the Appendix and Tables I and II.) By making differential measurements the net draft for no-wind conditions for different heights of chimney could be obtained without the necessity of building separate chimneys or having large openings in the chimney at various heights (cf. 1).*

Test results for the NRC chimney, with flue gas inlet temperatures of 350 and 750 F are given in Figs. 4 and 5. Chimney efficiencies for the 16.3-ft chimney are in fair agreement with the results of Achenbach and Cole. Results for all three heights at 350 F inlet temperature agreed poorly with the Schmitt and Engdahl design curves at the higher flow rates, and in general agreed only approximately at lower flow rates. The relative performance of the three heights was not regular: at low flow rates the 6.0-ft chimney had the greatest efficiencies, while at high flow rates the efficiencies for the 16.3-ft and 22.7-ft chimneys were greatest. To check the effect on performance caused by chimney inlet conditions, the air straightener was removed from the chimney thimble and tests

* Some authors (1, 4) claim a "stack effect" exists above the physical height of a chimney which causes an increase in draft in the absence of wind. However, there appears to be no experimental or theoretical evidence available to support this contention.

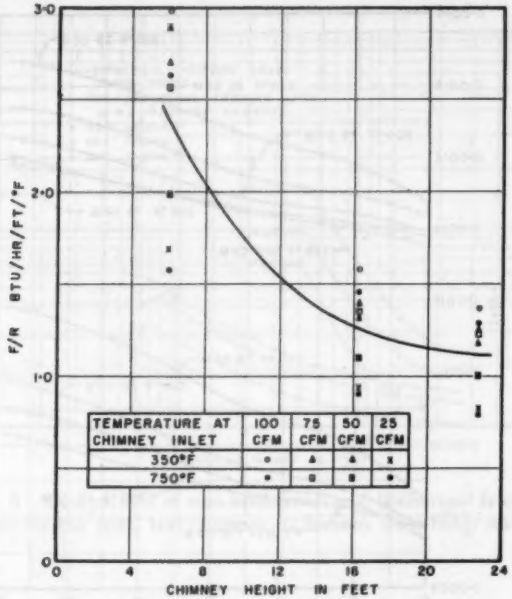

Fig. 6 F/R values for the NRC test chimney

repeated. Results were only slightly affected by this procedure. The values of F/R (Fig. 6) did not differ greatly from those of Achenbach and Cole, although values were somewhat greater for the 6.0-ft chimney than for the other two heights.

Since the differential method of obtaining draft measurements on the NRC chimney allowed more accurate results than previously obtained, an attempt was made to determine the actual friction losses occurring in non-isothermal flow. The measured value of ρ_m obtained from an average of the inverse of temperature at the chimney centerline (Fig. 7) was inserted into Equations (1) and (2), which were then solved for the non-isothermal friction factor K_n. Results (Figs. 8 and 9), although somewhat inconsistent, especially for the 6.0-ft chimney, show values much greater than for isothermal flow (model results given for comparison) except at high flow rates where convergence becomes apparent. Furthermore, it can be seen that the magnitude of K_n also depends on the chimney gas temperature.

The large friction factors obtained in non-isothermal flow can be clarified in part by a new theory for pressure loss and heat ex-

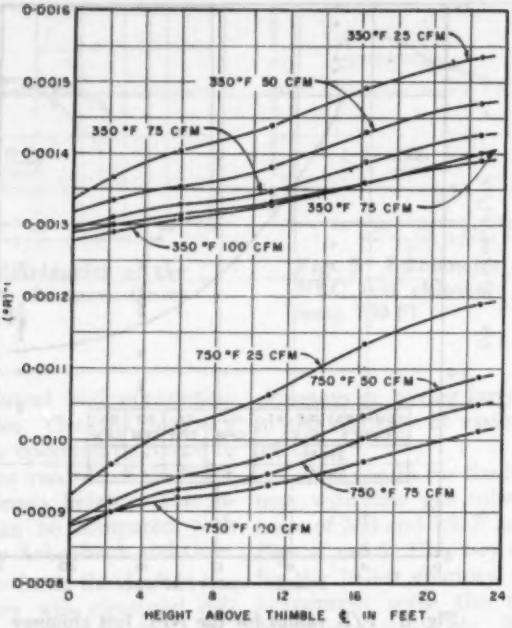

Fig. 7 Inverse of temperature at flue centerline in the NRC test chimney

change in vertical tubes,[9] which indicates that the Grashof number, $\frac{gd^3\beta\Delta T}{\nu^2}$, influences the friction pressure loss as well as the heat flow. At low flow rates in the chimney tests the Grashof number was large in comparison with the Reynolds number and greatly influenced the friction losses. At these low flow rates the turbulence due to instability was much greater than that occurring in the normal isothermal turbulent range and the friction loss was consequently increased.

Although calculated chimney performance based on the isothermal friction losses appeared to correlate fairly well in previous work,[8] it now becomes clear that this method is only applicable to high flow rates and to a quite limited range of chimney sizes. In the size range of domestic chimneys large errors in estimating the friction factor K_n do not greatly affect the calculated chimney efficiency. For extrapolation of results for other sizes of chimneys the method suggested previously[8] should be modified to incorporate the non-isothermal factor K_n instead of K for isothermal conditions. In the

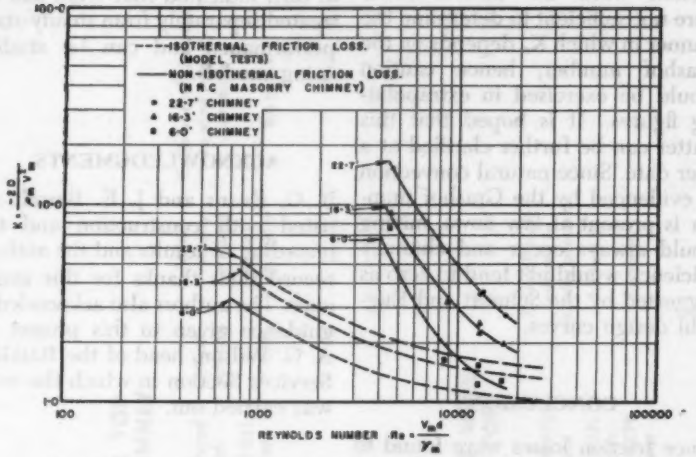

Fig. 8 Comparison of non-isothermal and isothermal friction losses for the NRC test chimney. (Chimney inlet temp 350 F)

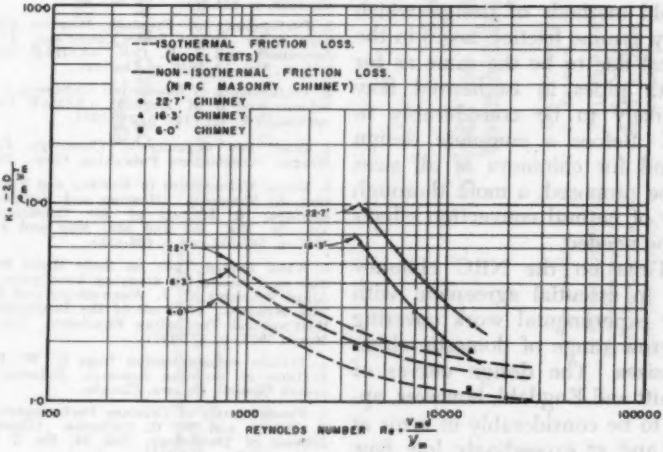

Fig. 9 Comparison of non-isothermal and isothermal friction losses for the NRC test chimney. (Chimney inlet temp 750 F)

present work the measurements were not sufficient to determine the manner in which K_n depends on the Grashof number, hence caution should be exercised in extrapolating figures. It is hoped that this matter can be further clarified at a later date. Since natural convection as evidenced by the Grashof number is present at low flows, mixing would always occur and chimney efficiency would not tend to zero as suggested by the Schmitt and Engdahl design curves.

CONCLUSIONS

Since friction losses were found to be much higher for non-isothermal flow than for isothermal flow, care should be exercised in extrapolating available results for other shapes and sizes of chimneys. In particular, old methods of design which simply assume friction losses in the vertical flue to be the same as for smooth pipes in isothermal flow are likely to be considerably in error. Before a complete design method for chimneys of all sizes can be proposed, a more thorough study of natural convection effects will be needed.

Tests on the NRC chimney were in essential agreement with other experimental work covering a narrow range of domestic chimney sizes. The design curves of Schmitt and Engdahl, however, appear to be considerably in error at high and at exceedingly low flow rates.

Incidental tests to study wind effects over the chimney top were verified by model results. This work in turn indicated that wind can be treated separately from steady-state performance and can be studied using models.

ACKNOWLEDGMENTS

R. G. Evans and J. E. Berndt assisted with construction and the recording of results and the authors record their thanks for this assistance. The authors also acknowledge guidance given to this project by A. G. Wilson, head of the Building Services Section in which the work was carried out.

REFERENCES

1. Observed Performance of Some Experimental Chimneys, R. S. Dill, P. R. Achenbach, and J. T. Duck. (ASHAE Transactions, Vol. 48, 1942, p. 351-368).

2. Performance of Fourteen Masonry Chimneys under Steady State Conditions, P. R. Achenbach and S. D. Cole. (ASHAE Transactions, Vol. 55, 1949, p. 129-154).

3. Performance of Residential Chimneys, L. B. Schmitt and R. B. Engdahl. (ASHAE Transactions, Vol. 55, 1949, p. 241-262).

4. Draft and Capacity of Chimneys, J. G. Mingle. (Combustion Publishing Corp., 1925).

5. Using Mathematics in Heating and Ventilation, E. Woodcock. (Heating and Ventilating Engineer & Journal of Air Conditioning. Vol. 30, Nos. 359 and 360. May and June, 1957, p. 547-553 and p. 606-612).

6. Wind Tunnel Tests on Scale Model Buildings as a Means for Studying Ventilation and Allied Problems, J. J. Wannenburg and J. F. Van Straaten. (Journal of the Institution of Heating and Ventilating Engineers, Vol. 24, March 1957, p. 477-492).

7. Private communication from D. W. Boyd, Division of Building Research, National Research Council, Ottawa, Canada.

8. Fundamentals of Chimney Performance, W. G. Brown and W. G. Colborne. (Canadian Journal of Technology, Vol. 34, No. 5, September 1956, p. 354-365).

9. Der Einfluss des Auftriebs auf Wärmeübergang und Druckgefälle bei erzwungener Strömung in senkrechten Rohren, W. G. Brown and P. Grassmann. (Forschung auf dem Gebiete des Ingenieurwesens, Vol. 25, No. 3, 1959, p. 63-78).

TABLE I

EFFECT OF WIND OVER TOP OF NRC MASONRY CHIMNEY

Draft measured differentially between thimble and a point 1 ft below chimney top	Draft measured between thimble and outside air	Draft induced by wind	Wind velocity	Wind velocity pressure	Ratio of draft induced to wind velocity pressure
0.012 to 0.014 in. water	0.039 in. water	0.025 to 0.027 in. water	9 mph	0.041 in. water	0.6 to 0.7

TABLE II

EFFECT OF A HORIZONTAL WIND OVER MODEL CHIMNEY TOP

Fan position	Draft induced by wind	Wind velocity pressure	Ratio of draft induced to velocity pressure
24 in. horizontally from chimney top	0.016 to 0.024 in. water	0.028 to 0.031 in. water	0.5 to 0.8
8 in. horizontally from chimney top	0.031 to 0.051 in. water	0.059 to 0.079 in. water	0.4 to 0.9

APPENDIX

EFFECT OF HORIZONTAL WIND OVER CHIMNEY TOP

Effect of horizontal wind over the top of the NRC masonry chimney was noted even at low wind velocities. Measurements of both wind speed and chimney draft were made with the chimney inoperative, i.e., no heating or air flow. Results are given in Table I. The calculated chimney draft, based on temperature of air in the chimney and room temperature, agreed with the draft measured differentially between the thimble and a point 1 ft below the chimney top. The draft measured in the usual way between thimble and outside air, however, was considerably greater, the net increase in draft due to wind being approximately 0.025 to 0.027 in. water. The wind speed during this test was somewhat irregular but averaged 9 miles per hour. The outside air temperature was approximately 40 F.

The theory for the effect of wind over a chimney top was given previously[6] as

$$\frac{(P_s - P_s')}{\rho_o V_o^2} = \phi\left(\frac{V_o d}{\nu}, \frac{T_s}{T_i}, \frac{V_s}{V_o}, \alpha\right)$$

where ϕ denotes functional dependence; $(P_s - P_s')$ is the difference in static pressure between ambient air and chimney exit at the same level, i.e., the increase or decrease in draft due to wind;
V_o and V_s are wind velocity and chimney exit velocity; α is the direction angle of the wind.
Other symbols are as previously used.

To ascertain whether the observed wind effect was represented by this equation the model of the NRC masonry chimney was subjected to simple tests with $V_s = 0$. For the conditions under study, the term V_s/V_o did not apply. The exit temperature of the masonry chimney and outside air temperature did not differ greatly, hence T_s/T_i was approximately the same for both the model and full-size chimneys. The Reynolds numbers were not the same for model and chimney, but dependence on this factor was not considered to be strong (this is generally true for all types of flow in the turbulent range). Under the circumstances the ratio of the increase in draft to wind velocity pressure was likely to be approximately equal for model and chimney.

Wind tests on the model, as on the full-size chimney, were carried out with the inlet blocked off, i.e., no air flow, and with the model in a horizontal position to avoid minor temperature induced draft. The room temperature was 70 F. Wind was provided by an ordinary domestic propeller fan and air velocity at the model top was measured with a pitot tube.

Model results (Table II) showed that the ratio of wind-induced draft to wind velocity pressure was about the same as for the full-size chimney, validating the theory suggested above. The results of these simple tests are not valid under conditions of actual chimney operation, since the effect of the ratios T_s/T_o and V_s/V_o is as yet unknown. It may be reiterated, however, that wind effects both over the chimney top and for inside/outside pressure differences in houses probably can be determined effectively by model tests for any type of building and chimney orientation.

1707

No. 1707

Saturated Steam Flow in Copper Tubing

C. M. HUMPHREYS
Member ASHRAE

J. T. BAKER
Member ASHRAE

B. H. JENNINGS
Member ASHRAE

Flow of saturated steam in pipes is not a simple phenomenon, as condensate is always present to a greater or less degree and the presence of this water converts ordinary vapor flow into a complex two-phase flow pattern. Nevertheless, if the amount of condensate is small (say less than 5 per cent of the total weight flow rate) and if the steam and condensate flow in the same direction the error introduced by treating the whole flow as simply vapor is not serious. Unfortunately, this simplification has not been applicable for many of the cases in which it has been employed.

The use of copper tubing for carrying steam has reached commercial significance only for small size tubing. This practice too is rather recent and consequently, data on steam flow in copper are almost lacking in the literature. Although it was not thought that great differences exist between flow in ferrous and copper tubing, some differences are known to exist, and at the start of this investigation there were definite uncertainties about both types. Consequently, this paper, although pointing out characteristics for copper, is applicable both to copper and steel.

The theory of flow of fluids in pipes has been studied intensively for many years. The work of Osborne Reynolds,[1] later expanded by Buckingham,[2] made possible the use of dimensionless parameters which could correlate the results of tests with one fluid to predict information for other fluids. The use of one of these dimensionless parameters, the Reynolds number, led to a method of indicating the friction factor, f, for quite a wide range of conditions and fluids. In turbulent flow, Nikuradze,[3] using water, first clearly demonstrated the effect of pipe roughness on flow characteristics. R. J. S. Pigott,[4] in 1933, made a broad contribution to this field when he prepared a chart

C. M. Humphreys is Assistant Director of Research; B. H. Jennings is Director of Research and J. T. Baker, Research Engineer, ASHRAE Research Laboratories. This paper was presented at the ASHRAE Semiannual Meeting in Dallas, Texas, February 1-4, 1960.

relating pipe roughness, Reynolds number and the friction factor, f. L. F. Moody,[5] in 1944 following a similar pattern to that developed by Pigott, expanded the friction chart to cover pipes having various degrees of roughness over a greater range. In fact, data from his chart are now used to such an extent that the friction factors are sometimes known as Moody Factors. It would be more accurate, however, to refer to them merely as friction factors.

Prior to this period of having the friction factor available in terms of the Reynolds number, for a wide range of conditions, various approximations for the value of f were in use. Most of these took the form

$$f = k\left(1 + \frac{B}{d}\right) \qquad (1)$$

where f represented the friction factor (dimensionless)

k and B were constants for a given medium

d was the pipe diameter in appropriate linear units

The pressure loss resulting from fluid flow was early observed to be proportional to pipe length, inversely proportional to pipe diameter, and to vary closely as the square of the mean fluid velocity. The resulting equation for pressure loss from flow, attributed probably first to H. d'Arcy[6] (1857), then to J. Weisbach and in slightly different form to Fanning, carries all three of these names, even including that of d'Arcy-Weisbach. For simplicity, we will here call it the d'Arcy equation, written thus

$$h = f\frac{L}{d}\frac{V^2}{2g} \qquad (2)$$

where

h = loss of head, in feet of fluid flowing

L = length of pipe run, feet

d = internal diameter of pipe, feet

V = fluid velocity in feet per second (fps)

g = 32.17, the gravitational constant

f = the friction factor, dimensionless, read from a friction factor chart such as that of Pigott or Moody in terms of the Reynolds number, N_{Re}

The Reynolds number is represented by the relationship

$$N_{Re} = \frac{Vd\rho}{\mu} \qquad (3)$$

where, with V and d having the units above

ρ the density, has units lb per cu ft

μ the viscosity, has units of lb per ft sec

With viscosity μ^1 expressed in centipoises

$$N_{Re} = 1488\frac{Vd\rho}{\mu^1} \qquad (4)$$

To express the pressure loss, Δp in lb per sq in. from h of the d'Arcy equation (2)

$$\Delta p = \frac{\rho h}{144} \qquad (5)$$

With the appropriate density and viscosity, of a given medium such as steam, water, ammonia or air, known, it is easy to calculate the Reynolds number for given velocity, and with the Reynolds number at hand, the friction factor can be found from a chart such as that of Pigott or Moody. With this

factor inserted in the d'Arcy equation, it is readily possible to obtain the pressure loss for a given set of flow conditions. The beauty of this approach is that even though the original test data were obtained for air or for water, if the appropriate viscosity and density of steam are known, it is possible to use such generalized data to determine values for steam.

This possibility of generalization has been a powerful tool in analysis. Unfortunately, as has been mentioned before, when a two-phase mixture of steam and water flows in a conduit, particularly with the ratio of steam to water varying, neither the viscosity of the mixture nor its density is known. Moreover, with two phases present, the liquid particles may exist as a fog or as is more usual in horizontal pipe, the liquid flows on the bottom of the pipe usually at a lower velocity than does the vapor.

Consequently, the need for experimentation to confirm the theory is definitely required. The experimentation described in this paper is quite closely in agreement with the aforementioned theory. In the case of dry saturated steam, no discrepancy occurs nor does it occur in terms of the dry portion of the two-phase mixture if the amounts of dry steam and liquid can be clearly determined.

During the first decade of this century many people became interested in developing a formulation for the pressure drop associated with flow of steam in pipes which by one simple equation would cover a range of flow conditions. W. C. Unwin developed an expression which was later adapted by G. H. Babcock[7] to cover the pressure loss under specified steam-flow conditions. This equation which still has limited utility is variously known as the Babcock equation, the Unwin equation, and the Unwin-Babcock equation. It is usually written as follows:

$$\Delta p = \frac{C_1 W^2 L}{\rho d^5} \left(1 + \frac{3.6}{d}\right) \qquad (6)$$

where

Δp = pressure drop in psi
C_1 = constant, used as 0.0001321 by Babcock, 0.0001306 by Unwin
W = steam flow rate in lb per minute
L = length of pipe run in feet
d = inside diameter of pipe, inches
ρ = average density of steam flowing, lb per cu ft

Many others followed the lead of Babcock and endeavored to find constants for the Babcock equation or new formulas that would represent steam flow over a greater range of values. In particular, G. F. Gebhardt[8] in 1909 summarized the constants for this equation. It is obvious that an equation, in which viscosity is not considered and the density, ρ, appears as the only variable related to the medium, can be applicable only under limited conditions. Nevertheless, this formula was widely used and is still employed at the present time in many places. In fact, until 1958, some of the steam-pipe capacity data in the ASHRAE GUIDE had been computed on the basis of this formulation. W. F. Kerka[9] recomputed data for the 1959 GUIDE using the

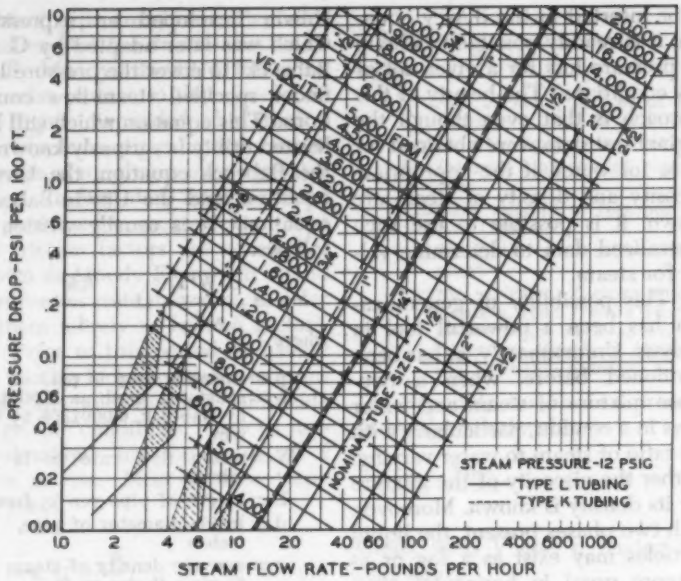

Fig. 1 Flow chart for 3.5 psig steam in copper tubing

d'Arcy-equation type of analysis and later published his results in a separate paper. Robert H. Page and S. Konzo[10] in 1951 prepared an exceptionally fine study of the problems relative to steam flow entitled, Analysis of Data on Flow of Steam in Pipes.

It should be realized that in using either the d'Arcy or Babcock equation to compute pressure drop, it is assumed that for the conditions under consideration the character of the medium is invariant, that is the fluid is incompressible. This is, of course, not true for steam but if the pressure drop is small, no serious error accrues when the mean density and mean viscosity are used in the computation. For large pressure drops, such as would arise in the case of a long pipe line, it would be advisable to break the computations into a number of steps.

The number of experimenters who have determined experimental data for friction factors of steam flow in pipes is not great, and the data found represent limited ranges used during the tests. One reason that more experimental data have not been obtained can be related to the fact that the generalizations relative to the dependence of the friction factor on the Reynolds number and pipe roughness are well established, and data deter-

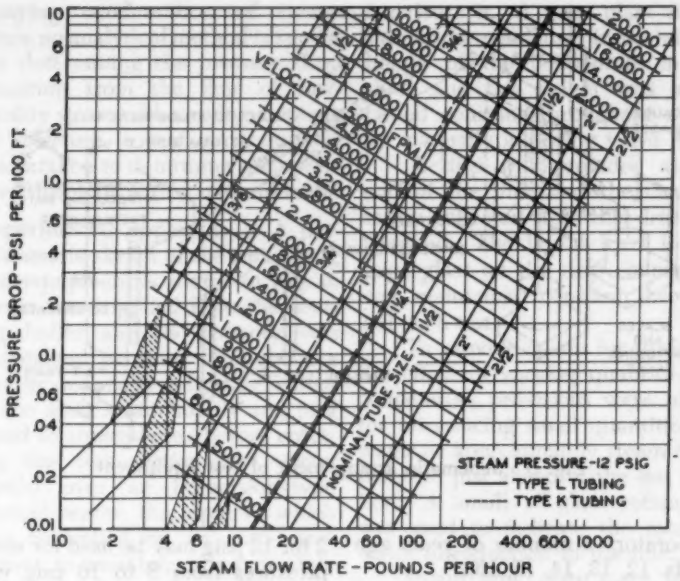

Fig. 2 Flow chart for 12 psig steam in copper tubing

mined for mediums other than steam are applicable. The other mediums usually employed are air or water. One paper on steam should be mentioned, namely that by J. H. Keenan, who, in 1939,[11] carried out a series of studies to measure friction coefficients for the flow of steam. His paper showed that the value of f bore a continuity relationship to the Reynolds number both for small pressure drops and for the large drops associated with velocities approaching the acoustic under which condition the steam has to be considered as a truly compressible fluid.

Computed capacity of copper tubing — Data on the capacity of supply and return piping in the various parts of a steam heating system are essential to the designer of such a system, and where steam and condensate are flowing in the same direction, it is customary to size the pipes on the basis of pressure loss.

However, for those parts of the steam piping in which steam and condensate flow in opposite directions, the steam velocity must be kept low enough so that it will not interfere with the counter-flow of condensate. For this condition which cannot be computed, data on the capacity of counter-flow steam lines were found from tests carried on at the ASHVE Research

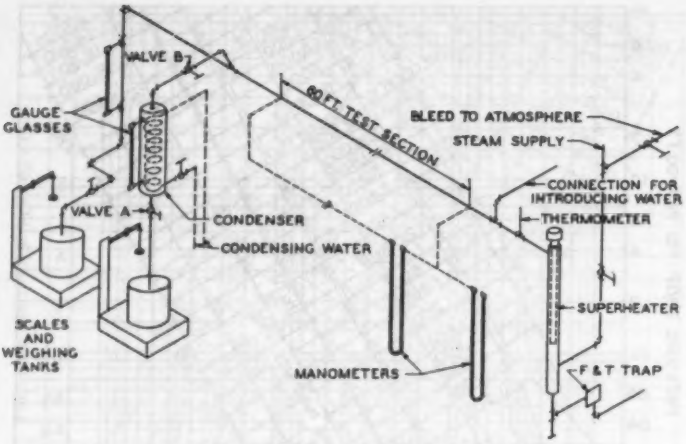

Fig. 3 Schematic arrangement of test equipment

Laboratory a number of years ago (Refs. 12, 13, 14, 15, 16).

A first step in the preparation of this paper was to use the analytical approach, described in the first part of this paper, to compute the capacity of small-size copper tubing (2½ in. and under). These computations were made by determining the Reynolds number, using it to find the friction factor and then by means of the d'Arcy equation, finding respective pressure drops. The results are plotted in Figs. 1 and 2.

Steam pressures of 3.5 and 12 psig were selected respectively for the computations for Fig. 1 and Fig. 2 to be consistent with tabular data on the steam flow in ferrous pipe in the 1959 GUIDE. As pointed out in the GUIDE, flow rates shown for 3.5 psig can be used for saturated steam at pressures from 1 to 6 psig, with an error not exceeding 8 per cent. Similarly, Fig. 2 for 12 psig may be used for steam pressures from 8 to 16 psig with the same accuracy. At low flow rates in some of the smaller tubes shown in Fig. 1 and 2, flow conditions are in the critical zone. In this zone, shown shaded in the figures, friction loss is unpredictable. Above this zone, the flow is turbulent, while below it, the flow is laminar.

It is recognized that the steam flow data presented in Figs. 1 and 2 are for idealized conditions which never exist in a heating system. They are strictly applicable only to the case where dry saturated steam is flowing throughout the length of the line. In practice, the steam entering the line from the average heating boiler is seldom completely dry, and the steam quality decreases as the distance from the boiler increases, because of heat loss from the line and the accom-

panying condensation of steam. Since no analytical method is known for determining the pressure drop resulting from the flow of low-quality steam with varying amounts of moisture, a test program was undertaken to determine such pressure drops by actual measurement.

Experimental apparatus – A diagrammatic sketch of the test piping and equipment is shown in Fig. 3. Steam was supplied from the heating boiler and its pressure was maintained constant throughout a test by manually adjusting valves in the main steam supply and in a bleed to atmosphere. Before entering the test section, the steam passed over an immersion-type electric heater, the input to which was controlled by an auto-transformer to maintain approximately 2 degrees of superheat. The temperature of the steam entering the test section was determined by means of a mercury-in-glass thermometer.

A pressure tap was located at each end of the 60-ft-long test section. The pressure of the steam at the entering end was determined by means of a mercury manometer. The pressure drop in the test section was indicated by a manometer filled with a fluid having a specific gravity of 1.75.

The rate of steam flow in the line was determined by condensing the steam and weighing the condensate over timed intervals of 20 to 60 min with the longer runs needed for exceedingly low flow rates. The capacity of the condenser could be varied by flooding a part of the condensing surface to inactivate it. A gage glass at the side of the condenser indicated the height of the condensate in the shell, and this height was maintained constant throughout a test by manually adjusting valve A.

A drip was provided at the end of the line, and the condensation collected from this drip was weighed. The liquid level in the gage glass on the drip connection was maintained constant throughout each test.

To provide means for studying the effect of varying quantities of condensate, provisions were made for introducing small quantities of water at approximately steam temperature just ahead of the test section. A small all-glass rotameter was used to indicate the rate of water introduction to the line.

Steam flow tests were made with ⅜, ½, ¾, 1, 1¼, and 1½-in. nominal-diameter Type L copper tubing. In all cases the test section was installed with a pitch of 1 in. in 20 ft-0 in., and was uninsulated.

Analysis of pressure loss data—Each tube size was tested at initial steam pressures of 2, 6 and 10 psig, and at a variety of flow rates. At least one no-flow test was made on each tube for each steam pressure to determine the amount of condensation occurring in the line. The no-flow tests were made by operating the system with valve B closed.

The test data were first analyzed on the basis of dry steam delivered at the downstream end of the test section. Since it was known that some of the condensation occurring in the pipe was being carried over with the steam into the

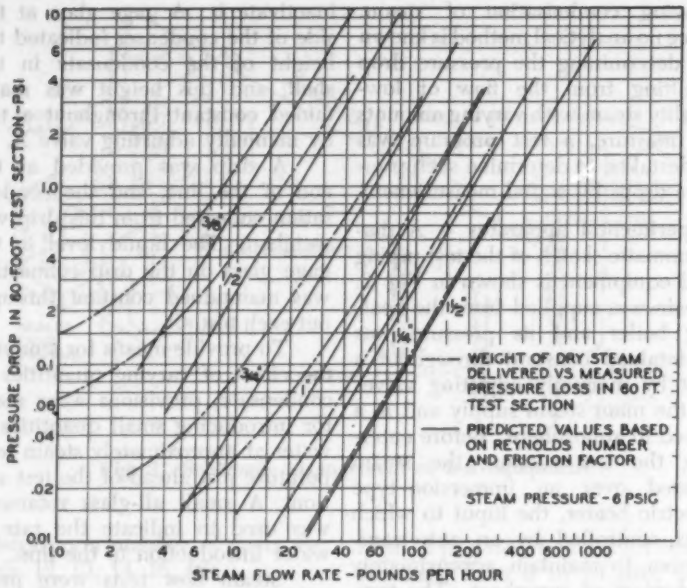

Fig. 4 Comparison of theoretical and experimental flow data

condenser, the weight of dry steam was calculated for each test by subtracting the condensation obtained in the no-flow run, from the sum of the weights of condensation obtained from the condenser and from the drip. In Fig. 4 these dry steam weights were plotted against the measured pressure loss in the 60-ft test section, for 6 psig. For comparison, the predicted curves based on the d'Arcy equation with appropriate friction factors are also shown. It will be noted that the differences between observed and predicted values are quite large for the smaller tubes and at the lower rates of flow.

One of the reasons for these large differences is immediately apparent. Although the steam flow at the downstream end of the line was as plotted, the flow at the upstream end was greater by the amount of the condensation collected in the no-flow run. On the assumption that the rate of condensation per foot of pipe was uniform throughout the line, the average steam flow in the test section during each test was calculated by subtracting one half of the condensation collected in the no-flow run, from the sum of the weights of condensation collected from the condenser and the drip. These average flow rates were plotted against pressure loss in Fig. 5. Here we find reasonably good

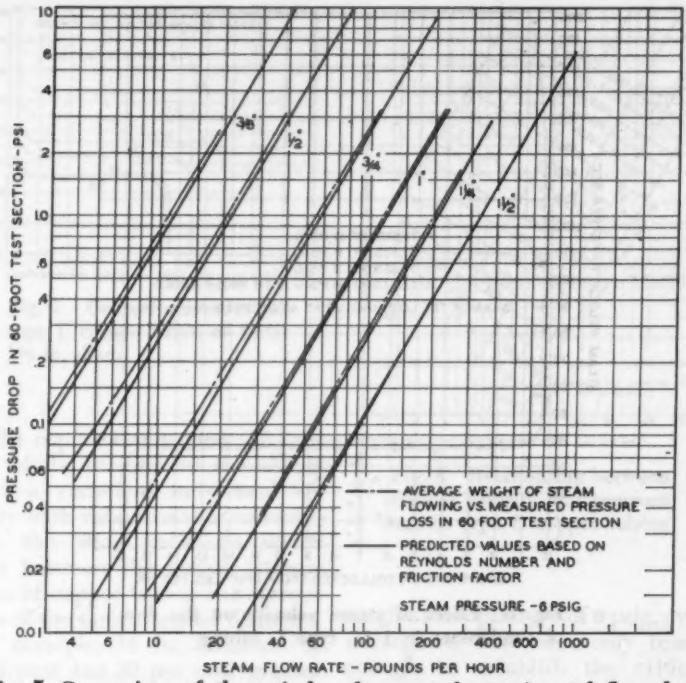

Fig. 5 Comparison of theoretical and corrected experimental flow data

agreement between the experimental and predicted values.

Condensation carry-over—As mentioned above, it was evident early in the program that some of the condensate which formed in the test line was being carried over into the condenser with the steam. A cursory examination of the data indicated sudden large scale differences in the amount of condensate collected from the drip, and a more thorough study of the phenomenon was undertaken.

The relationship between steam velocity in the 1-in. copper line and the weight of condensation collected from the drip is plotted in Fig. 6. It can be seen that for tests made with steam velocities above 40 ft per second, the condensate collected from the drip averaged only about ¼ pound per hour, but that at velocities below 35 fps, the rate of drip was approximately 7 pounds per hour. Different symbols have been used in the figure to plot the results obtained at steam pressures of 2, 6, and 10 psig. As may be seen from the distribution of the test points, no effect of steam pres-

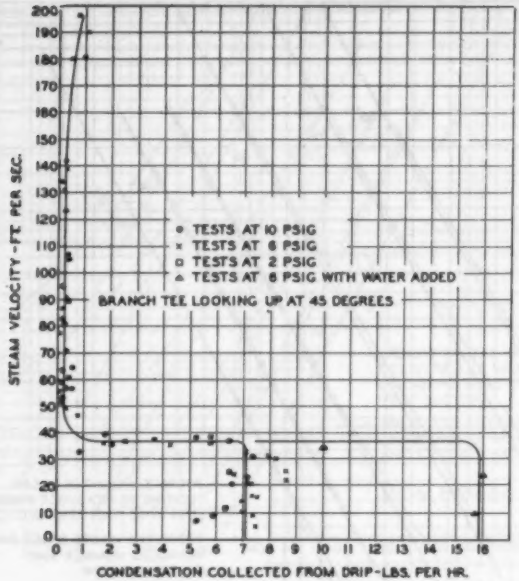
STEAM VELOCITY - FT. PER SEC.
CONDENSATION COLLECTED FROM DRIP - LBS. PER HR.
TESTS AT 10 PSIG
TESTS AT 6 PSIG
TESTS AT 2 PSIG
TESTS AT 6 PSIG WITH WATER ADDED
BRANCH TEE LOOKING UP AT 45 DEGREES

Fig. 6 Effect of steam velocity on the flow of condensate in 1 in. type L tubing

sure is indicated over this small pressure range.

A few points are shown in Fig. 6 for a series of tests in which water was added at the upstream end of the line at a rate of approximately 9 pounds per hour. These points follow the same pattern established by the other tests. At higher velocities the added moisture was carried over into the condenser with the steam, while at low velocities the water collected from the drip was increased by the amount of water added.

As originally installed, connections to the condenser and the drip at the end of the main were made with steel pipe and malleable fittings of the same nominal size as the copper test sections. The branch to the condenser was taken from the main with a tee looking up at 45 degrees. For these initial piping arrangements, although the general shape of the curves were identical to that of Fig. 6, the critical velocities determined for the various tube sizes, varied widely and unpredictably. The lowest critical velocity of 37 fps was obtained with 1-in. tubing while the maximum critical velocity of 65 fps was obtained with 1¼-in. tubing. These velocities were those prevailing in the downstream and

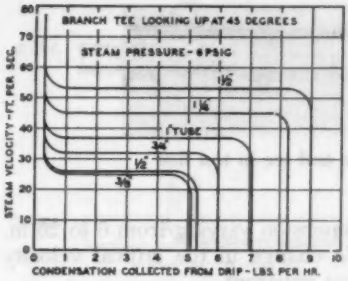

Fig. 7 Critical velocities for type L copper tubes of ⅜ to 1½ in. diam

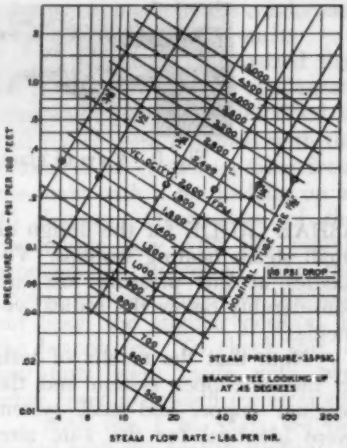
PRESSURE LOSS - PSI PER 100 FEET
STEAM FLOW RATE - LBS. PER HR.
VELOCITY - FEET PER SECOND
INCREASING TUBE SIZE
.06 PSI DROP
STEAM PRESSURE - 3.5 PSIG.
BRANCH TEE LOOKING UP AT 45 DEGREES

Fig. 8 Relationship between critical velocity and pressure loss in type L copper tubing

of the copper test section. At least one of the reasons for the almost random variations in critical velocity with tube size was undoubtedly the wide variations which exist between the actual internal areas of copper tubing and ferrous pipe of the same nominal diameter. For example, ½-in. Schedule-40 steel pipe has 30 per cent greater internal area than ½-in. type-L copper tubing, while the internal area of 1-in. steel pipe is only about 5 per cent greater than 1-in. type-L copper. However, a recalculation of the critical velocities based on the cross-sectional areas of ferrous pipe made only a slight improvement in the consistency of the relationship between pipe size and critical velocity.

After tests for determining pressure losses had been completed, the copper lines were reinstalled, with copper branches to the condenser taken from the copper main with sweat tees looking up at 45 degrees. Tests were made on these all-copper systems at a single steam pressure of 6 psig, over a range of flow rates only broad enough to establish the critical velocities. The results of these tests, plotted in Fig. 7, indicate that the critical velocity above which condensation is carried out of the branch with the steam, increases in a rather regular pattern with increasing tube diameter.

In Fig. 8 the points of critical velocity for the various tube sizes are indicated on a flow chart for steam at 3.5 psig. The locations of the points on this chart suggest that for a given steam pressure, the critical velocity occurs at an approximately constant pressure loss, regardless of tube size. The 1/16 psi pressure loss line is also prominently shown on Fig. 8. This is the pressure loss recommended in the

Fig. 9 View of glass pipe and tee in test line

ASHAE GUIDE for the design of small steam heating systems. Velocities at this pressure loss are considerably below the critical velocities.

Note that the results of tests in the all-copper system and the original copper-and-steel system were identical for the 1-in. size. This was undoubtedly due to the close agreement previously noted in the internal areas of 1-in. pipe and tubing. Fig. 6 includes test points from both series of tests.

Condensation flow into branches— It was thought that the velocity in the branch might have some effect on the pick-up of condensation by steam entering the branch. To check this, tests were made with 1¼-in. and ¾-in. branches taken from the 1¼-in. main, and with 1½-in., 1-in. and ¾-in. branches taken from the 1½-in. main. It was found that the critical velocity was independent of the branch size, or the velocity in the branch.

In most of the tests, the distance from the center line of the branch to the drip was 6 to 8 in. To make sure that the results obtained were not peculiar to this specific geometry, tests were made on the 1¼-in. main with both 1¼-in. and ¾-in. branches, with this dimension varying from 6 to 26 in. No change in the critical velocity was apparent.

Although the variation in weight of condensate collected from the drip indicated rather definitely that a change in direction of condensate flow took place at the critical velocity, the phenomenon by which this change was effected was a matter of conjecture. To investigate this, an 18-in.-long section of glass pipe was inserted in the 1-in. copper line just ahead of the branch to the condenser. However, this afforded no information on the subject. The stream of condensation could be observed flowing along the bottom of the pipe toward the branch and drip, at steam velocities well in excess of the critical velocity, but little or none of the liquid reached the drip.

A 1-in. glass tee was then installed in the line with the side outlet looking up at 45 degrees, and the connection to the condenser was taken from this outlet. The 18 in. long section of glass pipe was installed on the upstream side of the tee. A photograph of this glass piping and the near-by equipment and connections is shown in Fig. 9. With this installation, the flow of condensate could be clearly observed, but all at-

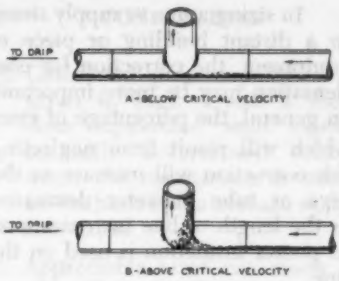

Fig. 10 Sketch of condensate flow observed in glass tee looking up at 45 deg

tempts to obtain clear photographs of the flow pattern were unsuccessful. The two sketches shown in Fig. 10 were, therefore, prepared.

As indicated in sketch A of Fig. 10, at steam velocities below the critical value, there was a tendency for the condensate level, just upstream from the center line of the branch to rise somewhat. However, the liquid continued to flow from this elevated area to the drip with no visible pick-up by the steam. As the critical velocity was approached this elevated area became more pronounced and more agitated, and occasional drops or small slugs were picked up by the steam and carried into the branch. A further increase in steam velocity caused a continuous film of water to flow up the sloping bottom of the branch following the path or pattern shown in Fig. 10B. With the establishment of this flow pattern, little or no condensate moved to the drip. Still further increases in steam velocity only tended to increase the abruptness of the turn made by the condensate as it flowed into the branch.

It should be emphasized that all results pertaining to condensate carry-over previously described in this paper were obtained with the branch to the condenser taken from the main with a tee looking up at 45 degrees. Observation of the condensate flow with this piping arrangement suggested that the critical velocity might be dependent upon the angular position of the branch tee. To check this, a few tests were made with two other types of branch connections.

With the 1 in. glass tee installed with the branch vertical, it was found that carry-over of condensate started at a steam velocity of approximately 40 fps, which was only 3 fps higher than the critical velocity determined with the branch tee looking up at 45 degrees. However, instead of a sudden sharp break in the flow pattern, it was found that the amount of carry-over increased with increasing velocity. Complete entrainment was reached at a velocity of approximately 80 fps. The condensate flow pattern, as observed in the glass tee, was very similar to that sketched in Fig. 10 for the 45-degree branch, except that the liquid was moving up both sides of the tee instead of flowing only along the bottom side.

The glass tee was then installed bullheaded at the end of the main, with the run of the tee in a vertical plane. The branch to the condenser was taken from the top of the tee and the drip from the bottom. With this arrange-

ment, carry-over started at a velocity of approximately 70 fps, and increased slowly with increasing velocity. Complete entrainment was reached at a velocity of approximately 175 fps.

Discussion of results – As pointed out earlier in the paper, the relationships shown in Figs. 1 and 2 are in good agreement with test results when comparison is made on the basis of the average steam flow rate. This average flow is the sum of the dry steam delivered at the end of the line, plus one half of the condensation occurring in the line. Usually the designer knows the weight of dry steam desired at various points along the line. The condensation rate can be estimated from data in the GUIDE.

In the design of the average steam heating system, the correction for condensation in the lines can usually be neglected because of a sizable safety factor which results from the common practice of considering published pipe capacities as maximum capacities for a given pressure drop. The load is usually distributed rather uniformly along the length of the main, and a main of a given size will supply several runouts. Only the section of a given size of main nearest the boiler is likely to be supplying a connected load approximately equal to its listed rating. Successive sections will be supplying progressively smaller loads, and the actual average pressure loss will be considerably less than the average drop for which the system is being sized.

In sizing a line to supply steam to a distant building or piece of equipment, the correction for condensation may be more important. In general, the percentage of error which will result from neglecting this correction will increase as the pipe or tube diameter decreases, as the length of line increases, and as poorer insulation is used on the line.

It is evident from Fig. 8 that the velocities in a small low-pressure steam system sized according to GUIDE recommendations of 1/16 psi drop per 100 ft, should be well below the critical velocities. However, many of the recently-installed small steam systems in which copper tubing has been used, have been designed for higher than normal pressure losses. There is little doubt that the critical velocities have been exceeded in these systems. Critical velocities are also exceeded in high-pressure steam systems where much higher pressure drops and steam velocities are commonly used.

Information regarding the critical velocity above which condensate is picked up by the steam, may have many applications, some of which may be economic. For example, where steam is purchased, and is measured by a condensation meter, the purchaser should be sure that the velocity in the branch supplying the steam is below the critical value at maximum load. Otherwise, part of his steam costs may be for steam which condensed in underground lines and not in his building.

CONCLUSIONS

1. Calculated pipe capacities as given in Figs. 1 and 2 show close agreement with experimentally determined values when the comparison is made on the basis of the average steam flow rates.

2. Appreciable error can result if steam flow charts such as Figs. 1 and 2 are used without making proper correction for the condensation occurring in the pipe. This error increases with decreasing pipe size, increasing length of run, and decreasing effectiveness of insulation.

3. For each size of pipe or tubing there is a critical steam velocity, above which condensation is picked up and carried through the branch with the steam instead of flowing along the bottom of the line to the drip.

4. The critical steam velocity described in the preceding conclusion increases with increasing tube size. For tube sizes from ⅜ to 1½-in., it occurs at a pressure loss of approximately 0.25 psi per 100 ft of length.

ACKNOWLEDGMENTS

The authors of this paper appreciate greatly the encouragement and advice given to them by the Research Advisory Committee on Hot Water and Steam Heating. Other members of the Laboratory staff were also most cooperative. In particular, William F. Kerka, who had previously developed flow data for steel pipes, was very helpful in his suggestions. In carrying out the experimental phases of this project, the excellent help given by William M. Cronin, Robert Balant, and Gary L. Smith, is worthy of note.

REFERENCES

1. Reynolds, O., *Trans. Royal Soc.* (London) V. 174, p. 935-82, 1883; summarized later *Proc Royal Soc.* (London) V. 56, p. 40 ff, 1894
2. Buckingham, E., Illustrations of the Use of Dimensional Equations, *Phys. Rev.*, V. 4, p. 345, 1914
3. Nikuradze, Jr., Stromungsgesetze in rauhen Rohren, VDI Forschungsheft 361, July-Aug. 1933
4. Pigott, R. J. S., The Flow of Fluids in Closed Conduits, *Mech. Engr.* V. 55, Aug. 1933
5. Moody, L. F., Friction Factors for Pipe Flows, *Trans. ASME*, V. 66, p. 671-94, Nov. 1944
6. d'Arcy, H., Recherches Experimental Relative an Movement de l'Eau dans les Tuyaux, 1857
7. Babcock, G. H., *Trans. ASME*, V. 7, p. 859, 1885
8. Gebhardt, G. F, Steam Power Plant Engineering, 1st Ed. p. 568, John Wiley & Sons, New York, 1909
9. Kerka, W. F., Re-evaluation of Steam-Pipe Size Tables for the ASHRAE GUIDE, *ASHRAE Trans.* 1960
10. Page, R. H. and Konzo, S., Analysis of Data on Flow of Steam in Pipes, *Heating and Ventilating Ref. Sect.*, V. 48, p. 86-104, Aug. 1951
11. Keenan, J. H., Friction Coefficients for the Compressible Flow of Steam, *ASME J. Appl. Mech.*, p. All-A20, Mar. 1939
12. Houghten, F. C. and Ebin, L., Capacities of Steam Heating Mains as Affected by Critical Velocities of Steam and Condensate Mixtures, *Trans. ASHVE*, V. 28, p. 295-300, 1922
13. Houghten, F. C. and Ebin, L., Capacities of Steam Heating Risers as Affected by Critical Velocity of Steam and Condensate Mixtures, *Trans. ASHVE*, V. 29, p. 109-128, 1923
14. Houghten, F. C. and Ebin, L., and Lincoln, R. L., Critical Velocity of Steam and Condensate Mixtures in Horizontal, Vertical and Inclined Pipes, *Trans. ASHVE*, V. 30, p. 139-156, 1924
15. Houghten, F. C. and O'Connell, M. E., Capacity of Up-Feed Steam Heating Risers for One- and Two-Pipe Systems, *Trans. ASHVE*, V. 33, p. 289-317, 1927
16. Houghten, F. C., O'Connell, M. E. and Gutberlet, C, Capacity of Radiator Supply Branches for One- and Two-Pipe Systems, *Trans. ASHVE*, V. 35, p. 389-418, 1929

DISCUSSION

H. L. GALSON, Syracuse, New York: The paper presented was very interesting and at this time I would like to ask whether the pipes were horizontal or whether they were sloped to provide for dripping.

CLOSURE BY AUTHOR JENNINGS: The pipes in this test were all essentially horizontal as the investigation of pipes at varying pitches is planned as part of a continuing program.

P. R. ACHENBACH, Washington, D. C.: Was additional water fed into the piping system when the critical velocity conditions were being explored or was the water in the system merely the normal condensate? Moreover, is it true that there was no through flow of steam?

Does the experiment indicate how the condensate is formed in the line, that is, are droplets of condensate formed and immediately collect on the surface of the pipe or do small droplets carry in the steam in the form of a fog?

AUTHOR JENNINGS: The only through flow of steam was that which went upward to the tee, and above critical velocity, essentially all of the condensate carried with the steam. The horizontal continuation of the pipe past the tee represented a static line as far as steam flow was concerned. To obtain heavy condensate loadings water at saturation temperature was fed into the test line near inlet. I cannot give a definite answer to what happened in the copper tubing itself but in the glass parts of the system which were toward the end of the line there was no active appearance of fog and the condensate was largely associated with and traveled on the inner surfaces of the tubing. Mr. Clark Humphreys, a co-author of the paper, will comment on this point.

AUTHOR HUMPHREYS: I don't think there is anything I can add to what Mr. Jennings has already stated. I do feel that in most cases the velocities we were using were high enough that as condensate formed it immediately started to move with the steam. I don't think that droplets or condensate remained static on the copper. There was no visible evidence of droplets or fog in the steam. In general, the condensate drained to the bottom of the tube and flowed there except at the tee itself.

L. S. O'BANNON, College Station, Texas: Experiments were made about 35 or 40 years ago (and published in the Journal) concerning the flow of steam and condensate in one-pipe steam systems. One of the tests which I supervised was on the simultaneous flow of air and water in horizontal pipe. The essential thing when both water and gas, such as steam or air, are flowing in a horizontal pipe is that the level of the water in the pipe increases as the pressure drops in the direction of the flow. The gas or steam above the water sets up wave motion in the water similar to the action of wind blowing over the ocean. The amplitude of waves increases as the velocity increases until the wave touches the top of the pipe. Then there is a solid flow of water which acts like the piston of an engine, and the slug of water moves through the pipe pushing water ahead of it. A section of pipe thus cleared of water, begins to fill up again and the phenomenon is repeated.

In vertical pipes where water and steam flow in opposite directions, such as water coming down and steam going up, the water will spiral around the circumference of the pipe, gradually increasing in volume until the inner edges of the spiral reach each other to form a solid block of water which in turn is forced to move in the direction of the pressure drop, that is, to rise until normal conditions are reestablished.

Obviously, for continuous steady flow, velocities must be either above or below a critical value depending upon whether the purpose is to convey both phases as a single fluid or whether it is desired that the gas and liquid flow separately in separate pipes.

AUTHOR JENNINGS: Thank you Professor O'Bannon for your comments, which are very pertinent. We did not see this happen in our particular system but I am familiar with what you have described. We are planning to carry on your investigations in this field and will undoubtedly encounter some of the phenomena you have described. I think it is unfortunate that some of your fine work was done so long ago that it has been lost sight of, however, I want you to know that we did examine your work and feel that it should be carefully re-explored in connection with any future studies in this field.

1708

No. 1708

Re-evaluation of the Steam-Pipe Size Tables for the ASHRAE GUIDE

WILLIAM F. KERKA
Member ASHRAE

In conjunction with the activities of the Research Advisory Committee on Hot Water and Steam Heating, the ASHRAE Laboratory began a survey late in 1956 directed toward determining the origin and validity of all of the information on steam and condensate flow that appeared in the ASHRAE GUIDE at that time. Simultaneous with this, a survey of manufacturers of steam-heating equipment was made in order to evaluate their comments on the steam-flow capacity tables.

The steam-flow data, in all GUIDES prior to 1959, were based on the commonly used Unwin-Babcock equation with its commonly accepted friction factor. This equation had been suspected for years of being unrealistically conservative in the smaller pipe sizes. The results of the industry survey also bore out this observation of conservatism that had resulted from the use of the Unwin-Babcock relationship in designing installations.

To bring the GUIDE material up to date, and more in line with the present theory of fluid flow, a program was initiated to revise all of steam-flow data in accordance with the Reynolds Number, friction-factor concept. The results of this effort were presented in Chapter 26 of the 1959 GUIDE.

Historical background—In 1857 the studies by Darcy,[1] and in 1870 the work of Weisbach (on water flow) resulted in an equation which related the pressure loss in piping to the fluid velocity, and the length and internal diameter of the pipe. The well-known Darcy-Weisbach equation is as follows:

$$h = \frac{fLV^2}{2gd} \qquad (1)$$

where

h = the head loss in feet of fluid
f = a friction factor

William F. Kerka is Research Engineer, ASHRAE Research Laboratory. The paper was presented by title only at the ASHRAE Semiannual Meeting, Dallas, Texas, February 1-4, 1960.

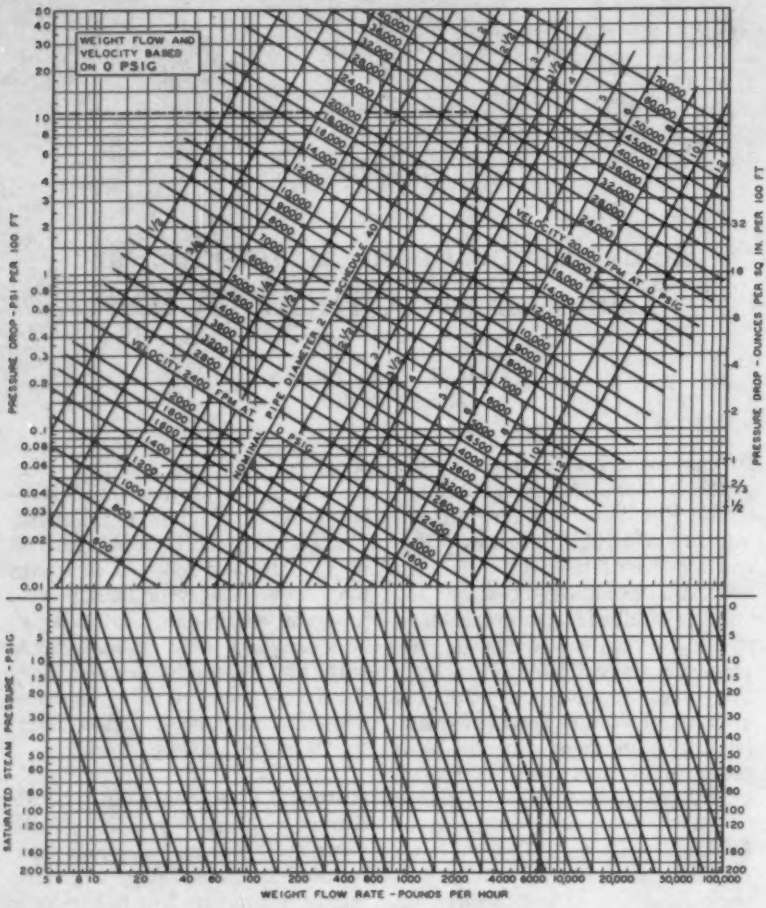
WEIGHT FLOW AND VELOCITY BASED ON 0 PSIG
PRESSURE DROP - PSI PER 100 FT
PRESSURE DROP - OUNCES PER SQ IN. PER 100 FT
SATURATED STEAM PRESSURE - PSIG
WEIGHT FLOW RATE - POUNDS PER HOUR
NOMINAL PIPE DIAMETER 2 IN SCHEDULE 40
VELOCITY 24,000 FPM AT 0 PSIG

Basic chart for weight-flow rate and velocity of steam in Schedule 40 pipe, based on saturation pressure of 0 psig (Fig. 22)

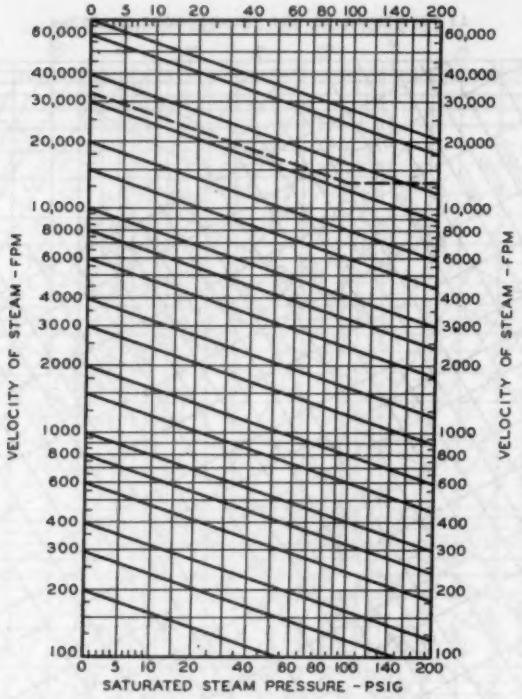

Velocity multiplier chart (Fig. 22 cont.)

L = length of pipe
V = velocity of fluid, feet per second
g = acceleration due to gravity
d = internal pipe diameter, feet

The relationship developed by Unwin in 1876 for the friction factor in the Darcy-Weisbach equation was based on the internal pipe diameter only, and was the result of experimentation conducted over a limited range of flow rates and pipe sizes. From his observations of the flow of water in piping, and also for the flow of air, Unwin concluded that the friction factor, f, was as follows:

$$f = K\left(1 + \frac{3.6}{d}\right) \qquad (2)$$

where

d = the internal pipe diameter in inches
K = a constant dependent upon the fluid

This friction-factor relationship was later adapted to steam flow by Babcock. In 1883 the pioneering work of Reynolds resulted in a bet-

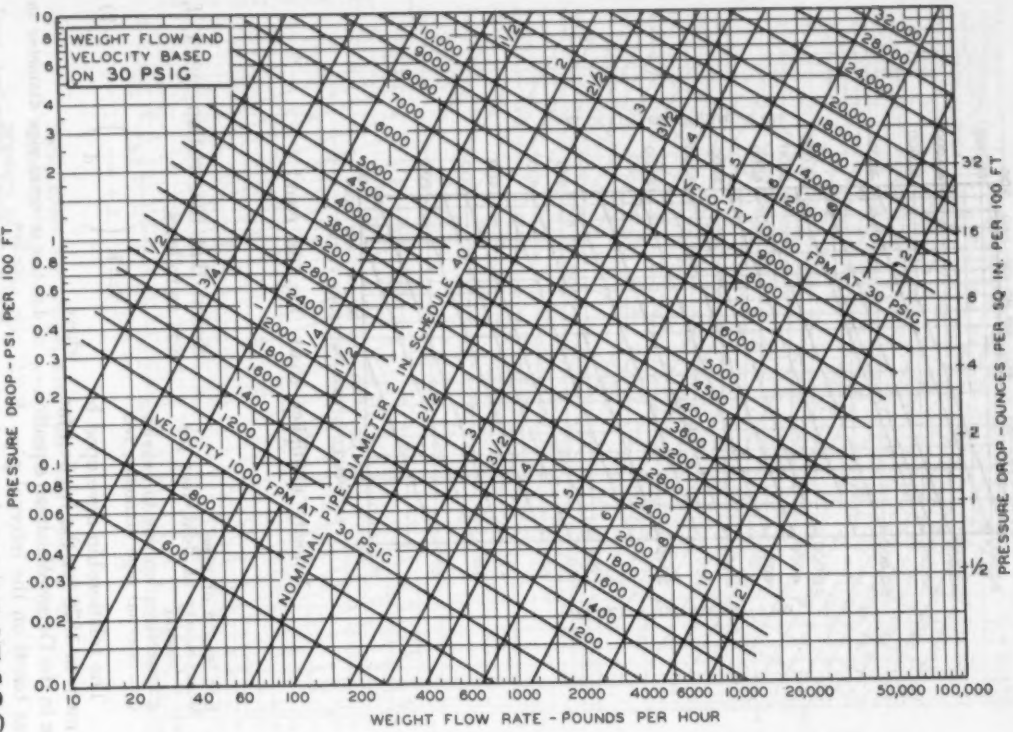
WEIGHT FLOW AND VELOCITY BASED ON 30 PSIG
PRESSURE DROP - PSI PER 100 FT
PRESSURE DROP - OUNCES PER SQ IN. PER 100 FT
WEIGHT FLOW RATE - POUNDS PER HOUR
NOMINAL PIPE DIAMETER 2 IN SCHEDULE 40
VELOCITY 1000 FPM AT 30 PSIG
VELOCITY 10,000 FPM AT 30 PSIG

Chart for weight - flow rate and velocity of steam in Schedule 40 pipe based on saturation pressure of 30 psig (Fig. 23)

WEIGHT FLOW AND VELOCITY BASED ON 50 PSIG
NOMINAL PIPE DIAMETER 2 IN SCHEDULE 40
50 PSIG
VELOCITY 1000 FPM AT
VELOCITY 7000 FPM AT 50 PSIG
PRESSURE DROP - PSI PER 100 FT
PRESSURE DROP - OUNCES PER SQ IN. PER 100 FT
WEIGHT FLOW RATE - POUNDS PER HOUR

Chart for weight - flow rate and velocity of steam in Schedule 40 pipe based on saturation pressure of 50 psig (Fig. 24)

ter understanding of the role of the viscous and inertia forces acting on a fluid. From his studies evolved the dimensionless parameter now known as the Reynolds Number:

$$N_{Re} = \frac{dV\rho}{\mu} \quad (3)$$

where

ρ = density of fluid
μ = absolute viscosity, pounds per foot-second

Blasius in 1912 showed that the friction factor from the Darcy-Weisbach equation was a function of the Reynolds Number, and thus proved that the flow of fluids in piping was a function of more than just the diameter.[1]

In 1944, L. F. Moody[2] published friction factors for pipe flow. It was presented in the form of a chart, with friction factor plotted versus N_{Re} for a range of relative roughness factors for the internal pipe surface. His work was based on the theories and experimental results of many investigators, mainly Stanton and Pigott.

Procedure used in revising GUIDE steam flow tables—In re-evaluating the steam-flow tables for the ASHRAE GUIDE, the friction-factor data as presented by Moody were thus used as the basis for all the calculations. Recent studies[3] at the ASHRAE Research Laboratories have borne out the validity of the Reynolds Number, friction-factor concept as applied to steam flow, where the flow of condensate does not inhibit the flow of steam.

Figs. 22 through 26 and Table 5 in Chapter 26 of the 1959 GUIDE were all derived from one master chart. The master chart was a plot (on log-log coordinates) of the absolute pressure of saturated steam as the ordinate versus the weight-flow rate of steam in pounds per hour for pipe sizes ranging from ¾ to 10 in. and for pressure drops of ⅛, ½, 2, 5 and 10 psi per 100 ft of pipe. The master chart was plotted from steam-flow calculations made at 1, 30 and 150 psig saturation pressure.

The reason for the master chart was that in the early stages of the program, the final working pressures that were to be reported in the GUIDE chapter were not definitely established, hence it was a simple matter to choose the flow rates at any desired saturation pressure from the chart (by interpolation) for use in the makeup of a chart for the particular pressure once it was selected.

As it turned out, however, the 30 and 150 psig pressures were among those chosen. In the master chart, the lines representing a particular pipe size and pressure drop plotted as straight lines with a slope of 2 to 1, although for pipe sizes above 6 in., a slight curvature in the lines was noted.

The steps used in calculating the steam flow rates are briefly outlined as follows:

For a given initial saturation pressure and pipe size, a weight-flow rate was arbitrarily chosen and the pressure drop corresponding to these given conditions was then calculated using the friction-factor data.

The steam velocity was derived from the weight-flow rate and the pipe size as follows:

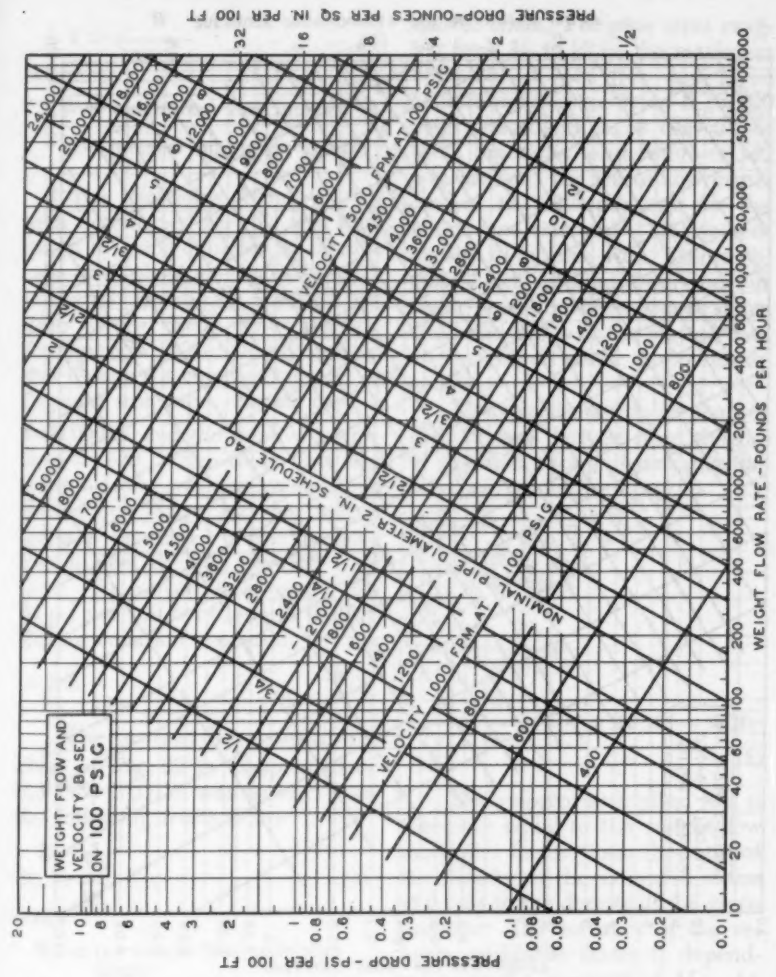
WEIGHT FLOW AND VELOCITY BASED ON 100 PSIG
NOMINAL PIPE DIAMETER 2 IN. SCHEDULE 40
VELOCITY 3000 FPM AT 100 PSIG
VELOCITY 1000 FPM AT 100 PSIG
PRESSURE DROP - PSI PER 100 FT
PRESSURE DROP - OUNCES PER SQ IN. PER 100 FT
WEIGHT FLOW RATE - POUNDS PER HOUR

Chart for weight - flow rate and velocity of steam in Schedule 40 pipe based on saturation pressure of 100 psig (Fig. 25)

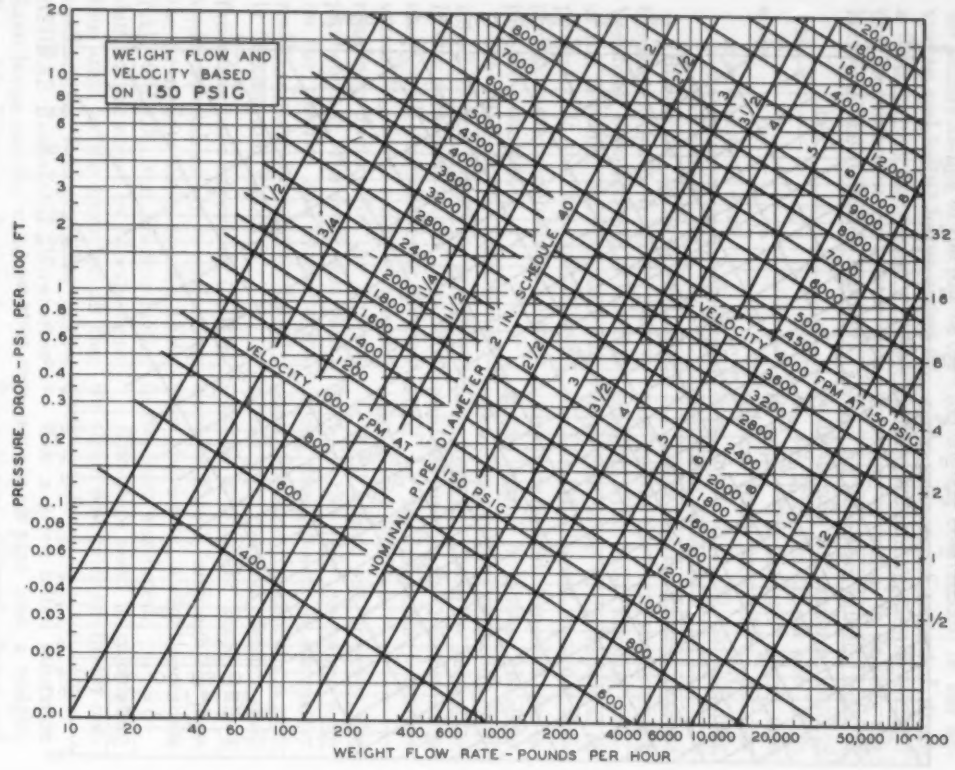
WEIGHT FLOW AND VELOCITY BASED ON 150 PSIG
PRESSURE DROP - PSI PER 100 FT
PRESSURE DROP - OUNCES PER SQ IN. PER 100 FT
WEIGHT FLOW RATE - POUNDS PER HOUR
NOMINAL PIPE DIAMETER 2 IN SCHEDULE 40
VELOCITY 1000 FPM AT 150 PSIG
VELOCITY 4000 FPM AT 150 PSIG

Chart for weight - flow rate and velocity of steam in Schedule 40 pipe based on saturation pressure of 150 psig (Fig. 26)

$$V = \frac{W}{3600\,\rho\,A} \qquad (4)$$

where

W = weight-flow rate, pounds per hour
A = internal pipe area, square feet

The Reynolds Number was then determined for this flow condition by using equation 3. In each case the absolute viscosities for saturated steam as reported by Lieb[4] were used. The absolute roughness, e, in the Moody method was chosen for commercial steel or wrought iron pipe. In this case, e = 0.00015, and the relative roughness = e/d. From these data, the friction factor was determined from the Moody chart, and was substituted in equation 1 to find the head loss in feet of fluid per 100 ft of pipe. To convert to pressure loss in psi per 100 ft of length, the following equation was used:

$$\Delta P = \frac{\rho h}{144} \qquad (5)$$

The weight-flow multiplier chart of Fig. 22 in Chapter 26 of the 1959 GUIDE was derived from the following relationship:

$$M_w = \frac{W_p}{W_o} \qquad (6)$$

where

M_w = the weight-flow multiplier factor
W_p = the weight-flow rate at a given saturation pressure, p, for a given pipe size and pressure drop
W_o = the weight-flow rate at 0 saturation pressure for the same pipe size and pressure drop

The numerical values of M_w were readily obtained from the master chart. For pipe sizes ranging from ¾ to 10 in. the maximum deviation of M_w (for any given saturation pressure from 0 to 200 psig) was found to be only 3 per cent. Since the mean value of M_w was chosen, the maximum errors amount to +1.5 per cent for the ¾-in. pipe size and −1.5 per cent for the 10-in. pipe size. This negligible error resulted from the but slight deviation from the straight-line relationship of the plotted data in the master chart, as previously noted.

The velocity-multiplier chart of Fig. 22 was derived from the use of equation 4 for a given saturation pressure, p, and for 0 psig.

thus

$$V_p = \frac{W_p}{3600\,\rho_p\,A}$$

and

$$V_o = \frac{W_o}{3600\,\rho_o\,A}$$

$$\frac{V_p}{V_o} = \frac{W_p}{W_o} \times \frac{\rho_o}{\rho_p} = M_w \times \frac{\rho_o}{\rho_p} = M_v \qquad (7)$$

The velocity multiplier, M_v, is therefore equal to the weight-flow multiplier factor times the ratio of the density of the saturated steam at 0 psig to the density at the given pressure. The accuracy of the velocity multiplier factor is dependent upon the accuracy of M_w. As noted, the maximum error amounts to ±1.5 per cent.

The steam-flow charts as present in the 1959 GUIDE now give the user a convenient means of determining steam pipe sizes over a wide range of working pressures.

The saturation pressures of 30, 50, 100 and 150 psig for Figs. 23, 24, 25 and 26 respectively, were chosen since they represent working steam pressures that are commonly used in the design of steam-heating systems. The weight-flow rates in Table 5 were presented in tabular form for those persons who find it more convenient to use the data in this manner in the design of low-pressure systems.

There is still a need for the study of condensate flow in return piping. The present tables in the GUIDE for the capacities of return piping are based on past work using the Unwin-Babcock relationship for friction factor. As new information, based on the more advanced theories of fluid flow, becomes available, it should be used to re-evaluate the condensate flow tables in future GUIDES.

BIBLIOGRAPHY

1. Page, R. H. and Konzo, S., "Analysis of Data on Flow of Steam in Pipes", Heating and Ventilating, Vol. 48, August 1951, p. 86.
2. Moody, L. F., "Friction Factors for Pipe Flows", Trans. ASME Vol. 66, p. 671-684, Nov. 1944.
3. Humphreys, C. M.; Baker, J. T.; and Jennings, B. H., "Saturated Steam Flow in Copper Tubing", a paper presented at this same meeting.
4. Lieb, ASME Trans. Vol. 62, p. 677, 1940; Combustion, Vol. 12, p. 45 Dec. 1940.

Example of Use of Basic and Velocity Multiplier Charts

Given:
a. Weight-Flow Rate = 6700 lb per hr.
b. Initial Steam Pressure = 100 psig.
c. Pressure Drop = 11 psi per 100 ft.

Find:
a. Size of Schedule 40 pipe required.
b. Velocity of steam in pipe.

Solution: The following steps are illustrated by the broken line on Fig. 22:

Step 1. Enter Fig. 22 at a weight-flow rate of 6700 lb per hr and move vertically to the horizontal line at 100 psig.

Step 2. Follow along inclined multiplier line (upward and to the left) to horizontal 0 psig line. The equivalent weight flow at 0 psig is about 2500 lb per hr.

Step 3. Follow the 2500 lb per hr line vertically until it intersects the horizontal line at 11 psi per 100 ft pressure drop. The nominal pipe size is 2½ in. The equivalent steam velocity at 0 psig is about 32,700 fpm.

Step 4. To find the steam velocity at 100 psig, locate the value of 32,700 fpm on the ordinate of the velocity multiplier chart at 0 psig.

Step 5. Move along the inclined multiplier line (downward and to the right) until it intersects the vertical 100 psig pressure line. The velocity as read from the right (or left) scale is about 13,000 fpm.

Note: The preceding Steps 1 to 5 would be rearranged or reversed if different data were given.

TABLE 5—WEIGHT FLOW RATE OF STEAM IN SCHEDULE 40 PIPE[a] AT INITIAL SATURATION PRESSURES OF 3.5 AND 12 PSIG.[b, c]

(Weight Flow Rate Expressed in Pounds per Hour)

	Pressure Drop—Psi Per 100 Ft in Length													
	1/16 Psi (1 oz.)		1/8 Psi (2 oz)		1/4 Psi (4 oz)		1/2 Psi (8 oz)		3/4 Psi (12 oz)		1 Psi		2 Psi	
Nom. Pipe Size Inches	Sat. press. psig		Sat. press. psig		Sat. press. psig		Sat. press. psig		Sat. press. psig		Sat. press. psig		Sat. press. psig	
	3.5	12	3.5	12	3.5	12	3.5	12	3.5	12	3.5	12	3.5	12
3/4	9	11	14	16	20	24	29	35	36	43	42	50	60	73
1	17	21	26	31	37	46	54	66	68	82	81	95	114	137
1 1/4	36	45	53	66	78	96	111	138	140	170	162	200	232	280
1 1/2	56	70	84	100	120	147	174	210	218	260	246	304	360	430
2	108	134	162	194	234	285	336	410	420	510	480	590	710	850
2 1/2	174	215	258	310	378	460	540	660	680	820	780	950	1150	1370
3	318	380	465	550	660	810	960	1160	1190	1430	1380	1670	1950	2400
3 1/2	462	550	670	800	990	1218	1410	1700	1740	2100	2000	2420	2950	3450
4	726	800	950	1160	1410	1690	1980	2400	2450	3000	2880	3460	4200	4900
5	1200	1430	1680	2100	2440	3000	3570	4250	4380	5250	5100	6100	7500	8600
6	1920	2300	2820	3350	3960	4850	5700	7000	7200	8600	8400	10,000	11,900	14,200
8	3900	4800	5570	7000	8100	10,000	11,400	14,300	14,500	17,700	16,500	20,500	24,000	29,500
10	7200	8800	10,200	12,600	15,000	18,200	21,000	26,000	26,200	32,000	30,000	37,000	42,700	52,000
12	11,400	13,700	16,500	19,500	23,400	28,400	33,000	40,000	41,000	49,500	48,000	57,500	67,800	81,000

[a] Based on Moody Friction Factor, where flow of condensate does not inhibit the flow of steam.
[b] The weight-flow rates at 3.5 psig can be used to cover sat. press. from 1 to 6 psig, and the rates at 12 psig can be used to cover sat. press. from 8 to 16 psig with an error not exceeding 8 percent.
[c] The steam velocities corresponding to the weight-flow rates given in this table can be found from the basic chart and velocity multiplier chart, Fig. 22.

1709

No. 1709

Effect of Compressor Characteristics on Motor Performance

ERIK H. JENSEN

The driving motor in a hermetic compressor is affected in many ways by the compressor design. Most of these are well known, but the effect of load impulses is only surmised. The primary purpose of the experiments here reported is to show a correlation between load type and motor performance.

Motor manufacturers and compressor manufacturers often find that their data on the same motor do not agree and attribute the difference to test errors. There is, however, a basic difference in the two methods of testing. The motor manufacturer tests the motor on a brake arrangement, which gives a continuous, steady load. The compressor manufacturer tests the motor in a compressor where the load varies from maximum to a much smaller value at least once per revolution.

The most obvious effect of the difference in the test methods is the difference in motor current measured. We have, therefore, based our experiments on measurements of instantaneous and rms motor currents. In order to measure the instantaneous current, a small resistor was placed in series with one of the power leads to the compressor. The voltage drop across the resistor was fed into an oscilloscope as shown in Fig. 1. With this arrangement we obtained pictures of the voltage drop across the resistor and since the resistance is constant, the pictures represent the current.

Fig. 2 illustrates the current for a 2-cyl, 90° V compressor with a single throw crankshaft arrangement, running at 1660 rpm. This

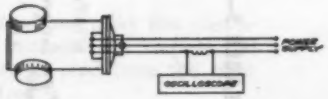

Fig. 1 Oscilloscope

E. H. Jensen is an Eng. Sect. Mgr. in the Air Conditioning Div. Westinghouse Electric Corporation. This paper was presented at the ASHRAE Semiannual Meeting in Dallas, February 1-4, 1960.

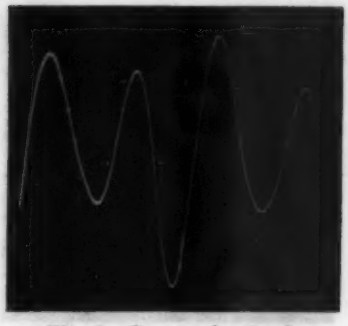

Fig. 2 Current for 2-cyl, 90° V compressor with single throw crankshaft. 1660 rpm

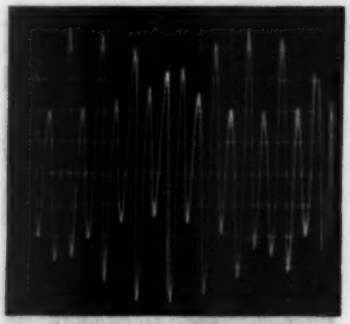

Fig. 3 Sweep time increased

differs materially from the simple curve which is obtained from a steady load. Note the change from low to high peaks and a variation from one low peak to the next low peak. In order to portray this better, the sweep time of the oscilloscope was increased, thereby bringing more current cycles within the picture, as shown in Fig. 3.

The pattern became more apparent when the sweep time was further increased, as in Fig. 4. Change in the peak value occurs because the compressor is running at less than synchronous speed. The basic wave represents the 60-cycle current. Superimposed on this is a wave which represents the compressor load variation. When the piston moves up and compresses the gas, it transfers energy from the motor and moving parts to the gas. On the downstroke no energy (or but little) is used. If the maximum piston load coincides with a peak of the ac, there will be a maximum current value. Since the current is 60 cps and the compressor speed a little less than 30 cps, the next peak will occur on the downstroke and it will therefore coincide with minimum torque and be a minimum peak. At the following peak, the piston load is a little behind because of the motor slip and the peak will be less than maximum. This goes on until a new maximum has been reached.

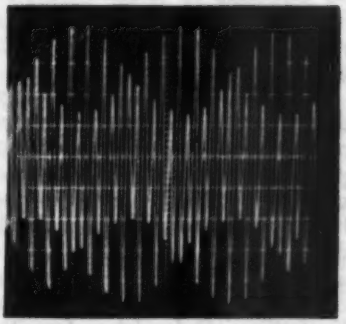

Fig. 4 Change in peak value

Notice that there is no evi-

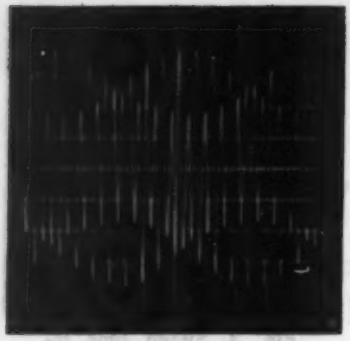

Fig. 5 Light load (110 F cond. temp., 20 F evap. temp.)

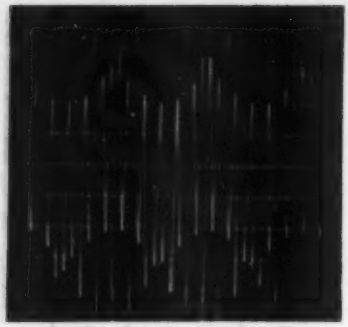

Fig. 6 Heavy load (130 F cond. temp., 50 F evap. temp.)

dence of two cylinder impulses. The reason is that the load from one cylinder overlaps that of the other cylinder in the 90° arrangement under most system conditions, so it may be considered as a single load impulse for the purpose of this investigation.

This cyclical curve traced by the current peaks can, incidentally, be used to determine the compressor speed. Since the distance between peaks represents ½ revolution of slip, one can count the peaks between maxima – in this case 12. Twelve peaks of 60-cycle current represent 1/5 and the slip is therefore ½ ÷ 1/5 = 2½ rps or 150 rpm. Synchronous speed is 1800 rpm. The compressor speed is then 1800 – 150 = 1650 rpm.

A current pattern similar to Figs. 2, 3 and 4 will always be present when a motor is subjected to a non-uniform load and it follows that the motor cannot perform the same under such condition as under a steady load like a brake.

The next experiments were directed to determining the effect of the size of the load. Fig. 5 shows the current picture at a light load (110 F cond. temp., 20 F evap. temp.) and may be compared with Fig. 6 which represents a heavy load (130 F cond. temp., 50 F evap. temp.).

As the load was increased, the current varied to greater extremes; or, expressed in another way, an increase in load caused the motor speed to vary more and more during one revolution of the shaft.

The following outlines a rough theory for the process during one revolution of the shaft and compares it with test results. The theory may not be absolutely correct, but it serves to show a probable detail picture of the compressor and motor behavior during one revolution. Conclusions, with some limitations, can be drawn from the detail picture to show what should

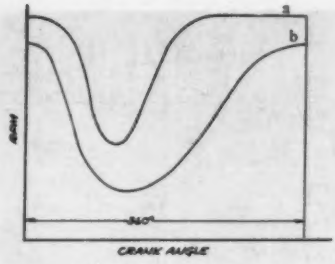

Fig. 7 Motor speed crank angle curves

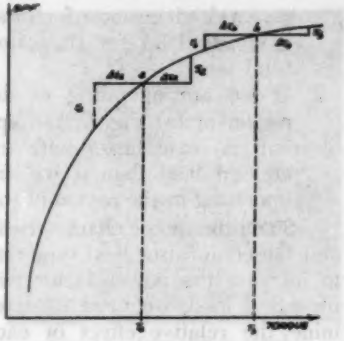

Fig. 8 Ordinary power factor curve as obtained on a brake

be expected in over-all or rms measurement. While the tests confirm the theory, it cannot be said that the theory has been proven.

A curve form is assumed for the shaft speed as a function of crank angle, as shown in Fig. 7: Going from left to right on curve (a), the load increases to a maximum, resulting in a minimum on the speed curve. As the load decreases again, the shaft picks up speed until it reaches the maximum value, where it stays until the load starts to build up again. A heavier load would shorten the time of maximum speed as indicated by curve (b).

Fig. 8 illustrates an ordinary type of power factor curve as obtained on a brake. In order to distinguish the pulsating load power factor and the brake load power factor, we will call the first compressor power factor cpf and the latter brake power factor bpf.

Point b is chosen on the bpf curve as representing the average torque of a pulsating load. If the load corresponds to curve (b) in Fig. 7, the torque variation will be approximately of the same size $\triangle t_b$ to either side of point b. The torque will also be lower than t_b for about the same length of time as it is higher than t_b. Had the bpf curve been a straight line, the resulting cpf would have been the same as the bpf. Since it is curved, however, the decrease r_b will be larger than the increase s_b and the resulting cpf will be lower than bpf.

Point a represents a different situation. It was chosen to correspond to the load represented by curve (a) Fig. 7. In this case the value of r_a is also larger than s_a, but the motor operates at the low torque for a longer period of time. The resulting cpf will therefore be reduced even more than at b. The amount of further reduction will depend on how large a portion of one shaft revolution is spent at minimum torque.

Using this theory, one should expect to find experimentally that:

1. A pulsating load will never

give as high a power factor as a steady load for the same total work.

2. If we are operating in the region of (a) Fig. 7, the cpf will increase faster with increased load than if we are operating in the region of (b).

Since the motor characteristics and the compressor load type tend to increase the power factor with increased load, we need to determine the relative effect of each. This may be done by dividing the cpf by the bpf. If they are identical, the value will be 1.00. If they are proportional, it will be a constant value. The value will always be less than 1.00 if statement 1 is correct. If statement 2 is true, then cpf/bpf should increase as the load increases, at least in region (a).

A sample calculation based on test values is shown in Table I.

Data from a series of tests were calculated in this manner and the resulting ratios of cpf/bpf were plotted as a function of motor watts. Watts were used to represent load since the power input is quite nearly a straight line function of the torque in the range covered by the tests.

The curves are shown in Fig. 9. Curve B Fig. 9 shows the results from tests of a 3½-ton compressor

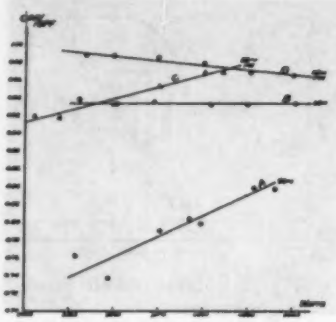

Fig. 9 Effect of compressor characteristics on motor performance

operating on 3-phase, 60-cycle, 220 volt. Curve A shows the results from the same compressor when it was operated at 3-phase, 50-cycle, 220 volt. The motor was not changed, but because of limiting test facilities the 50-cycle testing was done on 220 volts instead of the 190 volts which would have been proper for 50-cycle application. In most cases a motor will allow a higher loading at high voltage than at low voltage. The effect of applying a given motor to the same voltage on 50-cycle current is therefore the same as having a higher hp motor available for 50-cycle than for 60-cycle.

TABLE I

Compressor volt	222	Motor (brake) volt	222
Compressor amp	13.6	Motor (brake) amp	10.50
Compressor watt	3520	Motor (brake) watt	3520

$$cpf = \frac{3520}{222 \times 13.6 \times \sqrt{3}} = 0.680 \qquad bpf = \frac{3520}{222 \times 10.50 \times \sqrt{3}} = 0.870$$

$$cpf/bpf = \frac{0.680}{0.870} = 0.783$$

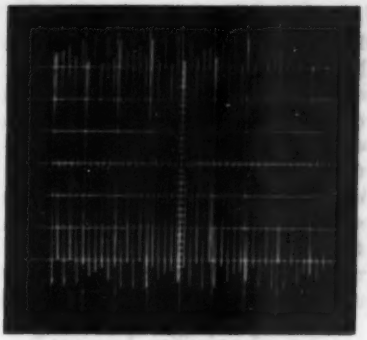

Fig. 10 Picture corresponding to the tests with the flywheel

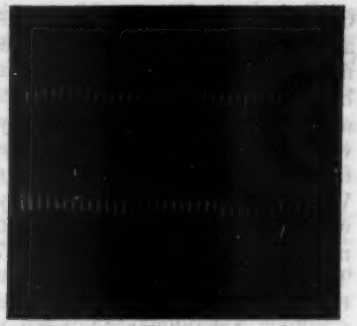

Fig. 11 Two throw crankshaft

With this in mind, it can be seen that curves A and B Fig. 9 indicate that statements 1 and 2 are true: Curve A (50-cycle) shows a definite increase of cpf/bpc with increased load. This would place curve A in the region of operation as (a) Fig. 7. Curve B Fig. 9 shows a nearly constant value of cpf/bpf with increased load. This would place Curve B in the region (b) Fig. 7. While we do not know that the Curves A and B are really the results of operations such as (a) and (b) Fig. 7, it can be seen that the 50-cycle operation, which has the motor with most excess torque available, also has a much greater slope than the 60-cycle operation. Noting that all values of curves A and B are below 1.00, both statements 1 and 2 are therefore supported.

For further confirmation a single test was run with 5 hp motor instead of the 3 hp motor previously used. The 5 hp motor was similar to the 3 hp motor in all respects and the test conditions were identical (60-cycle, 220 volt). The results are shown below:

Motor	3 hp	5 hp
cpf/bpf	0.933	0.710

In other words, by increasing the motor size in a different way, the cpf/bpf again decreased in accordance with the theory.

Three tests were run with the same compressor and the 3 hp motor at 60-cycle to establish the effect of voltage.

Volt	189	231	250
cpf/bpf	0.960	0.915	0.845

This also agrees with the previous findings, further supporting statement 2.

From the theory advanced it would seem that anything one can do to minimize the torque variation Δ_t Fig. 8 will improve the cpf and cpf/bpf. A series of tests were therefore made with the same compressor and 3 hp motor with a flywheel added to the crankshaft. This added about 30% to the moment of inertia of the moving parts. Curves C and D in Fig. 9 show the results.

Comparing Curve C with Curve A and Curve D with Curve B leaves little doubt that improvement has been made. Note also that the slope of cpf/bpf changes when the flywheel is added. We have not yet found the reason for this change. We suspect, however, that the flywheel makes the motor operate more in the region of (b) Fig. 7. This would also explain the negative slope of Curve D. Work is being done at the moment to separate the size effect in region (b) and region (a) Fig. 7 more clearly. Fig. 10 shows the picture corresponding to the tests with the flywheel:

It was previously mentioned that the two cylinders in a 90° V single crank arrangement act so that the motor receives the equivalent of a single load impulse. By making a 90° two throw crankshaft instead of the single throw shaft used in the previous tests, we constructed a compressor in which the crankshaft experienced two equally spaced impulses in each revolution. The compressor, motor and test conditions were otherwise the same. Table II shows a comparison of the two tests:

The current readings and oscilloscope pictures show the striking difference between uniform versus non-uniform loading of the shaft in its travel.

CONCLUSION

It is apparent that pulsating loads have a definite detrimental effect on motor performance, at least with respect to currents. The mechanical details of design and application of the compressor and motor can affect the motor performance substantially. In compressor design the most important points are:

1. The lowest current drawn for a given load will be obtained with pumping impulses equally spaced.
2. Larger moments of inertia will reduce the current. This may sometimes be accomplished by choosing the larger rotor diameter where more than one is available. It should also serve to caution against possible adverse effects of changes to lighter materials in the moving parts.
3. Since larger moments of inertia reduce the current, it follows that higher speeds will have the same effect.
4. Motors should be sized as closely as possible to the load and not oversized.
5. High voltages will cause more adverse effects on currents on a pulsating load than on a steady load.

This paper is based on tests which were mostly exploratory.

TABLE II

Arrangement	Single Throw Crankshaft	Two Throw Crankshaft
Impulse Spacing	90° & 270°	180°
cpf/bpf	0.898	0.995
Amp	14.3	12.9
Illustration	Fig. 4	Fig. 11

Most of the work has been focused on motor currents and it has been shown that the current drawn by a compressor can be varied 10-25% for the same compressor capacity by variations in compressor design only. Some test results, still preliminary and therefore not reported here, tentatively indicate that motor efficiency is affected in much the same manner and that similar but smaller changes can be made in power consumption.

More work should be done on this problem to show the effects more accurately, to determine how efficiency is affected and to find better criteria for motor arrangements. A relationship between the current variations shown on the illustrations and motor performance should also be established if possible. Such a relationship may provide a quick and direct answer to questions concerning the behavior of the motor-compressor combination.

DISCUSSION

DAVID V. JAHNS, Dayton, Ohio: Were the rotor temperatures controlled and/or measured during these particular tests?

CLOSURE BY AUTHOR JENSEN: They were not controlled or measured.

We used the same conditions for all the tests as far as we could but we did not measure rotor temperatures.

UNIDENTIFIED SPEAKER: Have you tested or given any thought to two pole motors running at twice the speed?

AUTHOR JENSEN: Yes, we have and we have tested some of them. The statement I made that higher speed will have an effect to improve the current characteristics was borne out by test.

1710

No. 1710

Muffler Analysis by Digital Computer

D. F. MILLER B. W. HATTEN

With the continuing emphasis on noise reduction, a designer of refrigeration compressors is faced with the problem of finding a satisfactory means of reducing the pulsating pressures and flows in intake and discharge lines. Mufflers are used for this purpose, but the results are not always completely satisfactory. Mufflers must be carefully analyzed and designed to avoid the coincidence of acoustic resonances with excitation frequencies, and to obtain satisfactory attenuation of the higher frequency components of the alternating flow. This paper presents an analytical method that accurately predicts muffler response up to fairly high frequencies. Computations are handled simply and rapidly by means of a high speed digital computer (in this case an IBM 704).

The condition of a non-reflecting termination of the muffler is often assumed. However, in practice, non-reflecting terminations seldom occur. Also, the head volumes and muffler tubes introduce effects which in many cases are not at all negligible. Therefore, in the approach to be described, the complete muffler system, including muffler inlet tubes and outlet tubes, head volumes, and shell volumes or condenser tubes are included. In this way, a more accurate representation of the effect of the muffler in the complete intake or discharge system is obtained.

Attention is given also to the middle or higher frequency ranges. It is shown that attenuations at higher frequencies are given correctly only if each tube element is considered as an element consisting of both distributed mass and compliance, not as a pure mass or compliance alone, as is assumed in the more familiar lumped element theory.

When large diameter tanks are used in the muffler, transverse wave effects due to three-dimensional wave motion occur in the higher frequency ranges. Trans-

D. F. Miller is associated with the Mechanics Dept., Westinghouse Research Laboratories, B. W. Hatten is with the Columbus Works, Westinghouse Electric Corporation. This paper was presented at the ASHRAE Semiannual Meeting, Dallas, Texas, February 1-4, 1960.

verse wave effects usually set the upper frequency limit of the calculations described in this paper. For refrigeration mufflers this is not usually a serious limitation.

ACOUSTIC EXCITATION

Gas flow from the discharge of a refrigeration compressor consists of a periodic train of pulses of both pressure and alternating flow. The wave shape of these pulses is dependent upon all the gas properties as well as the physical properties of the muffler system. However, no matter what the wave shape may be, it can be broken down into its Fourier series components. Thus, the alternating flow volume velocity, $U = Au$, at the excitation point of the system (usually taken as the valve port) can be written:

$$U_{IN} = U_o + U_1 \sin(\omega t + \phi_1) + U_2 \sin(2\omega t + \phi_2) + \ldots + U_n \sin(n\omega t + \phi_n) \quad (1)$$

where

U_{IN} = excitation volume velocity
U_o = steady flow component of volume velocity
$\phi_1 \ldots \phi_n$ = phase angles
ω = angular frequency of excitation

Similarly, the pressure-time wave can be written:

$$P_{IN} = P_o + P_1 \sin(\omega t + \phi_{1p}) + P_2 \sin(2\omega t + \phi_{2p}) + \ldots + P_n \sin(n\omega t + \phi_{np}) \quad (2)$$

The components $U_1, U_2, \ldots, U_n$ and $P_1, P_2, \ldots, P_n$ cause forced gas vibration at the frequencies ω, $2\omega, \ldots, n\omega$ throughout the entire intake or discharge system. Thus, no matter what the wave shape, only multiples of the fundamental excitation frequency occur in the system.

The system output at each excitation frequency, $n\omega$, is the product of the system response and the excitation at that frequency. The output wave shape is the sum of the outputs for each excitation frequency. In this paper we are primarily interested in the system response, not the output wave shape. The system response can be presented as a resonance curve showing at what frequencies resonances of the system would occur, whether excited or not. It is then possible to determine if the response is low at every excitation frequency. If it happens that some excitation frequency coincides with a peak in the system response curve, it is possible to determine what can be done to the system to shift the peak away from the excitation frequency. In practice the actual output wave shapes are not usually desired, and this is fortunate, as input wave shapes are difficult to determine in all but special cases.

RESPONSE CURVE METHOD

Response curves showing the magnitude (and phase angle if desired) of pressure or volume velocity versus frequency may be drawn for any point in an intake or discharge muffler system. The peaks in these curves are interpreted with respect to excitation frequencies. Response curves may be made dimensionless and plotted in decibels. In this paper the volume velocity curves are given as $20 \log_{10} (U/U_{IN})$, where U_{IN} is the input or excitation volume velocity. U is the volume velocity existing at the point in the

system under question. If this point happens to have a value of $U = U_{IN}$ at a certain frequency, the response curve is zero decibels at this point. Negative values of decibels in the response curve show that the volume velocity at the point in question is less than that at the input of the system. Muffler attenuation is given as the difference in decibels between muffler input and the muffler output. This may be obtained by subtraction of the input and output response curves. A negative attenuation is common at many frequencies as caused by resonances somewhere in the system.

The pressure response curves are made dimensionless by the use of the low frequency pressure, P_{LF}. If a system is closed, the static increase in pressure (corrected to adiabatic compression) caused by the piston moving from the midway position to top-dead-center is called P_{LF}. Since pressure response curves may be obtained experimentally by acoustic excitation of the system by a valveless compressor of constant displacement, P_{LF} may also be defined

$$P_{LF} = \frac{U_{IN}}{j\omega C_t} = \frac{j\omega A_p \xi}{j\omega C_t} = \frac{\xi A_p}{C_t} \tag{3}$$

Pressures obtained experimentally using a valveless pump, as indicated, are identical to the curves of P/P_{LF} obtained analytically, thus furnishing another reason for the definition of P_{LF}. The dimensionless pressure P/P_{LF}, defined only for a constant displacement pump and a closed system, approaches unity (zero decibels) at low frequencies. P/P_{LF} is also given in the following form

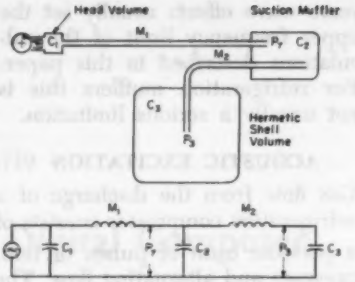

Fig. 1 Lumped element representation

$$\frac{P}{P_{LF}} = \frac{P}{U_{IN}} (j\omega C_t) \tag{4}$$

LUMPED ELEMENT CALCULATIONS

Each tube comprising the system is assumed to have only acoustic mass or acoustic compliance in a lumped analysis.

Acoustic mass is defined as

$$M_a = \frac{\rho l}{A} \tag{5}$$

Acoustic compliance is defined as

$$C_a = \frac{Al}{\gamma P_o} \tag{6}$$

It should be noted that acoustic mass differs from the actual mass of the gas in the tube, being A^2 smaller. A small area tube has high acoustic mass, but low actual gas mass. We refer to mass as always being acoustic mass. A large area

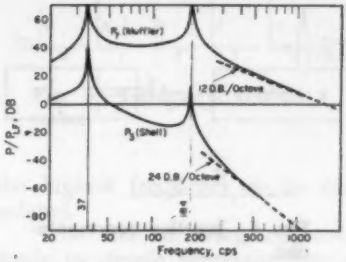

Fig. 2 Pressure response of lumped element representation of suction muffler

tube (tank) has acoustic compliance. Compliance is equal to A^2 divided by the mechanical spring constant of the gas in the tube.

In Fig. 1 is shown an intake muffler system and its lumped representation. The electrical symbols (derived from the analogy) for capacitance and inductance represent respectively compliance and mass.

The lower curve of Fig. 2 shows the system response for the alternating pressure in the hermetic shell (point 3). From lumped calculations it would appear that this muffler would attenuate at the rate of 24 db/octave, on the P_3/P_{LF} curve, and would become progressively more satisfactory for frequencies greater than 200 cps. That this is not the case shall be shown later. The resonances at 37 and 184 cps are due to the 2 masses resonating with the 3 compliances. For instance, the resonance at 37 cps is caused by the mass of the tube connecting muffler and hermetic shell resonating with the series compliance of the muffler and shell volumes.

Above 184 cps no resonances are shown, although in practice distributed effects cause resonances to occur near each half-wavelength frequency of every tube in the system. The effects of tube resonances may be included by using distributed element calculations.

DISTRIBUTED ELEMENT CALCULATIONS

One way of accounting for the distributed nature of mass and compliance of a tube is to subdivide each tube into a large number of sections. The mass and compliance of each section is then used in lumped calculations. This extended lumping procedure distributes the tube mass and compliance, but the accuracy is dependent upon the number of sections used. This method has been used successfully in electrical analogy representations.

A more satisfactory method, suitable for digital computation, is to use the solutions of the one-dimensional wave equation. Damping affects only the peak heights near resonance, therefore it is not included. The wave equation is then[1]

$$\frac{\partial^2 P}{\partial t^2} = c^2 \frac{\partial^2 P}{\partial x^2} \tag{7}$$

$$\frac{\partial^2 U}{\partial t^2} = c^2 \frac{\partial^2 U}{\partial x^2} \tag{8}$$

where

$$c = \sqrt{\frac{\gamma P_o}{\rho}} \tag{9}$$

The solution to these equations for

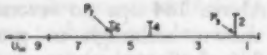

Tube	Description	Length	Area	γ	c	ρ	End
1	Hermetic Shell	.25	960.	1.123	2.887	20.	Closed
2	"	.25	960.	"	"	"	Closed
3	Shell-muffler	6.8	.052	"	"	"	
4	Muffler Tank	.5	2.0	"	"	"	Closed
5	"	1.5	2.67	"	"	"	
6	"	.5	2.67	"	"	"	Closed
7	Muffler-Head	6.5	.052	"	"	"	
9	Head	.67	.3	"	"	"	

Fig. 3 Line drawing of suction muffler shown in Fig. 1

steady state sinusoidal inputs is given by

$$P_i = DP_r + jBU_r \quad (10)$$

$$U_i = jCP_r + DU_r \quad (11)$$

$$D = \cos kl \quad (12)$$

$$B = Z_o \sin kl \quad (13)$$

$$C = (1/Z_o) \sin kl \quad (14)$$

$$k = 2\pi f/c. \quad (15)$$

$$Z_o = \rho c/A \quad (16)$$

Equations 10 and 11 are the basic equations of this paper. For a closed end tube $U_r = 0$ giving

$$P_i = P_r \cos kl$$

$$U_i = j\frac{P_r}{Z_o} \sin kl$$

so

$$\frac{P}{P_{LF}} = \frac{P}{U_{IN}} j\omega C_t = -\omega C_t Z_o \frac{\cos kl}{\sin kl} \quad (17)$$

Thus a closed tube has resonances in P/P_{LF} when

$$\sin kl = 0$$

$$kl = n\pi$$

$$\frac{2\pi fl}{c} = n\pi$$

$$f = \frac{nc}{2l} \quad (18)$$

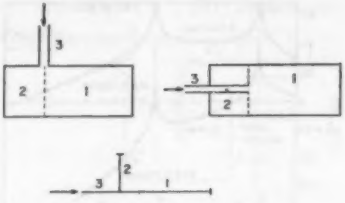

Fig. 4 Junction representation

These are the organ pipe half-wavelength fundamental and harmonics for a closed tube. Muffler systems are composed of many such tube elements connected together.

TANDEM-L CONFIGURATION

In the frequency range where one-dimensional wave equations are valid, expansion chamber-type muffler systems are simply a collection of tubes of different lengths and areas connected together in a given configuration. The intake muffler of Fig. 1 is shown in the line drawing of Fig. 3. The line drawing shows only the interconnection of tube elements. Tabulation of lengths, areas, gas properties and end conditions of the tubes, completes the necessary information defining the acoustic system.

Because of the irregular shape of hermetic shell with the pump inside, it was not desired to include wave effects in the shell, but to assume its effect was a pure compliance. Therefore, the total volume was kept the same, but the tube lengths were reduced to small enough values to make all wave effects in the shell negligible up to

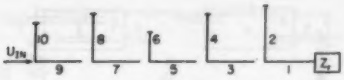

Fig. 5 Tandem-L configuration

the highest frequency to be calculated.

The line drawing approach leads to simple representation of more complex systems. The junctions of Fig. 4 both have the same line drawing because three-dimensional effects are not important in the frequency range considered. Pressures at all points in a given cross-section are the same. However, in Fig. 4, the diameter of the tube entering the side of the tank must be small compared to the tank diameter. Although tube 2 is represented by a side branch, the equations properly take account of the total length of tubes 1 and 2 to give the correct half-wave resonances. Tube 2 is an odd multiple of a quarter-wavelength at certain frequencies, causing the pressure to drop to zero at the junction.

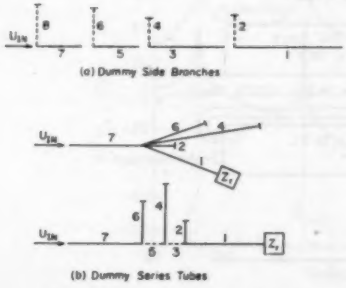

Fig. 7 Use of zero length tubes

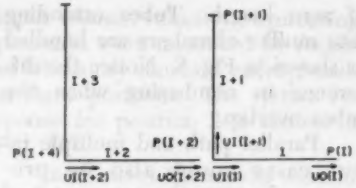

Fig. 6 Juncture of two L's

In developing a general purpose computer program, it is necessary to limit the number of possible tube configurations to be studied. The tandem-L configuration of Fig. 5 was chosen as it handles a great number of practical cases encountered at Westinghouse. All side branches are composed of one closed end tube. There is one system input and one termination point, which may have any value of impedance. Gas properties may be different for each tube. End corrections on tube lengths should be included where necessary.

The juncture between two L's composed of the tubes I, I + 1, I + 2, is shown in Fig. 6. The pressure at the junction, called P (I + 2) is the same for all three tubes. The positive directions of instantaneous volume velocity at the junction are also shown. Continuity of volume velocity makes the output volume velocity of tube I + 2 equal to the sum of the input volume velocities of tubes I and I + 1. The volume velocity out of tube I + 1 is always zero due to the closed end.

Any tube length may be set equal to zero, making possible many configurations as shown in Fig. 7. Dotted lines indicate tubes

of zero length. Tubes extending into muffler chambers are handled as shown in Fig. 8. Notice the difference in numbering when the tubes overlap.

Parallel path and multiple input cases could also be programmed using the same general theory.

For ease in programming, the equations 10 and 11 are separated into their real and imaginary parts. The equations necessary to complete the calculations for all pressures and volume velocities in the system at a given frequency of excitation are given in the appendix. In order to form a response curve, numerous such calculations must be performed at different frequencies to properly define the curve. Knowing the frequency range desired for a given case (e.g., 15 cps to 1500 cps) permits one to increase the frequency successively by Δf from the low frequency limit, until the high frequency limit is reached. A formula found useful for this purpose which was incorporated in

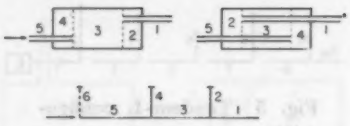

Fig. 8 Muffler representations

the digital program is

$$\Delta f = (C_1)\, f \log_{10} (C_2\, f_H/f) \qquad (19)$$

where C_1 and C_2 are constants determining the percent change in frequency at any frequency; f_H = high frequency limit at which calculation stops. The high frequency limit is usually set below the first transverse wave frequency expected to occur in the system. For round tanks with symmetric excitation this is[2]

$$f_H = 1.22\ c/d \qquad (20)$$

For unsymmetric excitation

$$f_H = .586\ c/d \qquad (21)$$

EXPERIMENTAL VERIFICATION

The digital results were compared

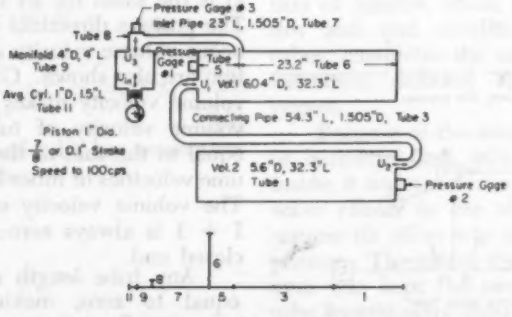

Fig. 9 Experimental test system and line drawing

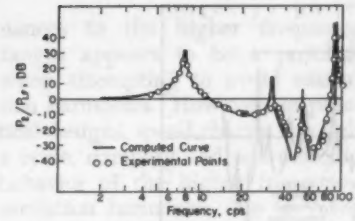

Fig. 10 Comparison of computer and test system results

with the results of an experimental test performed on a tube-tank system to verify the method. The test system with its line drawing is shown in Fig. 9. It is typical of a discharge system of a medium size refrigeration compressor with a two-stage muffler, except that the long pipe to condenser is omitted. Elbows, discontinuities, and off-center side entering positions of tanks are all included in the experimental test The system was excited by a small compressor with valves and valve plate removed, giving a sinusoidal input volume velocity. Alternating pressures were measured by means of laboratory standard microphones at three positions. The system response for position 2 is shown in Fig. 10.

In all cases, the results were in good agreement, considering the zero damping assumption made in the computer analysis. The sharp dip at 90 cps, which was noticed experimentally, was checked by the computer results. The computer provided pressures and volume velocities at every position in approximately two minutes running time, while several weeks' work was necessary to obtain the experimental pressure curves. The experimental volume velocity curves could not even be obtained with the equipment on hand.

In view of the close agreement obtained, the computer program was put to work on practical muffler design problems.

PRODUCTION COMPRESSOR

The first application of this ana-

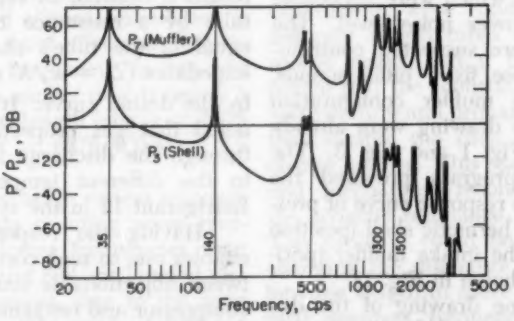

Fig. 11 Suction muffler response for two positions

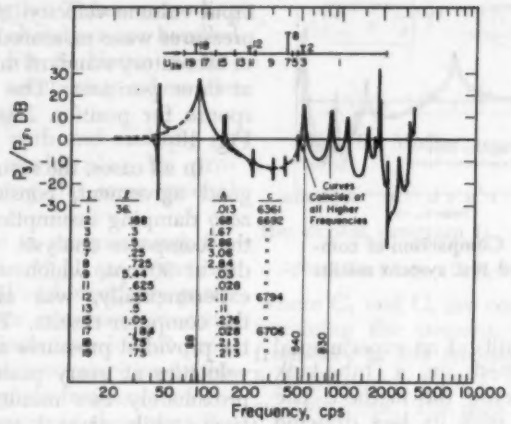

Fig. 12 Discharge system response

lytical tool at the Columbus Works was the study of a four pole internally spring mounted compressor which had recently been placed in production and was being used for refrigerators and freezers. In order to fully capitalize on the internal spring mounting improvement in the design, it was necessary to eliminate certain "buzzes" or "whines" which were noticeable with the lower noise level. The mufflers were suspected contributors to these fixed pitch sounds. The intake muffler configuration and its line drawing were already shown in Fig. 1 and Fig. 3. The computer program provided the data for the response curve of pressure in the hermetic shell (position 3) and in the intake muffler (position 7) as shown in Fig. 11.

The line drawing of the discharge system and the pressure response curve for the muffler output (position 3) is shown in Fig. 12. Tube 1 is the long discharge pipe to the condenser and includes part of the condenser tubing to near the liquid level. This 36-in. length tube gives resonances at every odd multiple of a quarter wavelength, accounting for the resonances shown at 44.2 cps, 132.6 cps, 221 cps, etc. These may be eliminated from the results if desired, by replacing the tube by a resistance termination equal to the tube's characteristic impedance ($Z_o = \rho c/A$) as is shown by the dotted curve. It should be noted that gas properties change through the discharge system due to the different temperatures of Refrigerant 12 in the system.

Having the response curves enables one to seek correlation between objectionable sounds in the compressor and resonance peaks in the acoustic system.

The large number of reso-

nances in the higher frequency ranges appears to be a problem when attempting to avoid excitation harmonics. However, in practical designs, speed change through a cycle, damping and non-periodic behavior of the higher frequency excitation harmonics due to valve motion, make it necessary only to obtain a high average attenuation.

INTERPRETATION OF RESULTS

The results of the lumped element calculations for the intake muffler (Fig. 2) and the distributed element calculations (Fig. 11) should be compared. It is evident that wave effects play an important part in the design of a muffler. Designs based on lumped element theory would predict a large attenuation of the higher frequency components, while in reality, the attenuation is not outstanding for this simple design. The second lumped element resonance, caused mainly by the resonance of the head volume with the head to muffler pipe, is correctly given as 140 cps in Fig. 11, although the lumped element calculation shows 184 cps. The lumped element calculation is in error as wave effects are important at this frequency. In this case the head to muffler pipe is nearly a quarter wavelength long ($c = 6578$ in./sec, $\lambda/4 = 6578/4(184) = 8.9$ in.).

The discharge system response (Fig. 12) has standing wave resonances at lower frequencies than the 88 cps and 830 cps lumped element resonances, due to the long 36-in. tube. The peak at 540 cps is of special interest as will be described.

Obviously, we cannot eliminate all resonances in a muffler system. The remedial approach is to identify a particular troublesome frequency and then either shift it, or to provide high muffler attenuation of the higher frequencies and thus make it negligible. The use of acoustic damping materials is possible, but generally involves expense which should be avoided if the product is to be priced competitively.

In the case of the subject compressor, audible resonance occurred in a significant number of units at 510 cps and at approximately 1300 cps, making remedial action necessary. Both mufflers possessed standing wave peaks near 510 cps which could respond to the higher excitation frequencies. The suction system has an inlet tube 6.8 in. long which produces a half-wavelength resonance at 490 cps as shown in Fig. 11. Similarly, the discharge muffler is connected to the head by tubes 9 and 11 having a combined length of 6.1 in. producing the peak at 540 cps in Fig. 12. Several experiments were conducted with different length tubes to shift response peaks, and it became apparent that the acoustic resonances were detrimental primarily because they excited the shell of the discharge muffler. This shell had several mechanical resonances near the acoustic resonance at 540 cps. This problem could be solved by changing the discharge muffler inlet tube length to move the acoustical resonant frequency, but an effective solution was obtained by changing the mechanical resonant

frequency of the discharge muffler shell. Doubling the muffler wall thickness virtually eliminated this frequency from the compressor noise spectrum. In production, an equivalent effect was obtained by brazing a steel slug to the muffler wall.

The 1300 cps noise was more elusive, but the computer analysis helped show potential noise sources. Fig. 12 shows clearly that trouble from acoustic excitation in the discharge system would not be anticipated. The suction muffler system has several resonances in the vicinity of 1300 cps. The 1300 cps peak is due to the half-wavelength of the 2.5-in. long muffler shell. The other peaks just below 1500 cps are the third harmonics of resonances near 500 cps. The design might have been modified to move these resonances to more favorable locations, however, it was found that the dominant share of the 1300 cps noise was due to the electric motor. Isolation of this source reduced the noise level to an acceptable level. Future conditions could renew the need for analysis of the suction muffler.

DEVELOPMENT COMPRESSOR

In undertaking the development of a new compressor, it was recognized that an opportunity existed to make use of muffler analysis before tooling commitments had been made. Therefore, a large number of computer runs were made to provide the following information:

1. Number of stages required for adequate high frequency attenuation.
2. Location of low frequency resonances and design parameters which could be altered to relocate these peaks.
3. Minimum size mufflers capable of fulfilling design objectives.
4. A basis for quickly evaluating proposed design changes which might influence noise.

The most urgent problem was that space requirements be established. Analysis of tentative muffler designs indicated that a reduction in muffler size was possible. Analysis also showed that 3-stage mufflers could attain greater attenuation. The multiple-stage benefit was considered essential in the discharge system where the high frequency noise could be conducted directly to the shell via the discharge tube.

Fig. 13 shows results for a 3-stage discharge muffler. Attenuations over 80 db are possible for muffler output pressure, P_3/P_{LF}, theoretically, for frequencies above 1500 cps. The muffler attenuation is the difference between P_{13} and P_3. Attenuations of this order may not be obtained, since in the analysis rigid walls and partitions were assumed, while in practice there will be mechanical transmission through partitions and along tank and tube walls. However, computer results show that multiple stages are a practical way to obtain high average attenuations even when wave effects are included.

The current version of the development compressor utilizing the discharge muffler discussed above and a single-stage suction muffler also based on computer analysis,

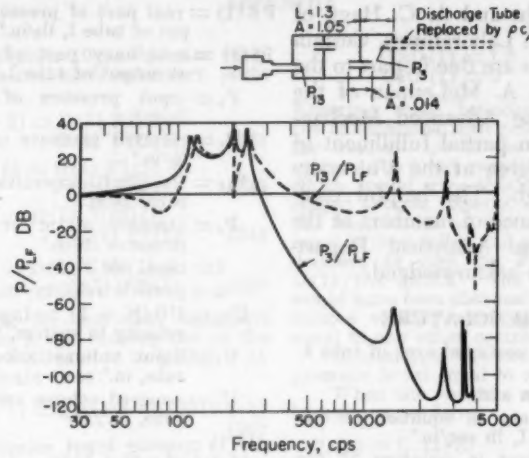

Fig. 13 Development discharge muffler

has produced excellent sound levels. The noise spectrum shows no consistent relationship of noise to peaks in the muffler response, thus indicating that adequate muffler attenuation has been provided, and that there is little excitation of muffler resonances by the excitation frequencies.

CONCLUSIONS

A method of obtaining muffler response curves by means of digital computation has been presented. The analysis is based on successive use of the undamped one-dimentional wave equation to represent each tube element in the muffler system. Wave effects play a most important part in determining the attenuation at the higher frequencies. Comparison of experimental and analytical curves shows good agreement.

Steady-state response curves are useful in analyzing mufflers, as they allow interpretation of resonance behavior whether these resonances are excited or not by the actual pulse type input from the valve. Response curves allow comparison of muffler designs, making it possible to explore quickly the effects of various muffler geometries. The tandem-L representation handles a large class of expansion muffler configurations. Other programs could be developed similarly to cover additional configurations not handled by the tandem-L analysis. Noise levels of production mufflers analyzed by the methods described, have been significantly improved.

ACKNOWLEDGMENTS

The authors acknowledge the assistance of their associates in Westinghouse, in particular the work of

D. V. Wright and A. C. Hagg of the Research Laboratories. Certain of the results are due in part to the thesis of G. A. McLennan of the Westinghouse Advanced Mechanics School in partial fulfillment of his M.S. degree at the University of Pittsburgh. The helpful computer assistance of members of the Westinghouse Analytical Department is also acknowledged.

NOMENCLATURE

$A(I)$ = cross sectional area of tube I, $in.^2$

A_p = piston area

$B(I)$ = constant in equation 10 for tube I, lb sec/$in.^4$

$C(I)$ = constant in equation 11 for tube I, $in.^5$/lb sec

$c(I)$ = sonic velocity for tube I, in./sec

C_a = acoustic compliance, $in.^5$/lb

C_1 = frequency constant in equation 19

C_2 = frequency constant in equation 19

C_t = total acoustic compliance of system, $in.^5$/lb

d = tube diam, in.

$D(I)$ = constant in equation 10 for tube I

f = frequency at which calculation is being performed, cps

f_L = lower frequency limit for calculations, cps

f_H = upper frequency limit for calculations, cps

I = number of tube I, integer

$I+1$ = number of tube after I, integer

$j = \sqrt{-1}$

$k(I) = 2\pi f/c(I)$ = wave number for tube I, rad/in.

$l(I)$ = length of tube I, in.

M_a = acoustic mass, lb $sec^2/in.^5$

N = number of last tube in system, integer

$P(I)$ = vector pressure at output of tube I, $lb/in.^2$

$PR(I)$ = real part of pressure at output of tube I, $lb/in.^2$

$PI(I)$ = imaginary part of pressure at output of tube I, $lb/in.^2$

P_i = input pressure of a tube, $lb/in.^2$

P_r = received pressure of a tube, $lb/in.^2$

$P_{LF} = U_{IN}/j2\pi fC_t$ = excitation pressure, $lb/in.^2$

P_o = absolute static or ambient pressure $lb/in.^2$

t = time, sec

u = particle velocity, in./sec

$U_{IN} = UO(N+1)$ = input volume velocity to system, $in.^3$/sec

U_i = input volume velocity to a tube, $in.^3$/sec

U_r = received volume velocity of a tube, $in.^3$/sec

$UI(I)$ = vector input volume velocity of tube I, $in.^3$/sec

$UO(I)$ = vector output volume velocity of tube I, $in.^3$/sec

$UII(I)$ = imaginary part of input volume capacity of tube I, $in.^3$/sec

$URI(I)$ = real part of input volume velocity of tube I, $in.^3$/sec

$URO(I)$ = real part of output volume velocity of tube I, $in.^3$/sec

$UIO(I)$ = imaginary part of output volume velocity of tube I, $in.^3$/sec

$v(I)$ = specific volume of gas in tube I, ft^3/lb

x = length variable, in.

Z_r = termination impedance of tube, sec/$in.^5$

$Z_o(I)$ = characteristic impedance of tube I, lb sec/$in.^5$

ZR = real or resistive parts of termination impedance, lb sec/$in.^5$

ZI = imaginary or reactive part of termination impedance, lb sec/$in.^5$

$\rho(I)$ = mass density in tube I, lb $sec^2/in.^4$

$\gamma(I)$ = adiabatic exponent for gas in tube I

ξ = particle displacement, in.

$\omega = 2\pi f$ = circular frequency, rad/sec

λ = wavelength, in.

APPENDIX

When equations 10 and 11 are separated into real and imaginary parts we obtain

$$PR(I+2) = D(I)\ PR(I) - B(I)\ UIO(I) \quad (22)$$

$$PI(I+2) = D(I)\ PI(I) + B(I)\ URO(I) \quad (23)$$

$$URI(I) = D(I)\ URO(I) - C(I)\ PI(I) \quad (24)$$

$$UII(I) = D(I)\ UIO(I) + C(I)\ PR(I) \quad (25)$$

Solving for the other equations defining an L and making use of the fact that $URO(I+1) = UIO(I+1) = 0$, we obtain

$$PR(I+1) = PR(I+2) / D(I+1) \quad (26)$$

$$PI(I+1) = PI(I+2) / D(I+1) \quad (27)$$

$$URI(I+I) = -\frac{C(I+1)}{PI(I+1)} \quad (28)$$

$$UII(I+1) = C(I+1)\ PR(I+1) \quad (29)$$

The coupling equations are

$$URO(I+2) = URI(I) + URI(I+1) \quad (30)$$

$$UIO(I+2) = UII(I) + UII(I+1) \quad (31)$$

The ten equations (22-31) allow the calculation of all quantities in an L for a given frequency if only the receiving end pressure and volume velocities are known (PR(I), PI (I), URO(I), UIO(I)). Since these equations are written for the general L section composed to tubes I and I + 1, they can be used successively from I = 1 to I = N to solve systems composed of tandem—L's. N is the total number of sections in the system.

The receiving end pressure and volume velocities are determined from the termination conditions. If the end is open, the pressure must always be zero at this point. The volume velocity is arbitrarily set equal to the real number one. That is

$$PR(1) = 0$$
$$PI(1) = 0$$
$$URO(1) = 1.0$$
$$UIO(1) = 0 \quad (32)$$

Knowing these boundary conditions the calculations then proceed through the tandem—L's to the input of the system. The input quantities are found which would give this assumed unit output volume velocity. The ratio of the magnitudes of the output to the input is then taken and converted into decibels, to give the $P(1)/P_{LF}$ and $U(1)/U_{IN}$ ratios. The same ratios would have been obtained if the output volume velocity were arbitrarily set equal to any other complex number.

Similarly, if the end is closed the pressure is set equal to one.

When the end has a terminating impedance, we have

$$P_r(1) = U_r(1) Z_r \quad (33)$$

Writing this equation in real and imaginary parts gives

$$PR(1) = URO(1)\ ZR - UIO(1)\ ZI$$
$$PI(1) = UIO(1)\ ZR + URO(1)\ ZI \quad (34)$$

Setting arbitrarily

$$URO(1) = 1.0$$
$$UIO(1) = 0 \quad (35)$$

we obtain

$$PR(1) = ZR$$
$$PI(1) = ZI \quad (36)$$

Equations 35 and 36 are then used as the boundary conditions when the termination is a constant impedance.

In all three types of terminations the ratios of P/P_{LF} or U/U_{IN} at any point in the system are calculated by the following equations

$$P(I)/P_{LF} \text{ in db} = 20 \log_{10} (\sqrt{[PR(I)]^2 + [PI(I)]^2}/P_{LF}) \quad (37)$$

$$U(I)/U_{IN} \text{ in db} = 20 \log_{10} (\sqrt{[UR(I)]^2 + [UI(I)]^2}/U_{IN}) \quad (38)$$

$$P_{LF} = U_{IN}/2\pi f C_t \quad (39)$$

$$U_{IN} = \sqrt{[URO(N+1)]^2 + [UIO(N+1)]^2} \quad (40)$$

$$C_t = \sum_{I=1}^{N} [A(I)\,l(I)] / [\rho(I)\,c(I)^2] \quad (41)$$

The phase angles of the quantities are also found in relation to the input P_{LF} or U_{IN}.

Phase angle of P/P_{LF} = arctan (PR(I)/PI(I)) — phase angle of P_{LF} (42)

Phase angle of U/U_{IN} = arctan (UR(I)/UI(I)) — phase angle of U_{IN} (43)

Phase angle of P_{LF} = phase angle of $U_{IN} - 90°$

Phase angle of U_{IN} = arctan (URO(N+1)/UIO(N+1)) (44)

The subsidiary calculations converting the input data are

$$\rho(I) = 1.498895 \times 10^{-4}/v(I) \quad (45)$$

$$c(I) = \sqrt{\gamma(I)\,P_s(I)/\rho(I)} \quad (46)$$

$$Z_s(I) = \rho(I)\,c(I)/A(I) \quad (47)$$

$$kl(I) = 2\pi fl(I)/c(I) \quad (48)$$

BIBLIOGRAPHY

1. Mason, W. P., "A Study of the Regular Combination of Acoustic Elements with Applications to Recurrent Acoustic Filters, Tapered Acoustic Filters and Horns," *Bell System Technical Journal*, Vol. 6, p. 258, 1927.

2. Morse, P. M. "Vibrations and Sound," 2nd Edition, McGraw-Hill, 1948, pp. 305-309.

DISCUSSION

UNIDENTIFIED SPEAKER: It was stated that the difference between the calculated results and the practical results was caused by the vibration transmitted through the separators of mufflers. Could this be greatly improved by variations in a choice of materials?

CLOSURE BY AUTHOR MILLER: It was assumed that the walls of the tubes and the separators were infinitely rigid so they did not vibrate. It is true that vibration transmission can be lessened by constructing the muffler from more rigid materials, using different materials, or by stiffeners. This is a problem that should be investigated further. Tests have confirmed that the full values of attenuations as given by the theoretical curves are not complete, but is it not felt that this is a deficiency in the method or in practical use.

W. F. KERKA: Cleveland, Ohio: Another problem to be considered is the fact that air flow through the muffler may generate noise in itself and hence give less attenuation than that determined from a no-flow analysis. High air flow rates in ducting also change the attenuation properties of absorbing materials as compared to a no-flow condition.

AUTHOR MILLER: Acoustic absorbing materials and noise generation due to the flow of gas are not considered in this paper. For refrigeration mufflers, absorbing materials are rarely used and flow velocities are kept low enough not to generate appreciable noise.

1711

No. 1711

Use of Activated Charcoal to Decrease Odor and Odor Transfer in Domestic Refrigerators

AARON L. BRODY JESS W. THOMAS LOIS LAFEBER

Problems in odor and odor transfer in domestic refrigerators have been reported for many years (Crocker, 1940; Nagy, 1956 a and b; Gutschmidt, 1958). These problems have generally fallen into two categories: a predominance of fresh and deteriorated food odor permeating the entire interior cabinet perceived upon opening; and a transfer of a strong odor from one food into another whose flavor is adversely affected by the transmitted odor.

Several methods have been devised in the past to alleviate the prevailing problem of food odor and odor transfer. Among these have been the oxidation of odor molecules by ozone (Nagy, 1956 a) and the adsorption of odorous materials by activated charcoal (Gutschmidt, 1958).

These are fundamental objections to the ozone method. The maximum allowable atmospheric concentration is about 0.1 parts per million (Hollaender, 1955). Previous studies have shown that at least 5 ppm are required for odor reduction (Gross, et al, 1947). Since ozone accelerates oxidation, undesirable effects such as rancidification of fatty foods may occur. Oxidized molecules may have more objectionable odors than their precursors; e.g., acetic acid, the oxidized form of ethyl alcohol, is more objectionable than ethyl alcohol.

Adsorbing agents have been successfully used to remove odors from commercial refrigerated storages (Smock and Southwick, 1945), but reported results indicated little success in domestic refrigerators (Gutschmidt, 1958).

A. L. Brody is a Food Technologist; J. W. Thomas is a Chemical Engineer; and L. M. Lafeber is Home Economist, Research Laboratories, Whirlpool Corporation. This paper was presented at the ASHRAE Semiannual Meeting in Dallas, Texas, February 1-4, 1960.

Since reported experiments in domestic refrigerators were conducted in units not equipped with forced air circulation, and since a large share of the American production of domestic refrigerators does incorporate this feature, it was felt that a re-evaluation of activated charcoal as an odor adsorbing agent in forced convection units would be desirable.

EXPERIMENTAL METHODS

Essentially, it was necessary to measure two phenomena: odor level intensity in refrigerators, and odor transfer from one food to another. Odors of a number of different foods typical of those causing problems in domestic refrigerators were measured. Since it would have been prohibitively expensive to develop physical or chemical indicators of odor level for each food odor, subjective methods were used with one exception.

Odor level intensity was evaluated by both a subjective and an objective method. In the former, odorous air from the refrigerator was passed through one of a series of six tubes containing successively decreasing amounts of activated charcoal. To start the test, odorous air was passed for a few seconds through the tube containing the most charcoal. A trained panelist then sniffed the effluent gas from the tube. If no odor was detected, the gas stream was shifted to the tube containing the next largest amount of charcoal, the effluent was sniffed, and the process was continued until a definite threshold level of odor was perceived. Assignment of consecutive numbers to the tubes permitted a semi-quantitative subjective evaluation of the refrigerator odor intensity.

Jarvis and Ranum (1958) used a similar method, except that odorous air was passed through all tubes simultaneously and continuously. In the present method, activated charcoal was exposed to odorous air for only a few seconds for each determination. Basically, the Jarvis and Ranum method measured the quantity of odorous air required to partially saturate a given quantity of activated charcoal. In the present work, odor intensity level was measured, since a given quantity of activated charcoal arranged in a thin bed removes a definite proportion of odor in odorous air passing through the bed. In order to understand the basis of this phenomenon and its limitations, it is necessary to consider the fundamental mechanism of odor removal from a flowing air stream by a thin bed of adsorbent.

An odor molecule will be permanently removed from an air stream only if it (1) contacts the surface of the activated charcoal enroute through the activated charcoal bed; (2), adheres, that is, does not ricochet or be desorbed. These two phenomena are quite distinct and depend on different parameters. The transport of the odor molecule to the surface depends only on the diffusion constant of the odor molecule, air velocity, and dimensions of the activated charcoal bed and activated charcoal granule. Transport is independent of chemical nature of the adsorb-

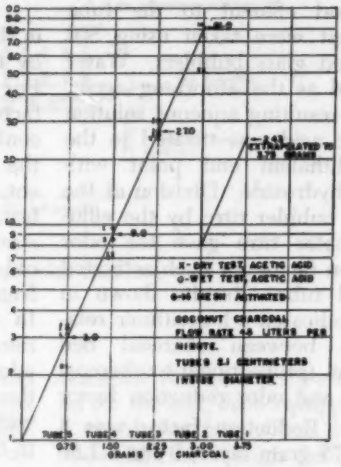

Fig. 1 Relationship between charcoal bed thickness and odor reduction factor

ent charcoal, or degree of charcoal activation. On the other hand, the quantity of gas that activated charcoal will hold is dependent on degree of charcoal activation, and of saturation of the activated charcoal bed.

Conditions in the activated charcoal odorometer were controlled so that the activated charcoal was far removed from saturation. Hence transport properties alone determined the fraction of odor getting through the activated charcoal bed. For a given odor, and given activated charcoal mesh size and air velocity, the fraction of odor removed should be a logarithmic function of bed thickness. Molecular properties of odor molecules are independent of the number (i.e., concentration) of odor molecules, which implies that the number of odor molecule collisions with the activated chaircoal is proportional to odor molecule concentration, C. In a differential bed thickness, dz, therefore, there will be kC dz collisions with the activated charcoal, and $-dC = kCdz$.

Integration gives $\ln (C_1/C_2) = kz$. As will be shown subsequently, this logarithmic relation holds.

To apply the activated charcoal tube method it is necessary to know the odor reduction factor for each tube. This was determined using acetic acid vapor as a representative odor.

Flow rate through all tubes was standardized at 4.5 1/min. Activated charcoal was 6 x 14 mesh, and amount in each tube varied from 0.75 to 3.75 gram in increments of 0.75 gram. Tests were made using both dry air and air saturated with water vapor. Acetic acid vapor was obtained by bubbling dry air through glacial acetic acid. After dilution with air to the required flow rate of 4.5 1/min., concentration samples in-

fluent and effluent to the tube under test were taken using 500 ml. fritted glass bubblers. Water was used as the absorbing agent, and the resulting aqueous solution of acetic acid was titrated to the phenolphthalein end point with sodium hydroxide. Division of the influent bubbler titre by the effluent bubbler titre gave the odor reduction factor for each activated charcoal tube. Results shown in Fig. 1 indicated a logarithmic relationship between charcoal bed thickness, (proportional to charcoal weight) and odor reduction factor (C_1/C_2). Reduction factor was 3 for a 0.75 gram layer; 9 for a 1.50 gram layer, etc., and was independent of relative humidity conditions.

These values apply only to acetic acid vapor which has a diffusion constant of 0.11 cm^2/sec at room temperature and pressure (Sherwood, 1937). For other odors, the reduction factors probably would be not much different, since most gaseous odors have diffusion constants between 0.04 and 0.15 (Sherwood, 1937). Even though the odor reduction factor varies somewhat for different odors, these differences tend to cancel out when comparing two different refrigerators.

In order to assign a number to the odor intensity, the threshold unit concept (Hopper, 1959) was used. For example, an odor having five times the concentration of odor molecules necessary to be just detectable is said to have an odor level intensity of five threshold units.

Activated charcoal tubes used in this work caused odor reduction by factor of 243, 81, 27, 9 and 3. For the tube having a reduction factor of 9, the odor molecule concentration in the influent is 9 times the odor concentration in the effluent, etc. Hence, in a refrigerator test, if panelists found that the air stream from this tube had a threshold odor, the odor level in the refrigerator was 9 threshold units. In comparing refrigerator odors, results are reported in terms of odor intensity ratios or ratios of threshold units in the refrigerator without charcoal to threshold units in the refrigerator with charcoal.

Odor level intensity was also evaluated using an objective method, reduction of potassium permanganate. Since many food products, and especially those which are generally agreed to have strong food odors, contain substances volatile at ambient temperatures which are able to reduce alkaline permanganate solutions, the concentration of these volatile reducing substances (VRS) was measured. The measures had been previously correlated to organoleptic evaluations (Farber, 1957). Air from refrigerators under test was bubbled through alkaline 0.001 N potassium permanganate for one hour. Reduction of the permanganate was measured by light transmission through the solution in a Klett-Summerson colorimeter using a green filter.

Odor transfer was measured by groups of trained panelists sniffing various food materials placed in sealed refrigerators with odor-

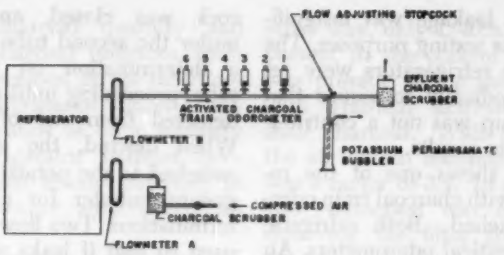

Fig. 2 Refrigerator with charcoal train odorometer attached

ous foods, doors being opened and food load removed and replaced at intervals to simulate household use. Two groups of panelists were selected from volunteers on the basis of their acuity for onion odor Odor intensity differences were measured using the triangle test (Peryam, 1958).

Two odor receiver food samples from the control refrigerator and one from the activated charcoal equipped unit or vice-versa, were smelled in succession, and the panelist was asked to select the odd sample and state whether it had more or less odor than the other sample. The correct triangle selection could be made in three times by chance, and the correct intensity judgment would arise by chance once in six tries. Thus, a result showing 16.7% correct intensity judgment could be considered as arising by chance. Significance of results was determined by a standard statistical chi-square technique (Guilford, 1954).

TEST PROCEDURE

Two identical 12 cu ft production domestic refrigerators were selected for the test, each equipped with a circulating fan, which delivered about 22 cfm through the installed ductwork. Screen wire canisters 1.75 x 6.00, 0.875 in. in direction of air flow, were used to contain the activated charcoal. Installation of these canisters in the ductwork naturally caused a reduction in the air volume delivered, to about 9 cfm with one canister in the ductwork, and to about 5 cfm with two canisters installed in series. Each canister contained about 70 grams of charcoal. The one pass efficiency of a single canister was estimated to be over 90% at a flow rate of 9 cfm.

In most of the tests two canisters in series were used. The canister or canisters were placed in one refrigerator only. The other refrigerator had none, and served as a control. Granular 6 x 14 mesh activated coconut shell charcoal, 50 minute test, was selected for trial because it was recommended as the best material available for odor adsorption (Barneby, 1957). Refrigerator cabinets were sealed

so that gas leakage was insignificant for odor testing purposes. The roles of the refrigerators were reversed periodically to assure that odor build-up was not a contributory factor to results.

Fig. 2 shows one of the refrigerators with charcoal train odorometer attached. Both refrigerators had identical odorometers. Air entered refrigerator continuously at the bottom after purification by passage through an activated charcoal scrubber. In the standby position, the air passed through the effluent charcoal scrubber. When a panelist was available for test, the stopcock below the first tube was opened for a few seconds, and a panelist sniffed the emerging air. If no odor was detected, the stopcock was closed, and stopcock under the second tube opened for a determination on the second tube, proceeding until an odor was detected from one of the tubes. When desired, the effluent was switched to the potassium permanganate bubbler for chemical determinations. Two flowmeters were used so that if leaks were present they were detected. For example, if flowmeter B read consistently differently than A, a leak was present.

RESULTS

Odor intensity reduction: Results of subjective tests, using trained panelists and the odorometer just described, are given in Table I. Four different combinations of

TABLE I

REDUCTION OF REFRIGERATOR ODOR BY ACTIVATED CHARCOAL, ODOROMETER TEST

Odor Produced By	Odor Intensity Ratio* A	B	C	D
400 ml onion juice	40			
200 ml onion juice	13		2.4	6.1
100 ml onion juice		5.8	3.2	
200 ml garlic juice	24	3.0		
100 ml garlic juice			3.0	
400 g onion slices	17			
300 g onion slices	4.9			
200 g onion slices	3.4		4.2	
7 oz limburger cheese	11			
200 ml cider vinegar	7.3			
200 ml wine vinegar	4.1			
200 ml cider-tarragon vinegar	5.5			
1 lb fish	31			
Chemical fish odor (TMA)	13			

* Ratio of odor intensity in refrigerator without activated charcoal to odor in refrigerator with activated charcoal.

A. Air circulating fan on, 2 charcoal canisters in series in air duct from fan.
B. Air circulating fan off, 2 charcoal canisters placed on refrigerator shelf.
C. Air circulating fan on, 2 charcoal canisters placed on refrigerator shelf.
D. Air circulating fan on, 1 charcoal canister placed in air duct from fan.

activated charcoal quantity and activated charcoal positions were used, as described in the table notations. Performance figures in the table give ratios of odor intensity in the refrigerator without activated charcoal to odor intensity in the refrigerator with activated charcoal.

For example, in the case of 400 ml of onion juice in refrigerators with 140 g of activated charcoal in the air stream, the amount of odor present in the refrigerator without activated charcoal was forty times greater than that present in the unit with the activated charcoal filter. Expressed in another way, only 1/40th of the odor present in the control refrigerator was present in the unit equipped with granular activated coconut shell charcoal. With the filter in the air stream minimum reduction was a factor of 3.4. In general, less odor reduction was obtained by removing the filter from the air stream, and greater odor reductions were obtained with stronger odors.

Results of odor intensity tests, using the objective potassium permanganate method, are presented in Table II. Again, greater odor reductions were evident in the unit containing activated charcoal in

TABLE II

REDUCTION OF REFRIGERATOR ODOR BY ACTIVATED CHARCOAL, VRS TEST*

Odor Produced By	Odor Intensity Ratio** A	B	C	D
400 ml onion juice	1.5			
200 ml onion juice	4.2	1.2		10
100 ml onion juice		1.3	1.3	
200 ml garlic juice	3.7	1.2		
100 ml garlic juice			none	
400 g onion slices	3.1	3.5	none	
300 g onion slices	1.8			
200 g onion slices			1.8	
7 oz limburger cheese	2.9	1.3	none	
200 ml cider vinegar	8.3			
200 ml wine vinegar	complete			
200 ml cider-tarragon vinegar		1.2		
1 lb fish	4.8			
Chemical fish odor—0.05 % TMA***	complete			
Chemical fish odor—0.1 % TMA	complete			

* Measurement of volatile reducing substance with $KMnO_4$.
** Ratio of odor intensity in refrigerator without activated charcoal to odor intensity in refrigerator with activated charcoal.
*** Trimethyl amine.

A. Air circulating fan on, 2 charcoal canisters in series in air duct from fan.
B. Air circulating fan off, 2 charcoal canisters placed on refrigerator shelf.
C. Air circulating fan on, 2 charcoal canisters placed on refrigerator shelf.
D. Air circulating fan on, 1 charcoal canister placed in air duct from fan.

TABLE III

DECREASE OF ODOR INTO WATER IN REFRIGERATOR WITH USE OF ACTIVATED CHARCOAL

Odor Produced By	Percentage of Judgment Indicating Decrease of Odor Transfer A	B	C	D
200 ml onion juice	80	56		94
100 ml onion juice		94	53	
200 ml garlic juice	90	41		
100 ml garlic juice			44	
400 g onion slices	95		13	
300 g onion slices	67			
200 g onion slices	56		80	
7 oz limburger cheese		29	47	
200 ml cider vinegar	100			
200 ml cider-tarragon vinegar		67		
1 lb fish	90			
Total Percentage	87	57	46	94
Total Judgments	(178)	(65)	(61)	(17)

A. Air circulating fan on, 2 charcoal canisters in series in air duct from fan.
B. Air circulating fan off, 2 charcoal canisters placed on refrigerator shelf.
C. Air circulating fan on, 2 charcoal canisters placed on refrigerator shelf.
D. Air circulating fan on, 1 charcoal canister placed in air duct from fan.

TABLE IV

DECREASE OF ODOR TRANSFER INTO VARIOUS FOODS IN REFRIGERATOR WITH USE OF ACTIVATED CHARCOAL

Odor Produced By	Percentage of Judgments Indicating Decrease of Odor Transfer Water	Whole Milk	Skim Milk	Butter in Open Butter	Butter in Keeper
200 g sliced onion	71	94	67	72	
30 g chopped garlic	64	82		50	
1 lb fish	47		60	49	41
Chemical fish odor (TMA)*	89				
Sliced apples	56				78
Acetic acid (Glacial)		70		80	
100 ml vinegar				82	81
3½ oz. limburger cheese		90	75	51	38
Total percentage	66	85	69	63	61
Total judgment	(109)	(53)	(39)	(254)	(93)

* Trimethyl amine.

the air stream, and lesser reductions were found with activated charcoal in other positions. Direct correlation between panel and chemical tests could not be found since this volatile reducing substances method (VRS) measures only a fraction, albeit a significant fraction, of total odor present. For purposes of these studies, VRS may be considered an approximate index of gross odor rather than an exact measure of relative odor intensities which could not be obtained since potassium permanganate measures only one odor property, chemical reduction.

Results of odor transfer tests are given in Tables III, IV and V. Table III shows the decrease of odor transfer of given odorous materials into water in sealed refrigerators.

As with refrigerator odor, odor transfer was decreased the greatest amount by activated charcoal in the air stream, and lesser amounts by placement in other positions. In all cases except the 400 g of onion slices in a unit with activated charcoal removed from the air stream, the probability of any of the results arising by chance alone was less than one in one thousand. Total percentage of correct judgments was so high for each activated charcoal variation that decrease of odor transfer was conclusive.

Table IV shows results of a series of odor transfer tests run in paired closed conventional (unsealed) domestic refrigerators. One was used as a control and the other had an activated charcoal filter weighing approximately 100 g placed over one of the air circulating system's outlet ducts.

The remaining outlet ducts in both units were sealed so that all of the air in the control unit would take a similar path. Results in Table IV are expressed as percentage correct judgments with 16.7% correct being the base which could

TABLE V

DECREASE OF ODOR TRANSFER INTO VARIOUS FOODS IN REFRIGERATORS UNDER SIMULATED HOUSEHOLD CONDITIONS WITH USE OF ACTIVATED CHARCOAL

Odor Produced By	Water	Percentage of Judgments Indicating Decrease of Odor Transfer: Whole Milk	Skim Milk	Butter in Open	Butter in Keeper
200 g sliced onion			70	63	67
100 ml cider vinegar				73	45
200 ml cider vinegar	84				62
3½ oz. limburger cheese		80	80	44	
Grape drink				65	
Total percentage	84	80	75	67	59
Total judgments	(19)	(10)	(20)	(58)	(32)

arise by chance alone. In every case, results were highly significant, indicating decrease in transfer of odors to the designated receivers.

Table V indicates results obtained using the same equipment and techniques used to obtain data of Table IV except that the refrigerators were operated under simulated household conditions with door openings and dummy food loads. Results were highly significant in favor of activated charcoal as a means of decreasing odor transfer.

USEFUL LIFE

Activated charcoal removes water vapor from the atmosphere, but preferentially adsorbs higher molecular weight molecules such as odors and emits water vapor. On the other hand, odor molecules generally are not emitted from activated charcoal even when saturated.

Activated coconut shell charcoal will adsorb about 25% of its own weight in odor molecules. Since odors are emitted from foods in microgram quantities, a 100 g charge of activated charcoal could continue to adsorb odor for an extended period prior to saturation.

Generally, about one year's life under continuous operation is expected from a quantity of adsorbent sufficient for refrigerator odor removal (Barneby, 1958). However, actual life varies depending upon specific odors being removed, quantity of odor removed, operating conditions, etc.

CONCLUSIONS

Granular activated coconut shell charcoal, used under both extreme and simulated household conditions, significantly reduced refrigerator odor and odor transfer between foods. Most efficient odor decreases were found when activated charcoal was placed in the path of forced air used for cooling; activated charcoal out of the path of forced air was less efficient, as was activated charcoal in a cabinet without forced air, but all three are significantly superior in odor removal performance to controls with no adsorbent present.

REFERENCES

Barneby, H. L., "Activated Charcoal for Air Purification", *Heating, Piping and Air Conditioning*, 64, 481. (1958).

Crocker, Ernest C., "Flavor Transfer in Refrigerated Storage", *Proc. Inst. of Food Tech.*, 195, 1941.

Ewell, A. W., "Ozone and Light", *Refrigerating Data Book, Appl. Vol., 2nd. Ed.*, ASRE: 1946.

Farber, Lionel, "Chemical Evaluation of Pungency of Onion and Garlic by the Content of Volatile Reducing Substances", *Food Tech., 11*, 621, (1957).

Gross, C. R., G. O. Hall, and R. M. Smock, "Odor Sources in Egg Storage and Methods of Removal", *Food Industries, 19*, 919 (1947)

Guilford, J. P., *Psychrometric Methods*, N. Y.: McGraw-Hill, 1954.

Gutschmidt, J., "Untersuchen uber die Gernchs-und Geschmacksubertragung in Kunlschranken", *Kaltetechnik*, 10 Jahrgang, 255, Heft 8 1958.

Hollaender, Alexander, *Radiation Biology, Vol. II, Ultraviolet and Related Radiations*, N. Y. p. 65, McGraw-Hill, 1955.

Hopper, W. F., "Surface Odor Adsorption", *ASHRAE Journal*, Vol. 1, No. 3, p. 92 (1959).

Jarvis, L. A. and R. I. Ranum, "Investigation of Quantitative Odor Measurement by Dynamic Dilution of Odor Adsorption Methods", Presented before 18th Annual Meeting, Institute of Food Technologists, Chicago, 27 May 1958.

Moncrieff, R. W., *The Chemical Senses*, N. Y.: John Wiley, 1944.

Nagy, Rudolph, "Application of Germicidal Lamps in the Domestic Refrigerator", Bloomfield, N. J.: Westinghouse, 1956.

Nagy, Rudolph, "Application of Germicidal Lamps", Presented before International Ozone Conference, Chicago, 28 November 1956.

Peryam, David R., "Sensory Difference Tests", *Food Technology 12*, 231, 1958.
Sherwood, T. K., *Absorption and Extraction*, N. Y.: McGraw-Hill, 1937.
Smock, R. M. and F. W. Southwick, "Air Purification in Apple Storage", Bulletin 843, Cornell University, Ithaca, N. Y.: 1948.

DISCUSSION

R. C. EDWARDS, Pompton Plains, N. J.: In food holding refrigerators is the problem of odor transfer from one stored food to another more serious with refrigerators equipped with forced convection evaporators as compared to refrigerators equipped with gravity operated evaporators?

What is the physical mechanism of the phenomena of adsorption of gases by activated carbon?

Is ammonia the only hydrocarbon that will not be adsorbed?

CLOSURE BY AUTHOR BRODY: On the basis of the theory of odor and odor transfer, there might possibly be an increase in odor transfer from one material to another due to forced air circulation. There also might be increased absorption in the evaporator which reduces the problem. According to field complaints, forced air circulation presents a problem, but I have no direct experience or knowledge of it.

The mechanism of odor adsorption is not really known. Essentially, the activation process removes hydrocarbons and everything but pure carbon from the system, leaving a porous pure carbon structure. There is an electrical charge on the carbon surface, and since odor molecules are usually polar, there is an attraction of mobile odor molecules for charcoal surfaces. Bonding, while fairly good, is not true chemical bonding, so the odor can be desorbed by heating. The bonding is sufficiently strong to retain the odor on the surface of the activated charcoal for an indefinite period under normal conditions.

Ammonia is not a hydrocarbon, but it is one of the few food degradation odors which is not adsorbed except by specially-treated activated charcoal.

UNIDENTIFIED SPEAKER: At one time there was much excitement in the scientific world to clarify the basis of odor using an infrared spectrum. Is this being used today?

AUTHOR BRODY: Many odoriferous materials have been classified on the basis of their infrared spectra. There is a theory that infrared emission of a molecule is that which is sensed by the olfactory nerve endings and transmitted to the brain as odor. There has been some experimental work which separated bees from the odor source by salt crystals which transmitted infrared. The major objection to this theory is that no one can conceive of body temperature differential causing black body radiation sufficiently high enough to create a detectable sensation.

1712

No. 1712

Solar Heat Gain Factors for Windows with Drapes

N. OZISIK

L. F. SCHUTRUM
Member ASHRAE

Effectiveness of drapes in reducing solar heat gain through sunlit glass windows was investigated experimentally by testing drapes of different materials and colors in combination with a regular plate glass and a heat absorbing glass. The results are presented in terms of the solar heat transfer factor, K, defined as the ratio of the solar heat gain through a glass and a drape combination to the incident solar radiation on the glass surface. The K factor curves are given for the entire range of solar reflectance and absorptance of the shade materials and for different glasses. Knowing the type of glass and solar properties of the shade material, the solar heat gain can be determined from the curves.

The over-all coefficients of heat transfer based on indoor and outdoor air temperature differences are also given.

This paper presents the results of an investigation on the effect of drapes on heat flow through a sunlit glass. The investigation was carried out at the ASHRAE Research Laboratory under the guidance of the former TAC on Heat Transfer Through Fenestration.*

The results of similar research for roller shades was presented in an earlier paper,[1] and the present work is a part of the continuing program of research to develop data on heat flow through shading devices.

The materials commonly used as drapes ranged in transmittance for solar radiation from about 70 per cent to almost opaque, and reflectance and absorptance were

N. Ozisik is a Research Engineer and L. F. Schutrum a Research Supervisor, ASHRAE Research Laboratory. This paper was presented at the ASHRAE Semiannual Meeting in Dallas, Texas, February 1-4, 1960.

* D. D'Eustachio, Chairman; R. C. Jordan, Vice Chairman; F. L. Bishop; T. C. Carson; O. D. Englehart; W. B. Ewing; C. W. Kelly; J. B. Leavy; E. C. Miles; Bruno Morabito; F. W. Mowrey; G. R. Munger; O. L. Pierson; D. J. Vild; O. F. Wenzler; C. J. Youngblood.

TABLE I

SOLAR PROPERTIES OF DRAPERY MATERIALS AND GLASSES

Material	Transmittance	Absorptance	Reflectance
Cotton, dark green	0.05	0.80	0.15
Cotton dark green, vinylcoated	0	0.85	0.15
Cotton, beige	0.23	0.26	0.51
Fiber glass, dark grey	0.11	0.60	0.29
Fiber glass, tan	0.14	0.44	0.42
Fiber glass, light grey	0.23	0.30	0.47
Fiber glass, off white	0.35	0.05	0.60
Glass cloth*, white with golden stripes	0.54	0.05	0.41
Dacron, white	0.70	0.02	0.28
Glasses			
Ordinary window	0.87	0.05	0.08
Regular plate	0.77	0.16	0.07
Heat absorbing	0.41	0.53	0.06

Note: All values are for normal incidence.
* Same material as used in Reference 3.

variables for a given transmittance. The types of materials tested were selected with the advice of the manufacturers of drapery materials, to cover the range of these variables.

A 100 per cent fullness** was used for all the drapes tested except one. Separate tests were made to investigate the effect of pleating on the transmittance and reflectance.

TYPES OF MATERIALS TESTED

Drapery materials selected for testing included the following types:

1) Cotton, dark green, 6.06 oz per sq yd, yarn counts: 91 warp-36 filling.
2) Cotton, dark green, vinyl coated (same material as used for roller shade studies).
3) Cotton, beige, 6.18 oz per sq yd, yarn counts: 91 warp-36 filling.
4) Fiber glass, dark grey.
5) Fiber glass, tan, 7.55 oz per sq yd, yarn counts: 57 warp-29 filling.
6) Fiber glass, light grey.
7) Fiber glass, off white, 5.72 oz per sq yd, yarn counts: 61 warp-58 filling.
8) Glass cloth, white with golden stripes.
9) Dacron, white, 1.8 oz per sq yd, yarn counts: 86 warp-81 filling.

The solar reflectance and transmittance of the materials tested were measured at the Laboratory using a pyrheliometer. Solar reflectance of the flat material was determined by comparing reflectance with that of a magnesium carbonate block, for which the reflectance was approximately 0.95. The solar transmittance of the flat material is the ratio of the sun's energy

** Width of cloth was twice that of drape for a 100 per cent fullness, and three times for a 200 per cent fullness.

passing through the cloth to the energy incident upon the cloth. The solar transmittance and reflectance of the drapery materials thus tested are given in Table I.

Similar tests were made to determine the transmittance and reflectance of the materials when pleated like a drape. The pleated form was produced by fixing the material between two imposed frames 25 in. sq, the intermatching edges of which were cut to simulate the pleats of a drape. The reflectance and transmittance of the pleated material were compared with those of the flat material by alternate readings of the pyrheliometer. In the range of transmittances from 20 to 50 per cent, the direct normal transmittance of a drape with 100 per cent fullness was almost the same as that of the flat material, but at 45 deg. incidence was about 20 per cent less. For diffuse solar radiation, the transmittance of a drape was about 20 per cent less than that of the flat material. The reflectance of the drape was about 15 to 20 per cent less than that of the flat material for normal incidence and 5 to 10 per cent less for 45-deg. incidence.

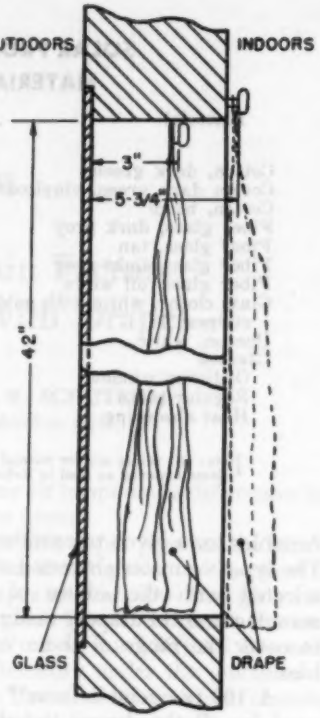

Fig. 1 Position of drapes

Test apparatus—The solar calorimeter used in these studies was described in an earlier publication.[3] The 42 in. sq opening of the calorimeter, covered with a ¼-in. thick glass, was used as the test window through which heat gain was measured. The properties of the glasses used are given in Table I.

The drape was hung with a standard light weight rod behind the glass as shown in Fig. 1, and the distance between the rod and glass was either 3 or 5¾ in. Heat passing through the glass and shade was collected by the fluid circulating in the tubes of the calorimeter, and the inlet temperature of the circulating liquid could be controlled as desired.

Intensity of direct and diffuse solar radiation was measured with two Eppley thermo-electric type pyrheliometers. The amount of heat transfer was obtained from the tem-

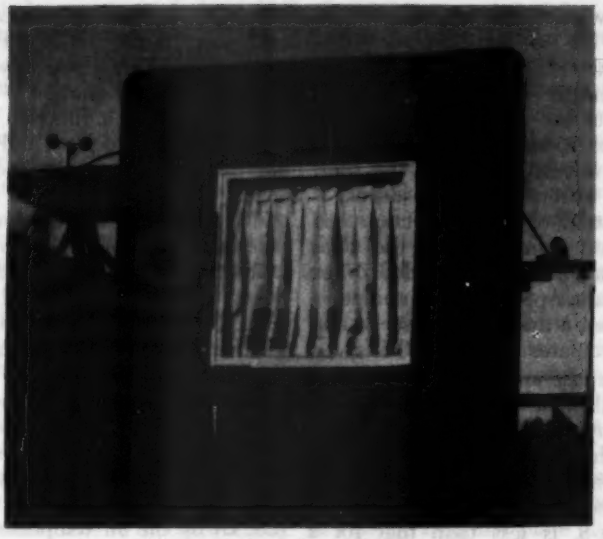

Fig. 2 The solar calorimeter

perature rise and the flow rate of the circulating liquid. All temperatures were measured by means of copper-constantan thermocouples. A view of the solar calorimeter with a drape in the window is shown in Fig. 2.

Test procedure — Over-all coefficients of heat transfer for a glass and drape combination were determined from the winter tests with an average outdoor air temperature of about 25 F and without solar radiation. Effect of spacing between the glass and drape on the U values was investigated by varying the rod to glass spacing from 3 to 5¼ in.

The summer heat gains were investigated with solar radiation, and tests were made either with the calorimeter following the sun or with a fixed orientation. Drapes from nine different materials were tested in combination with regular plate and/or heat absorbing glass. The inside surface of the solar calorimeter was kept at a nominal temperature of 75 F.

Analysis of solar heat gain — When solar radiation falls upon a glass with a drape, part of this radiation is transmitted through the glass and drape, unless the drape is opaque, part is reflected back, and the remainder is absorbed by the glass and drape. Knowing the transmittances and reflectances of the glass and drape and the intensity of the solar radiation, the energy transmitted can be calculated. If the edges of the drape were sealed

to the window frame so that there would be no air circulation between the glass-drape spacing and the room, it would be possible to calculate the amount of heat flow into the room by convection and radiation resulting from the solar energy absorption of the drape. A calculation of the convection and radiation component of the solar heat gain for such a sealed drape is given in Appendix A. In practice, however, a drape hangs freely, and air circulates between the glass-drape space and the room, and additional heat is carried into the room by the circulating air. Therefore, the convection and radiation component of solar heat gain with a sealed drape, as given by Equation A-8, is less than that for a freely hanging drape, but the additional heat gain due to air circulation could not be calculated.

RATIO FROM TESTS

Here, the ratio of the convection and radiation component of the solar heat gain with a freely hanging drape to that with a sealed drape as obtained from Equation A-8 was determined from the test data. Hence, the convection and radiation component of the solar heat gain with a freely-hanging drape can be calculated by multiplying Equation A-8 by this ratio.

Total solar heat gain is the sum of the transmitted and convection-radiation components of the solar heat gain. In order to simplify the heat gain calculations, a solar heat transfer factor K, defined as the ratio of the solar heat gain through a glass and drape (freely hanging) combination to the incident solar radiation on the outer surface of the glass was developed in Appendix B. Equation B-7 gives this K factor as a function of the solar properties of glass and drape, the indoor and outdoor conductances, the conductances of the sealed space, and an experimentally determined factor which is above unity for unsealed drape and reduces to unity for a sealed drape. This K factor, when multiplied by the incident solar radiation gives the total solar heat gain.

There is also the conduction heat gain due to the indoor-outdoor air temperature differences. This can be obtained by multiplying the over-all coefficient of heat transfer (i.e. U) by the air temperature difference.

Thus, the total heat gain through a glass and drape combination can be expressed by the following equation:

$$Q = K\,I\,A + U\,(t_o - t_i)\,A \qquad (1)$$

Note, however, that K values are different for diffuse and direct solar radiation. Furthermore, if only a portion of the glass surface is irradiated by the direct solar radiation, the Equation 1 can be written as follows:

$$Q = K_D\,I_D\,A\,(1 - P) + K_d\,I_d\,A + U\,(t_o - t_i)\,A \qquad (2)$$

where P is the fraction of the glass surface in shade.

TEST RESULTS

Over-all coefficients of heat transfer, U, for glass and drape combinations were determined from the winter tests with an average out-

door air temperature of about 25 F with no solar radiation. The U value for materials of medium transmittance, after being adjusted for an outdoor conductance of 3 Btu per (hr) (sq ft) (F), was 0.76. Note that this value is the same as that for a glass with a roller shade. For materials with low or high transmittance, the over-all coefficients of heat transfer were about 5 per cent lower or higher than this respectively. These results are for a rod located 3 in. from the glass; with the rod at 5¾ in., U values were about 10 per cent higher.

As indicated above, the total heat gain measured by the calorimeter was the sum of conduction heat transfer due to indoor-outdoor air temperature difference, and the transmitted and convection-radiation components of the solar heat gain. The conduction heat transfer and the transmitted component could be calculated from the known values of the over-all coefficient of heat transfer, indoor and outdoor air temperature difference, and the transmittance of the drape and glass. The convection and radiation component of the solar heat gain could, therefore, be determined by deducting from the total heat gain the conduction and transmitted components. The experimental value thus obtained was then compared with the convection and radiation component of solar heat gain for a sealed drape as calculated from Equation A-8. In this equation, the value of space conductance h_a was taken the same as that suggested in the ASHRAE GUIDE for a vertical ¾- to 4-in. air space with a mean emmisivity of about 0.83; and the solar absorptance of the drape material with 100 per cent fullness was used.

The ratio of the convection and radiation component of the solar heat gain with an unsealed drape to that of a sealed drape was determined for over 150 tests made with nine different materials. As shown in Table I, the solar absorptances of these materials ranged from 5 to 85 per cent, transmittances from zero to 70 per cent, and the emissivity for long-wave radiation was about 0.9 on both sides of the material.

For all the drapes tested, this ratio averaged within ± 6 per cent of 1.25 for a regular plate glass and 1.35 for a heat absorbing glass. Knowing this ratio, the solar properties of the glass and drape material, and taking the space conductance h_a, indicated above, the solar heat gain factor K could be calculated from Equation B-7 for any indoor and outdoor conductances. Fig. 3 gives the K factors thus calculated for an outdoor conductance of 3 Btu per (hr) (sq ft) (F) and an indoor conductance referred to in Ref. 1, for a heat absorbing, a regular plate and an ordinary window* glass, as a function of solar absorptance and transmittance of the flat material. Fig. 4 shows the data in Fig. 3 replotted as a function of the solar reflectance of the material. Since the sum of reflectance, transmittance and absorptance is unity,

* Although no tests were made with an ordinary window glass, K values are included for this glass in order to complete the data for the commonly used types of glasses.

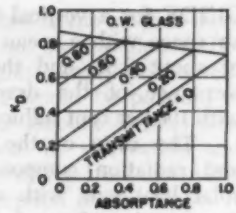

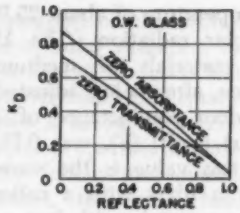

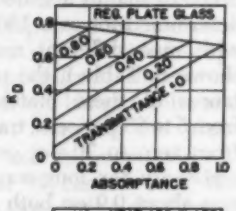

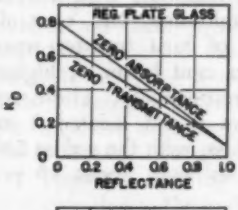

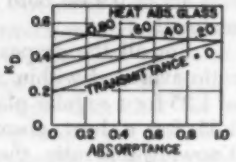

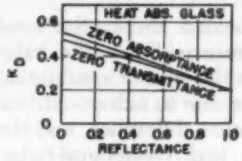

Fig. 3 Fig. 4

Fig. 3 and 4 Values of the solar heat-transfer factor K_D for direct solar radiation and incidence angles ranging from 0 to 50 deg

Note 1: For incidence angles in the range 50 to 85 deg, decrease K_D by 10 per cent, for each 10 deg increase in incidence angle above 50 per cent.
Note 2: K_d values for diffuse solar radiation are 10 per cent less than the values of K_D given in the graphs.

with a given reflectance many combinations of transmittance and absorptance are possible. With a given reflectance, however, a zero transmittance and a zero absorptance are the two limiting conditions. Therefore, K curves in Fig. 4 are for these limiting cases, and K values for all combinations of transmittance and absorptance lie between these two curves. The band between the two limiting curves is considerably reduced by plotting K against the solar reflectance. This indicates that the solar reflectance of the material is the predominant variable influencing the K factor. With a maximum deviation of about 10 per cent, these two limiting curves could even be represented by a mean curve; such an approximation could be useful in estimating K values for practical purposes, knowing only the solar reflectance

of the flat material.

The K factors given in Figs. 3 and 4 are for direct solar radiation and for incidence angles* from zero to 50 deg. For incidence angles above 50 deg., K values in these figures should be decreased by 10 per cent for each 10 deg. increase in incidence angles. K factors for diffuse solar radiation are about 10 per cent less than Fig. 3 or 4 values.

The drape temperature was measured with thermocouples at different points. With solar radiation, however, the temperature reading of each thermocouple varied considerably depending on the location of the junction on the pleats. No satisfactory average could be obtained. Furthermore, with translucent materials, the thermocouple readings were influenced by the bonding material which attached the junction to the drape. However, it was concluded that the average temperature of a drape was a little less than that of a roller shade[1] of the same material.

Application of data—The heat flow through a glass with a drape can be calculated with Equation 2, knowing the intensity of incident solar radiation on the glass surface, indoor and outdoor air temperatures, and the K and U values. The K values for incidence angles 0 to 50 deg. can be taken directly from Figs. 3 or 4; for incidence angles above 50 deg., Fig. 3 or 4 values should be adjusted by decreasing K by 10 per cent for each 10 deg. increase in incidence angle above 50 deg. The K value for the diffuse solar radiation can be taken as 10 per cent less than the Fig. 3 and 4 values. The U value for a drape with glass can be taken as 0.76.

The application is illustrated in the following example: Calculate the total heat gain at 1 p.m. through a south facing, 3 ft wide x 5 ft high regular plate glass window covered by a fully drawn drape made of a material with a solar absorptance 0.40 and transmittance 0.15. The window set back is such that at 1 p.m., 10 per cent of the surface of the glass is in shadow. The intensities of the solar radiation are 285 Btu per (hr) (sq ft) for direct (normal), and 28 Btu per (hr) (sq ft) for diffuse on a south wall. The incidence angle of the direct beam on the south wall is 69.3 deg., and the cosine of the incidence angle 0.3535. Indoor and outdoor air temperatures are 75 F and 93 F respectively.

Solution — The total heat gain through a glass with drape can be calculated from Equation 2:

$$Q = K_D I_D A (1 - P) + K_d I_d A + U (t_o - t_i) A$$

For a given example, $A = 3 \times 5 = 15$ sq ft, $P = 0.10$, $I_D = 285 \times 0.3535 = 101$ Btu per (hr) (sq ft), $t_o = 93$ F and $t_i = 75$ F. For a material with solar absorptance 0.40, transmittance 0.15 and in combination with a regular plate glass, from Fig. 3, $K = 0.42$. This K value, however, is for incidence angles from 0 to 50 deg.; and for a 69.3 deg. incidence angle $K_D = 0.34$ (i.e. decreasing K by 10 per cent for each 10 deg. increase in inci-

* Angle between the sun's beam and the normal to the glass surface.

dence angle above 50 deg.). For diffuse solar radiation $K_d = 0.38$. Substituting the foregoing values in Equation 2: $Q = 0.34 \times 101 \times 15 \times (1 - 0.10) + 0.38 \times 28 \times 15 + 0.76 \times (93 - 75) \times 15 = 828$ Btu/hr, the total heat gain.

RESULTS

The solar heat gain factor K given in Figs. 3 and 4 is a direct measure of effectiveness of a glass and a drape combination in excluding solar heat; the smaller the K, the smaller is the solar heat gain. However, considering the fact that a shading device should permit transmission of a reasonable amount of daylight into the room while excluding the solar heat, the smallest K value accompanied with a zero transmission is not necessarily a desirable property. A compromise is needed. The two curves in Fig. 4 give K values as a function of the solar reflectance of material for a zero transmittance (i.e. opaque) and a zero absorptance.

K values for an opaque material are on the zero transmittance curve, and those for translucent materials are between the zero transmittance and zero absorptance curves. Since a translucent material permits daylight to enter a room, such a material with reasonable solar reflectance may be a good compromise between heat exclusion and light transmission requirements of a drape.

The K value of a drape can be determined from Fig. 4, knowing solar reflectance of the material. The reflectance for the visible range of the spectrum, however, is a more commonly used property than the solar reflectance. Therefore, if a relation were known between these reflectances, Fig. 4 would have a more practical application in determining the K value. Furthermore, knowing the relation between the transmittances of the material in the solar and visible range of the spectrum, Fig. 3 or 4 would serve to indicate the amount of light as well as the solar heat entering the specific room.

This phase of the problem is not included in the present investigation; it can be a subject of a separate investigation.

All drapes tested except one had 100 per cent fullness. The K values for these drapes were not appreciably different from those given in an earlier paper[1] for roller shades of the same material. Similarly, an increase in the amount of fullness up to 200 per cent w[illegible] not significantly influenced th[illegible] value.

The data in Fig. 4 indicate that the K value is smaller for materials with a high solar reflectance; and such materials usually are the light colored materials, (i.e. white, light beige, cream, etc.). A light colored material with a medium transmittance will let daylight into the room and exclude more solar heat than a dark material. With a white drape of medium to zero (opaque) transmittance, the K value is slightly higher with a heat absorbing glass than with an ordinary window glass. However, with dark materials (i.e. low solar reflectance) the K value is lower with a heat absorbing glass than with an ordinary window glass.

CONCLUSIONS

Solar heat gain through a single glass with a drape can be obtained by multiplying the incident solar radiation on the glass by the K factor.

K factors are given as a function of the solar properties of drape materials for an ordinary window, a regular plate and a heat absorbing glass in Figs. 3 and 4.

The solar reflectance of a material on the glass side largely determines the solar heat gain. A material with a high solar reflectance on the glass side excludes more solar heat than a material with a low reflectance.

Effectiveness of glass and drape combinations in excluding solar heat can be compared directly by their K factors. For the draperies tested with regular plate glass, solar heat gains ranged from about 45 to 75 per cent of those for unshaded glass with white (60 per cent reflectance) to dark green (15 per cent reflectance) drapes respectively.

ACKNOWLEDGMENT

The authors acknowledge with thanks the suggestions and guidance of the Technical Advisory Committee on Heat Transfer Through Fenestration and the assistance and helpful criticism of their colleagues of the ASHRAE Research Laboratory staff. Special thanks are due to the Qwens-Corning Fiberglas Corporation and the S. M. Hexter Company for their advice in selecting and identifying the materials.

REFERENCES

1. *Heat Gain through a Glass with a Roller Shade*, by N. Ozisik and L. F. Schutrum, ASHRAE Journal, April, 1959.
2. *Heat Gain through Windows Shaded by Canvas Awnings*, by N. Ozisik and L. F. Schutrum, *Heating, Piping & Air Conditioning*, ASHAE Journal Section, May, 1958.
3. *Solar Radiant Gains through Directional Glass Exposure*, by R. D. Crammer and L. W. Neubauer, *Heating, Piping & Air Conditioning*, ASHAE Journal Section, November, 1958.

NOMENCLATURE

A = Area of glass surface, sq ft
CR = Convection and radiation heat gain into the room with a freely-hanging drape, Btu per (hr) (sq ft)
CR' = Convection and radiation heat gain into the room with a sealed drape, Btu per (hr) (sq ft)
f = CR/CR' = a ratio
h = Thermal conductance, Btu per (hr) (sq ft) (F)
I = Intensity of solar radiation on a vertical wall, Btu per (hr) (sq ft)
I_D = Intensity of direct solar radiation on a vertical wall, Btu per (hr) (sq ft)
I_d = Intensity of diffuse solar radiation on a vertical wall, Btu per (hr) (sq ft)
αI_g = Solar energy absorbed by the glass, Btu per (hr) (sq ft)
αI_s = Solar energy absorbed by the drape, Btu per (hr) (sq ft)
αI_{gs} = Solar energy absorbed by glass drape combination, Btu per (hr) (sq ft)
K = Solar heat transfer factor, dimensionless
P = Fraction of the glass surface in shade, dimensionless
Q = Total heat gain into the room, Btu per hr
T = Solar transmittance, dimensionless
U = Over-all coefficient of heat transfer, Btu per (hr) (sq ft) (F)
U' = Over-all coefficient of heat transfer, for a sealed drape, Btu per (hr) (sq ft) (F)
α = Solar absorptance, dimensionless
r = Solar reflectance, dimensionless
t = Temperature, Fahrenheit degree
a, g, s = space between glass and drape, glass, and drape
i, o = inside and outside

APPENDIX A

Convection and radiation heat gain with a sealed drape – Consider a single glass and a drape with sealed edges so that no air is circulating from the glass-drape space into the room. With solar radiation falling

upon the glass surface, the energy balance equations for the glass and drape are:

$$\alpha I_g = h_o (t_g - t_o) + h_a (t_g - t_a) \quad \text{(A-1)}$$

$$\alpha I_a = CR' + h_a (t_a - t_g) \quad \text{(A-2)}$$

From equations (A-1) and (A-2), eliminating t_g:

$$\left(\frac{1}{h_o} + \frac{1}{h_a}\right) CR' + t_a = \frac{1}{h_o} \alpha I_g + \left(\frac{1}{h_o} + \frac{1}{h_a}\right) \alpha I_a + t_o \quad \text{(A-3)}$$

also, $CR' = h_i (t_a - t_i)$ (A-4)

From equations (A-3) and (A-4), eliminating t_a:

$$\left(\frac{1}{h_o} + \frac{1}{h_a} + \frac{1}{h_i}\right) CR' + t_i = \frac{1}{h_o} \alpha I_g + \left(\frac{1}{h_o} + \frac{1}{h_a}\right) \alpha I_a + t_o \quad \text{(A-5)}$$

let, $$\frac{1}{h_o} + \frac{1}{h_a} + \frac{1}{h_i} = \frac{1}{U'} \quad \text{(A-6)}$$

U' = over-all coefficient of heat transfer for a glass with a sealed drape.

Substituting (A-6) in (A-5) and rearranging

$$CR' = U' \left[\frac{1}{h_o} \alpha I_g + \left(\frac{1}{h_o} + \frac{1}{h_a}\right) \alpha I_a + (t_o - t_i)\right] \quad \text{(A-7)}$$

or, when $t_i = t_o$:

$$CR' = U' \left[\frac{1}{h_o} \alpha I_g + \left(\frac{1}{h_o} + \frac{1}{h_a}\right) \alpha I_a\right] \quad \text{(A-8)}$$

and this is the convection-radiation component of the solar heat gain for a glass and a drape with sealed edges.

APPENDIX B

The K factor – In Appendix A it was shown that the convection and radiation component of the solar heat gain for a glass and drape with sealed edges was

$$CR' = U' \left[\frac{1}{h_o} \alpha I_g + \left(\frac{1}{h_o} + \frac{1}{h_a}\right) \alpha I_a\right] \quad \text{(B-1)}$$

and experimentally it was shown that the ratio of the convection-radiation component of the solar heat gain with an unsealed drape to that for a sealed drape was constant. Hence,

$$CR = f.CR' = f.U' \left[\frac{1}{h_o} \alpha I_g + \left(\frac{1}{h_o} + \frac{1}{h_a}\right) \alpha I_a\right] \quad \text{(B-2)}$$

where

$$\alpha I_g = I . \alpha_g . \left(1 + T_g \frac{r_a}{1 - r_g r_a}\right) \quad \text{(B-3)}$$

$$\alpha I_a = I . \alpha_a . \frac{T_g}{1 - r_g r_a} \quad \text{(B-4)}$$

Transmitted component of the solar radiation is:

$$\text{Trans.} = I . T_g . T_a \frac{1}{1 - r_g r_a} \quad \text{(B-5)}$$

Defining the solar heat transfer factor, K, as follows:

$$K = \frac{CR + Trans}{I} \qquad \text{(B-6)}$$

We get from equations B-2, B-3, B-4, B-5, and B-6:

$$K = f \cdot U' \left[a_g \cdot \frac{1}{h_o} \left(1 + T_g \frac{r_s}{1 - r_g r_s} \right) + a_s \left(\frac{1}{h_o} + \frac{1}{h_s} \right) \frac{T_g}{1 - r_g r_s} \right] + \frac{T_g T_s}{1 - r_g r_s} \qquad \text{(B-7)}$$

where, $U' = 1 / \left(\frac{1}{h_o} + \frac{1}{h_s} + \frac{1}{h_i} \right)$

f = experimentally determined factor.

DISCUSSION

C. L. BROWN, Memphis, Tenn.: In Table I, dacron has a transmittance of 0.70 and a reflectance of 0.28 Cotton-beige has a reflectance of 0.51. Is there a difference in density, or is the material itself that much different in its ability to absorb or reflect heat?

CLOSURE BY C. M. HUMPHREYS: No attempt was made to determine why each of the fabrics behaved the way it did. In general, the higher transmittance values seemed to be associated with lighter weight, lighter colored and loosely-woven fabrics. That portion of the solar energy not transmitted through the fabric was either reflected or absorbed. Reflectance was high for lighter colors, while the darker colors showed high absorbance.

K. D. SIMON, Van Nuys, Calif.: Is there a comparison in broad percentages of the drapes versus Venetian blinds? Within about 15 or 20%?

C. M. HUMPHREYS: Data on other shading devices is available and may readily be compared with the data presented here on drapes. The tests have shown that the effectiveness of drapes may vary from 45-75%, depending upon color, location, and other factors. Similarly, wide variations were found in other types of shading devices. In view of these wide variations it would be impossible to say that one type of sun shade excels another by any particular amount.

However, the data are available for comparing a particular shade of one type with a particular shade of another type. This is the only kind of comparison that has any real merit.

1713

is a ground-water temperature recommended by the U. S. Geological Survey, Water Resources Division, Anchorage, Alaska.[2]

Ground temperature for Fairbanks is an average monthly temperature taken at a depth of 15 ft for a two year period, from October, 1946, to September, 1948.[3] A permafrost, or year-round frost condition exists in the Fairbanks area, from about the 6 to the 420 ft level. As one progresses further north the condition is found to exist nearer the surface. Other factors, such as vegetation and habitation, affect its nature.

Ground temperature for Juneau is the same as the ground-water temperature for Seattle, Washington, as recommended by the Snow, Ice and Permafrost Research Establishment, Corp of Engineers, U. S. Army, Wilmette, Illinois.[4]

Wind velocity (Column 7): The wind velocity to be used in design, as recommended by TAC is the average of the summer wind velocities, recorded hourly, for the period of record. In the table the period of record is from June, 1953, to August, 1955.[1] In 1953, a new form enabled the climatologist to record wind velocities along with temperatures. The previous forms contained space for temperatures and precipitation data.

Daily range of temperatures (Column 9): The daily range of temperatures for Anchorage, Fairbanks and Juneau is taken as the difference between the average of the average monthly maxima and the average of the average monthly

TABLE II

VALUES OF "K", THE COSINE OF THE INCIDENT ANGLE, FOR VARIOUSLY ORIENTED WALLS AND A HORIZONTAL SURFACE*

Lat.	Sun Time AM		Values of K, Cosine of the Incident Angle N	NE	E	SE	S	SW	Horiz.
	5	7	0.436	0.940	0.890	0.325			0.104
	6	6	0.184	0.802	0.948	0.540			0.250
	7	5		0.683	0.927	0.678	0.031		0.374
60 deg. N.	8	4		0.435	0.840	0.753	0.224		0.492
	9	3		0.208	0.700	0.780	0.404		0.587
	10	2			0.507	0.743	0.543	0.025	0.669
	11	1			0.282	0.648	0.663	0.250	0.719
	12					0.472	0.670	0.472	0.743
	5	7	0.435	0.935	0.888	0.322			0.139
	6	6	0.168	0.792	0.950	0.548			0.258
	7	5		0.606	0.925	0.700	0.064		0.374
65 deg. N.	8	4		0.400	0.838	0.785	0.272		0.469
	9	3		0.172	0.698	0.815	0.455		0.552
	10	2			0.505	0.785	0.603	0.068	0.615
	11	1			0.289	0.688	0.693	0.304	0.662
	12					0.516	0.731	0.516	0.682
	PM		N	NW	W	SW	S	SE	

* This table is a continuation of Table V, Chapter 13, *ASHAE Guide*, 1958.

minima for the month of July. The period of record is from the time the station came into existence to July, 1955.[5]

SUMMER SOLAR HEAT DATA

In order to arrive at working data from which solar heat gains through glass under summer conditions in the Alaskan cities can be found, it was necessary to establish the basic solar data for the latitudes of these cities. Since the existing data in the current edition of the GUIDE cover the North Latitudes up to 50 deg., it was clear that if the corresponding data were determined for 60 and 65 deg. North Latitude, the range would be extended sufficiently to cover most of Alaska.

The first step was to establish values of K, the cosine of the incident angle for various wall orientations and for 60 and 65 deg. North Latitude. This would amount to an extension of Table V, Chapter 13, ASHRAE GUIDE, 1958, and the extension appears in this paper as Table II.

The next step was similarly to extend Table VI, Chapter 13, 1958 GUIDE, so that values of γ, the wall solar azimuth, would be available for 60 and 65 deg. North Latitude. This extension appears as Table III of this paper.

Completion of Table III necessitated the determination of the solar altitudes, β, and the wall solar azimuths, γ, for 60 and 65 deg. North Latitudes. To accomplish this, values were needed from the hours 0500 to 1900 (24-hr clock system). The Greenwich Hours Angle (GHA) for each hour, for August 1st, for the star SUN is found in the

TABLE III
VALUES OF THE WALL SOLAR AZIMUTH, γ, FOR VARIOUSLY ORIENTED WALLS AND SOLAR ALTITUDE*

Lat.	Sun Time AM	Solar Alt., β Deg.	Azimuth Angle, Degrees N	NE	E	SE	S	SW
	5 7	6.0	64	19	26	71		
	6 6	14.5	79	34	11	56	Shade	
	7 5	22.0	Shade	47	2	43	88	
60 deg. N.	8 4	29.5		60	15	30	75	
	9 3	36.0		75	30	15	60	Shade
	10 2	42.0		Shade	47	2	43	88
	11 1	46.0			66	21	24	69
	12	48.0			90	45	0	45
	5 7	8.0	64	19	26	71		
	6 6	15.0	80	35	10	55	Shade	
	7 5	22.0	Shade	49	4	41	86	
65 deg. N.	8 4	28.0		63	18	27	72	
	9 3	33.5		78	33	12	57	Shade
	10 2	38.0		Shade	50	5	40	85
	11 1	41.5			68	23	22	67
	12	43.0			90	45	0	45
	PM		N	NW	W	SW	S	SE

* This table is a continuation of Table VI, Chapter 13, *ASHAE Guide*, 1958.

No. 1713

Alaska Summer Weather Data

ROBERT BURGGRAAF

The current edition of ASHRAE GUIDE does not contain weather data for either summer or winter conditions in the territory of Alaska. Now that the territory has attained statehood there is increased reason for including this information in the GUIDE. An additional consideration is that since 1941, the United States Government has placed more and more importance on the territory of Alaska, as a key to the national defense effort.

Due to this policy, areas of major population have grown up, principally around the capital city of Juneau, the seaport of Anchorage and in the agricultural district around Fairbanks. The Matanuska Valley and Kenai Peninsula, north and south of Anchorage, show the potential of large agricultural areas. Also, the Southeastern Peninsula and other interior areas show promise of becoming the most productive lumber, pulp and paper districts in the United States. A large food freezing business has, also, made a beachhead along the coastal region as a result of the growing $20,000,000 annual fishing business.

Available literature bears no evidence of summer outdoor design conditions having been established for the Alaskan cities. Also, there is no published information on Solar Heat Gain Values for locations further north than 50 deg. North Latitude. The most populated region of Alaska lies between the 56 deg. and 66 deg. North Latitude lines.

This paper aims to supply this missing information so far as existing available data permit.

SUMMER CLIMATIC DATA

In examining and analyzing the available summer weather data, the aim was to follow the recommendations of the TAC on Weather Design Conditions as far as possible. It was intended that in doing so a tabulation of data for the Alaskan cities would result essentially simi-

R. Burggraaf is with Harmon & Beckett, Inc.
This paper was presented at the ASHRAE Semiannual Meeting in Dallas, Texas, February 1-4, 1960.

lar to that appearing in Table II, page 291, of the 1958 edition of the GUIDE. This tabulation is presented here as Table I. The following comments are applicable to this Table.

Dry-bulb temperature (Column 5): The Technical Advisory Committee on Weather Data has recommended that the summer design dry-bulb temperature be the maximum hourly outdoor temperature which has been equalled or exceeded in 2½ per cent of the total hours of June, July, August and September for the period of record.

Due to the lack of complete information for the month of September and the fact that complete weather observations were taken only four times daily at Alaskan weather stations, the method of determination was necessarily altered in the present study. The summer design dry-bulb temperature shown in Column 5 of Table I is the maximum 6-hourly outdoor temperature which has been equalled or exceeded 2½ per cent of the total period of record in the months of June, July and August.[1]

Wet-bulb temperature (Column 6): The TAC has recommended that the summer design wet-bulb temperature be taken as that wet-bulb temperature which has been equalled or exceeded in 5 per cent of the hours during the months of the period of record. In view of the conditions under which the summer design dry-bulb temperature was determined, the summer design wet-bulb temperature is the maximum 6-hourly wet-bulb temperature which has been equalled or exceeded in 5 per cent of the total period of record in the months of June, July and August.[1]

Ground temperature (Column 8): Ground temperature for Anchorage

[1] Exponent numerals refer to References

TABLE I
WEATHER DATA FOR ANCHORAGE, FAIRBANKS AND JUNEAU

(all temperatures F)

1	2	3	4	5	6	7	8	9	10
City	Elev above sea, ft	Highest temp of record	Lowest temp of record	Design dry-bulb temp	Design wet-bulb temp	Avg wind vel, mph	Ground temp	Daily range of temp	Period of record[a]
Anchorage	134	84	—32	72	58	6.5	37	16.3	From 12/50 to 8/55
Fairbanks	434	92	—55	78	59	5.5	31	22.5	From 12/50 to 8/55
Juneau	24	82	—13	75	56	7.5	52	16.6	From 12/50 to 8/55

[a] Period of record does not include ground temperature and daily range of temperature.

is a ground-water temperature recommended by the U. S. Geological Survey, Water Resources Division, Anchorage, Alaska.[2]

Ground temperature for Fairbanks is an average monthly temperature taken at a depth of 15 ft for a two year period, from October, 1946, to September, 1948.[3] A permafrost, or year-round frost condition exists in the Fairbanks area, from about the 6 to the 420 ft level. As one progresses further north the condition is found to exist nearer the surface. Other factors, such as vegetation and habitation, affect its nature.

Ground temperature for Juneau is the same as the ground-water temperature for Seattle, Washington, as recommended by the Snow, Ice and Permafrost Research Establishment, Corp of Engineers, U. S. Army, Wilmette, Illinois.[4]

Wind velocity (Column 7): The wind velocity to be used in design, as recommended by TAC is the average of the summer wind velocities, recorded hourly, for the period of record. In the table the period of record is from June, 1953, to August, 1955.[1] In 1953, a new form enabled the climatologist to record wind velocities along with temperatures. The previous forms contained space for temperatures and precipitation data.

Daily range of temperatures (Column 9): The daily range of temperatures for Anchorage, Fairbanks and Juneau is taken as the difference between the average of the average monthly maxima and the average of the average monthly

TABLE II

VALUES OF "K", THE COSINE OF THE INCIDENT ANGLE, FOR VARIOUSLY ORIENTED WALLS AND A HORIZONTAL SURFACE*

Lat.	Sun Time AM	Values of K, Cosine of the Incident Angle N	NE	E	SE	S	SW	Horiz.
	5 7	0.436	0.940	0.890	0.325			0.104
	6 6	0.184	0.802	0.948	0.540			0.250
	7 5		0.683	0.927	0.678	0.031		0.374
60 deg. N.	8 4		0.435	0.840	0.753	0.224		0.492
	9 3		0.208	0.700	0.780	0.404		0.587
	10 2			0.507	0.743	0.543	0.025	0.669
	11 1			0.282	0.648	0.663	0.250	0.719
	12				0.472	0.670	0.472	0.743
	5 7	0.435	0.935	0.888	0.322			0.139
	6 6	0.168	0.792	0.950	0.548			0.258
	7 5		0.606	0.925	0.700	0.064		0.374
65 deg. N.	8 4		0.400	0.838	0.785	0.272		0.469
	9 3		0.172	0.698	0.815	0.455		0.552
	10 2			0.505	0.785	0.603	0.068	0.615
	11 1			0.289	0.688	0.693	0.304	0.662
	12				0.516	0.731	0.516	0.682
	PM	N	NW	W	SW	S	SE	

* This table is a continuation of Table V, Chapter 13, *ASHAE Guide*, 1958.

minima for the month of July. The period of record is from the time the station came into existence to July, 1955.[5]

SUMMER SOLAR HEAT DATA

In order to arrive at working data from which solar heat gains through glass under summer conditions in the Alaskan cities can be found, it was necessary to establish the basic solar data for the latitudes of these cities. Since the existing data in the current edition of the GUIDE cover the North Latitudes up to 50 deg., it was clear that if the corresponding data were determined for 60 and 65 deg. North Latitude, the range would be extended sufficiently to cover most of Alaska.

The first step was to establish values of K, the cosine of the incident angle for various wall orientations and for 60 and 65 deg. North Latitude. This would amount to an extension of Table V, Chapter 13, ASHRAE GUIDE, 1958, and the extension appears in this paper as Table II.

The next step was similarly to extend Table VI, Chapter 13, 1958 GUIDE, so that values of γ, the wall solar azimuth, would be available for 60 and 65 deg. North Latitude. This extension appears as Table III of this paper.

Completion of Table III necessitated the determination of the solar altitudes, β, and the wall solar azimuths, γ, for 60 and 65 deg. North Latitudes. To accomplish this, values were needed from the hours 0500 to 1900 (24-hr clock system). The Greenwich Hours Angle (GHA) for each hour, for August 1st, for the star SUN is found in the

TABLE III
VALUES OF THE WALL SOLAR AZIMUTH, γ, FOR VARIOUSLY ORIENTED WALLS AND SOLAR ALTITUDE*

Lat.	Sun Time AM	Solar Alt., ρ Deg.	Azimuth Angle, Degrees N	NE	E	SE	S	SW
	5 7	6.0	64	19	26	71		
	6 6	14.5	79	34	11	56	Shade	
	7 5	22.0	Shade	47	2	43	88	
60 deg. N.	8 4	29.5		60	15	30	75	
	9 3	36.0		75	30	15	60	Shade
	10 2	42.0		Shade	47	2	43	88
	11 1	46.0			66	21	24	69
	12	48.0			90	45	0	45
	5 7	8.0	64	19	26	71		
	6 6	15.0	80	35	10	55	Shade	
	7 5	22.0	Shade	49	4	41	86	
65 deg. N.	8 4	28.0		63	18	27	72	
	9 3	33.5		78	33	12	57	Shade
	10 2	38.0		Shade	50	5	40	85
	11 1	41.5			68	23	22	67
	12	43.0			90	45	0	45
	PM		N	NW	W	SW	S	SE

* This table is a continuation of Table VI, Chapter 13, *ASHAE Guide*, 1958.

TABLE IV

SOLAR ALTITUDES AND WALL SOLAR AZIMUTHS RELATIVE TO NORTH

Greenwich Mean Time, GMT	Hour Angle, HA	60 deg. N			65 deg. N		
		Altitude		Azimuth	Altitude		Azimuth
0500-1900	110	6 deg.	01.5'	64.0 deg.	8 deg.	11.9'	64.5 deg.
0600-1800	92	14	32.3	79.1	15	25.7	80.4
0700-1700	77	21	59.9	91.9	21	44.7	93.9
0800-1600	62	29	23.8	105.9	27	57.2	108.1
0900-1500	47	36	17.6	120.3	33	33.9	123.3
1000-1400	32	42	08.1	137.2	38	23.0	140.0
1100-1300	17	46	15.0	156.3	41	38.3	158.2
1200	00	47	58.5	180.0	42	58.8	180.0

American Air Almanac.[6] To obtain an Hour Angle (HA) before 1200 hours Greenwich Mean Time (GMT), the GHA is subtracted from 360. For an HA after 1200 hours GMT, GHA is the HA. The altitude and azimuth for each HA is found in the tables in Ref. 7. Table IV of this paper was prepared from these data. To obtain the altitudes and azimuths other than North, β and γ for North from Table IV were plotted on polar co-ordinates (Fig. 1) and interpolated relative to the desired points of Table III.

To understand what further data are needed to calculate solar gains through glass at the Alaska

TABLE V

INSTANTANEOUS RATES OF HEAT GAIN DUE TO TRANSMITTED DIRECT AND DIFFUSE OR SKY SOLAR RADIATION BY A SINGLE SHEET OF UNSHADED COMMON WINDOW GLASS*

Lat.	Sun Time AM	Instantaneous Heat Gain in BTU per (hr) (sq ft) N	NE	E	SE	S	SW
	5 7	32	67	66	22		
	6 6	23	118	145	74		
	7 5		139	195	138	10	
60 deg. N.	8 4		105	198	172	37	
	9 3		45	176	189	90	
	10 2			133	188	131	15
	11 1			68	168	160	53
	12			26	121	171	116
	5 7	38	90	89	30		
	6 6	22	129	157	89		
	7 5		124	198	142	14	
65 deg. N.	8 4		86	179	174	49	
	9 3		38	172	191	99	
	10 2			130	196	142	18
	11 1			71	173	170	65
	12			28	129	182	123
	PM	N	NW	W	SW	S	SE

* This table is a continuation of Table XII, Chapter 13, *ASHAE Guide*, 1958.

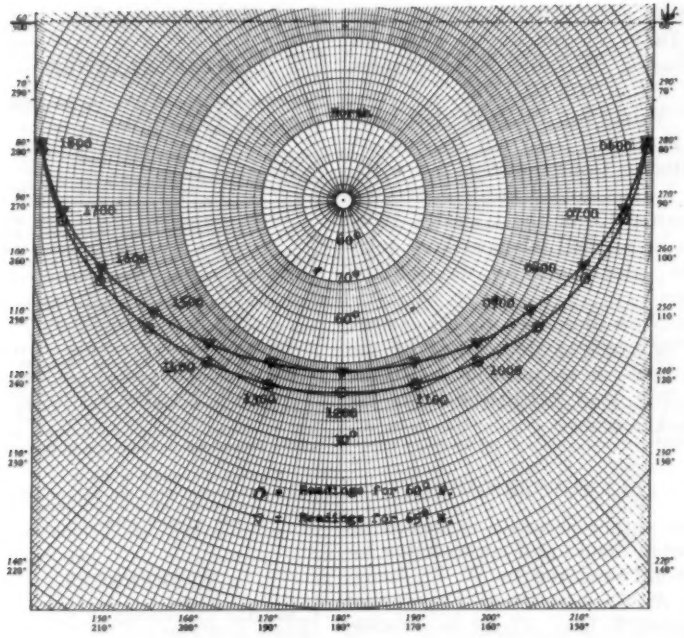

Fig. 1 Trace of the sun's path across the sky at 60 and 65 deg. North Latitude on August 1

latitudes, the heat balance equation for a section of glass is helpful. This equation can be stated for a unit time interval as:

$$\left[\begin{matrix}\text{Total heat flow,}\\ \text{through glass section}\end{matrix}\right] = \left[\begin{matrix}\text{Transmitted}\\ \text{Solar radiation}\end{matrix}\right] + \left[\begin{matrix}\text{Absorbed}\\ \text{Solar radiation}\end{matrix}\right] + \left[\begin{matrix}\text{Convective and radiative exchanges}\\ \text{between outer surfaces of glass and}\\ \text{outdoor surroundings}\end{matrix}\right] \quad (1)$$

To obtain values for the first term on the right side of Equation 1 it is necessary to have instantaneous rates of heat gain for the Alaska latitudes similar to the values found in Table XII, Chapter 13, of the GUIDE, 1958, for the more southerly latitudes. These values for 60 and 65 deg. North Latitude have been calculated by Equation 2:

$$I_T = I_{DT} + I_{dT} = (K)\ (I_{DN})\ (\tau_d) + (I_d)\ (\tau_d) \quad (2)$$

The resulting values are tabulated as Table V.

Values for use in the second right-hand term of Equation 1 were found by use of Equation 3:

$$I_A = I_{DA} + I_{dA} = (K)\ (I_{DN})\ (d_D) + (I_d)\ (\alpha_d) \quad (3)$$

These values for 60 and 65 deg.

North Latitude appear in this paper as Table VI and are in effect an extension of Table XVI, Chapter 13, of the 1958 GUIDE.

Values for use in the last term of Equation 1 do not depend on latitude. Consequently, the value of I_{CR} as found in Table XIII, Chapter 13, of the GUIDE, 1958, can be applied when making solar gain calculations for the Alaskan cities.

With the data in this paper to supplement that given in the GUIDE it is possible to make cooling load calculations for the Alaskan cities.

ACKNOWLEDGMENT

The author herewith expresses his sincere thanks and appreciation for the aid rendered by W. M. Laughlin, Alaska Agricultural Experiment Station, Palmer, Alaska, in securing many of the needed data.

NOMENCLATURE

α_d, α_D = absorptance of glass for diffuse and direct radiation.
β = solar altitude.
γ = wall solar azimuth.
GMT = greenwich mean time.
HA = hour angle.
I_A = heat absorbed in glass, Btu per (hr) (sq ft).
I_{ET} = instantaneous rate of heat gain, by convection and radiation from a single sheet of unshaded common window glass, Btu per hr (sq ft).
I_d, I_D = diffuse and direct solar radiation, Btu per (hr) (sq ft).
I_{dA}, I_{DA} = heat absorbed in glass due to diffuse and direct radiation, Btu per (hr) (sq ft).
I_{DN} = direct solar radiation normal to sun's rays, Btu per (hr) (sq ft).
I_{dT}, I_{DT} = transmitted diffuse and direct solar radiation, Btu per (hr) (sq ft).
I_T = instantaneous rate of heat gain, due to transmitted diffuse and direct solar radiation by a single sheet of unshaded window glass, Btu per (hr) (sq ft).
$K = \cos\theta = \cos\beta \times \overline{\cos}\,\gamma$
τ_d, τ_D = transmittance for diffuse and direct radiation of a single sheet of common window glass.
θ = angle of incidence.

REFERENCES

1. Monthly Climatological Summary for Juneau, Anchorage and Fairbanks, Alaska,

TABLE VI

HEAT ABSORBED IN GLASS*

Lat.	Sun Time AM		Heat Absorbed in Glass, Btu per (hr) (sq ft) N	NE	E	SE	S	SW
	5	7	2	4	4	2		
	6	6	3	8	9	6		
	7	5		10	12	9	1	
60deg. N.	8	4		8	14	13	4	
	9	3		5	13	14	7	
	10	2			10	14	10	1
	11	1			7	12	11	5
	12				2	10	12	9
	5	7	2	5	5	3		
	6	6	3	9	10	6		
	7	5		9	12	10	2	
65deg. N.	8	4		8	13	12	5	
	9	3		4	13	14	8	
	10	2			10	14	10	2
	11	1			7	13	12	6
	12				2	10	13	9
		PM	N	NW	W	SW	S	SE

* This table is a continuation of Table V, Chapter 13, *ASHAB Guide*, 1958.

for months of December 1950, and for the December, January, February June, July and August for each year 1951 to 1955 inclusive; (U. S. Dept of Commerce, Weather Bureau, Asheville, N. C.).
2. Letter to author from R. M. Waller, geologist, Ground Water Branch, Geological Survey, Anchorage, Alaska.
3. Letter to author from W. K. Boyd, Snow, Ice and Permafrost Research Establishment, U. S. A. Wilmette, Ill.
4. Investigation of Military Construction in Arctic and Subarctic Regions, 1945-1948, Plates III—10, 11, 13, 14, 15, 16 and 17, Airfield Branch, Engineering Div, Military Construction, St. Paul District for Office of Chief of Engineers, U. S. Army.
5. *Local Climatological Data with Comparative Data for Anchorage, Fairbanks and Juneau,* 1955 (U. S. Dept of Commerce, Weather Bureau, Asheville, N. C.)
6. *American Air Almanac* (U. S. Government Printing Office, Washington, D. C., 1955).
7. *H .O. Pub #214, Vol. VII,* (U. S. Government Printing Office, Washington, D. C., 1955).
8. ASHRAE GUIDE 1956 Chap 13.

DISCUSSION

W. L. HOLLADAY, Los Angeles, Calif. (Written): The lack of September data in the summer tabulations may result in figures which are in error. The method in the ASHRAE GUIDE lists all four months.

The following tabulation compares the author's data with that of the Weather Bureau publication 60-49 "Climates of the States—Alaska" published in September 1959;

		High temp of record	Lowest temp of record	Daily range July	Period of record
Anchorage:	Burggraaf	84	−32	16.3	
	60-49	86	−38	18.3	35 yr
Fairbanks:	Burggraaf	92	−55	22.5	
	60-49	93	−66	20.7	28 yr
Juneau:	Burggraaf	82	−13	16.6	
	60-49	84	−21	18.5	14 yr

It is understood that this paper was prepared several years ago, but all the record highs and lows were registered in 1955 or earlier, except the high for Juneau, which occurred in July 1956.

Fluor's "Evaluated Weather Data for Cooling Equipment Design" gives the following 5% wet-bulb design temperatures for two of the three localities:

	Burggraaf	Fluor
Anchorage	58F	59.4F
Fairbanks	59F	61.9F

Since the Fluor figures were developed by machine tabulation of thousands of individual readings per station, they probably represent better temperature values than those of the author.

A spot check of Table II with some of the values of K in the ASHRAE GUIDE Table 5 which were plotted against latitude showed. that the values developed in this paper for the higher latitudes do not make smooth curves with those published in the GUIDE, nor are they consistent with each other. As an example, the difference between the "11 a.m. to 1 p.m." line and the "12" line, south wall, are:

Latidude		11-1	12	Difference
30 deg	GUIDE	.192	.208	.016
40 deg	GUIDE	.354	.375	.021
50 deg	GUIDE	.505	.530	.025
60 deg	BURGGRAAF	.663	.670	.007
65 deg	BURGGRAAF	.693	.731	.038

Table III presents some figures for the Azimuth angle, γ, (only the South direction was checked) not consistent with the GUIDE. The values of β, the solar altitude, are in close agreement with GUIDE figures for all hours except the 7 a.m. and 5 p.m. values.

Table V, a continuation of GUIDE Table 12, gives numbers much below even conservative extrapolation of GUIDE values to higher latitudes, and one set (South direction for 7 a.m. and 5 p.m.) is inconsistent: 60 deg is below the 50 deg GUIDE figure, 65 deg is higher than the 50 deg figure.

Before these data are included in the GUIDE, careful checking of values is required.

AUTHOR BURGGRAAF: Summarizing Mr. Holladay's comments, the author wishes to thank him for the thorough and detailed check made of this paper. The errors can only be accounted for by the lack of experience and crude hand methods used in making the calculations. The author also wishes to point out that the paper was first used as an undergraduate thesis where primary emphasis was placed upon establishing a proper method for compiling and analyzing the necessary raw material, setting up a correct calculation procedure and organizing the results (this does not mean that accuracy was disregarded, it was not).

For further discussion of this paper, see the comments of Mr. John Everetts, Jr. following the paper of Mr. H. C. S. Thom.

1714

No. 1714

A Rational Method of Determining Summer Weather Design Data

H. C. S. THOM

The load on air conditioning equipment involves a number of other factors besides weather conditions. Weather factors are: dry bulb temperature, humidity as measured by wet bulb temperature and solar radiation. The latter is not as subject to random variability and has usually been treated as a constant extreme value depending mostly on location. Only the wet bulb and dry bulb temperature design values will be discussed here.

Wet and dry bulb temperatures vary through the day, through the summer and through the years. These variations are to a great extent random in nature as all weather variations in a particular climate are and hence involve contingency or probability. Since the air conditioning system load carrying capacity is related in part to the wet and dry bulb temperatures, the capacity of the system also has a contingency on satisfactory operation, i.e., there must be some small probability of the system being unable to meet the load imposed by weather conditions.

The selection of this probability is not a climatological problem but is an engineering problem which involves many factors such as economy, use, customer satisfaction, etc. The best the climatologist can do is to furnish the engineer with a practical set of probability values from which he can make the proper selection for design. Although it has not often been recognized in the past, there are three contingencies in summer weather design data; these are associated with variation within the day, variation within the summer season, and variation between years. All three will be considered in this study.

There have been a number of published studies on prevailing methods of computing summer weather design data. Certain of these methods will be reviewed

H. C. S. Thom is Chief Climatologist, Office of Climatology, U. S. Weather Bureau. This paper was presented at the ASHRAE Semiannual Meeting in Dallas, Texas, February 1-4, 1960.

briefly to show how the discovery of their deficiencies led to a more rational approach to the weather design data problem.

Design variable problem — Some general consideration has been given to the problem of the single design variable.[1,2] The present problem, however, is complicated by the need to consider two weather variables simultaneously, wet bulb and dry bulb temperature. In previous studies, and in present practice, these two variables are considered independently although no purely statistical justification for this practice was found. Some efforts have been made toward considering these variables jointly, but these have been little more than presentations of data since no clear illustration of engineering design uses have been given.

Usually, these presentations of data take the form of joint frequency counts tallied on a dry bulb temperature-wet bulb temperature rectangular coordinate system. Sometimes the coordinate system has been these two variables on a psychrometric chart. The futility of such presentations can be seen easily from the fact that for any given dry bulb temperature t the wet bulb temperature t′ can range over its entire possible scale and vice versa. Hence, in order to be useful in design both t and t′ must be fixed on the basis of some joint probability which in design would be the probability of failure of the system to meet the load. However, there is an infinite number of combinations of t and t′ for a given design probability, hence, no design value can come from joint frequency presentations or joint probability distributions. This is not to imply that such presentations may not have some interest and possibly be of use in operating problems where fixed t and t′ are available, however, some other approach must be followed if design data are to be obtained.

The procedure followed at present is to select t and t′ independently. This has meant that some kind of a contingency of exceeding the design value (however loosely defined) was associated with the dry bulb and wet bulb temperatures individually. This, in effect, is equivalent to considering the contingencies independently in which case the joint contingency of failure as a result of t and t′ exceeding design values could be far different than the contingency associated with t and t′ separately. This may be easily appreciated by considering two dice: The probability of getting a five or greater with a single die is clearly 2/6. (The analogy with the design problem is obtained by simply assuming 5 as the dry bulb design value in some arbitrary temperature units.) Now if the second die represents t′, and five is again the design value in some appropriate units, the probability of equaling or exceeding this design value is again 2/6 as for the first die. Now it is certainly true that the outside air load is a function of both t and t′ as ordinarily considered; hence the contingency of failure to meet load would be analogous to some joint

consideration of t and t' or a joint tossing of the two dice. A simple and natural assumption would be that the joint design value or design load should be 5 + 5 = 10. Now tossing the two dice together it is seen that the probability of a 10 or greater is 6/36. This is made up of the possibilities of a 5 on the first die and a 5 on the second called (5, 5) plus five other possibilities as follows (6, 4), (4, 6), (5, 6), (6, 5), and (6, 6) all of which add to 10 or greater divided by the total number of ways that two dice can fall together $6 \times 6 = 36$. But 6/36 or 1/6 is much less than 2/6 or 1/3 so while the designer chose 1/3 each for design dry bulb and wet bulb, the contingency on design load was reduced to 1/6. This raises the possibility that the present practice could lead to unanticipated design contingencies although this is not definitely known since the problem has not been examined from this angle. Certainly, when the objective is to rationalize summer weather design data so that engineers have a full understanding of the contingencies involved, it is imperative that the practice of selecting the dry bulb and wet bulb design temperatures independently be analyzed completely. The die analogy simply points to possible difficulties, for the load is not a simple function of the sum of dry bulb and wet bulb temperatures as will be seen presently.

It is clear from the above discussion that the designer must have the contingency or probability on the heat load to evaluate properly a proposed design. The total outdoor heat load may be expressed[3] by the relationship

$$q_t = q_s + q_l \quad (1)$$

Here q_s is the sensible heat load, q_l is the latent heat load, and q_t is the total heat load. The present discussion need only be concerned with a unit air movement, for the total outside air intake multiplies both the unit sensible heat load and the unit latent heat load and can therefore be factored out. Thus the q's in (1) would correspond to q/Q of Ref. [3], equation (9) page 196.

From considerations discussed above and general principles given,[1,2] it follows that to solve the present design problem, probabilities must be found for the occurrence of the unit total load exceeding various values of q_t. These will be given by the statistical distribution of q_t expressed by the equation

$$P = G(q_t) \quad (2)$$

Here P is the probability of a value of total load exceeding q_t. The solution to the design problem is given by the inverse of (2) or

$$q_t = G^{-1}(P) \quad (3)$$

If the probability of system failure as a result of the unit load exceeding a value of q_t is chosen by the engineer to be P_d (the design probability), then the unit design total outside air load is given by

$$q_{td} = G^{-1}(P_d) \quad (4)$$

The design total outside air load is found by multiplying this value by Q the total air intake in cfm.

By reason of equation (1) the

distribution (2) may be expressed as

$$P = G\,(q_s + q_e) \qquad (5)$$

To gain further insight of the problem the q_s and q_e must be expressed as functions of t and t'. From equations (7) and (8),[3] page 196, it is seen that for unit air intake

$$q_s + q_e = 1.08\,(t_o - t_i) + 4840\,(W_o - W_i) \qquad (6)$$

Here the subscripts o and i refer to outside and inside conditions, t is the dry bulb temperature at those conditions, and W is the humidity ratio (mixing ratio to the meteorologist).

It is apparent from (6) that q_t is not a simple function of the dry bulb and wet bulb temperatures since, although q_s is a simple function of t_o and t_i, q_e is a function of W_o and W_i both of which are functions of t_o and t'_o and t_i and t'_i through the psychrometric chart, a complicated diagram. Notwithstanding, the distribution of q_t could be found directly from transforming the meteorological data by equation (6) were it not for the fact that a separate distribution would be required for each set of inside design conditions (t_i, W_i). This would specialize resulting design data too greatly and result in much extensive climatological work to produce a suitable selection of q_{td}. Thus, it seems most reasonable to determine what effect the independent selection of design wet and dry bulb values t_{od} and t'_{od} at the same probability (as is now the practice) has on the probability of the design unit total heat load q_{td} being exceeded, and if necessary to adjust the probabilities for t_o and t'_o to give the prescribed probability on q_{td}.

As seen by equation (6), in order to make q_t a function of t and t', W must be made a function of t and t'. This may appear to be an insuperable task in view of the complicated empirical relationship between temperature and humidity ratio at saturation. However, for the present purpose of getting a look at what might happen to the probabilities an approximate relationship would be quite adequate.

An examination of the psychrometric chart accompanying Ref. 3 shows that the t'-lines are not far from straight and parallel, sloping negatively with respect to the t and W axes. Hence, they may be considered as approximately straight and parallel contours on the t-W plane. From this it would be expected that the function is approximately linear of the form

$$W = k_1 + k_2\,t' - k_3 t \qquad (7)$$

The coefficients k could be estimated by ordinary regression procedures from a sample of data read from the psychrometric chart.[3] However, since the true functional relationship is physically exact and the present need is only for an approximation, the k's were determined from three carefully read points in the ordinary range of design values. The solution of the three resulting simultaneous equations in the k's gave the following relationship for W:

$$W = -.02891 + .000871\,t' - .000232\,t \qquad (8)$$

Independent pairs of t and t' in the design range substituted in (8) gave W values to within less than 2% of the chart values, which is adequate for the present purpose. Substitution of the value of W from equation (8) into equation (6) to eliminate W_o gives after some simplification

$$q_t = -.0430\, t_o + 4.216\, t_o' - 139.92 - 1.08\, t_i - 4840\, W_i \qquad (9)$$

The preponderant importance of t'_o is clear in this equation; t_o actually is a negative component. Note that t_i and W_i are fixed values for a given design hence W_i need not be expressed as a function of t_i and t'_i.

A further check on this development was obtained by using the design conditions of Example 11 beginning on page 202 of Ref. [3]. On page 204 one finds $t_o = 95$, $t'_o = 78$, $t_i = 80$, $t'_i = 65$, $W_o = 0.0168$, and $W_i = 0.0098$. Substitution of the inside design values in equation (9) gave

$$q_t = -.0430\, t_o + 4.216\, t_o' - 273.75 \qquad (10)$$

This equation will be useful since the present demonstration will be based on the foregoing inside design values although it will eventually be found to be independent of them.

Substituting further Example 11 values for t_o and t'_o in (10) gives

$$q_t = 0.430 \times 95 + 4.216 \times 78 - 273.75 = 50.97$$

This is the unit total outside air heat load. Multiplying by Q = 1275 of Example 11 gives 64,987 Btuh. Using equation (6) multiplied by Q directly with the t's and W's of Example 11 gives

$$q_t = 1275 \times 1.08 \times 15 + 1275 \times 4840 \times .0070 = 63,852$$

The former is again less than 2% from the latter more exact value.

The methods which will be proposed later to obtain design values are such that, to an approximation adequate in the present demonstration, the distributions of t_o and t'_o may be treated as normal distributions. This simplifies the analysis greatly without detracting significantly from the demonstration. Since a linear function of normally distributed variables is normally distributed, q_t will have a normal distribution with mean $\overline{q_t}$ and standard deviation $a(q_t)$.

The mean of a linear function is that linear function of the means of the variables; hence

$$\overline{q_t} = -.0430\, \overline{t_o} + 4.216\, \overline{t_o'} - 273.75 \qquad (11)$$

The variance of q_t i.e., the square of the standard deviation, is also found by standard methods to be:

$$v(q_t) = (.0430)^2 v(t_o) + (4.216)^2 v(t_o') - 2 \times .0430 \times 4.216\, r(t_o, t_o')\, s(t_o)\, s(t_o')$$

Here $r(t_o, t'_o)$ is the correlation coefficient between t_o and t'_o, $v(t_o)$ and $v(t'_o)$ are the variances of t_o and t'_o. The sq roots of the variances are the standard deviations $s(t_o)$ and $s(t'_o)$. After some simplification the variance of q_t may be written as

$$v(q_t) = .001849\, v(t_o) + 17.7713 \times v(t_o') - .3626\, r(t_o, t_o')\, s(t_o)\, s(t_o') \qquad (12)$$

Note again in this equation the lack of importance of term involving only t_o i.e., $v(t_o)$.

The standardized variable of the normal distribution of q_t may be expressed as

$$u_G = \frac{q_{tG} - \bar{q}_t}{s(q_t)} \quad (13)$$

Here u_G is the independent variable of the ordinary normal probability table and q_{tG} is the corresponding value of the unstandardized variable. Since u_G corresponds to a probability G, i.e., the probability of exceeding u_G, q_{tG} also corresponds to the probability G and is called a quantile with associated probability G.

By equation (10)

$$q_{tG} = .0430\, t_{oP} + 4.216 \times t'_{oP} - 273.75 \quad (14)$$

Subtracting equation (11) from equation (14) yields after some rearrangement

$$q_{tG} - \bar{q}_t = .0430\,(\bar{t}_o - t_{oP}) + 4.216\,(t'_{oP} - \bar{t}'_o) \quad (15)$$

Expressing t_o in standard form for probability P gives

$$u_P = \frac{t_{oP} - \bar{t}_o}{s(t_o)}$$

Rearranging yields

$$(\bar{t}_o - t_{oP}) = -u_P\, s(t_o) \quad (16)$$

Similarly again for probability P

$$u_P = \frac{t'_{oP} - \bar{t}'_o}{s(t'_o)}$$

and

$$(t'_{oP} - t'_o) = u_P\, s(t'_o) \quad (17)$$

Substituting (16) and (17) in equation (15) and dividing both sides of the resulting equation by $s(q_t)$ gives

$$u_G = \frac{-.0430\, u_P\, s(t_o) + 4.2156\, u_P\, s(t'_o)}{s(q_t)} \quad (18)$$

This is the expression needed to determine what the probability G of exceeding q_t is when t_o and t'_o are chosen independently with probability P. Since $s(t_o)$ is at most roughly 5 times $s(t'_o)$, it is seen that the first term in the numerator is only about 0.05 as large as the second term. In equation (12) it is also seen that the term involving $v(t'_o)$ is also the predominant term, consequently, the denominator of equation (18) depends mostly on the size of $v(t'_o)$ or $s(t'_o)$. Thus, for a given station it would be expected that u_G would be approximately equal to u_P and hence G = P. To check this at several stations the central design probability 0.075 for winter outside design temperatures was employed[2,3] to check the closeness of u_G to this probability. For P = 0.075, u_P = 1.4395. Substituting this value in equation (18) gives

$$u_G = \frac{-.0619\, s(t_o) + 6.0684\, s(t'_o)}{s(q_t)} \quad (19)$$

Data for St. Louis, Miami, and Los Angeles were used as examples of a wide range of climatic conditions. For St. Louis $s(t_o)$ = 3.42 and $s(t'_o)$ = 1.37. This gives u_G = 1.42 or G = 0.078 which is quite close to 0.075, the probability chosen for t_o and t'_o independently. For Miami $s(t_o)$ = 1.14 and $s(t'_o)$ = 0.610 giving u_G = 1.44 and G = 0.075. For Los Angeles $s(t_o)$ = 4.19 and $s(t'_o)$ = 0.685 consequently u_G

= 1.42 and G = 0.078. It is clear from these examples that if the probabilities of the wet bulb and dry bulb design values are chosen separately the design outside air heat load will have close to the same probability. That this is independent of the probability may be seen by dividing both sides of equation (18) by u_P giving

$$\frac{u_G}{u_P} = \frac{-.0430\, s(t_o) + 4.2156\, s(t'_o)}{s(q_i)} \qquad (20)$$

Thus, for a wide range of climatic conditions u_G/u_P is approximately unity which extends the above results to all design probabilities.

The foregoing analysis is only meant to demonstrate that G will be quite close to P. It is not to be inferred that equation (9) is recommended for use in place of the methods discussed in Chapter 13, Ref. [3].

Average frequency design variables — Beginning with the publication of "Summer Weather Data,"[4] average frequency design variables began to be proposed. The usual average frequency design variable is obtained by making a frequency distribution of the dry bulb temperature for all hours of the day during June, July, August, and September for a period of years. Usually five years were used and more recently records up to 10 years have been employed. From this frequency distribution a cumulative distribution was formed and a value of temperature was chosen so that a given number of hours exceeded it usually in 5% or 2.5% of the hours. Since the hours for all years are lumped, the resulting design value is determined by a total or average frequency which does **not** estimate a probability which is useful to the designer in measuring the risk of failure of a system to meet load. The designer may think on the basis of such design values, e.g., the 2.5% value, that he can assure a customer of only 2.5% failure of the system. And this will be true, for example, on the average for a 30-year period where a total of 2.5% of the hours in 30 years the system will not carry the load. However, there will be many individual years when the percentage hours of failure will be much higher than 2.5% due to the tendency of hot weather to run in spells. That is, warm summers tend to have a high frequency of hot days and therefore have a high frequency of hours in which the 2.5% value is exceeded. Thus, the average frequency design value does not reflect what happens in the individual summer which is what mainly interests the customer. He would have good reason to label the design inadequate if, as could easily happen, in the first year of operation the 2.5% value of hours of failure were far exceeded. On the basis of the average frequency design value the probability of this happening is high although it could be said that the factor of safety in the design would take care of a good proportion of the failure hours. However, letting the factor of safety take care of components of the design which can be analyzed is not rational design.

Some years ago the writer tabulated the 5% summer dry bulb temperature values at Des Moines for a 20 year record 1925-44 both for each year and for the record.[5] The latter is the average frequency design value which was found to be 93.9 F. Eight of the 20 individual summer values were above the design value and three of these were above 100 F, one being 104.8 F. Thus, as was to be expected, about half the annual values were above the average frequency design value. A similar analysis was made of the wet bulb temperature at New York for 1925-34. In this case the average frequency design value was 74.8 F. Of the 10 summer 5% values five exceeded the 10 year average frequency design value. Both analyses showed that the average frequency design value percentages do not indicate the contingency of design failure.

The old TAC design values are the most widely known average frequency design values. Although a considerable effort was put forth in obtaining them, they never attained widespread acceptance. This is perhaps due to their being lower than design values in common use just as the winter TAC values were too high. The dry bulb temperature TAC values have been published in the ASHRAE Guide[3] but did not replace the values in common use. The wet bulb TAC values are not given in the Guide. In order to make the TAC type design values comparable to those in common use the percentages must be lowered to 1% or less. At this point the percentages bear little relation to the actual contingency which the customer experiences. One per cent average frequency design values give the impression of low risk of failure when actually the risk is quite ordinary. Part of this deflation of the percentages is due to including the night and morning hours which all fall at the lower end of the frequency curve. This requires lower TAC values in order to still include the proper percentage above the TAC value.

Some years ago the writer participated in the preparation of the climatic portion of the Canadian Building Code. At that time[6] it was not known how to handle conveniently the difficulties found. Two steps to rectify the difficulties were recommended and adopted: Data for the month of July only were used and the 1% value was added to the range of percentages. With these modifications the resulting 1% design values are higher than the ordinary TAC values and appear to be in agreement with rationally derived values in the United States although, of course, the 1% is as pointed out above an unrealistic measure of the contingency of failure the customer faces.

From the above discussion it appears that good weather design values must meet four requirements: (1) Give proper weight to the high load parts of the day viz., afternoon and evening. (2) Limit the within season risk i.e., the risk of repeated failure to meet the load day after day within a summer due to the tendency of hot weather to occur in spells. (3) Provide realistic

probability measures of the year to year contingency of failure to meet load. (4) Be based on a climatologically satisfactory length of record, preferably the standard record of 30 years. The average frequency design values cannot meet the first three requirements by their very nature and cannot meet the fourth because 30 years of hourly data is not available. It is apparent then that some new approach is needed.

RATIONAL DESIGN VARIABLES

Hours when high loads are prevalent will be considered rather than all hours of the day when most air-conditioning loads are either low or non-existent. Keeping in mind the feasibility of later climatological analysis only maximum load conditions from outside air was considered. This immediately leads to maximum daily dry bulb temperature for which there is adequate record length but raises a problem with respect to the wet bulb. No maximum daily wet bulb temperature is available, and if it were, it would not always occur at the same hour as the maximum dry bulb temperature although they are highly correlated. However, the p.m. variation of the wet bulb is small compared to the dry bulb and usually attains its maximum value in later afternoon. It seemed reasonable, therefore, to choose the 7-8 p.m. daily synoptic wet bulb temperature for which an adequate record exists at many stations. This reading was taken at 7-8 p.m. E.S.T., 6-7 p.m. C.S.T., 5-6 p.m. M.S.T., and 4-5 p.m. P.S.T. This variation in time has little effect because of the small diurnal variation and because all times are within the period when wet bulb maxima usually occur. It is also much to be preferred to the mixing of all 24 hours together as is done in the compilation of average frequency design wet bulb temperature.

When it was found that the average frequency design data do not limit the within season risk of failure,[5] the obvious solution was to consider compiling a percentage value for each summer season. This would ensure that no summer had greater than a fixed percentage of the daily maxima above the design value during the sample record. However, this solution was not feasible because the problem of climatological analysis could not be solved in any but a highly complex manner. Not until sometime later was it realized that the variable could be thrown into a slightly different form for which the climatological analysis was more easily developed. If, as above, the series of 2.5% values for the summer seasons of June, July, August, and September is considered, and since these months contain 122 days, 2.5% of this is close to three days, on which the maxima will equal or exceed the 2.5% value for that summer. Hence, it is only necessary to arrange the temperatures in each summer in decreasing order of magnitude and count down from the highest value to the third value in each season to obtain a series equivalent to the 2.5% series. Counting down to the 6th highest value will produce the 5% series and in

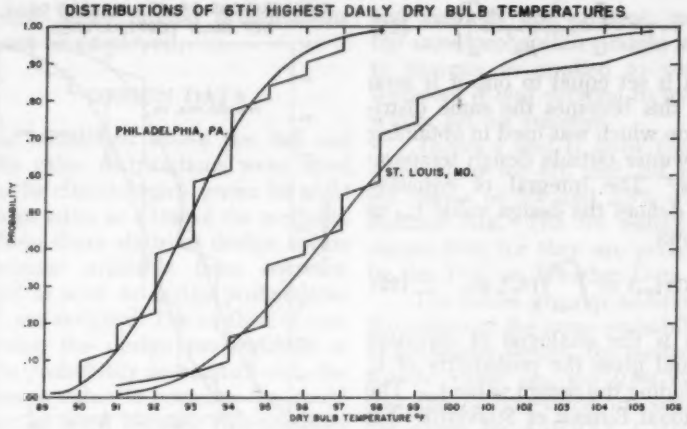

Fig. 1 Dry bulb temperature

general counting down to the mth will produce the (100m/122)% series. When such series are fitted with frequency distributions the probability of the 2.5% or 3rd highest value in any summer exceeding a particular value may be obtained. In general, the probability of the (100m/122)% value or mth highest value in any summer exceeding a specified value may be calculated. This is now a rational solution to the design variable problem since the within season risk is limited by a definite percentage or mth value each season and the between year risk is defined by a probability of these individual year percentages or mth values exceeding a specified value e.g., the design value. The engineer, therefore, has control over both seasonal and annual risks of failure to meet load, these design variables are for near maximum load conditions, and there is adequate climatological record.

CLIMATOLOGICAL ANALYSIS

The climatological series under consideration is the series of mth highest dry bulb and wet bulb temperatures for 30 year records. Gumbel[6] developed an mth value distribution which was found to fit these series well. Available methods of fitting this distribution, however, were not found to be efficient; hence, new methods were derived[7] which give near optimum estimates of the parameters of the distribution. The Gumbel frequency distribution, or probability density function, may be expressed in the form

$$f(t_m) = \frac{m^m}{\beta_m \Gamma(m)} \exp \left\{ \frac{-m\,(t_m - \alpha_m)}{\beta_m} - m \exp \right.$$

$$\left[-\frac{t_m - \alpha_m}{\beta_m}\right]\Bigg\} \qquad (21)$$

If m is set equal to one it is seen that this becomes the same distribution which was used in obtaining the winter outside design temperatures.[2] The integral of equation (21) defines the design value t_{md} as follows

$$G(t_{md}) = \int_{t_{md}}^{\infty} f(t_m)\, dt_m \qquad (22)$$

This is the analogue of equation (2) and gives the probability of t_m exceeding the design value t_{md}. The National Bureau of Standards[8] has prepared convenient tables of this integral which greatly simplify the application of the distribution. If P_d is the probability of exceeding the design value t_{md} given by (22) then the explicit solution for the design value is the analogue of equation (4) or

$$t_{md} = G^{-1}(P_d) \qquad (23)$$

In the above development t represents either the outside dry bulb or wet bulb temperature.

Using the methods of Ref. [7] the distribution (21) was fitted to the 3rd and 6th highest value series for eight cities. The mth value distribution provided good fits to the data in all instances. Fig. 1 shows the distributions for the 6th highest annual dry bulb temperature for Philadelphia and St. Louis. The broken lines connect the empirical data, and the smooth curves are plots of one minus the probability given by equation (22) with t_{md} as the independent variable. The ordinate gives the probability that t_{md} will be less than a specified value. This is one minus the design probability P_d. Note the much greater spread of the St. Louis distribution indicating the continental type climate with variable temperatures as contrasted to Philadelphia where the proximity to an ocean tempers the variability.

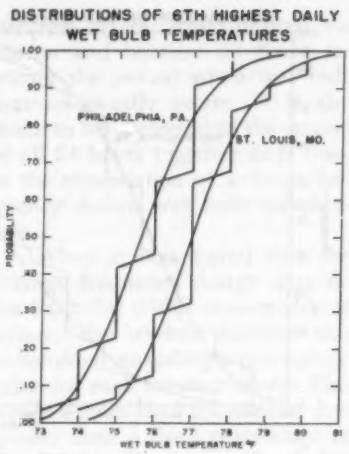

Fig. 2 Wet bulb temperature

Fig. 2 gives similar distribution curves for the 6th highest wet bulb temperatures. Here the curves are nearly parallel, but the curve for St. Louis is displaced toward higher values indicating that the wet bulb temperature averages considerably higher at St. Louis. It is noted that the wet bulb temperature tends to be less variable than the dry bulb in both cities.

The distribution curves of Figs. 1 and 2 define all possible design values, however, graphs would take too much space to be used in presenting data for a large number of

cities; hence tabular presentations must be employed.

DESIGN DATA

As mentioned above the 3rd and 6th value distributions were fitted to the climatological series for eight large cities as a test of the methods. From these statistics design values become available from equation (23) as soon as design probabilities P_d are assigned. The method of centering the design probabilities or the probability associated with the design value in common use could not be used because this required data for a larger number of stations than was available. Also the summer weather design values in common use, Ref. 3, p. 170, might be more variable because of the shorter period in which they have been developed. If, however, the present methods are rational, nearly the same probabilities might apply to summer as applied to winter; therefore it was decided to try the winter set for summer.

Tables I and II show the design values for 6th and 3rd highest values or 5% and 2.5% within summer risk. The 5% values are shown first, for they are preferred by the TAC on Weather Data.

The tables give, in addition to the values at the same probabilities as for winter design, the median or middle value i.e., the 0.50 value, and the design value in common use given by ASHRAE GUIDE.[8] Note that the 5% within summer risk central (0.075) wet bulb design values correspond closely to the wet bulb design values in common use. These differ on the average by only 0.4 F. The dry bulb values tend to be higher than those in

TABLE I

SUMMER WEATHER DESIGN DATA FOR SELECTED CITIES
6TH HIGHEST DRY BULB TEMPERATURE
5% WITHIN SUMMER RISK

Station	.025	0.05	.075	0.10	0.20	0.50	Guide Value (Common Use)
Chicago, Ill.	98.3	97.5	96.9	96.5	95.3	93.4	95
Fort Worth, Texas	105.8	105.2	104.7	104.3	103.4	101.6	100
Miami, Fla.	92.1	91.6	91.3	91.1	90.5	89.5	91
New Orleans, La.	97.8	97.3	97.0	96.8	96.2	95.1	95
New York, N. Y.	94.1	93.3	92.9	92.6	91.8	90.3	95
Philadelphia, Pa.	97.2	96.4	95.9	95.6	94.6	93.0	95
St. Louis, Mo.	104.1	102.6	101.8	101.2	99.9	97.0	95
Washington, D. C.	98.7	98.1	97.7	97.4	96.6	95.2	95
6th Highest Wet Bulb Temperature							
Chicago, Ill.	77.5	76.9	76.6	76.3	75.6	74.3	75
Fort Worth, Texas	79.4	78.9	78.6	78.4	77.8	76.7	78
Miami, Fla.	79.3	79.0	78.8	78.7	78.3	77.7	79
New Orleans, La.	80.1	79.8	79.6	79.4	79.0	78.3	80
New York, N. Y.	76.0	75.6	75.3	75.1	74.5	73.6	75
Philadelphia, Pa.	78.7	78.2	77.8	77.6	76.9	75.7	78
St. Louis, Mo.	80.1	79.5	79.2	78.9	78.2	77.0	78
Washington, D. C.	78.6	78.2	77.9	77.7	77.2	76.3	78

common use. However, the dry bulb values in common use are less refined than the wet bulb values since all but one value is given only to the nearest 5 deg. If the 0.075 values are rounded to the nearest 5 deg. the 0.075 values are in agreement with all common use values except that at St. Louis where the GUIDE value is 95 F and the 0.075 value is 100 F. There appears to be an agreement between the values of Table I at the same probability levels as for winter design data and the summer design values in common use. The complexity of the analysis prevented any foretelling of such a result. It is one of those comparisons which can only be made when the final results are available. Thus the proposed design values of Table I are consistent in design risk with already adopted winter design values.

Table II gives similar data for the 2.5% within summer risk. This may be of interest where more stringent control on this risk is desired. These values are to a large extent by-products of the 5% or 6th values, since in performing the main task, the compilation of the climatological series, the 3rd value is passed when counting to the 6th.

ACKNOWLEDGMENTS

The author wishes to thank John Everetts, Jr., for his constant technical guidance and unfailing encouragement and patience without which this study could not have been completed. Sincere appreciation to the members of the TAC on Weather Data and especially to Paul R. Achenbach, J. B. Graham, and David L. Fiske whose keen understanding of different aspects

TABLE II

SUMMER WEATHER DESIGN DATA FOR SELECTED CITIES
3RD HIGHEST DRY BULB TEMPERATURE
2.5% WITHIN SUMMER RISK

Station	.025	0.05	.075	0.10	0.20	0.50	Guide Value (Common Use)
Chicago, Ill	102.5	101.0	100.2	99.7	98.2	95.7	95
Fort Worth, Tex.	108.4	107.1	106.5	106.1	104.9	102.9	100
Miami, Fla.	94.0	93.2	92.8	92.5	91.7	90.2	91
New Orleans, La.	99.4	98.7	98.3	98.0	97.2	95.9	95
New York, N. Y.	98.5	97.1	96.4	95.9	94.6	92.4	95
Philadelphia, Pa.	100.2	99.2	98.5	98.1	96.8	94.9	95
St. Louis, Mo.	105.7	104.4	103.5	102.9	101.3	98.7	95
Washington, D. C.	100.9	100.1	99.5	99.2	98.3	96.7	95
3rd Highest Wet Bulb Temperature							
Chicago, Ill.	79.2	78.6	78.2	77.8	77.0	75.7	75
Fort Worth, Tex.	80.8	80.2	79.8	79.4	78.6	77.3	78
Miami, Fla.	79.5	79.2	79.1	79.0	78.6	78.0	79
New Orleans, La.	81.1	80.7	80.4	80.2	80.7	78.8	80
New York, N. Y.	78.5	77.7	77.4	77.1	76.3	75.0	75
Philadelphia, Pa.	80.4	79.8	79.4	79.1	78.3	77.1	78
St. Louis, Mo.	81.5	80.9	80.4	80.1	79.3	77.9	78
Washington, D. C.	80.8	80.1	79.8	79.5	78.8	77.6	78

of the basic problems was helpful. Sincere appreciation also must go to the National Weather Records Center, Asheville, for compiling part of the basic climatological data and to my assistant Maurice Kasinoff for performing all computations.

REFERENCES

1. H. C. S. Thom, "Frequency of Maximum Wind Speeds", *Proc. A. S. C. E.*, Vol. 80, November 1954, Separate No. 539.
2. H. C. S. Thom, "Revised Winter Outside Design Temperatures"," *Trans. ASHAE*, Vol. 63, pp. 111-128 (1957).
3. ASHAE, *Guide*, 37th Ed., 1959, ASHAE, New York.
4. J. C. Albright, "Summer Weather Data", 1939, The Marley Co., Kansas City.
5. H. C. S. Thom, "Preliminary Report on the Analysis of WB-WPA-ASHVE Weather Design Data" (Manuscript), Des Moines, Iowa, 1945.
6. E. J. Gumbel, "Les valeurs extremes des distributions statistique", Ann. de l'Institute Henri Poincaré, Vol. V, pp. 115-158, 1935.
7. H. C. S. Thom, "Maximum Likelihood Estimates for the Gumbel Distribution", U. S. Weather Bureau Manuscript, 1959, (Multilith).
8. National Bureau of Standards, "Probability Tables for the Analysis of Extreme Value Data", Applied Math. Series 22, 1953.

DISCUSSION

JOHN EVERETTS, JR., Philadelphia, Pa.: I would like to take this opportunity to thank both speakers for the contributions they have made to a most important factor in the design problems of our industry, namely, weather data.

Twenty-nine years ago, April 1931 to be more exact, Joseph C. Albright proposed to me that we make a study of weather data to try to bring some order out of chaos for establishing a wet-bulb temperature which would be reasonable for the design of cooling towers. In New York, for example, at that time engineers were specifying anything from 70 deg WB to 80 deg WB for cooling towers, which made a difference of approximately 100% in the cost of the tower. By 1932, we had studied weather data from some 67 different cities in the United States and published a wet-bulb map in which the wet-bulb isotherms were plotted on a map of the U.S.

The basis for selecting the value of the wet-bulb was purely arbitrary. After determining the number of hours each wet-bulb temperature existed, we then looked to the general design temperature used by most engineers in the various cities studied and found that a temperature which was not exceeded more than 5% of the total hours of the four summer months of June through September was the generally accepted value. Q.E.D. .5% was the magic number.

The acceptance of our wet-bulb map was beyond our greatest expectations. We received many requests from all over the country asking us to continue our work in dry-bulb, dewpoint, solar, and wind data. By the end of 1932, we decided to make a comprehensive study of these data and obtained through the Weather Bureau the data for some 220 cities for the period of 1930 to 1934 inclusive. After analyzing over 2,000,000 readings over the period of six years, the results of this study were presented to the Society at the Annual Meeting in Pittsburgh in January 1939. Subsequent to that time the book "Summer Weather Data" was published by the Marley Company of Kansas City. For several years these data were considered the best available and yet there were certain inconsistencies which we could not ignore nor could we reconcile them. These inconsistencies were mainly in the use of the arbitrary value of 2½% for the dry-bulb and 5% for the wet-bulb.

In previous papers as well as the paper presented by Mr. Thom today, it very forcibly points out that values based upon these criteria are a function of the number of years considered and the relation of those years to long term cycle of weather. There is also the consecutive number of hours at which a given condition exists and whether that was taken into account in establishing the design.

The Table which I have made for New York City for a twenty-year period from 1922 to 1941 inclusive brings out these points rather vividly. The values which Albright and I took for the years 1930 to 1934 inclusive show that 90 deg DB was equalled or exceeded 2.33% of the time, and 75 deg WB 4.49% of the time. This is as close to the 2½% and 5% values that we could get so these temperatures were set as design for New York.

An examination of the Table will show that if the years 1935-1939 were used, the 90 deg DB would be exceeded only 2.05% of the time but the 75 deg WB would be exceeded 6.62% of the time. The difference between 4.49% and 6.62% is too great to ignore. It is therefore important that as many years as possible be considered for a proper analysis.

It will also be noted from the Table that the design dry-bulb varies in percent from

WEATHER DATA NEW YORK CITY JUNE-JULY-AUG-SEPT 1922-1941

DB = Dry-Bulb 90 deg & Above WB = Wet-Bulb 75 deg & Above

Year	Total Hours DB	Total Hours WB	% Hours DB	% Hours WB	Year	Total Hours DB	Total Hours WB	% Hours DB	% Hours WB	Con-Sec. Hours	No. of Incid. DB	No. of Incid. WB	Con-Sec. Hours	No. of Incid. DB	No. of Incid. WB	
1922	20	98	.67	3.26	1932	23	78	.76	2.60	1	38	73	13	1	10	
1923	48	43	1.60	1.43	1933	92	199	3.03	6.63	2	35	58	14		6	
1924	46	86	1.51	2.83	1934	69	177	2.30	5.90	3	25	44	15		10	
1925	66	95	2.20	3.16	1935	26	175	.86	5.83	4	30	38	16		5	
1926	56	175	1.86	5.83	1936	77	118	2.60	3.93	5	30	29	17		2	
1927	19	75	.63	2.50	1937	93	269	3.10	8.96	6	33	47	18		3	
1928	34	196	1.10	6.53	1938	59	252	1.96	8.40	7	27	32	19		4	
1929	87	111	2.90	3.70	1939	52	180	1.73	6.00	8	14	27	20		2	
1930	80	103	2.67	3.43	1940	61	191	2.03	6.36	9	9	21	32		1	'26
1931	87	117	2.90	3.90	1941	107	103	3.60	3.33	10	9	16	34		1	'28
					Total	1202	2841			11	3	21	38		2	'33
					AVG.	60	142	2.0	4.73	12	3	13				'34

0.63% for 1927 to a high of 3.6% for 1941. The wet-bulb design varies from a minimum of 1.43% for 1923 to a maximum of 8.96% for 1937.

The second point which the Table shows is the number of consecutive hours over the twenty-year period that each design temperature existed. It is interesting to note that the 90 deg DB value only extends to a maximum of 13 hours for only one time in twenty years. On the other hand, the design wet-bulb was exceeded for 32 consecutive hours in 1926, 34 consecutive hours in 1928, and 38 consecutive hours in both 1933 and 1934. As the wet-bulb temperature affects the refrigeration load to a much greater extent than the dry-bulb, except for residential applications, this information becomes extremely important to the design engineer. With the use of Mr. Thom's method for determining weather data, the previous inconsistencies will be greatly reduced and the engineer will have data from which he can determine his own calculated risk to a much greater degree than is now possible.

With reference to Mr. Burggraaf's paper, I do not wish to detract from the many hours of work he put into this; because up to now there were no data for Alaska, he has at least presented data which will give an order of magnitude of design criteria even though they may not be as accurate as they should. For example, if the wet-bulb happens to be 3 to 4 deg higher than those shown, the refrigeration load for ventilation will be doubled for a system maintaining a 52 or 53 deg dewpoint. It is, therefore, important that until further data are available on the basis of Mr. Thom's method, the Alaska data be used with caution.

CLOSURE BY AUTHOR THOM: Jack Everetts is a pioneer in the preparation of weather design data. Without his enthusiastic efforts there would be little weather design data for use in air conditioning problems today. Without his technical help and encouragement this paper would never have been written. Mr. Everetts has presented a very interesting illustration from actual data of the basic reasons for undertaking this study, that is, the necessity for limiting the within year risk.

AUTHOR BURGGRAAF: Summarizing Mr. Everetts' comments, the author agrees that Alaska Weather Data, as well as that from other areas, should be calculated on the basis of Mr. Thom's method, which the author believes to be one of the most significant contributions to the air conditioning industry.

H. T. GILKEY, Cleveland, Ohio (Written): Once again, Mr. Thom has presented us with a detailed and complete analysis of a statistical approach to the problem of establishing design temperatures. This paper, which discusses summer design dry-bulb and wet-bulb temperatures, places in our hands the tools for determining rationally derived design values and builds upon the winter design value groundwork which Mr. Thom has laid previously.

I believe that Technical Committee 1.5, Meteorology and Weather Data, could advance this on a nation-wide basis by outlining an exact procedure which might be followed in order to come up with data similar to those presented in Tables I and II. Possibly, suggested tabulation sheets could be prepared, which could be used by interested Chapters and others in working up new and more complete information applicable to specific areas. Additionally, the Technical Committee could set up an example, including the integration of equation 22 of the paper, to show how the final design data were obtained.

It is recognized that this would be a "cook book" approach. Nevertheless, it would permit an interested group to perform such an analysis.

Each Chapter should be encouraged to perform these operations for as many stations in its area as possible. In mountainous areas or in areas in which rapid changes in elevation occur within a relatively short distance,

significant variations in design temperatures, both summer and winter, can occur within a few miles.

AUTHOR THOM: I appreciate the kind remarks of Mr. Gilkey. As he recommends, the results presented must be reduced to a "cook book" approach and they must be extended to a much more detailed network. Mr. Gilkey makes an important point when he calls for studies of local variations. The first step, however, is the preparation of data to replace material now published in the GUIDE, which is the objective of the methods presented.

W. L. HOLLADAY, Los Angeles, Calif. (Written): The mathematical proof of the independence of design dry-bulb and wet-bulb temperatures is unique. Most design engineers have felt that if they had a good design dry-bulb and a good design wet-bulb, it was unlikely that both would be exceeded simultaneously. Our office made some studies of temperatures at Burbank, Calif. which apparently verified, but did not prove, this contention. Mr. Thom's analysis is ingenious and valuable.

There are still some reservations about this paper which apply to the statistical approach and the winter design temperature method. No one except the author is able to arrive at these esoteric calculations, which do not help obtain the summer design temperatures for Los Angeles, Burbank or Bakersfield. In this connection, it is necessary to explain that summer dry-bulb temperatures in Southern California vary as much as one deg per mile.

Is it better to use the sixth highest dry-bulbs and wet-bulbs at a central probability of .075, or the third highest with a probability of .20? Since the figures are about the same, which is the better path to follow and why?

The author's method of using the sixth highest or third highest seems to be sounder than the method of choosing the coldest day or the mean of the high and the low, as in the winter design method. The m^{th} values are easier to choose from published weather data and they automatically eliminate the effect of diurnal change. I think it would be preferable to have the winter design temperatures based on the m^{th} lowest value instead of the coldest day which would result in unwarranted high design levels (less safe levels) for localities with high diurnal change.

AUTHOR THOM: When Mr. Everetts explained the independence of the dry- and wet-bulb to me I couldn't understand the reasoning until the mathematics verified his conclusions. I thought it would be well to present the argument in terms that others of a mathematical bent will find convenient to follow.

In reply to Mr. Holladay's same point, the theoretical development in this paper has been proven valid and valuable by specialists, and a discussion of micro-variations of design values was not a part of this paper. This is a problem for specialized local study.

In the third point, if the designer properly starts from a within-year percentage risk and a between-year probability based on engineering judgment not from temperatures, the fact that two combinations of these risks give the same design temperature simply means that within-year and between-year risks are compensatory. This gives a more refined basis for design as well as greater flexibility of interpretation.

Mr. Holladay's last point is an interesting suggestion. It was not followed because it was thought that the lowest daily temperature would occur too often outside the diurnal period of normal operation of heating equipment. The m^{th} value would reflect a diurnal time shift dependent upon climatic conditions which would make it necessary to use a different value of m for different climates, especially the West Coast. This could be overcome by working with the temperatures for a particular hour appropriate for a particular place for the heating season. This offers an interesting possibility for future study.

No. 1715

Environmental Study II — Sensation Responses to Temperature and Humidity under Still Air Conditions in the Comfort Range

WALTER KOCH B. H. JENNINGS C. M. HUMPHREYS

The reaction of man to his environment has been a subject of intense interest to the Society for many years. In the decade between 1920 and 1930, the Society carried out work which led to the development of the Comfort Chart. Houghten and Yaglou[1,2] in 1923, combined temperature and humidity into an index of thermal comfort called Effective Temperature (ET). The ASHRAE Comfort Chart for Still Air, shown in the 1959 GUIDE,[3] also indicates the percentages of subjects feeling comfortable in summer and winter. This has served as a widely used standard since its appearance. However, it was felt that additional knowledge on the subject was needed, and in 1956 at the ASHRAE Research Laboratory, construction was started on an environment laboratory in which the needed data could be obtained.

A comprehensive program was planned to carry out studies on the effects of environmental conditions on human comfort, productivity, and learning rate. The first phase of the program, conducted at temperatures considerably above the comfort level, was completed in 1958 and was presented before the Society in January, 1959.[4] The second phase of the study, the results of which are reported in this paper, is concerned with the effects of environmental conditions at or near the comfort level.

It is unfortunate that environmental studies cannot be con-

W. Koch is a Medical Research Supervisor; B. H. Jennings is Director of Research and C. M. Humphreys is Assistant Director of Research, ASHRAE Research Laboratory. This paper was presented at the ASHRAE Semiannual Meeting in Dallas, Texas, February 1-4, 1960.

ducted at a more rapid pace, but working with subject panels is an extremely slow process. Consequently, this paper, as was true of the preceding one, represents a limited contribution to our knowledge of human responses to thermal environment. It applies to individuals under essentially still-air conditions in a uniform environment with the mean radiant temperature maintained close to the dry-bulb temperature. The results are further limited to individuals who have come to equilibrium with the environment after stabilization periods of approximately three hours. Thus, this research covers the responses of subjects to temperature and humidity with the other variables of the environment being so adjusted as to have minimum effect on subjective reactions.

Factors controlling the sensation of comfort – The sensation of comfort in a thermal sense implies the absence of discomfort due to temperature or other atmospheric effects. The average individual will adapt readily to environmental conditions in the comfort range, and this makes the establishment of an optimum line difficult. There is a wide range of temperatures over which an individual will vote "comfortable," and the range for a group of individuals is still wider. Thus, it is obvious that there is no single temperature which elicits the response of "comfortable" from every individual.

There are also factors unrelated to the ambient air that have a marked effect on human comfort. People prefer lower temperatures when heavily dressed or when they are active, and vice versa. Heat output decreases with age and hence, older people often feel "cold" and add additional layers of clothing. A thermal sensation vote immediately following a change in activity may be at variance with a vote cast after equilibrium has been attained, even though no change has taken place in the environmental conditions. For instance, after walking outdoors, a room may appear to be too hot immediately upon entering, whereas, it may prove comfortable after occupancy of an hour or so.

The feeling of comfort is also influenced by radiation to or from surroundings, and by the air movement over the body. In this study, the effect of radiant environment has been minimized by keeping room surface temperatures close to the dry-bulb temperature. Nevertheless, radiation is a significant factor and many investigators have considered it. It should be mentioned that the effective temperature scale does not take into account thermal radiation. Vernon[5] applied a radiation correction to effective temperatures by using readings of a globe thermometer instead of the dry-bulb temperatures.

Environment Laboratory and test facility – The entire experimental program reported in this paper was carried out in the Society's Environment Laboratory. A floor plan of this and the adjoining rooms is shown in Fig. 1.

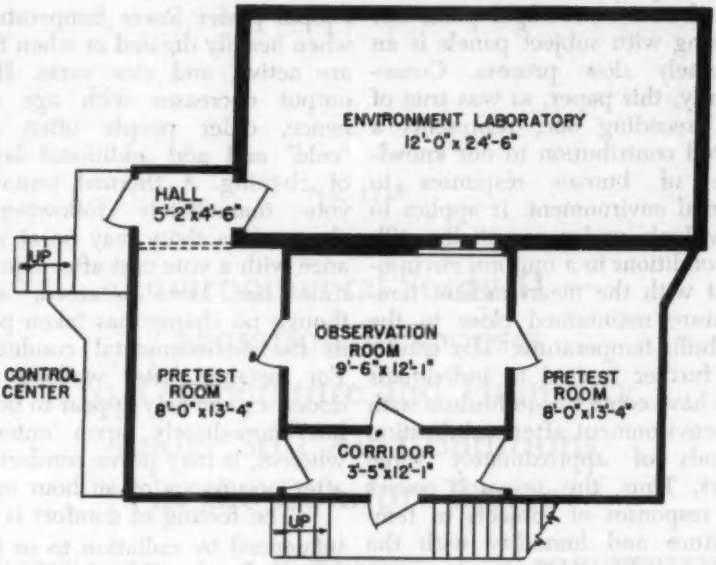

Fig. 1 Floor plan of ASHRAE Environment Laboratory

The shell of the environment room was constructed about ten years ago, and was originally used in a panel heating project. It is 12 ft wide and 24½ ft long, and the ceiling height can be adjusted from a low setting of 6 ft to a high setting of 11 ft. All interior surfaces are made of metal panels, to the back of which are fastened copper tubes through which heated or chilled liquid can be circulated to provide controlled surface temperatures. The liquid circuits are so arranged that different temperatures can be maintained on different surfaces to simulate various room conditions. In the tests described in this paper, all surface temperatures were held essentially equal to the dry-bulb temperature being maintained in the room. Further details regarding the general room construction and the piping circuits to the surface panels may be found in an earlier paper.[6]

In preparation for the physiological program, two pretest rooms and an observation room were constructed adjacent to the original Environment Laboratory as shown in Fig. 1, and all of the areas shown in the figure were air conditioned. An exterior view of the completed facilities is shown in Fig. 2; Fig. 3 shows the interior of the Environment Laboratory.

The air-conditioning system for the environment room is quite elaborate, and can maintain the dry-bulb temperature at any desired level from 40 to 140 F. The relative humidity can be controlled as desired throughout this wide

Fig. 2 Outside view of Environment Laboratory showing supervisory data center and instrumentation

dry-bulb temperature range by means of a capillary-type washer and a sorption-type dehumidifier. The air washer and some of the duct work for the air-conditioning system may be seen at the left of Fig. 2. Air is introduced into the room through perforated inlet strips located between the ceiling panels, and is exhausted from a continuous slot around the bottom periphery of the room, Fig. 3. Provision is made for circulating up to 50 air changes per hr.

An elaborate system of electronic-pneumatic control equipment has been provided to control, record and indicate test conditions. The space can be completely controlled from outside the test room so that minimum entry and exit is required by those in attendance. The central control panel may be seen in Fig. 2. The two instruments at the top of the center module are electronic, process-type controller-recorders, which control the dry-bulb and wet-bulb temperatures in the test room. The sensing elements for these two units are aspirated resistance thermometers located in the conditioned space. These may be seen in Fig. 3.

Below the two controllers are an electronic-indicating potentiometer and an electronic-multipoint recorder. By means of the numerous switches on the left-hand module of the control panel, the wall-surface-temperature thermocouples, and any other thermocouples or other electrical inputs can be connected into either of these instruments.

On the right-hand module of the control panel is a graphic representation of the air-conditioning system showing the air circuits, the heated and chilled liquid circuits, and the fans, coils and other major pieces of equipment. The pneumatic control lines are also outlined on this panel. Lights indicate those parts of the system

Fig. 3 Environment test room showing locations used by test subjects and some instrumentation

which are in operation, and air or liquid temperatures at various points in the system can readily be checked.

Participating subjects — Three groups of subjects were used in the project. The first group, which served from September 23 to December 23, 1958 consisted of six high school graduates who were enrolled in evening school. The second group, which varied from six to eight subjects, served from January 5 to March 13, 1959. This group was made up of some of the subjects from the first group and four older subjects. The third group, which worked from June 15 to August 28 consisted of one of the older subjects from Group 2, and seven college students on summer vacation. It was necessary to make a few changes in personnel in each of the groups. Pertinent data regarding the subjects are given in Table I.

Basal metabolism tests and physical examinations — Each subject underwent a physical examination and, with the exception of Subject No. 1, each was given one or more basal metabolism tests. There were two cases of hypertension, No. 9 (185/120) and No. 11 (195/90). In neither of these cases was the subject under medication and neither showed any signs of decompensation or even slight impairment; consequently, they were admitted as subjects. Basal metabolism rates

TABLE I—GENERAL DATA ON SUBJECTS

Subject Number	Name	Period of Participation	Sex	Age	Height cm	Height Inches	Weight kg	Weight Lbs.	Percentage Deviation*	Date of Metabolism Test
1	CT	9/23/58-11/25/58	F	18	149.9	59	43.50	95.8		
2	JC	9/23/58- 3/13/59	F	18	157.5	62	50.85	112.0	— 1.2	1/ 7/59
3	FB	9/23/58- 1/ 6/59	F	19	165.1	65	60.84	134.0	+ 4.4	1/ 6/59
4	SN	9/23/58-12/19/59	F	18½	164.2	65	50.39	111.0	— 8.4	12/19/58
5	GD	9/23/58- 3/13/59	M	19	173.4	68	60.65	133.6	—12.6	1/ 8/59
6	TR	9/23/58- 3/13/59	M	18	189.6	75	85.62	188.6	—23.4	1/ 9/59
"									—22.8	1/16/59
7	MR	1/19/59- 3/13/59	F	47	163.8	64	49.03	108.0	+ 9.0	1/29/59
8	BE	1/ 5/59- 3/13/59	F	53	153.0	60	53.84	118.6	—16.9	1/15/59
9	WK	1/ 5/59- 3/13/59	F	50	165.1	65	80.49	177.3	— 4.2	1/14/59
10	MJ	1/ 5/59- 3/13/59	F	18	167.6	66	65.74	144.8	+10.9	1/12/59
11	PH	2/16/59- 8/28/59	M	65	160.0	63	55.25	121.7	+ 0.5	2/12/59
"				66			54.84	120.8	— 7.1	9/ 2/59
12	BK	6/15/59- 7/12/59	M	20	173.4	68	62.70	138.1	— 8.3	6/18/59
13	CB	6/15/59- 8/28/59	F	19	164.5	65	55.12	121.4	— 6.5	6/23/59
14	BM	6/15/59- 8/26/59	F	18½	174.0	69	58.52	128.9	— 7.5	6/22/59
"									— 3.5	9/ 8/59
15	BB	6/15/59- 8/21/59	M	19	170.2	67	57.43	126.5	—15.8	6/22/59
16	KP	6/18/59- 8/28/59	F	18	158.8	63	46.76	103.0	—15.6	6/24/59
"							51.03	112.4	— 1.9	8/31/59
17	RC	6/30/59- 7/ 2/59	M	20½	186.7	74	65.78	144.9	— 5.0	6/30/59
18	SJ	7/ 1/59- 8/28/59	F	19½	163.2	64	53.16	117.1	— 6.4	7/ 1/59
"							54.43	119.9	—10.9	8/31/59
19	HD	7/ 9/59- 8/21/59	M	19	172.7	68	62.91	138.6	— 7.4	7/13/59
20	HD	7/20/59- 8/28/59	F	19	168.3	66	56.21	123.8	— 6.3	7/20/59

* Percentage deviation of basal metabolic rate from that predicted on basis of surface area and age

were calculated from at least three breathing periods, each exceeding 6 min.

Perusing Table I, it will be noticed that negative deviations prevail when using the Dubois Body Surface Chart and the Mayo Foundation Normal Standards for Predicting the Basal Metabolic Rate. Means and Lerman[7] found their peak for normal cases at about −4% and not at zero; their zone of no symptoms of hypothyroidism extends to −20%, while their zone of symptoms of thyrotoxicosis starts at +10%. These limits are similar to those of Cleveland Clinic (Courtesy Dr. O. P. Schumacher), namely that 95% of all cases fall between −20% and +15% of their predicted B.M.R.'s. According to Dr. Schumacher, a B.M.R. of −15%, especially in females, is a rather common experience. Among our participants, only one exceeded these limits (No. 6, B.M.R., in two tests, −22.8% and −23.4% respectively).

Clothing — An investigation of thermal responses of subjects to their environment can more accurately be carried out with subjects in the nude. However, in temperate climates, clothing is always worn

both in summer and winter, and it is in connection with clothed subjects that specific data are needed. Consequently, even though clothing presents an additional variable which must be considered, these tests were carried out with clothed subjects. To minimize variation due to clothing, customary indoor summer clothing (men without coats) was specified for both summer and winter, and subjects were asked to wear the same or similar outfits for all tests. The weight of clothing was checked frequently to make certain that this factor remained reasonably constant. It was found that the mean weight of clothing, exclusive of shoes, for the summer and winter groups, was 351.4 and 333.6 grams per square meter of subject surface area, respectively. The difference between these two values was not statistically significant ($P=0.694$). From the air temperature at which the occupants voted thermal comfort, it was estimated that the clothing represented an insulating value of about ½ clo. unit[8].

Room arrangement — The subjects were seated on typical college-type classroom chairs, having a wide right-hand arm rest for writing. The chairs were not fastened but could be moved from place to place in the room. However, a fixed position was indicated for each chair.

It was recognized that by increasing the number of subjects in the test room, the reliability of the mean votes could be increased. However, it was essential that the population density be kept low enough that radiation between subjects would not influence their sensation of warmth or comfort. The maximum number of subjects used at any time was 8, and with the observer, this made a maximum of 9 occupants. Thus, in a 12 x 24.5 ft room, 32.7 sq ft of floor area was available per person. Yaglou and Drinker[9] found that with a gross floor area of 25 sq ft per person, no effect of radiation was evident.

Air velocities throughout the occupied zone of the test room were found to be remarkably uniform. Measurements made with a heated-thermocouple-type anemometer at various locations in the room indicated that velocities at all points were less than 20 ft per min. At one location, the anemometer, which was not calibrated below 10 ft per min., was checked against a rhodium-plated Kata thermometer[10] calibrated for low air speeds. The anemometer indicated a velocity of 0 to 16 ft per min., the Kata thermometer indicated 14 ft per min.

The original paper on the effective temperature index by Houghten and Yaglou[1] did not indicate the actual air velocities which existed in their psychrometric rooms. It was only stated that the air velocities were negligibly small. The present effective temperature chart for still-air defines still-air as having a velocity of 15 to 25 ft per min.

Effect of radiation — The importance of radiation on comfort has already been mentioned. It has

also been stated that the six room surfaces were held at the same temperature as the room air. However, because of radiation from lights and occupants, the globe thermometer temperature was usually slightly higher than the air temperature. To evaluate the possible effect of this difference between globe and air temperature, a series of tests was conducted with the second group of subjects, in which the room surfaces were maintained at temperatures either above or below the air temperature. These preliminary tests seem to indicate that the effect on human comfort of a 3-degree elevation of room surface temperature over air temperature is approximately equal to the effect of a one degree increase in the dry-bulb temperature. It was therefore decided to maintain air and room surfaces at the same temperature and to neglect minor sources of radiation. This effect was further minimized by excluding data from all tests in which the difference between globe and air temperatures exceeded 1.2 F.

It should be emphasized that the study of radiation effects was made only to determine an approximate order of magnitude. A more exhaustive study of the subject is contemplated. It should also be pointed out that the results of these tests have not been included in the analysis presented in this paper.

EXPERIMENTAL PROCEDURE

Length of test period – Two test periods were held each working day. The morning period ran from 9 a.m. to 12:15 p.m. and the afternoon period from 1 to 4:15 p.m. The occupants remained in the environment room continuously during each test period and were discouraged from leaving their chairs except at ½ hour intervals when data were taken. They were allowed to read, talk, write, engage in table games, knit or sew as they desired. Smoking was not permitted. In order to assure complete equilibrium, the occupants were exposed to only one dry- and wet-bulb combination in each session.

Sensation scales and voting – Each subject was asked to report his impressions on a number of scales which included thermal sensation, sensation of humidity, sensible perspiration, pleasantness, air motion and sensation of warmth or coolness from surrounding surfaces. Of these, the first four were the most significant, and specific details of these scales are listed below. As previously indicated, the effect of air motion and radiation had been purposely minimized so as to have little effect on the subjects, and they are not reported here. It should be mentioned that each of these scales is arbitrary. A seven-point scale was used for thermal sensations. Both 7-point and 5-point scales have been used by prior investigators and both have been found to be satisfactory.

Thermal Sensation
1. Cold
2. Cool
3. Slightly Cool
4. Comfortable
5. Slightly Warm
6. Warm
7. Hot

Sensible Perspiration
0. Forehead or Body Dry
1. Forehead or Body Clammy (Surface feels moist to touch)
2. Forehead or Body Damp (Perspiration just visible)
3. Forehead or Body Wet (Sweat covering the surface, frequently in drops)
4. Parts of the Clothing Wet
5. Most, or All of the Clothing Wet

Humidity Sensation
The rooms seems to be
1. Painfully Dry
2. Very Dry
3. Dry
4. Normal
5. Humid
6. Very Humid
7. Wet

Pleasantness
1. Pleasant
2. Indifferent
3. Unpleasant
4. Very Unpleasant

Votes on the above scales were cast by the subjects every half hour throughout each test period. A perusal of the data indicated that the most stable votes were those which were cast toward the end of the session after the subjects had

TABLE II—COMPARISON OF MEAN AIR TEMPERATURES EVOKING VOTES "3", "4" and "5" IN WINTER GROUP (UP TO DEC. 19, 1958)

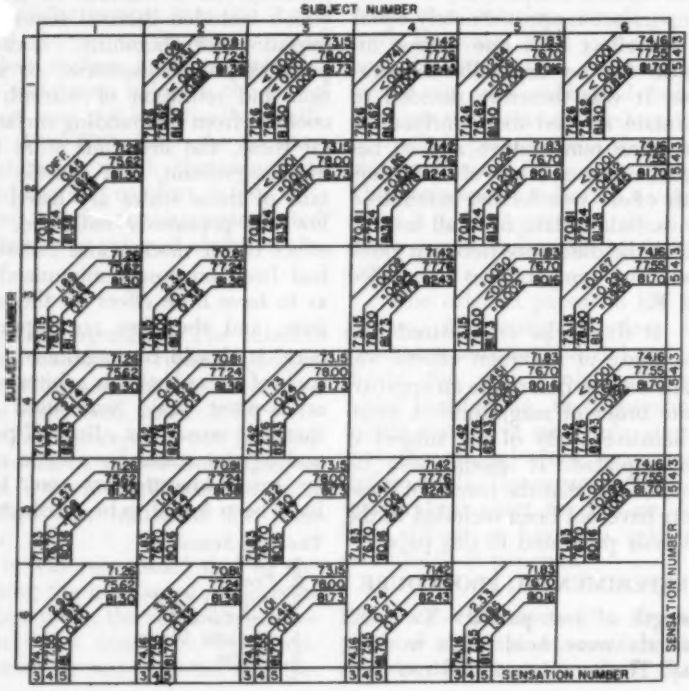

reached a state of thermal equilibrium.

Data and programming – The pulse rate and oral temperature of each subject were recorded at half hour intervals and the weight of the subject was taken at the beginning and end of each session.

Outdoor dry- and wet-bulb temtemperatures were taken and the weather conditions were noted before each session. In the environmental room itself both dry- and wet-bulb temperatures were taken at half hour intervals, using an aspirated psychrometer with mercury-in-glass thermometers. Wet- and dry-bulb resistance thermometers located in the same air stream were connected to electronic controller-recorders on the main control panel where both temperatures were indicated and recorded. Check readings were also taken frequently with a sling psychrometer. Wall-surface temperatures were determined by means of thermocouples on the surfaces, which were connected to the electronic recording and indicating potentiometers on the control panel. The globe temperature was obtained by reading a mercury thermometer having its bulb at the middle of the globe, or by thermocouples soldered to the globe and connected to the potentiometer.

The test points were first chosen by selecting conditions slightly cooler or warmer than comfortable. The range around sensation "comfortable" was then continuously narrowed. A similar pattern was followed to define the areas corresponding to conditions slightly cool and slightly warm. Later in the program additional test points were selected to provide a regular distribution of data along several relative humidity lines.

Data analysis and results—The several sensation votes cast simultaneously by each subject were transferred to a single index card. Also entered on the card were the date, time of day, number of subject, and the dry-bulb, wet-bulb and globe temperatures. Each card was numbered in chronological order.

There are several methods which can be followed in analyzing the votes. For example, the votes cast by each participant can be treated separately and for each sensation the mean dry-bulb and mean wet-bulb temperatures can be found. This method is applied when a comparison between participants is needed. Such a comparison was made for subjects numbers 1 to 6 of the first or winter group, for the period up to December 19, 1958. The results are shown in Table II, and are arranged to permit easy comparison. The rows and columns are numbered 1 to 6 to identify the subjects whose data appear in them.

In each square, two subjects are compared. The horizontal figures in each square are the mean air temperatures corresponding to sensations 3, 4 and 5 for the subject whose number appears at the top of the column. Similarly, the vertical figures are the mean air temperatures corresponding to the three sensations for the subject

whose number appears at the left of the row.

The sloped figures between the horizontal and vertical figures in the left lower part of the table are the differences in mean dry-bulb temperatures for the two participants. In the right upper part of the table, these sloped figures indicate the significance of these differences. For example, in the first square in the bottom row, mean air temperatures evoking sensation 3 in subjects 1 and 6 are shown to differ by 2.9 F. In the last square of the top row, the probability of such a difference occurring by chance is shown to be less than 0.001.

It may be noted from row 6 and column 6 of Table II that the subject, who had a slightly lowered metabolism, required a significantly higher temperature than Subjects 1, 2, 4 and 5 for Sensation 3. However, the temperature for Sensation 4 differed significantly only from that of Subject No. 1, and for Sensation 5, only from that of Subject No. 5.

The analysis of individual votes becomes difficult when a subject is absent from a test and leaves a blank for this test condition. It cannot be predicted what his vote might have been because of the wide overlap in air temperatures between sensations. Consequently, to minimize the effect of missing votes, it was decided to analyze the data on the basis of mean votes obtained by averaging all votes cast simultaneously.

A complete tabulation of individual votes would require excessive space, and a condensation of them has therefore been presented in Tables III, IV and V.

TABLE III—DRY-BULB AND WET-BULB TEMPERATURES EVOKING VOTE "3" FROM EACH PARTICIPANT (F)

Subj. No.	No. of Votes	Mean Dry Bulb	Mean Wet Bulb	Standard Deviation Dry Bulb	Standard Deviation Wet Bulb	Dry Bulb Extremes	Dry Bulb Range	Dry Bulb Overlap Sens. 3 & 4	Dry Bulb Overlap Sens. 3 & 5
1	29	71.26	56.65	1.808	7.768	69.0-75.1	6.1	4.5	0.2
2	42	70.82	56.95	1.095	6.966	69.2-74.0	4.8	4.6	0.0
3	43	73.15	63.10	2.891	7.835	69.2-78.0	8.8	5.7	0.0
4	44	71.42	60.83	2.318	8.366	69.2-76.0	6.8	4.6	0.0
5	39	71.83	59.16	2.607	7.456	69.2-77.2	8.0	8.0	5.2
6	96	74.16	62.45	3.228	7.697	69.1-79.4	10.3	7.9	4.3
7	4	71.95	61.58	1.204	1.208	70.9-74.0	3.1	2.4	0.0
8	14	74.06	61.19	1.086	1.625	72.5-75.5	3.0	3.0	1.0
9	29	73.33	62.51	1.609	2.234	71.0-76.4	5.4	5.0	1.9
10	16	72.43	61.65	2.045	2.315	69.2-75.5	6.3	4.1	0.0
11	34	73.69	63.69	2.470	6.240	70.0-78.0	8.0	5.5	0.0
12	8	71.25	63.95	1.131	2.751	70.0-73.2	3.2	3.0	0.0
13	11	71.68	59.18	2.150	4.298	68.9-74.6	5.7	4.4	0.0
14	23	71.93	60.29	2.399	4.121	68.0-76.1	8.1	3.7	0.0
15	15	71.23	64.46	3.413	4.972	68.0-77.6	9.6	8.7	3.1
16	10	71.64	61.60	1.292	6.412	70.1-74.0	3.9	3.5	0.0
18	12	77.02	63.36	2.608	6.531	73.9-82.0	8.1	8.5	2.0
19	10	71.56	58.79	2.278	7.449	68.9-75.0	6.1	5.0	0.0
20	7	72.84	56.87	2.498	4.008	68.9-76.0	7.1	2.7	0.0

Table III gives the mean dry-bulb and mean wet-bulb temperatures which evoked the sensation—"slightly cool" (3), and their standard deviations. The highest and lowest dry-bulb temperatures (dry-bulb extremes) at which "3" was voted, the difference between the extremes (dry-bulb range), and the temperature overlap of sensations are also given. Tables IV and V give similar information on sensations "comfortable" (4) and "slightly warm" (5). It will be noted from the last column of Table II that some overlap exists between sensations "3" and "5" even though they are not adjacent.

It should be kept in mind that the number which was assigned to each thermal sensation is not a true number but a rank. Objection therefore could be raised to treating these ranks like ordinary numbers, to forming their mean, and to reassigning to this mean a position on the rank scale. It was found, however, that within the comfort range, ranks may be treated like numbers without an appreciable error. Caution is, however, indicated near either end of the scale. Sensation "cold" (1) and "hot" (7) may be considered collective votes in the sense that whatever the degree of cold or heat, a person cannot vote lower than 1 or higher than 7. This does not mean that it is impossible to find lines of equal thermal sensation in the hot or cold regions. However, when working in the hot or cold region only, in the absence of "comfortable" as a base line, the temperatures associated with sensation ranks may differ from those shown in this paper.

Most of the votes cast were

TABLE IV—DRY- AND WET-BULB TEMPERATURES EVOKING VOTE "4" FROM EACH PARTICIPANT (F)

Subj. No.	No. of Votes	Mean Dry Bulb	Mean Wet Bulb	Standard Deviation Dry Bulb	Standard Deviation Wet Bulb	Dry Bulb Extremes	Dry Bulb Range	Dry Bulb Overlap Sens. 3 & 4	Dry Bulb Overlap Sens. 3 & 5
1	44	75.62	59.79	2.955	6.981	70.6-80.2	9.6	4.5	5.3
2	139	76.20	63.65	2.322	4.985	69.4-82.5	13.1	4.6	5.5
3	104	78.00	66.33	2.564	5.560	72.3-82.2	9.9	5.7	4.2
4	119	77.76	65.34	2.734	6.550	71.4-82.8	11.4	4.6	3.7
5	120	75.50	62.69	3.023	4.734	69.2-82.8	13.6	8.0	10.8
6	70	76.95	63.10	2.614	5.326	71.5-82.5	11.0	7.9	7.4
7	23	74.97	63.13	1.552	1.083	71.6-77.8	6.2	2.4	0.0
8	38	77.47	63.42	3.339	2.272	72.5-85.0	12.5	3.0	10.5
9	36	76.49	62.65	2.834	1.867	71.4-85.0	13.6	5.0	10.5
10	52	74.86	62.49	2.249	1.800	71.4-80.5	9.1	4.1	3.5
11	30	76.48	62.07	2.966	4.724	72.5-82.0	9.5	5.5	3.4
12	20	76.59	65.29	3.365	6.618	70.2-82.0	11.8	3.0	3.9
13	36	75.08	63.96	2.761	7.855	70.2-80.0	9.8	4.4	4.0
14	54	77.55	64.72	3.676	6.480	72.4-85.5	13.1	3.7	6.7
15	99	78.71	64.45	4.926	6.557	68.9-88.0	19.1	8.7	13.5
16	55	77.04	63.53	3.525	6.111	70.5-83.6	13.1	3.5	9.2
18	29	79.62	66.14	3.781	5.821	73.5-83.9	10.4	8.5	3.9
19	26	75.71	61.82	2.569	4.525	71.0-80.0	9.0	5.0	2.5
20	29	78.24	62.78	3.000	5.113	73.3-82.2	8.9	2.7	1.5

integer numbers. The participants were encouraged to express their sensations more accurately by using half-unit votes (e.g. 3.5, 4.5, etc.), but few such votes were cast.

When simultaneous votes are averaged, the mean vote is not likely to be an integer. However, it is possible to interpolate between such mean votes to determine the location of the integer vote lying between them. The premises for linear interpolation are equidistant spacing of the thermal sensation lines on the dry- and wet-bulb scales, and the absence of differences in curvature. Although neither of these was strictly true, cross checking indicated that no serious error was caused by this approach if the interpolations were made over small intervals. This method of interpolation has been successfully used by T. Bedford[11] and R. G. Nevins.[12] As an example of such interpolation, if at a certain relative humidity, the mean vote of the group at a dry-bulb temperature t_1 is 3.8 and at a temperature t_2 is 4.3, then the mean vote 4.0 would be located at an air temperature $t_1 + (t_2 - t_1)\ 2/5$; for 0.2 sensational unit out of 0.5 has to be added to 3.8 in order to obtain 4. Similar interpolations may also be carried out for dissimilar relative humidities or wet bulbs.

Fitting of interpolated points by straight lines – With the lower thermal sensations ("3" and "4") an approximately linear course soon was apparent. Linear regression lines were fitted by calculating the coefficient of correlation (r) as well as the coefficients of regression, $r\frac{\sigma_y}{\sigma_x}$, and $r\frac{\sigma_x}{\sigma_y}$, in which σ_x is the

TABLE V—DRY-BULB AND WET-BULB TEMPERATURES EVOKING VOTE "5" FROM EACH PARTICIPANT (F)

Subj. No.	No. of Votes	Mean Dry Bulb	Mean Wet Bulb	Standard Deviation Dry Bulb	Standard Deviation Wet Bulb	Dry Bulb Extremes	Dry Bulb Range	Dry Bulb Overlap Sens. 3 & 5	Dry Bulb Overlap Sens. 4 & 5
1	49	81.30	68.11	2.246	7.083	74.9-85.1	10.2	0.2	5.3
2	65	81.11	67.50	2.844	6.093	77.0-88.0	11.0	0.0	5.5
3	46	81.73	69.41	2.532	7.344	78.0-88.2	10.2	0.0	4.2
4	53	82.43	69.13	3.247	7.301	79.1-88.0	8.9	0.0	3.7
5	108	80.16	68.64	3.978	6.735	72.0-89.3	17.3	5.2	10.8
6	69	81.66	68.57	3.374	5.846	75.1-89.2	14.1	4.3	7.4
7	1	82.00	65.80			82.0-82.0	0.0	0.0	0.0
8	13	80.08	65.02	3.025	2.924	74.5-85.5	11.0	1.0	10.5
9	12	79.26	64.46	2.778	1.597	74.5-84.8	10.3	1.9	10.5
10	14	79.06	64.30	2.057	1.257	77.0-82.2	5.2	0.0	3.5
11	18	81.53	69.12	1.781	5.743	78.6-85.1	6.5	0.0	3.4
12	6	79.87	68.23	1.826	6.672	78.1-82.4	4.3	0.0	3.9
13	29	81.05	67.31	1.950	6.344	76.0-83.9	7.9	0.0	4.0
14	36	85.02	71.49	2.839	6.366	78.8-90.0	11.2	0.0	6.7
15	32	85.78	72.23	3.483	5.599	74.5-91.0	16.5	3.1	13.5
16	36	82.98	68.57	3.017	5.814	74.4-87.6	13.2	0.0	9.2
18	32	83.80	68.79	2.555	5.551	80.0-88.0	8.0	2.0	3.9
19	39	82.86	70.28	3.104	5.284	77.5-90.0	12.5	0.0	2.5
20	21	82.22	71.43	4.648	5.136	80.7-87.0	6.3	0.0	1.5

standard deviation of dry-bulb temperatures and σ_y the standard deviation of wet-bulb temperatures. The two regression lines intersect at a point whose ordinates are the mean dry-bulb and the mean wet-bulb temperatures. The angles which the regression lines make to the horizontal and vertical respectively are measured by the coefficients of regression. Both regression lines are not always of equal standing, and one may have a definite physical meaning, while the other has only conventional meaning given to it by mathematical definition.[13] Of the two regression lines which were calculated, the one showing the mean values of dry-bulb for regularly increasing values of wet-bulb was used.

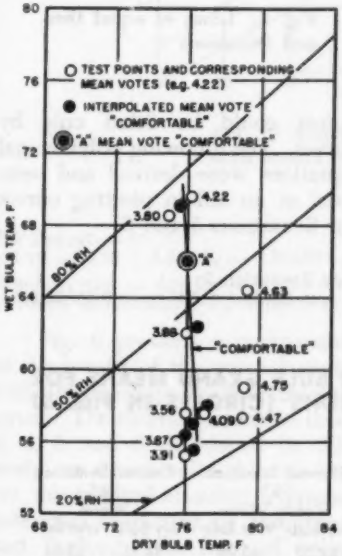

Fig. 4 Method employed in locating sensation line by interpolation

Fig. 4 has been prepared to illustrate the method of data analysis. The circles on the figure show the various environmental conditions for a short series of tests, and the adjacent figures are the mean votes of the groups at these conditions. The dot noted A is a mean vote which happened to be 4.0. All other dots represent the location of "4" votes which have been determined by linear interpolation between two circles with which they are in line.

The regression lines were calculated as indicated above from the dry-bulb and wet-bulb coordinates of the dots, and the relevant regression line is shown. This is the straight line of best fit for the plotted data. It should be pointed out that this example was worked out for a relatively small number of tests, and the results therefore differ somewhat from those found for the complete study.

Though curvature was evident for sensations "5" and "6," coefficients of correlation and regression coefficients were also calculated, though the latter served only as indicators of direction.

As indicated earlier, test points were chosen to provide a distribution of data along selected relative humidity lines. At the completion of the test program a great number of individual votes were available along each of these lines. This mass of data was reduced by three successive steps. First the individual votes were converted to group

means. Next, from the group means, integer votes of sensations 3, 4, 5 and 6 were determined by interpolation as described above. Grand means were then determined by averaging the temperature and humidity coordinates of each group of integer votes at the four or five humidity levels. The ordinates of these grand means are listed in Table VI and the points are shown in Fig. 5.

Sensation lines 3 and 4 on Fig. 5 are the relevant regression lines for the points shown. It should be pointed out that the line of optimum comfort is based on both winter and summer data. Separate treatment of the winter and summer data indicated a difference of approximately 1.2 degrees ($P = 0.0057$) in the mean dry-bulb temperatures for the two seasons. Thus, the winter comfort line would be 0.6 F lower, and the summer line 0.6 F higher than the mean comfort line shown in Figs. 5 and 6.

Thermal sensations 5 and 6 depended on humidity as well as air temperature, and the plotted points could be fitted only by curves. The following polynominal equations were derived and were used as an aid in plotting curves for Sensations 5 and 6.

For Sensation 5:

$$t_s = 20.22 + 1.983\, t_w - 0.01576\, t_w^2$$

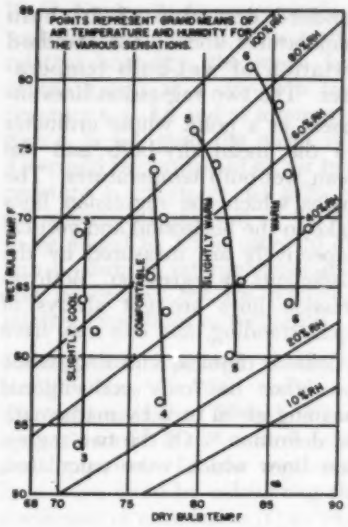

Fig. 5 Lines of equal thermal sensations

TABLE VI—DRY BULB AND WET BULB GRAND MEANS FOR DIFFERENT THERMAL SENSATIONS (CIRCLES IN FIG. 5)

Thermal Sensation "3" Slightly Cool		Thermal Sensation "4" Comfortable		Thermal Sensation "5" Slightly Warm		Thermal Sensation "6" Warm	
Dry Bulb	Wet Bulb	Dry Bulb	Wet Bulb	Dry Bulb	Wet Bulb	Dry Bulb	Wet Bulb
71.35	53.59	77.22	56.69	82.20	60.08	86.36	63.86
72.52	61.82	77.61	63.25	82.89	65.38	87.68	69.28
71.60	64.10	76.42	65.66	81.92	68.28	86.12	73.25
71.22	68.94	77.32	69.98	81.03	73.86	85.38	78.22
		76.57	73.53	79.36	76.38	83.35	80.95

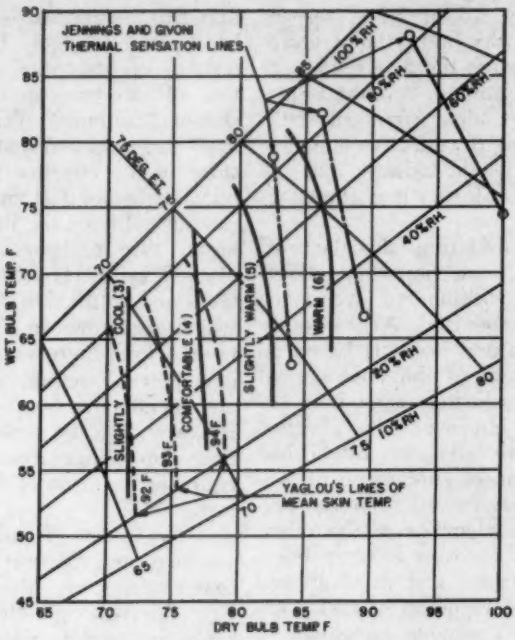

Fig. 6 Comparison of new data with results of former investigators

For Sensation 6:

$t_s = -29.20 + 3.384\, t_w - 0.02459\, t_w^2$

Where t_s and t_w are the dry-bulb and wet-bulb temperatures F, respectively.

Fig. 6 presents a comparison of the results of the present study with the findings of other investigators. The thermal sensation lines 3, 4, 5 and 6 developed in this study are shown solid. Also shown are the original effective temperature lines developed by Houghten and Yaglou,[1,2] the lines of mean skin temperature as established by Yaglou,[14] and the thermal sensation lines of Jennings and Givoni.[4]

Discussion of results – From Fig. 6, it is immediately apparent that the slope of the new sensation "4" line and the effective temperature lines differ appreciably. A critical comparison is therefore indicated.

It may be seen that along the line of optimum comfort (Sensation 4), a change from 20 to 80% relative humidity is compensated by a drop of approximately 1.5 F in dry-bulb temperature. A similar change in relative humidity along the 68 F ET winter comfort line or the 71 F ET summer comfort line would require a change of ap-

proximately 6.5 or 7.7 F, respectively in dry-bulb temperature. Thus, although the new data indicate that optimum comfort is primarily dependent upon dry-bulb temperature, the effective temperature lines would indicate that the humidity is also an important factor.

In considering this lack of agreement, one important difference in conditions of occupancy must be recognized. As previously stated, the new work is based on the appraisal of the environment after approximately three-hour occupancy. However, the effective temperature index was established on instantaneous judgments of subjects as they moved from one psychrometric chamber to the other. The chambers were held at different combinations of dry-bulb and wet-bulb temperatures, and were adjusted to provide an equal, or nearly equal, feeling of warmth. Thus, the findings were based on a quick comparison of the rooms with the reaction of the subjects being stated as the same, warmer, or cooler. Dr. E. V. Hill,[1] in discussing the paper, commented that the curves obtained were lines of immediate temperature perception and not equal comfort lines.

A number of previous investigators have felt that the effective temperature lines overestimated the effect of relative humidity. C. P. Yaglou,[15] who was one of the authors of the original paper, stated in 1954, that in his opinion the influence of relative humidity was only about half of that indicated by the original work. He suggested that this overestimation can now be explained largely by the phenomena of adsorption and desorption of moisture on the exposed skin and clothing.[16] Professor Yaglou[14] also proposed that the correct slope of the effective temperature lines in the comfort zone could be established from the lines of equal mean skin temperature of the clothed body. His lines of 92 F, 93 F and 94 F skin temperature, which are shown in Fig. 6, are in much closer agreement with the new thermal sensation lines than are the effective temperature lines. However, it is not generally agreed that skin temperature is an unequivocal measure of thermal comfort.

The results of earlier work by Jennings and Givoni[4] at elevated temperatures are also plotted on Fig. 6. Although the numerical ranks assigned to similar environments by the two groups of subjects varied considerably, the lines of equal thermal sensation as found in the two studies have approximately the same slope. Since the Jennings and Givoni tests were made at only two relative humidities, only two points can be plotted for each sensation line, and these two points have been connected by straight lines.

The experiences of engineers in the field also indicate that comfort is dependent primarily on the dry-bulb temperature, and is so little dependent on humidity that this factor is frequently not even mentioned. Field experience also confirms the fact that comfort is attained at essentially the same

dry-bulb temperature, both in winter and summer. W. L. Fleisher[15] stated that his field experiences indicated that maximum thermal comfort was experienced between 74 and 76 F dry bulb during both summer and winter. In the discussion of a paper, L. T. Avery[17] described an installation in which approximately 2000 people had found optimum comfort at 76 F and 35% relative humidity, regardless of the season or outside weather conditions. C. S. Leopold[18] described similar findings in his paper and cites instances of buildings that are operated at 76 or 77 F throughout the year.

Fig. 1 in the recent paper by Werden, Fahnestock and Galbraith[19] shows that a comfort vote of 4 was obtained by their subject panels at 76 F dry-bulb temperatures and 40% r.h., and at 75 F dry-bulb and 80% relative humidity. These two points would set the slope of their "4," or comfort line, at exactly the same angle as found in the studies reported here. Their line is not drawn on Fig. 6 of this paper because copy of their work was not available until after the graphs of this paper had been finished.

Over the years, there has been a gradual increase in the optimum winter temperature. Research prior to 1932 indicated that optimum conditions in winter were to be found along the 66 F ET line. In 1941[20] a shift to 67 F ET was reported, and the comfort chart which has been included in the GUIDE since 1951 locates the winter comfort line at 68 ET. This increase in optimum winter temperature is probably due primarily to the lighter winter clothing now being worn. This change in clothing is undoubtedly the result of the widespread improvements in heating in this country.

CONCLUSIONS

1. Lines of equal thermal sensations for continued occupancy have been determined which are applicable to sedentary (inactive) individuals, lightly clothed in still-air conditions, in a uniform radiant environment with the temperature of the surroundings maintained approximately equal to the air temperature.

2. The line of optimum comfort for both winter and summer is approximately straight and ranges from 77.6 F at 30% relative humidity to 76.5 F at 85% relative humidity. It is only slightly dependent on humidity.

ACKNOWLEDGMENTS

The authors are indebted to a number of individuals for giving assistance on this project. Members of the RAC on Physiological Research and Human Comfort were most helpful in planning of the project and following its progress. This was also true of the other members of the Laboratory staff. The twenty men and women who served as subjects were patient and conscientious throughout the many tests.

Dr. L. A. Doty of Western Reserve University served as consult-

ing psychologist throughout the whole program. Dr. Thomas Bedford of London, England, spent two days at the Laboratory in helpful consultation. A number of others, too numerous to mention, made significant suggestions during the research by correspondence.

REFERENCES

1. Houghten, F. C. and Yaglou, C. P.—Determining Lines of Equal Comfort, Trans. ASHVE, v. 29, p. 163-176, 1923.
2. Houghten, F. C. and Yaglou, C. P.—Determination of the Comfort Zone, Trans. ASHVE, v. 29, p. 361-384, 1923.
3. Heating, Ventilating, and Air Conditioning GUIDE, Annual Publication of ASHRAE, p. 70, 1959.
4. Jennings, B. H. and Givoni, B.—Environment Reactions in the 80 to 105F Zone, ASHAE Journal, p. 3-10, January, 1959.
5. Vernon, H. M.—Measurement of Radiant Heat in Relation of Human Comfort, Jour. Inst. Hygiene, v. 14, p. 95, 1932.
6. Tasker, C., Humphreys, C. M., Parmelee, G. V., Schutrum, L. F.—The ASHVE Environment Laboratory, Trans. ASHVE, v. 58, p. 139-154, 1952.
7. Dubois, E. F.—Basal Metabolism in Health and Disease. Lea and Febiger, p. 322-324, 1936.
8. Herrington, L. P. and Hardy, J. D.—Temperature and Humidity in Relation to the Thermal Interchange between the Human Body and the Environment. Human Factors in Undersea Warfare, National Research Council, Chap. 13, p. 305.
9. Yaglou, C. P. and Drinker, P.—The Summer Comfort Zone: Climate and Clothing, Trans. ASHVE, v. 35, p. 269-286, 1929.
10. Koch, W. and Kaplan, D.—A Rhodium Plated Kata Thermometer for Measuring True Air Velocity, Jour. of Scientific Instr., v. 35, p. 8-11, 1958.
11. Bedford, Thomas—Private Communication, 1958.
12. Nevins, R. G., Flinner, A. O.—Effect of Heated-Floor Temperatures on Comfort, Trans. ASHAE, v. 64, p. 175-188, 1958.
13. Fisher, R. A.—Statistical Methods for Research Workers, Oliver and Boyd, 1946.
14. Yaglou, C. P.—A Method for Improving the Effective Temperature Index, Trans. ASHVE, v. 53, p. 307-326, 1947.
15. Minutes of the Technical Advisory Committee on Comfort, June 28, 1954.
16. Newburch, L. H.—Physiology of Heat Regulation and the Science of Clothing, W. B. Saunders Co., p. 280, 1949.
17. Glickman, N. et al—Comparison of Physiological Adjustments of Human Beings during Summer and Winter, Trans. ASHVE, v. 54, p. 307-320, 1948.
18. Leopold, C. S.—Conditions for Comfort, Trans. ASHVE, v. 53, p. 295-306, 1947.
19. Warden, Jane E., Fahnestock, M. K. and Galbraith, Ruth L.—Thermal Comfort of Clothing of Varying Fiber Content, Textile Research Journal, v. XXIX, No. 8, Aug. 1959.
20. Houghten, F. C., Gunst, S B. and Suciu, J. Jr.—Radiation as a Factor in the Sensation of Warmth, Trans. ASHVE, v. 47, p. 93, 1941.

DISCUSSION

W. H. MULLIN, Philadelphia, Pa. (Written): This article states ". . . comfort is primarily dependent upon the dry-bulb temperature and is so little dependent upon the humidity that this factor is frequently not even mentioned." To design for a latent load means some consideration of humidity and its control, and also often requires an elaborate control system to give a desired humidity. If this humidity factor were disregarded and only the dry-bulb temperature used as a design criterion, many poor air-conditioning systems would be the result, particularly in areas where 90% relative humidity is experienced over extended periods. The paper indicates a change in optimum winter time temperature from a 66 F effective temperature line to a 68 F temperature line. This is attributed to a change in the type and weight of clothing worn. Wouldn't a similar change to lighter summer clothing also influence the results presented here, causing them to differ from previous work which may have used different type and weight of clothing. This being the case, a repeat of your tests may not completely correlate if the weight and type of clothing is not held constant.

In the optimum comfort region, line 4, Fig. 6, humidity has less effect on comfort than at higher dry-bulb temperatures; this is confirmed in the study. However, the humidity effect seems to be overly-minimized, a very slight change in dry-bulb will compensate for a large change in wet-bulb. Engineers, through experience, recognize the shortcomings of the present comfort tables and have made their own corrections and allowances. Only time and experience with the use of new information can prove its practicality.

CLOSURE BY AUTHOR HUMPHREYS: We agree that almost every comfort air-conditioning system is designed to handle some latent load. We believe that this is the proper procedure and nothing in this paper should be interpreted as indicating otherwise. On a hot, humid day, if the dry-bulb were lowered sufficiently to produce a comfortable temperature without the removal of moisture, serious problems could develop. It is both possible and customary to define comfort conditions in terms of dry-bulb only. At higher temperatures, relative humidity becomes a second parameter which must be included.

In referring to the effect of clothing in changing the optimum E. T. from 66 F to 68 F, we also were suggesting the possibility of a shift to still higher temperatures because

of the light clothing being worn today. This paper reports on only one small facet of the extensive problem related to the effect of environmental conditions on human comfort. The data apply only to the limited conditions in the paper. As further data are obtained on the other parts of the problem, a more comprehensive picture will become apparent.

R. G. NEVINS, Manhattan, Kansas (Written): Many members of our Society will be pleased to note that the environmental program for revaluation of the comfort chart is well underway and that this paper is the second in a comprehensive program. The Laboratory has excellent facilities for these studies, and we should commend the staff and past members of the TAC on Physiological Research for their efforts in preparing and initiating the program. However, the subject is so complex that more data are needed if we are to provide the members of the Society with a complete and accurate picture of man's response to this thermal environment. This paper represents an important part of this picture and it is satisfying to see the progress being made.

However, the authors' conclusions should be studied with care and in context. Serious misapplication of these data could result if the limitations imposed by the conditions of these tests are not recognized. These limitations are presented in the paper and include: sedentary, seated subjects, limited in number (13 female and 7 male), lightly clothed individuals, 16 of college age and 4 in the 47 to 66 year age group, still air conditions with the MRT equal to the air temperature.

Data are not presented which will allow one to estimate effects of radiation although mention is made of this factor.

It is gratifying to see reported some of the data used in preparing the curves shown in Fig. 6. The discussion of the statistical methods used in data analysis is also of value. This information will be of interest to those who wish to critically examine the conclusions.

It is hoped that future studies will remove many of the limitations imposed on these tests and that sometime in the future a comfort chart will be presented which may include corrections for air velocity, radiation, and activity. Prof. Jennings, Mr. Humphreys and Dr. Koch are to be congratulated for the work they and the laboratory staff are doing to make this possible.

I have two questions to ask the authors, first, what use, if any, was made of the subject votes regarding sensible perspiration, humidity sensations and pleasantness? And, secondly, to what degree do the authors feel these data are of value in comfort studies?

AUTHOR HUMPHREYS: Thank you Dr. Nevins for your kind and encouraging remarks, and for so clearly restating and stressing the limitations imposed on the data by the conditions of the tests. This paper is only a first step toward a more complete understanding of the complex relationships which exist between man's environment and his degree of comfort. Data on other facets of the problem will be developed at the Laboratory as rapidly as possible.

To answer your first question, to date no use has been made of the subjects' votes on sensible perspiration, humidity sensation and pleasantness.

Your second question is not easy to answer. We cannot be sure that these data for comfort level tests will ever have great value. However, it costs little or nothing to gather this additional information while the tests are being run.

BARUCH GIVONI, Haifa, Israel (Written): A former study from the ASHRAE Research Laboratory indicated that increasing humidity below 85 F has much more effect on the sensible perspiration than on the thermal sensation, and the feeling of wetness might be the main cause of discomfort associated with high humidity. Does the present investigation confirm this supposition?

The slopes of the weight loss lines in the Laboratory study published in January 1959 suggested that below 80 F, increasing the humidity reduces the weight loss. This is confirmed by the data published by Inouge et al., "Effect of RH on Heat Loss of Man Exposed to Environments of 80, 76 and 72 F" (ASHVE TRANSACTIONS 1953), and by Werden, Fahnestock and Galbraith in the article "Thermal Comfort of Clothing of Varying Fiber Content" (*Textile Journal*, August 1959). It would be of interest to compare the present results with those above.

Also, in the January 1959 paper of the Laboratory, it seemed that although the pulse rate and oral temperature did not change with sufficient significance as a response to the change in air temperature in this zone, they responded more significantly to changes in humidity. What are the results of the present study in this connection?

AUTHOR HUMPHREYS: The January 1959 paper presented the results of tests made at temperatures ranging from 80 to 105 F. In these tests, in which the conditions were above the comfort level, sensible perspiration, weight loss, and changes in pulse rate and oral temperature were significant variables. However, in the series of tests at or near the comfort level, the values of these variables were minimal. These data have not yet been completely analyzed but they will be studied, and if any significant trends are indicated, they will be reported at a later date.

JOHN EVERETTS, JR., Philadelphia, Pa. (Written): Since the presentation of the subject paper at the Dallas meeting, I have endeavored to analyze the data presented in this paper and compare it with the data presented a year ago in the progress report entitled Environment Reactions in the 80 to 105 F Zone, by Jennings and Givoni,[15] presented at the Annual Meeting of ASHAE in Philadelphia in January, 1959. I have also tried to compare the data presented in these papers with some of the previous work in the Laboratory and others.

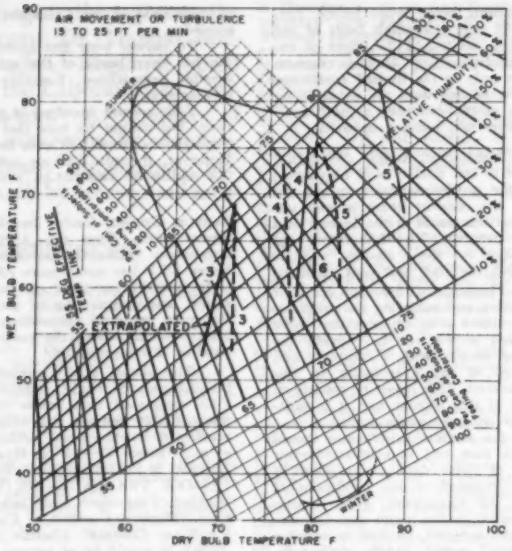

Fig. A ASHRAE Comfort Chart, 1958 GUIDE, with superposed lines used in discussion of John Everetts, Jr.

Fig. A shows a copy of the Comfort Chart in which the results of both papers are overlaid in terms of the "sensation numbers" as they were presented. No. 3 is stated colder than optimum, No. 4 is supposed to be optimum, and No. 5 is warmer than optimum. Also included is a dash line, numbered 6, which is vertical (no humidity effect) from the 1959 data.[15] The solid lines are from the 1959 report, and the broken lines from the 1960 paper.[16] Sensation No. 3 for the 1959 report has been extrapolated from Fig. 5 of the report from 75 to 68 F at 33%, and from 80 to 71 F at 85%.

The findings for sensation No. 5 are 7 F higher in the 1959 report[15] than for the 1960 paper.[16] Sensation No. 4 is in close agreement at 33% RH, but 2½ F off at 85% RH. The findings for sensation No. 3 show a close agreement at 85% RH but are off over 4 F at 33% RH. Since the major conclusion is the absence of humidity effect and the lines on Fig. No. A are straight, the extrapolation for sensation No. 3 appears to be justified.

The vertical line indicating no sensation reaction to humidity (for the 1959 report) is at 80 F, which is 4 F over the generally accepted optimum, while the vertical line in the 1960 paper is at approximately 72, which is 4 F below the accepted optimum.

The 1959 report indicates an optimum of 79 F at 85% RH, and 78 F at 33% RH. The 1960 paper concludes the optimum to be 77.6 F at 30% RH, and 76.5 F at 85% RH and "only slightly dependent on humidity."

In the 1959 report, the clothing for the men consisted of a sports-type shirt with short sleeves, light underpants, socks, and according to the photograph, long trousers.

In the tests conducted at the Laboratory in 1936, referring to Page 217 of the Transactions for that year, it will be noted that the clothing worn consisted of athletic underwear, a light-weight shirt with collar attached, tie, light socks, light-weight summer coat and light flannel trousers. There is certainly a great deal of difference in the sensation of comfort between a long-sleeved shirt with collar and tie which fits snugly around the neck, compared to a short-sleeved sports shirt with open collar. As far as my observations are concerned, I have rarely seen a man in an office building who does not wear a long-sleeved shirt with collar and tie. In some cases, he does not wear a coat and may roll up his shirt sleeves.

The results of the tests made at the University of Illinois and reported in Paper No. 1480 in Transactions No. 59, 1953, pages 329-346, with subjects clad only in union suits showed practically no effect of relative humidity between 30 and 80% at 72 and 76 F but a decided difference was noted at 80 F. (Sensation No. 4.4 at 30% to No. 5.4

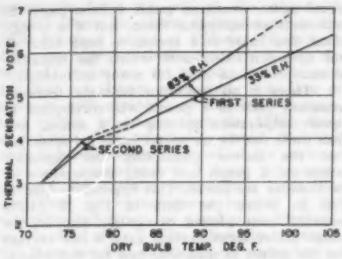

Fig. 4 Thermal sensation lines at a high and low relative humidity plotted from the Data of Environmental Studies I and II at a high and low relative humidity, Refs. 14 and 15

at 80%, Fig. 1, page 333.)

The following observation is quoted from page 337: "Immediately upon entrance into the psychrometric room from the staff office, the men still dressed in their street clothes always felt the environment with an 80% RH to be warmer than the one with a 30% RH. In an environment maintained at 80 F, the difference in sensations, persisted throughout the exposure."

In the 1959 report, the last sentence on page 9, referring to thermal sensation number vs. sensible perspiration number, states as follows: "One basic difference between these responses is that the thermal sensation is almost instantaneous and does not change appreciably with time of exposure in a constant environment."

In the middle of first column of page 7 of the 1960 paper, the following statement is made: "As previously stated, the new work is based on the appraisal of the environment after approximately three hours occupancy. However, the effective temperature index was established on instantaneous judging as the subject moved from one psychrometric chamber to the other."

These two statements appear to be contradictory. Furthermore, the 1936 work of Houghten reported in Paper No. 1035, on page 215 of the 1936 Transactions, specifically shows that the subjects were tested over a three-hour period and the elapsed time for the subject to establish a complete sensation equilibrium was seldom less than a 30-min period.

There is nothing in these publications to indicate that these inconsistencies were considered or resolved in the conclusions. The differences are so great that I feel they should be considered in light of previous work to determine wherein the deviations occur and how they may be resolved, if possible.

AUTHOR HUMPHREYS: Much of this discussion is based on the assumption that data determined in one regime are applicable to a distinctly different regime. This is somewhat surprising, as the pitfalls of extrapolation are normally so well recognized that most engineers studiously avoid the practice. It is not, then, surprising that the extrapolation carried out in the discussion produces irrelevant and erroneous conclusions. The discussor has presented his work in Fig. A which contains his lines and some from the papers. Those from the papers reading from left to right are the second No. 3 line (dotted), the first No. 4 line (dotted), the first No. 5 line (dotted), and the last No. 5 line (solid). The remaining lines on this chart result from the discussor's extrapolation and represent his own thinking but, as will be shown, are not conclusions implied in either paper. In particular his solid lines 3 and 4 are the result of extrapolation and the dash line No. 6 which the discussor states is a "vertical line indicating no sensation reaction to humidity" is similarly a limiting condition from the 1959 data. Factually, the 1959 data for the hot region showed that humidity had a great effect on response in its full spread, but relative-humidity effect minimizes as the severity of the conditions becomes less.

Before discussing further comparisons of the extrapolated lines, it is necessary to explore the significance of the sensation numbers, as in particular he makes a statement, which should be answered, that sensation No. 5 in the 1959 report is 7 F higher than in the 1960 paper. This he points out as an inconsistency. Before reaching a conclusion in this regard, let us analyze what is meant by the sensation numbers. The basic scale for thermal sensation used by the subjects is as follows:

1. Cold
2. Cool
3. Slightly Cool
4. Comfortable
5. Slightly Warm
6. Warm
7. Hot

On this scale, No. 4 is the number representing comfort which may be described simply as the absence of discomfort. In terms of this scale, to a group of subjects habituated to the comfort region, No. 5 (slightly warm) applies to any condition that is even slightly warm. Thus sensation No. 5 approached from the viewpoint of the comfort range will be only a few degrees above the optimum line of comfort. Consider, however, approaching sensation No. 5 from the opposite direction; for example, from the viewpoint of a subject in an environment at perhaps 95 F. To this subject a change of environment even to 88 F would be a great relief, and it is highly probable that a change of one point in his recorded sensation would take place. Let us now consider the maximum sensation No. 7 (hot). Depending upon the subject's viewpoint, hot may be anywhere from say 95 F to the highest temperature that could be endured for short periods of time, say 135 F

Yet, from another viewpoint, the subject might consider that the lower part of this range is merely warm, giving it a No. 6 value. The important thing is that, in any group of tests, consistent values must be established relative to the subject's frame of reference.

The fact then that the No. 5 sensation is different when approached from the hot region than when approached from the comfort region leads to the obvious conclusion that it is purely fortuitous if the same value is given to No. 5 under different testing regimes. In addition to the two papers in which it was mentioned that No. 5 differed by 7 degrees, attention might be called to the paper of Professor Ralph Nevins, No. 1630 (1958 Transactions),[17] where from the one point of his tests that can be compared, his No. 5 value is approximately 3 degrees higher than the 1960 data indicate and 3 degrees lower than the 1959 degree data. Should we, therefore, conclude that his work is questionable, because it does not agree with either of the Laboratory values, or must we arrive at the conclusion that any of the three values are satisfactory provided the data on which they are determined are internally consistent?

Let us now consider the discussor's extrapolation of hot-region data to show that the optimum comfort line as indicated from the extrapolation is not in agreement with the optimum comfort line as determined from the 1960 series of carefully conducted tests. If they should agree, it would be only by happenstance and for no other reason. The authors of the hot-region paper would have been wise to have completely stopped their graphs above 90 F, as it was there the testing was really concentrated. As comfort was not a part of this paper, the authors felt absolutely no justification at this point in making any comfort conclusions based on inadequate data.

However, because the discussor has brought up the question of extrapolation, it appeared advisable to explore the data of both papers; and in Fig. B, pertinent data have been plotted to bring out what was involved. The two solid lines at the right of the figure show the relationship determined for the hot environments of the earlier paper[15] between dry-bulb temperature and thermal-sensation vote for the 83 and 33% relative-humidity conditions. The solid lines at the left of the graph show similar relations obtained at, or near, comfort levels in the second paper.[16] The solid lines from the earlier paper apply to the range over which the subjects were actively tested; namely, 82 F to 95 F and 82 F to 102 F and above. Dotted lines were then used to connect the two testing regimes, as it is obvious that for the complete spread from hot to cool conditions the plots are far from linear in character. Fig. B shows how the striking effect of relative humidity in the hot region gradually minimizes for inactive subjects as conditions become more comfortable. If, however, the diverging lines from the hot region are erroneously continued as being linear, they quickly intersect in the region of the 4 sensation to indicate an untenable conclusion. From an analytical sense, sensation point 4 from paper II represents an optimum value, but it is recognized that there is a spread to both sides of this optimum value over which the sensation of comfort would hold for many individuals.

There is no assurance that the thermal-sensation scale of 7 points will correspond to equal temperature spacing on a graph, and thus there can be no sound basis for assuming that the curves connecting the sensation points on a graph and using temperatures at its abscissa are linear. This appears to hold in Fig. B. When the data of Fig. 5 (1959 paper)[15] were plotted, a straight line for the range under consideration gave a fair average for the points in question; and for this reason, lines were thus drawn without curvature and without endeavoring to distort the data by changing slope to make them agree with what the value 4 might have been thought to be. Considering the form that the data actually take, the point of extrapolating to predict the cold No. 3 sensation from subjects tested in a hot range certainly appears to be ill-advised and without justification. Moreover with the high- and low-relative humidity lines converging as they do, any conclusions after they intersect would be highly suspect. In the minds of the authors, the only point which can be concluded from the data as they appear is that as the dry-bulb temperature lowers there appears to be less influence of relative humidity in determining the comfort of an individual.

The discussor raises the question of type of clothing used by the subjects. This is a very important item and one to which we have given the greatest thought. We recognize that other tests need to be run with subjects more heavily clothed, as it is important that our industry have knowledge as to the manner in which clothing affects subjective response. At the present time, the only conclusion that we have made in these papers is that the results reported are for lightly-clothed individuals. We certainly agree wholeheartedly with the discussor that an office worker wearing a coat with collar and tie will react differently to environmental conditions than will the lightly-clothed individual. Moreover, we fully realize that the degree of activity of the subject is important and that subjects walking around, working on files, operating machines or carrying out assembly processes will require lower temperatures for comfort than will lightly-clothed, seated subjects engaged in restricted activity.

We certainly agree with the discussor's comment relative to the test at the University of Illinois, paper No. 1480, which indicates that the humidity effect is noted at 80 F. This point is definitely outside of the comfort region even for inactive individuals, and the problem of dissipation of sweat generated for removal of heat cannot be disregarded. A study of Fig. 6 of the 1960 paper (shown on page 279) shows that this is definitely in agreement with our findings, and the same result appears in the interconnected graphs of Fig. B.

Let us now reply to the fourth and fifth

paragraphs from the end of the discussor's remarks where he quotes the statement in the 1959 hot-zone paper as follows: "One basic difference between these responses is that the thermal sensation is almost instantaneous and does not change appreciably with time of exposure with constant environment." In contrast to this, he quotes from the 1960 paper as follows: "As previously stated the new work is based on the appraisal of the environment after approximately 3 hours occupancy; however, the effective temperature index was established on instantaneous judging as the subject moved from one psychrometric chamber to the other." The discussor contends that these two statements appear contradictory which is certainly the case if you take them out of context.

The truth of the matter is that our tests show a subject has an instantaneous thermal-sensation response on entering any room, but this is not necessarily a response which remains invariant throughout a test. The constancy of the sensation depends upon a number of factors, one of the most significant being the temperature in the space. For example, consider a space at 90 F and 80% relative humidity. A subject on entry receives an immediate hot impression when he enters the space, and the same impression continues although the body quickly brings into play its heat-dissipating forces to make it possible to exist in this uncomfortable environment. Our tests show that equilibrium is reached in a very short time under such hot conditions, varying from 30 min to an hour; and a subject's vote which starts off in these hot-range conditions at No. 5 or No. 6 remains there as long as he stays in the hot environment. On the other hand, consider the case of the subject entering an environment that is in or almost in the comfort range as was treated in the 1960 data. The initial impression of the subject may be that of true comfort, slightly cool or slightly warm. The environmental conditions are never very far from the conditions under which the subject's system can obtain a good balance and when the temperature is near to optimum for comfort, the time response is definitely lengthened. The following unpublished analysis of our data[15] brings out this point very clearly as it shows the test averages over the full period of occupancy. The first row represents a slightly cool condition, the second row almost comfort, and the third row an overly warm condition.

A study of these averaged values shows that equilibrium is not completely reached even after three hours; however, at this time the data are rapidly becoming asymptotic, and there is no reason to run a longer period. It is interesting to note that, in the case of warm environment (lower line), the difference between the initial reading and the final reading is much less than in the other cases; and an extension of the warm data into the hot region as was done in the first series of tests confirms the accuracy of both statements for the ranges to which they apply.

In his next to the last paragraph, the discussor comments on the 1936 work of Houghten reported in paper No. 1035 (Ref. 6) and states that the subjects were tested over a three-hour period. The point we raise is the fact that paper No. 1035, as quoted above, had nothing to do with the establishment of the present comfort chart as this was developed and described in References 1 and 2 of the 1923 and 3 of the 1925 ASHVE Transactions, at much earlier dates and the applicable quotation from Reference 1 reads as follows: "The dry- or wet-bulb temperature, or both, of the first chamber are then allowed to slowly rise while the judges pass back and forth from one chamber to the other, each time recording their judgment as to the relative feeling of warmth of the two conditions." A number of two-hour tests were also run by these authors in connection with the reported data of Reference 2 and the resultant comfort chart did give some effect to longer period testing, although it was overweighted with short-impression valuations. It is interesting to note that even at this time (1923) the problem of initial impression in relation to longer-term occupancy was receiving attention. The work of the later 1936 paper[6] related to cooling shock, and the statement from the authors of that paper that comfort can be expected after "20 to 40" min (30 min average) is not unreasonable. The curves of that paper interestingly enough do show in Figs. 3 to 7 that body temperature, however, had not stabilized even after 2.5 hours.

AVERAGE VOTES CAST BY SUBJECTS

No. of Tests	Time of Voting 9:15	9:45	10:15	10:45	11:15	11:45	12:15	Differences Between 9:15 & 12:15 Votes
24	3.60	3.49	3.52	3.31	3.28	3.16	2.92	0.68
35	4.35	4.25	4.20	4.10	3.97	3.94	3.89	0.46
21	5.12	5.10	5.20	5.08	5.02	4.90	4.86	0.28

REFERENCES

15. Jennings, B. H. and Givoni, B.—Environment Reactions in the 80 to 105F Zone, ASHRAE Journal, v. 1, p. 3-10, January, 1959.

16. Koch, Walter, Jennings, B. H. and Humphreys, C. M.—Environmental Study II—Sensation Responses to Temperature and Humidity under Still Air Conditions in the Comfort Range, ASHRAE Journal, v. 2, p. 63-68, April, 1960.

17. Nevins, R. G., Flinner, A. O.—Effect of Heated Floor Temperatures on Comfort, Transactions, ASHAE, v. 64, p. 175-188, 1958.

6. Houghten, F. C. and Gutberlet, Carl—Comfort Standards for Summer Air Conditioning, Transactions, ASHVE, v. 42, p. 215-229, 1936.

No. 1716

Proposed Humidity Standard

C. E. TILL

G. O. HANDEGORD

Water vapor, as a universal component of the atmosphere in which we live, is an important factor to be considered in many fields of research activity. This is particularly true in the field of building research, where the properties of materials and their performance in buildings may be determined by the humidity of the environment to which they are exposed.

The accurate measurement of humidity is a problem that has faced the investigators for some time, and many instruments and techniques have been developed. Each has its particular advantages and disadvantages, and each has its own restricted range of application. A number of principles of operation are involved in the various instruments, and they vary widely in accuracy, sensitivity, and ease of application.

C. E. Till was formerly Research Officer, and G. O. Handegord is with the Prairie Regional Station, Div. of Building Research. This paper is a contribution from the Div. of Building Research, National Research Council of Canada, and is published with the approval of the division. It was presented at the ASHRAE Semiannual Meeting in Dallas, Texas, February 1-4, 1960.

It is recognized generally that many of the instruments and techniques proposed measure humidity indirectly and must be calibrated in terms of the desired thermodynamic property. Some of the instruments have come to be regarded as "standards," on the assumption that they measure a particular moist air property directly. Such instruments are accepted frequently as standards without proper regard for the definitions of the thermodynamic properties involved or discrepancies between various published definitions. This lack of appreciation of fundamental requirements becomes increasingly apparent as more precise calibration work is attempted.

The analysis presented in this paper is the result of an attempt to provide calibration facilities for electrical resistance type instruments within an accuracy of 0.2 per cent. The project involved a review and assessment of existing instruments and subsequent design and construction of a suitable ap-

paratus. In this work the appraisal of methods and the formulation of design criteria were based on the definitions of the properties of moist air as given by the International Joint Committee on Psychrometric Data.

Measurement of the thermodynamic properties of moist air—The Final Report of the Working Subcommittee, International Joint Committee on Psychrometric Data, sets forth a standard formulation of the thermodynamic properties of moist air, which can claim general acceptance as a standard on the ground that it is thermodynamically consistent within the accuracy of existing knowledge.[1] Although inconsistencies appear throughout the literature, this formulation is now generally accepted in most engineering fields. Definitions of the terms that are frequently used in describing the condition of moist air, and that are in harmony with the standard formulation, are listed in the ASHRAE GUIDE.[2]

A knowledge of the thermodynamic properties of any atmosphere must first include the temperature and the total pressure. Accurate standards and precise measuring instruments have been developed that make the accurate measurement of these quantities a relatively simple task. Under the standard formulation,[1] all that is necessary to complete the knowledge of the thermodynamic properties of any atmosphere is an accurate numerical value of either of two fundamental thermodynamic properties of the vapor component, the vapor pressure, or the humidity ratio, or an accurate numerical value of either of two derived thermodynamic properties, the wet bulb temperature, or the dewpoint temperature. An instrument capable of providing any one of these values is, therefore, all that is necessary for a complete knowledge of the thermodynamic properties of any atmosphere.

Any one of many instruments could be used to provide the required values, but each would require calibration unless it actually indicates the measured quantity by definition. Any instrument that requires no calibration must actually be used to define the quantity it is to measure or, in other words, the measured quantity must be defined in terms of the principle of operation of the instrument. In illustration, the absolute temperature scale can be shown to be identical to a temperature scale defined in terms of the constant-volume ideal gas thermometer.[3] This thermometer, therefore, requires no calibration, as it provides the numerical value of the temperature by definition. All other thermometers require calibration, however, and must be compared to the constant-volume gas thermometer. A similar principle applies to the measurement of the necessary thermodynamic properties of the vapor component of the atmosphere.

A number of practical instruments and techniques have been developed that attempt to measure directly some thermodynamic prop-

1716

No. 1716

Proposed Humidity Standard

C. E. TILL

G. O. HANDEGORD

Water vapor, as a universal component of the atmosphere in which we live, is an important factor to be considered in many fields of research activity. This is particularly true in the field of building research, where the properties of materials and their performance in buildings may be determined by the humidity of the environment to which they are exposed.

The accurate measurement of humidity is a problem that has faced the investigators for some time, and many instruments and techniques have been developed. Each has its particular advantages and disadvantages, and each has its own restricted range of application. A number of principles of operation are involved in the various instruments, and they vary widely in accuracy, sensitivity, and ease of application.

C. E. Till was formerly Research Officer, and G. O. Handegord is with the Prairie Regional Station, Div. of Building Research. This paper is a contribution from the Div. of Building Research, National Research Council of Canada, and is published with the approval of the division. It was presented at the ASHRAE Semiannual Meeting in Dallas, Texas, February 1-4, 1960.

It is recognized generally that many of the instruments and techniques proposed measure humidity indirectly and must be calibrated in terms of the desired thermodynamic property. Some of the instruments have come to be regarded as "standards," on the assumption that they measure a particular moist air property directly. Such instruments are accepted frequently as standards without proper regard for the definitions of the thermodynamic properties involved or discrepancies between various published definitions. This lack of appreciation of fundamental requirements becomes increasingly apparent as more precise calibration work is attempted.

The analysis presented in this paper is the result of an attempt to provide calibration facilities for electrical resistance type instruments within an accuracy of 0.2 per cent. The project involved a review and assessment of existing instruments and subsequent design and construction of a suitable ap-

paratus. In this work the appraisal of methods and the formulation of design criteria were based on the definitions of the properties of moist air as given by the International Joint Committee on Psychrometric Data.

Measurement of the thermodynamic properties of moist air—The Final Report of the Working Subcommittee, International Joint Committee on Psychrometric Data, sets forth a standard formulation of the thermodynamic properties of moist air, which can claim general acceptance as a standard on the ground that it is thermodynamically consistent within the accuracy of existing knowledge.[1] Although inconsistencies appear throughout the literature, this formulation is now generally accepted in most engineering fields. Definitions of the terms that are frequently used in describing the condition of moist air, and that are in harmony with the standard formulation, are listed in the ASHRAE GUIDE.[2]

A knowledge of the thermodynamic properties of any atmosphere must first include the temperature and the total pressure. Accurate standards and precise measuring instruments have been developed that make the accurate measurement of these quantities a relatively simple task. Under the standard formulation,[1] all that is necessary to complete the knowledge of the thermodynamic properties of any atmosphere is an accurate numerical value of either of two fundamental thermodynamic properties of the vapor component, the vapor pressure, or the humidity ratio, or an accurate numerical value of either of two derived thermodynamic properties, the wet bulb temperature, or the dewpoint temperature. An instrument capable of providing any one of these values is, therefore, all that is necessary for a complete knowledge of the thermodynamic properties of any atmosphere.

Any one of many instruments could be used to provide the required values, but each would require calibration unless it actually indicates the measured quantity by definition. Any instrument that requires no calibration must actually be used to define the quantity it is to measure or, in other words, the measured quantity must be defined in terms of the principle of operation of the instrument. In illustration, the absolute temperature scale can be shown to be identical to a temperature scale defined in terms of the constant-volume ideal gas thermometer.[3] This thermometer, therefore, requires no calibration, as it provides the numerical value of the temperature by definition. All other thermometers require calibration, however, and must be compared to the constant-volume gas thermometer. A similar principle applies to the measurement of the necessary thermodynamic properties of the vapor component of the atmosphere.

A number of practical instruments and techniques have been developed that attempt to measure directly some thermodynamic prop-

erty of the vapor component of the atmosphere. The acceptance of the definitions of the thermodynamic properties contained in the Report,[1] however, precludes the acceptance of the values given by most, if not all, of these instruments, unless they have been suitably calibrated. The instruments may be divided into four general groups: those that attempt to measure (a) the thermodynamic dew-point, (b) the thermodynamic wet bulb temperature T_w, (c) the vapor pressure p_w, and (d) the humidity ratio W.

(a) **Dew-point hygrometer** — The following statement appears in the Final Report regarding the measurement of dew-point:

> "It is a problem belonging properly to practical hygrometry to design and construct dew-point hygrometers capable of reading values of the thermodynamic dew-point temperatures as defined by the solution $T_d(p,W)$ of the equation $W_s(p,T_d) = W$, after suitable calibration."

All the many forms of the dew-point hygrometer that are described in the literature[4,5,6,7,8,9] function on the same basic principle: an alteration of the temperature or total pressure of the gas sample until the first detection of the appearance of condensation, usually on a polished metal surface. The various forms possess practical limitations. In the majority of cases the precision of measurement depends upon the skill and patience of the operator.

A more basic objection to the acceptance of the dew-point method as a fundamental standard of humidity is the fact that no practical dew-point hygrometer provides the thermodynamic dew-point by definition. All, in fact, require calibration. The temperature, T_d, as defined in the above equation, is mathematically exact and may be calculated for any given combination of the total pressure p and humidity ratio W. The temperature of a polished metal surface, on the other hand, is dependent upon a variety of other factors related to the specific experimental arrangement.

(b) **Psychrometer** — The wet and dry bulb psychrometer consists of two thermometers: the bulb of one is covered with a moistened wick, while the bulb of the other is left bare. The heat required for the evaporation of water from the moistened wick is supplied by its environment until a thermal balance is attained and the thermometer remains at constant temperature. This temperature is related to the original moisture content of the air and is assumed to be the thermodynamic wet-bulb temperature. The psychrometer takes a variety of forms,[10,11,12,13,14,15,16] and considerable work has been done on psychrometric theory.[17,18,19,20] The true thermodynamic wet-bulb temperature is defined as "the temperature at which liquid or solid water, by evaporating into air, can bring the air to saturation adiabatically at the same temperature."[1] The experimental wet-bulb temperature obtained from the

psychrometer, however, is influenced by many other extraneous factors. Among these are the velocity of the air past the wet-bulb thermometer, radiation, conduction down the thermometer stem, the size, shape, material and wetting properties of the wick, and the temperature and purity of the water used in wetting the wick. The process is not adiabatic and the wet- and dry-bulb psychrometer, therefore, cannot be accepted as a fundamental standard of humidity.

(c) **Vapor pressure hygrometers** — The basic requirement of any instrument that is to measure vapor pressure is that it must measure the partial pressure of the water vapor in the presence of air. If this is not done the air and vapor must be separated, some sort of measurement of the pressures made, and some assumption made concerning the interaction between the air and water vapor when the two were mixed. In those instruments described in the literature,[21,22] the separation is made by absorbing the water, and Dalton's Law is assumed to be valid. In the usual form of these instruments, the pressure of water vapor in the sample is assumed to be equal to the measured change in total pressure, when the volume is held constant and the water is absorbed.

The fundamental objection to the acceptance as a primary standard of humidity of instruments of this type is that in all the validity of Dalton's Law tacitly is assumed. The total pressure is assumed to be the sum of the pressures that the water vapor and the air would individually exert, if each separately occupied the container. Therefore, upon absorption of the water vapor, the total pressure, minus the pressure of the air alone, would be equal to the pressure of the water vapor that was originally in the sample.

This ignores the interaction between the air and vapor molecules. In practice, the assumption of the validity of Dalton's Law is probably well within the limits of accuracy of the instrument itself, for there are many difficulties that arise in the practical operation of these instruments that dissipate much of their accuracy. The main difficulties are directly attributable to the small magnitude of the vapor pressure of water throughout the usual range at atmospheric temperatures.

(d) **Gravimetric hygrometer** — The gravimetric technique[23,24,25] has often been accepted as a primary standard of absolute humidity, and has been applied to the fundamental calibration of instruments and to exact determinations of water vapor content. The gravimetric hygrometer attempts to measure directly the humidity ratio from the weight of water vapor in a measured quantity of air that is absorbed by some chemical. In the usual form of the gravimetric hygrometer, the sample to be analyzed is passed through a series of tubes containing an absorbent. The dried air sample is then metered in some way to permit the calculation of the quantity of air involved.

Thus, the quantities actually measured are the increase in weight of the absorbent tubes and the metered quantity or air. The gravimetric technique is thus extremely simple in principle, but the difficulties that are inherent in the method and the painstaking care and patience that are necessary in order to obtain precise results severely limit its usefulness. Indeed, the complexity of the extraneous factors that are inherent in the method make it highly questionable as to just what, in fact, is being measured.

In the weighing of the absorbent tubes, for example, some of the quantities that are actually weighed, in addition to the moisture from the air, include any impurities from the air, the sorption of water, and the deposition or removal of other foreign matter on the outside surface of the tubes, changes in apparent weight due to electrostatic charge, and temperature and pressure changes of the air inside the tubes. Factors of this kind, that influence the accuracy of weighing in any gravimetric method, are magnified in importance in applying such a method to the measurement of water vapor in air because of the small concentrations of water that are present for determination.

A number of assumptions must also be made in the calculation of the quantity of air involved. The number and plausibility of the assumptions vary with the metering method used, but at the least, the average temperature, pressure and degree of saturation of the mass of air are involved. The final assumption that must be made is that sufficiently accurate corrections can be applied so that the resultant numerical value is equal to the humidity ratio. The number and the complexity of the factors influencing the results make precise determinations a near impossibility. The difficulties increase rapidly with decrease in temperature of the gas sample and subsequent reduction in water concentration. From the standpoint of its use as a humidity standard, another undesirable feature of the gravimetric technique is that the sample is destroyed in evaluating it.

In applying the gravimetric technique, therefore, it must first be shown that the measurement of the weight of moisture removed from the atmosphere in question does, in fact, represent the total weight of water in that atmosphere and nothing else. Secondly, it must be shown that the metered quantity of air represents the weight of dry air associated with the measured weight of moisture and nothing else. Only then is there basis for the acceptance of the gravimetric technique as a fundamental standard of humidity. From a practical standpoint, however, the gravimetric technique is so subject to error and so awkward in application that its usefulness as a primary standard is greatly limited.

There is therefore some serious fundamental objection to every instrument that attempts to measure directly a basic thermodynamic property associated with the vapor component of an air-vapor atmos-

phere. In the measurement of most physical quantities, however, the quantity to be measured is compared with some other quantity of the same kind, which is used as a basis for comparison. The measurement of length is a simple example. This principle may also be applied to the measurement of the thermodynamic properties of moist air by reference to a standard atmosphere of known thermodynamic properties. The accuracy of the method, however, will be directly dependent on the accuracy to which the thermodynamic properties of the standard atmosphere are known.

Production of standard atmospheres — Any standard atmosphere must be defined in terms of an atmosphere in a saturated condition. All definitions and tabulated values of the thermodynamic properties of the vapor component of air-vapor mixtures are directly related to saturation, for it is the only fixed point of reference upon which calculations may be based. For saturation, the condition of moist air must be such that it can coexist in neutral equilibrium with the associated condensed phase presenting a flat surface to it.

Some rather stringent requirements are thus imposed on any saturating device that is to be used to produce standard atmospheres. The water itself must be as pure as is practicable, and it must be shown that any possible impurities will not appreciably affect the vapor pressure over the surface. The surface of the water must be clean and must present a plane surface to the atmosphere. This does not imply planeness in the usual sense, for a radius of curvature of the order of 10^{-4} cm will only introduce an error of 0.1 per cent. The requirement raises questions in regard to the use of any spraying devices, since droplets having smaller dimensions than this might be formed. The most important requirement, however, is that of equilibrium, for only under equilibrium conditions can the saturation properties of moist air be defined.

The production of saturated atmospheres alone is not sufficient for practical purposes since most calibration work must be carried out at unsaturated conditions. The saturator must be used to establish the initial condition and a second component is required in which the moist air may be brought to an unsaturated condition through a known and calculable thermodynamic process. Any practical device must therefore satisfy these two requirements to be acceptable as a standard.

There are a number of types of apparatus described in the literature as suitable for the calibration of humidity sensing devices.[24, 25, 26, 27, 28, 29, 30, 31, 32, 33] Most of these provide an acceptable means for bringing the moist air to the unsaturated condition from initial saturation, but the degree to which initial saturation is achieved may not always be calculable.

Most of the systems proposed utilize a continuous flow process, air from one source being passed

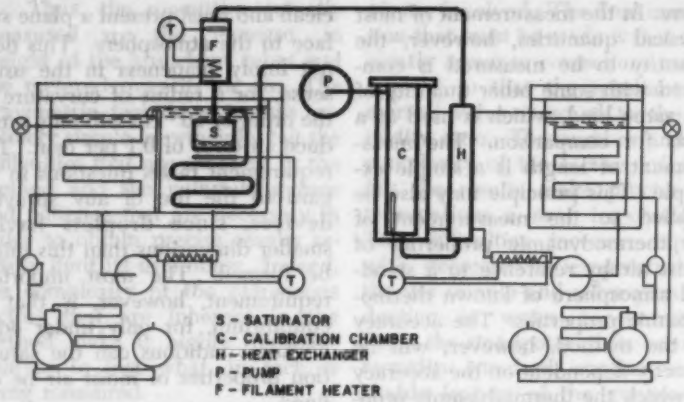

Fig. 1 Schematic diagram of atmosphere producer

through a series of saturating devices, then brought to the desired unsaturated condition, and exhausted to the atmosphere or some other sink. These systems operate on a dynamic, non-equilibrium basis, with water or ice being continuously added or removed from the moist air in the saturator section. In this non-equilibrium situation it is difficult to evaluate exactly the condition of the air effluent from the final saturator. The definition of a saturated atmosphere is not satisfied, owing to the non-equilibrium nature of the process.

The requirements of the definition of a saturated atmosphere can best be met in a practical apparatus by using the recirculation principle. Such an apparatus involves a closed system in which moist air is continuously recirculated over the surface of water or ice in a saturator. The moist air will thus eventually come to neutral equilibrium with the water or ice surface as required by the definition of saturation. The devices utilizing this principle which are described in the literature[22,23] employ a heating process to bring the air to the desired unsaturated condition. It could also be attained through a change in total pressure between saturator and calibration chamber. Regardless of the technique employed to bring the air stream to the unsaturated condition, the recirculation principle offers the one sound basis for attaining saturation. In a practical atmosphere producer using this principle, complete saturation may not be achieved, but the degree to which it is achieved can be determined and the accuracy of the apparatus definitely established.

Description of the apparatus—The apparatus proposed as a standard in this paper is based on the two-

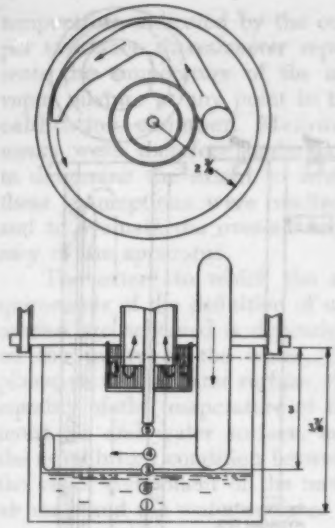

Fig. 2 Saturator for proposed humidity standard

temperature principle, since this lends itself more suitably to recirculation of moist air. A schematic diagram of the apparatus is shown in Fig. 1. It consists essentially of two controlled-temperature liquid sources which maintain the saturator section and calibration section at different temperature levels. Heat exchangers located immediately before the saturator and calibration chamber serve to bring the temperature of the moist air to the required entrance conditions.

The saturator design is patterned after that described by Wexler.[33] It is a cylindrical copper chamber, 5 in. diam and 5 in. high, filled with water to a level just below that of the air inlet nozzle, as shown in Fig. 2. The air first passes through a heat exchanger consisting of 40 ft of ¾-in. OD copper tubing and is discharged from the saturator nozzle parallel to the water surface and tangential to the wall of the saturator. The resultant vortex action in the saturator induces good mixing and serves as a centrifugal separator before the air leaves through a centrally located discharge port at top of the chamber. A slotted screen surrounding the exhaust port is a further guard against the possibility of droplet carry-over.

The saturator and its surrounding heat exchanger are immersed in a glycol-water bath which is continuously cooled to slightly below the desired temperature by a 1½ hp single-stage Refrigerant 12 condensing unit. A 1500-watt immersion heater, controlled by a sensitive on-off resistance bridge controller, raises the brine temperature to the desired control point.

The air from the saturator passes over a bare nickel-chrome alloy wire heater where its temperature is raised to approximately the desired level, this heater being operated by a proportional resistance bridge controller. The air then passes through an extended surface heat exchanger to a jacketed calibration chamber. Ethylene glycol-water brine from a second controlled-temperature liquid source is circulated through this heat exchanger and through the jacket surrounding the calibration chamber in order to bring the air temperature to the desired level.

Temperature control in this section is accomplished using a reheating principle similar to that employed in the saturator system. Rather than on-off control, a proportional control system with derivative and integral action is used, having the sensing element located in the calibration chamber.

The calibration chamber consists of a jacketed copper cylinder, 4 in. ID and 28 in. long, shown schematically in Fig. 3. Access to this chamber is provided by a removable transparent plastics head which is bolted to the top of the chamber through a gasket seal. A sword arrangement secured to the head and extending into the chamber serves as a support for the humidity elements under test. Provision is also made for the insertion of other humidity sensing devices in the exit tube of the chamber.

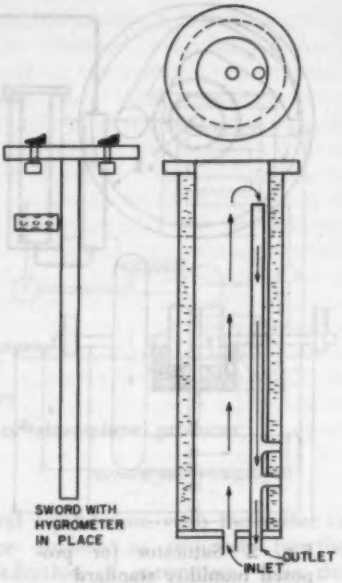

Fig. 3 Calibration chamber with sword removed

The air circulation pump consists of two diaphragm-type paint spray compressors operated in tandem. The pumps are arranged to operate 180 degrees out of phase to reduce pressure fluctuation. These pumps were found to be the only type available which satisfied the combined requirements of negligible leakage and contamination in the desired flow range of 3 to 4 cfm. Connections between the various components of the air circulation system are made with flexible polyethylene pipe and hose clamps.

The temperature of the saturator bath is measured using a calibrated platinum resistance thermometer and precision Mueller bridge. A calibrated copper resistance thermometer is used to measure the air temperature in the calibration chamber. Pressure measurements in the calibration chamber and saturator are indicated by simple "U" tube oil manometers.

Performance of the apparatus — Calculation of the humidity of the test atmosphere in the calibration chamber is based on the assumption that the moist air in the system is in neutral equilibrium with the water surface in the saturator at the temperature indicated by the platinum resistance thermometer. It is further assumed that the

temperature indicated by the copper resistance thermometer represents the temperature of the air-vapor mixture at any point in the calibration chamber. Measurements were therefore undertaken to determine the extent to which these assumptions were realized, and to evaluate the over-all accuracy of the apparatus.

The extent to which the requirements of the definition of saturation are achieved is dependent on the purity of the water, the planeness of the water surface, the equality of the temperature of the moist air and water surface, and the equilibrium condition between the vapor component of the moist air mass and the water surface.

(a) **Purity of the water**—The purest water available at the laboratory was triple distilled water. This was used as a standard against which to compare water that had been in use for some time in the atmosphere producer. The method employed was a comparison of the readings of a sensitive electrolytic hygrometer when the atmosphere producer had come to its steady-state condition, first with water in the saturator that had been used for some time, then with fresh triple-distilled water, all other conditions being maintained constant The electrolytic hygrometer used was sensitive to changes in vapor pressure of less than 0.1 per cent.

In some of the tests the water had been in use for approximately a month; in others the water had been in use for only a few days. In no case was there any detectable difference in vapor pressure of the test atmosphere provided by the fresh distilled water and that provided by water that had been in use for some time.

(b) **Planeness of the water surface** — Observations were made of the condition of the water surface under various air flow rates using a glass-walled saturator. At the desired air flow rates of 3 to 5 cfm, the water surface was only slightly disturbed and no agitation sufficient to cause droplet formation occurred until much higher flow rates were used. Since extremely small droplets would have to be formed to introduce significant errors, the requirement of planeness of the water surface was considered satisfied.

(c) **Equality of the temperature of moist air and water surface** — The transfer of heat to the saturator from its outlet connection, by conduction or by radiation, is minimized in the design of the apparatus. The saturator is immersed to a depth of at least 3 in. in the controlled temperature fluid and the interior is shielded from exposure to any outlet component which is at a higher temperature than that of the bath.

The saturator heat exchanger was completely immersed in the bath and proved to be of ample capacity to bring the air to the average bath temperature with the flow rates employed. Measurements with calibrated thermocouples and a precision potentiometer indicated that, with 100 F differ-

ence between inlet air and saturator temperature, air entering the saturator was within ±0.01 F of the average bath temperature.

A series of measurements was made of the temperature of the water and of the air-vapor mass above the surface of the water in the saturator. Thirty-gage thermocouples, calibrated against a platinum resistance thermometer to ±0.01 F, were used in conjunction with a precision potentiometer sensitive to temperature fluctuations of less than 0.01 F. Five thermocouples were used: two measured water temperature and three the temperature of the air-vapor mass at points above the water surface as indicated in Fig. 2.

The saturator bath temperature was measured with the platinum resistance thermometer and Mueller bridge. In each case the calibration chamber temperature was 70.0 F, the flow rate was 3.6 cfm, and the depth of the water in the saturator was ¾ in. The procedure in each case was to calibrate the thermocouples against the platinum resistance thermometer and then to place the thermocouples in the saturator. After a period sufficient for the attainment of the steady-state condition the temperature readings were taken. The thermocouples were then recalibrated.

Table I provides four typical conditions through the full range of relative humidities. The deviations shown are maximum deviations. Case A represents an extreme condition, corresponding to a relative humidity of about 4 per cent, which approaches the most rigorous condition the saturator heat exchanger encounters in practice. Even at this extreme, the average bath temperature, the water temperature, and the temperature of the air-vapor mass agreed to within 0.05 F. In the other three cases the largest observed deviation was 0.02 F. Thus the temperature of the air-vapor mass over the water surface is substantially equal to the average temperature of the saturator bath.

It was difficult to make an accurate direct measurement of the water surface temperature. Thermojunction 2 was just under the water surface and thermojunction 3 was just above it. In no case was there any evidence of a temperature effect owing to evaporation or condensation, and the temperature

TABLE I

SPATIAL VARIATIONS IN SATURATOR TEMPERATURE

	A	B	C	D
Saturator Bath Temperature F	−2.22 ± 0.06	36.50 ± 0.05	43.48 ± 0.04	64.88 ± 0.04
Thermocouple #1	−2.22 ± 0.02	36.50 ± 0.01	43.48 ± 0.02	64.88 ± 0.01
Thermocouple #2	−2.18 ± 0.03	36.50 ± 0.00	43.50 ± 0.02	64.88 ± 0.01
Thermocouple #3	−2.21 ± 0.01	36.50 ± 0.01	43.48 ± 0.01	64.88 ± 0.01
Thermocouple #4	−2.16 ± 0.02	36.50 ± 0.03	43.48 ± 0.01	64.88 ± 0.01
Thermocouple #5	−2.17 ± 0.02	36.50 ± 0.01	43.50 ± 0.02	64.86 ± 0.01

of the air-vapor mass was substantially equal to the bulk temperature of the water. As there is no possibility of a net radiation exchange with the surface, the surface temperature must be equal to that of the air-vapor mass.

(d) **Equilibrium condition between the vapor component of the air-vapor mixture and the water surface** – The moist air in the system is recirculated repeatedly over the water surface. The steady-state condition of the vapor component must be that of neutral equilibrium with the water surface if there are no sources or sinks present in the recirculation system other than the saturator. Any source or sink that tends to change the relative proportions of air and vapor in the air-vapor mixture tends to upset the neutral equilibrium condition in the saturator. There are two possibilities: (1) a net exchange of moisture between the air-vapor mixture and any moisture sources or sinks, other than the saturator, within the recirculation system; (2) a mass exchange between the air-vapor mixture in the recirculation system and the ambient atmosphere, caused by leakage.

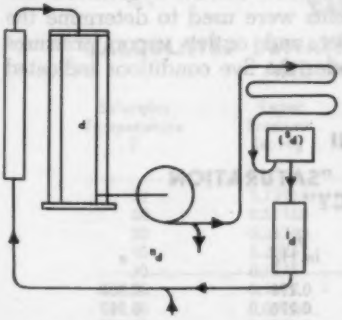

Fig. 4 Leakage in recirculation system

(1) **Moisture exchange**—Aside from the presence of an open liquid or solid water surface, the only appreciable moisture source would be the presence of hygroscopic materials. The recirculation system is made up almost entirely of metals, clear plastics, and polyethylene. The amount of moisture sorbed on these surfaces would be entirely negligible in comparison with the magnitude of the air-vapor mass. Under steady-state conditions there is no source of liquid or solid water within the recirculation system other than the saturator itself. The possibility of a serious moisture sink exists only if the saturator is operated at temperatures above the temperature of the room. Condensation on certain of the recirculation system boundary surfaces might occur. This effect limits the operation of the atmosphere producer to the production of atmospheres in which the dew-point is below the ambient temperature.

(2) **Leakage** – The magnitude of the effect of leakage is dependent upon the amount of moist air that is exchanged with the ambient atmosphere relative to the amount that is recirculated. The case shown in Fig. 4 represents the most severe condition whereby room air enters the system between saturator and calibration chamber and leaves at the pump discharge. The

moist air entering the saturator is not in true equilibrium with the water surface, and leaves the saturator at a condition dependent on the efficiency of the saturator. Its vapor pressure is further modified before entering the calibration chamber by mixing with the room air. An expression that may be used to evaluate the error resulting from this condition may be derived as follows:

If p = vapor pressure in calibration chamber,
p_s = vapor pressure after the saturator, and
p_* = vapor pressure corresponding to saturation at the temperature of the saturator,

then

$$p_s = p + e\,(p_* - p) \qquad (1)$$

where

e = "saturation efficiency"

If p_a = water vapor pressure in the ambient atmosphere

and g = mass of air exchanged with the room / mass of air circulated in the system

then, to a sufficiently close approximation,

$$p = \frac{p_s + g p_a}{g + 1} \qquad (2)$$

Substituting Equation (1) in Equation (2) and reducing,

$$p = \frac{e p_* + g p_a}{g + e} \qquad (3)$$

The leakage of the apparatus was estimated by pressurizing the system to a gage pressure of 0.6 in. Hg, which was the maximum pressure observed at any point under operating conditions. The decay in pressure, as determined by an oil manometer, was then found to be 0.074 in. Hg in 2.0 min. Assuming the volume of the manometer fluid to be insignificant compared with the volume of the apparatus and assuming a barometric pressure of 28 in. Hg, the leakage may be calculated as 1.31×10^{-3} air changes per min. This value could represent twice the leakage experienced under operating conditions and may safely be assumed as a maximum for purposes of this discussion.

The leakage ratio, g, for the design flow rate of 3.6 cfm and for a system volume of 0.5 cu ft, may be calculated as 1.82×10^{-4}.

The saturation efficiency was determined by opening the system at point "A" in Fig. 4 and circulating room air through the apparatus at the design flow rate. Calibrated electric hygrometer elements were used to determine the inlet and outlet vapor pressures under the five conditions indicated

TABLE II

DETERMINATION OF "SATURATION EFFICIENCY"

p_s in. Hg	p_* in. Hg	p_r in. Hg	e
0.638	0.208	0.298	0.208
0.436	0.212	0.276	0.287
0.256	0.159	0.185	0.275
0.058	0.131	0.056	1.03
0.064	0.270	0.065	0.995

in Table II, and the corresponding "saturation efficiencies" calculated using Equation (1).

It will be noted that when the saturator temperature corresponds to a saturation vapor pressure lower than the vapor pressure of the room air, the "saturation efficiency" is unity. This is no doubt caused by the increase in dehumidifying surface afforded by the heat exchanger. While it is not inconceivable that the accumulation of water or frost on this surface will affect the performance over long periods, it is extremely unlikely that such effects will be significant under a normal calibration program.

The error introduced by leakage is of concern when the room air vapor pressure is lower than that in the saturator, being a maximum when p_s is zero. The ambient atmosphere is maintained at a vapor pressure of approximately 0.2 in. Hg and this value has been employed in determining the error in vapor pressure and dew-point for the range of operation of the apparatus shown in Table III. A tolerance of ± 0.02 F in saturator temperature was also assumed in the preparation of this table, the sign chosen being the one to result in a maximum error.

(e) **Calibration chamber temperatures**—Investigation of the calibration chamber condition was made with 30-gage thermocouples calibrated and used in a manner similar to that used in making the saturator temperature measurements. The temperatures of the air-vapor mass were taken at four positions in the calibration chamber. At each position two thermocouples were used, one shielded from radiation, the other unshielded. Two thermocouples, secured directly to the interior walls, were used to indicate the temperatures of the calibration chamber boundaries. The final thermocouple was inserted in the air stream at the inlet to the

TABLE III

CALCULATED DEVIATION IN VAPOR PRESSURE AND DEW-POINT

Saturator Temperature F	Vapor Pressure in. Hg	Maximum Deviation in Vapor Pressure %	Maximum Deviation in Dew-point F
70	0.73916	−0.12	−0.04
60	0.52160	−0.11	−0.03
50	0.36240	−0.10	−0.03
40	0.24767	−0.09	−0.02
30	0.1645	+0.09	+0.02
20	0.1027	+0.11	+0.03
10	0.06286	+0.14	+0.03
0	0.03764	+0.19	+0.03
−10	0.02203	+0.26	+0.04
−20	0.01259	+0.39	+0.07

heat exchanger. The positions of the thermojunctions are shown in Fig. 3.

The filament heater was found to cause a cyclical temperature variation in the air stream entering the heat exchanger. The amplitude was approximately ±0.4 F, and the period was approximately 10 sec. The maximum "droop" observed was in the order of 2 F when the saturator bath temperature was varied through a range of temperatures corresponding to the full range of relative humidities at 70 F.

The spatial variation in the temperature of the air-vapor mass in the calibration chamber and the variation in the temperature of the walls of the calibration chamber for a 12-hour period of test are shown in Table IV. The copper resistance thermometer measuring the calibration chamber temperature read 69.52 ± 0.03 F during this period. The average temperature of the air stream at the heat exchanger inlet varied from 68.7 to 70.3 F as the load on the system was varied by changing the saturator bath temperature. The cyclical variation was ±0.4 F. The tolerances quoted in Table IV are maximum deviations.

The results show that the spatial variation in the average temperature of the air-vapor mass were no worse than ±0.02 F and the total fluctuation in temperature over the 12-hour period was ±0.05 F at the maximum. The copper resistance thermometer measured the average temperature to an accuracy within its rated sensitivity of 0.03 F.

(f) **Over-all accuracy of the apparatus**—The primary function of the atmosphere producer is in the calibration of electric hygrometer sensing elements in terms of relative humidity. The maximum uncertainty in the values obtained are shown in Table V, based on the possible errors in vapor pressure taken from Table III and assuming an error of ±0.05 F in the calibration chamber temperature.

The errors listed in Table V represent maximum values determined using the worst possible

TABLE IV

CALIBRATION CHAMBER TEMPERATURES

Thermocouple Position	Details	Temperature °F
A	Shielded from radiation	69.54 ± 0.03
A	Unshielded	69.54 ± 0.03
B	Shielded from radiation	69.52 ± 0.03
B	Unshielded	69.51 ± 0.02
C	Shielded from radiation	69.52 ± 0.05
C	Unshielded	69.53 ± 0.02
D	Shielded from radiation	69.51 ± 0.04
D	Unshielded	69.52 ± 0.02
E	Wall temperature	69.5 ±0.1
F	Wall temperature	69.5 ±0.1

combination of errors. The probable error will be less for each case. These inaccuracies are a result of the effect of leakage and the present practical limits of temperature control and measurement, and are not caused by any fundamental characteristic of the method. It is anticipated that improvements to the present model will be made with a view to the elimination of leakage and to more precise measurement and control of temperature.

CONCLUSIONS

1. The definitions of the thermodynamic properties of moist air given in the Final Report of the International Joint Committee on Psychrometric Data leave little scope for the establishment of a fundamental standard of humidity other than by the production of a standard atmosphere.

2. The definitions given in the Report are such that no practical form of humidity measuring instrument can be used to provide a fundamental humidity standard. Such instruments, with one possible exception, must be calibrated in terms of a standard atmosphere.

3. The gravimetric hygrometer, as the exception, although potentially a fundamental standard, is of restricted use as a practical standard, and requires a constant atmosphere for its application.

4. An atmosphere producer, employing recirculation of moist air in a closed system, provides a practical fundamental standard for humidity which is consistent, in principle, with the definitions given by the Report of the International Joint Committee on Psychrometric Data.

5. The condition of the air-vapor mass in the recirculation system of the atmosphere producer described in this paper necessarily satisfies the definition of an atmosphere saturated at the measured temperature T_1 and the measured total pressure P_a, within a small tolerance. This tolerance arises from the practical limitations in temperature control and the practical limitations on the establishment of the neutral equilibrium condition.

6. In contrast to those systems that do not involve recirculation, the limitations on the knowledge of the condition of the air-vapor mixture in this atmosphere producer

TABLE V

MAXIMUM UNCERTAINTY IN THE RELATIVE HUMIDITY EXPRESSED IN PER CENT R.H.

Temperature °F	Relative Humidity 10% R.H.	25% R.H.	50% R.H.	75% R.H.	100% R.H.
90	0.03	0.06	0.14	—	—
70	0.03	0.06	0.14	0.20	0.29
50	0.04	0.08	0.14	0.21	0.29
30	0.06	0.11	0.18	0.25	0.33
10	—	0.17	0.24	0.34	0.40

may be precisely evaluated. The maximum uncertainty in the vapor pressure of the test atmosphere is in the order of 0.1 per cent in the temperature range from 0 to 70 F. The maximum uncertainty in the dew-point is in the order of 0.03 F in the same temperature range. The maximum uncertainty in relative humidity is, on the average, 0.2 per cent R.H. through the full range of the relative humidities at temperatures from 10 to 70 F.

7. The range of humidities that the atmosphere producer is capable of producing is limited in the present arrangement to dew-points between −20 and 70 F. The lower limit is fixed by the capacity of the saturator bath refrigeration unit, and the upper limit is fixed by the ambient temperature. The lower limit of the dry-bulb temperature is 10 F, set by the capacity of the air-temperature bath refrigeration unit. The upper limit is presumably fixed only by the boiling point of the glycol-water mixture.

8. Although the atmosphere producer was developed for a specific purpose in studies in the field of building research, it provides a reference standard of humidity which has much broader application. There is no doubt that the accurate calibration of humidity-sensing instruments would be of value to research workers in other fields, and the availability of a standardization facility would be useful to any investigator concerned with humidity measurement. An atmosphere producer of the accuracy described is of necessity too large, complex, and expensive for acceptance as a standard piece of equipment in all laboratories. It is to be hoped, however, that the provision of one such apparatus in the National Research Council Laboratories will satisfy most of the needs for a standardization facility in Canada.

ACKNOWLEDGMENTS

The work reported in this paper was done by the senior author while on the staff of the Prairie Regional Station of the Div of Building Research, National Research Council, at Saskatoon, Canada. The paper is based on a thesis prepared by the senior author under Dr. B. W. Currie of the Department of Physics and submitted to the Faculty of Graduate Studies, University of Saskatchewan, in partial fulfillment of the requirements for the degree of Master of Science.

The authors express their appreciation to D. G. Cole and other members of the staff of the Prairie Regional Station for the valued assistance given them in the design and construction of the apparatus.

REFERENCES

1. Standardization of Thermodynamic Properties of Moist Air, by J. A. Goff, ASHVE Transactions, Vol. 55, 1949, p. 459.
2. Heating, Ventilating and Air Conditioning Guide, 1958, p. 25. (American Society of Heating and Air Conditioning Engineers).
3. Introduction to Thermodynamics, the Kinetic Theory of Gases, and Statistical Mechanics, by F. W. Sears, Addison-Wesley Publishing Company, 1953, p. 7-9.
4. Accurate Determination of Dewpoints, by A. W. Hixson and G. E. White, Industrial Engineering Chemistry, Analytical Edition, Vol. 10, 1938, p. 235.
5. Dew-point Hygrometer for Use at Low Temperatures, by C. A. Winkler, Canadian Journal of Research, Vol. 17, Sec. D, 1939, p. 35.

6. Moisture Measurement with an Electronic Dewpoint Indicator, by V. E. Soumi, Instruments, Vol. 21, 1948, p. 178.
7 Improved Electronic Dewpoint Hygrometer, by E. W. Barrett and L. R. Herndon, Journal of Meteorology, Vol. 8, 1951, p. 40-51.
8. Further Improvements in the Electronic Dewpoint Hygrometer, by E. W. Barrett, R. L. Slater and K. E. Newton, Journal of Meteorology, Vol. 12, August 1955, p. 308.
9. Illinois Testing Laboratories Dewpoint Indicator, Instruments, Vol. 19, 1946, p. 278.
10. Industrial Humidity Instruments, by M. P. Behar, Instruments, Vol. 3, 1930, p. 549, 605, 659.
11. Resistance Thermometers for the Measurement of Relative Humidity or Small Temperature Differences, by D. C. Rose, Canadian Journal of Research, Vol 5, 1931, p. 156.
12. Determination of Relative Humidities by Means of Thermocouples, by J. G. Lanning, Industrial and Engineering Chemistry, Analytical Edition, Vol. 4, 1932, p. 286.
13. Thin-Film Psychrometer for Measuring Relative Humidity in Small Spaces, by W. A. Wink and J. A. Van Den Akker, TAPPI, Technical Section, Vol. 39, September 1956, p. 647.
14. Constant-Feed All Temperature Wet Bulb, by S. M. Henderson, Agricultural Engineering, October 1952. p. 644.
15. Construction and Use of a Thermoelectric Psychrometer, by C. Lorensen Jr. Temperature—Its Measurement and Control in Science and Industry, American Institute of Physics, 1941, p. 660.
16. Psychrometry in the Frost Zone, by D. D. Wile, Refrigerating Engineering, Vol. 48, 1944, p. 291.
17. Theory of the Psychrometer, by J. H. Arnold, Physics, Vol. 4, 1933, p. 255, 334.
18. Effect of Radiation on Psychrometer Readings, by D. Dropkin, Cornell University Engineering Experimental Station, Bulletin No. 26, 1939.
19. Review of Existing Psychrometric Data in Relation to Practical Engineering Problems, by W. H. Carrier and C. O. Mackey, A.S.M.E. Transactions, Vol. 59, 1937, p. 32 and 528.
20 Deviation of the Actual Wet Bulb Temperature from the Temperature of Adiabatic Saturation, by D. Dropkin, Cornell University Engineering Experimental Station, Bulletin No. 23, 1936.
21. Tilting Hygrometer: a New Form of Absorption Hygrometer, by H. G. Mayo and A. M. Tyndall, Proceedings of Physical Society London, Vol. 34, 1921-22, p. 67.
22. Studies with the Condensation Hygrometer, by T. Okada and M. Tamura, Proceedings Imperial Academy, Tokyo, Vol. 16, 1940, p. 141 and 208.
23. Water Content of Saturated Air at Temperatures up to 100°C, by J. H. Awberry, Proceedings Physical Society London, Vol. 44, 1932, p. 143.
24. Divided Flow Type, Low Temperature Humidity Test Apparatus, by A. Wexler, Journal of Research, National Bureau of Standards, Vol. 40, 1948, p. 479.
25. Two Pressure Humidity Atmosphere Producer, by R. S. Feigal and E. J. Amdur, Minneapolis Honeywell Research Report GR2998-R1.
26. Supplying Atmospheres of Known Humidity, by A. C. Walker, Bell Laboratory Record VII, 1933, p. 169.
27. Investigation on Absorption Hygrometers at Low Temperatures, by E. Gluckauf, Proceedings Physical Society London, Vol. 59, 1947, p. 344.
28. Apparatus for Producing Air of Controlled Relative Humidity for Hygrometer Calibration and Testing by L. A. Gram, Journal of Scientific Instruments, Vol. 33, 1956, p. 273.
29. Measurement of Water in Gases by Electrical Conduction in a Film of Hygroscopic Material and the Use of Pressure Changes in Calibrations, by E. R. Weaver and R. Riley, Journal of Research, National Bureau of Standards, Vol. 40, 1948, p. 169.
30. Electrical Measurement of Water Vapour with a Hygroscopic Film, by E. R. Weaver, Analytical Chemistry, Vol. 23, 1951, p. 1076.
31. Pressure-Humidity Apparatus, by A. Wexler and R. D. Daniels, Journal of Research, National Burau of Standards, Nov. 48, 1952, p. 265.
32. Equipment for Conditioning Materials at Constant Humidities and at Elevated Temperature, by J. G. Wiegerink, Journal of Research, National Bureau of Standards, Vol. 24, 1940, p. 639.
33. Recirculating Apparatus for Testing Hygrometers, by A. Wexler, Journal of Research, National Bureau of Standards, Vol. 45, 1950, p. 357.

DISCUSSION

E. J. AMDUR, Minneapolis, Minn. (Written): While electrical sensors of the Dunmore type are the most sensitive and precise of available hygrometric devices, in certain types of research it is desirable to calibrate these sensors before and after a test procedure. The authors describe a two temperature calibration device which is relatively inexpensive to construct, and which is probably sufficiently precise for the type of work which it will be called upon to do. It is, however, difficult to accept the device described as a "fundamental" or "primary" standard of relative humidity, or even as the best "practical" standard device.

In 1955 a two pressure atmosphere producer was built at the Research Center of the Minneapolis Honeywell Regulator Company. This instrument[1], has been rather thoroughly investigated and tested by continuous use. A similar model was supplied to the U.S. Signal Corps at Fort Monmouth, N. J. in 1957. It is this type of atmosphere producer which we feel to be a candidate primary standard of relative humidity. Experience with these devices as well as with a two temperature atmosphere producer affect the comments given on the following page.

[1] E. J. Amdur, The Research Center Two Pressure Atmosphere Producer, Minneapolis, The Minneapolis-Honeywell Regulator Company, January 16, 1956.

To summarize the objections to this paper and the device it describes:

1. The two temperature atmosphere producer does not conform to the requirements for a fundamental standard of relative humidity because the relative humidity cannot be directly calculated from physical measurements. One does not utilize only the two temperature measurements taken but must accept vapor pressure tables as intermediary.

2. While gravimetric measurements seem to confirm the Goff and Gratch tables at temperatures above freezing, determinations in our laboratory indicate a fairly constant deviation of 1.5% below 32 F, the actual vapor pressure values being larger than the tabulated values.** As a practical standard the two temperature atmosphere producer is probably satisfactory when used with test chamber and saturator temperatures both above freezing, and with little error if both temperatures are below 32 F. When the test chamber is above the freezing point and the saturator is below it, the possible error may be 1.5% rh from this source. A program of precise gravimetric evaluation of below freezing vapor pressure tables appears necessary in order to remove this ambiguity.

3. It is true that absolute, primary, or fundamental standards do not by definition require calibration. Nevertheless, it is essential that such standards be tested against alternative primary standards. While the physical theory which forms the basis for the standard may be impeccable, the apparatus and operations required to use this theory frequently are less so.

The question is which alternative primary standard one is to use. It is difficult to avoid the use of the gravimetric determination of the moisture content in a volume of air. It is the only alternative method which may be applied with sufficient precision to constitute an adequate test of a candidate primary standard method in the humidity field.

It must be recognized that the gravimetric procedure is an analytical method of determining the vapor density (weight per unit volume) rather than vapor pressure, and relative humidity values calculated from vapor density measurements may differ slightly from those obtained from an atmosphere producer operating on a vapor pressure principle. The gravimetric method itself is, as the authors indicate, not an easy procedure. It is time consuming and requires a high standard of manipulation if precise results are to be obtained. Nevertheless, it is necessary to resort to this procedure before the validity of the two temperature atmosphere producer may be admitted.

** The Goff and Gratch tables give values for the vapor pressure of ice below 32 F. The values of the vapor pressure of water below 32 F are higher, and the deviation becomes greater at lower temperatures. Values determined at the Minneapolis-Honeywell laboratories lie between those for ice and water, about 1.5% above those for ice.

4. Messrs. Till and Handegord devote some effort to arguments that there is some merit in the type of saturation obtained in their recirculation apparatus as compared to that achieved in a continuous flow saturator. These arguments apparently result from a confusion between their device and a static equilibrium system. It can be shown that their system is in fact no different in behavior from a continuous saturator having a great number of evaporators except that some in and out leakage occurs on each trip around the apparatus. This is less likely to occur with the straight line or continuous device. Actually, neither of these methods, both approaching saturation by evaporation of water into the air, is as satisfactory as the method used in the Honeywell device according to our test results. In this apparatus saturated air is cooled to the desired temperature, both heat and moisture being simultaneously removed.

5. In addition to the above points a purely practical objection exists to the Till device if operated as described. The passage of 3 cfm of air through tubes of the size indicated will result in a fractional air pressure loss of some magnitude between the saturator and the test chamber. This change in pressure will introduce an error in the relative humidity calculation. It may be taken into consideration in the calculation if the pressure drop is measured, but apparently Messrs. Till and Handegord have not done so.

6. The time response of the device has not been reported and should be quite long as compared to that of the two pressure system. A slowly responding device tends to be used less frequently because its use is tedious. One avoids investigations which one might otherwise undertake. While a slow response rate does not affect the validity of the apparatus it does therefore tend to affect the amount and quality of the work of a laboratory.

An ideal instrument should be accurate, easy to use and rapid in response. The two pressure device appears to be superior on these counts to the Till and Handegord apparatus. The two pressure device is more expensive to construct, although this might not be true on the basis of work output capacity. Persons contemplating the construction of an atmosphere producer should also consider the two pressure principle seriously in the light of their particular requirements.

CLOSURE BY AUTHORS TILL and HANDEGORD: The authors wish to thank Dr. Amdur for his comments on their paper and would also like to acknowledge the co-operation extended to them in the past by Dr. Amdur and his colleague, Mr. H. Lofgren, of the Applied Research Division of Minneapolis-Honeywell. Their private comments and suggestions regarding humidity instrumentation have been of considerable assistance in planning research in this field at Saskatoon.

Dr. Amdur has raised several objections to the paper and to the acceptance of a two temperature recirculating apparatus of the type described as a humidity standard. He suggests

further that the atmosphere producer developed at Honeywell and described in a company report more properly meets the requirements. In dealing with these criticisms in the order in which they were presented, the authors would also like to comment on the characteristics of the Honeywell apparatus as they relate to the requirements for a fundamental standard.

1. Contrary to Dr. Amdur's suggestion, the authors do not claim that the apparatus described is a standard for relative humidity. The term "humidity standard", involving a broader connotation, was used since it was recognized that psychrometric tables were required to calculate relative humidity and that the present tables were to some degree based on empirical formulae. This use of empirical psychrometric tables is given by Dr. Amdur as the reason why the apparatus described cannot be accepted as a standard. It is important to note, however, that the Honeywell two pressure system requires the use of an empirical equation in the determination of relative humidity and may be criticized on exactly the same basis.

The authors propose the two temperature recirculation system as a humidity standard on the basis that moist air is brought to equilibrium with a flat water surface at a known temperature and pressure in accordance with the definition of saturation given by the I.J.C.P.D. and then brought to a higher temperature (and slightly lower pressure) by means of a known thermodynamic process. In the authors' view, a knowledge of these conditions properly describes the state of the moist air in the calibration chamber. The calculation of the particular thermodynamic property desired may only be as precise as the accuracy of the psychrometric tables available at the time, but the principle of the apparatus and the basic measurements made are unaffected by any changes that might be made in such tables. From a purely practical point of view, researchers concerned with moist air conditions and the use of humidity sensing devices will normally be using the accepted psychrometric tables of the day as a standard for measurement and calculation.

2. The Goff and Gratch Tables are presently accepted as standard on the grounds that they are based on formulations which are thermodynamically consistent within the accuracy of existing knowledge. The authors feel that it is reasonable to accept these tables as such until it is definitely established that they are in error. They respectfully suggest that Dr. Amdur should properly present his criticism of the tables to those responsible for their compilation.

3. The authors cannot agree with the principle that a primary standard need be checked by an alternative method to be accepted as such. This is not to suggest that a test of this nature would not be desirable, but the authors are not prepared to accept the gravimetric method in its common form as the alternative primary standard for a serious practical reason. The great difficulties in manipulation and measurement involved in the method were described in the paper under discussion. Their effect is to cast doubt on whether the measured weight change of the absorbent and container represents only the weight gain of the absorber. Aside from these difficulties, it must always be shown that the weight gain of the absorbent results only from water vapor and nothing else. This involves the use of air which has essentially no particulate matter or other impurities which may be sorbed or retained by the dessicant. The problem becomes particularly significant when small amounts of water vapor are involved and raises serious implications in regard to the acceptance of the gravimetric method as a practical primary standard, even for purposes of checking other methods.

There are practical accuracy limitations to the data obtained from an atmosphere producer such as the one described in this paper. It is important to note, however, in contrast to the gravimetric method, the error involved can be estimated and the maximum value definitely established using simple instrumentation.

4. The authors maintain their view that the recirculating principle offers the best practical means for achieving saturation on an atmosphere producer in accordance with the I.J.C.P.D. definition. In a completely closed system of this type the recirculating air will eventually come to equilibrium with the water surface and the degree to which saturation is achieved can be established by temperature measurement alone. The saturator heat exchanger can thus be sized so that the temperature difference between entering air and water surface is reduced to a negligible, known value. In a non-recirculating continuous flow system, the degree of saturation achieved can only be evaluated by measurement of the humidity of the effluent air stream. This fact, in the authors' opinion, is the fundamental difference between the two systems and represents the chief advantage of the recirculation principle.

The type of system which has been developed at Honeywell is of the non-recirculating, continuous flow type, in which dehumidification by cooling is employed in an attempt to insure saturation. The authors do not suggest that saturation cannot be achieved in this way, but do maintain that cooling of high humidity air in a chamber below its dewpoint is not in itself proof that the effluent air is saturated.

5. The fact that a total pressure difference exists between the saturator and calibration chamber in the two temperature system could perhaps have been emphasized if space had permitted. The authors did indicate in the paper that such measurements were taken, as may be noted by reference to the last sentence under the section "Description of the Apparatus". This pressure difference is, of course, taken into account in calculation of the relative humidity in the calibration chamber.

6. It is quite likely that the time

response of the two temperature recirculating apparatus is longer than that of the two pressure Honeywell system. The authors would agree that this slow response may reduce the rate at which calibration work may be done in a laboratory, but it seems unreasonable to suggest that it would affect the quality of the work.

1717

No. 1717

ASHRAE 67th Annual Meeting, 1960

VANCOUVER, B. C.

The program for the 67th Annual Meeting, held at the Vancouver Hotel, June 13-15, consisted of four Technical Sessions, a Domestic Refrigerator Engineering Symposium, a Commercial Refrigeration Symposium and seven Forums. A total of 15 papers was presented at the Technical Sessions; the full texts of these papers appear in this volume of TRANSACTIONS. Additionally, seven papers were presented at the Symposiums.

The Vancouver Meeting attracted a relatively large attendance for a somewhat remote location. There were 593 registrations of members and guests.

The General Assembly convened at 9 a.m. on Monday, June 13, called to order by President Daniel D. Wile. A warm welcome to members attending the meeting was extended by Charles L. Hall, Director, Region X. Mr. Wile then introduced Executive Secretary R. C. Cross who read certain proposed amendments to the By-laws which will be voted upon at the Semiannual Meeting in February, 1961. In closing, Mr. Wile announced that polls were open until 2 p.m. for the election of officers and members of the Board of Directors.

President Wile presided at the Welcome Luncheon, held on Monday at 12:30 p.m. Following the playing of the Canadian and American national anthems, Rev. J. Whinfield Robinson, Rector, St. Helen's Anglican Church, delivered the invocation. Mr. Wile welcomed everyone in attendance and acknowledged the work of the Program Committee and the local Host Committees. S. J. Williams, Chairman of the Program Committee, requested that the speakers at the Technical Sessions and Symposiums rise and be acknowledged. Before proceeding with the program, President Wile reviewed events and progress within the Society during his term in office.

Various honors and awards in recognition of distinguished service to ASHRAE were made by President Wile. Certificates of Appreciation to retiring members of the Board of Directors were presented to: F. Y. Carter, C. L. Hall, H. M. Hendrickson, P. J. Marschall, G. W. F. Myers, R. S. Stover, S. J. Williams and W. F. Wischmeyer.

Fellow Certificates were given to: Axel B. Algren, John Everetts, Jr., M. K. Fahnestock, P. B. Gordon, Walter A. Grant, Linn Helander, John W. James, R. D. Madison, P. J. Marschall, W. T. Miller, E. B. Nottage, E. R. Queer and E. F. Snyder. A Life Member Certificate was presented to R. W. Ayres.

Other annual awards presented were:

1959 ASHRAE Klixon Award to John F. Harris and C. B. Sonnino, for their paper, "New Insulating Media for Hermetic Motors Require New Tests", published in the March 1959 issue of the ASHRAE JOURNAL. This award is sponsored by Texas

Instruments, Inc., Metals and Controls Div., Spencer Products Group for the best paper appearing in the JOURNAL, March through February, on a subject relating to electric motors or controls. The authors received $150 and a certificate.

Wolverine—ASHRAE Diamond Key Award to P. H. Ziel and J. S. Blossom, for their paper, "Pressurizing High Temperature Water Systems", published in the November 1959 issue of the JOURNAL. Sponsored by the Wolverine Tube Division of Calumet and Hecla, a gold key with a diamond inset is awarded to the authors of the best paper presented in the JOURNAL, March through February.

ASHRAE Willis H. Carrier Award to Aaron L. Brody, senior author of the paper, "Use of Activated Charcoal to Decrease Odor and Odor Transfer in Domestic Refrigerators", presented at the Dallas Semiannual Meeting and published in the April 1960 issue of the JOURNAL. This award is sponsored by the Carrier Corporation for the best paper presented at a national meeting by an Associate Member under 30 years of age and consists of a cash award in the amount of $250 plus a scroll.

ASHRAE Homer Addams Award for 1959 to Frank D. Farrington. Sponsored by the Addams Memorial Fund, $600 and a certificate are given to a graduate student working on an ASHRAE project. The committee selects the school, which recommends the student.

As his last official duty, President Wile introduced and installed new ASHRAE officers as provided by the Plan for Reorganization in the fourth step of succession. John E. Dube, the new Treasurer, was also introduced. Following his induction, incoming President Walter A. Grant presented a pin and a certificate to retiring President Wile. Mr. Grant then addressed the audience:

INAUGURAL ADDRESS—WALTER A. GRANT, PRESIDENT

First, I want to tell you how perfectly delighted I am to be privileged to advance to our Society's top office in the most beautiful city of your great country, and among the members of one of Canada's foremost Chapters.

I must also tell you that election to the Presidency is an overwhelming experience. It is, of course, a great honor, and I give you my pledge that I shall do everything in my power to prove that your trust in me has been well placed.

Even more importantly, the position is today one of great responsibility for the future of our 20,000 members. It will require qualities of leadership and judgment beyond the capacity of any single individual. Here I am fortunate to have as my associates a group of Officers and Board Members and committee chairmen and members of exceptional ability and devotion.

Eighteen months have passed since the combination of ASHAE and ASRE. Our Society has come a long way. Once the merger vote was taken, the membership at both Chapter and national levels closed ranks and resolved to make it work.

Nevertheless, we are confronted with problems. A few of these problems are serious. Many of them are difficult and complicated. All of the important ones had their roots in the previous organizations long before the merger. In the months to come, your Officers and Board of Directors propose to face these problems squarely, and with your help determine the best possible solutions.

The basic question is simply stated: Is your Society management—technical and non-technical, at all levels, nationally, and locally—advancing the wishes of, and the best long-range interests of, the membership? While experienced leaders in any organization will necessarily be buffeted by the cross-currents of events, in the long run they should and must determine a consistent course in tune with the desires of the membership.

Stemming from this basic question are a number of problem areas.

We have a financial problem which cannot be swept under the rug. I might add that so has every other technical society today—we're not unique and we're in good company. During the coming fiscal year we will give every member $60 value in services for his $25 annual dues. This is much better value than most organizations give. But to sustain our sources of income supplementary to dues requires a tremendous effort on the part of many devoted members. What services in the way of publications, long-range research, meetings, and expositions do our members really want to continue and support during the years to come?

The Society By-laws have built-in safeguards to assure adequate service to the three major areas of membership interest; namely, heating, refrigeration, and air conditioning and ventilation. If you will review the meeting programs, publications, and committee memberships since the merger, you will discover that each of these broad areas is, in actual fact, well represented and actively served.

But have we set up adequate machinery to satisfy the needs of particular segments of these

broad areas? What about cryogenics? Air pollution? Food processing and storage? What about programs at the Chapter level which will satisfy specialized groups, and still maintain the interest of the average member? While the problems of special-interest groups existed long before the merger, it remains a continuing challenge to find the right solutions.

We have problems in the area of publications. What policy goals should we establish for the JOURNAL in order to make it the outstanding engineering publication on the continent? Do our members want to continue the Society TRANSACTIONS? How well is the GUIDE AND DATA BOOK serving you?

In our Research Laboratory at Cleveland, we possess an organization unique among engineering societies. For many years it has made notable contributions to our industry. Toward what areas of research should its future efforts be directed? Should the operation be increased in size and scope? These are questions not to be answered lightly on the basis of personal opinion, but only after the most searching examination of our long-range policy and objectives.

Finally, is our organization structure suited to the needs of a fast-moving engineering society? Shouldn't we look in the mirror at our administrative and committee organizations to be sure they are serving us as effectively as possible, consistent with needs of the Society?

In the months to come, your Officers, Board of Directors, committees at interest, and Headquarters Staff will be devoting much time and effort to bring about wise solutions to these problems. I sincerely believe that you have a competent and devoted administration at the helm, determined to respond to the membership, and at the same time maintain the high standards expected of an engineering society. We need your active interest and your constructive suggestions to help us set the long-range goals needed for our Society's future growth.

Now, I should like to turn for a moment to the industry which our Society serves. The growth of the heating, refrigerating and air-conditioning business has been almost explosive in the past 15 years. There is every reason to believe that it will continue for a long time. I don't believe this is over-optimism, for history shows that the limitation on industry growth is market saturation. For example, of the three major air conditioning markets—commercial, industrial, and residential—only commercial has received substantial coverage, but it is by no means saturated. The market for factories and homes has just begun to open up, and so far the surface has barely been scratched.

My company has just completed a study of the heating, refrigerating and air-conditioning business in Canada, to determine its growth potential. It is our conclusion that sales by Canadian industry will double during the next five years. As you might expect, the largest rate of growth will be in the air conditioning segment.

Figures from the Dominion Bureau of Statistics bear out this forecast. Sales of self-contained air conditioners increased 34% from 1958 to 1959, and room air conditioners 82%. So far the evidence is that this growth is continuing in 1960. Moreover, the impetus to sales will increase as more Canadian manufacturing and assembly operations come into being.

This explosive growth rate is opening up employment opportunities which people in Canada and the United States have not fully realized. The air-conditioning industry in the United States already employs a quarter of a million people. Yet it faces serious limitations to its growth from a shortage of trained installation and service personnel, and this shortage is virtually nation-wide.

A similar growth rate is foreseeable in the Dominion during the next decade. The population ratio of our two countries indicates a manpower requirement for Canadian industry of at least 25,000 trained persons. It seems certain that aggressive steps should be taken by your educational and business leaders to increase the number of trained personnel, particularly for installation and service.

I believe we need a stepped-up extension school program for adults, and a vocational program for young men who will enter industry upon graduation from high school.

Of nearly as great importance is the need to increase the flow of high school students into the engineering colleges. We need to build a closer liaison between our Chapters and our colleges, and bring more engineering graduates into our industry.

I hope that our Canadian members will become increasingly active in the affairs of our Society, and keep pace with the industry's growth which we foresee so clearly ahead. We are in process of doubling the number of Canadians on General Committees of the Society, to bring your representation more in line with the size of your membership.

In closing, I simply must tell you, on behalf of all of our national members and their wives, and particularly Mrs. Grant and myself, how much we are enjoying the privilege of meeting here in your beautiful city, and how much we appreciate the warmth of your greeting and your generous hospitality.

Thank you again for putting your confidence in me as President. I shall work hard to merit it.

President Grant officially welcomed everyone attending the dinner-dance on Wednesday, at 7:30 p.m. New members of the Board of Directors were introduced: Warren S. Harris, W. L. McGrath, Axel Marin, James W. May, James F. Naylor, Jr., George B. Rottman, Thomas J. White and V. Dale Wissmiller. W. J. Collins was reelected to the Board.

A Memory Book was presented to 1958 ASHAE President E. R. Queer.

Professor Queer was the last recipient of this memento of Society activities during a President's term of office.

President Grant, on behalf of the members of ASHRAE, presented Mr. Wile with a token of the Society's appreciation and esteem.

Former President P. B. Gordon received the ASHRAE F. Paul Anderson Award for outstanding service in heating, ventilating, air conditioning or refrigeration. Sponsored by the Society, this award consists of a gold medal.

The First Technical Session was called to order by President Wile at 9:30 a.m. on Monday, June 13. He introduced S. J. Williams, who served as Chairman for this Session, where four papers were presented.

Held concurrently, the Domestic Refrigerator Engineering Symposium had H. P. Harle as Chairman. Four speakers discussed "Human Engineering and Its Demands on Refrigerator Design". These papers do not appear in this volume of TRANSACTIONS and are not planned for preparation as a Bulletin.

The Second Technical Session was held at 9:30 a.m. on Tuesday, June 14; President Grant presided. Before proceeding with the scheduled papers, Secretary Cross announced the results of the election. The Report of the Inspectors of Election follows:

REPORT OF INSPECTORS OF ELECTION

Ballot for Treasurer and Regional Directors

	Total Votes
Treasurer (Term: June 1960 to Jan. 1961), John E. Dube	3773
Regional Director—Region VII (Term: June 1960 to June 1962), James F. Naylor, Jr.	3772
Regional Director—Region VIII (Term: June 1960 to June 1962), William J. Collins, Jr.	3772
Regional Director—Region X (Term: June 1960 to June 1962), Thomas J. White	3771
Directors-at-Large (Term: June 1960 to June 1962)	
George B. Rottman	3771
Warren S. Harris	3770
William L. McGrath	3769
V. Dale Wissmiller	3771
James W. May	3768
Axel Marin	3771

By-law Amendments

		For	*Against*
1.	*Section* 4.4	3685	87
2.	*Section* 5.14	3727	45
3.	*Section* 8.5	3464	308
4.	*Section* 8.8.1	3719	53
5.	*Section* 8.8.24	3674	98
6.	*Section* 8.9	3737	35
7.	*Section* 8.12	3711	61
8.	*Section* 9.6	3610	162
9.	*Section* 11.1	3732	40
Invalid Ballots		46	

Respectfully Submitted

A. T. BOGGS
G. J. FINCK
W. J. OLVANY
Inspectors

President Grant then introduced R. A. Line, Chairman of this Session; four papers were presented.

The Commercial Refrigeration Symposium, with J. H. Rainwater as Chairman, was held concurrently. Three speakers discussed the "Effect of Air Conditioning in Food Stores on Open Display Cases". Condensed versions of the papers presented here appear in the September 1960 issue of the ASHRAE JOURNAL, pages 62-66. The

full texts of these papers do not appear in this volume of TRANSACTIONS and are not planned as a Bulletin.

Tuesday afternoon, starting at 2:00, was for Forums, with E. N. Johnson in charge. Since Forums are highly informal discussions for the exchange of ideas, there are no prepared papers and no notes or minutes are taken.

The Third Technical Session was called to order by First Vice President R. H. Tull and G. F. Carlson was Chairman. As scheduled, four papers were presented here.

The Fourth Technical Session was a concurrent one. At this Session, Second Vice President John Everetts, Jr., presided and R. S. Buchanan was Chairman. Three papers were presented.

Numerous committee meetings were scheduled during the course of the meeting.

In addition to the technical program, a full schedule of social events took place.

PROGRAM—ANNUAL MEETING

Vancouver Hotel, Vancouver, B. C.

June 13-15, 1960

Saturday, June 11

8:00 a.m	Advertising Committee breakfast-meeting.
9:00 a.m.	Finance Committee.
12 noon	Executive Committee luncheon-meeting.
2:00 p.m.	Program Committee. Research and Technical Executive Committee.
4:00 p.m.	Regions Central Committee dinner-meeting.

Sunday, June 12

10:00 a.m	Advance Registration, Main Mezzanine. Research and Technical Committee.
12:30 p.m.	Board of Directors luncheon-meeting.
2:00 p.m.	Meeting Arrangements Committee. Standards Committee.
2:00 p.m. to 5:00 p.m.	Informal Reception, B. C. Chapter.

Monday, June 13

7:30 a.m.	Speakers' Breakfasts: First Technical Session. Domestic Refrigerator Symposium.
8:30 a.m.	REGISTRATION, Main Mezzanine.
9:00 a.m	GENERAL ASSEMBLY Opening of the 67th Annual Meeting of the Society. Remarks by President D. D. Wile.

Address of Welcome by C. L. Hall, Director, Region X.
Polls Open for Election of Officers and Members of Board of Directors.

9:30 a.m. FIRST TECHNICAL SESSION
D. D. Wile, President, officer-in-charge.
Chairman, S. J. Williams, Si Williams Co.
Gas-Fired Open Cycle Air Conditioner, B. E. Eakin, Supervisor, Reservoir Engrg. Research, and R. T. Ellington, Asst. Res. Dir., Inst. of Gas Technology.

10:15 a.m. An Air-Cooled Absorption Cycle, R. H. Merrick, Chief Engr. and R. A. English, Sr. Dev. Engr., Gas Air Cond., Bryant Mfg. Co.

11:00 a.m. Dual Solution System, F. H. Hibberd, Air Conditioning Development Co.

11:45 a.m. Solar Heat Gains through Slat-Type, Between-Glass Shading Devices, N. Ozisik (formerly with ASHRAE Laboratory) and L. F. Schutrum, Res. Supervisor, ASHRAE Research Laboratory. Presented by C. M. Humphreys.

9:30 a.m. DOMESTIC REFRIGERATOR ENGINEERING SYMPOSIUM
Chairman, H. P. Harle, Prod. Engr., Household Refrig. Dept., General Elec. Co.

HUMAN ENGINEERING AND ITS DEMANDS ON REFRIGERATOR DESIGN
Keynoter: Mrs. Virginia Thabet Habeeb, Home Equip. Editor, American Home Magazine.
Styling and Features for Household Refrigeration Appliances, E. V. Sutin, Associate, Walter Dorwin Teague Associates.
Underwriters' Requirements for Refrigerators and Freezers, G. H. Pope, Managing Engr., Casualty and Automotive Dept., Underwriters' Laboratories, Inc.
C.S.A. Requirements, D. C. King, Engr. in charge of the light industrial section, Engrg. Dept., Canadian Standards Assn.

10:00 a.m. Coffee Hour, Ladies, Hospitality Room.

12:30 p.m. WELCOME LUNCHEON
Canadian and U.S. national anthems.
Installation of Officers.
Presentations.
Announcements.

2:00 p.m Polls close for Election of Officers and Members of Board of Directors.

2:30 p.m. Divisional Advisory Committee.
Domestic Refrigerator Symposium.
Honors and Awards Committee.
Publications Committee.
Public Relations Committee.
Research Exhibit Committee.

3:00 p.m. Ladies' Tea and Summer Fashion Excitement.
Childrens' Swim Party.

7:00 p.m. Moonlight Cruise aboard S.S. Princess Patricia on Howe Sound.

Tuesday, June 14

7:30 a.m. Speakers' Breakfasts:
Second Technical Session.
Commercial Refrign. Symposium.
Forum Moderators.

8:30 a.m. REGISTRATION, Main Mezzanine.

9:30 a.m. SECOND TECHNICAL SESSION
Walter A. Grant, President, officer-in-charge.
Election results announced by Executive Secretary Cross.
Chairman, R. A. Line, Engineer, Hussmann Refrig. Co.
A Proposed Pipe Friction Chart for High Temperature Water Systems, Prof. T. C. Min, Dept. of Mech. Engrg., Auburn Univ. and Prof. P. J. Potter, formerly Head, Dept. of Mech. Engrg., Alabama Polytechnic Institute.

10:15 a.m. Reaction Forces in A Scotch Yoke, V. G. Foris and B. W. Hatten, Refrig.-Freezer Engrg. Dept., Westinghouse Elec. Corp. Presented by B. W. Hatten.

11:00 a.m. Heat Loss from a Heated Basement, J. M. Elliott, Asst. Prof., University of Kentucky and Dr. Merl Baker, Executive Director, Kentucky Research Foundation. Presented by Merl Baker.

11:45 a.m. Cooling Rates of Apples Packed in Different Bushel Containers and Stacked at Different Spacings in Cold Storage, D. V. Fisher, Head, Pomology Section, Canada Dept. of Agriculture.

9:30 a.m. COMMERCIAL REFRIGERATION SYMPOSIUM
Chairman, J. H. Rainwater, Dir. of Engrg., The Warren Co., Inc.

EFFECT OF AIR CONDITIONING IN FOOD STORES ON OPEN DISPLAY CASES
Inter Effects of Air Conditioning and Open Display Refrigerators, D. E. Friedman, Chief Engr., Hussmann Refrig. Co.
Air Conditioning in Food Stores and Its Effects on the Operation of Open Display Equipment, T. L. Tyler, Prod. Dev. Engr., Tyler Refrigeration Corp.
Condensation In and On Open Display Equipment as Related to Air-Conditioned Stores, J. A. Biggers, Dir. of Engrg., Friedrich Refrigerators, Inc.

10:00 a.m. Golf Tournament.

2:00 p.m. Ladies' Sightseeing Tour.

2:00 p.m. FORUMS
E. N. Johnson, Engineer, Swift and Co., Chicago, Ill., *in charge*
1. Cryogenics
Moderator: V. J. Johnson, Chief, Gas Liquefaction Sec., Cryogenics Engrg. Lab., Natl. Bur. of Standards.
2. Corrosion with Window Air Conditioners
Moderator: C. O. Hutchinson, Mgr., Industrial Sales, The Glidden Co.
3. Practical Applications of Foam Insulation
Moderator: V. L. Miller, Asst. Mgr., Tech. Services Dept., Pittsburgh Corning Corp.
4. Economics of Electric Heating vs. Fossil Fuels for School Buildings
Moderator: Lincoln Bouillon, Bouillon, Griffith, Christofferson & Schairer.

3:00 p.m. 5. Aluminum Tube Refrigeration Coils
Moderator: O. J. Nussbaum, Chief Engr., Kramer-Trenton Co.
6. Reducing Power Needs for Hot Water Systems
Moderator: C. W. Pollock, Manager, Air Cond. & Refrign. Div., Crane Co.
7. Noise in Ventilating Systems
Moderator: D. P. Dakos, Koppers Co.

2:30 p.m. Children's Trip to Grouse Mt. Ski Lift.

3:00 p.m. TC-1.5, Meteorology & Weather Data.

7:30 p.m. Dinner-Dance, Ballroom.
Presentations.
Announcements.
Dancing.
Barber Shop Quartette.

Wednesday, June 15

7:30 a.m. Speakers' Breakfasts:
Third Technical Session.
Fourth Technical Session.

8:30 a.m. REGISTRATION, Main Mezzanine.
General Administrative & Coordinating Committee.
Technical Coordinating Committee.

9:30 a.m. THIRD TECHNICAL SESSION
Robert H. Tull, First Vice-President, officer-in-charge.
Chairman, G. F. Carlson, Chief Engr., Specialty Div., Bell and Gossett Co., Inc.
Solubility of Refrigerants 11, 21, and 22 in Organic Solvents Containing an Oxygen Atom, Prof. L. F. Albright, Asst. Prof. T. C. Doody, and Graduate Students P. C. Buclez and C. R. Pluche, School of Chem. Engrg., Purdue Univ.

10:15 a.m. Determination of Moisture in Fluorocarbons, J. D. Morton and L. K. Fuchs, Development Dept., Union Carbide Chemicals Co., Div. of Union Carbide Corp. Presented by W. S. Engle.

11:00 a.m. A Study of the Factors Influencing the Stability of Mixtures of Refrigerant 22 and Refrigerating Oils, Dr. W. O. Walker, Dean, Div. of Research and Industry, and Shelvin Rosen, Ind. Chem. Res. Lab., Univ. of Miami, and S. L. Levy, Res. Lab., Gen. Chem. Div., Allied Chemical Corp.

11:45 a.m. Time Factors in the Removal of Moisture from Refrigerating Systems with Desiccant-Type Driers, W. O. Krause, Section Head, Refrign. Research; A. B. Guise, Dir., Dev. and Design; and E. A. Beacham, Refrign. Sales Dev., Ansul Chemical Corp.

9:30 a.m. FOURTH TECHNICAL SESSION
John Everetts, Jr., Second Vice-President, officer-in-charge.
Chairman, R. S. Buchanan, Asst. Dir. Engr. and Res., Kelvinator Div., American Motors Corp.
Production Control Testing of Thermoelectric Materials, Dr. G. V.

Downing, Jr., Physical and Inorganic Chem. Res., Merck, Sharp, and Dohme Res. Labs., Div. of Merck and Company.

10:15 a.m. A Simplified Engineering Approach to Thermoelectric Heat Pumping, W. V. Huck, Applied Res. Supvr., Minnesota Mining and Mfg. Co.

11:00 a.m. A Comparative Study of the Manufacturing Costs of Thermoelectric and Mechanical Refrigerating Systems, D. W. Scofield, Proj. Engr., Dr. P. F. Taylor, Proj. Scientist, and L. A. Staebler, Manager, Advanced Dev. Dept., Philco Corp. Presented by L. A. Staebler.
Adjournment of the 67th Annual Meeting of the Society.

12:30 p.m. Board of Directors luncheon-meeting.

HOST CHAPTER
BRITISH COLUMBIA

OFFICERS

W. F. Wiggins, President
D. B. Leaney, First Vice President
R. W. Hole, Second Vice President
William Baker, Secretary
M. J. Phillipson, Treasurer
F. J. Dwyer, Board of Governors
R. S. Millar, Board of Governors
C. H. White, Past-President
C. L. Hall, Regional Director

MEETING ARRANGEMENTS COMMITTEE

A. C. Martin, General Chairman
C. W. Leek, Co-Chairman
F. J. Dwyer, Co-Chairman
D. W. Thomson, Reception
C. T. Hamilton, Reception
P. H. Snider, Sessions
A. S. Lewis, Transportation
R. B. McDonnell, Entertainment
R. B. Butler, Finance
R. W. Racine, Publicity
E. E. Renouf, Golf Tournament
Clarence Van Boeyen, Children's Events
Mrs. H. E. McConaghy, Ladies

The following resolutions were duly made, seconded and adopted by the membership at the 67th Annual Meeting.

RESOLUTIONS

WHEREAS, Almighty God in His infinite wisdom saw fit on June 6, 1960 to remove from our midst Aubry Vaughn Hutchinson, Secretary Emeritus of our Society, and

WHEREAS, the departed served the AMERICAN SOCIETY OF HEATING AND VENTILATING ENGINEERS since 1922; first as Manager of Publications; was appointed Secretary 1926; Executive Secretary 1950, and

WHEREAS, he served the AMERICAN SOCIETY OF HEATING AND AIR-CONDITIONING ENGINEERS as Executive Secretary 1955-1959 and as Executive Secretary of the AMERICAN SOCIETY OF HEATING, REFRIGERATING AND AIR-CONDITIONING ENGINEERS until his retirement as Secretary Emeritus in June 1959, a total of 38 years of continuous service,

BE IT RESOLVED THAT, in recognition of his long and faithful devotion to the interests of our Society, his painstaking and monumental attention to the development of the GUIDE, the

JOURNAL and TRANSACTIONS, the encouragement of Chapters and his capable and resourceful arranging for National Meetings, the

BOARD OF DIRECTORS in session at this 67th Annual Meeting at Vancouver, B.C. takes recognition of his lifetime of devoted service, does enter this resolution upon the minutes of this meeting and does extend, upon its own behalf and that of the members, expressions of deepest sympathy to Mrs. Hutchinson in her bereavement.

WHEREAS, Almighty God in His infinite wisdom saw fit on June 3, 1960 to remove from our midst, Dr. Constantin P. Yaglou, a distinguished and long time participant in activities of our Society, and

WHEREAS, the departed received the F. Paul Anderson Award of the A.S.H.R.A.E. in 1950 in recognition of outstanding work in his chosen field and research particularly in the hygienic aspects of human comfort, and

WHEREAS, he served on the staff of the Research Laboratory of our Society for several years during which time he was closely associated with most of the pioneering studies in the development of the original Effective Temperature Scale, determination of the Comfort Zone, and

WHEREAS, in his work as Professor of Industrial Hygiene at the Harvard University, School of Public Health he did conduct important studies in the comfort, health and therapeutic aspects of air conditioning and worker efficiency under temperature extremes, and

WHEREAS, he did serve on the GUIDE Publication Committee, on the Nominating Committee and numerous Technical Advisory Committees of our Society and as an officer of the Massachusetts Chapter,

BE IT RESOLVED that the Board of Directors in session at the 67th Annual Meeting at Vancouver, British Columbia takes further recognition of his life time of accomplishments and contributions and does enter this resolution upon the minutes of this meeting, and a copy be sent to his family.

WHEREAS, the 67th Annual Meeting of the AMERICAN SOCIETY OF HEATING, REFRIGERATING AND AIR-CONDITIONING ENGINEERS was assembled in solemn and at times not so solemn conclave, in Vancouver from June 13 to 15, 1960, and

WHEREAS, no assemblage of such numbers and persons of prestige is possible of accomplishment without much planning and preparation, and

WHEREAS, when all provisions has been made for personal and bodily comforts, all with an admixture of sunshine, and moist mists by nature proportioned throughout the meeting, and

WHEREAS, when moonlight cruises have been provided on the good ship "Princess Patricia" sailing on quiet seas, amidst unparalleled scenery, and

WHEREAS, our ladies, visiting with us, were at all times graciously entertained by the good ladies of British Columbia, and

WHEREAS, there was an ever abundant and adequate provision for those participants of the cup that cheers, and

WHEREAS, provision was also made for the royal and ancient game of "golf" on a sporty course with some of the "Pacific mists" to make even a modest handicap insufficient, and

WHEREAS, when all of the pleasures of good fellowship, gay conversation and the company of fair ladies are combined with the principal purpose for our gathering—the presentation of papers dealing with highly technical subjects, presented within the palatial accommodations of the Hotel Vancouver,

BE IT RESOLVED that a most hearty and sincere vote of thanks be extended to Chairman Red Martin and his Meeting Arrangements Committee and to President Wiggins and all members of the British Columbia Chapter, our hosts,

May this resolution be inscribed on the permanent records of our Society in regard to this meeting for the information of our Society membership at large.

1718

No. 1718

Gas-Fired Open Cycle Air Conditioner

B. E. EAKIN R. T. ELLINGTON

Air conditioning by liquid-desiccant-drying and adiabatic partial-resaturation of the circulated air has aspects of continued interest to designers of commercial and industrial systems. In such a unit the relative humidity as well as the temperature of the air can be controlled, and dust and odors are effectively removed in the dual washing the air receives. A particular advantage for small commercial or domestic applications, is the ease with which an open-cycle system can be adapted to year-round operation providing summer cooling and winter space-heating, with complete humidity control.

Few regions in the country have climates sufficiently dry to permit cooling of the air directly by partial-resaturation. When the air must be dehumidified prior to the evaporative cooling, this conditioning technique has proved to have disadvantages from the standpoint of complete gas-firing. When moisture is removed from air, the heat which is liberated raises the temperature of the dried air sufficiently that mechanical refrigeration is often required for effective cycle operation.

The benefits that might be attained through the use of internal cooling in the dehumidifier to remove the liberated heat were discussed by Bichowski[1] prior to World War II, but there is no evidence that such a unit was constructed. In 1948, Peck and Ryant[2] constructed an apparatus for a feasibility study of the open cycle, which included a water-cooled dehumidifier, and employed lithium chloride solution as the sorbent. This equipment utilized an absorber-heat-exchanger fabricated of automobile radiator core sections with horizontal passes for the cooling water. The results obtained[2] indicated that the open cycle with a water-cooled dehumidifier had distinct advantages over compression-refrigeration air-conditioning cycles, if a sorbent could be found

B. E. Eakin is Supervisor, Reservoir Engineering Research, and R. T. Ellington is Assistant Research Director and Chairman of the Education Program, Institute of Gas Technology. This paper was presented at the ASHRAE Annual Meeting, Vancouver, B.C., June 13-15, 1960.

that was as effective as, but less corrosive than, the lithium chloride solutions utilized. This would be especially true in view of prevailing ratio of energy costs.

The individual operations which would be employed in a gas-fired open cycle have all been previously utilized. However, the literature contains no description or analysis of a system employing all these processes in a single cycle for operation under the conditions and requirements encountered in residential cooling. Large-scale units have employed some of the newly-developed liquid sorbents for air dehumidification, but insufficient data have been published to permit analysis of their performance in other applications.

The calculated results of thermodynamic analyses of liquid-sorbent open air-conditioning cycles, and experimental results obtained by use of a laboratory pilot unit utilizing one of these cycles are reported here. This investigation of the open cycle was conducted as a part of the PAR (Promotion-Advertising-Research) Plan of the American Gas Association under the sponsorship of the General Research Planning Committee.†

PROPERTIES OF THE IDEAL SORBENT

To determine the types of compounds most promising for use in dehumidification, the properties of an ideal sorbent should be considered. These have been treated in detail elsewhere[4] and will only be summarized.

† American Gas Association, Project ZB-22.

The sorbent must be chemically stable over the temperature range of operation, and not corrosive to any of the materials in the systems. The boiling point of the sorbent should be high to insure low vapor pressure at all operating temperatures. This will minimize sorbent carryover into the air being conditioned and air which might be used for sorbent reconcentration, and will reduce the energy expended to separate the sorbent and absorbed water by distillation.

The sorbent solution should have a low viscosity, to reduce the energy required for circulation and improve heat transfer coefficients. Low viscosity also increases the rate of mixing as the solution absorbs moisture, thus increasing the rate of solution. A low heat capacity is advantageous in reducing the heat lost in warming and cooling the sorbent in its circulation cycle.

The sorbent must be completely miscible with water over the temperatures and concentrations employed. The vapor pressure of water over the solution at a given temperature then becomes the major consideration, This vapor pressure should be low, so the dehumidifier can operate at or above atmospheric temperature while reducing the moisture content of the air to a low value. For ideal solutions in which there is no attraction between solute and solvent molecules, the vapor pressure of solute over a solution is equal to its vapor pressure in the pure state, times its mole fraction in the solution. In an ideal sorbent solution, the vapor pressure of the sorbent

should be negligible compared to that of water, and the total pressure over the solution will then be due to water vapor.

To be effective, however, the vapor pressure of water in the solution must be lower than that for ideal behavior so that at a given temperature a reduced amount of sorbent is needed per lb of water removed from the air; less pumping energy and smaller units will result, and less heat will be required to raise the solution to reconcentration temperature.

The solutions that provide these negative deviations from ideal behavior are those in which there is attraction between the solute and solvent molecules. Such attraction may be provided by the electrical nature of the molecules, wherein they are considered to possess electric dipoles and are referred to as polar molecules.

The attraction between polar solute and polar solvent molecules is usually greatest when one of the pair possesses a hydrogen atom and a negative group while the other contains an electronegative atom such as fluorine, oxygen or nitrogen. The hydrogen becomes relatively positive and acts as a bond between the two molecules which are said to be "hydrogen bonded." This phenomenon has been employed by Zellhoefer[8] to explain the enhanced solubility or vapor pressure lowering of dichloromonofluoromethane in ethers. This factor may also account for the decreased vapor pressure of water in glycols.

Another chemical effect that may account for enhanced solubility or vapor pressure lowering is exemplified by the formation of solvates. Many positive metal ions form a bond with the negative end of polar solvents, such as water, ammonia and the alcohols. These bonds are referred to as ion-dipole bonds and result from electrostatic forces. This may account for the large solubility of lithium salts in water and ammonia.[9]

An indication of the deviation of a solution from ideal behavior is the amount of heat evolved on forming a solution; the greater the heat evolved, the greater the negative deviation. A rough general rule has been offered by Hainsworth[7] that the temperature rise should be 15 to 20 F deg on the mixing of equal portions of solute and solvent. This serves as a quick and easy method for elimination of less favorable sorbents.

SELECTION OF SORBENT

Lithium salts have been used in various absorption cycles, but they possess certain undesirable properties. Lithium bromide is a good absorbent, but is toxic and therefore cannot be used in open cycles. Lithium chloride is nearly as good an absorbent, but solutions of it are quite corrosive. Various investigations are under way to determine methods of corrosion inhibition for lithium chloride solutions, but until an effective method is found, the cost of the special materials of construction required precludes use of these solutions in domestic and commercial units.

The natural gas industry has utilized both solid and liquid desic-

cants for dehydration of pipeline gas, modifying the cycles as new and better desiccants were developed. Recently several dehydration cycles were developed utilizing triethylene glycol (TEG) as the sorbent.[8] Data on the physical properties of TEG[9, 10] indicated these solutions might satisfy the requirements for the sorbent in an open cycle air conditioner.

Some of the properties of TEG that make it a desirable dehumidifying agent are:

(a) Good dew-point depression. The vapor pressures of aqueous solutions in the concentration range 90 to 99% TEG are very much lower than that for pure water: i.e., 98% TEG solution has a vapor pressure of 9 mm Hg at 100 F compared to 49 mm for water.

(b) The equilibrium TEG vapor concentration in treated air is low. The glycol is relatively nonvolatile, having a normal boiling point of approximately 530 F.

(c) Solutions have desirable properties for pumping. Pure TEG has a viscosity of 49 centipoises at 20 C, compared to 35.7 centipoises for diethylene glycol, or 1 centipoise for water. Concentrated TEG solutions have specific gravities of about 1.1.

(d) TEG has low heat capacity. The specific heat of aqueous solutions is 0.5 to 0.6 Btu/lb/F.

(e) TEG is chemically and thermally inert. Concentrated solutions may be considered non-corrosive at room temperature, and much less corrosive than lithium salts or other glycol splutions at elevated temperatures. Aqueous solutions are relatively inert and chemically stable up to about 400 F.

(f) Reasonable cost may be expected. Currently TEG costs approximately $0.19/lb.

An additional advantage of TEG solution is that the small amounts retained in the conditioned air have a beneficial effect as a bactericide.[11, 12] The principal disadvantage of TEG solution is that highly concentrated solutions are required in order to effect adequate moisture dew-point depression. A 95% TEG solution is required to effect the same water vapor pressure reduction as can be obtained with a 40% solution of either lithium bromide or chloride at the same temperature. Therefore, circulation rates of lithium salt solutions would be much lower, and more thorough dehumidification could be obtained with consequent increase in capacity and higher efficiencies, than with the sorbent now selected.

Existing data on heats of dilution and heat capacity of TEG solution, obtained from primary suppliers,[9, 10] were evaluated and judged sufficiently accurate for use in cycle thermodynamic calculations. However the vapor pressure and phase equilibrium concentration data[13] were conflicting in the range of interest for air conditioning. Therefore experimental vapor pressure data were obtained for concentrations of 93 to 99% by

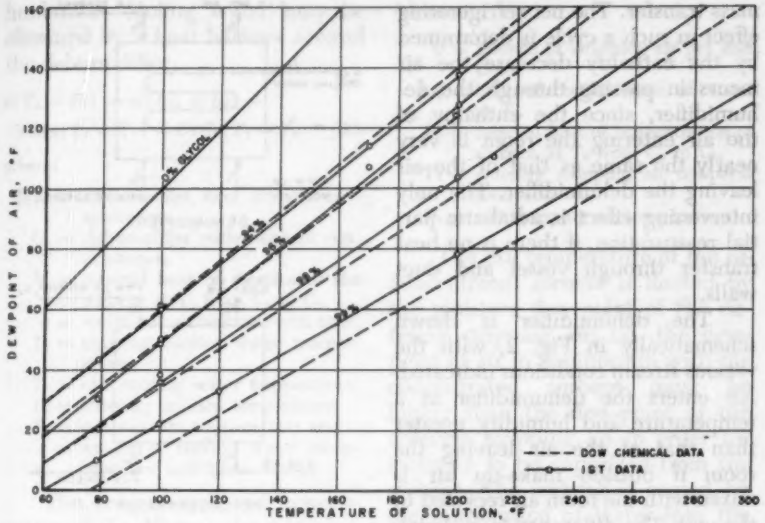

Fig. 1. Dew-point of equilibrium air as a function of glycol solution temperature

weight TEG at temperatures from 78 to 120 F. A few data were also obtained for temperatures of 170 to 205 F. A plot of equilibrium air dew-point as a function of TEG solution concentration and temperature is given in Fig. 1, and compares the IGT data with those presented by Dow Chemical Company. Satisfactory agreement exists between the data for all solutions tested except for 99%, where the IGT data indicate considerably less favorable dew-point depressions than the Dow data. The experimental technique utilized was a modification of the gas transport method of Bent and Krinbill[4] which has proven quite accurate for systems of similar behavior.

THERMODYNAMIC ANALYSIS OF IDEAL OPEN CYCLE

The thermal efficiency of an open absorption cooling cycle is dependent on the operating temperatures in the various units, inlet and outlet air temperatures, cooling water temperature, method of sorbent reconcentration, and the non-ideal behavior of sorbent solution. Therefore, determination of the cycle thermal efficiency for a given set of operating conditions necessitates calculation of the heat and material flows in each component of the proposed system.

A detailed consideration of an ideal cycle was made without restriction to temperature and humidity gradients necessary for heat and

mass transfer. The net refrigerating effect in such a cycle is determined by the enthalpy decrease the air incurs in passing through the dehumidifier, since the enthalpy of the air entering the room is very nearly the same as that of the air leaving the dehumidifier. The only intervening effect is adiabatic partial resaturation, if there is no heat transfer through vessel and duct walls.

The dehumidifier is shown schematically in Fig. 2, with the various stream conditions indicated. Air enters the dehumidifier at a temperature and humidity greater than that of the air leaving the room if outside make-up air is mixed with the room air recycled to the unit. The difference in enthalpy between the air leaving the room or occupied space, and that entering the dehumidifier is lost as regards refrigerating effect in the room, and is thus an extra burden on the system.

The air entering the dehumidifier loses water to the absorbent solution, which is consequently warmed by liberation of an amount of heat equal to the heat of condensation of the water plus the heat of dilution of the solution. The solution is cooled to some extent by releasing some of this heat to the air and warming it to exit temperature. The solution is further cooled by transfer of heat from the solution to water circulated through cooling coils in the dehumidifier. The net refrigerating effect on the air, Q_1, may be taken to be:

$$Q_1 = wh_{fg} - 0.24a(T_2 - T_1) \quad (1)$$

where:

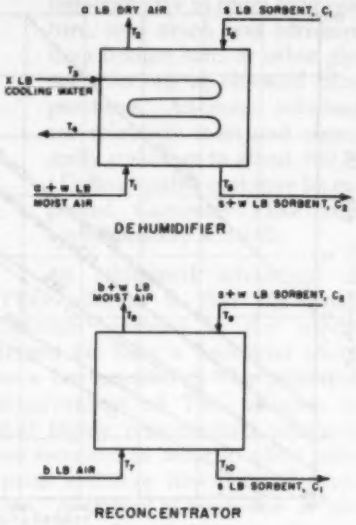

Fig. 2. Schematic diagram of water-cooled dehumidifier and stripping-air reconcentrator flow conditions

a = pounds of air dehumidified per unit time.
h_{fg} = heat of condensation of water at T_1.
T_1 = entering air temperature.
T_2 = exit air temperature, and
w = weight of water removed from "a" pounds of air.

In this expression the specific heat of air is taken as 0.24 Btu/lb/F (corresponding to dry air), instead of the humid heat, and the enthalpy change corresponding to temperature change of the liquid-phase has been neglected. These simplifications, also used in the remainder of the enthalpy balances, have little effect on the dehumidifier heat balance.

The heat removed by the de-

humidifier cooling water may be obtained by a heat balance around the dehumidifier:

$$x(T_4 - T_3) = w(h_{fg} + h_s) - 0.24a(T_3 - T_1) - 0.65s(T_6 - T_5) \quad (2)$$

where:

C_1 = dehumidifier inlet sorbent concentration.
C_2 = dehumidifier outlet sorbent concentration.
h_s = integral heat of dilution of the sorbent at T_1 from C_1 to C_2.
s = weight of sorbent per unit time.
T_3 = entering cooling water temperature.
T_4 = exit cooling water temperature.
T_5 = entering solution temperature.
T_6 = exit solution temperature, and
x = weight of cooling water circulated per unit time.

The temperature and concentration of the dilute sorbent leaving the dehumidifier are limited by the moisture dew-point temperature of the entering air, i.e., the dew-point of air in equilibrium with the dilute sorbent must be lower than the entering air dew-point in order for moisture to be absorbed. If the dilute sorbent concentration is fixed, the exit temperature and solution flow rate will therefore be determined by the entering air rate, temperature, and humidity.

In the reconcentrator, also shown schematically in Fig. 2, the amount of water absorbed in the dehumidifier, w, must be expelled from the dilute sorbent. For the case of air stripping, neglecting the heat content of the water vapor in the stripping air, the overall reconcentrator heat requirement, Q_2, may be taken to be:

$$Q_2 = w(h_{fg} + h_s) + 0.24b(T_8 - T_7) \quad (3)$$

where:

b = pounds of stripping air per unit time.
h_{fg} = heat of condensation of water at T_8.
h_s = integral heat of concentration of sorbent at T_8 from C_2 to C_1.
T_7 = entering stripping air temperature, and
T_8 = exit stripping air temperature.

The exit temperature of the reconcentrated sorbent is limited by the moisture dew-point of the entering stripping air; i.e., the dew-point of air in equilibrium with the concentrated sorbent must be higher than the dew-point of the entering stripping air in order for moisture to be vaporized from the sorbent. The sorbent is cooled by the evaporation of water into the stripping air and also supplies heat to raise the stripping air to its exit temperature. Therefore the required stripping-air flow rate, b, and the dilute sorbent entering temperature are calculated from a heat balance on the reconcentrator.

Neglecting losses in heat exchange, a gross thermal efficiency may be calculated for this simple cycle by dividing the effective air refrigeration obtained in the dehumidifier, Q_1, by the heat required for operation of the reconcentrator, Q_2:

$$\frac{Q_1}{Q_2} = \frac{wh_{fg} - 0.24a(T_3 - T_1)}{w(h_{fg} + h_s) + 0.24b(T_8 - T_7)} \quad (4)$$

The open cycle described has two inherent characteristics which reduce efficiency; (a) heat is absorbed by the recirculated air as it passes through the dehumidifier, and (b) heat is required to warm

TABLE I. SUMMARY OF FLOW CONDITIONS*, HEAT, AND COOLING WATER REQUIREMENTS FOR VARIOUS OPEN CYCLES

Condition	I	II	III	IV	V	VI
Recirculated air to unit, cfm	1200	1200	1200	1200	1200	1200
Outside air to unit, cfm	0	0	0	0	155	446
99% Solution to dehumidifier:						
Rate, lb/min	27.1	20.2	24.0	27.1	22.9	29.1
Temperature, F	85	85	85	85	85	85
Dilution to, %	96	96	96	96	95	95
Outside stripping air, cfm	25	25	25	0	28	34
Room air:						
dry-bulb temp., F	75	80	76	75	75	75
wet-bulb temp., F	62.6	63.5	64	62.6	62.6	62.6
Sp. humidity, lb/lb	0.0093	0.0087	0.0100	0.0093	0.0093	0.0093
Air entering dehumidifier:						
dry-bulb temp., F	80	80	76	80	81.6	84.0
wet-bulb temp., F	67	63.5	64	67	67.9	69.3
Sp. humidity, lb/lb	0.0112	0.0087	0.0100	0.0112	0.0115	0.0120
Air leaving dehumidifier:						
dry-bulb temp., F	88	88	88	88	88	88
wet-bulb temp., F	54.7	54.7	54.7	54.7	55.2	55.2
Sp. humidity, lb/lb	0.0016	0.0016	0.0016	0.0016	0.0018	0.0018
Air leaving subcooler:						
dry-bulb temp., F	----	----	----	----	80	65
wet-bulb temp., F	----	----	----	----	51.8	45.1
Sp. humidity, lb/lb	----	----	----	----	0.0018	0.0018
Gross refrig., Btu/min	720	496	534	720	863	1179
Net room refrig., Btu/min	435	496	534	435	578	895
Heat added in cycle, Btu/min	1178	876	1033	1250	1347	1710
Cooling water, gal/min	3.53	3.56	3.07	3.53	5.10	6.68
Gross cycle efficiency, %	61.0	56.6	51.7	57.6	64.0	68.9
Net cycle efficiency, %	36.9	56.6	51.7	34.8	43.0	52.3
Cooling water heat load:						
Outside tower, Btu/min	873	604	662	1036	849	1196
Internal cycle, Btu/min	----	----	----	----	168	484
Temperature approach:						
Sorbent-sorbent, F	5	5	5	15	5	5
Sorbent-water, F	5	5	5	5	5	5
Air-sorbent, F	3	3	3	3	3	3
Dewpoint approach to equil., F	3	3	3	3	3	3

I. Original cycle, 25% outside air and 75% room air to unit, regeneration by air stripping.
II and III. Original cycle, 100% room air to unit, regeneration by air stripping.
IV. Original cycle, 25% outside air and 75% room air to unit, regeneration by direct distillation.
V and VI. Modified cycle, 25% outside air and 75% room air to unit, internal subcooler cycle, regeneration by air stripping.

* Outside air was assumed the same for all calculations: dry-bulb temperature, 95 F; wet-bulb temperature, 75 F; specific humidity, 0.0141 lb/lb.

the stripping air stream in the reconcentrator. Some of the heat in the stripping air could be recovered if it were utilized to heat the dilute sorbent entering the reconcentrator, or to preheat the stripping

air. This loss would be completely eliminated if the solution could be reconcentrated by distillation rather than by air stripping.

RESULTS OF OPEN CYCLE CALCULATION

The flow rates and heat and cooling water requirements were calculated for 32 sets of operating conditions or cycle modifications utilizing TEG solutions as the sorbent liquid. The most favorable results are summarized in Table I for the original open cycle for three sets of conditions with air stripping regeneration and one for direct distillation regeneration, and for the recommended modification of the open cycle for two conditions. The modified open cycle is shown schematically in Fig. 3.

To perform the cycle calculations, temperature approach of 5 F deg was assumed for streams in heat exchangers, and an approach of 3 F deg for air and liquid in contact. It was also assumed that the dew-point of the air leaving the dehumidifier was 3 F deg higher than the dew-point of air in equilibrium with the entering TEG solution.

Conditions I, II and III illustrate the effect of varying the condition of the recycled and room air on cycle efficiency and capacity for the original open cycle with air stripping regeneration. The air recirculated to the unit in Condition I is composed of 75% room air and 25% outside make-up air. Conditions II and III are for slightly higher room air temperature and for 100% recycle of room air.

Conditions I and IV represent a comparison of the effect on cycle efficiency, of varying the methods of regeneration of the spent sorbent, with all other conditions held constant. The assumed temperature approach in the sorbent-sorbent heat exchanger, for the direct distillation regeneration, IV, was increased to 15 F deg, due to the high heat load imposed on this exchanger in the direct distillation cycle. Also, the heat requirement in Condition IV includes an allowance of 5% to make up for reflux in the distillation column. The two regeneration techniques result in comparable cycle efficiencies, although the equipment for direct distillation regeneration should require less space than for air stripping regeneration. Introduction of an inert stripping gas into the vapor phase would reduce the volumetric efficiency of the regeneration column.

The efforts of this project were directed toward improving the efficiency of cycles utilizing air-stripping regeneration, since, for efficient cycle operation, a TEG concentration of 99% is required in the regenerated stream. In order to achieve this concentration by direct distillation at atmospheric pressure, the solution would have to be heated to about 420 F, at which point thermal decomposition proceeds at a fairly rapid rate. Field dehydration units have operated at reboiler temperatures of 380 F satisfactorily, but the TEG concentration is only 98.0 to 98.3%.

Conditions V and VI illustrate the effect of internal dry-air sub-

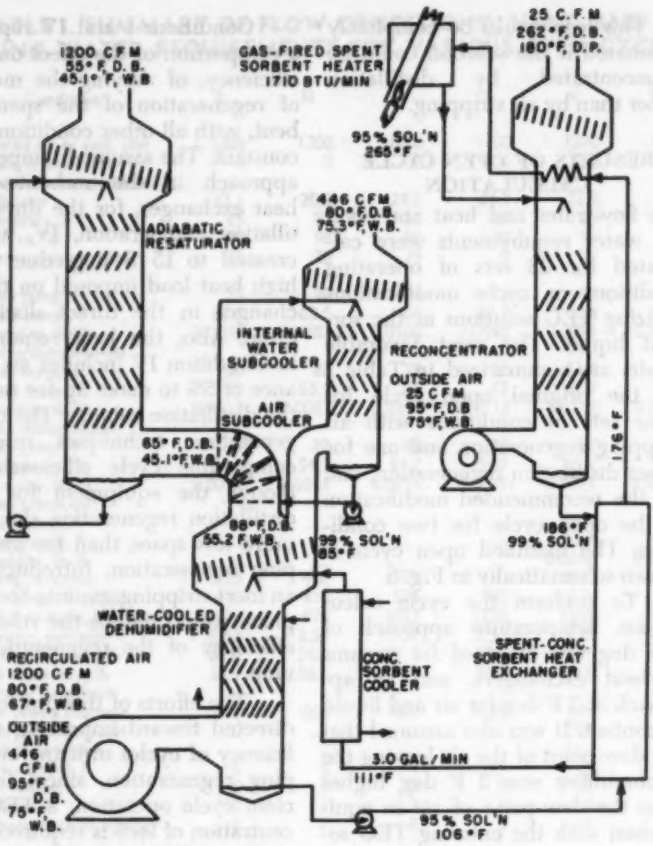

Fig. 3. Schematic diagram of modified open cycle with reconcentration by use of outside stripping air

cooling on the net room refrigeration efficiency for the best modified open cycle. The modified open cycle, illustrated schematically in Fig. 3, uses the original cycle operated at optimum conditions (Condition I, Table I) with an internal water-cooled air sub-cooler between the dehumidifier and partial resaturator. This cycle modification results in the largest amount of room refrigeration per cu ft of air circulated and also has the highest calculated thermal efficiency. It is be-

lieved that the cost of the additional equipment would be more than compensated by increased efficiency of operation.

In this modified cycle, Fig. 3, the recirculated air (1200 cfm) plus outside air (446 cfm) enters near the bottom and rises through the water-cooled dehumidifier. The dry air from the dehumidifier is split into two streams: the main (room air) stream (1200 cfm) and the internal water subcooler air stream (446 cfm). The dry air to the subcooler rises countercurrent to the warm water from the air subcooler, and is vented. The dry room air is cooled in the air subcooler (from 88 to 65 F) by heat exchange with the cold water, and then partially resaturated in an adiabatic cooling tower, lowering its temperature to about 55 F. The cold air is then recirculated to the room.

Cold, concentrated (99%) sorbent is sprayed into the top of the water cooled dehumidifier. The dilute (95%) warmed sorbent (106 F) is heated by countercurrent heat exchange with the concentrated sorbent stream (176 F). The spent sorbent is heated further in a direct gas-fired tube furnace (265 F) and sprayed into a packed column where the absorbed water vapor is stripped from the sorbent by a rising stream (about 25 cfm). The latent heat of vaporization and integral heat of solution for evaporating the moisture from the sorbent are supplied by the hot sorbent; the concentrated sorbent leaves the bottom of the column at 186 F. The concentrated sorbent is cooled by heat exchange with the dilute sorbent (111 F), further cooled with cooling water (85 F) and the cold concentrated sorbent is then ready to be sprayed into the dehumidifier.

The outside air used for stripping (95 F) enters the bottom of the reconcentrator, and hot moist air (262 F dry-bulb, 180 F dew-point), is discharged to the economizer. In the economizer the dry-bulb temperature of the stripping air is reduced to its dew-point for recovery of vaporized sorbent from the air. The sorbent-rich liquid condensed from the exhaust stripping air is returned to the top of the reconcentrator.

The reconcentrator required for this cycle will have a cross-sectional area about 2½ times as large as the direct distillation column, and will have to be longer, as the stripping air not only increases the volume of the vapor phase but also reduces the volumetric efficiency of the column. This cycle also requires the use of a cooled contactor section (economizer) to reduce the loss of vaporized sorbent in the stripping air. However, the temperature level at which this economizer operates permits the spent sorbent to be used as the coolant, thereby reducing the spent-liquid heater load.

DESIGN AND OPERATION OF PILOT UNIT

A search of the literature indicated a paucity of data on which the design of a prototype open-cycle unit could be based. Therefore, a pilot-unit was designed, with a nominal

capacity of 300 cfm, to obtain data on the operation of the water-cooled dehumidifier, heat exchangers, and regeneration equipment, under heat and mass transfer conditions simulating those to be encountered in domestic or small commercial units. An exploded view of the pilot unit is shown in Fig. 4, indicating the location of thermocouples (T.C.) for temperature measurement, and the various pumps, valves and rotameters for control of the stream flow rates.

The water-cooled contactor in the dehumidifier was composed of stacked truck radiator core sections, 10- x 9-in. x 3⅝-in. deep. Each flat copper finned section was provided with 4 water tube sets, manifolded together so that the cooling water flow was in the same direction in all the tubes in any one section. The fin spacing was approximately 3/32-in., providing an estimated sorbent-air contact area of 135 sq ft. A steel-wool filter was provided above the contactor to eliminate carryover of sorbent by entrainment in the dried air. The bottom well of the dehumidifier provided for drainage of the sorbent holdup in the contactor when the unit was shut down.

A fairly uniform distribution of the cool concentrated sorbent to the top of the core sections was provided by 5 parallel ¼-in. copper tubes each provided with 20 No. 68 holes. Various solid-cone type spray nozzles which were tried would not operate properly with TEG at the pressure heads available in the pilot unit.

A divided cocurrent-countercurrent type resaturator equipped with water spray nozzles and redistribution screens was provided. However, most of the data for the pilot unit were obtained without operating the resaturator, since sufficient literature data are available for the engineering design of this component.

The spent solution heater was formed from three 15-ft lengths of ¼-in. I.D. copper tubing manifolded together, and formed to fit in a space 15- x 3-in. x 18-in. high. A modulating control valve was provided on the gas supply to the heater, operated by a temperature sensing element in the hot solution line leaving the heater, and provided control of the exit solution temperature within ±2 F deg of the set point for temperatures from 250 to 300 F.

The 4.5-in. diam stripping-air regeneration column was composed of three sections: (a) a 9-in. high accumulator for concentrated sorbent at the column bottom; (b) a 33-in. stripping section packed with ½-in. Berl saddles where the sorbent regeneration was effected; and, (c) a water-cooled partial condenser to recover vaporized sorbent from the stripping air. The Berl saddles were supported on a metal gird separating the accumulator from the column; the stripping-air inlet was located just below this gird. The hot spent sorbent entered the column at the top of the stripping section with 4 wire-mesh screens used to improve liquid distribution. The section above the feed inlet was packed to a depth of 14 in. with copper lathe-turnings, and topped

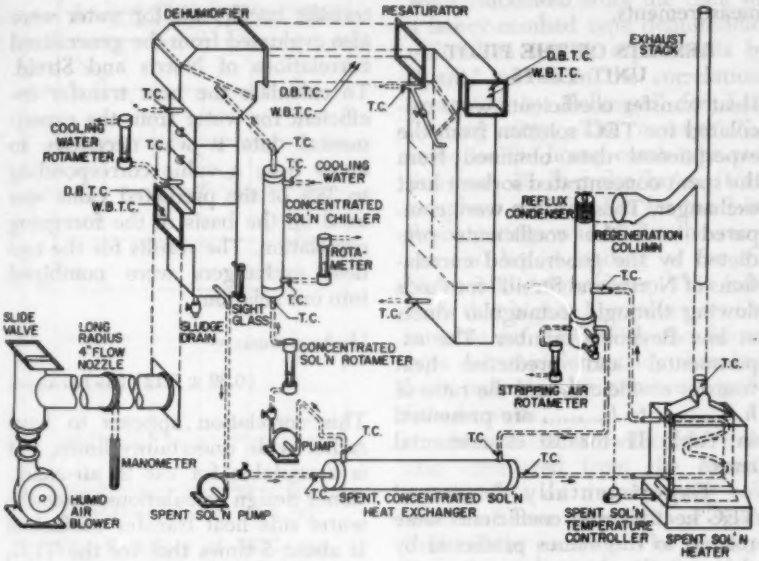

Fig. 4. Exploded view of pilot unit of open-cycle liquid sorbent air-conditioning system

with a water-cooled heat exchanger, to provide a rectification section and partial condenser for recovery of sorbent vapor from the stripping air.

Air with wet- and dry-bulb temperatures controlled within ±1 F deg was supplied to the unit from a conditioned test cell. From two to four hours were required to achieve steady-state conditions, and the pilot-unit was operated for at least one half-hour at steady state conditions before recording of data. From one to three hours were required to obtain the experimental measurements.

Temperatures were measured to ±0.1 F deg at 19 points in the system by use of copper-constantan thermocouples, a K-2 potentiometer, and a precision galvanometer. The air stream wet-bulb temperatures were measured to ±0.1 F deg with calibrated thermometers. The air rate to the pilot-unit was measured by use of a 4-in. long-radius flow nozzle, calibrated by means of a precision anemometer. Glycol and cooling water flow rates were measured by use of calibrated rotameters. Samples of the concentrated and spent sorbent were withdrawn near the end of each run, and the TEG concentrations determined from refractive index

measurements.

RESULTS OF THE PILOT UNIT TESTS

Heat transfer coefficients were calculated for TEG solution from the experimental data obtained from the spent-concentrated sorbent heat exchanger. These values were compared with the coefficients predicted by the generalized correlations of Norris and Streid[8] for fluids flowing through rectangular ducts at low Reynolds number. The experimental and predicted heat transfer coefficients and the ratio of $h_{experimental}$ to $h_{predicted}$ are presented in Table II for 10 experimental runs.

Experimentally determined TEG heat transfer coefficients were related to the values predicted by the generalized correlation:

$$(h_{TEG})_{experimental} = (0.88 \pm 0.05)\ (h_{TEG})_{predicted}$$

These values were obtained with normal fouling resulting from use of TEG without a corrosion inhibitor.

Heat transfer coefficients were calculated for water from the experimental data obtained from the concentrated solution cooler and chiller heat exchangers. The heat transfer coefficients for water were also evaluated from the generalized correlations of Norris and Streid. To calculate the heat transfer coefficient for water from the experimental data it was necessary to know h_{TEG}; a value corresponding to 38% of the predicted value was used on the basis of the foregoing correlation. The results for the two heat exchangers were combined into one relation:

$$(h_w)_{experimental} = (0.39 \pm 0.12)\ (h_w)_{correlation}$$

This correlation appears to have rather wide uncertainty limits, but is acceptable for use in air-conditioner design calculations, since the water side heat transfer coefficient is about 5 times that for the TEG, and therefore the overall heat transfer coefficient is almost entirely determined by the value of h_{TEG}.

Mass transfer coefficients were calculated from the experimental data for the finned dehumidifier section and for the packed regeneration stripping column. The value of the mass transfer coefficient ($K_x a$) for the dehumidifier was found to be slightly dependent on concentration of entering TEG solution, as shown in Fig. 5, but to be

TABLE II. COMPARISON OF EXPERIMENTAL AND PREDICTED TEG HEAT TRANSFER COEFFICIENTS

h_{expt}	14.1	13.2	13.5	13.9	12.4	14.2	12.1	11.2	11.0	10.7
h_{pred}	16.5	15.3	14.2	14.7	14.1	15.3	13.7	13.6	14.0	11.9
$\frac{h_{expt}}{h_{pred}}$	0.855	0.864	0.950	0.945	0.880	0.927	0.884	0.824	0.787	0.900

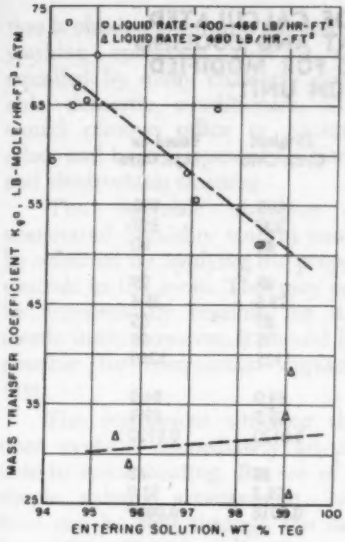

Fig. 5. Effect of TEG concentration on K_xa for two ranges of liquid flow rates

principally dependent on liquid flow rate. The data for liquid rates from 400 to 466 lb/hr/sq ft is represented by the upper curve in Fig. 5, and the data for flow rate above 480 lb/hr/sq ft by the lower curve. The region of flow between 460 and 480 apparently represents the range between liquid loading and flooding rates, as indicated by the large change in average K_xa values. The average K_xa value for the region of high liquid loading is 61.8 ± 6.2 lb-moles/hr/cu ft/atmosphere compared to a K_xa value of 31.6 ± 3.4 for the region of liquid flooding in the dehumidifier.

As a check on the operation of the experimental unit, K_xa values were calculated from the data for a honey-combed type dehumidifier utilized in similar experiments by Ryant,[9] and from the correlations presented by Fellinger[10] for 1-in. Raschig rings. The average K_xa value for the honey-comb type section was 32 lb-moles/hr/cu ft/atmosphere and the K_xa for the 1-in. Raschig rings was 16 for the same gas and liquid loading as the experimental dehumidifier. This indicates that higher K_xa values are obtainable for TEG with the finned type dehumidifier section than had been indicated by previously published results.[8]

Mass transfer coefficients were also calculated from the experimental data on the stripping column for 8 runs with 33 in. of ½-in. Berl saddle packing. The average K_xa value was 40.0 ± 9.5 lb-moles/hr/cu ft/atmosphere. There was no observable correlation between inlet TEG concentration and K_xa values for the stripping column, and the gas and liquid flow rates encountered were considered to be below the flooding values given in the literature[10] for ½-in. Berl saddles. The corresponding K_xa value estimated from the literature for ½-in. Berl saddles was 13.

The experimental data also verified that the loss of sorbent vaporized into the stripping air could be held to an acceptable value by use of a short packed rectification section and a refluxing partial condenser for the stripping air. This system reduced sorbent loss to less than one-hundreth the equilibrium vapor concentration in air leaving the column.

TABLE III. SUMMARY OF CALCULATED FLOW CONDITIONS, HEAT AND COOLING WATER REQUIREMENTS FOR MODIFIED OPEN CYCLE 3-TON UNIT*

Condition	Original Cycle Calc.	Based on Expt. Data
Recirculated air to unit, cfm	805	910
Outside air to unit, cfm	300	350
Cooling water temperature, F	80	80
Solution to dehumidifier:		
Concentration, % TEG	99	99
Rate, lb per min	19.6	28.4
Temperature, F	85	85
Dilution to, % TEG	95	96
Air conditioned, cfm	1105	1260
Air entering dehumidifier		
dry-bulb temperature, F	84.0	84.0
wet-bulb temperature, F	69.3	69.3
specific humidity, lb/lb	0.0120	0.0120
Air leaving dehumidifier		
dry-bulb temperature, F	88	88
wet-bulb temperature, F	55.2	57.0
specific humidity, lb/lb	0.0018	0.0029
Air leaving subcooler		
dry-bulb temperature, F	65	65
wet-bulb temperature, F	45.1	47.4
specific humidity, lb/lb	0.0018	0.0029
Gross refrigeration, Btu/min	800	837
Net room refrigeration, Btu/min	600	600
Heat added in cycle, Btu/min	1145	1360
Outside cooling water, gal/min	4.48	5.17
Gross cycle efficiency, %	68.9	61.5
Net cycle efficiency, %	52.3	44.1
Heat removed by cooling water		
outside tower, Btu/min	801	647
subcooling section, Btu/min	323	367
Temperature approach		
sorbent-sorbent exchanger, F	5.0	15.5
sorbent cooler, F	5.0	7.5
Air-liquid in contact, F	3.0	3.0
TEG-air equilibrium D.P., F	3.0	13.0

* The room air, outside air, and recirculation air to unit are assumed to be the same conditions for both calculations:

	Room Air	*Outside Air*	*Recirculated Air*
dry-bulb temperature, F	75	95	80
wet-bulb temperature, F	62.5	75	67
specific humidity, lb/lb	0.0093	0.0141	0.0112

OPEN CYCLE FLEXIBILITY

Consideration of the open cycle indicates that it has a number of attributes that should add to its attractiveness for domestic and commercial applications. Air purifica-

tion is obtained, through the double washing operation, that is not equalled by many currently available domestic conditioners. This would remove office or cooking odors and bacteria passed by filters and electrostatic cleaning.

The desirable objective of year-round humidity control could be achieved by applying the proper controls to the cycle. This may not be economically feasible for domestic units; however, it should be possible for commercial application.

The equipment utilizing the open cycle is immediately adaptable to space heating. By use of a simple valving arrangement, hot fluid can be sent through the dehumidifier contactor directly and the heat exchangers, reconcentrator and other units cut out of the circuit. The 80,000 Btu minimum input necessary for 3 tons of cooling matches well with the heat loss of homes and commercial spaces in many parts of the country. Thus, a single direct-fired unit can provide year-round conditioning.

Slight refinement of the switch-over procedure could provide year-round humidity control and retention of some TEG in the room air to take advantage of its germicidal properties.

GENERAL DESIGN OF A 3-TON UNIT

The results obtained in the experimental program were applied to the sizing of the principal components for a 3-ton unit based on the modified open cycle. A summary of the calculated flow conditions and cycle efficiency is presented in Table III based on the components described below, with the results of the previous cycle calculations for the same conditions included for comparison.

For design of the water cooled dehumidifier a mass transfer coefficient, $K_x a$, of 60 lb-moles/hr/cu ft/atmosphere was used, at a liquid loading of 340 lb TEG solution/hr/sq ft cross sectional area. A total of 0.885 lb of water would be removed from the 1260 cu ft of air processed each minute, reducing the air dew-point from 62.2 F entering to 26.2 F at the exit. The 99% TEG solution flow rate required would therefore be 28.4 lb/min, if the solution leaves the dehumidifier as 96% TEG. A dehumidifier volume of 13 cu ft would be required to effect this dew-point depression, with a required cross sectional area of 5 sq ft. This dehumidifier volume is based on the use of vertical parallel fins spaced 10 per in., which results in a contact area of 216 sq ft per cu ft. If this contact area per cu ft can be increased, the $K_x a$ value will increase proportionally, requiring less dehumidifier volume for the same dew-point depression.

The air subcooler would reduce the temperature of 910 cu ft of dehumidified air per min from 88 to 65 F. This requires a heat transfer of 22,000 Btu/hr from the air to the cooling water. If an overall heat transfer coefficient of 7 Btu/hr/sq ft/F, and a 5 F deg temperature approach are assumed, an air side heat-transfer area of 630 sq ft would be required. If the subcooler

is constructed of flat fins spaced 8 to the in., the required subcooler volume would be 3.3 cu ft.

The air from the subcooler is cooled from 65 to 55 F by adiabatic partial-resaturation. The heat load on this unit is 9600 Btu/hr, with an average temperature difference of about 13 F deg. The volumetric vaporization coefficient for spray-cooling of air generally applied to void volumes is about 90 Btu/hr/cu ft/F which would result in this partial resaturator requiring a volume of 8.2 cu ft. Recent manufacturers' literature has reported various packing materials, and equipment modifications which have increased the vaporization coefficient several fold, and which would materially reduce the required volume for this unit.

It is proposed that the heat exchangers be slightly modified from those used in the pilot unit. If the heat transfer surface is corrugated, instead of flat, the heat transfer area will be increased about two-fold for the same volume and spacing, and the mechanical strength of the exchanger will also be greatly improved. For the heat exchangers to operate efficiently it is necessary that the liquid mass flow rate be reasonably large. Therefore, the unit described here is based on use of 6-in. square exchangers 30-in. long, which provides a sorbent flow rate of about 14,000 lb/hr/sq ft cross sectional area.

The sorbent-sorbent exchanger would be composed of two such units in series. This would provide sufficient heat exchange area for warming of the lean 96% TEG from 100 F (as it leaves the dehumidifier) to 179 F (when it enters the stripping air partial condenser) by cooling the concentrated 99% TEG from 197 F (as it leaves the reconcentrator) to 113 F. The sorbent-sorbent exchanger heat load would be about 81,000 Btu/hr.

The concentrated sorbent chiller would be composed of one such heat exchanger, and would cool the 99% TEG from 113 to 85 F. The cooling water would be warmed from 80 to 103 F. The heat load on this exchanger would be about 27,000 Btu/hr.

Spent solution from the sorbent-sorbent exchanger would flow through cooling coils in the stripping air partial condenser where it would be warmed 2 to 3 F deg. This would provide the cooling required for recovery of TEG vapor from the stripping air leaving the reconcentrator.

The reconcentrator design is based on the use of ½-in. Berl saddles for packing in the stripping section, and copper lathe-turnings in the top rectification section. A mass transfer coefficient of 40 lb-moles/hr/sq ft/atmosphere was utilized for the stripping section. This resulted in an 8-in. diam column having 33 in. of stripping and 8 in. of rectification section. The spent 96% TEG would enter at the top of the stripping section at 255 F and would require about 18 to 20 cu ft of outside air per min to effect the regeneration, with the concentrated 99% TEG solution leaving the accumulator at the bottom of the column at 197 F.

The specific design of the spent

solution heater is quite flexible. This heater raises the temperature of the spent solution from 181 or 182 to 225 F, and for this particular unit would have a heat load of 82,000 Btu/hr, which represents a thermal efficiency for the cycle of 44.1%.

The 3-ton air conditioner described here is not to be taken as representing the optimum design for the modified open cycle, but rather to indicate the approximate sizes for the various components for this one particular set of operating conditions. This description also demonstrates the need for development of a more efficient dehumidifier contactor design to reduce the size of the equipment. No efforts are made to show year-round cycle applications and control refinements. These would vary markedly with the equipment and fabrication methods of the individual manufacturer.

CONCLUSIONS

The cycle calculations and experimental pilot unit data show that:

1. An efficient modified open air-conditioning cycle can be based on the use of triethylene glycol as the sorbent liquid.

2. Sufficient experimental data are now available for the engineering design of a unit based on this modified open cycle.

3. A more efficient dehumidifier contactor design should be developed to make such a unit sufficiently compact for the domestic market.

The contactor utilized in the pilot unit was constructed of flat parallel fins, which represents only a first effort. Highly efficient packing materials and contacting techniques are available industrially which could be applied to this operation.

ACKNOWLEDGMENT

This paper summarizes the results of a study of "Improved Liquid Sorbent Dehydration—Partial Resaturation Domestic Air-Conditioning System,"[7][7] sponsored by Coleman Company from March, 1955 until April, 1957, and continued through June, 1958 as "Investigation of a Liquid Sorbent Open-Cycle Air Conditioner" sponsored by the American Gas Association. The authors wish to acknowledge the contributions of Drs. H. R. Linden, R. E. Peck, and M. A. Elliott in the formulation and analysis of the experimental program. D. A. Worcester assisted in operation of the pilot unit.

REFERENCES

1. F. R. Bichowsky: Chemical dehumidification agents (*Heating, Piping, and Air Conditioning*, Vol. 12, 1940, p. 627).
2. R. E. Peck and C. J. Ryant, Jr.: Conditioning of hot humid air (*Refrigerating Engineering*, Vol. 56, 1948, p. 417).
3. C. J. Ryant, Jr.: *Heat Transfer in a Double Exchanger* (Unpublished Ph.D. thesis in Chemical Engineering, Illinois Institute of Technology, June 1947).
4. R. T. Ellington, G. Kunst, R. E. Peck, and J. F. Reed: *The Absorption Cooling Process* (Institute of Gas Technology, Research Bulletin No. 14).
5. G. F. Zellhoefer, M. J. Copley, and C. S. Marvel: Hydrogen bonds involving the C-H link (*Journal Amer. Chem. Soc.*, Vol. 60, 1938, p. 1337).
6. N. V. Sidgwick: *The Chemical Elements and Their Compounds*, Vol. 1, p. 98 (Oxford University Press, London, 1950).
7. W. R. Hainsworth: Refrigerants and absorbents, parts I and II, (*Refrigerating Engineering*, Vol. 48, August, 1944, p. 97; ibid September, 1944, p. 201).
8. L. H. Peahl: Skid-mounted gas-dehydration plant (*Oil and Gas Journal*, Vol. 49, July 13, 1950, p. 92).
9. *Glycols* (Carbide and Carbon Chemicals Co., New York, 1955).

10. L. D. Polderman: Private communication of July 19 (Carbide and Carbon Chemicals Co., New York, 1955).
11. G. O. Curme, Jr., and F. Johnston: *Glycols* (Reinhold, New York, 1952).
12. L. D. Polderman: Triethylene glycol for air sanitation (*Soap and Sanitary Chemicals*, Vol. 23, July 1947, p. 133; Vol. 25, November 1949, p. 120; Vol. 25, December 1949, p. 129).
13. A. F. Gallaugher and H. Hibbert: Vapor pressures of polyethylene glycols and their derivatives. (*Journal Amer. Chem. Soc.*, Vol. 59, 1937, p. 2521).
14. H. E. Bent and C. A. Krinbill, Jr.: Vapor pressure determination by comparison with a standard liquid (*Journal Amer. Chem. Soc.*, Vol. 72, 1950, p. 2757).
15. R. H. Norris and D. D. Streid: Laminar-flow heat-transfer coefficients for ducts (*ASME Transactions*, Vol. 62, August 1940, p. 523).
16. L. L. Fellinger: (Unpublished Sc.D. Dissertation in Chemical Engineering, Massachusetts Institute of Technology, Cambridge, Mass., 1941).
17. B. E. Eakin, R. T. Ellington, R. E. Peck, and J. F. Reed: *Improved Liquid Sorbent Dehydration—Partial Resaturation Domestic Air Conditioning System* (Unpublished Progress Report No. 1, Project S-104, Institute of Gas Technology, 1956).

DISCUSSION

G. B. PRIESTER, Baltimore, Md. (Written): What are the economics of the manufacturing cost? Can this unit be made and sold for less money than the 3-ton closed-absorption units or gas engine units now on the market? Will it be competitive in first cost?

What are the plans for future work and reporting on this equipment?

CLOSURE BY AUTHOR EAKIN: It is difficult to make a good cost estimate to determine whether it would be possible to place this unit on a competitive basis. In operation it certainly should be competitive, but I don't know about a first cost basis. The advantage of the unit is that it could be made for both summer and winter temperature control and give complete humidity control all year round.

As to future work, the American Gas Association has sponsored a considerable volume of research on gas-fired air conditioners. This is a continuing effort, but, as far as I know, there is no further work planned on this particular cycle, even though the economics do appear reasonable.

FRANK H. BRIDGERS, Albuquerque, N. M.: What would be the lowest practical temperature of the sorbent heater for the solution? At 165 F you are getting into the practical range of sorbent heat for solar refrigeration.

AUTHOR EAKIN: On the experimental unit, we ran at about 265 to 275 F. At this temperature only a very small quantity of stripping air is required; 25 cfm stripping air compared to 1600 cfm in the recirculation system for a full scale unit. It is necessary to effect a balance in this type unit between the vapor losses, cycle efficiency, and heat exchanger requirements. The lower the maximum temperature of the air passed through the sorbent on reconcentration, the more moisture removed from the sorbent. However, lower maximum temperatures require a larger volume of air to remove the moisture, and the more air put through, the more sorbent vapor loss. If you use a fairly large amount of air for regeneration, it is possible to eliminate the spent solution-concentrated solution heat exchanger entirely, with a resulting lower cycle efficiency. In this case, it is possible to regenerate with a sorbent temperature of 160 F.

We mentioned carryover of the sorbent vapor in the stripping air stream. In order to reduce this loss, we placed a small partial condenser on the stripping air outlet which reduced the air temperature to its dew point. Even though only a very small fraction of the total moisture in the air was condensed and refluxed to the stripping unit, the tri-ethylene glycol concentration was reduced to 1/1000 equilibrium concentration in the air.

DONALD F. DEVINE, Portland, Ore.: What is the approximate total size and weight of your experimental pilot unit?

AUTHOR EAKIN: Since the pilot unit was designed strictly to take data, it was built oversize and the parts strung out to make it easy to take measurements. The pilot unit was about 6 ft high, 8 ft wide and 2 ft thick.

1719

No. 1719

An Air-Cooled Absorption Cycle

R. H. MERRICK
Member ASHRAE

R. A. ENGLISH
Member ASHRAE

This paper covers a specific type of air-cooled absorption refrigeration cycle with application to air conditioning equipment now in production. This unit is manufactured in 3 and 4½-ton sizes. It comprises an outdoor, air-cooled water chilling section, as shown in Fig. 1, which circulates chilled water to furnace, duct or fan coils serving the conditioned space.

Design objectives called for an air-cooled, hermetic absorption cycle. A new cycle development was required as a review of familiar cycles disclosed the following limitations:

1—Cycles evolving from the lithium bromide water combination require low absorber temperatures which cannot be maintained practically by air cooling.

2—Cycles employing halogenated hydrocarbon refrigerants fail on one or more of the following points:
   a. Air cooling is not practical
   b. Poor chemical stability and/or compatability with ordinary materials of construction
   c. Exorbitant solution heat exchange and pumping requirements

3—The Platen-Munters, ammonia-water-hydrogen cycle has poor heat transfer rates and geometric limitations

4. The conventional ammonia-water cycle has thus far not been hermetic owing to pump shaft seal and has not been fully exploited thermodynamically

This review disclosed a potential in an air-cooled ammonia-water combination if a hermetic circulation means were developed and performance-improving heat exchange relationships introduced. In the description to follow, the solution return trap and the solution cooled rectifier piped in parallel

R. H. Merrick is Chief Engineer, R. A. English is Senior Development Engineer, Gas Air Conditioning, Bryant Manufacturing Company.
This paper was presented at the ASHRAE 67th Annual Meeting, Vancouver, B. C., June 13-15, 1960.

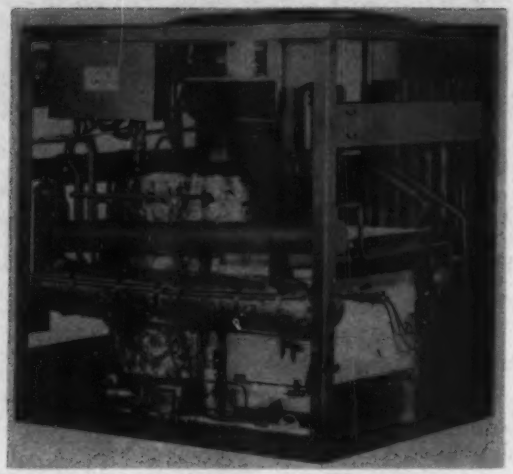

Fig. 1 Outdoor, air-cooled water chiller section

with the heat exchanger answer these conditions.

Cycle Description—The cycle is diagramed in Fig. 2. To be consistent with previous absorption refrigeration literature terminology, in this paper strong solution is that rich in solute, which in this case is ammonia. Weak solution is, therefore, poor in ammonia.

Strong solution entering the generator is heated and the resulting vapor and weak solution are separated in the separator. The vapor, a mixture of ammonia and water, leaves from the top of the separator and travels to the analyzer across the top of the generator reservoir. It passes through the analyzer in intimate contact with returning strong solution, approaching equilibrium with the solution and leaving richer in ammonia.

Then the vapor passes through the rectifier where it is cooled and partially condensed by returning strong solution. The condensate has a high percentage of water so the leaving vapor is now nearly pure ammonia. The ammonia is then condensed in the condenser and passes through a fixed restrictor to the chiller. Here the refrigerant vapor then goes into the bottom of the absorber.

The hot weak solution that leaves the bottom of the generator separator passes through the heat exchanger where it gives up its heat to returning strong solution not used to cool the rectifier. It is then metered through a fixed restrictor into the subcooled absorber and to the bottom of the absorber.

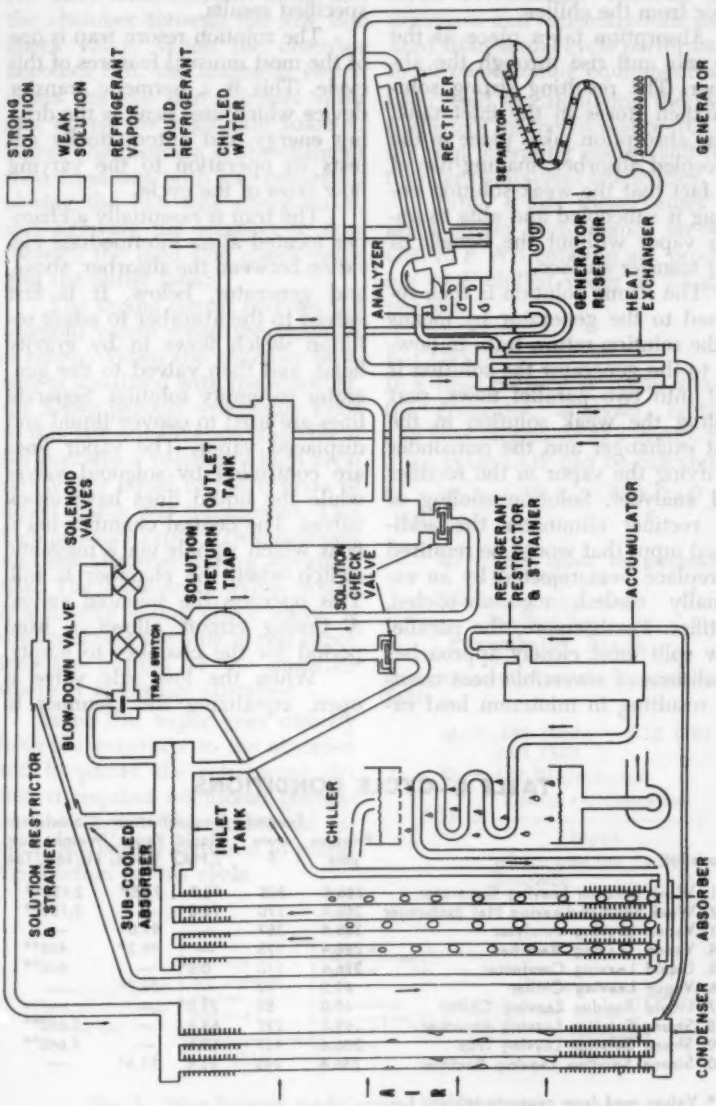

Fig. 2 Cycle diagram

Here it comes in contact with the vapor from the chiller.

Absorption takes place as the two mix and rise through the absorber. The resulting strong solution then stores in the inlet tank. Some absorption takes place in the subcooled absorber, making use of the fact that the weak solution entering is subcooled and able to absorb vapor without the benefit of heat transfer surface.

The strong solution is then returned to the generator by means of the solution return trap. In flowing to the generator the solution is split into two parallel flows, part cooling the weak solution in the heat exchanger and the remainder purifying the vapor in the rectifier and analyzer. Solution cooling of the rectifier eliminates the additional input that would be required to replace heat rejected by an externally cooled, e.g. air-cooled, rectifier. Furthermore, the parallel flow split most closely approaches conditions of reversible heat transfer resulting in minimum heat exchanger and rectifier sizing for specified results.

The solution return trap is one of the most unusual features of this cycle. This is a hermetic transfer device which uses heat as the driving energy and automatically adjusts its operation to the varying flow rates of the cycle.

The trap is essentially a chamber located at an intermediate elevation between the absorber, above, and generator, below. It is first valved to the absorber to admit solution which flows in by gravity head, and then valved to the generator to empty solution. Separate lines are used to convey liquid and displaced vapor. The vapor lines are controlled by solenoid valves while the liquid lines have check valves. The central chamber has a float which signals via a magnetic switch when the chamber is full. This operates the solenoid valves. A timing circuit allows a fixed period for the chamber to empty.

When the low side valve is open, equalizing the chamber to

TABLE I—CYCLE CONDITIONS

Location	Pressure psia	Temperature F	Concentration Liquid %H_2O	Concentration Vapor %NH_3	Calculated Weight Flow Lb/Min/Ton
1. Weak Solution Leaving Generator	286.4	305	78.0	76.5*	2.150**
2. Weak Solution Leaving Hat Exchanger	286.4	170	78.0	—	2.150**
3. Vapor Leaving Analyzer	286.4	257	—	91.0*	—
4. Vapor Leaving Rectifier	286.4	175	—	99.2*	.488**
5. Liquid Leaving Condenser	286.4	110	0.8*	—	.448**
6. Vapor Leaving Chiller	69.0	52	—	100.0*	—
7. Liquid Residue Leaving Chiller	69.0	52	23.0*	—	—
8. Strong Solution Leaving Absorber	69.0	137	63.6	—	2.640**
9. Strong Solution Leaving Trap	286.4	137	63.6	—	2.640**
10. Strong Solution Leaving Rectifier	286.4	245	63.6	93.4*	—

* Values read from property tables.

** Values calculated in Appendix.

the inlet tank, solution flows into the chamber through the low side check valve. When the chamber becomes full, the magnetic switch closes the low side solenoid valve and opens the high side solenoid valve. The pressure in the chamber then equalizes with the generator, closing the low side check valve, and allowing the solution to flow through the high side check valve into the outlet tank.

The timing circuit reverses the solenoid valves when the chamber is empty. When the chamber pressure is equalized with the absorber, the filling process will begin. Prior to this last equalization, the chamber contains a volume of high pressure vapor equal to the volume of liquid which was transported. This high pressure vapor is then dumped into the absorber during equalization. The blow-down valve, which is a double acting check valve, is used to divert the bulk of this vapor into the bottom of the absorber where it is readily absorbed.

Since this vapor goes directly from the generator to the absorber and by-passes the refrigerant circuit, it requires additional generator heat input. This additional input is the energy required to pump the solution in this cycle.

Cycle Performance—Pressure temperatures and concentrations measured from actual cycle performance in air conditioning equipment have been used in calculating the cycle coefficient of performance (COP), the trap operating energy and heat transfer component efficiencies.

Table I lists these values for rated chiller performance on 95 F DB, 75 F WB entering air, producing 44 F chilled water at 2.5 gpm per ton.

1—COP:

If a heat balance is made around the generator, analyzer, rectifier and heat exchanger as a group, Fig. 3 the cycle COP can be calculated.

$$Q_g + W_9 h_9 + W_4 h_4 + W_3 h_3 = 0$$

Where:

Q_g = heat input to generator, Btu/min/ton
W = mass flow rate, lbs/min/ton
h = enthalpy, Btu/lb

Subscripts refer to the conditions in Table 1.

$$Q_g = .488\ (603) + 2.15\ (76) - 2.64\ (10)$$

$$Q_g = 432 \text{ Btu/min/ton}$$

$$COP = \frac{\text{Useful refrigeration}}{\text{Input}};$$

where one ton = 200 Btu/min

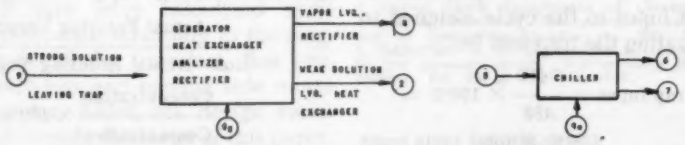

Fig. 3 Heat balance made around the generator, analyzer, rectifier and heat exchanger as a group

$$COP = \frac{200}{432} = .462$$

This calculated COP includes the trap operating energy as determined next. It does not include vagrant heat losses from the cycle or any efficiency involved in converting fuel to actual generator heat input.

2—Trap Operating Energy:
Ideally, the trap allows a volume of vapor equal to the volume of strong solution transferred to go directly to the absorber from the rectifier, by-passing the refrigerant circuit. Actually, the trap never completely fills with solution so that a volumetric efficiency must be applied, which in this case, has been measured at .96.

$$\text{Trap vapor flow} = \frac{1}{E} \times W_s \times \frac{d_s}{d_a}$$

Where:

E = trap volumetric efficiency
d_s = density of vapor, lb/cu ft
d_a = density of solution, lb/cu ft

$$\text{Trap vapor flow} = \frac{1}{.96} \times 2.64 \times \frac{.81}{54.5} = .0418 \text{ lb vapor/min/ton}$$

Comparing this to the total vapor flow leaving the rectifier, Point-4, Table I, the per cent of heat input to the cycle assigned to operating the trap will be:

$$\text{Trap input} = \frac{.0418}{.488} \times 100\% = 8.36\% \text{ of total cycle input}$$

In the equipment where this cycle is used, a trap efficiency of less than 96% is realized which, of course, increases the trap operating energy value shown here and correspondingly decreases the COP value calculated previously. The magnitude of this disparity is a design variable associated with an absorption-desorption process occurring during trap operation. While emptying, high pressure vapor is absorbed into solution residues in the float chamber and later released when the chamber is equalized to the absorber pressure.

3—Heat Transfer Component Efficiencies:
a. Absorber efficiency is defined by,

$$\frac{\text{Actual Entering Solution Concentration—Actual Leaving Solution}}{\text{Actual Entering Solution Concentration—Saturated Leaving Solution}} \times 100\% = \frac{\text{Concentration}}{\text{Concentration}} \times 100\% = \frac{.780 - .636}{.780 - .620} \times 100\% = 90\%$$

Concentrations in terms of water.
b. Analyzer efficiency is defined by,

$$\frac{\text{Actual Leaving Vapor Concentration—Actual Entering Vapor}}{\text{Saturated Leaving Vapor Concentration—Actual Entering Vapor}} \times 100\% = \frac{\text{Concentration}}{\text{Concentration}} \times 100\% = \frac{.910 - .765}{.934 - .765} \times 100\% = 85.8\%$$

Concentrations in terms of ammonia.

c. Heat exchanger efficiency is defined by,

$$\frac{\text{Entering Weak Solution Temperature} - \text{Leaving Weak Solution Temperature}}{\text{Entering Weak Solution Temperature} - \text{Entering Strong Solution Temperature}} \times 100\% =$$

$$\frac{305 - 170}{305 - 137} \times 100\% = 80.4\%$$

d. Rectifier efficiency is defined by,

$$\frac{\text{Entering Vapor Temperature} - \text{Leaving Strong Solution Temperature}}{\text{Entering Vapor Temperature} - \text{Entering Vapor Temperature}} \times 100\% = \frac{257 - 175}{257 - 137} \times 100\% = 68.3\%$$

CONCLUSIONS

The discussion has been directed specifically at the operation of the cycle and has avoided construction details of the cycle and the air conditioners in which it has been applied. It should be recognized that actual air conditioner performance will vary from calculated cycle performance according to the magnitude of the trap loss, flue loss, jacket loss and cooling side motor energies, which are design variables outside the scope of this paper.

It is natural to wonder about cycle performance with a pump replacing the solution return trap. This can be readily calculated once a pump performance is assumed along with relative costs of heat and electrical energy. However, this is a difficult high-head, low-flow pumping job involving a saturated liquid with approximately the viscosity of water. Pump performance assumptions could be extremely hypothetical.

ACKNOWLEDGMENT

The authors acknowledge the contributions of the many who contributed importantly to this development and particularly the work of John E. Ebertz, Leonard A. Hall and Frederick W. Moth, their associates on the original project team, and William L. McGrath, under whose direction this activity originated.

REFERENCES

1. Eiseman, B. J., Jr. Why refrigerant 22 should be favored for absorption refrigeration. ASHRAE JOURNAL, Vol. 1, p. 45, Dec. 1959
2. Kohloss, F. H., Jr. and Scott, G. L. Equilibrium properties of aqua ammonia in chart form. Refrigerating Engineering, Vol. 58, p. 970, Oct. 1950.
3. Mastrangelo, S. V. R. Solubility of some chlorofluorohydrocarbons in tetraethylene glycol dimethyl ether. ASHRAE JOURNAL, Vol. 1, pp. 64-68, Oct. 1959.
4. Scatchard, G. et al., Thermodynamic properties—saturated liquid for vapor of ammonia water mixtures. Refrigerating Engineering, Vol. 53, p. 38, May 1947.
5. Taylor, R. S. Heat operated absorption units. Refrigerating Engineering, Vol. 49, p. 188, March 1945.
6. United States Department of Commerce, Bureau of Standards. Thermodynamic properties of ammonia. Circular no. 142, 1923.
7. Zellhoefer, G. S. Commercial refrigeration by low pressure steam. Refrigerating Engineering, Vol. 33, p. 217, May 1937.

APPENDIX

Nomenclature:

Q = heat transferred, Btu/min/ton
q = heat transferred, Btu/lb

W = mass flow rate, lb/min/ton
w_r = mass flow rate, lb/lb refrigerant vapor
w_v = mass flow rate, lb/lb rectifier vapor
h = enthalpy, Btu/lb
X = water concentration by weight

Subscripts:

e = chiller
g = generator

Numbers refer to Table I

Calculations in support of Table I:

1—Refrigerant flow rate through chiller

A mass balance based on the flow of the water component of the solution can be used to solve for the flow of liquid residue (W_{r1}) leaving the chiller in pounds per pound of refrigerant entering the chiller.

$$W_7 X_3 + W_{r3} X_3 + W_{r1} X_1 = 0$$

let $W_{r3} = 1$ lb

assume $W_{r3} X_3$ is zero

$$W_{r1} = 1 \frac{(.008)}{(.230)}$$

$W_{r1} = .0348$ lb/lb refrigerant

Using a total mass balance, the weight of vapor leaving the chiller (W_{r2}) per pound of refrigerant entering can be found.

$$W_{r3} + W_{r2} + W_{r1} = 0$$

$W_{r2} = .9652$ lb/lb refrigerant

Now a heat balance can be used to find the heat added per pound of refrigerant (q_g).

$$q_g + W_{r3} h_3 + W_{r1} h_1 + W_{r2} h_2 = 0$$

$q_g = .0348 (-44) + .9652 (564) - 1(86)$

$q_g = 446.5$ Btu/lb refrigerant

Knowing the heat added per pound of refrigerant, the entering refrigerant flow rate in pounds per minute per ton can be determined.

$$W_3 = \frac{200}{446.5} = .448 \text{ lb refrigerant/min/ton}$$

Where: one ton = 200 Btu/min/ton

2—Solution circulating rates

If the generator, heat exchanger, analyzer and rectifier are taken as a group (Fig. 3) the solution circulating rates per pound of vapor leaving the rectifier (W_{v2} and w_{v2}) can be found by solving simultaneously a total mass balance and a mass balance based on the water component of the solution.

$$W_{r2} + W_{v2} + W_{v1} = 0$$

$$W_{r2} X_2 + W_{v2} X_2 + W_{v1} X_1 = 0$$

let $W_{v1} = 1$ lb

assume $W_{v1} X_1$ is zero

Then,

$$W_{r2} = \frac{X_2}{X_2 - X_3}$$

$$W_{v2} = \frac{.636}{.78 - .636} = 4.41 \text{ lb weak solution/lb vapor}$$

$w_{v2} = 5.41$ lb strong solution/lb vapor

Since the vapor leaving the rectifier supplies both the trap and refrigeration circuit, the trap flow rate per pound of vapor has to be found.

$$\text{Trap vapor flow} = \frac{1}{E} \times w_{v2} \times \frac{d_1}{d_2} \text{ (see text)}$$

Where:

E = trap volumetric efficiency = .96
d_1 = density vapor, lb/cu ft
d_2 = density strong solution, lb/cu ft

$$\text{Trap vapor flow} = \frac{1}{.96} \times 5.41 \times \frac{.81}{54.5}$$

$$= .0836 \text{lb/lb vapor}$$

The remainder of the vapor is useful refrigerant.

Refrigerant flow = .9164 lb/lb vapor

The total vapor flow rate in pounds per minute per ton is:

$$W_4 = \frac{W_3}{.9164} = \frac{.4475}{.9164} = .488 \text{ lb of vapor lvg. rectifier/min/ton}$$

The solution circulation rates in pounds per minute per ton are:

$$W_2 = w_{v2} W_4 = 4.41 \times .488 = 2.15 \text{ lb weak solution/min/ton}$$

$$W_9 = w_{v2} W_4 = 5.41 \times .488 = 2.64 \text{ lb strong solution/min/ton}$$

DISCUSSION

G. R. MUNGER, Toledo, Ohio: What are the prospects for marketable units with a smaller capacity than 3 tons?

Is there any difficulty in selling the current unit?

CLOSURE BY AUTHOR MERRICK: There is no limitation to making a smaller capacity unit, but it is not our immediate intention to do this.

Selling is not a problem we face at the moment. Right now, our problem is making as many as we can sell.

FRANK J. FORD, Chicago, Ill: Are these units strictly for residential use or do they have commercial applications? Will these units be suitable in a city such as Chicago where there are large ventilation requirements for commercial establishments? Can they be used in multiples?

Has any consideration been given to noise levels and exhaust combustion gases?

Is there a specific distance one has to stand from adjoining pieces of property to safeguard against possible nuisance?

AUTHOR MERRICK: Initially, the unit was developed with the residential market in mind. However, it is adaptable for commercial jobs as these units can be used in multiples for sizeable jobs. Their ability to cool and dehumidify is comparable to what is now accomplished with conventional compression refrigeration equipment. The largest application that I know of is in Florida where 11 units were used: eight units of 4½ tons and three units of 3 tons. There are individual zones for each unit. Any size of job could be handled.

I do not have any figures concerning the sound power level of the unit. Because we move a large quantity of air with this equip-

ment and do not wish to expend too much electrical energy in doing so, the noise level is low as we have to use a low pressure drop system. This would compare favorably with an atttic fan in a house which is rather quiet by comparison to the type of fan used in a typical outdoor compression type condensing unit which has been compacted and, as a result, has a higher air pressure drop.

As far as the fume or combustion products are concerned, the flue gas effluent from the generator dilutes into the air quantity leaving the condenser and absorber coils, and goes out the top. This raises the air temperature going through by only a few degrees, so there is no hot flue pipe projecting to the exterior of the equipment.

People have generally felt that this was an exceptionally quiet piece of equipment.

A. P. BOEHMER, Des Plaines, Ill.: What performance data have you determined on either tonnage per cu ft of gas or a C.O.P. of this equipment?

Do you also use it for heating?

AUTHOR MERRICK: The unit has been approved and rated by A. G. A. in the smaller size at 34,000 Btu/hr with an input of 120,000 Btu/hr. In the larger size unit: 52,000 Btu/hr with an input of 180,000 Btu/hr.

The unit is not used for heating but is strictly an add-on piece of equipment.

O. J. NUSSBAUM, Trenton, N. J.: What has been done to apply this system for freezing temperatures when the water chiller is installed outside? How is the water protected against freezing?

Will you explain the ammonia condenser a little further?

AUTHOR MERRICK: The operation of the equipment in the winter is not contemplated, so it is not necessary to add anti-freeze to the water circuit to keep it in a fluid state. There are jobs that have been operated in freezing conditions and the problem was solved with anti-freeze. Our concern with freezing is limited to withstanding the sub-freezing temperatures during shut-down in the winter and we have designed the machine to overcome this problem.

Flexible members in the chilled water pump will permit expansion of the freezing water to take place without building up forces that can do any damage. Insulation is placed in the bottom of the chiller tank which is compressible by nature. The insulation is a close-cell material which is able to absorb the expanding water as it freezes. For chilled water piping flexible polyethylene pipe is recommended, which is able to withstand the expansion of the water as it freezes.

1720

No. 1720

The Dual Solution System — a Different Approach to Some of the Problems of Air Conditioning

F. H. HIBBERD

Essentially, the dual solution system is of the open absorption type. Air to be conditioned is brought into direct contact with a hygroscopic solution. The dual solution system differs from other open absorption systems in that the hygroscopic solution is cooled continuously so that it simultaneously cools and dehumidifies the air. As both strength and temperature of the solution are controllable readily within limits, the temperature and moisture content of the conditioned air likewise are controllable individually. This patently valuable asset is secured, however, at the cost of a relatively complex cycle and apparatus.

In discussing various types of absorption refrigeration methods, differing meanings have been assigned to the terms used to denote the condition of the solutions at various points in the cycle. Here the term "strong" is taken to mean a solution which is relatively concentrated as to its hygroscopic component. For example, a solution containing 40% lithium chloride is said to be relatively strong while one containing 15% is said to be relatively weak.

The system described herein is not limited inherently to a specific hygroscopic material. Furthermore, as there are in fact two separate solution circuits it is possible, probably for some applications desirable, to use different substances in the two circuits. However, for reasons hereinafter discussed, lithium chloride has been used in the experimental equipment and will be assumed in discussing the operation.

In Fig. 1, the hygroscopic, relatively weak, primary solution cools and dehumidifies the air being con-

H. F. Hibberd is with the Air Conditioning Development Company. This paper was presented at the ASHRAE 67th Annual Meeting, Vancouver, B. C., June 13-15, 1960.

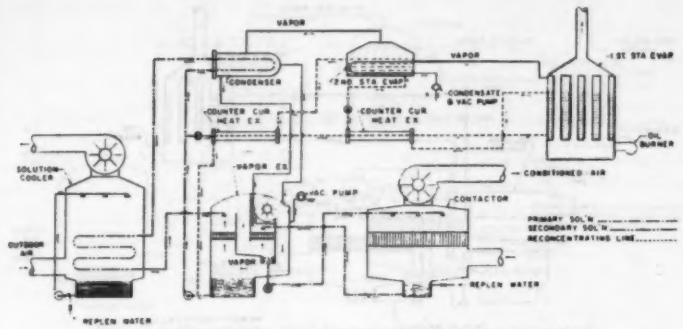

Fig. 1 Arrangement of the double effect evaporator system

ditioned in the contactor. Having absorbed sensible heat and been diluted it is drawn by vacuum into the vapor exchanger where it loses water by evaporation resulting in cooling and restoration of strength. It is removed continuously by a pump and reused.

Conditions in the vapor exchanger favor evaporation from the primary solution because a vacuum is maintained therein and a fan continuously recirculates air between contact with the sprayed primary solution and a spray of secondary solution, which although relatively warm is relatively strong enough to absorb the water vapor picked up from the primary solution. Thus, the primary solution is continuously cooled and reconcentrated while the secondary solution is continuously warmed and diluted. The degree of vacuum is not critical for this purpose but it must be high enough to minimize the carry back of sensible heat by the air stream from the warm secondary to the cold primary solution. In practice a vacuum of about 27.5 in. is satisfactory.

The secondary solution is continuously recooled by passing it through the solution cooler where it is in indirect heat exchange with a stream of water saturated outdoor air. It is reconcentrated by withdrawing a small portion—about 6% of total flow—and passing through a double effect evaporator. In the experimental unit the first effect was oil fired. Gas fuel would be suitable and more easily controlled. As the first evaporator is maintained at a temperature approaching 260 F, steam could only be used at a pressure of 25 psig or more.

Fig. 1 shows diagrammatically the arrangement of the double effect evaporator system. Feed to the first evaporator is preheated by two countercurrent heat exchangers in series. The first evaporator is maintained at about 10 in. vacuum by a small combined condensate and vacuum pump. The second effect evaporator is at approxi-

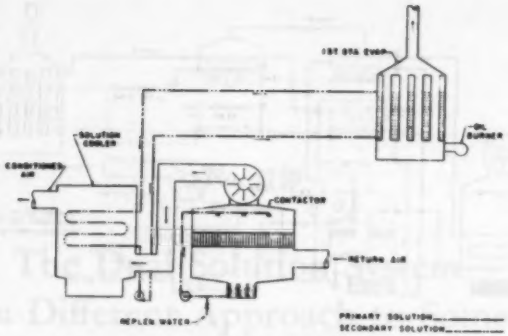

Fig. 2 Heating and humidifying cycle

mately vapor exchanger vacuum which is maintained by a sliding vane pump controlled by a vacuum switch.

The heating and humidifying cycle, although it utilizes much of the same equipment, is somewhat more orthodox. By shifting valves and dampers the solution cooler becomes the means of heating air to be conditioned. The solution (actually that which is the "secondary" solution when cooling) is now recirculated directly between the oil fired first evaporator and the solution cooler. Humidification is accomplished with same pumps and sprays used with the primary solution when cooling.

The heating and humidifying cycle is shown in Fig. 2.

Efficiency and Performance – The primary justifications for considering the dual solution system are its low operating cost and independent control of humidity and temperature within limits.

To establish the potentialities with regard to operating cost, a representative set of conditions has been established and the predicted temperatures and quantities throughout the system indicated in Fig. 3. The following assumptions were made.

60,000 Btu/hr removed from air by reducing it from 80 db 68.8 F wb (50% rh 60 F dp) to 65 db 60.7 F wb (78% rh 58 F dp).

Heat removed from secondary solution by cooling it from 95 to 83 F using outdoor air at 95 db 75 F wb water saturated.

Oil or gas fired first effect evaporator – 75% furnace off.

These will be recognized as moderate design specifications for a home air conditioner. They will be used to indicate normal maximum fuel and power requirements which can be compared with conventional equipment of similar ca-

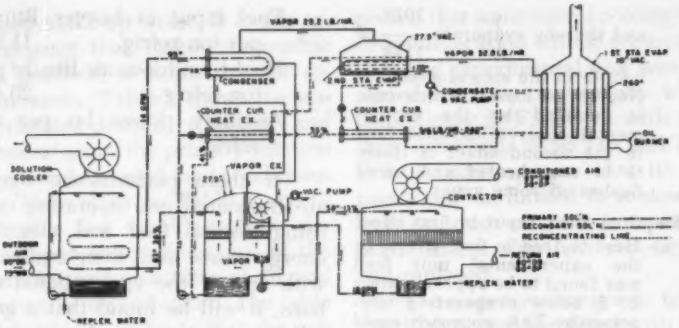

Fig. 3 Quantities and temperatures to be expected

pacity. The possibilities of the dual solution system in meeting more unusual conditions will then be explored.

Quantities and temperatures to be expected are indicated in Fig. 3. Demonstration of the entire heat balance is complex and believed to be unnecessary for the present purposes, but some calculations are pertinent to justifying the quantities of Fig. 3 as follows:

1—Water absorbed by secondary solution.

a) Equiv. of 60,000 Btu/hr $= \frac{60{,}000}{1060} = 56.5$ lb/hr

b) Loss due to air recirculation in vapor exchanger. Approx. 3300 cfm at 2.5 in. Abs cooled from 85 to 65 F = 5800 Btu/hr equiv to 5.5 additional lb/hr water

c) Total absorbed by secondary $= 56.5 + 5.5 = 62.0$ lb/hr

2—Quantities fed to concentration system

Secondary solution strength 36 %
Returning concentrated solution 41 % (limited to avoid solidification during shutdown)
X = lb/hr LiCl in feed
Y = lb/hr H_2O in feed

$$\frac{X}{X+Y} = 0.36$$

$$\frac{X}{X+(Y-62.0)} = 0.41$$

X = 186 lb/hr
Y = 330 lb/hr
Feed = 516 lb/hr

3—Evaporation in each effect

a) Latent heats of evaporation

	First effect	Second effect
Vacuum	10 in.	27.5 in.
Solution temperature	260 F	170 F
Heats Btu/hr/lb		
Evaporation—water from water	983	1033
Heat of solution approx.	80	80
Heat to superheat vapor—approx.	33	35
Total latent heat evap. fr. solution	1096	1148

b) Latent heats of condensation 1016 1068

c) Each pound of vapor evaporated in the first effect will (neglecting losses) condense

and thereby evaporate $\frac{1016}{1148} =$ 0.89 lb in the second effect. Neglect of losses in this case is justified by the experimental observation that feed to the second effect is likely to be superheated and hence flashes off some vapor.

4—Required Heat Input to first effect

a) Heat to feed in first effect. In the experimental unit feed was found to be approximately 20 F below evaporating temperature. This approach could be considerably improved by insulation etc. but is assumed for these calculations

Specific heat of strong LiCl solution is approximately 0.6
First effect heat to feed = $516 \times 20 \times 0.6 = 6{,}200$ Btu/hr

b) Required evaporation in first effect $= \frac{1.0}{1.89} \times 62.0 = 32.8$ lb/hr

c) Total net input to first evaporator $= 32\,8 \times 1096 + 6{,}200 = 42{,}100$ Btu/hr

5—Heat input to burner $= \frac{42{,}100}{0.75} =$ 56,200 Btu/hr

6—Heat rejected to outdoor air = 60,000 + 42,100 = 102,100 Btu/hr

7—Auxiliary power

Small pumps operating continuously require an aggregate of about 0.4 hp. Vacuum pump drive ¼ hp intermittent. Vapor exchanger fan less than 0.07/hp continuous.

The foregoing has been assembled for a 5 ton (60,000 Btu/hr) system as this was the design capacity of the experimental unit, and in general, the experimental results support this analysis although no attempt has yet been made at an accurate heat balance or other performance test. The above figures can be summarized as follows:

Fuel input to burner Btu/hr per ton refrig.	11,200
Heat to outdoor air Btu/hr per ton refrig.	20,400
Auxiliary power hp per ton refrig.	0.1

If these performance figures are translated into operating costs using normal fuel and electrical energy costs and then compared with any of the conventional systems, it will be found that a great advantage appears to be available.

The second outstanding asset of the dual solution is its ability independently to control moisture content and temperature of conditioned air. This control is achieved through the primary solution. As has been shown, the water evaporated from the primary solution in the vapor exchanger accounts for the entire refrigerating load—both sensible and latent—plus some losses. Consequently, if no make-up is provided the primary solution will tend to become more and more concentrated.

As the limit on evaporation from the primary solution is a function of the vapor pressure maintained by the secondary solution in the vapor exchanger, the effect of concentrating the primary solution will also be to allow its temperature to rise. The end result would then be that the primary solution would greatly increase its capacity for absorbing moisture at the expense of its ability to remove sensible heat.

To control the proportions of sensible and latent heat removed from the air, the primary solution is rediluted continuously by con-

trolled make-up water. It is this arrangement that makes it possible and practical to adjust to suit requirements. Table I shows the approximate desired strength and temperature of the primary solution for several assumed load conditions.

The values in Table I are illustrative but would actually depend upon the performance of the contactor and quantities of air and solution being circulated. The table is intended to indicate that the system has an inherent capacity to adjust itself to a wide range of requirements.

The Experimental Unit — Figs. 1 and 2 show the experimental unit as set up in the author's home. The supply and return air connections were made in parallel with the existing forced warm air heating unit. As the house duct sizes and grille locations were not planned with summer air conditioning in mind, the experimental unit was not expected to air condition the house effectively but the arrangement does provide a means of loading the experimental unit and it is expected that some useful cooling and dehumidification will be secured.

TABLE I

General Condition	Design Maximum Day	Light Load	High Moisture Load
Return Air			
Temp db	80	75	80
Rel. Hum.	50%	50%	50%
Supply Air			
Temp db	65	70	70
Dew Point	58	55.5	55
Prim. Soln.			
Temp.	58	65	65
Strength	13%	21%	23%
Equiv. dew point	53	52	50

The experimental unit was designed for five ton capacity when maintaining 80 F, 50% rh with outdoor conditions of 95 DB and 75 F WB. It now appears that its capacity will be limited to somewhat less by one or two component parts, unless they are redesigned and replaced.

The vapor exchanger is fabricated from steel and fitted with two sets of sprays, contact material, and a motor driven fan. Epoxy and synthetic rubber coatings have been successful deterrents of corrosion.

The first effect evaporator uses a low pressure type oil burner. All parts in contact with solution are silicon bronze with welded or silver soldered joints.

The condenser and heat exchangers are copper throughout with brazed or silver soldered joints. The means of treating the air to be conditioned (the "contactor") is a substantially standard capillary air washer with sprays and glass fibre contact cells. The solution cooler is a standard evaporative condenser. The main solution pumps are centrifugal. Small positive displacement pumps control flow in the concentration circuit. The vacuum pump is of the sliding vane type with its individual motor but the other pumps are driven by a single motor.

Hose was used for the main primary and secondary solution connections. Copper tubing and brass pipe and fittings were used for smaller connections. Although there are no significant pressures

in the system most lines must withstand collapsing forces due to vacuum.

Lithium Chloride Used – The system as described could be made to function with any one of several hygroscopic solutions. However, lithium chloride was chosen for several reasons for both primary and secondary solutions. Lithium chloride has been widely used for conditioning air for many years. It has been applied for human comfort and for industrial purposes. It has had no deleterious effect on either humans or products and in fact is said to have beneficial germicidal properties.

Among the hygroscopic liquids it is especially attractive because it retains reasonably good flow characteristics even at high concentrations and because, although an electrolyte, its corrosive tendencies have been found to be controllable. Lithium bromide, a similar material, has been favored for sealed absorption systems presumably because of a better corrosion behavior.

Installation of the equipment was completed in 1954. Trials, tests and development have continued since then. From the outset it was recognized that a primary objective was to achieve substantially automatic functioning of the entire system including the double effect evaporator. Furthermore, there must be reasonable assurance of freedom from mechanical or corrosive failure. For these reasons, rather costly materials and fabrication methods were used, with the hope and expectation that substitutions could be made when the basic system had been proven. The satisfactory use of lithium chloride in such a system could not be taken for granted.

CONTROLS

Automatic control of the unit was provided even where it resulted in complexity incommensurate with the capacity of the unit. It was felt to be important to first determine whether the relatively complex system was amenable to automatic operation and to thereafter seek ways to reduce cost and complexity.

The first stage evaporator temperature is maintained by aquastat for either cooling or heating conditions. For the cooling cycle, vacuum is normally maintained in the vapor exchanger continuously. Upon demand for cooling the vapor exchanger fan and pumps are started, setting the cycle in motion. The conditioned air fan may be run continuously or not as desired. Careful attention to gravity flow and air entrapment, where necessary, have resulted in quite satisfactory automatic operation of the evaporator circuit.

Although no such controls were installed, it is apparent that by regulating water return to the primary solution, (for which water loss by evaporating corresponds to the total refrigerating load) its strength and resultant dehumidifying capacity can be controlled over fairly wide limits. Its temperature can be controlled by conventional bypassing.

Safety controls consist of the

usual ones on the first evaporator plus a low vacuum cutout of pumps, responsive to vapor exchanger vacuum.

The experimental unit has not been equipped to convert quickly from cooling to heating or vice versa although it has functioned successfully in both capacities. Provisions for rapid and easy conversion of this unit would entail rather elaborate motorized valve and damper linkages. Much could undoubtedly be accomplished with further testing and design studies but it may well prove to be a rather costly provision in a small system.

Test Results and Limitations – As stated, the primary objective of these first tests was to establish feasibility. No attempt was made to achieve optimum conditioned air temperature or humidity. To do so, it was soon apparent that a major rearrangement of the internal structure of the vapor exchanger would be required. However, enough experience was gained to indicate what was possible and practical.

The dual solution system, since it interposes another solution and an inert vacuum air stream between the strong solution and the air being conditioned, limits the obtainable moisture reduction for a given strong solution strength and temperature. Furthermore, it imposes practical limits on the strength of the secondary solution, since it must be restorable to required strength by extracting and further concentrating a small portion, without that portion being concentrated enough to solidify and plug the system during shutdown.

There are no precise limits to obtainable temperatures and humidities as they are influenced by design and acceptable losses in efficiency. The tests indicated that the dual solution system is quite able to satisfy usual requirements for human comfort air conditioning when the secondary solution is cooled to temperatures obtainable from evaporative condenser-like equipment supplied with saturated air at 80 F wet bulb or less.

It is significant that because the dual solution system controls temperature and humidity independently and without "bypassing" of air it should achieve a better control of humidity within its limits than do other systems. This is especially true in comparison with direct expansion fluorocarbon or sealed lithium bromide types.

Disadvantages – The outstanding disadvantage of the dual system should be recognized at the outset; probably inherent, it would be a vital factor in establishing applicability. Many parts are required; some of which are bulky. This implies added first cost and added space requirements.

As compared to compression refrigeration, the heat rejection is considerably higher. For this reason straight water cooling is not proposed for normal applications of the dual solution system. It might be attractive where there is ample water, such as sea water, available. The system as herein described requires only a little more make-up water than a compression unit

served by a cooling tower but it must have that much water. The arrangement shown cannot operate on dry air cooling under normal conditions.

There are many applications of air conditioning, especially in vehicles, where pumps and sprays are not acceptable. For such applications, direct expansion compression refrigeration is about the only answer.

As compared with presently used open absorption systems it lacks the ability to achieve extremely low humidities sometimes required in process industries. These rather low humidities are only obtainable with any system at relatively high first cost and operating cost.

Advantages—The disadvantages are serious and assuredly would prevent any considerable application of the dual solution system were there not compensating advantages. It does have many potential advantages but probably no one of them is outstanding,

First, consider comparison with compression refrigeration, specifically of the direct expansion type including the heat pump. The dual solution system provides independent control within its capacity. It is able to take care of that difficult condition of high latent and low sensible heat loads on the "muggy" days. It avoids the difficulties of wet cooling coils after compressor cut off on intermittent operation.

Relative operating costs are dependent on fuel and electric power costs, but it appears that the dual solution system will have a large advantage under usual conditions. Gas utilities and the fuel oil industry are known to be seeking more summer load and the dual solution system offers one approach. An important asset of the dual solution system is that it does not require a large increase in electrical service or consumption. This can be quite important where either wiring or generating capacity is limited. It might make quite a difference in some of the undeveloped areas near the oil fields.

In the combined heating and cooling configuration the dual solution system, as does the heat pump, utilizes the same equipment for heating and for cooling. An advantage over the heat pump, however, is that there need be no limitation on heating capacity with reference to cooling capacity. This means that the system can be applied economically in localities or under conditions where the heating load may be expected to be large compared to the cooling load.

Consider the dual solution system in comparison with other open absorption systems. An outstanding asset is that it avoids heating and evaporation from an aerated and contaminated solution. Experience with the experimental unit indicates this to be quite significant. The strong secondary solution recirculates within a clean system and is deaerated continuously in the vapor exchanger. The weak primary solution is never heated. After several years of intermittent experimental operation there is no indication of corrosion or plugging.

The efficiency of the dual solution system is far higher than that of conventional open absorption systems. It is customary in such systems to reconcentrate the solution by causing it to flow over heated contact material countercurrent to a stream of air. This, aside from other inefficiencies, causes a loss of heat to the air stream carrying off the water vapor.

Furthermore, the solution used for air treatment cannot, without the use of refrigeration, be colder than the available cooling water. Under normal conditions this results in heating the air while drying it. The open absorption system as just described does not take advantage of multiple effect evaporation and cannot readily do so.

The dual solution system permits treating the air with a primary solution of different composition than that of the high strength secondary solution. Thus, the solution used to treat the air may have special germicidal or other properties but need not be highly hygroscopic nor need it be exposed to heat. This indicates possibilities in some special applications such as in hospitals. In practice the two solutions must be reasonably compatible as there is likely to be some carry-over in the vapor exchanger.

Finally, consider the advantages of the dual solution system compared with sealed heat powered systems such as those currently in use employing lithium bromide. The latter systems avoid moving parts but are thereby denied the advantages of multiple effect evaporation and forced flow through heat exchangers. The consequence is a large difference in efficiency in favor of the dual solution system.

The dual solution system avoids the problem of establishing and maintaining an extremely high vacuum over a period of years. Even minor internal corrosion can add to this problem as the products of corrosion are in part gaseous.

By achieving a large reduction in heat input, the dual solution system requires a far smaller cooling tower or its equivalent. If cooling water from another source is to be used the dual solution system needs far less of it.

The dual solution system has about the same advantages as to humidity control over the sealed absorption systems as it does over compression refrigeration.

General Advantages – The dual solution system imposes no unusual standards of workmanship or material. The experimental unit was assembled with no unusual precautions as to tightness. Standard plumbing and tubing fittings were used in making connections. It has been taken apart and reassembled many times without difficulty.

In general comparison with other systems including heating systems it is significant that the dual solution system employs no pressures at any time and that there is no hazard from rupture. The liquid and vacuum pumps operate at low heads and moderate vacuums.

As to freedom from noise and

vibration, the dual solution system is almost, but not quite, as favorably endowed as the sealed absorption systems. It is at a definite advantage when compared with the other systems.

CONCLUSIONS

The dual solution system cannot be expected to find a place among room units or small simple systems where size and cost are paramount considerations. There are many transportation and similar applications for which it is unsuited. It lacks the ability to produce extremely low humidities needed for some processes. The most attractive possibilities are probably for those somewhat unusual human comfort applications where, for one or more reasons, we can accept a degree of complexity in return for:

Unusual control of conditioned air humidity
Efficiency (low operating cost)
Reduced vibration and noise
Low electrical load
Absence of pressure
Combined heating and cooling if required
Moderate standards of tightness
Germicidal treatment of air if desired

DISCUSSION

FRANK H. BRIDGERS, Albuquerque, N. M.: Do the C.O.P. calculations include the vacuum pumps and other electrical components such as fans?

CLOSURE BY AUTHOR HIBBERD: No, they do not, but they are very small. The figures in the paper give the total electrical requirements as 1/10 hp per ton, making a very negligible effect on the C.O.P.

1721

No. 1721

Solar Heat Gains through Slat-Type Between-Glass Shading Devices

N. OZISIK

L. F. SCHUTRUM
Member ASHRAE

The increased use of and widespread interest in slat-type sun screens positioned between two sheets of glass as a means of controlling solar heat gains led to this research program which was conducted at the ASHRAE Research Laboratory in Cleveland, Ohio. The research has had the benefit of the guidance of the former RAC on Energy Transfer through Fenestration* and has been a continuation of the general study on solar heat gains through windows. Considerable data[1,2,3] have been published for slat-type shades located either inside or outside of single glass, and the excellent analysis given in Ref. 1 has been drawn upon extensively for this study of shades positioned between two sheets of glass.

*D. D'Eustachio, Chairman
O. L. Pierson, Vice Chairman
F. L. Bishop — Bruno Morabito
E. M. Burke — F. W. Mowrey
T. C. Carson — G. R. Munger
O. D. Englehart — D. J. Vild
W. B. Ewing — O. F. Wenzler
E. C. Miles — C. J. Youngblood

N. Ozisik was formerly Research Engineer and L. F. Schutrum is a Research Supervisor, ASHRAE Research Laboratory. This paper was presented at the 67th ASHRAE Annual Meeting, Vancouver, B. C., June 13-15, 1960.

EXPERIMENTAL EQUIPMENT

Shading devices tested consisted of commercial sun screens positioned between two sheets of common window glass (Normal Transmittance about 0.87) in the following manner: (1) the sun screen in direct contact with both sheets of glass; (2) in direct contact with both sheets of glass and having the sun screens embedded in plastics; (3) with a small space between the sun screen and the two glasses. These three shading devices were commercially available. A fourth type consisting of venetian blind slats between two sheets of glass was constructed at the Laboratory. These four types of shading devices are illustrated in Fig. 1, and a description of the shades tested is given in Table I.

The shading devices were

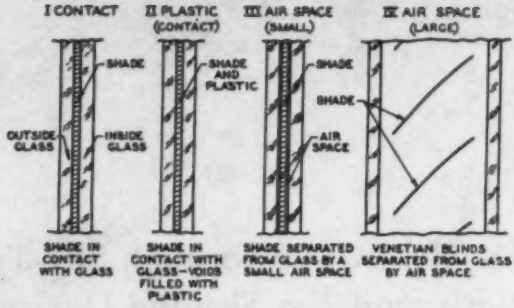

Fig. 1 Illustration of types of shading devices tested

tested under natural weather conditions by means of the Solar Calorimeter[4] which was first put into use in 1947. The calorimeter can be rotated to any desired orientation and tilted to any position from horizontal to vertical. The test window opening was 44¼ x 44¼ in., and was essentially flush with the outer surface of the 8-ft sq surrounding well.

The heat gained by the calorimeter was absorbed by a temperature-controlled mixture of ethylene glycol and water which was circulated through tubes soldered to the inside surface of the calorimeter. Solar radiation measurements were made with Eppley pyrheliometers mounted symmetrically on the wall. One pyrheliometer was positioned 12 in. above and the other 12 in. below the window. A 16-point recorder provided continuous readings throughout the test.

TEST PROCEDURE

All tests were made with the window glass in a vertical position and with the calorimeter continuously adjusted to follow the sun or with a fixed orientation. During the 10 or 15-min test intervals, records were kept of the altitude of the sun, the wall solar azimuth, wind velocity and direction, and the condition of the sky, as well as temperature and solar radiation measurements.

The total heat gain of the calorimeter was determined by computation from the quantity and temperature rise of the circulating fluid and was adjusted for the small heat flow through the back of the apparatus. This total heat gain is the sum of the solar radiation transmitted through the window and the convection-radiation gain from the warm glass.

The convection-radiation gain was determined from previously established calibration curves based on the temperature of the inner glass and the temperature of the heat absorbing surface of the calorimeter. The transmitted solar energy was then determined by

TABLE 1 DESCRIPTION OF SLAT-TYPE SUNSHADES

Type	Color or Appearance	Solar[a] Absorptance α	Slats Per Inch	Slat Spacing Inches	Slat Width In.	Slat Thickness In.	Slat Angle Degrees	Degrees Cut Off Angle[d] Air	Plastic[e]
A) Kaiser	Aluminum	0.37[b]	17½	0.057	0.057	0.0085	17	32	52
B) Reflectal	Black	0.8	23	0.043	0.047	0.0051	17	29	47
C) Reflectal	Black	0.8	17	0.059	0.047	0.0075	17	42	83
Venetian Blinds	Dark Green	0.7[c]	0.6	1.67	2.0	——	45	10	—

a Values of 0.37 and 0.8 taken from Ref. 2
b The room side of some of the screens tested were painted black. 0.8 was assumed fog absorptance
c Measured with pyrheliometer, compared with magnesium carbonate
d Minimum profile angle at which none of the sun's rays pass between the slats.
e Computed for index of refraction of 1.49

subtracting the convection-radiation gain from the total calorimeter gain.

ANALYSIS

Part of the solar radiation falling on a sun screen is transmitted through, another portion is reflected back, and the remainder is absorbed by the screen. These three properties of the sun screens, solar transmittance, reflectance, and absorptance were calculated by means of the analysis given in Ref. 1.

With the screen positioned between two sheets of glass, the sun's rays must first pass through the outer glass, then the sun shade, and finally the inner glass before entering the room. The incident solar radiation reflected from the outer glass passes to the exterior of the building and is no longer considered. Of the remaining radiation, part is absorbed and warms the glass, and a portion is transmitted through to the sun shade. The sun shade, in turn, either reflects, absorbs, or transmits this solar energy. Part of the energy reflected from the sun shade passes through the outer glass to the exterior, part is absorbed by the glass, and the remainder is re-reflected to the sun shade. The solar energy that is absorbed by the sun shade will increase its temperature. The radiation passing through the sun screen falls on the inner glass and again the phenomenon of reflection, absorption and transmission occurs.

The combined transmittances and absorptances of the sun screen between two sheets of glass were determined as described in Appendix A. Now, recall that the total heat gain measured by the solar calorimeter consisted of transmitted solar energy and a convection-radiation component. The transmitted component can be determined analytically from Equation A-2 of Appendix A.

The convection-radiation component is the result of the warm glass radiating to the room surfaces and convecting to the room air. The temperature of this inside glass is

dependent upon the solar energy absorbed by it, and upon the heat exchange with the sun shade and with the room. Similarly, the temperature of the sun shade depends upon the absorbed solar energy and the heat exchange with both inner and outer glasses. The temperature of the outer glass results from the balance of absorbed solar energy and heat exchange with the sun shade and with the outdoors. These heat exchanges between the glasses and shade occur by various combinations of convection, conduction and radiation, depending upon the construction of the between-glass shading device. The convection-radiation component can be determined analytically from Equation B-7 of Appendix B.

The purpose of the theoretical analysis was to be able to extend the data beyond the confinements of the experiments, but first the theory had to be confirmed by comparison with experimental data. From Fig. 2, the calculated total heat gains as obtained by the methods referred to above can be compared with the total heat gains measured by means of the solar calorimeter under natural weather conditions. We conclude from Fig. 2 that the theoretical analysis is satisfactory.

DESIGN FACTORS

The analytical Equations A-2 and B-7 can be consolidated into the following relatively simple form for the total heat gain into the room per unit area of glass (Derivation in Appendix C):

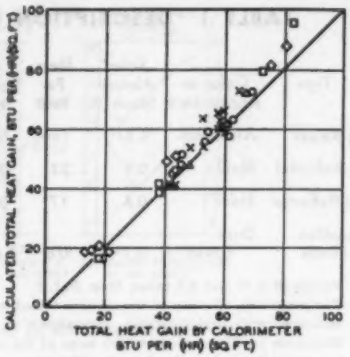

Fig. 2 Comparison of calculated total heat gains with heat gains measured by means of the solar calorimeter

$$Q = K_D I_D + K_d I_d + U(t_o - t_i) \qquad \text{Eq. 1}$$

K_D and K_d are dimensionless solar heat transfer factors for direct and diffuse solar radiation respectively; they depend upon the type of fenestration as well as the angular relation between the window and the sun. I_D and I_d are the intensity of the direct and diffuse solar radiation falling upon the glass surface. U is the conventional overall heat transfer coefficient and t_o and t_i are the outside and inside air temperatures respectively.

The K_D, K_d and U values for various slat-type between-glass shading devices are given in Fig. 3. Note that the value of K_D depends upon the profile angle which is defined in Fig. 4. The U-values were calculated by combining an inside overall coefficient of 1.5 Btu/hr/ft²/F and an outside coefficient of 3.0, with the thermal conductance of each window.

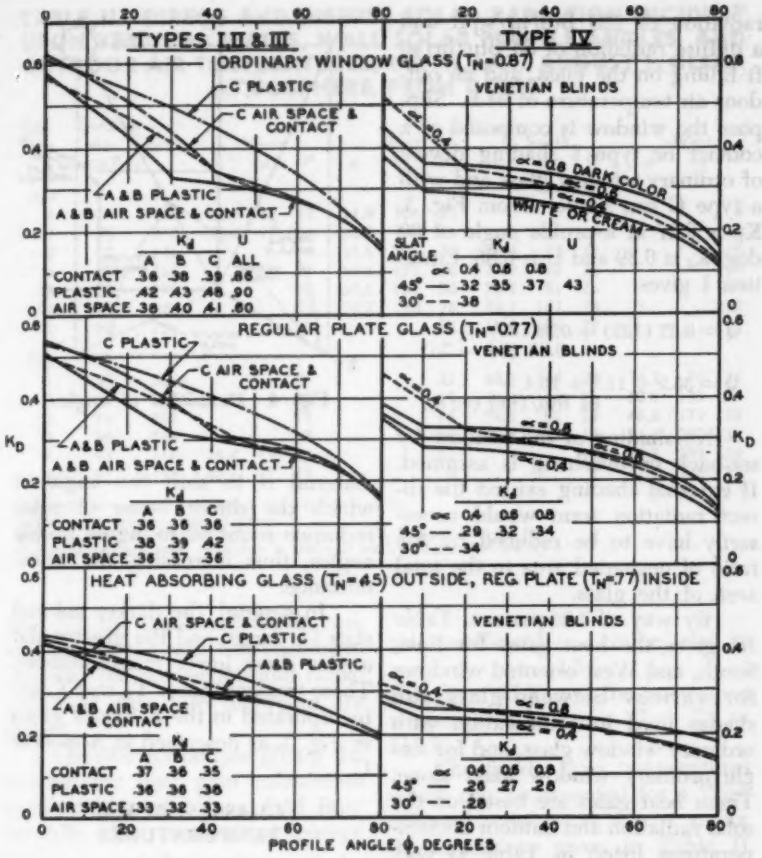

Fig. 3 K and U values for between-glass slat-type sunshade devices (For description of A, B, C type shades—see Table I)

The thermal conductances were measured in the calorimeter under night-time conditions and/or in a special set-up used to measure the conductances of one-foot square samples. The intensities of direct and diffuse solar radiation, outdoor air temperatures and profile angles taken from the GUIDE are given in Table II for 40° N. Lat., August 1.

Example of Heat Gain Calculation —A West-facing window on August 1, 40° N. Lat., at 2 p.m., according to Table II, has a profile angle of 60 deg with the sun, a direct solar

radiation of 133 Btu/hr/sq ft and a diffuse radiation of 30 Btu/hr/sq ft falling on the glass, and an outdoor air temperature of 94 F. Suppose the window is composed of a contact or type I shading device of ordinary window glass and with a type C sun shade. From Fig. 3, K_D is 0.27 at a profile angle of 60 deg, K_d is 0.39 and U is 0.86. Equation 1 gives:

$$Q = 0.27\ (133) + 0.39\ (30) + 0.86\ (94 - 75)$$

$$Q = 35.9 + 11.7 + 16.4 = 64\ \text{Btu/(hr) (sq ft)}$$

No shading of the window by set-back or overhang is assumed. If external shading existed the direct radiation term would necessarily have to be reduced by the ratio of unshaded area to the total area of the glass.

By way of comparison, Table III gives the heat gains for East, South, and West oriented windows for various between-glass sun shades used in combination with ordinary window glass, and for single ordinary window glass alone. These heat gains are based on the solar radiation and outdoor air temperatures listed in Table II and, except for the single glass, were calculated by means of Equation 1 and Fig. 3.

Transmitted Component—The magnitude of the transmitted solar energy is an indication of the amount of light or visible energy entering the room through the window. The calculated transmittances of these fenestrations are given in Fig. 5. The effect of the plastics material is to shift the angle at which the direct beam of solar radiation is cut off to higher profile angles, thus increasing the transmittance.

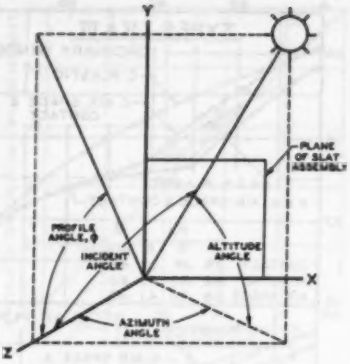

Fig. 4 Definition of angles

In general, the darker colored slats (α large) and the greater slat angles show lower transmittances. These transmittances T_D and T_d are incorporated in the K values given in Fig. 3, as described in Appendix C.

GLASS SURFACE TEMPERATURES

The comfort of the occupants may be influenced by the surface temperature of the inner glass if the glass area is large or the persons are near the window. The total convection and radiation gain from the window, excluding transmitted solar radiation, is the result of the inner glass radiating to other room surfaces and convecting heat to the room air. The glass temperature can be found if the room tempera-

TABLE II DIRECT AND DIFFUSE SOLAR RADIATION INCIDENT UPON VERTICAL WALLS, WALL SOLAR PROFILE ANGLES, AND OUTDOOR AIR TEMPERATURES, (40° N. LAT., AUGUST 1, CLEAR ATMOSPHERE, FROM GUIDE)

Sun Time	Outdoor Air Temp, F, t_o	I_{ND}[a]	North			East			South			West		
			ϕ[b]	I_D[c]	I_d[d]	ϕ	I_D	I_d	ϕ	I_D	I_d	ϕ	I_D	I_d
AM														
6	74	133	40.1	32	12	11.8	126	22			9			8
7	75	210	78.4	17	16	23.2	193	34			14			12
8	77	246			17	34.6	203	36	82.8	17	19			16
9	80	266			19	46.6	179	35	74.8	52	23			18
10	83	279			20	60.0	133	30	70.8	81	26			19
11	87	286			21	74.7	70	26	68.7	101	28			22
12	90	288			22			23	68.0	108	29			23
PM														
1	93	286			21			22	68.7	101	28	74.7	70	26
2	94	279			20			19	70.8	81	26	60.0	133	30
3	95	266			19			18	74.8	52	23	46.6	179	35
4	94	246			17			16	82.8	17	19	34.6	203	36
5	93	210	78.4	17	16			12			14	23.2	193	34
6	91	133	40.1	32	12			8			9	11.8	126	22

a Direct normal solar radiation Btu per (hr) (sq ft)
b Wall solar profile angle, degrees
c Direct incident solar radiation in plane of wall, Btu per (hr) (sq ft)
d Diffuse incident solar radiation in plane of wall, Btu per (hr) (sq ft)

ture (t_o), the combined inside convection and the radiation coefficient (h_o), and the convection and radiation heat gain into the room are known.

The above example giving the method for heat gain calculation resulted in a total gain of 64 Btu/hr/sq ft. The transmitted energy is the sum of the products of the direct and diffuse solar intensities given in the example, and the direct and diffuse transmittances given in Fig. 5. This amounts to about 8.5 Btu/hr/sq ft for the example. Then the convection-radiation gain is 64-8.5 or 55.5 Btu/hr/sq ft.

The temperature difference between the inner glass and the room is equal to the convection-radiation gain divided by the combined inside coefficient $\frac{55.5}{1.5}$ (value used in Fig. 3) = 37 F, and the inner glass temperature becomes 37 + 75 = 112 F.

The inside glass temperatures which can be expected for a West oriented window at 4 p.m. under the conditions given in Table II would be from about 108 F to 131 F for ordinary window glass, with the lower temperatures corresponding approximately to the sun screen having the lower solar absorptances. The temperature of inner and outer glasses would be nearly the same.

With heat absorbing glass outside and regular plate inside the range of temperature for the inside glass would be about 112 to 130 F and the outside or heat absorbing

glass from 125 to slightly under 150 F. For the higher thermal conductance devices types II and I (plastics and contact), the outside glass is only slightly warmer than the inside.

The inside to outside glass temperature difference is greatest for venetian blind devices (type IV) which have comparatively low conductances. This temperature difference increases as the solar adsorptance of the slats decreases.

RESULTS

All of the test data were taken with both glasses approximately equivalent to common window glass; however, it is believed that calculated K values are also reasonably accurate for the regular plate (Normal transmittance 0.77) and heat absorbing glasses (Normal transmittance 0.45). No adjustment was made for the selective transmittances[8] of two sheets of glass which is relatively more important for higher absorbing glasses.

The solar properties of the sun screens depend upon the profile angle which was defined in Fig. 4, but the solar properties of the glass are dependent upon the incident angle. Thus both profile and incident angles should be used to determine the thermal performance of a between-glass shading device; however, for the sake of simplicity, it was decided to accept the error involved and neglect the effect of change with incident angle.

Consequently, the transmittance of the outer glass was taken at an incident angle equal to the profile angle and a small error would then occur for only those angles of incidence much greater than the profile angle. The calculated values shown in Fig. 2, which are slightly higher on the average than the experimental data, were based on the profile angle for the transmittance of the glass.

A correction for the true incidence angle would bring some of the calculated points closer to the experimental values. Also the storage of heat in the glass and shade has been neglected in presenting the K factor. The magnitude of the storage, determined in the solar calorimeter, was less than 10% of

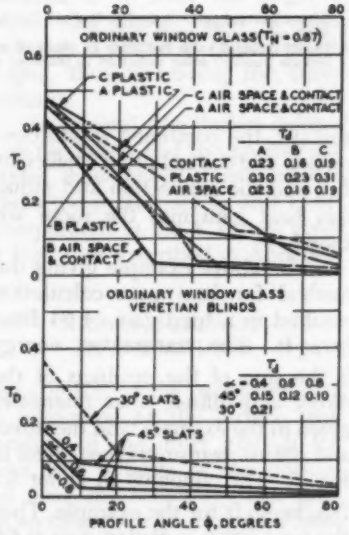

Fig. 5 Transmittance of between-glass slat-type sunshade devices

Note: For Regular plate glass multiply T_D by 0.75. For Heat absorbing—Regular plate multiply T_D by 0.4 for direct and T_d by 0.45 for diffuse radiation.

the total gain. Adjustment to the data for storage effects tends to better the agreement shown in Fig. 2.

The K and U values given in Fig. 3 were based on an overall outside coefficient of 3 Btu/hr/sq ft/F between the outer glass and the outdoor air. Calorimeter data indicate outdoor coefficients lower than 3 on an average (also see Ref. 7). The outdoor coefficient does not influence the transmitted component of heat transfer but only the convection and radiation gains. Thus in Fig. 6, which shows the trend of the K_D value with the outdoor coefficient, a greater change is shown for the higher profile angles where the convection and radiation component of the total solar gains is proportionately larger.

The slat-type shading devices (horizontal slats) have greater transmittances for radiation from below the horizon and, consequently, the amount of solar radiation reflected from the foreground will influence the diffuse transmitted component

TABLE III HEAT GAIN FOR SLAT-TYPE BETWEEN-GLASS SHADING DEVICES AND FOR ORDINARY WINDOW GLASS, BTU/(HR) (SQ FT) (AUGUST 1, 40° N LAT., CLEAR ATMOSPHERE, INDOOR TEMP. 75 F)

Orientation & Sun Time	SLAT-TYPE BETWEEN-GLASS SHADING DEVICE WITH ORDINARY WINDOW GLASS					Single Ordinary Window Glass
	Air Space & Contact[a]		Plastics		45° White Venetian Blinds	
	A & B	C	A & B[a]	C		
EAST						
6 AM	69	78	73	82	43	128
7	89	108	102	118	66	199
8	81	97	95	116	68	211
9	71	76	75	96	59	187
10	53	54	56	66	42	137
11	33	33	36	39	25	71
12 Noon	20	20	23	25	14	33
SOUTH						
8 AM	11	11	12	13	9	20
9	23	23	25	27	18	48
10	34	35	37	40	26	78
11	43	44	47	52	33	104
12 Noon	48	48	52	57	37	115
1 PM	48	48	52	57	36	110
2	42	43	47	50	31	90
3	34	34	38	40	25	63
4	23	23	27	29	16	37
WEST						
12 Noon	20	20	23	24	14	33
1 PM	37	38	42	44	27	77
2	61	62	66	76	47	147
3	82	87	89	109	65	204
4	93	109	110	131	76	228
5	102	121	118	134	74	217
6	82	90	88	97	51	144

[a] Average K & U values used for computation because of small differences.

(included in K_d). For this diffuse component it was assumed that 75 per cent of the diffuse or sky radiation came uniformly from above the horizontal, and 25 per cent from below.[3, 6, 7]

Venetian blinds with the slats mounted vertically were also tested in the solar calorimeter with a fixed slat angle of 45 deg. The conductance of the device was about the same with the venetian blind slats either vertical or horizontal. The predicted solar heat gains based on K and U values agreed with the measured total gain. However, for blinds with vertical slats set to exclude the sun, the wall solar azimuth angle should be used in Fig. 3, in place of the profile angle.

Difference in the diffuse K_d terms for vertical and horizontal slats should be secondary in magnitude as long as the bright portion of the sky (near the sun) does not radiate directly through the shade because of slat angle, and extremely bright foregrounds are avoided.

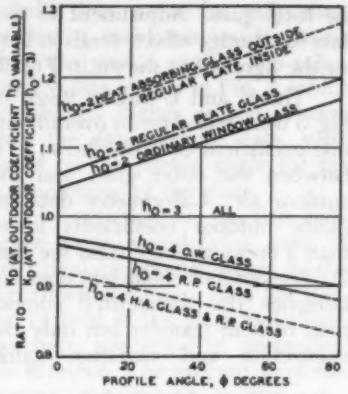

Fig. 6 Approximate effect of combined outdoor coefficient of heat transfer h_o, on the K_D factor for between-glass shading devices

CONCLUSIONS

1. Instantaneous heat gains through slat-type between-glass shading devices have been predicted with engineering accuracy from the incident solar radiation, the outdoor air temperature, and the K and U values reported in the paper.

2. The use of these shading devices results in a reduction of instantaneous heat gains as compared with a window of single glass. For a west-oriented window, the design (Aug. 1, 40° N. Lat.) instantaneous heat gain from 12 noon to 5 p.m., using a slat-type between-glass shading device constructed with ordinary window glass, would be about 35 to 60 per cent of the gain through a window of single regular plate glass. These percentages also hold for the maximum instantaneous heat gains.

NOMENCLATURE

A	Solar absorptance of an element when in combination with other elements of the fenestration, dimensionless
C	Conductance of shading device (outside surface to inside surface) Btu/(hr) (sq ft) (F)
CR	Combined convection and radiation exchange, Btu/(hr) (sq ft)
G	Thermal resistance from an element of the fenestration to inside (F) (hr) (sq ft) per Btu
h	Thermal conductance Btu/(hr) (sq ft) (F)

I_D Intensity of direct solar radiation on a vertical wall, Btu/(hr) (sq ft)

I_d Intensity of diffuse solar radiation on a vertical wall, Btu/(hr) (sq ft)

K Solar heat transfer factor, dimensionless

Q Total heat gain into room per unit area of the window, Btu/(hr) (sq ft)

q Transmitted solar energy Btu/(hr) (sq ft)

R Radiation exchange Btu/(hr) (sq ft)

ρ Reflectance for solar radiation, dimensionless

T Solar Transmittance, dimensionless

t Temperature, Fahrenheit degree

U Over-all coefficient of heat transfer, Btu/(hr) (sq ft) (F)

α Solar absorptance, dimensionless

αI Solar energy absorbed by the glass or shade Btu/(hr) (sq ft)

ϕ Wall solar profile angle, degrees

Subscripts

1, 2, 3 Refer to indoor glass, shade screen, and outdoor glass respectively

22, 33 For solar radiation, refers to the combined property

21, 32, 21, etc. For convection, radiation and thermal conductance, refers to exchange between elements

c Convection

cr Convection and radiation

D Direct solar radiation

d Diffuse solar radiation

N Normal incidence

r Radiation

i, o Inside and outside

ACKNOWLEDGMENTS

The authors acknowledge the valuable suggestions and guidance of the Research Advisory Committee on Energy Transfer through Fenestration and express their gratitude to the many technicians who made the extremely extensive calculations, and to Mr. Edward Burke for his liaison with industry.

REFERENCES

1. ASHVE Research Report 1460, The Shading of Sunlit Glass—An Analysis of the Effect of Uniformly Spaced Flat Opaque Slats by G. W. Parmelee and W. W. Aubele (ASHVE Transactions, Vol. 58, 1952, p. 377)

2. ASHVE Research Report 1474, The Shading of Sunlit Glass—An Experimental Study of Slat-Type Sun Shades by G. V. Parmelee, W. W. Aubele and D. J. Vild (ASHVE Transactions, Vol. 59, 1953, p. 221)

3. ASHVE Research Report 1485, Design Data for Slat-Type Sun Shades for Use in Load Estimating by G. V. Parmelee and D. J. Vild (ASHVE Transactions, Vol. 59, 1953, p. 403)

4. ASHVE Research Report 1333, Measurements of Solar Heat Transmission through Flat Glass by G. V. Parmelee, W. W. Aubele and R. G. Huebscher (ASHVE Transactions, Vol. 54, 1948, p. 165)

5. ASHVE Research Report 1348, Solar and Total Heat Gain through Double Flat Glass by G. V. Parmelee and W. W. Aubele (ASHVE Transactions, Vol. 54, 1948, p. 407)

6. Research Report 1510, Irradiation of Vertical and Horizontal Surfaces by Diffuse Solar Radiation from Cloudless Skies by G. V. Parmelee (ASHVE Transactions, Vol. 60, 1954, p. 341)

7. ASHAE Research Report 1645, Heat Gain through Windows Shaded by Canvas Awnings by Necati Ozisik and L. F. Schutrum (ASHAE Transactions, Vol. 64, 1958, p. 463)

APPENDIX A

Transmittance and Absorptance of Between-Glass Slat-Type Shading Devices —Designating the inner glass as 1, the shade as 2, and the outer glass as 3, the transmittance of the combination was determined as follows:

For a unit solar energy falling on the outer glass a portion of T_3 is transmitted through the glass 3. After an infinite series of reflections between glass 3 and shade 2 a portion $T_{32} = T_3\ T_2/(1 - \rho_2\rho_3)$ is transmitted through the shade 2.

Another infinite series of reflections between the shade and inner glass 1 results in a portion $T_{32}\ T_1/(1 - \rho_2\rho_1)$ passing through glass 1. However, part of these interflections between the shade 2 and glass 1 pass back through the shade and are reflected from glass 3. Repeating this phenomena infinitely results in the solar transmittance of the combination as:

$$T_{321} = T_{32} \cdot \frac{T_1}{1 - \rho_1\rho_1} \cdot \frac{1}{1 - \frac{\rho_1 T_2}{1 - \rho_2\rho_1} \cdot \frac{\rho_3 T_2}{1 - \rho_2\rho_3}}$$

Eq. A1

and the transmitted energy per unit area of the window becomes

$$q = I_D\ T_{321} \qquad \text{Eq. A2}$$

By a similar treatment, the solar absorptance of each of the combinations is:

$$A_2 = \alpha_2 \left[1 + T_{32} \frac{\rho_1 T_2}{1 - \rho_2\rho_1} \cdot \frac{1}{1 - \rho_2\rho_2} \cdot \frac{1}{1 - \frac{\rho_1 T_2}{1 - \rho_2\rho_1} \cdot \frac{\rho_3 T_2}{1 - \rho_2\rho_3}} + \frac{\rho_3 T_2}{1 - \rho_2\rho_3} \right]$$

Eq. A3

$$A_3 = \alpha_3 \left[\frac{T_{32}}{T_3} + \frac{\rho_1 T_{32}}{1 - \rho_3\rho_1} \right] \frac{1}{1 - \frac{\rho_1 T_2}{1 - \rho_2\rho_1} \cdot \frac{\rho_3 T_2}{1 - \rho_3\rho_3}}$$

Eq. A4

$$A_1 = \alpha_1 \left(\frac{T_{32}}{1 - \rho_3\rho_1} \cdot \frac{1}{1 - \frac{\rho_1 T_2}{1 - \rho_2\rho_1} \cdot \frac{\rho_3 T_2}{1 - \rho_2\rho_3}} \right)$$

Eq. A5

In evaluating these equations for the transmittance and absorptance of direct radiation, t_2, t_3, ρ_2 and α_2 were calculated using the direct solar radiation properties of the glass and shade. All other terms were calculated on the basis of the diffuse radiation properties.

The effect of spectral variation resulting from selective absorptances of the shade or glasses was beyond the scope of this investigation.

The transmittance and absorptances of the shade depends upon the profile angle, and the transmittance of the glass upon the incidence angle. For design purposes the incidence angle was taken the same as the profile angle.

The transmittances and absorptances for diffuse radiation are integrated values based on a uniform irradiation and ¾ of the diffuse radiation coming from the sky (¼ from below the horizon).

Since the plastics used in the Type II shading devices had high transmittance and low absorptance, the effect of the plastics was neglected in the calculation.

APPENDIX B

Convection and Radiation Gain—For this analysis, the arrangement shown in Fig. B1 was assumed in which a radiation but no convection exchange existed between surfaces 3 and 1. The glasses (3 and 1) were assumed to be infinitely thin as was the shade (2).

The energy balance for a unit area is:

For 1 $\alpha I_1 = CR_1 + CR_{12} + R_{13}$ Eq. B1
For 2 $\alpha I_2 = CR_{23} + CR_{21}$ Eq. B2
For 3 $\alpha I_3 \; CR_o + CR_{32} + R_{31}$ Eq. B3
For 3 $\alpha I_3 = CR_o + CR_{32} + R_{31}$ Eq. B3

where for the outer glass (Eq. B3)

$CR_o = h_o (t_o - t_o)$ Eq. B4
$CR_{32} = (h_{cr32} + h_{rr32})(t_3 - t_2)$ Eq. B5
$R_{31} = h_{rr31} (t_3 - t_1)$ Eq. B6

The terms in equations B1 and B2 were similarly expressed as a product of a heat transfer coefficient and a temperature difference. Assuming that the convection coefficients and the radiation coefficient for heat exchange between 3 and 2 are equal respectively to convection and radiation coefficients for 2 and 1, the solution in terms of the convection radiation gain to the room per unit area of the window is:

$$CR_1 = U\left[\frac{\alpha I_3}{h_o} + \alpha I_3 \left(\frac{1}{h_o} + \frac{1}{h_{cr32} + 2\,h_{rr31}}\right) + \alpha I_1 \left(\frac{1}{h_o} + \frac{2}{h_{cr32} + 2\,h_{rr31}}\right)\right] + U\,(t_o - t_1) \quad \text{Eq. B7}$$

where, $\alpha I_3 = A_3 I$, $\alpha I_2 = A_2 I$, $\alpha I_1 = A_1 I$ and A_3, A_2, A_1, are defined by equations A3, A4, A5 of Appendix A respectively.

The radiation coefficient h_{rr31} was estimated by calculating the net exchange for low temperature radiation between 3 and 1 by a method similar to that described in Appendix A. For the shades tested, h_{rr31} was computed to be approximately 0.3 Btu/(hr)(sq ft)(F).

The thermal conductances of the between-glass shading devices were measured in order that the U values and the coefficients h_{cr32} could be calculated. The thermal conductances measured from the outside of the outer glass to the room side of the inner glass are given in Table B1.

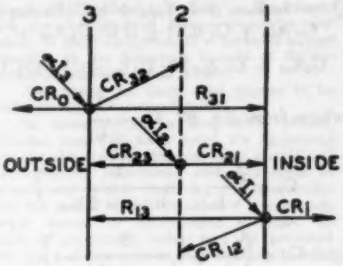

Fig. B1

TABLE B1

Type Fig. 1	Description	Conductance, C, BTU/(hr)(sq ft)(F)
I	Shade contacts glass	4-8
II	Shade and plastics, contact	8-12
III	Shade separated from glass—(Small space)	1.5
IV	Venetion Blinds (Large space)	0.7

The U value is defined as:

$$U = \frac{1}{\frac{1}{h_o} + \frac{2}{h_{cr32} + 2\,h_{rr31}} + \frac{1}{h_i}}$$

and $C = \dfrac{h_{cr32} + 2\,h_{rr31}}{2}$

APPENDIX C

Design Equation—The design equation (Eq. 1) given in the paper was determined from the equations developed in Appendices A and B.

Q (Total heat gain per unit area of window =

Transmitted direct and diffuse radiation (Eq. A2) +

Convection and radiation from the inside glass (Eq. B7)

Eq. C1

$$Q = I_D T_{\tau\alpha D} + I_d T_{\tau\alpha d} + I_D U(G_2 A_{2D} + G_2 A_{2D} + G_1 A_{1D}) + I_d U(G_2 A_{2d} + G_2 A_{2d} + G_1 A_{1d}) + U(t_o - t_i) \quad \text{Eq. C2}$$

where from Eq. B7, $G_2 = \frac{1}{h_o}$,

$$G_2 = \left(\frac{1}{h_o} + \frac{1}{h_{crss} + 2\,h_{rss}}\right)$$

and $$G_1 = \left(\frac{1}{h_o} + \frac{2}{h_{crss} + 2\,h_{rss}}\right)$$

(F)(hr)(sq ft) per Btu

Collecting Terms

$$Q = I_D[T_{\tau\alpha D} + U(G_2 A_{2D} + G_2 A_{2D} + G_1 A_{1D})] + I_d[T_{\tau\alpha d} + U(G_2 A_{2d} + G_2 A_{2d} + G_1 A_{1d}] + U(t_o - t_i) \quad \text{Eq. C3}$$

where the terms in the brackets are assumed to vary only with the profile angle.

$$Q = I_D K_D + I_d K_d + U(t_o - t_i)$$

Eq. C4 and Eq. 1

The transmittances and absorptances included in the K values depend upon the incidence angle as well as the profile angle and upon the spectral distribution of the radiation. The G_2, G_2, and G_1 terms, of course, vary with temperature because convection and radiation coefficients are involved, and also with the outdoor coefficient of heat transfer.

The U value varies with temperature and with the outdoor and indoor coefficients. Consequently the K_D and K_d values which are recommended for design are compromised and are approximate.

DISCUSSION

ERWIN L. WEBER, Seattle, Wash.: Do these figures take into consideration the fact that when the sun is near the setting point, its rays penetrate under the angle at which the plates are set and strike walls and objects in the room, rapidly raising the temperature? Or are these conduction figures?

CLOSURE BY AUTHOR HUMPHREYS: The figures in the paper include the direct transmittance of solar energy through the shades at low profile angles. You will note that there is a definite break in the curves of Fig. 3. This break occurs at the point at which the sun's rays start to pass directly between the slats.

W. L. HOLLADAY, Altadena, Calif.: Is there a comparison between the curves for within glass shading devices and the conventional method of placing window glass with a similar shading device outside the window?

AUTHOR HUMPHREYS: There is no direct comparison made in this paper. You will have to refer to other papers for different types of devices and then make your own comparison.

W. BRUCE MORRISON, Portland, Ore.: Have any firms marketed a between-glass shading device?

AUTHOR HUMPHREYS: The first three types of between-glass shading devices shown in Fig. 1 of the paper are commercially available. All three use some type of commercial sun screen. I believe that these commercial units are now being made only with ordinary window glass. However, our analysis has been extended to include units constructed with regular plate glass and with a combination of regular plate and heat absorbing glass.

E. J. OVERMYER, Seattle, Wash.: What is the loss of visibility through these slats?

AUTHOR HUMPHREYS: These screens are similar to "Cool-Shade" screens. There is some reduction in visibility, but I have no figures on the extent of the reduction.

FRANK H. BRIDGERS, Albuquerque, N. M.: The calculated inside temperature of 108-131 F is rather high for someone sitting next to a window at that temperature. Was any attempt made to measure the inside temperature?

AUTHOR HUMPHREYS: The temperatures of both the inner and outer glasses were measured in all of the calorimeter tests. The temperatures calculated in the example in the paper are in good agreement with the temperatures determined by test for similar conditions.

RICHARD M. STERN, Seattle, Wash.: How did the test results compare with manufacturers' claims for the same?

AUTHOR HUMPHREYS: The manufacturers did not furnish any performance data on the between-glass shading devices. We had nothing with which we could compare our results.

ARTHUR E. SPOWAGE, Vancouver, B. C.: The GUIDE shows a 70% saving in heat gain can be effected by outside shading of the window glass. Does this mean a 70% saving in this case?

AUTHOR HUMPHREYS: A sun screen between glass is not as effective as a similar screen on the outdoor side of a glass. As indicated in the paper, the heat gain through a west-oriented slat-type between-glass shading device from 12 noon to 5:00 p.m. would be from 35 to 60% of the gain through an unshaded window.

CHARLES S. LEOPOLD, Philadelphia, Pa. (Written): We first used the white venetian blind with double fenestration, consisting of wire glass outside, ordinary window glass inside, in 1937 for the old Bulletin Building in Philadelphia. At that time it was necessary to estimate the solar heat gain.

In 1947 we performed a number of experiments on various types of fenestration and shading devices using a scale model and artificial sun. The results on a venetian blind and double fenestration were presented at the annual meeting in 1951[1]. This paper indicated a transmittance of 25% of the normal incident solar radiation on the outside surface of the outer glass. Experiments were made at a solar altitude of 35 deg.

In a number of installations since then, we have used and have recommended to others a factor of 30% normal incident. The reason for using 30% instead of 25% is partly for a margin of safety because of the experimental method and partly in accordance with the reasoning of Messrs. Parmelee and Ashley in their discussion of a previous paper[2] presented to the American Society of Refrigerating Engineers on this subject.

The values we have used appear to be confirmed by the present study.

In Research Paper No. 1485[3] Messrs. Parmelee and Vild have noted the agreement between the results with our solar model and the laboratory calorimeter on other types of fenestration, which leads to the conclusion that the solar model would be a relatively simple means of establishing at least an order of magnitude value for any proposed new types of fenestration and shading devices.

CLOSURE BY AUTHOR SCHUTRUM: Mr. Leopold has pointed out that there is good agreement between the results of his early study and this present study. In his paper Test E, column 29 of Table A-3 shows a calculated room load of 30%. A KD value estimated from this study for the 55 degree slat angle would be about 0.25. The diffuse factor would be considerably higher making the total solar gain in the order of 30%, depending upon the amount of diffuse radiation. It is reassuring that these results agree so closely. I must apologize for overlooking this excellent paper of Mr. Leopold's.

[1] Design Factors in Panel and Air Cooling Systems, by Charles S. Leopold. Transactions Vol. 57, 1951; Paper No. 1409.

[2] Mechanism of Heat Transfer, Panel Cooling, Heat Storage, Part II, Solar Radiation by Charles S. Leopold. June 1948 issue of REFRIGERATING ENGINEERING.

[3] Design Data for Slat-Type Sun Shades for Use in Load Estimating, by Messrs. C. V. Parmelee and D. J. Vild. 1953 Transactions, Vol. 59.

1722

No. 1722

Proposed Pipe Friction Chart for High-Temperature Water Systems

T. C. MIN
Member ASHRAE

P. J. POTTER
Member ASHRAE

The friction chart is a fundamental tool for designing any fluid system. Especially in a high-temperature system, it is almost indispensable due to the wide range of water temperature and density. The friction loss for 300 F water, for instance, flowing through a 3-in. pipe at a mass flow rate of 20,000 lb-mass per hr differs from that for 500 F water flowing through the same size of pipe at the same mass flow rate because of the differences in the thermal-physical properties of the water. Likewise, for the same pipe and velocity, the mass flow rate of 300 F water differs from that for 500 F water.

Since the calculation of friction losses for a wide range of temperature, velocity and pipe sizes is tedious and troublesome, the need of a friction chart becomes apparent.

T. C. Min is Associate Professor, Mechanical Engineering, Auburn University. P. J. Potter was formerly Head Professor of Mechanical Engineering, Alabama Polytechnic Institute. This paper was presented at the ASHRAE Annual Meeting, Vancouver, B.C., June 13-15, 1960.

Currently available friction charts for high-temperature water systems[1, 2, 3, 4, 5] appear to have two disadvantages: first, they cover a range of temperatures up to only 350 F, and secondly, their theoretical development is open to question[6, 7, 8, 9, 10, 11].

It is, therefore, the purpose of this paper to present a friction chart which would fulfill the following requirements[5, 12]:

1. Applicable for overall system design.
2. Cover the wide temperature range (200-500 F) encountered in practice in high-temperature water systems.
3. Applicable for a wide range of sizes and water velocities, and be independent of pipe wall thickness.
4. Based upon currently accepted friction data.
5. Consistent with indisputable engineering principles.
6. Styled for convenient use

and simplicity without sacrificing engineering accuracy.

Any chart which is to be of real value must have distinct features which aid functionally in problem analysis. This is particularly true of the proposed chart and will be demonstrated later in the paper.

PROPOSED CHART

The calculation for the loss of pressure head due to friction for fluid flowing in a pipe is quite straightforward. The equation used for the calculation is generally known as the Darcy-Weisbach equation.

$$\Delta P = f_{DW}\left(\frac{L}{D}\right)\frac{\rho_t U^2}{2g_c} \qquad (1)$$

or

$$H_{t(t)} = \frac{\Delta P}{\rho_t}\frac{g_c}{g} = f_{DW}\left(\frac{L}{D}\right)\frac{U^2}{2g} \qquad (2)$$

The chart is made for steady flow of water in commercially clean steel or wrought iron pipe*, running full and using 1.5×10^{-4} ft as its absolute roughness, e[10, 14]. The thermal-physical properties of water are taken from References (1, 15, 16). If the velocity, the size of the pipe, and water temperature (the temperature determining the density and absolute viscosity) are known, the Reynolds number N_{Re} can be determined. Knowing the Reynolds number and relative roughness e/D the Darcy-Weisbach friction factor f_{DW}† can be found in Reference 14.

The friction loss is then computed by Equation 1 if it is expressed in lb/sq ft. If the friction loss in feet of head of the water flowing is desired, then Equation 2 may be used. In the case of expressing friction loss in terms of feet of 62 F water, the conversion may be accomplished by the relation

$$h_{w(t)} = \frac{h_{t(t)}\rho_t}{\rho_w} \qquad (3)$$

The mass flow rate in lb_m per hr is calculated by

$$M_t = \frac{3600\pi D^2 U_{\rho t}}{4} \qquad (4)$$

In terms of the volume flow (in U.S. gallons per minute), Equation 6 becomes

$$V = \frac{60\pi D^2 U}{4 \times 0.1337} \qquad (7)$$

The chart as shown in Fig. 1 is plotted on logarithmic coordinates. There are 2 horizontal scales and 3 vertical scales. The lower horizontal coordinate is the mass flow rate of water in lb_m/hr, hereafter referred to as scale (a).

In low-temperature water systems, the heat conveyed in Btu/hr is usually employed as one coordinate of the friction chart. Thus, for the customray 20 F temperature drop, each U.S. gal of water pro-

* Copper pipe deteriorates rapidly under high temperature and is not suitable for high-temperature water application (13).

† Should one use Fanning's equation for the calculation of friction loss

$$\Delta P = 4fr\left(\frac{L}{D}\right)\frac{\rho_t U^2}{2g_c} \qquad (5)$$

or

$$H_{t(t)} = 4fr\left(\frac{L}{D}\right)\frac{U^2}{2g} \qquad (6)$$

then the friction factor f_{DW} found in Reference 14 should be divided by 4 to obtain Fanning friction factor f_t or a special chart for Fanning friction factor such as the one in Reference 17 should be consulted.

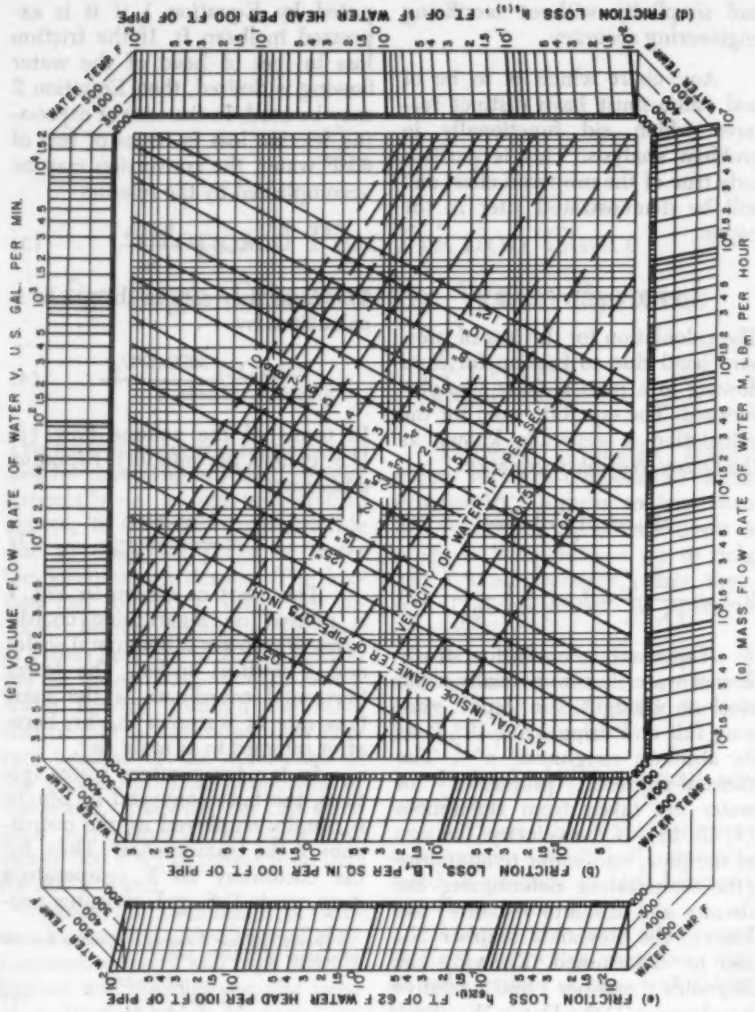
(d) FRICTION LOSS $h_{f(t)}$, FT OF IF WATER HEAD PER 100 FT OF PIPE
(c) VOLUME FLOW RATE OF WATER V, U.S. GAL. PER MIN.
(e) MASS FLOW RATE OF WATER M, LB_m PER HOUR
(b) FRICTION LOSS, LB/SQ IN PER 100 FT OF PIPE
(a) FRICTION LOSS h_{f62^0}, FT OF 62 F WATER HEAD PER 100 FT OF PIPE
WATER TEMP F
ACTUAL INSIDE DIAMETER OF PIPE, INCH
VELOCITY OF WATER, FT PER SEC

Fig. 1. Friction loss for high-temperature water in commercial steel pipe (pipe sizes are referred to actual inside diameters)

vides approximately 10,000 Btu/hr of heating[1, 18, 19, 20]. The temperature drop employed in high-temperature water systems may vary up to 200 F deg[1, 21]. Therefore, the heat conveyed certainly is no longer a parameter for friction loss.

Three friction loss scales are employed as vertical coordinates. The use of absolute units of pressure loss is desirable for pipe sizing when the fluid temperature varies throughout the system. Scale (b) expresses friction loss in lb-force/sq in. per 100 ft equivalent length of pipe. Scale (e) uses another absolute system of units, i.e., feet of head of 62 F water/100 ft equivalent length. The temperature of 62 F has become accepted because at that temperature a British Imperial gal of water (277.42 cu in.) weighs 10 lb. Therefore, 62 F is still an accepted standard in England[10]. There were also charts[1, 2, 3] prepared in this country that adopted the 62 F water as the unit for pipe friction.

The other scales on the chart, Fig. 1, are: scale (d) employing units of feet of water at its actual temperature per 100 ft of equivalent pipe for friction loss, and scale (c) in which the volume flow is given in US gpm. Use of all of the scales is illustrated later.

In each of the 5 coordinates just mentioned, 4 temperature subscales, 200, 300, 400, and 500 F are provided.

The pipe sizes cover a range from ½ in. up to 12 in. of the actual inside diam. This was selected as one parameter instead of nominal size so that the chart would be independent of pipe wall thickness. A table of dimensions of welded and seamless steel pipe based on ASA Standard B.36-10 is included as Table I for reference. It is under-

TABLE I. DIMENSIONS OF WELDED AND SEAMLESS STEEL PIPE[a]

Normal Pipe Size, Inches	Outside Diameter, Inches	Inside Diameter, Inches								
		Sched 20	Sched 30	Sched 40	Sched 60	Sched 80	Sched 100	Sched 120	Sched 140	Sched 160
½	0.840	—	—	0.622	—	0.546	—	—	—	0.466
¾	1.050	—	—	0.824	—	0.742	—	—	—	0.614
1	1.315	—	—	1.049	—	0.957	—	—	—	0.815
1¼	1.660	—	—	1.380	—	1.278	—	—	—	1.160
1½	1.900	—	—	1.610	—	1.500	—	—	—	1.338
2	2.375	—	—	2.067	—	1.939	—	—	—	1.689
2½	2.875	—	—	2.469	—	2.323	—	—	—	2.125
3	3.500	—	—	3.068	—	2.900	—	—	—	2.624
3½	4.000	—	—	3.548	—	3.364	—	—	—	—
4	4.500	—	—	4.026	—	3.826	—	3.624	—	3.438
5	5.563	—	—	5.047	—	4.813	—	4.563	—	4.313
6	6.625	—	—	6.065	—	5.761	—	5.501	—	5.189
8	8.625	8.125	8.071	7.891	7.813	7.625	7.439	7.189	7.001	6.813
10	10.750	10.250	10.136	10.020	9.750	9.564	9.314	9.064	8.750	8.500
12	12.750	12.250	12.090	11.938	11.626	11.376	11.064	10.750	10.500	10.126

[a] Based on ASA Standard B36.10–1950.

[b] The Schedule Numbers are approximate values of 1000 P/S, where P = maximum internal service pressure, psi, and S = allowable stress in material, psi. The dimensions of "standard-weight" steel pipe, which has been the traditional commercial terminology, in sizes 10 in. and smaller are identical with those for Schedule 40 of ASA-B36.10. The dimensions of "extra-strong" pipe 8 in. and smaller are identical with Schedule 80 of ASA-B36.10. "Double-extra-strong" pipe has no corresponding schedule number.

TABLE II[a] (CONDENSED) FRICTION LOSS DUE TO FLOW OF HIGH-TEMPERATURE WATER IN COMMERCIAL STEEL PIPE

Velocity of Water, Feet Per Second	Actual Inside Diam. of Pipe, Inches	Water Temperatures: 200 F — Friction Loss, Ft of Head Per 100 Ft of Pipe: 200 F Water	200 F — 62 F Water	Water Flow Rate, Lbm Per Hour	Water Temperatures: 300 F — Friction Loss, Ft of Head Per 100 Ft of Pipe: 300 F Water	300 F — 62 F Water
V	d	$h_{(200)(200)}$	$h_{(62)(200)}$	$M_{(200)}$	$h_{(300)(300)}$	$h_{(62)(300)}$
↑	½	1.01×10^{1}	9.71×10^{0}	8.90×10^{3}	9.96×10^{0}	9.16×10^{0}
	¾	6.09×10^{0}	5.87×10^{0}	1.99×10^{3}	5.93×10^{0}	5.45×10^{0}
	1	4.21×10^{0}	4.06×10^{0}	3.57×10^{3}	4.15×10^{0}	3.81×10^{0}
	1¼	3.15×10^{0}	3.04×10^{0}	5.54×10^{3}	3.09×10^{0}	2.84×10^{0}
	1½	2.54×10^{0}	2.45×10^{0}	7.97×10^{3}	2.41×10^{0}	2.21×10^{0}
	2	1.77×10^{0}	1.71×10^{0}	1.42×10^{4}	1.72×10^{0}	1.58×10^{0}
3	2½	1.34×10^{0}	1.29×10^{0}	2.21×10^{4}	1.31×10^{0}	1.20×10^{0}
fps	3	1.07×10^{0}	1.03×10^{0}	3.19×10^{4}	1.05×10^{0}	9.67×10^{-1}
	4	7.55×10^{-1}	7.29×10^{-1}	5.67×10^{4}	7.22×10^{-1}	6.64×10^{-1}
	5	5.71×10^{-1}	5.51×10^{-1}	8.86×10^{4}	5.64×10^{-1}	5.19×10^{-1}
	6	4.59×10^{-1}	4.43×10^{-1}	1.28×10^{5}	4.48×10^{-1}	4.12×10^{-1}
	8	3.27×10^{-1}	3.16×10^{-1}	2.27×10^{5}	3.15×10^{-1}	2.89×10^{-1}
	10	2.48×10^{-1}	2.40×10^{-1}	3.54×10^{5}	2.43×10^{-1}	2.24×10^{-1}
↓	12	1.97×10^{-1}	1.90×10^{-1}	4.93×10^{5}	1.94×10^{-1}	1.79×10^{-1}
↑	½	1.74×10^{1}	1.67×10^{1}	1.19×10^{3}	1.72×10^{1}	1.58×10^{1}
	¾	1.05×10^{1}	1.01×10^{1}	2.66×10^{3}	1.03×10^{1}	9.51×10^{0}
	1	7.43×10^{0}	7.17×10^{0}	4.76×10^{3}	7.22×10^{0}	6.64×10^{0}
	1¼	5.46×10^{0}	5.27×10^{0}	7.39×10^{3}	5.25×10^{0}	4.83×10^{0}
	1½	4.38×10^{0}	4.22×10^{0}	1.06×10^{4}	4.22×10^{0}	3.88×10^{0}
	2	3.25×10^{0}	3.14×10^{0}	1.89×10^{4}	3.01×10^{0}	2.77×10^{0}
4	2½	2.33×10^{0}	2.25×10^{0}	2.95×10^{4}	2.27×10^{0}	2.09×10^{0}
fps	3	1.88×10^{0}	1.81×10^{0}	4.25×10^{4}	1.81×10^{0}	1.66×10^{0}
	4	1.31×10^{0}	1.26×10^{0}	7.56×10^{4}	1.27×10^{0}	1.17×10^{0}
	5	9.91×10^{-1}	0.96×10^{0}	1.18×10^{5}	9.61×10^{-1}	0.88×10^{0}
	6	7.96×10^{-1}	0.77×10^{0}	1.70×10^{5}	7.71×10^{-1}	0.71×10^{0}
	8	5.63×10^{-1}	0.54×10^{0}	3.02×10^{5}	5.56×10^{-1}	0.51×10^{0}
	10	4.36×10^{-1}	0.42×10^{0}	4.72×10^{5}	4.21×10^{-1}	0.39×10^{0}
↓	12	3.48×10^{-1}	0.34×10^{0}	6.57×10^{5}	3.43×10^{-1}	0.32×10^{0}
↑	½	2.70×10^{1}	2.61×10^{1}	1.48×10^{3}	2.61×10^{1}	2.40×10^{1}
	¾	1.63×10^{1}	1.57×10^{1}	3.32×10^{3}	1.60×10^{1}	1.47×10^{1}
	1	1.16×10^{1}	1.12×10^{1}	5.95×10^{3}	1.12×10^{1}	1.03×10^{1}
	1¼	8.31×10^{0}	8.02×10^{0}	9.23×10^{3}	8.17×10^{0}	7.51×10^{0}
	1½	6.65×10^{0}	6.42×10^{0}	1.33×10^{4}	6.53×10^{0}	6.00×10^{0}
	2	4.78×10^{0}	4.61×10^{0}	2.36×10^{4}	4.66×10^{0}	4.29×10^{0}
5	2½	3.62×10^{0}	3.49×10^{0}	3.69×10^{4}	3.53×10^{0}	3.24×10^{0}
fps	3	2.87×10^{0}	2.77×10^{0}	5.31×10^{4}	2.81×10^{0}	2.59×10^{0}
	4	2.00×10^{0}	1.93×10^{0}	9.45×10^{4}	1.97×10^{0}	1.81×10^{0}
	5	1.54×10^{0}	1.48×10^{0}	1.48×10^{5}	1.48×10^{0}	1.36×10^{0}
	6	1.22×10^{0}	1.18×10^{0}	2.13×10^{5}	1.18×10^{0}	1.09×10^{0}
	8	8.74×10^{-1}	0.84×10^{0}	3.78×10^{5}	8.62×10^{-1}	0.79×10^{0}
	10	6.76×10^{-1}	0.65×10^{0}	5.90×10^{5}	6.48×10^{-1}	0.60×10^{0}
↓	12	5.40×10^{-1}	0.52×10^{0}	8.21×10^{5}	5.24×10^{-1}	0.48×10^{0}

[a] Table II as presented herewith is condensed from the Complete Table II as prepared by the authors. The complete table is arranged for water temperatures of 200, 250, 300, 350, 400, 450, and 500 F, whereas the condensed table omits the 250, 350, and 450 columns. Also the condensed table shows values only for water velocities of 3, 4, and 5 fps, but the complete table includes values for ½, 1, 1½, 2, 3, 4, 5, 6, 7, 8, 9, and 10 fps. Processed copies of complete Table II are obtainable from ASHRAE Headquarters for $1.00 each.

stood, however, that the actual inside diam of pipe would vary with manufacturer's tolerance and temperature effect on the pipe material[12].

Also included is Table II, which provides more precise direct reading of friction loss in pipe either in head of actual water, or 62 F water, with water temperatures at intervals of every 50 deg. The table is included here for dual

TABLE II (Continued)

Water Temperatures							
300 F	400 F			500 F			
Water Flow Rate, Lb_m Per Hour	Friction Loss, Ft of Head Per 100 Ft of Pipe		Water Flow Rate, Lb_m Per Hour	Friction Loss, Ft of Head Per 100 Ft of Pipe		Water Flow Rate, Lb_m Per Hour
	400 F Water	62 F Water		500 F Water	62 F Water	
$M_{(300)}$	$h_{f(400)\,(400)}$	$h_{f(62)\,(400)}$	$M_{(400)}$	$h_{f(500)\,(500)}$	$h_{f(62)\,(500)}$	$M_{(500)}$
8.48×10^3	9.56×10^0	8.23×10^0	7.94×10^3	9.56×10^0	7.52×10^0	7.25×10^3
1.90×10^4	5.82×10^0	5.01×10^0	1.78×10^4	5.82×10^0	4.58×10^0	1.63×10^4
3.40×10^4	4.08×10^0	3.51×10^0	3.19×10^4	4.03×10^0	3.17×10^0	2.91×10^4
5.28×10^4	2.95×10^0	2.54×10^0	4.94×10^4	2.94×10^0	2.31×10^0	4.52×10^4
7.59×10^4	2.39×10^0	2.06×10^0	7.11×10^4	2.37×10^0	1.87×10^0	6.50×10^4
1.35×10^5	1.69×10^0	1.45×10^0	1.26×10^5	1.69×10^0	1.33×10^0	1.15×10^5
2.11×10^5	1.28×10^0	1.10×10^0	1.97×10^5	1.27×10^0	9.98×10^{-1}	1.80×10^5
3.04×10^5	1.02×10^0	8.77×10^{-1}	2.84×10^5	1.01×10^0	7.92×10^{-1}	2.60×10^5
5.40×10^5	7.18×10^{-1}	6.18×10^{-1}	5.06×10^5	7.13×10^{-1}	5.61×10^{-1}	4.62×10^5
8.44×10^5	5.37×10^{-1}	4.62×10^{-1}	7.90×10^5	5.37×10^{-1}	4.22×10^{-1}	7.62×10^5
1.22×10^6	4.36×10^{-1}	3.75×10^{-1}	1.14×10^6	4.31×10^{-1}	3.39×10^{-1}	1.04×10^6
2.16×10^6	3.15×10^{-1}	2.71×10^{-1}	2.02×10^6	3.13×10^{-1}	2.46×10^{-1}	1.85×10^6
3.38×10^6	2.37×10^{-1}	2.04×10^{-1}	3.16×10^6	2.33×10^{-1}	1.84×10^{-1}	2.89×10^6
4.69×10^6	1.92×10^{-1}	1.65×10^{-1}	4.39×10^6	1.90×10^{-1}	1.50×10^{-1}	4.02×10^6
1.13×10^3	1.67×10^1	1.44×10^1	1.06×10^3	1.65×10^1	1.30×10^1	9.67×10^2
2.53×10^3	1.02×10^1	8.80×10^0	2.37×10^3	1.02×10^1	8.04×10^0	2.17×10^3
4.54×10^3	7.16×10^0	6.17×10^0	4.25×10^3	7.01×10^0	5.52×10^0	3.88×10^3
7.04×10^3	5.23×10^0	4.50×10^0	6.59×10^3	5.13×10^0	4.04×10^0	6.02×10^3
1.05×10^4	4.18×10^0	3.60×10^0	9.48×10^3	4.18×10^0	3.29×10^0	8.66×10^3
1.80×10^4	3.13×10^0	2.70×10^0	1.68×10^4	2.95×10^0	2.32×10^0	1.54×10^4
2.81×10^4	2.22×10^0	1.91×10^0	2.63×10^4	2.22×10^0	1.75×10^0	2.41×10^4
4.05×10^4	1.79×10^0	1.54×10^0	3.79×10^4	1.79×10^0	1.41×10^0	3.47×10^4
7.21×10^4	1.26×10^0	1.09×10^0	6.74×10^4	1.26×10^0	0.99×10^0	6.16×10^4
1.13×10^5	9.49×10^{-1}	0.82×10^0	1.05×10^5	9.49×10^{-1}	0.75×10^0	9.63×10^4
1.62×10^5	7.61×10^{-1}	0.66×10^0	1.52×10^5	7.56×10^{-1}	0.59×10^0	1.39×10^5
2.88×10^5	5.52×10^{-1}	0.48×10^0	2.70×10^5	5.48×10^{-1}	0.43×10^0	2.47×10^5
4.50×10^5	4.18×10^{-1}	0.36×10^0	4.21×10^5	4.12×10^{-1}	0.32×10^0	3.85×10^5
6.26×10^5	3.38×10^{-1}	0.29×10^0	5.86×10^5	3.33×10^{-1}	0.26×10^0	5.35×10^5
1.41×10^3	2.60×10^1	2.24×10^1	1.32×10^3	2.57×10^1	2.02×10^1	1.21×10^3
3.17×10^3	1.57×10^1	1.35×10^1	2.96×10^3	1.56×10^1	1.23×10^1	2.71×10^3
5.67×10^3	1.11×10^1	9.56×10^0	5.31×10^3	1.08×10^1	8.51×10^0	4.85×10^3
8.80×10^3	8.05×10^0	6.93×10^0	8.24×10^3	7.87×10^0	6.19×10^0	7.53×10^3
1.27×10^4	6.50×10^0	5.59×10^0	1.18×10^4	6.46×10^0	5.09×10^0	1.08×10^4
2.25×10^4	4.59×10^0	3.95×10^0	2.11×10^4	4.54×10^0	3.57×10^0	1.92×10^4
3.52×10^4	3.45×10^0	2.97×10^0	3.27×10^4	3.43×10^0	2.70×10^0	3.01×10^4
5.06×10^4	2.80×10^0	2.41×10^0	4.74×10^4	2.80×10^0	2.20×10^0	4.33×10^4
9.01×10^4	1.95×10^0	1.68×10^0	8.43×10^4	1.96×10^0	1.54×10^0	7.70×10^4
1.45×10^5	1.47×10^0	1.27×10^0	1.32×10^5	1.47×10^0	1.16×10^0	1.20×10^5
2.03×10^5	1.17×10^0	1.01×10^0	1.90×10^5	1.17×10^0	0.92×10^0	1.73×10^5
3.60×10^5	8.33×10^{-1}	0.72×10^0	3.37×10^5	8.51×10^{-1}	0.67×10^0	3.08×10^5
5.63×10^5	6.48×10^{-1}	0.56×10^0	5.27×10^5	6.81×10^{-1}	0.54×10^0	4.81×10^5
7.82×10^5	5.21×10^{-1}	0.45×10^0	7.32×10^5	5.17×10^{-1}	0.41×10^0	6.69×10^5

purposes: first, for the substantiation of the data of the original calculation from which the chart was made; and second, for those who prefer to use a table instead of a chart.

USE OF THE FRICTION CHART

Example 1: Find the friction loss for a flow of 30,000 lb_m/hr of 400 F water through 100 feet of 2½-in. Schedule-80 pipe (2.323 in. ID).

Solution: From the intersection on scale (a) of the lines for 3×10^4 lb_m flow and for 400 F, proceed vertically to an imaginary diagonal line representing an inside diam of 2.323 in. A velocity of 5.3 fps is indicated for this point. From this point, proceed horizontally to the 400 F line of scale (b) to read a friction loss of 1.6 lb_f/sq in./100 ft of pipe.

If it is preferable to obtain the friction loss in units of ft of 62 F water ($h_{f(62)}$), proceed horizontally to the 400 F line of scale (c) to read 3.8 ft of 62 F

water. For the friction loss in ft of 400 F water ($h_{f(w)}$), use the 400 F line of scale (d) to read 4.4 ft of 400 F water per 100 ft of pipe.

When specifying pumps, it is advisable to give the flow in gpm rather than in lb_m/hr. The flow of 30,000 lb_m per hr may be converted into the flow in gpm by proceeding vertically from the original intersection of the 400 F and the 3 x 10^4 flow lines on scale (a) to scale (c) to obtain a value of 70 US gpm.

Example 2: Find the friction loss and volume flow of 30,000 lb_m/hr of 200 F water flowing through 2-in. Schedule-80 pipe (1.939-in. ID) which has an equivalent length of 150 ft.

Solution: From the intersection of the 200 F line and the 3 x 10^4 lb_m/hr flow line of scale (a), proceed vertically to an imaginary line for 1.939-in. inside pipe diam. From this intersection, which indicates a velocity of 6.8 fps, proceed horizontally to the left to read a friction loss per 100 ft of pipe of 3.8 psi on scale (b) or 8.9 ft of 62 F water on scale (e). Proceeding horizontally to the right indicates a friction loss of 9 ft of 200 F water on scale (d).

Since the pipe has an equivalent length of 150 ft, the friction loss will be 1.5 x 3.8 = 5.7 psi, or 13.3 ft of 62 F water, or 13.5 ft of 200 F water.

Scale (c) indicates a flow of 60 US gpm.

Example 3: A high-temperature hot water system includes the supply piping as given in Example 1, the return piping of Example 2, a pump* handling the water at 400 F, and heat exchangers having a pressure drop of 5 psi. Find the pump capacity, pump developed head, and pump input horsepower if the pump efficiency is 70%.

Solution: Since the pump is handling the water at 400 F, the capacity will be 70 US gpm from Example 1.

Where the system involves water at several temperatures, it is most convenient to use head in either psi or ft of 62 F water. Selecting the former, the pump developed head will be 1.6 + 5.7 + 5 = 12.3 psi. Converting this into ft of 400 F water (since the pump operates at 400 F), produces 12.3 x 144/53.65 = 33 ft. (53.65 is the density of 400 F water). The pump input is

$$\frac{\text{gpm x developed head in psi}}{1714 \times \text{efficiency}} = \frac{70 \times 12.3}{1714 \times 0.70} = 0.71 \text{ hp.}$$

Note that no allowance has been made on the pump head or capacity for pump wear or contingencies, since this is a matter of engineering judgment.

FRICTION FACTORS

Since the reliability of a friction chart depends upon that of the friction factor data on which it was based, it seems in order to discuss first the friction factor. For the flow of a fluid in long, straight, uniform pipes, the relationship of friction factor, Reynolds Number and relative roughness was first used by Stanton in 1914[22]. The only difficulty was the definition of a reliable index of pipe roughness. Nikuradse[23] used pipes of an artificially-made roughness pattern and by his systematic tests demonstrated the relationship between f_{DW} and N_{Re} and relative roughness e/D. His artificially-made roughness pattern was obtained by fixing a coating of uniform sand grains to the pipe wall, thus giving an easily measurable index of absolute roughness e, the diameter of the sand grain. Although the sand grain roughness of Nikuradse is quite different from that of commercial pipes, it provides a solid basis for quantitative measurement of roughness effects.

* For location of pump relative to the compression tank and boiler, see Reference 21a.

Colebrook[24, 25] used the concept of absolute and relative roughness by Nikuradse and applied it toward a quantitative measurement of commercial pipe roughness. He compared his data on friction loss of commercial pipes with Nikuradse's data on pipes with artificially-made roughness and computed an equivalent sand grain size or equivalent absolute roughness, e, of the pipes.

In his paper, Colebrook presented his data by plotting $1\sqrt{f_{DW}} - 2 \log_{10} D/e$ vs $(e/D)(N_{Re}\sqrt{f_{DW}})$ in a single curve which may be expressed

$$\frac{1}{\sqrt{f_{DW}}} - 2 \log_{10} \frac{D}{e} = 1.14 - 2 \log_{10} \left[1 + \frac{9.35}{N_{Re} \left(\frac{e}{D}\right) \sqrt{f_{DW}}} \right] \quad (8)$$

or simply

$$\frac{1}{\sqrt{f_{DW}}} = -2 \log_{10} \left[\frac{2517}{N_{Re}\sqrt{f_{DW}}} + \frac{0.269e}{D} \right] \quad (8a)$$

This equation, known as the Colebrook and White function, is hardly suitable for engineering use[14, 26]. Rouse[14, 27, 29, 30] replotted it into a family of curves with different values of $2D/e$ with $1\sqrt{f_{DW}}$ as abscissa and $N_{Re}\sqrt{f_{DW}}$ as ordinate. He also adopted a curved logarithmic coordinate by plotting N_{Re} vs f_{DW} in the same figure. The plot, however, was considered inconvenient and troublesome for practical usage.

Moody[14] later modified the presentation by plotting the same data in conventional rectangular coordinates using f_{DW} vs N_{Re} in a family of curves with different relative roughness e/D. The latter apparently is more convenient to use and has won general acceptance in both elementary[16, 28] and advanced[20, 21] engineering literature here and in England[10, 12].

The proposed chart presented with this paper was prepared by using Moody's friction factor chart. As just mentioned, however, the pressure drop due to friction should be the same regardless of the use of friction factor from Colebrook's, Rouse's or Moody's paper.

There are a few other friction factor data upon which some friction charts[1, 2, 3, 4, 5] were based. One of the empirical formulas used for pipe friction calculation in engineering practice is the Hazen-Williams equation (Reference 32) which is applicable for flow of water only, as follows:

$$U = 1.318 C_{HW} (r_h)^{0.63} \left(\frac{h_{f(l)}}{L}\right)^{0.54} \quad (9)$$

where C_{HW} is a roughness coefficient. It is, however, not evident whether C_{HW} is a measure of absolute or relative roughness, whether there is any effect of Reynolds number in the equation, and whether it applied only to the turbulent region.

In order to be comparable with other friction factor data[3, 14, 25, 27, 32, 34, 35], Vennard[28] transformed the Hazen-Williams equation to

$$f_{DW} = \frac{1090}{C_{HW}^{1.85} N_{Re}^{0.15}} \quad (10)$$

For clean new steel pipe, C_{HW} is 140

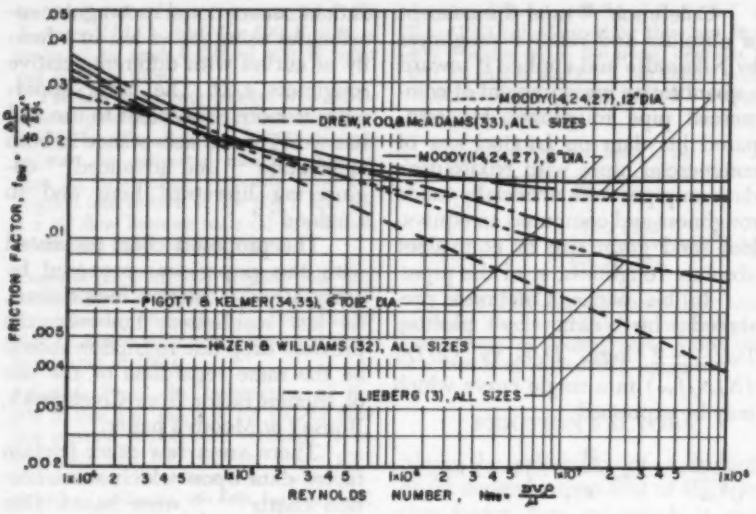

Fig. 2. Comparison of friction factor (f_{DW}) for fluid flowing in new clean commercial steel pipe

(5) and therefore

$$f_{DW} = \frac{0.1556}{N_{Re}^{0.16}} \qquad (11)$$

Equation 11 implies that the size of the pipe does not have an effect on the friction factor so long as the material of the pipe and the Reynolds number remain unchanged. Furthermore, the values of C_{HW} given for different pipe materials imply that brass is rougher than the best cast iron, which is not[24].

Krew, Koo, and McAdams[33] gave an equation of friction factor for turbulent flow in clean commercial steel pipe as

$$f_F = 0.00307 + 0.1886N_{Re}^{-0.32} \qquad (12)$$

or

$$f_{DW} = 0.01228 + 0.7544N_{Re}^{-0.32} \qquad (13)$$

Leiberg[3] used a friction factor as follows

$$f_F = \frac{0.0650}{N_{Re}^{0.230}} \qquad (14)$$

or

$$f_{DW} = \frac{0.26}{N_{Re}^{0.230}} \qquad (15)$$

for the base of his friction chart. The source of the equation is not given.

All the previously mentioned 3 sources of information on friction factor appear to be lacking of a logical basis as pipe size and, consequently, the relative roughness is completely disregarded.

Piggott and Kemler[34,35] presented the friction factor data by charts and plotted the f_{DW} vs N_{Re} for different material of pipe and a certain range of pipe size. How-

ever, they recognized the relative roughness to only a certain extent. For instance, in the range 6- to 12-in. pipe, the friction factors are the same for fluids flowing in steel pipe at a given Reynolds number.

Fig. 2 shows the friction factors f_{DW} vs N_{Re} for all of the investigators mentioned.

In view of this comparison, the friction factor chart prepared by Moody has been used in the calculations presented with this paper because it includes the effects of relative roughness and Reynolds number and has been generally accepted as being the most reliable[10, 20, 20, 21]

FRICTION CHART

In order to justify the proposal of a new chart, critical appraisal of presently available friction charts was made.

One—Reference 1—provides a friction chart for 300 F water flowing through Schedule-40 steel pipes. The values given in the chart are based on the absolute roughness, e, of steel pipe of 0.000015 ft which is considered too low[4, 7, 8, 10, 14]. The generally accepted absolute roughness for new clean steel or wrought iron pipe is 0.00015 ft[5, 10]. Due to the low absolute roughness used in making the chart of Ref. (1), the friction loss values are about 35% too low.

Another continental reference (2) gives a friction chart for 300 F water through pipes. The material of pipe, its absolute roughness, the thickness of the pipe, and the friction factor used are not given. The values for 300 F water are also too low (varying 23 to 30% low) for steel pipe.

A third, Reference 3, also gives a friction resistance chart for 300 F water in Schedule-40 steel pipe. It is based on Equation 14, and the values are about 20% too low. Recently, two more friction charts became available. One[4], based on Piggott and Kemler friction data, appears to give low values of friction loss. The other[9] was based on the Williams-Hazen equation. The water temperature, upon which the chart was based, was not designated. Also, the thickness of pipe wall was not given. Although it is shown in Fig. 2 that the friction factor f_{DW} obtained from the Williams-Hazen equation is lower than that from Moody's or Colebrook-White's data, the friction loss from the chart in Reference 5 is slightly greater than the authors' proposed chart which is based upon Moody's friction factor. The reason for this is not readily understandable.

Table III shows a comparison of values of friction loss from available friction charts. In order to make all data comparable, the friction loss was converted to feet of head of 62 F water when the water flowing in the pipe is at 300 F. Also, new clean Schedule-40 steel pipe, designated as nominal diam, was used.

The previously mentioned continental Reference 2 also gives a correction factor chart for water temperature of 200, 250 and 350 F. The chart appears to be confusing and could easily be misinterpreted. While it is actually based on constant mass flow rate, the param-

TABLE III. COMPARISON OF VALUES OF FRICTION LOSS FROM AVAILABLE FRICTION CHARTS FOR 300 F WATER IN SCHEDULE -40 COMMERCIAL PIPE

Pipe Size, Nominal	Velocity, fps	Friction Loss $h_{300/62}$, Ft of 62 F Water Head Per 100 Ft Pipe					
		Authors	ASHRAE Guide (1)	Sturdevant (4)	Lieberg (3)	Carrier (5)	Faber & Kell (2)
3 in.	0.5	0.032	0.028	—	—	—	—
	1	0.115	0.1	0.1292	—	0.1414	0.21
	2	0.445	0.35	0.43	0.44	0.546	0.483
	5	2.63	1.8	2.31	2.333	2.83	1.99
	8	6.5	4.2	5.43	5.33	6.95	4.59
	10	10.0	6.3	8.54	8.66	10.18	—
6 in.	0.5	0.0135	0.012	—	—	—	—
	1	0.0495	0.043	0.0556	—	0.0695	—
	2	0.188	0.15	0.178	—	0.2383	0.23
	5	1.13	0.78	1.062	1.024	1.29	0.919
	8	2.75	1.8	2.38	2.42	3.08	1.99
	10	4.3	2.6	3.445	3.665	4.66	—
12 in.	0.5	—	—	—	—	—	—
	1	0.022	0.018	0.0208	—	—	—
	2	0.084	0.064	0.0775	—	—	—
	5	0.50	0.34	0.421	0.433	—	0.459
	8	1.23	0.78	1.016	1.033	—	0.919
	10	1.9	1.2	1.438	1.6	—	—

eters used are velocity and pipe size instead of mass flow rate and pipe size. In addition, the parameter velocity in the chart is not the average velocity of water at its actual temperature flowing in a certain size of pipe; rather it is the average velocity of 300 F water flowing in the same pipe with the same mass flow rate. Besides, the code of pipe applicable to this chart is not given (presumably class C or B black steel pipe of British standards).

References 1 and 3 also employ the temperature correction factor chart originally given in Reference 2. With no explanation of the intricate use of the chart given in the mentioned references, one would presume that the velocity in the chart is the actual average velocity of water at its temperature flowing in the pipe. The correction thus obtained would be entirely different from that intended.

In a recent revision[20] of Reference 2 the temperature correction chart is deleted. Replacing the old friction loss table for 300 F water is a new one also for 300 F water. In the new table, the parameters used are pipe size in inches (nominal) of black steel Class C pipe and the mass flow rate. No velocity scale is provided. The mass flow rates are essentially expressed in an auxiliary manner as they are not designated in a round number of lb-mass/hr. The values of friction loss in pipe in the table based on 62 F water head seem to be slightly low (varying from 10 to 20%); besides, the range of mass flow rate (velocity in actual sense) is relatively small.

From the foregoing discussion, it is indicated that values from other friction charts are generally too low and could lead to underdesigning a system. Those charts cover a range of temperature up to 350 F only, and apply to a speci-

fied thickness of steel pipe.

In closing, the authors do not claim to offer anything particularly new and original; their aim merely being to furnish, by the use of the now accepted friction factor data with relative roughness concept[14, 20, 27, 29, 31], a friction chart for overall system design in a manner consistent with engineering principles.

The high-temperature water system holds considerable promise for large installations. It has recently received more attention, particularly since the High-Temperature Water Symposium held at the Annual Meeting of the American Society of Heating and Air-Conditioning Engineers at Pittsburgh in January, 1958. The authors trust that this paper may also indirectly stimulate more interest in the high-temperature water system.

ACKNOWLEDGMENT

It is a pleasure to acknowledge the suggestions and encouragement received from the members of the Research Advisory Committee on Steam and Hot Water Heating ASHRAE. The authors wish to thank particularly G. F. Carlson and H. A. Lockhart of Bell and Gossett Co.; H. G. Mitchell of the University of Minnesota; and Professor J. R. Carroll of the University of Illinois for their review of the manuscript and for their discussions which contributed to the preparation of the paper. To B. H. Marvet of Tennessee Valley Authority, appreciation is due for his helpful suggestion. Appreciation is also expressed to Dr. N. Ozisik, L. F. Schutrum, C. M. Humphreys and Director B. H. Jennings of the ASHRAE Research Laboratory for their comments and for checking the calculations.

NOMENCLATURE

C_{HW} = Hazen-Williams roughness coefficient, dimensionless.

D = Inside diameter of pipe, feet.

d = Inside diameter of pipe, inches.

d_n = Nominal diameter of pipe, inches.

f_{DW} = Darcy-Weisbach friction factor, dimensionless.

f_F = Fanning's friction factor, dimensionless.

g = Acceleration of gravity, 32.1739, feet per (second) (second).

g_c = Dimensional constant, 32.1739 (lb_m/lb_f) feet per (second) (second).

$H_{t_1(t_2)}$ = Loss of pressure head due to friction for water of temperature t_2 flowing in a pipe L feet long, feet of head of water at t_1.

$h_{t_1(t_2)}$ = Loss of pressure head in 100 feet of pipe due to friction for water of temperature t_2 flowing in a pipe, feet of head of water at t_1.

L = Equivalent length of pipe, feet.

M_t = Mass flow rate of water at temperature t, pounds-mass per hour.

N_{Re} = Reynolds number, $D\,U\rho/\mu$, dimensionless.

ΔP = Pressure drop due to friction for water flowing in a pipe L feet long, pounds-force per square foot.

r_h = Hydraulic radius, feet; (equals cross-section of stream divided by wetted perimeter; for a circular pipe $r_h = D/4$).

t = Temperature of water, Fahrenheit.

V = Volume flow rate of water, US gallons per minute.

U = Velocity of water, feet per second.

e = Absolute roughness, feet.

ρ_t = Density of water at temperature t, pounds-mass per cubic foot.

μ = Viscosity of water, pounds-mass per (foot) (second).

REFERENCES

1. HEATING, VENTILATING, AIR CONDITIONING GUIDE, 1959 (published by AMERICAN SOCIETY OF HEATING AND AIR-CONDITIONING ENGINEERS, pp. 414-415, 391-396, 405-406, 410).

2. *Heating and Air Conditioning of Buildings*, by Oscar Faber and J. R. Kell, (Published by The Architectural-Press, Westminster, England, 1943, p. 385, 386, 387, 388).

3. High Temperature Water, Part III and IV Piping and Distribution Design, by Owen S. Lieberg (*Air Conditioning, Heating and Ventilating*, Vol. 52, No. 11, November 1955, p. 86).

4. Personal Communication (with B. L. Sturdevant of Stanley Engineering Company, Muscatine, Iowa, March 11, 1959).

5. Modern Air Conditioning, Heating, and Ventilating, by W. H. Carrier, R. E. Cherne, W. A. Grant, W. H. Roberts, (published by Pitman Publishing Corporation, 3rd edition, 1959, pp. 228-229).

6. Personal Communication (with C. M. Humphreys of ASHRAE Research Laboratory, Cleveland, Ohio, March 18, 1958).

7. Personal Communication (from N. Ozisik of ASHRAE Research Laboratory, Cleveland, Ohio, March 26, 1958).

8. Personal Communication (from B. H. Marvet of Tennessee Valley Authority, Knoxville, Tennessee, February 13, 1958).

9. Personal Communication (with G. F. Carlson of Bell and Gossett Co., Morton Grove, Illinois, December 30, 1958).

10. New IHVE Pipe Sizing Data for Water Flow, by P. L. Martin, (*IHVE Journal*, Vol. 23, February, 1956, p. 401).

11. High-Temperature Water—A Symposium Bulletin (published by AMERICAN SOCIETY OF HEATING AND AIR-CONDITIONING ENGINEERS, 1958).

12. An Inquiry into the Possibility of Presenting Unified Fluid Flow in Pipes Data, by H. G. Mitchell, (prepared for the Sub-Committee on High-Temperature Water of the ASHRAE Research Advisory Committee on Steam and Hot Water Heating and Professor J. R. Carroll, Sub-Committee Chairman, April, 1959, University of Illionis).

13. *Mechanical Engineers' Handbook*, by L. S. Marks, (published by McGraw-Hill Book Co., Inc., New York, N. Y., 6th edition, 1958, pp. 8-176).

14. Friction Factors for Pipe Flows, by L. F. Moody, (*ASME Transactions*, Vol. 66, 1944, pp. 671-694).

15. *International Critical Tables*, (published by McGraw-Hill Book Co., Inc., New York, N. Y., 1926-30).

16. *Introduction to Heat Transfer*, by A. I. Brown and S. M. Marco, (published by McGraw-Hill Book Co., Inc., New York, N. Y., 3rd edition, 1958, p. 82, 107-109, 305).

17. *Heat Transmission*, by W. H. McAdams, (published by McGraw-Hill Book Co., 3rd edition, 1954, p. 145, 156).

18. *Heating and Air Conditioning*, by B. H. Jennings, (published by International Textbook Co., Scranton, Pa., 1956, p. 254-255).

19. *Handbook of Air Conditioning Heating and Ventilating*, by Clifford Strock and W. B. Foxhall, (published by Industrial Press, New York, N. Y., 1959, p. 4.153-154).

20. *Air Conditioning* and *Refrigeration*, by Burgess H. Jennings and Samuel R. Lewis, (published by International Textbook Co., Scranton, Pa., 4th edition, 1958, p. 252, 264).

21. Hydronic Systems, by G. F. Carlson, (paper presented at the Marquette University Institute on Heating, Air Conditioning and Refrigeration, February, 1959).

21a. Pressure Effects of Pump Location Relative to the Compression Tank (Bulletin No. HR-456, Bell & Gossett Co., Morton Grove, Illinois).

22. Similarity of Motion in Relation to the Surface Friction of Fluids, by T. E. Stanton and J. R. Pannell, (*Transactions of Royal Society of London* (A), Vol. 214, 1914, p. 199).

23. Laws of Flow in Rough Pipes, by J. Nikuradse; translation of Stromungsgetze in Rauhen Rohren, *VDI-Forschungsheft*, 361, Beilage Zu "Forschung auf dem Gebiete des Ingenieurwesens" Ausgabe B Band 4, July/August, 1933, (*NACA* TM 1292, November, 1950).

24. Experiments with Fluid Friction in Roughened Pipes, by C. F. Colebrook and C. M. White, (*Proc. Roy. Soc.* (A), Vol. 161, (1937). pp. 367, 381).

25. Turbulent Flow in Pipes With Particular Reference to the Transition Region Between the Smooth and Rough Pipe Laws, by C. F. Colebrook, (*Journal Inst. Civil Eng.* (London), February, 1939, Vol. 11, p. 133).

26. *Elementary Fluid Mechanics*, by J. K. Vennard, (published by John Wiley & Sons, Inc., New York, N. Y., 1954, 3rd edition, pp. 189, 191).

27. Evaluation of Boundary Roughness, by H. Rouse, (*Proceedings* Second Hydraulic Conference, *University of Iowa Bulletin* 27, 1943).

28. Discussion of Friction Factors for Pipe Flow—by L. F. Moody, by H. Rouse, (*ASME Transactions*, Vol. 66, 1944, p. 680-682).

29. *Elementary Mechanics of Fluids*, by Hunter Rouse, (published by John Wiley & Sons, Inc., New York, N. Y., 1946, p. 201).

30. *The Dynamics and Thermodynamics of Compressible Fluid Flow*, by Ascher H. Shapiro, (published by The Ronald Press Co., New York, N. Y., Vol. 1, 1953, p. 184-185).

31. *Fluid Dynamics and Heat Transfer*, by James Knudsen and Donald L. Katz, (published by McGraw-Hill Book Co., New York, N. Y., 1958, p. 176-178).

32. *Hydraulic Tables*, by A. Hazen and G. S. Williams, (published by John Wiley & Sons, New York, N. Y., 3rd edition, 1920).

33. The Friction Factors for Clean Round Pipes, by T. B. Drew, E. C. Koo, and W. H. McAdams, (*Trans. Am. Inst. of Chem. Engrs.*, Vol. 28, 1932, p. 56-72).

34. The Flow of Fluids in Closed Conduits, by R. J. S. Piggott, (*Mechanical Engineering*, Vol. 55, 1933, pp. 497-501, 515).

35. A Study of the Data on the Flow of Fluid in Pipes, by E. Kemler, (*ASME Transactions*, Vol. 55, 1933, paper Hyd. 55-2, p. 7-32).

36. *Heating and Air Conditioning of Buildings*, by Oscar Faber and J. R. Kell, (published by The Architectural Press, Westminster, England, 3rd edition, 1957, p. 407).

DISCUSSION

PAUL L. GEIRINGER, Long Island City, N. Y. (Written): This paper by Professors Min and Potter presents a friction chart and table in a very convenient form, to estimate the pressure drop in pipe lines of high temperature water systems. These tables give friction drops for different water temperatures from 200 to 500 F. The form of the table and the presentation are very commendable.

Equally interesting is the comparison of the literature of the various friction factors. However, German and Swiss engineering literature, which is intimately connected with high temperature water design, and where high temperature water design originated, is not included in the list of references.

In general, calculations for water at a mean temperature of 300 F are sufficiently exact to estimate the pressure drop in district heating systems. 300 F represents a good and safe average between a supply temperature of 400 F and a return temperature of 220 to 250 F. Even in systems with somewhat lower supply temperatures, where the return temperature will be higher, a selection and calculation of resistances at a temperature around 300 F give friction factors which are only slightly above those which may be obtained by exact evaluation of assumed supply and return temperatures. To correctly estimate the return temperature is a considerable problem in itself, because the quality of water passing through the pipe lines tends to be overestimated and because the accumulation of the water, as well as the diversity factor, cannot be accurately determined.

It has been further experienced that high temperature water smooths out piping so that, after starting operation, the pressure drop in the line is reduced. A pressure drop reduction of 5% and more has been observed after several years.

We have designed high temperature water systems for about thirty years, and have found in general that the danger of overdesigning is much greater than that of underdesigning.

Moody and the authors of this paper recommend a roughness factor of 0.000150.

The authors also point out that the GUIDE table of the ASHRAE (1959) is based on a roughness factor of 1/10 of the above value, equal to 0.000015 ft. German publications give, for seamless steel pipe, roughness values of 0.01 to 0.05 mm, equal to 0.000033 to 0.000164 ft. (See Otto Kirschner, *Gas und Wasserfach* (1953) and Bruno Eck, *Technische Stroemungslehre* (1957)). It can be assumed that American pipe corresponds to the same roughness factor, especially if it has been subjected to the smoothing out action of the alkaline high temperature water. Whether the roughness value of the GUIDE, or the factor used by Kirschner, Moody, or others, are applicable, can be determined only by practical tests.

To the best of my knowledge, only few tests have been made. Around 1928-29, the Caliqua Waermegesellschaft, Berlin, conducted tests, based on which nomograms were prepared, which were used for thousands of high temperature water designs during the last thirty years. They have proven quite accurate, and their friction values do not deviate from the figures published in the ASHRAE GUIDE. On a few pipe dimensions they show higher pressure drop values. Some values of the GUIDE graph fall below the smooth line, which should be corrected. The data in the GUIDE are close to the smooth line.

Thorough tests were made at the Eidg. Technische Hochschule in Zurich, by Prof. Dr. Bruno Bauer and Ing. F. Galavics (published in 1936). These tests were conducted on a long district heating line and exact measurements were taken applying various water temperatures on a 106.5 mm (4.2 in.) line.

To compare the values obtained by Bauer and Galavics, and the data of the ASHRAE 1959 GUIDE, and those of Moody, I give in Table I the values for the same pipe diameters of 106.55 mm, equal to 4.2 in. The f values of the smooth curve are also given to show the deviation of the Bauer and Galavics results, and the Moody computation, from the smooth curve. This comparison indicates a 20% to 30% variation between the Moody data and data based on actual tests. No new tests with

TABLE 1

τ = ft²/sec. Kin. Viscosity at 300 F = 2.17 x 10⁻⁵ D = 106.5 mm = 4.2 in. V in ft/sec.	f = Value of Friction Factor of Darcy Equation			
	Re = 0.02 x 10⁵ V = 1.24 ft	Re = 0.398 x 10⁵ V = 2.47 ft	Re = 1 x 10⁵ V = 6.2 ft	Re = 2 x 10⁵ V = 12.4 ft
Bauer and Galavics	0.0155 100%	0.0141 100%	0.0130 100%	0.0128 100%
ASHRAE Guide	0.0157	0.0139	0.01205	0.0108
Smooth Line	0.0155	0.0137	0.0115	0.0103
Min & Potter (Moody	0.0185	0.0178	0.0172	0.0168
Deviation of Bauer & Galavics from Smooth Line	0.0000 0 %	0.0004 2.9 %	0.0015 13.1 %	0.0025 24.6 %
Deviation of Min and Potter from Smooth Line	0.0030 19.4	0.0041 30	0.0057 49.5	0.0065 64

high temperature water have been made to justify the increase of 20% to 30% of the friction factor beyond the presently-used values, as suggested by the authors.

It seems, therefore, that establishing friction factor curves based on essentially theoretical calculations does not yield satisfactory results in this case.

A further explanation why values of friction head used in high temperature water design do not deviate too far from the smooth line follows:

High temperature water design utilizes generally for smaller lines installed in heat exchangers, air heaters, etc., steel, arsenical copper, cupro-nickel, or Admiralty tubing. This tubing in sizes below 1 in. uses high velocities. Seamless pipe is used for piping and, here again, in the lower dimensions, low velocities are used and only in higher dimensions, higher velocities. The Reynolds Number exceeds rarely 5×10^5 and goes not far below 2×10^4. The lower Reynolds Numbers are always close to the smooth line, and the deviation becomes apparent only in the higher Reynolds Numbers in excess of 1.5×10^5, which correspond to the larger sizes and higher velocities.

The old tables which have served successfully for more than thirty years seem to present more closely the physical behavior of high temperature water. Nevertheless, at the moment I am preparing new tests to check the figures given in the light of the present knowledge. These data will be published shortly.

G. F. CARLSON, Skokie, Ill. (Written): Professors Min and Potter are to be congratulated on this paper. It is an important step toward the comparison of the various pressure drop charts and values which are now in common use. It can be presently said that there is no common denominator for pressure heads used in selection of pumps for hydronic systems and that the selected head will vary depending on which particular chart is used by the engineer. Discrepancies in various pressure drop charts applicable to high temperature water systems have been pointed out in this paper. There is a need for similar work on lower temperature systems in which even greater discrepancies would be found between the various charts now in use.

Professors Min and Potter have shown that pressure drop increases as temperature increases for a given mass flow rate at temperatures beyond approximately 250 F. This disproves some presently prevalent ideas that pressure drop decreases with increasing temperature because of a reduction in viscosity.

This paper is an important contribution to our knowledge concerning pressure drop, but contains some information and methods of presentation which should be discussed.

The pipe sizes are indicated as being "actual" rather than "nominal". This presents some problems in terms of use of the chart since the engineer must extrapolate between the lines shown to the imaginary nominal pipe size line that would actually be installed. In other words, the chart is based on ¾ in. pipe as having ¾ in. ID rather than the .824 dimension which applies to nominal Sch. 40 pipe size. This point should be made more strongly in the paper to avoid the possibility of engineers using the pipe size lines shown for nominal pipe size.

The paper contains a formula relating pump input power to developed head in psi. It would seem that the factor 1714 used in this formula applies only to a pump operating at 400 F. It should be pointed out that this is not a general formula but rather a specific relationship.

The paper contains three different expressions for pressure drop: friction loss, ft of water head per 100 ft of pipe; friction loss lb per sq in. per 100 ft of pipe; and friction loss in ft of 62 F water. As is pointed out in the paper, this chart is indicated for use on water systems which can have a considerable temperature difference between the supply and return piping. Professor Min and I have had previous discussions concerning the question of how the pressure drop for a 400 F supply main can be added to that for a 200 F return main so as to obtain the total pressure drop against which a pump must operate and for which a pump must be selected.

Professor Min has indicated in his paper that when supply and return main temperatures differ, it is most convenient to use pressure drops based on either psi or ft of 62 F water. It is my opinion that pump selection based on the use of either 62 F water head or psi is theoretically incorrect and that the chart illustrated in the paper would be simplified and made theoretically correct were the friction loss shown only in ft of water head (ft of water head at the water temperature flowing).

This is based on a belief that pump selection is a simple application of the first law of thermodynamics: energy in = energy out. The pressure drop chart is a description of energy lost by water as it flows through the piping circuit. In terms of energy, it is my belief that psi, when used in a friction loss sense, is an expression stating ft lb energy loss per cu ft volume flowing. If this is true, we cannot add supply main pressure drop in psi to return main pressure drop directly because the unit volumes change between the supply and the return mains. This would seem to be true for charts based on mass flow.

When piping pressure drop is expressed in ft head, the energy statement is ft lb energy loss per lb of water flowing. Since the mass flow rate through a piping circuit remains constant despite temperature change it is, in my opinion, consistent to add ft head to ft head without correction. This is because we are simply adding energy to energy.

Friction loss expressed in ft of 62 F water is a "corrected" expression for ft head at the water temperature flowing. Since ft head at the water temperature flowing is, in my opinion, a direct energy expression, the correction to 62 F water head converts something which is energy to a relationship which is not. Water head expressed in ft of 62 F water cannot be added directly when water

temperatures vary between supply and return mains without recorrection to the actual temperatures flowing.

It is my opinion that the theoretical hp required to pump water through a piping circuit must be constant regardless of pump location and for fixed temperature conditions of the supply and return piping. It will be found that theoretical required water hp changes depending on pump location when pipe temperature drops are defined in terms of either psi or ft of 62 F water and when supply and return main temperatures differ. It seems to me impossible for the total energy requirement to change because of pump location since the energy requirement is not dependent on the pump. The pump only supplies the necessary energy or power for a stated flow through a fixed piping circuit.

This discussion concerning friction drop nomenclature is not of great importance in terms of practical application since the difference between the various methods of describing pipe pressure drop is not large enough to cause real concern. It seems to me, however, that if pipe friction drop charts for hydronic systems are based only on ft of head at the water temperature flowing, a simplification of the pressure drop chart and of the method for pump selection will result. I cannot agree that the complications which result when pressure drop charts are based on either psi or ft of 62 F water are either necessary or correct.

It is hoped that the important work started by Professors Min and Potter in terms of evaluation of pressure drop charts will be continued. The next step would seem to be an evaluation of all the pressure drop charts which are now in use for the lower water temperature systems.

CLOSURE BY AUTHOR MIN: We wish to thank Mr. Geiringer and Mr. Carlson for their interest and remarks. Mr. Geiringer indicated that, from his experience, a pressure drop reduction of 5% and more was observed after several years. He found that, in general, the danger of over-designing is much greater than that of under-designing. However, A. T. Ippen* reported a 20% increase of surface roughness over a three-year period on a 4-in. diam galvanized steel pipe, while J. H. Keenan** reported a 15% increase of surface roughness over eighteen months on a 1-in. diam steel pipe. Furthermore, when the system is new, the pressure-drop reduction has not yet developed. When it becomes old, the pump wears off and its efficiency would likely drop off thus, perhaps, compensating if there is any reduction in pressure drop. In either case, it is questionable that a pump selected on the basis of 5% or more anticipated pressure reduction would work satisfactorily.

The justification of taking up the pipe friction chart in the present ASHAE GUIDE to prove the good agreement with German 1928-1929 nomograms*** is also debatable. After perusing Chapters 4 and 29 of the 1959 ASHAE GUIDE, Mr. Geiringer would probably agree with us that the chart in the GUIDE was prepared with the intention of employing the absolute roughness of 1.5×10^{-4} ft for commercial steel pipe. Nowhere in Chapters 4 and 29 (including references and bibliography) is mentioned the use of 1.5×10^{-5} ft as the absolute roughness for commercial steel pipe. The use of 1.5×10^{-5} ft for commercial steel pipe as the basis of the pipe friction chart in the GUIDE was interpreted in an authoritative correspondence (7)* to us merely as a probable incident, and was not backed by experimental data as far as we know. Incidentally, this same value of 1.5×10^{-4} ft was adopted by the Institute of Heating and Ventilating Engineers in England (10, 12) as the absolute roughness for commercial steel pipe.

Mr. Geiringer's remark on Moody's friction factor curves as the result of theoretical calculation needs to be certified. As mentioned in the paper, these curves were based upon the extensive experimental data from Colebrook and White in 1937 (24) and 1939 (25).

Mr. Geiringer also stated "very thorough tests were made at the Eidg. Technische Hochschule in Zurich, by Professor Dr. Bruno Bauer and Ing. F. Galavics (published in 1936)." Since neither the complete information necessary for searching the publication was given, nor the copies of original articles were made available upon our recent request to the discussor**, we are handicapped to make any concrete comment on this.

Nevertheless, we feel that any "reduction" to pipe surface roughness or to pressure-drop under actual operating conditions due to the effect of temperature or otherwise (aging, deterioration, etc.) must be handled with extreme care because of the inherent uncertainties involved, such as the homogeneity of pipe material, constituents of water, pipe fitting, and workmanship of installation. It is comparable to "correcting" the published thermal

* A. T. Ippen, "Discussion of Friction Factors for Pipe Flow", *Transactions of American Society of Mechanical Engineers*, Vol. 66, 1944, pp. 678-679.

** J. H. Keenan, "Friction Coefficients for the Compressible Fow of Steam", *Journal of Applied Mechanics*, Vol. 6, No. 1, March 1939, pp. A-11 to A-20.

* Numbers in parentheses apply to references in the text of the paper.

** See Footnote***.

*** Mr. Geiringer referred to four German publications in his written discussion. However, complete information necessary for searching the articles such as titles of the articles, names of the authors, names of the journals, numbers and months of the issues, years and page numbers were not given.

We requested this information and/or the copies of original articles from him about four weeks ago. Up to this writing we have not received any word about this essential information to warrant our effort to library search for foreign publications.

conductivity, K, and overall heat transfer coefficient, U, values of various insulations when designing a building to the anticipated deduction or increasing under actual weather conditions and after years of operation without ascertaining the contingency inherited, such as homogeneity of material, moisture content, workmanship of installation of insulation etc. It is certainly an area needing further research. We would invite Mr. Geiringer to publish his research as a paper for the Society.

Mr. Carlson stated that if pressure drops are expressed in ft head, they are direct energy expression, and could and should be added directly without correcting to ft head of same fluid and same temperature. We believe, however, pressure and energy are two entirely different properties. When pressure drops are expressed in ft head of fluid at certain temperatures, they are in relative units and can only be added when they are converted to the same base, i. e. expressed in ft head of same fluid and same temperature.

The other question was concerned with the variation of water hp of the pump with respect to pump location. The fact that water hp varies with pump location in a system with a constant mass flow rate but different supply and return water temperature, may at first seem to be apparently incorrect and in violation of the first law of thermodynamics. However, we must be reminded of the limitation of classical thermodynamics.

Thermodynamics deals only with states of systems, and makes no reference about the structure and thermal physical properties of matter and the mechanism of momentum, heat, and mass transfer. It is not concerned with the details of a process or cycle, but rather the states and relations among them.

For a HTW system with pipe friction loss of 112 ft head of 350 F water in the supply line, 106 ft head of 250 F water in the return line, and a mass flow rate of 400,000 lb_m/hr, for instance, the WHP for pump installed in supply line is

$$WHP = \frac{86.56 \times 897 \times 0.1337 \times 144}{33{,}000} = 45.4 \text{ hp}$$

or

$$WHP = \frac{224 \times 400{,}000}{33{,}000 \times 60} = 45.4 \text{ hp}$$

and WHP for pump in the return line

$$WHP = \frac{86.56 \times 847 \times 0.1337 \times 144}{33{,}000} = 42.8 \text{ hp}$$

or

$$WHP = \frac{215 \times 400{,}000}{33{,}000 \times 60} = 42.8 \text{ hp}$$

Considering this example of HTW circuit at a thermodynamic system, the thermodynamic analysis, or the first law of thermodynamics, would only reveal that the work done by the pump on the system equals the net heat subtracted from the system and nothing else. It is known from the fluid mechanics that the water hp required is 45.4 hp for a pump located in the supply line of the system, and 42.8 hp for a pump located in the return line. In other words, the net heat subtracted from the system using a supply pump is 2.6 x 42.4 x 60 or 6620 Btu/hr more than one using a return pump. But, this does not mean it is in violation of the first law. It merely indicates that the water temperature in the supply line after the pump should theoretically be about

$$\frac{45.4 \times 42.4 \times 60}{400{,}00 \times 1.044} + 350 \text{ or } 350.276 \text{ F}$$

instead of 350 F with a supply pump in the system; the return water remains at 250 F. Similarly, the water temperature in the return line after the pump should be about

$$\frac{42.8 \times 42.4 \times 60}{400{,}000 \times 1.0128} + 250 \text{ or } 250.268 \text{ F}$$

instead of 250 F if a return pump is installed; the supply water in this case remains at 350 F. Assumption of no heat loss or gain in the pipe line and pump housing is understood in both cases. Heat is added only at boiler and is subtracted at heat exchanger.

The example further demonstrates that the thermodynamic analysis will not reveal whether (or how) it could be accomplished in two identical HTW systems with a mass flow of 400,000 lb_m/hr, return water of 250 F and supply water of 350 F, but wherein a return pump is installed in one system and a supply pump of same WHP in the other (obviously, it is theoretically impossible). Problems of transport type are not capable of solution by thermodynamic reasoning alone, but require, in addition, analysis based on fluid mechanics, heat transfer, and mass transfer, depending upon the transport process involved.

We would like to point out, that even in an unusually large system such as the one given above, the difference in WHP based on supply or return water is within 5%. It is therefore only a matter of theoretical correctness and practical tolerableness.

We appreciate Mr. Carlson's suggestions and encouragement that we extend the pipe friction chart to include chilled-water, low temperature water, intermediate temperature, in addition to the high temperature system. A chart for a unified water system as such is under preparation.

1723

No. 1723

Electronic Computer Aids Calculation of Reaction Forces in a Scotch Yoke

V. G. FORIS B. W. HATTEN
Member ASHRAE

The Scotch yoke is a time-honored, simple mechanism for converting rotational to reciprocating motion. Its chief characteristics are that it provides simple harmonic motion with respect to crank rotation, and is capable of accommodating relatively large variations in perpendicularity between the cylinder bore and the crankshaft.

The yoke has found its way into countless applications, but the primary concern here is with the small compressors used in household refrigerators and freezers. Specifically, the objective is to reduce the magnitude of the restraining loads on the piston and other parts of the Scotch yoke, and thus minimize noise, wear, and power consumption.

This analysis is relatively straightforward, but the numerous combinations of variables and the complexities introduced by friction characteristics made extensive calculations necessary. Such work is not only tedious, but involves a high probability of error. Consequently, use was made of a digital type electronic computer (in this case an IBM 704) to accomplish a thorough investigation with accuracy and in a short time. Use of the computer also means that new questions covered by the existing program could be resolved promptly.

The practicality of the computer application is further evidenced by the fact that after the initial set-up and confirming runs, new cases with revised data were run in 5.7 sec each at a cost of approximately 53 cents, as compared with several hours of manual calculation.

V. G. Foris and B. W. Hatten are with the Refrigerator-Freezer Engineering Dept., Westinghouse Electric Corp. This paper was presented at the ASHRAE Annual Meeting, Vancouver, B.C., June 13-15, 1960.

ANALYSIS

Equilibrium Equations—The elements of the problem are sketched in Fig. 1. The rotational motion of

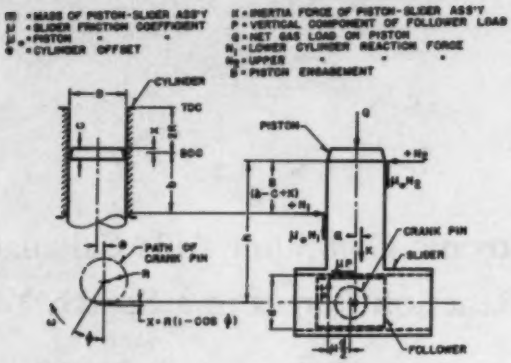

Fig. 1 Scotch yoke forces and dimensions

the crank pin is converted to translation of the piston by means of the Scotch yoke which consists of a "slider" rigidly attached to the bottom of the piston, and a "follower" which rides on the crank pin and reciprocates in the slider. Note that the vertical component P of the follower force is displaced from the center of the crank pin by a distance $\mu d/2$, assuming negligible crank pin friction.

The three basic equations determining equilibrium conditions are as follows:

Horizontal Forces:

$$N_1 - N_2 - \mu|P| = 0 \qquad (1)$$

Vertical Forces:

$$Q + K + \mu_o|N_1| + \mu_o|N_2| - P = 0 \qquad (2)$$

Moments about intersection of piston and slider centerlines:

$$Ka - N_2 h + N_1 (h - B) + \tfrac{1}{2}\mu_o D (N_2 - N_1) + P (R \sin \phi - e) = 0 \qquad (3)$$

with

μ positive $270° < \phi < 90°$
(follower moving to left)

negative $90° < \phi < 270°$
(follower moving to right)

μ_o positive $0° < \phi < 180°$
(piston moving upward)

negative $180° < \phi < 360°$
(piston moving downward)

and where

$$B = b - c + x \qquad (4)$$

$$x = R(1 - \cos \phi) \qquad (5)$$

$$K = mR\omega^2 \cos \phi = m\omega^2 (R - x) \qquad (6)$$

$$\omega = 2\pi N/60 \quad (N = \text{rpm}) \qquad (7)$$

The static weight of the piston is neglected on the basis of a horizontal piston axis. Note that in Eq. (3) the friction torque $-\mu P\, d/2$ was cancelled by the term $\mu d/2$ in the moment arm of the force P, making the solution independent of the slider diameter.

In Eqs. (1) and (2) the absolute values of the N's and P appear wherever a negative value of that

TABLE I

SOLUTIONS TO EQUILIBRIUM EQUATIONS

	Signs P	N_1	N_2	Solutions P	N_1	N_2
1.	+	+	+	$\dfrac{Q_o + 2\mu_o C_o}{1 + \mu\mu_o - 2\mu_o C_1}$	$C_o + C_1 P$	$N_1 - \mu P$
2.	+	−	+	$\dfrac{Q_o}{1 + \mu\mu_o}$	"	"
3.	+	+	−	$\dfrac{Q_o}{1 - \mu\mu_o}$	"	"
4.	+	−	−	$\dfrac{Q_o - 2\mu_o C_o}{1 - \mu\mu_o + 2\mu_o C_1}$	"	"
5.	−	+	+	$\dfrac{Q_o + 2\mu_o C_o}{1 - \mu\mu_o + 2\mu_o C_2}$	$C_o + C_2 P$	$N_1 + \mu P$
6.	−	−	+	$\dfrac{Q_o}{1 - \mu\mu_o}$	"	"
7.	−	+	−	$\dfrac{Q_o}{1 + \mu\mu_o}$	"	"
8.	−	−	−	$\dfrac{Q_o - 2\mu_o C_o}{1 + \mu\mu_o + 2\mu_o C_2}$	"	"

Constants

$$Q_o = .Q + K$$

$$C_o = K\,a/B$$

$$C_1 = \frac{R\sin\phi - e + \mu h - \mu\mu_o D/2}{B}$$

$$C_2 = \frac{R\sin\phi - e - \mu h + \mu\mu_o D/2}{B}$$

Friction Coefficient Signs

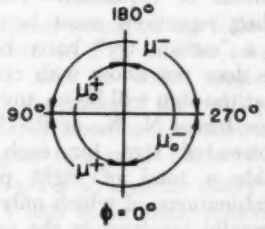

particular normal force would produce an incorrect direction of the corresponding friction force. For instance, when the load N_2 reverses it is applied to the opposite side of the piston, but the direction of the friction force $\mu_o N_2$ is unchanged. To solve the simultaneous equations for a negative N_2 condition, one would alter Eq. (2) by changing the fourth term from $+\ \mu_o N_2$ to $-\ \mu_o N_2$. Similar revisions are re-

quired for negative values of N_1 and P.

The fact that the friction force also moves to the opposite side when a normal force reverses is significant only in Eq. (3) where the negative sign of the force automatically indicates the reversal of the torque. The intersection of the piston and slider centerlines is selected as the center of moments in Eq. (3) to avoid any change in magnitude of a friction torque term whenever the friction force changes location.

The additional restrictions preceding Eq. (4) must be placed on the basic equations to account for the change in direction of friction forces whenever relative motion reverses.

Oil films cause the reaction forces to be distributed away from the points shown in Fig. 1, but this effect can be observed by reducing the piston engagement and the cylinder bore (with unchanged gas loads).

Solution of Equations—The preceding equations must be solved on a "cut-and-try" basis because one does not know with certainty what the sign will be on any of the three forces N_1, N_2, or P. The two choices of sign for each force yields a total of eight possible combinations, of which only one is normally involved in the solution. Formulas for each combination of force signs are listed in Table I.

To systematize the search for the correct solution at each crank position, the complete array of possible answers was programmed, and the computer was instructed to try all such formulas and print out the results.

A large number of cases was analyzed on the computer in an attempt to observe the primary effects of every important variable. Calculations were made at increments of 15° crank rotation except at multiples of 90° where, to avoid ambiguity at reversal of motion, points were investigated at 1° each side of the critical angle. The value of the gas load at each point in the cycle was determined from a typical pressure diagram obtained experimentally from a refrigeration compressor operating with Refrigerant 12 discharged at 180 psi above suction pressure, and with 1.5 psi maximum drop in the suction system.

The curves presented in Fig. 2 show characteristic plots of data obtained from the computer. The calculations are based on a four-pole compressor with 0.75-in. stroke. The cylinder offset is 0.12, and the friction coefficients are each 0.1, except as stated in Fig. 2. The force units are pounds.

Piston Binding—With sufficiently high friction, it is possible for the parts of the Scotch yoke to bind such that the forces required to produce motion become infinite. In order to obtain a general picture of the possible binding conditions, a complete survey was made of all denominators of P in Table I. (The force P becomes infinite when the denominator approaches zero.) Plots of these data—of which Fig. 3 is an example—indicate that fric-

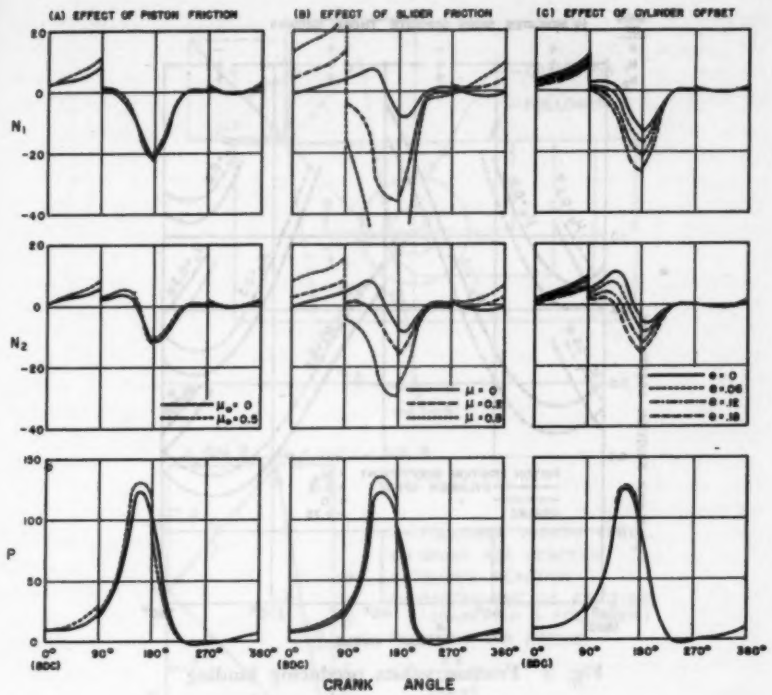

Fig. 2 Calculated reaction forces on piston

tion coefficients in the vicinity of 0.3 or higher are required before binding occurs. Critical regions exist at BDC and at crank angles 45° either side of BDC. The computer confirmed their effect by printing "no solution" (or dual solutions in some instances). A positive cylinder offset increases the hazard at some of the worst points.

Crank Pin Friction—In accounting for friction between the crank pin and follower, one must also consider the inertia of the follower. All of the forces acting on the follower are shown in Fig. 4. The inertia force J acts at crank angle ϕ through the center of the crank pin. The pin reaction S can be shown to be tangent to a small circle of radius $r\psi/\sqrt{1+\psi^2}$, and the slider reaction T acts at an angle ρ having tangent equal to μ. For equilibrium, these three forces intersect at a point designated by the large dot. From this diagram, and a consideration of reversed motion and the sign of P, one can establish the location of the follower load as

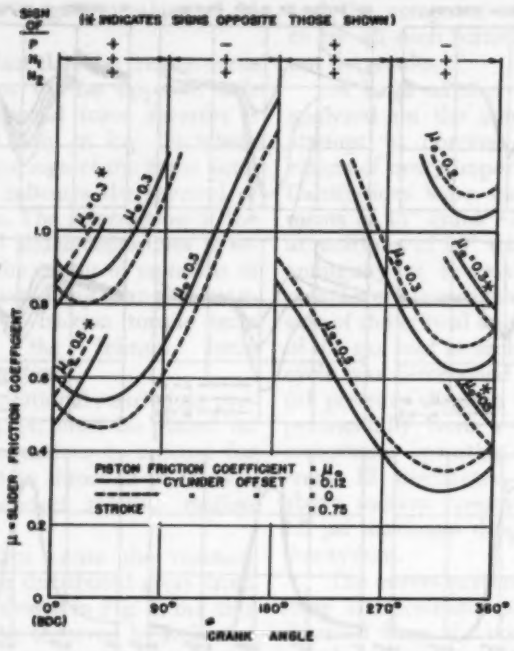

Fig. 3 Friction values producing binding

$$b_1 = \mu \frac{d}{2} \pm r\psi$$

$$\sqrt{\frac{1 + \mu^2 + 2J_o(\cos\phi \mp \mu \sin\phi) + J_o^2}{1 + \psi^2}} \qquad (8)$$

where the lower alternate signs apply for negative values of P, and $J_o = J/P$. This equation reveals that the location of P in Fig. 1 is in error by the amount of the above departure from $\mu d/2$, but that the error is zero with negligible crank pin friction.

The effect of this friction and inertia can be added to the solutions in Table I by adding the last term in Eq. (8) to the numerators of C_1 and C_2, respectively. However, the solutions then become a little cumbersome and involve successive approximations of P. This amount of computation did not appear warranted in view of the values of the terms involved. Noting that the extreme values of the factor multiplying $r\psi$ are

$$F = \frac{\sqrt{1 + \mu^2 \pm 2J_o\sqrt{1 + \mu^2} + J_o^2}}{1 + \psi^2} \qquad (9)$$

we calculate the curves in Fig. 5

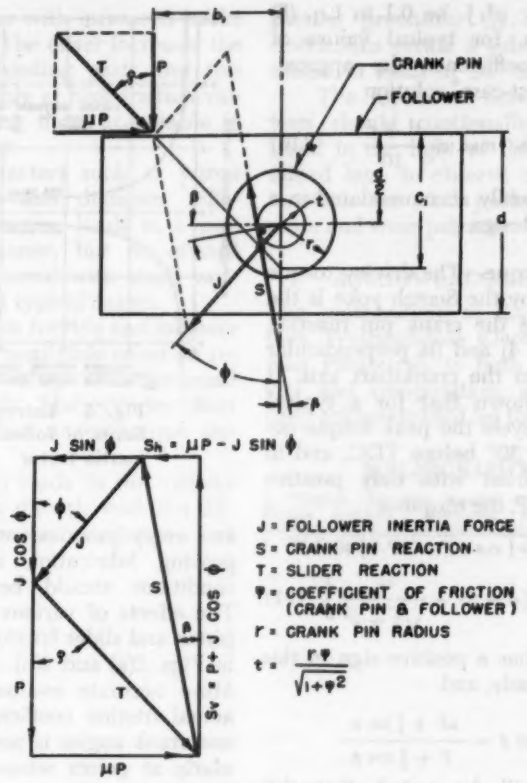

Fig. 4 Forces acting on follower

for a wide range of friction coefficients. The value of the factor F is always in the bounded region, and does not depart greatly from unity except at relatively low values of P/J.

The value of $r\psi$ in Eq. (8) is about equal to the manufacturing tolerance on the cylinder offset, so the error in neglecting it is quite small even when the factor F is appreciably different from unity.

Length of Follower—It is assumed that the follower has sufficient length such that the force P is always between the ends of the follower, thus avoiding a moment which would cause contact at both the top and bottom of the slider.

Neglecting extremely small values of P/J by letting the maxi-

mum value of J_o be 0.1 in Eq. (8) we obtain, for typical values of friction coefficients, the approximate "worst-case" solution

$$|b_1|_{max.} \cong \frac{d+r}{10} \qquad (10)$$

which is easily accommodated in a practical design.

Motor Torque—The driving torque required by the Scotch yoke is the product of the crank pin reaction (S in Fig. 4) and its perpendicular distance to the crankshaft axis. It can be shown that for a typical pressure cycle the peak torque occurs near 30° before TDC, and in this quadrant with only positive values of P, the torque is

$$T_m = \sqrt{(P+J\cos\phi)^2+(\mu P+J\sin\phi)^2}\left[R\sin(\phi-\beta)+\frac{r\psi}{\sqrt{1+\psi^2}}\right] \qquad (11)$$

where μ has a positive sign in this instance only, and

$$\tan\beta = \frac{\mu P + J\sin\phi}{P + J\cos\phi}$$

It will be noted that this torque is independent of the offset e except to the extent that e (and associated value of distance a) influences P. Inspection of the formulas for P in Table I indicates that this influence is small (becoming zero without friction). Fig. 2(c) shows that the effect was negligible in a typical case.

CONCLUSIONS

Friction—especially that occurring in the slider—is the most critical factor influencing reaction forces,

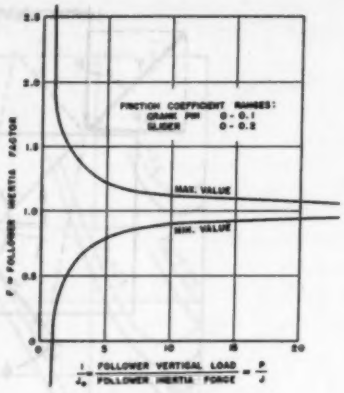

Fig. 5 Extreme limits of follower inertia factor

and every practical means of improving lubrication and surface conditions should be employed. The effects of various amounts of piston and slider friction are shown in Figs. 2(a) and 2(b), respectively. More accurate evaluation of the actual friction coefficients at various crank angles is needed, particularly at points where motion reverses.

Offsetting the cylinder with respect to the crankshaft provides a means of equalizing peak loads as shown in Fig. 2(c). Positive offset reduces piston side loads at bottom dead center (BDC) and during compression, but increases them (in the opposite direction) while maximum gas pressures exist at top dead center (TDC). Note that the values of these loads must be interpreted in terms of actual friction coefficients.

The need for the cylinder off-

set is greater with increased stroke and speed. The offset increases the hazard of binding parts, but this can occur only at high friction values exceeding those acceptable in a compressor.

Other factors such as piston engagement and diameter influence the reaction loads in a predictable manner, but no critical changes occurred with small variations from a typical design.

Crank pin friction and follower inertia have negligible effect on reaction loads except at rather small follower loads. The cylinder offset does not affect motor torque significantly.

Reaction loads in the vicinity of TDC vary directly with the difference between discharge and suction pressures. Cylinder inlet restrictions create a substantial increase in loads at 90° after TDC.

The results of noise and life tests should continually be analyzed in the light of the data obtained here to observe correlation between the load peaks and the noise and wear patterns.

ACKNOWLEDGMENT

The contributions of R. L. Chambers, Westinghouse Electric Corp., East Pittsburgh, to both the analysis and computation, are gratefully acknowledged by the authors.

BIBLIOGRAPHY

1. "Digital Computer Applied to Compressor Design Analysis", Soumerai, Kusuda, and Dittfach. ASHRAE JOURNAL, July, 1959, Vol. 1, No. 7, p. 43.

1724

No. 1724

Heat Loss from a Heated Basement

J. M. ELLIOTT

MERL BAKER
Member ASHRAE

The heat loss from a heated basement is usually a small percentage of the total heating requirements of a building. This fact coupled with the experimental difficulties encountered in measuring the heat transfer which takes place through the walls and floor of a basement has resulted in a neglect of the problem. A deficiency of reliable design data exists on which to base an estimate of basement heat losses. These data are needed in the determination of a design to avoid condensation on the basement walls and floors.

The magnitude of the heat loss depends on the type of construction, the thermal conductivity of the soil and the climatic conditions. The maximum, or design, loss will occur when steady state conditions are approached; that is, when the outdoor temperature drops and remains low for a considerable length of time.

J. M. Elliott is Assistant Professor, Mechanical Engineering, University of Kentucky. Merl Baker is Executive Director, Kentucky Research Foundation. This paper was presented at the ASHRAE Annual Meeting, Vancouver, B. C. June 13-15, 1960.

To evaluate the heat flow, consider a vertical section cut through the walls, floor and surrounding earth. The heat transfer is limited to 2 dimensions if the basement has an infinite length in the direction perpendicular to the section. Since the temperature field is symmetrical, the losses can be determined by analyzing one side only. The heat transfer from the basement may be expressed as

$$q' = -k_s \int_D \frac{\partial t}{\partial n} dD \qquad (1)$$

where

q' = heat transferred per unit time per foot of perimeter.
k_s = thermal conductivity of the soil and the basement wall and floor.
D = depth of the basement plus one-half the width of the basement floor.
t = temperature at any point.
n = direction normal to the surface.

The temperature distribution may be expressed by the Laplace equation as

$$\frac{\partial^2 t}{\partial x^2} + \frac{\partial^2 t}{\partial y^2} = 0 \qquad (2)$$

for steady state conditions. Introducing a new variable

$$\theta = \frac{t - t_o}{t_i - t_o} \qquad (3)$$

where

t_o = outdoor air temperature.
t_i = air temperature inside the basement.

By combining Equations 1 and 3, the heat flow rate can be expressed as

$$q' = k_s(t_i - t_o)\int_D -\frac{\partial\theta}{\partial n}dD \qquad (4)$$

or

$$q' = Fk_s(t_i - t_o) \qquad (5)$$

and

$$F = -\int_D \frac{\partial\theta}{\partial n}dD \qquad (6)$$

Where F is dimensionless and is a ratio of the depth plus one-half the floor width of the basement to an effective length of the flow path. In keeping with the terminology used by Jakob[1] and others, the factor F is designated the shape factor. The value of the integral in Equations 4 or 6 does not depend on the temperature t_i or t_o, but only upon the geometrical configuration of the basement. The integral is difficult to evaluate by analytical means; but since it is independent of temperature, any experimental method based on Equations 1 and 2 is feasible.

For steady state 2-dimensional conditions, both the electrical potential (voltage) and the thermal potential (temperature) satisfy the Laplace equation. If a model is constructed from an electrically conducting material and the model dimensions are proportional to those of the basement section, then the voltage at any point in the model will be proportional to the temperature at a corresponding point in the basement wall or soil. The flow of current in the electrical system is analogous to the flow of heat in the thermal system. Ohm's law for a steady state 2-dimensional model may be written as

$$\frac{I}{S} = -\lambda\int_{D_1} \frac{\partial e}{\partial n_1}dD_1 \qquad (7)$$

where

I = current.
S = thickness of the model.
λ = the electrical conductivity of the model.
e = voltage.
n_1 = direction normal to the surface.
D_1 = dimension of the model analogous to the basement depth plus one-half the floor width.

Since voltage and temperature are proportional at all points, the variable θ may also be expressed as:

$$\theta = \frac{e - e_1}{e_1 - e_o} \qquad (8)$$

where

e_1 = voltage analogous to t_i.
e_o = voltage analogous to t_o.

Using Equation 8, the current flow per foot of thickness may be expressed as

$$\frac{I}{S} = \lambda(e_1 - e_o)\int_{D_1} -\frac{\partial\theta}{\partial n_1}dD_1 \qquad (9)$$

or

$$F = -\int_{D_1} \frac{\partial\theta}{\partial n_1}dD_1 = \frac{I}{S\lambda(e_1 - e_o)} \qquad (10)$$

The determination of the

shape factor is then reduced to the measurement of current and voltage provided the electrical conductivity is known.

An electrical analogue known as the conductive sheet method is used in this research. The electrical model is made to scale from a thin continuous sheet. Since the model retains geometric similarity, temperature fields may be obtained directly by plotting the constant voltage lines on the model.

The use of a wall or floor construction for a basement that has a lower thermal conductivity than the surrounding soil causes increased resistance in the heat flow path from the heated space. Increased resistance to current flow in the model may be accomplished by altering the effective unit resistance. Kayan[8] suggests that this be done by carefully cutting the sheet into a mesh pattern, the electrical resistance increasing as the amount of material cut out increases. The resistance of the perforated sheet is measured by direct electrical measurements until the desired resistance ratio is obtained.

Equations 1 and 7 are based on a homogeneous material of uniform resistance in the flow path and do not apply to the perforated model. The total electrical resistance is still analogous to the total thermal resistance. Consider two electrical models that are identical except for the strip of increased resistance in one model. The ratio of the total electrical resistances may be determined by electrical measurements;

$$X = \frac{r_1}{r_2} \tag{11}$$

where

r_1 = the total electrical resistance of the model with perforated strip.
r_2 = the total electrical resistance of the homogeneous model.

This dimensionless electrical ratio is analogous to thermal resistance ratio, which may also be expressed as;

$$X = \frac{R_1}{R_2} \tag{12}$$

where

R_1 = total thermal resistance of the basement with insulated walls.
R_2 = total thermal resistance of basement with walls having a thermal conductivity equal to that of the soil.

The heat transfer rate from the basement is given by

$$q' = \frac{t_i - t_o}{R_1} \tag{13}$$

The objective of this research is to construct electrical models and use these models in analyzing the heat loss and plotting the temperature field for basements of different wall constructions.

REVIEW OF EXPERIMENTAL INVESTIGATIONS

The experimental difficulties in evaluating basement heat losses and the lack of design data have resulted in the use of a "rule of the thumb" method in determining the heating requirements. The method most frequently used is that of assuming the transmittance coefficient for the walls and floor and an estimated soil temperature equal to ground water temperature for the

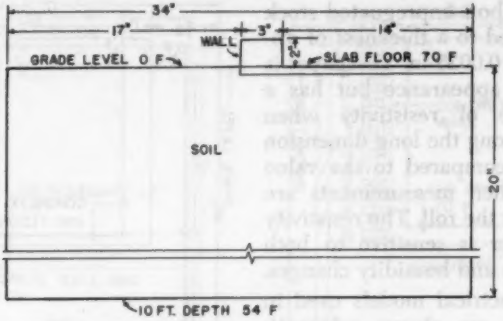

Fig. 1. Model A representing an uninsulated slab floor

locality in which the installation was built. Houghten, Taimuty, Gutberlet and Brown[3] in 1942 reported a wide discrepancy between calculated and measured values of basement heat loss. They published results obtained from an experimental basement constructed at the ASHVE Research Laboratory at the Pittsburgh Experiment Station. The total measured heat loss for February 11, 1941, was 1747 Btu/hr compared to a calculated value of 13,734 Btu/hr. The use of actual full scale basements is an excellent method of determining losses; but since the heat loss depends on the type of construction and the thermal conductivity of the soil, extrapolation of experimental data to conditions different from the tests may be very uncertain.

Baker, O'Byrne and Levy[4] in 1952 presented an equation for figuring the design loss from an uninsulated basement in a moderately cold climate. The heat loss from a basement with a depth of 7 ft and including a 2.5 ft floor band was given by

$$q = 135\,KL \qquad (14)$$

where

q = heat transfer rate.
K = thermal conductivity of the soil.
L = perimeter length of the basement.

The constant is the product of the shape factor and the temperature difference between inside and outside air. The equation was based on a temperature field obtained by application of the relaxation method. Use of the proposed equation results in a more conservative heating load than the "rule of the thumb" method; however, the loss obtained from Equation 14 may be excessive because of neglecting the surface film.

DESCRIPTION OF ELECTRICAL MODELS

The models used in this project were made from a continuous sheet of Teledeltos paper, type L. The paper available commercially is

made of carbon impregnated stock and is formed to a thickness of approximately 0.0035 in. The paper is uniform in appearance but has a lower value of resistivity when measured along the long dimension of the roll compared to the value obtained when measurements are made across the roll. The resistivity of the paper is sensitive to both temperature and humidity changes.

The electrical models used in this project are shown schematically in Figs. 1 to 4. To maintain geometrical model requirements, the proportions were made to scale. The ratio of lengths in the actual building to those of the model was 6:1 in all cases except model B, for which the scale factor was 12:1. The following assumptions are common to all models: (a) no contact resistance at the interface between the concrete slabs and the soil; (b) the thermal conductivity of the poured concrete walls and floor is equal to the thermal conductivity of the soil; (c) the outdoor air temperature is zero F; (d) the basement or inside air temperature is 70 F; (e) the thermal conductivity of the soil is 1 Btu/sq ft/hr/F/ft. Figs. 1 to 4 also contain actual model dimensions.

Model A (Fig. 1) represents an uninsulated slab floor. The building wall thickness was taken as 15 in. and specific assumptions are (a) the temperature gradient is uniform at a distance of 9.5 ft from the center line of the building wall; (b) the floor surface temperature and the outdoor soil surface temperature are constant and equal to 70 F and zero F respectively;

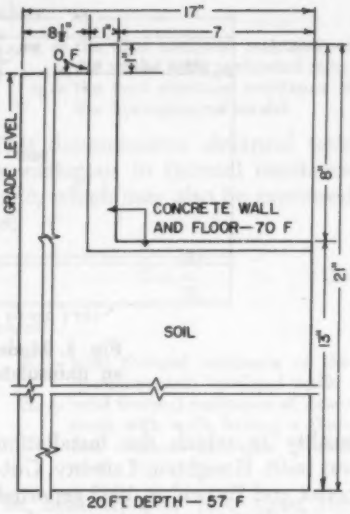

Fig. 2. Model B, for a basement with concrete wall and floor

(c) the soil temperature is constant and at 54 F at a depth of 10 ft.

Model B (Fig. 2) depicts an uninsulated basement with a depth below grade level of 7 ft and a wall thickness above grade of 12 in. The assumptions used were the same as those for Model A except that the temperature of the soil was constant and 57 F at a depth of 20 ft.

The assumptions used in the preceding 2 models were essentially the same as those used by Baker[4] for obtaining a numerical solution. Repetition of his work was performed to provide a check on the conductive sheet method used in this project. The slab floor model was used because of a lack of data for basement losses.

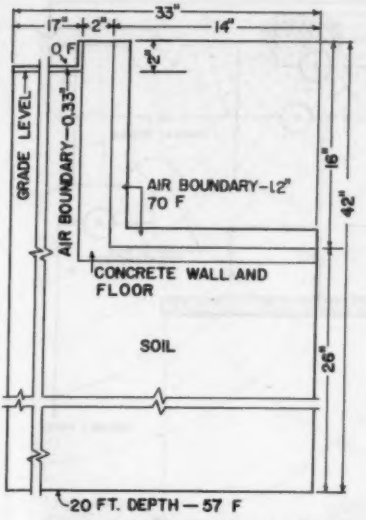

Fig. 3. Model C—like Model B but with fluid boundaries included in the construction

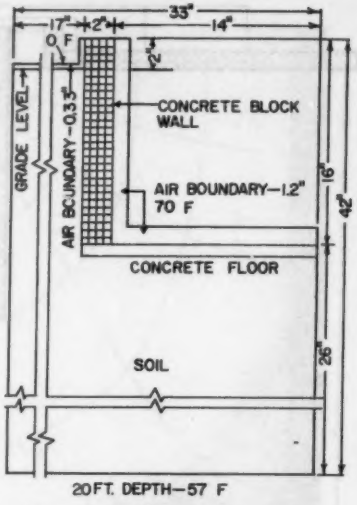

Fig. 4. Model D—for same size basement but with wall construction of 12-in. concrete blocks

Model C (Fig. 3) represents a basement of the same dimensions and wall construction used in Model B, but fluid boundaries are included in the construction. Surface conductance values were taken from the ASHAE GUIDE[5]; and the values selected were, for inside air, $h_i = 1.67$ Btu/sq ft/hr/F and for outside air, $h_o = 6.0$ Btu/sq ft/hr/F. The surface films were replaced with an equivalent length of soil. The inside film is represented on the model by an additional 1.2 in. of material at the basement wall and floor, while the outdoor boundary was displaced a distance of 0.33 in.

Model D (Fig. 4) is for a basement of the same size but with a different wall construction. The wall was assumed to be built from 12-in. concrete blocks for which the thermal conductivity was 0.445 Btu/sq ft/hr/F/ft. The ratio of the thermal resistance of the wall section to that of the soil was 2.25. The unit resistance of the conductive sheet was altered by carefully cutting a square mesh until this resistance ratio was achieved for the model. For a one-in. mesh, 0.6-in. square holes and a 0.4 in. web, the measured electrical resistance ratio was 2.25.

The resistivity of the sheets was determined by using 12-in. square sections. The resistivity was measured both along and crosswise of the length of the roll.

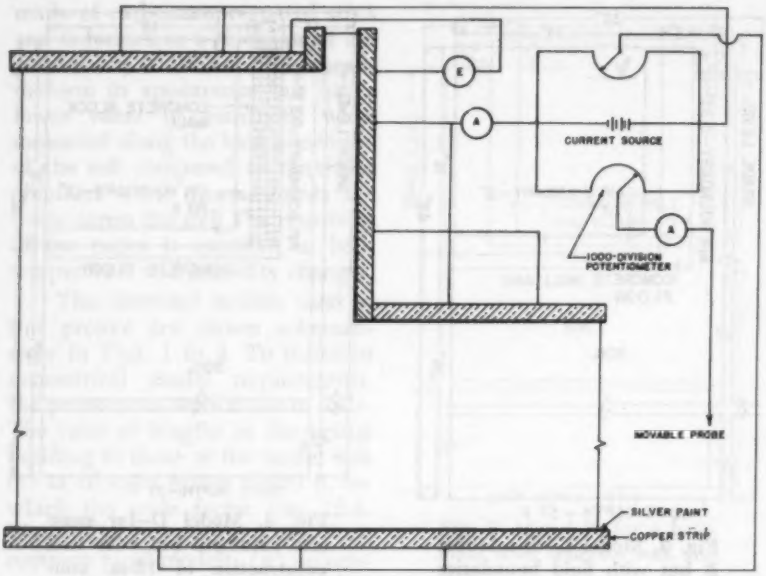

Fig. 5. Schematic diagram of test apparatus

TEST PROCEDURE

The test setup is shown schematically in Fig. 5. The boundary electrodes consisted of copper strips placed about 0.375 in. from the actual boundaries. The strips were held firmly in place by thumb tacks at approximately 2-in. intervals along the length of the strip. The space between the strips and the actual boundary was painted with a high silver content paint to obtain good electrical contact with both the copper and the paper. The potential at the boundary was checked with the probe and additional layers of paint applied until there was no detectable voltage drop in the boundary electrodes.

Direct current was supplied to the models from a 7-volt dc source. The current flow to the boundary representing the inside surface of the basement was measured with a milliammeter. The voltage difference between the two surface electrodes was measured with a dc voltmeter. The percent of the voltage difference necessary at the boundary representing the constant temperature in the soil at a depth of 20 ft was determined by Equations 3 and 8 as $\theta_b = (e_b - e_2)/(e_1 - e_2) = (t_b - t_o)/(t_i - t_o) = 0.814$, where the subscript b refers to the boundary. The variable resistor was

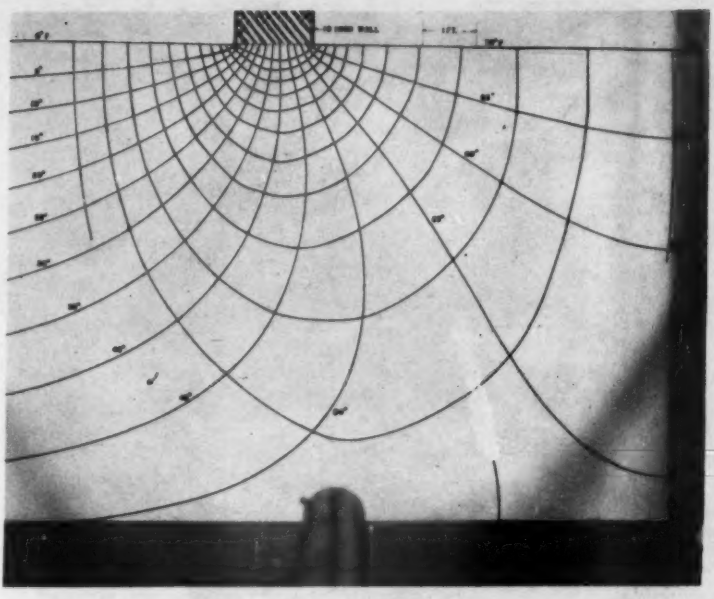

Fig. 6. Heat flow paths and isotherms in the soil below a slab floor, $k_s/k_w = 1$

adjusted until the voltage at this boundary was 81.4% of the total voltage.

The isopotential lines were located on the models using the probe in series with the 1000-division potentiometer and a microammeter. The potentiometer divisions made it possible to set the potential at any point to the nearest 0.1% of the total voltage anywhere between zero and 100%.

While each test was being conducted, electrical measurements were made on the square models to determine the unit resistivity of the paper. Wet- and dry-bulb temperatures were recorded for each set of electrical measurements.

EXPERIMENTAL RESULTS

The results are best shown by the isopotential lines drawn from the models. These maps are shown in Figs. 6 through 9. For models A and B, which were used as a check on the conductive sheet method, the network of curvilinear squares was completed by careful sketching of the adiabatic lines. The heat transfer rate was calculated from the curvilinear squares and also from electrical measurements. Table

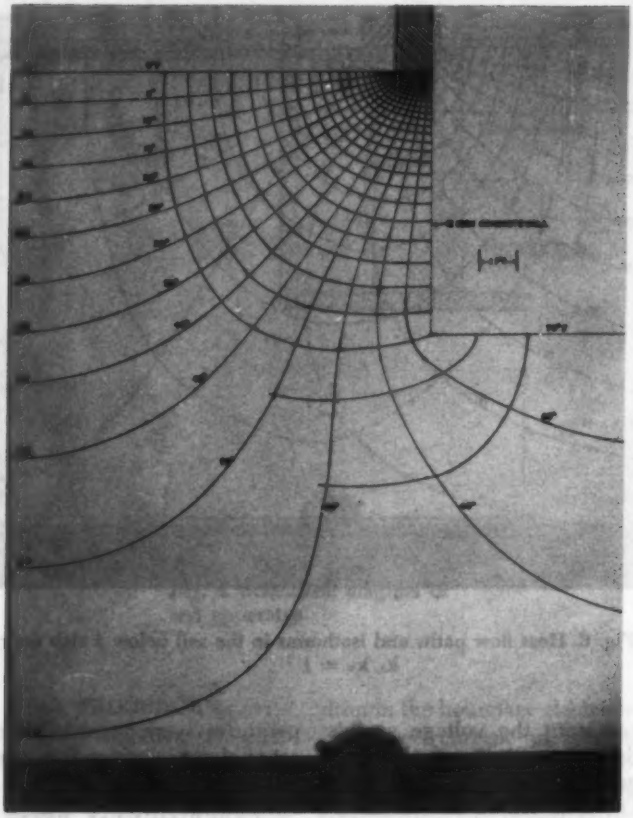

Fig. 7. Heat flow paths and isotherms in the soil surrounding a basement, $k_s/k_w = 1$

I allows a comparison of these results with those obtained by Baker[4] for similar conditions. The heat loss listed per ft of perimeter is for a floor width of 7 ft and for the basement includes a wall height of 7 ft.

The excellent agreement between the two graphical methods indicates that the isopotential lines plotted on the models compare favorably with the calculated value from the relaxation method. The heat transfer calculated from the electrical measurements also shows good agreement with the graphical solutions, the maximum difference

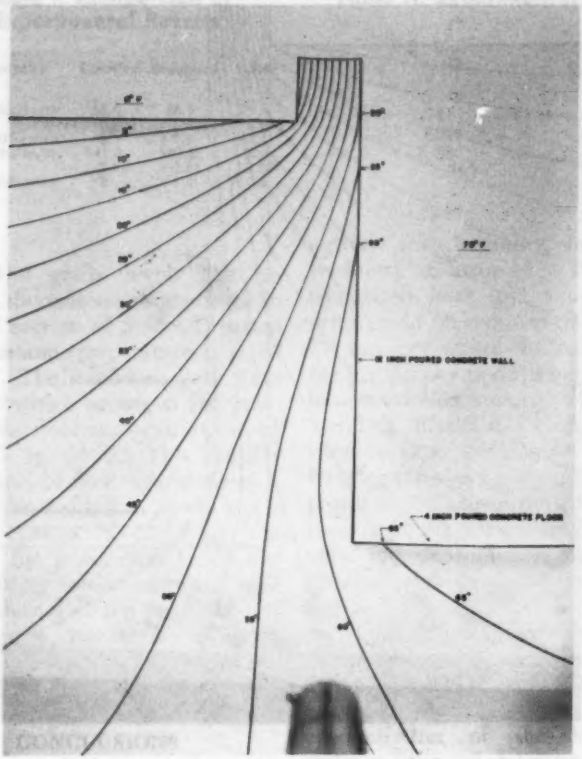

Fig. 8. Isotherms in the soil surrounding a basement, $k_s/k_w = 1$

being 2.8% for the basement models.

Karplus[8] gives a temperature coefficient of resistance of approximately 0.1% per degree Fahrenheit for the Teledeltos paper. For the temperature changes encountered during the tests, the temperature coefficient introduced a change of less than one percent in the resistance value. The paper was found to be sensitive to moisture and changes in relative humidity caused a variation of plus or minus 3% from a mean value of 1576 ohm per sq. The resistivity was 3% lower along the roll compared to values crosswise to the roll. Since the heat flow was not predominately in either direction, the resistances were combined to give a mean value.

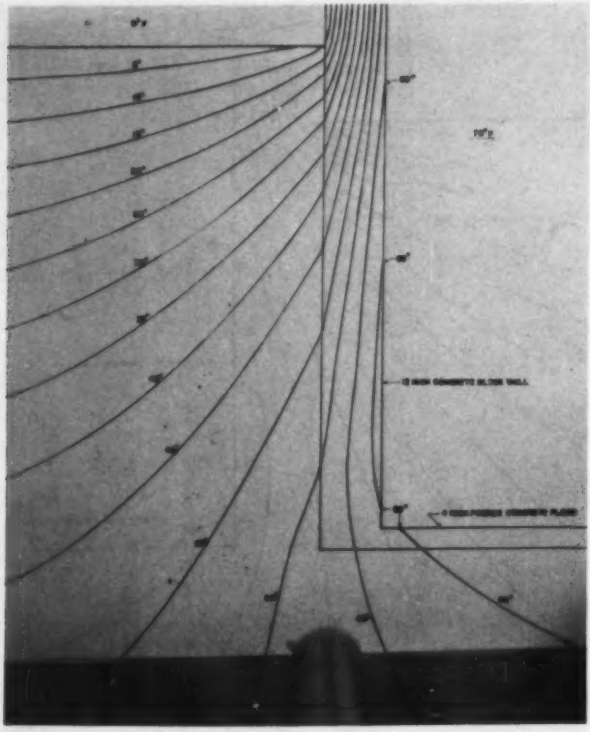

Fig. 9. Isotherms in the soil surrounding a basement, $k_s/k_w = 2.25$

The results obtained from models C and D show that the design heat loss for an uninsulated basement may be determined by

$$q' = 1.50\, k_s(t_i - t_o)L \qquad (15)$$

and for the basement with the concrete block wall by

$$q' = 1.25\, k_s(t_i - t_o)L \qquad (16)$$

where

L = perimeter length.

The design heat loss calculated by Equation 15 will be 25% less than the loss determined by neglecting the film coefficient. The results from the 3 basement models are listed in Table II for comparative purposes.

Inspection of the isothermal lines plotted for models C and D and shown in Figs. 8 and 9 shows that the minimum wall surface temperature occurs at a point just

Table I. Comparison of Experimental Results

Model	Quantity	Electrical	Graphical	Baker[4]
A	q', Btu/hr/ft	56.0	56.5	55.4
	F	0.800	0.806	0.796
	% difference	0	+0.9	−1.1
B	q', Btu/hr/ft	141.0	142.5	145.0
	F	2.01	2.03	2.07
	% difference	0	+1.0	+2.8

Table II. Experimental Results

Model	Q', Btu/hr/ft	F	Percent Difference
B	141	2.01	0
C	104	1.50	−25.5
D	88	1.25	−34.0

above the grade level. The increased thermal resistance used in the wall section of model D raised this minimum temperature from 50 to 58 F. The minimum floor temperature which occurs at the junction of the floor and wall increased from 63 to 64 F. This smaller change for the floor temperatures is due to the insulation producing a smaller change in the heat loss through the lower portion of the wall. Adding insulation to the wall section decreases the possibility of condensation; but to be effective for this purpose, it should also extend under the floor.

CONCLUSIONS

The electrical geometrical analogue using the conductive sheet method proved to be an excellent method for evaluating basement heat losses. The paper used for the models is inexpensive and easily cut to any desired shape. The isopotential lines which constitute the measured field are recorded directly on the conductive sheets. The points located in plotting the constant voltage lines could be checked within 0.01 in. with the tracing probe.

The variation of electrical resistivity with humidity changes introduced an error of ±3% in the calculated heat loss values. This error could be reduced to less than 1% in cases where the refinements are justified by performing the tests in a controlled atmosphere.

The maximum electrical resistance ratio obtainable by perforating the sheet is about 5:1. This prohibits the use of the conductive sheet method with a single thickness for determining the losses through well insulated walls and floors.

The shape factors presented are independent of the thermal conductivity of the soil but are dependent on the ratio of the thermal conductivities of the basement walls and the soil. Interpolation between the values given may be performed with a reasonable degree of accuracy, but extrapolation will produce uncertain results.

REFERENCES

[1] Max Jakob; *Heat Transfer* (John Wiley & Sons, Inc., New York, 1949, Vol. 1).

[2] Carl F. Kayan: An electrical geometrical analogue for complex heat flow (*ASME Transactions*, Vol. 67, 1945, p. 713).

[3] F. C. Houghten, S. I. Taimuty, Carl Gutberlet, and C. J. Brown: ASHVE Research Report No. 1213—Heat loss through basement walls and floors (ASHVE Transactions, Vol. 48, 1942, p. 369).

[4] Merl Baker, J. M. O'Byrne, and A. M. Levy; Estimating the heat loss from slab floors and basements (*Heating, Piping & Air Conditioning*, Nov., 1952, p. 95).

[5] ASHAE Guide (AMERICAN SOCIETY OF HEATING AND AIR-CONDITIONING ENGINEERS, 1950, Chapter 9, p. 170).

[6] Walter J. Karplus: *Analog Simulation* (McGraw-Hill Book Co., Inc., New York, N. Y. 1958).

BIBLIOGRAPHY

Paul J. Schneider: *Conduction Heat Transfer* (Addison-Wesley, Cambridge, Mass., 1955).

Neville S. Billington: Heat loss through solid ground floors (*IHVE Journal*, Vol. 19, 1951).

Carl F. Kayan: Electrical analogger studies on panels with imbedded tubes (ASHVE TRANSACTIONS, Vol. 56, 1950, p. 205).

Carl F. Kayan: Temperature patterns and heat transfer for a wall containing a submerged metal member (*Refrigerating Engineering*, Vol. 51, 1946, p. 533).

DISCUSSION

R. G. HUEBSCHER, Cleveland, Ohio (Written): Since basement heat loss is studied as a two-dimensional heat flow field, a logical extension of the work would be the investigation of the corner-effect, essentially a three-dimensional heat flow problem. Total heat loss can be obtained using an electrolytic analog. Is any additional work planned to study this?

The replacement of surface film resistances by an equivalent thickness of soil seems open to question. In a two-dimensional analog, some means must be provided to prevent current flow transverse to the plane of the boundary within the conductive medium simulating the film resistance.

CLOSURE BY AUTHOR BAKER: I fully agree that in small basements the corner effects should be considered. The analog method can be used effectively to consider three-dimensional flow, and I am hopeful that we will be able to conduct additional experiments in this direction.

In some cases, the criticism relative to the surface conductance would be quite valid. In our particular experiments, the assumption of one-dimensional flow through the film did not produce any significant error, but it is well to point out the possible danger.

W. G. BROWN, Ottawa, Canada (Written): It is hoped that this paper will stimulate an increased interest in the problem of heat exchange under buildings. It was pointed out that the ground heat loss is usually a small percentage of the total heating requirement, when actually it is seldom less than about 10% of the total heat load and deserves considerable attention.

Since the mathematical solutions for the annual weather cycle are greatly complicated, steady-state operation must be assumed. What is not always realized is that the heat flow can be thought of as having two sink temperatures: the outside air temperature and the mean undisturbed ground temperature. The heat flow in the ground near the edge of a building has the outside air temperature as sink; the heat flow near the building center has the mean annual temperature as sink. The influence of these two temperatures can be illustrated by considering a very large and a very small building having the same geometry and shape factor F. If t_i = 70F, t_o = OF, and the mean annual temperature is 50F, the heat flow per foot of width in the small building is proportional to 70 − 0 = 70F, and that in the large building is proportional to 70 − 50 = 20F. The resulting error in the calculated heat flow could be as much as 350%. Another minor source of error is that of obtaining the total heat loss for the building by multiplying the loss per foot of section by the perimeter. An additional shape factor has been suggested for a square building which amounts to about 0.8, takes into account the additional distortion of the head flow path in three dimensions. How do these sources of error compare to the studies shown in this paper?

The good agreement for the results of Model A (basementless building) compared with the paper by Baker, O'Byrne and Levy are difficult to understand. In describing Model A, the wall thickness is first stated as 15 in., but in Fig. 6 it appears as 18 in. How was a uniform gradient obtained at a distance of 9.5 ft from the wall center-line? These discrepancies are minor but Table 2 shows that small differences in geometry or boundary conditions can have appreciable effects.

AUTHOR BAKER: I would like to correct an error in Fig. 6 of the text in which the wall thickness should have been 15 in. and not 18 in. The model was constructed in consideration of a 15-in. wall.

The analog described in our paper does consider the existence of two heat sinks. As pointed out by Mr. Brown, these are 1) outside air and 2) undisturbed earth. The only thing omitted from our analog is the consideration of corner effects. This omission becomes significant only for very small buildings. The basement models considered that the earth beneath the basement floor was at a uniform undisturbed temperature of 57 F at a depth of 20 ft. In preliminary studies we found it made little difference whether this uniform temperature was assumed to be at 20 ft or 40 ft. For all practical purposes to this problem, a 20-ft depth is infinity.

The perimetric method of analysis includes both the heat that is transferred through the soil and eventually to the air at the earth surface, and also that which is transferred into the depth of the earth. We do not understand Mr. Brown's reference to the resulting error of 350%.

Except in very small buildings, the additional shape factors for three dimensional flow, occurring at the corners only, does not significantly alter the loss.

It must be kept in mind that the analysis presented in our paper pertains to a maximum or designed heat loss. It is appreciated that because of thermal lag in the soil, the heat loss at any particular time might be substantially less than predicted from the model analysis. However, the maximum loss would occur when steady state conditions are reached and this analysis is then appropriate for designed purposes.

1725

No. 1725

Cooling Rates of Apples Packed in Different Bushel Containers and Stacked at Different Spacings in Cold Storage

D. V. FISHER

Until recent years western apples have been packed exclusively in wooden bushel boxes, with apples paper-wrapped and tightly placed in the container to produce a high crown bulge. The boxes were stacked in cold storage at a space of 3½ in. between rows and the stacks placed bulge to bulge in the rows. This resulted in fairly satisfactory cooling rates because of exposure of 4 out of 6 sides of the box to cooling air. Under these conditions reduction of fruit temperature from field heat to 32 F was normally accomplished in one week.

The present day packing method is to place apples unwrapped in cells or trays in corrugated cardboard bushel containers. These containers are of various lengths depending on the number of apples in them. When placed in cold storage, stacks of containers are spaced at distances varying from one to four in. With narrower spacings, poor row alignment often causes blockage of air flow between adjacent rows of stacks. Furthermore, since cardboard containers have no "bulge" they are often placed tightly stack to stack in rows, thus reducing the number of air-free surfaces around the box from six to two. The result has often been that cardboard containers have not cooled satisfactorily.

Following complaints from packing house operators of poor cooling in the 1957 season, a series of cooling tests was carried out using wood boxes with cardboard tray packs and cardboard cell packs with various types of pads and partitions.

Work reported by Sainsbury

D. V. Fisher is Head, Pomology Section, Canada Department of Agriculture. This paper was presented at the ASHRAE 67th Annual Meeting, Vancouver, B. C., June 13-15, 1960.

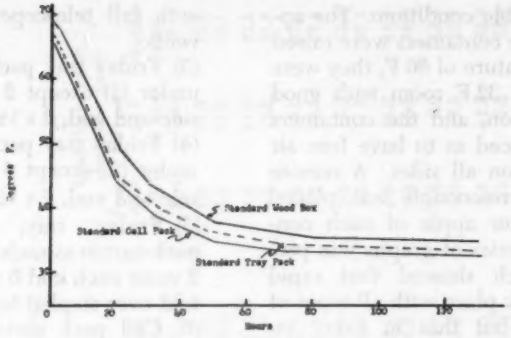

Fig. 1 Cooling time required to reduce temperature of standard cell packs, tray packs and wood boxes from 66 F to equilibrium with full exposure of all surfaces of containers to 32 F air

and Schomer[2] on cooling of pears in wood and cardboard cartons using different stacking arrangements, indicated that tight stacking impeded heat loss, more so with cardboard than wood. The greater number of sides exposed to air movement the faster was the heat loss. Differences between stabilized storage temperatures of pears in cardboard cartons and those in wood boxes were much greater when the containers were tightly stacked than when more of their surface was exposed to air flow. Large differences were found in rate of fruit cooling between different storage plants, probably attributable to degree of efficiency of air circulation within the plants.

Further data by Sainsbury[1] on the use of vents in cardboard cartons to improve cooling of apples indicated that apples in unvented cartons often took three times longer to cool than those packed in wooden boxes, and that the fruit remained on the average 2 F warmer than in wooden boxes.

Cartons with large vents plus perforated trays, cooled in about the same time as fruit in standard wooden packs. Smaller vents and absence of vents increased cooling time. With a stacking pattern exposing both ends of the cartons, the best venting resulted in a temperature difference between carton and air of 0.8 F and poorest venting, 2.0 F.

EXPERIMENTAL

Cooling of well spaced individual wood and cardboard containers—In a preliminary study of cooling rates of apples in cardboard vs wood containers, the object was to determine rate of heat loss under the

most favorable conditions. The apples in these containers were raised to a temperature of 66 F, they were placed in a 32 F room with good air circulation, and the containers were so placed as to have free air circulation on all sides. A remote reading thermocouple was placed in the center apple of each container. A series of graphs was prepared which showed that rapid cooling took place with all types of containers but that in every instance wood boxes were slightly slower in cooling than cardboard boxes.

A typical graph is given in Fig. 1. In each run, temperatures of approximately 33 F were realized in 80 hrs. The slightly faster cooling performance with cardboard might be explained by absence of insulating effect of paper wraps used in wood boxes and by thinner sides, bottoms and ends with cardboard.

Cooling of wood box and cardboard containers using different stacking methods—In the winter of 1958 a comprehensive cooling experiment was set up in the B.C. Fruit Shippers Summerland cold storage plant to compare cooling rates of Rome apples in wooden boxes and in various vented and unvented tray and cell cartons. All containers held 120 or 125 pieces of fruit except for the frame-end cell pack which held 200 apples. All of the fruit was unwrapped except in the standard wood boxes. The following containers were used in the experiment:

(1) Standard wood box.
(2) Friday tray pack carton with full telescope top — no vents.
(3) Friday tray pack carton as under (2) except 2 vents each side and end, 2 x ½ in.
(4) Friday tray pack carton as under (2) except 4 vents each side and end, 2 x ½ in.
(5) Friday tray, frame-end pack carton as under (2) except 2 vents each end 6 x ¼ in. and fold-over stapled top.
(6) Cell pack carton with no vents.
(7) Cell pack carton with 2 vents, each side and end, 2 x ½ in.
(8) Cell pack carton with 4 vents, each side and end, 2 x ½ in.
(9) Cell pack carton, frame-end, 4 vents each end, 2 x ½ in.

The fruit was heated to approximately 64 F and placed in 6-high stacks within regular warehouse rows of fruit of the same package size in the commercial 31 F storage to which reference has been made. The block containing experimental packs was buffered on either side with regular commercial fruit, and buffer stacks were placed between the experimental stacks in the rows to complete the row arrangement and to provide for commercial cooling conditions.

Air circulation was representative of good commercial practice at about 1100 cfm per ton of refrigeration with air delivery parallel to row alignment. A thermocouple was inserted into the apple nearest the center of the package in each top

TABLE I

EFFECT OF CONTAINER CONSTRUCTION AND SPACING ARRANGEMENT ON COOLING OF APPLES AT AIR TEMPERATURE OF 31 F

Container Description		COOLING PERFORMANCE A Rows 3½ in. apart, stacks ¾ in. apart From 64 F to 35 F Days	A From 64 F to equil. Days	A Equil. temp. F	B Rows 3½ in. apart, stacks 0 in. apart, From 64 F to 35 F Days	B From 64 F to equil. Days	B Equil. temp. F	C Rows 1½ in. apart, stacks 0 in. apart From 64 F to 35 F Days	C From 64 F to equil. Days	C Equil. temp. F
Tray pack unvented	Top pack	4.5	8.0	32.0	6.5	10.0	32.6	6.0	11.0	32.8
	Centre pack	5.5	10.0	32.8	8.5	11.5	33.6	7.5	13.5	33.1
Tray pack with 2 side and 2 end vents	Top pack	2.5	8.0	31.1	4.0	10.0	32.3	4.5	11.0	32.5
	Centre pack	4.5	9.0	32.7	8.5	11.5	33.7	4.0	10.0	31.9
Tray pack with 4 side and 4 end vents	Top pack	3.5	7.0	32.3	5.5	11.5	32.1	4.5	10.0	32.3
	Centre pack	4.5	12.0	32.7	8.0	12.5	33.4	5.5	12.5	33.6
Tray pack, frame-end with 2 end vents	Top pack	4.0	7.0	33.5	3.0	9.0	31.7	5.5	10.0	32.9
	Centre pack	3.5	8.0	32.0	4.0	10.0	32.0	7.0	11.5	33.1
Cell pack unvented	Top box	4.0	11.0	32.6	5.0	9.0	32.6	6.0	10.0	33.1
	Centre box	6.0	11.5	33.0	8.0	11.5	34.0	9.5	10.5	34.4
Cell pack with 2 side and 2 end vents	Top pack	2.5	11.0	32.0	3.0	9.0	31.7	3.5	8.0	32.3
	Centre pack	3.5	8.0	32.5	4.5	10.5	32.3	6.0	9.5	33.2
Cell pack with 4 side and 4 end vents	Top pack	3.0	7.0	32.0	7.0	10.0	33.0	3.5	12.5	32.9
	Centre pack	4.5	12.0	32.0	6.5	11.5	32.9	7.0	12.0	32.6
Cell pack, frame-end with 4 end vents	Top pack	3.0	7.0	32.7	4.0	9.0	32.7	6.0	11.0	32.9
	Centre pack	5.5	12.0	32.9	9.0	10.5	34.1	9.5	12.5	33.7
Standard wood box	Top pack	4.5	9.0	32.8	4.0	10.0	32.3	6.0	11.0	33.7
	Centre pack	4.5	11.5	32.2	4.5	12.5	32.0	6.5	12.5	32.6

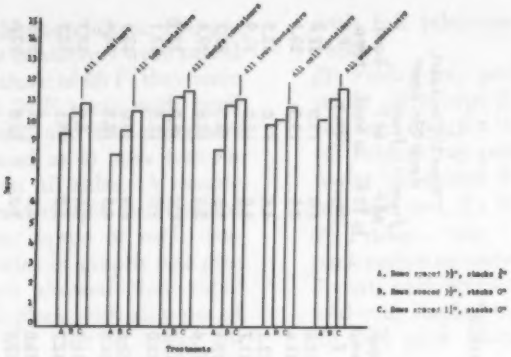

Fig. 2 Comparison of cooling rates of apples from 64 F to equilibrium in an air temperature of 31 F with different containers, stack spacing arrangements and container location in the stack

and middle box of each experimental stack of fruit. Using remote leads resistance readings were taken daily until an equilibrium temperature had been achieved.

Three separate cooling runs were performed, in each case with the same fruit and thermocouples. After completion of a run the containers were removed from storage, warmed to a temperature of 64 F and then replaced in storage for the succeeding tests. The three tests reported on represent:

(A) Stacks ¾ in. apart, rows 3½ in. apart.
(B) No space between stacks, rows 3½ in. apart.
(C) No space between stacks, rows 1½ in. apart.

The data from this experiment are presented in summarized form in Table I and Fig. 2 showing cooling time (to the nearest half day) from 64 to 35 F and from 64 F to the final equilibrium temperature attained by each package.

These data have been further statistically examined (Tables II, III, IV) showing means for all packages, for locations and for spacings with appropriate L.S.D.'s.

Packages – Table II indicates that unvented tray and cell packs took 6.42 days to cool from 64 to 35 F compared with 5.00 days for the standard wood box and close to this time for most other containers. The differences in cooling rates between unvented tray and wood containers were significant at the $P = 0.05$ level.

Those between unvented cells and wood containers were significant at the $P = 0.05$ level. The cell

TABLE II

STATISTICAL SIGNIFICANCE OF DIFFERENCES IN COOLING RATES OF DIFFERENT PACKAGES

Packages	Means, cooling time from 64 to 35 F Days	Means, cooling time from 64 F to equilibrium Days	Mean temp. at equilibrium F
Tray pack, unvented	6.42	10.67	32.82
Tray pack with 2 side and 2 end vents	4.67	9.92	32.37
Tray pack with 4 side and 4 end vents	5.25	10.92	32.73
Tray pack, frame-end, with 2 end vents	4.50	9.25	32.53
Cell pack, unvented	6.42	10.58	33.28
Cell pack with 2 side and 2 end vents	3.83	9.33	32.33
Cell pack with 4 side and 4 end vents	5.25	10.83	32.57
Cell pack, frame-end, with 4 end vents	6.17	10.33	33.17
Standard wood box	5.00	11.08	32.60
L.S.D.'s			
P = .05	1.09	1.14	.54
P = .01	1.50	1.57	.75

pack frame-end, vented package was also significantly slower in cooling than the wood container but this is probably explained by it being the only container holding 200 apples, all other packages holding 120 or 125 apples.

The additional number of cells would result in a slower rate of heat release. On the other hand, the cell pack with 2 side and 2 end vents cooled significantly faster from 64 to 35 F than the standard wood box (3.83 vs 5.00 days).

The period from start of cooling to attainment of equilibrium temperature ranged on the average from 9.25 to 11.08 days for different packages. The tray pack with 2 side and 2 end vents, the frame-end tray pack with 2 end vents, and the cell pack with 2 side and 2 end vents cooled slightly but significantly faster than the standard wood box.

The only significant difference found between final equilibrium temperature of the standard wood box (32.60 F) and other packages was that of the frame-end cell pack with 4 end vents (33.17 F). This was probably the result of greater insulation from having 200 fruit cells in the latter compared with only 125 apples in the former packages. Where packages with equal fruit counts were compared, cooling performance was almost as good in one package as the other, and final temperatures similar.

Box location in stack – Table III provides a comparison between rate of cooling of apples in top containers and those in center containers of stacks. The cooling time averaged 1.5 days longer in center than in top stacks and the equilibrium temperature was 0.43 F higher. These differences were both highly significant.

Stack and container spacing – Data are presented in Table IV to show the effect of spacing on package cooling performance. Wide (A) spacing gave a highly significant improvement in rate of cooling and in final fruit temperature compared with narrow (B and C) spacing. The mean time required for all packages to drop in temperature from 64 to 35 F was 4.08, 5.75 and 6.00 days respectively for A, B and C spacing.

To reach final equilibrium temperatures of 32.43, 32.72 and 32.98 F, required 8.3, 9.7 and 10.5 days respectively for A, B and C spacing. The higher final temperatures associated with close spacing are probably of much more practical importance than the slightly slower cooling rates.

Cooling of cartons of apples stacked in pallets in commercial storages – Information on cooling rates of apples, 120 to the carton, packed in cardboard cartons and stacked on pallets in a commercial cold storage is presented herewith. The test included:

(1) Fruit in frame-end tray cartons, placed solidly, 8 to a layer, 5 layers high on 43 x 49 in. pallets, stacked 3 high.

(2) Fruit in frame-end tray cartons, placed 7 to a layer for ventilation, 5 layers high, on 43 x 49 in. pallets, stacked 3 high.

(3) Fruit in ordinary tray cartons, lock-stacked to provide air spaces between cartons for cooling and placed 7 to a layer.

Thermocouples were placed in the center of an outside and inside carton, both on the top pallet and the bottom pallet, with similar pallet stacks surrounding the test stack on all sides. Air temperature in the room was 30.5 F and varied little between top and bottom pallets be-

TABLE III

STATISTICAL SIGNIFICANCE OF DIFFERENCES IN COOLING RATES OF TOP AND CENTER CONTAINERS IN STACKS

Location	Means, cooling time from 64 to 35 F Days	Means, cooling time from 64 F to equilibrium Days	Mean temp. at equilibrium F
Top container	4.41	9.52	32.50
Centre container	6.15	11.13	32.93
L.S.D.'s P = .01	.71	.75	.36

cause of good circulation from an effective forced air circulation system.

Cooling times reported are for reducing fruit temperature from 64 to 35 F and to final equilibrium temperature. The results are summarized in Table V. It is apparent that cooling time, from 64 F to either 35 F or equilibrium, was twice as long with tight as with loose spacing, and equilibrium temperatures with solid loading were 1 F higher than with spaced loading. With both types of spacing, top pallet loads averaged 1 F lower in temperature than bottom pallet loads.

The cooling performance of regular cardboard tray cartons on pallets spaced 7 to a layer was similar to that of the frame-end cartons similarly spaced. The advantage of frame-end cartons is their resistance to crushing when pallet is loaded; and the main disadvantage, instability of pallet loads when lock stacked.

DISCUSSION

Studies on cooling rates of containers freely exposed on all sides to good air movement pointed to the fact that with good surface exposure quite rapid cooling took place (66 to 33 F in 80 hr). This was confirmed in actual warehouse tests where various containers were stacked 6 high at different spacings in a commercial cold storage plant. Cooling tests in another storage using fruit loaded on pallets stacked solidly and spaced on pallets (lock stacks) demonstrated that spacing of containers reduced cooling time by 50 per cent, and lowered final holding temperature by about 1 F.

Cartons with vents of various sizes and numbers differed little from wood boxes in cooling efficiency. This is probably explained by the blockage of ventilation within containers by the presence of cells, trays and fruit.

REFERENCES

1. Salnsbury, G. F. Vents improve cooling in

TABLE IV

STATISTICAL SIGNIFICANCE OF DIFFERENCES IN COOLING RATES OF PACKAGES SUBJECTED TO DIFFERENT SPACING ARRANGEMENTS

Spacing	Means, cooling time from 64 to 35 F Days	Means, cooling time from 64 F to equilibrium Days	Mean temp. at equilibrium F
A. Rows 3½ in. apart stacks ¼ in. apart ...	4.08	9.39	32.43
B. Rows 3½ in. apart, stacks 0 in. apart	5.75	10.53	32.72
C. Rows 1½ in. apart, stacks 0 in. apart	6.00	11.06	32.98
L.S.D.'s			
P = .05	.63	.66	.31
P = .01	.87	.89	.42

TABLE V

COOLING RATES OF APPLES PACKED IN CARDBOARD CARTONS AND PLACED WITH DIFFERENT SPACINGS ON PALLETS SET THREE HIGH

Container and type of stacking	Thermistor location	Time to Cool from 64 F to: 35 F Days	Equilibrium Days	Equilibrium temperature F
Frame-end tray carton, 8 cartons per pallet layer, no air spaces	Top pallet, centre	10.0	15.0	32.4
	Top pallet, outside	7.0	15.0	32.3
	Bottom pallet, centre	9.5	14.5	33.4
	Bottom pallet, outside	8.0	14.0	33.4
Frame-end tray carton, 7 cartons per pallet layer, lock-stacked to provide air spaces	Top pallet, centre	4.0	7.0	31.5
	Top pallet, outside	4.0	7.0	31.1
	Bottom pallet, centre	4.5	8.0	32.3
	Bottom pallet, outside	4.5	8.0	32.8
Tray carton, 7 cartons per pallet layer, lock-stacked to provide air spaces	Top pallet, centre	4.5	9.5	31.5
	Top pallet, outside	3.5	6.5	31.2
	Bottom pallet, centre	3.5	7.0	31.2
	Bottom pallet, outside	4.0	8.6	32.0

cartons. Agric. Mark. U.S.D.A. Marketing Service, Oct 1957.
2. Sainsbury, G. F., and H. A. Schomer. Influence of stacking patterns on pear cooling rates. Marketing Research Rept. No. 171, U.S.D.A. Marketing Service, 1957.

DISCUSSION

G. F. SAINSBURY, Seattle, Wash. (Written): Was cooling better with vented cartons in stacks?

With the instrumentation and observation procedures used, the comparisons based on the cooling time from 64-35 F seem more reliable than those based on cooling from 64 F to equilibrium temperature.

CLOSURE BY AUTHOR FISHER: Cooling with vented cartons in stacks was slightly faster, perhaps a day or a day and a half, to pull the fruit down to 35 F or to a final equilibrium temperature than with unvented cartons. But in the final holding temperature achieved, there was little difference with vented vs. unvented cartons.

W. T. PENTZER, Washington, D. C. (Written): Since the best cooling was obtained by exposing all surfaces to air and equilibrium temperatures was achieved in about 80 hr, and the best time recorded was 224 hr when ¾ in. was left between stacks and 3½ in. between rows, would dunnage strips used between layers to expose tops and bottoms of packages to air come near the 80 hr cooling time?

Were there any differences in the condition of apples as a result of worst cooling (10 days to reach 35 F) and the best cooling (3.5 days to reach 35 F)?

AUTHOR FISHER: Using dunnage strips would reduce the cooling time to 80 hr or come quite close to it. It must be remembered that packing houses are sensitive to packing costs and this stripping would probably cost a cent or two a box. Unless everyone did it, no one would want to do it.

The experiments were made in January and February, cooling and rewarming the same apples for all three runs, so we couldn't determine from this particular work what effect the speed of cooling had upon fruit condition.

RONALD A. WILLIAMS, Edmonton, Canada: Can any improvement in cooling be made in air distribution?

AUTHOR FISHER: The air distribution in the conventional type storage used was about as good as could be obtained, roughly 1000 cfm per ton of refrigeration. The new type of storages built today are for palletized or bin operation and in many cases deliver air volumes of 3000 cfm per ton of refrigeration. Under those conditions, cooling is more rapid with more uniform load temperatures since the split is reduced with the higher volume of air.

1726

No. 1726

Solubility of Refrigerants 11, 21, and 22 in Organic Solvents Containing an Oxygen Atom

L. F. ALBRIGHT T. C. DOODY
P. C. BUCLEZ C. R. PLUCHE

Absorption refrigeration and air conditioning systems potentially offer several advantages as compared to vapor-compression type systems. Although the initial cost of the absorption systems is at present higher, their operating expenses are often appreciably lower. Even better advantages for the absorption systems would be possible if better chemical combinations were available as the solvent and refrigerant. Buffington[3] and Ellington[4] have outlined the major requirements for suitable chemicals for these systems, and the solubility characteristics of the refrigerant gas in the solvents are probably the single most important consideration.[10,11] The mixture should be non-ideal exhibiting large negative deviations from Raoult's law, i.e. the amount of refrigerant absorbed is larger than that predicted for ideal solutions.

Extensive studies to find suitable chemicals for absorption refrigeration were conducted about twenty years ago by Zellhoefer and associates,[12,13,14] who limited their solubility measurements for a given binary system to one temperature and one pressure. Although this information is useful as a rough screening technique for suitable binary systems, more elaborate investigations now seem necessary in order to learn more of the fundamentals of the absorption phenomena.

Extensive studies concerning the solubility characteristics of several binary systems have been made[11] and some appliance manufacturers are showing considerable interest in this area of research. Mastrangelo[7,8] and Albright[1,2] re-

L. F. Albright, Professor, and T. C. Doody, Assistant Professor, School of Chemical Engineering, Purdue University. P. C. Buclez and C. R. Pluche are graduate students at Purdue.
This paper was presented at the ASHRAE 67th Annual Meeting in Vancouver, B. C., June 13-15, 1960.

cently have investigated the solubility characteristics of several fluorocarbon refrigerants in some organic solvents. Hydrogen bonding or lack of hydrogen bonding is a significant factor in explaining the solubility characteristics noted in these solutions.

The present investigation was made in order to determine systematically the solubility characteristics of three fluorocarbon refrigerants in polar organic solvents, which contain an oxygen atom, over a wide range of temperatures and pressures. The results obtained help evaluate the factors of importance in the solubility phenomenon and in addition will aid in directing future research for finding better chemical combinations for absorption refrigeration.

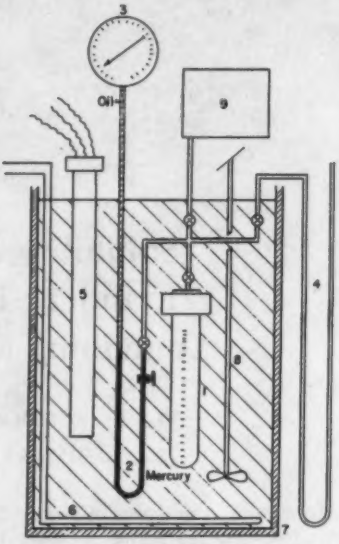

Fig. 1 Vapor pressure equipment

Equipment and operating procedures — Solubility measurements were made in static equilibrium cells with internal volumes of 50-100 ml (Fig. 1). The cells for the measurements up to 100 psig were Aerosol-type glass tubes. A neoprene gasket and Teflon insert were used to obtain a seal between the tube and the metal top and flange arrangement. A ¼ in. Hoke valve was provided in the opening at the top of the cell. For the higher pressure studies, the cell was machined from stainless steel, and the top was then welded to it.

The valve on the equilibrium cell was connected through a metal cross and tubing to an open-end manometer, a vacuum pump, and an oil-mercury leg on which was mounted a pressure gauge. This leg allowed the pressure in the equilibrium cell to be transmitted to the pressure gauge, and yet restricted the fluids of the equilibrium cell to equipment immersed in the oil bath. The pressure gauge assembled on the oil-mercury leg was calibrated in situ.

The oil bath temperature was controlled manually to within 0.1 F by means of electric heaters and a heating coil immersed in the bath. Mechanical agitation maintained temperature differences in the bath to less than 0.1 F as measured by calibrated mercury thermometers.

TABLE I
BINARY SYSTEMS INVESTIGATED

Solvent	Refrigerants
Diethyl oxalate	21, 22
Diethyl malonate	11, 21, 22
Dimethyl malonate	21
Diethyl adipate	21
Ethyl benzoate	21, 22
n-butyl benzoate	21
Triacetin	21, 22
Ethyl laurate	21
n-heptyl alcohol	11, 21
Ethylene glycol	22
Glycerine	22
Oleic acid	21
Linoleic acid	11, 21, 22
Valeric acid	21, 22
2-octanone	11, 21
Benzaldehyde	21, 22
Acetophenone	21, 22
2, 4-pentanedione	21, 22
Dimethyl ether or tetraethylene glycol	11, 21, 22

At the beginning of a run, the equilibrium cell was disconnected from the apparatus and cleaned. It was then weighed to within 0.005 g, and was next filled with about 10-20 ml of the high-boiling organic solvent to be tested. The cell was evacuated for several minutes by means of a vacuum pump and was weighed to determine the amount of solvent in the cell. The cell was then connected to a refrigerant cylinder, and some refrigerant was condensed in the cell. The cell was next disconnected, and some refrigerant gas in the cell was vented to remove any air that might have accidentally entered the cell. The cell was weighed again to determine the amount of refrigerant in the cell.

The loaded cell was connected to the solubility apparatus (Fig. 1) and the lines to the oil-mercury leg were evacuated by means of the vacuum pump. The valves to the vacuum pump and the manometer were closed, and the valve on top of the equilibrium cell was opened allowing the pressure in the cell to be read on the pressure gauge. The bath temperature was adjusted to the desired level, and equilibrium in the cell was reached after the pressure readings were constant for at least five minutes.

Equilibrium was promoted by tapping or slightly shaking the cell, and it usually occurred within 15 to 30 min. In general, the bath temperature was raised to the desired temperature during the course of a run since equilibrium was reached more quickly in this manner. Occasionally, however, the bath was cooled to a desired temperature, and an equilibrium pressure was again obtained and compared to the previous reading at the same temperature. Such a procedure checked the accuracy of the previous reading and indicated if any leaks had occurred in the equipment.

When the equilibrium pressure readings had been completed at the desired temperatures, the valve of the equilibrium cell was closed. The cell was then disconnected from the apparatus and reweighed. In all cases the final weight of the cell agreed with the initial weight except for the small amount of refrigerant lost in the connecting line to the oil-mercury leg.

For each measurement, the temperature and total pressure of the system (psia) were obtained directly. The solvent in the cell

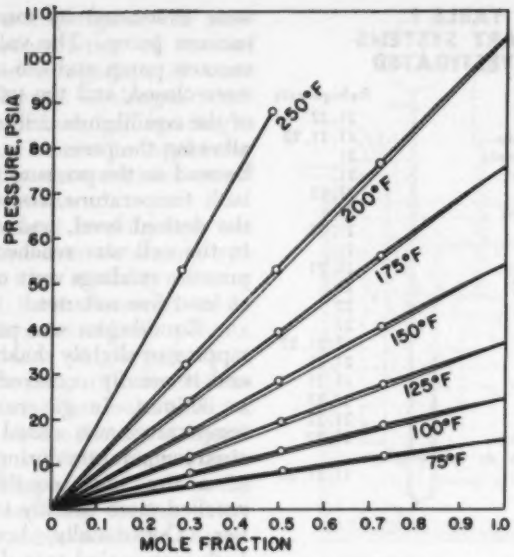

Fig 2 Solubility of Refrigerant 11 in dimethyl ether of tetraethylene glycol

was assumed to be entirely in the liquid phase. This assumption in general is quite acceptable since the vapor pressure of the solvent is quite low in the temperature range of this investigation. Since the volume of the cell plus the connecting lines had been determined to within 0.3 cc, the entire volume of the gas and liquid phases was known.

When the glass equilibrium cell was employed, the liquid volume and hence the gas volume could be easily determined since the cell was graduated. The amount of refrigerant in the gas phase was calculated from P-V-T relationships, and by difference the amount of refrigerant in the liquid was determined. The concentration of refrigerant in the liquid could then be calculated on either a weight or mole basis. When the metal equilibrium cell was used, the volume of liquid could not be determined visually. It was assumed that the solvent and refrigerant liquid volumes were additive, and calculations were made on that basis. The results in the glass cell indicate that this assumption results in only an insignificant error.

RESULTS

Thirty-four binary systems were investigated as indicated in Table I. In general, solubility data were

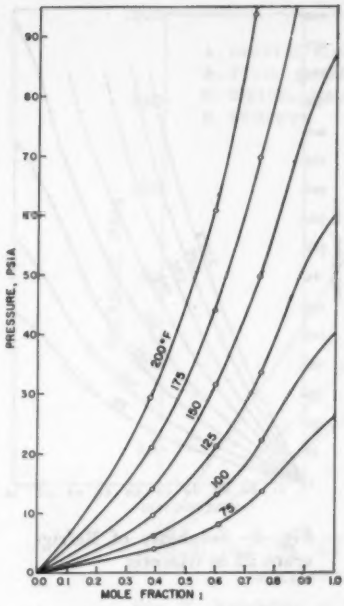

Fig. 3 Solubility of Refrigerant 21 in diethyl adipate

collected at temperature intervals of 25 F from 75 F up to 200-250 F. Three to six measurements were made at relatively different compositions for each temperature investigated, and at pressures up to those approaching the vapor pressure of the refrigerants.

Refrigerant 11 (CCl_3F) was investigated with several types of solvents: an ester (diethyl malonate), an alcohol (n-heptyl alcohol), a ketone (2-octanone), and an ether (dimethyl ether of tetraethylene glycol). The solutions formed in all cases indicated positive deviations from Raoult's Law, i.e. the pressure of the system was higher than predicted for an ideal solution, or less refrigerant was dissolved than expected. Fig. 2 shows the solubility results plotted as the pressure of the mixture versus the molal concentration of refrigerant in the mixture of Refrigerant 11 and dimethyl ether of tetraethylene glycol.

The constant temperature lines of this graph were extended to mole fractions of 0.0 and 1.0 where the pressures are the vapor pressure of the pure solvent and the pure refrigerant respectively. Fig. 2 shows slight positive deviations, and the pressure values for ideal solutions as predicted by Raoult's Law are shown as the straight lines just slightly below the smooth curves for the experimental data. The solutions of Refrigerant 11 with the other solvents, especially n-heptyl alcohol, had even higher positive deviations than shown in Fig. 2.

Refrigerant 21 ($CHCl_2F$) and Refrigerant 22 ($CHClF_2$) formed solutions with negative deviations from Raoult's Law with esters, carbonyl compounds (ketones and aldehydes) and the dimethyl ether of tetraethylene glycol. These refrigerants, however, formed solutions with positive deviations with alcohols and glycols. Solutions with acids were relatively ideal, in some cases showing positive deviations and in other cases negative deviations. All solutions of esters and Refrigerants 21 or 22 investigated had relatively high negative deviations. Typical examples of the results obtained for esters are shown in Fig. 3 (diethyl adipate and Re-

frigerant 21) and Fig. 4 (triacetin and Refrigerant 22).

The number of ester groups in a molecule is an important factor regarding the refrigerant solubility as shown in Fig. 5. Triacetin with three ester groups dissolves more refrigerant than does diethyl malonate, which has two ester groups, or ethyl benzoate, which has only one ester group.

Calculations were made to determine the amount of refrigerant dissolved per ester group in the solvent; in general the effectiveness of each ester group decreases as the number of ester groups in the solvent molecule increases. In diester molecules, the solubility of the refrigerant increases on a mole basis, but not necessarily a weight basis, as the following factors vary:

(1) As the number of methylene groups between the ester groups increases;

(2) When ethyl and especially higher alkyl esters are used instead of methyl esters;

(3) When aliphatic esters are employed instead of aromatic esters.

High positive deviations occurred for mixtures of n-heptyl alcohol and Refrigerants 21 or 22 (Fig. 5). Tests with ethylene glycol and glycerine indicated that immiscible liquid phases sometimes formed, which indicates extremely high positive deviations.

Fig. 6 compares the solubility results of three organic acids with Refrigerant 21 at 100 F. The results seem to indicate that double bonds in the acid improve the solubility characteristics. Note that

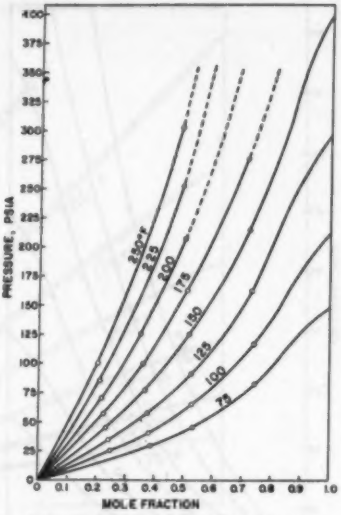

Fig. 4 Solubility of Refrigerant 22 in triacetin

linoleic and oleic acids produce negative deviations from Raoult's Law but valeric acid gives positive deviation.

Carbonyl-type solvents dissolve relatively large amounts of Refrigerants 21 and 22 (Fig. 7). Of the carbonyl compounds studied, the refrigerants were most soluble in 2-octanone. Less solubility was obtained in 2, 4-pentanedione, which contains two carbonyl groups; apparently the carbonyl groups are close enough together so that an interaction occurs between them to give an enol form.[9] Less refrigerant solubility was obtained in aromatic carbonyl compounds such as acetophenone and benzaldehyde.

The dimethyl ether of tetra-

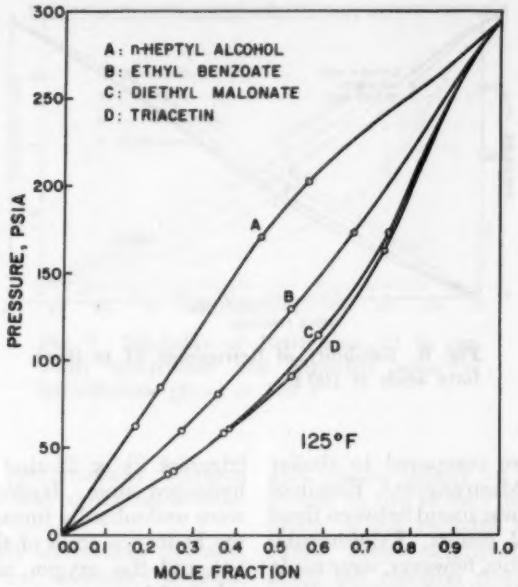

Fig. 5 Solubility of Refrigerant 22 in esters and heptyl alcohol at 125 F

ethylene glycol was found to be the best solvent of those studied for Refrigerants 11, 21, and 22. Fig. 8, which shows the results with Refrigerant 22, indicates the large negative deviations from the ideal solution curves. Curve A on Fig. 7 indicates the significantly better solubility of Refrigerant 21 in this ether as compared to the carbonyl compounds.

CAUSE AND EFFECT

Solubility data of this investigation were found to be reproducible within about 2% as indicated by frequent repeat runs and the good correlation of the experimental data by graphs such as Figs. 2 to 8. In addition cross plots of the data at constant composition yielded smooth curves of pressure versus temperature. Inaccuracies of the pressure, temperature, weight, and volume measurements would perhaps account for additional errors as high as 1%. Furthermore, the assumption that no solvent is present in the gas phase would cause a small error particularly at higher temperatures. The overall accuracy of the solubility results is thought to be within 4%.

The solubility results for the mixture of the dimethyl ether of tetraethylene glycol and Refriger-

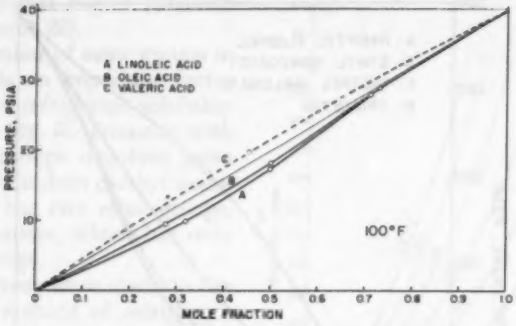

Fig. 6 Solubility of Refrigerant 21 in three fatty acids at 100 F

ant 22 were compared to similar results of Mastrangelo.[8] Excellent agreement was found between these two sets of results. Experimental measurements, however, were made at higher refrigerant concentrations than in the previous study, and the extrapolated curves of that study do not agree too well with the present data.

It was possible to compare the present results with those of Zellhoefer[12,14] in several cases. The relative amounts of Refrigerant 22 absorbed by several solvents were similar in the two investigations. However, the absolute amounts of refrigerant absorbed as reported by Zellhoefer were often 5-6% lower than those of this investigation. His experimental technique is thought to be less accurate than the one employed here.

The present investigation was limited to polar solvents that contain oxygen atoms, and the results definitely indicate the importance of using a refrigerant such as Refrigerant 21 or 22 that contains a hydrogen atom. Hydrogen bonds were undoubtedly formed between the hydrogen atom of the refrigerant and the oxygen atom of the solvent.[5,6]

These bonds obviously account for the improved solubility characteristics of Refrigerants 21 and 22 as compared to Refrigerant 11. Previous data of Albright and associates[1,2] indicate that halogenated methanes and ethanes are less soluble in non-polar hydrocarbon oils than in the solvents of the present investigation. In the case of the non-polar solvents, the hydrogen atom of the refrigerant can not form a hydrogen bond with the solvent.

The poor solubility characteristics of alcohols and acids is probably because these compounds tend to associate or hydrogen bond with themselves rather than with the refrigerant. In the case of the ethers, esters, and carbonyl compounds, the hydrogen bonding is

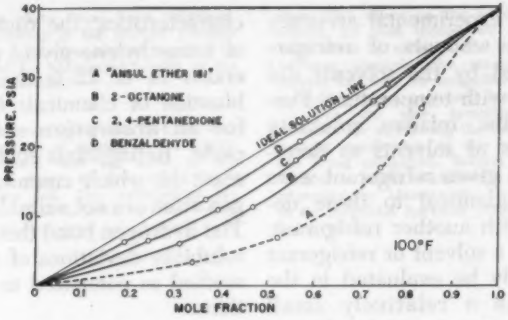

Fig. 7 Solubility of Refrigerant 21 in carbonyl compounds and dimethyl ether of tetraethylene glycol at 100 F

apparently preferentially between the solvent and refrigerant molecules.

Solubility differences between related solvent molecules is probably caused mainly by the atomic groups in the vicinity of the polar group, which contains the oxygen atom. These neighboring groups affect the electron density of the polar group and hence the strength of the hydrogen bond. In addition, they may have a significant effect on the spatial configuration of the solvent molecule so that steric hindrances may prevent good utilization of all polar groups.

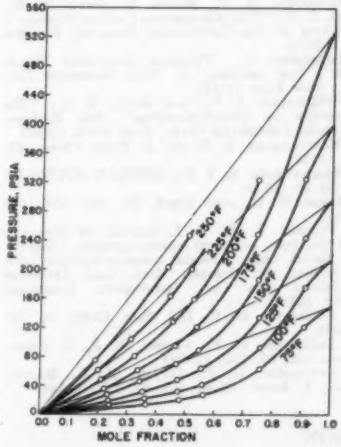

Fig. 8 Solubility of Refrigerant 22 in dimethyl ether of tetraethylene glycol

This reason may be important for solvent molecules containing more than one polar group. For example, Mastrangelo[7] reports that only two or three of the five oxygen atoms of the dimethyl ether of tetraethylene glycol are being utilized. It is quite possible then that related ether molecules might exhibit better solubility characteristics and minimize steric hindrances.

Numerous comparisons were made between the solubility results of mixtures of various solvents and a given refrigerant. It was found

that within experimental accuracy the relative amounts of refrigerant absorbed by the solvents did not change with temperature. Furthermore, the relative solubility effectiveness of solvents as determined for a given refrigerant were essentially identical to those determined with another refrigerant. As a result, a solvent or refrigerant can probably be evaluated in the future with a relatively small amount of experimental information.

The results as shown in Figs. 2 to 8 are presented on a mole basis since it is possible to compare the results to Raoult's Law and since the data can be better evaluated in a theoretical manner. From a practical standpoint in regard to absorption refrigeration, the results are more meaningful on a weight or volume basis. Calculations indicate, however, that the dimethyl ether of tetraethylene glycol is still the best solvent on these bases. Based only on the solubility results of this study, this ether and Refrigerants 21 or 22 should prove to be a relatively good system, and an actual coefficient of performance of about 0.35 may be possible.[8, 10]

CONCLUSIONS

Esters, carbonyl compounds, and particularly ethers are good solvents for refrigerants containing a hydrogen atom such as Refrigerants 21 or 22. Based only on solubility characteristics, the dimethyl ether of tetraethylene glycol and Refrigerants 21 or 22 is the best combination of chemicals investigated for an absorption refrigeration cycle. Refrigerants such as Refrigerant 11 which contain no hydrogen atom are not suitable, however, The hydrogen bond theory explains solubility deviations of the systems studied as compared to ideal solutions.

ACKNOWLEDGMENT

This research was sponsored by the Indiana Gas Association and the commercial-grade refrigerants were furnished by E. I. du Pont de Nemours and Co., Inc.

REFERENCES

1. Albright, L. F., Mandelbaum, A. S., Refrig. Eng. 64 (10), 37 (1956)
2. Albright, L. F., Lawyer, J. D., ASHRAE JOURNAL 1 (4), 67 (1959)
3. Buffington, R. M., Refrig. Eng. 57, 343 (1949)
4. Ellington, R. T., Kunst, G., Peck, R. E., Reed, J. F., "The Absorption Cooling Process", Institute of Gas Technology Research Bulletin 14, (1957)
5. Glasstone, S., "Physical Chemistry Handbook", 2nd Edition, D. Van Nostrand Co., Inc., New York (1946)
6. Hildebrand, J. H., and Scott, R. L., "The Solubility of Nonelectrolytes", 3rd Edition, Reinhold Publishing Corp., New York (1950)
7. Mastrangelo, S. V. R., J. Phys. Chem. 63, 608 (1959)
8. Mastrangelo, S. V R., ASHRAE JOURNAL 1 (10) 64 (1959)
9 Meyer, K. H., and Hopff, H., Ber. 54B, 579 (1921)
10. Palmer, F. S., E. I. duPont de Nemours and Co, Inc., personal communication (1958)
11. Servel, Inc., personal communications with Whirlpool, St. Joseph, Mich. and Arkansas Louisiana Gas Co., Shreveport, Louisiana (1958, 1959)
12. Zellhoefer, G. F., Ind. Eng. Chem. 29, 548 (1937)
13. Zellhoefer, G. F., Copley, M. J., J. Amer. Chem. Soc. 60, 1343 (1938)
14. Zellhoefer, G. F., Copley, M. J., Marvel, C. S., J. Amer. Chem. Soc 60, 1337 (1938)

DISCUSSION

H. O. SPAUSCHUS, Louisville, Ky.: You assumed that the volume of mixing of the two components was ideal. For solutions of the type you have studied, particularly those involving hydrogen bonding, it is known that the volume change on mixing can be as large as 10-15%. How does this affect your results?

With the data you have obtained, wouldn't the plotting of the activity (instead of pressure) as a function of mol fractions be a better method for comparing results of the various systems studied?

CLOSURE BY AUTHOR ALBRIGHT: You are correct that the volume of mixing in the binary systems investigated was not ideal as we discovered in a series of runs made in a glass equilibrium cell. Our calculations indicated that a 15-20% error of the vapor volume will have, however, only a small (less than 1%) effect on the calculated solubility values. So even though we were unable in most cases to measure the liquid and vapor volumes precisely, the assumption of ideal mixing had only an insignificant effect on the solubility values presented here.

We are now investigating improved methods for correlating the data. Activity and activity coefficients of the refrigerant gases are being calculated. Several techniques, including a slight modification of the method presented by Mastrangelo in a recent paper in the ASHRAE JOURNAL (October 1959), are being tested.

1727

No. 1727

Determination of Moisture in Fluorocarbons

JOSEPH D. MORTON LAURA K. FUCHS

A method generally recommended throughout the industry for determining traces of water in refined fluorocarbons (refrigerants or aerosol propellants) is the phosphorus pentoxide absorption procedure. Using this procedure, approximately 300 g of specification grade sample is necessary to obtain a net increase of only 2 to 3 mg in the weight of the absorption bulbs. The method is extremely time consuming for routine analyses since a single determination requires from 3 to 16 hr depending upon the flow rates used in different laboratories.

Other methods, utilizing the Karl Fischer reagent,[1,2] lack the required accuracy and sensitivity for determining water in the 1 to 20 ppm range and are difficult to apply to materials which are gases under ordinary conditions. Infrared spectrophotometric methods[3] and the use of the electrolytic water analyzer[4,5] both have certain disadvantages when applied to the routine analysis of a wide variety of discrete samples.

The cost of infrared equipment may preclude its use in smaller laboratories. The electrolytic analyzer is affected by changes in temperature and precautions in varying degree must be taken regarding the sample and instrument temperature. The need for a faster, more accurate method of analysis that could be applied to a variety of discrete samples on a routine basis initiated this investigation.

In the investigation reported here, the sensitivity of the Karl Fischer method for water was increased approximately 100 fold by a simple dilution of the reagent with methanol neutralized with Karl Fischer reagent. A cooled, pressurized titration apparatus was designed which allowed the samples to be analyzed from the liquid phase and provided maximum pro-

J. D. Morton and L. K. Fuchs are with the Development Department of the Union Carbide Chemicals Company, a division of Union Carbide Corporation. This paper was presented at the ASHRAE 67th Annual Meeting, Vancouver, B. C., June 13-15, 1960.

tection from atmospheric contamination during the sample addition and titration procedure. The method can be performed rapidly in a routine analytical laboratory and is applicable to Refrigerants (refrigerants or aerosol propellants) 11, 12, 22, 113, and 114, as well as to many other compounds which are liquids at 0 C and 60 psi, pressure.

The average standard deviation of the procedure is 0.6 ppm and the accuracy is ± 1 ppm water in the 1.0 to 20 ppm range. All of the components required to fabricate this apparatus can be purchased at a total cost of approximately $600.

REAGENTS

Standard Reagent (equivalent to approximately 2 mg of water per ml of reagent.)

Dilute reagent (equivalent to approximately 35 micrograms of water per ml of reagent). Mix 200 ml of redistilled pyridine and 700 ml of anhydrous methanol (containing no more than 30 ppm carbonyl as acetaldehyde) in the reservoir of a 10-ml automatic buret. Titrate with standard reagent to the visual end point. Add additional standard reagent equivalent to 1/50 of the volume of the neutralized methanol-pyridine solution, and mix well. Store in a 10-ml automatic microburet equipped with drying tubes which are refilled daily with Drierite or other suitable desiccant. Use polyethylene grease on the ground-glass joints.

Standard Methanol-Water Solution—Fill an 8-ounce bottle with anhydrous methanol which contains between 300 and 1000 ppm water and no more than 30 ppm carbonyl as acetaldehyde. Add distilled water to the methanol if the water content is too low. Stopper the bottle with a rubber serum bottle cap. Do not open the bottle to the air thereafter. Allow the methanol-water solution to stand in the bottle at least one hour before using.

APPARATUS

A pressure titration flask was designed and built as shown in Fig. 1. The pressure chamber was constructed with a cooling jacket to avoid excessively high pressures. The highest anticipated pressure is 60 psi, the vapor pressure of Refrigerant 22 at 0 C. The pressure chamber was tested hydrostatically for 100 psi.

The pressure titration flask is attached to a 10-ml automatic microburet as shown in Fig. 2. The leads from the electrodes of the pressure titration flask are attached to the voltage source and a volt-ohmmeter as shown in Fig. 3.

The 50-ml sampling tube for handling liquid samples is made by adding a pressure stopcock to each end of the bulb of a 50-ml pipet. One stopcock is provided with a 5/20 standard taper joint to which a No. 22 hypodermic needle can be fitted. A short section of 6-mm tubing is added to the other stopcock for attaching to the sample cylinder with a suitable connector.

A 9-in. hypodermic needle is made from a section of stainless

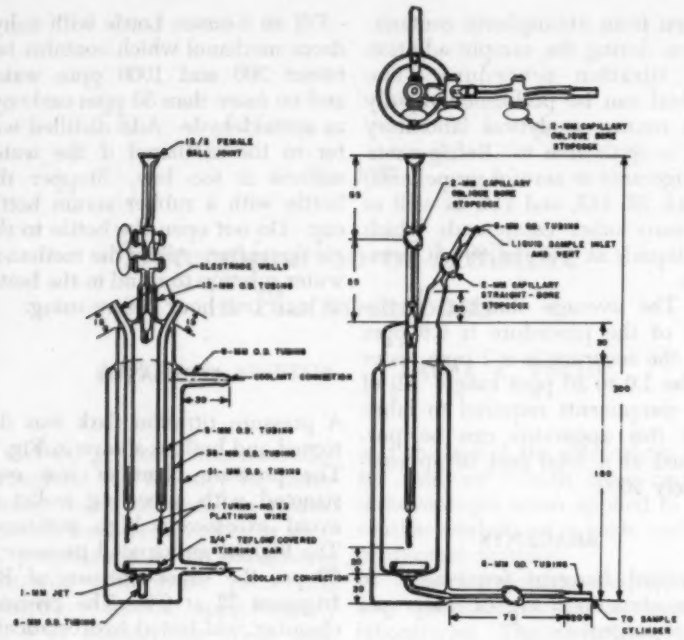

GENERAL NOTES

All dimensions given in millimeters

All Pyrex construction

Stopcocks may be secured with an Emil Grenier stopcock pressure adapter

Test inner - chamber of cell at 100 psi hydrostatic

Fig. 1 Pressure titration flask

steel capillary tubing (0.050 in. O.D., 0.017 in. I.D.) silver-soldered to the base of a No. 22 hypodermic needle.

Anyone wishing to set up this apparatus should consult a reliable glass blowing shop to have the pressure titration flask and other specialized glassware fabricated. Most of the other glass equipment can be purchased from any reliable laboratory supply house. The components of the voltage source and a voltohmmeter can be purchased from any one of a number of the larger instrument companies or electronic parts supply houses.

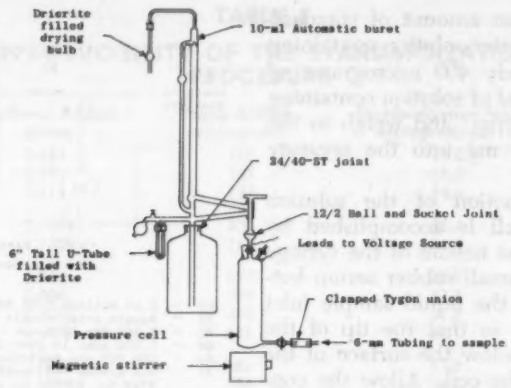

Fig. 2 Flask attached to 10 ml automatic microburet

STANDARDIZATION OF REAGENTS

Standard Reagent—Standardize this reagent against distilled water.

Dilute reagent — Prepare a pressure cell (Fig. 1) by drying it overnight in a 200 C oven and cooling to room temperature with a stream of nitrogen which has been passed through a U-tube filled with a 50-50 mixture of phosphorus pentoxide and asbestos fiber. Immediately close the stopcocks, which have been lubricated with polyethylene grease, and insert a rubber serum cap in the liquid sample inlet. Fill the electrode wells with sufficient mercury to make contact with the platinum wires attached to the leads from the voltage source. Protect the openings of the cell with drying tubes containing a suitable desiccant.

Inject approximately 30 ml of anhydrous methanol through the liquid sample inlet into the cell, so that the electrodes are completely covered. Attach the leads from the voltage source (Fig. 3) and start the magnetic stirrer. Apply a potential of 0.6 volt to the leads by adjusting the regulator knob on the voltage source (resistor R2 in the circuit diagram).

Equip a 5-ml syringe with a 2-in. long No. 22 hypodermic needle and fill the syringe with standard reagent. Add the reagent dropwise to the cell through the liquid sample inlet until the voltage approaches 0.1 volt. Attach the 10-ml automatic buret to the cell (Fig. 2) and titrate the contents of the cell with dilute reagent until the voltage remains at 0.1 volt or lower for 60 ± 5 seconds.

Rinse a 2-ml syringe fitted with a 9-in. hypodermic needle four times with the standard methanol-water solution by withdrawing and discarding portions of the solution.

Withdraw an amount of standard methanol-water solution containing approximately 400 micrograms of water (0.8 ml of solution containing 500 ppm water) and weigh to the nearest 0.1 mg into the pressure cell.

Introduction of the solution into the cell is accomplished by inserting the needle of the syringe through a small rubber serum bottle cap on the liquid sample inlet of the cell so that the tip of the needle is below the surface of the liquid in the cell. Allow the contents of the cell to mix for one minute and titrate with dilute reagent until the voltage remains at 0.1 volt or less for 60 ± 5 sec.

Record the volume of reagent and the weight of the standard methanol-water solution used. Make a duplicate determination by adding more standard methanol-water solution to the same cell and repeating the titration procedure. Duplicate determinations should agree within 2 micrograms of water per ml of reagent.

If the factor for the dilute reagent does not fall between 30 and 45 micrograms of water per ml, add more standard reagent or more anhydrous methanol as required to bring the factor within range. This factor should be checked approximately every three weeks.

Standard Methanol-Water Solution – Determine the concentration of the water in the methanol using the standard reagent.

PROCEDURE

Procedure for Refrigerants 11 and 113 – Follow the previous instructions to prepare the pressure cell for use. For Refrigerant 11, circulate coolant at 0 C through the jacket around the cell. No coolant is required for Refrigerant 113. Attach the 9-in. hypodermic needle to the sample cylinder of Refrigerant 11 and weigh to the nearest 0.1 gm. If the sample cylinder is too large to weigh to the nearest 0.1 gm, rinse a 50-ml glass sampling tube four times with portions of the sample, and fill the tube with sample leaving a small vapor space at the top. Weigh the tube to the nearest 0.1 gm. Refrigerant 113 is most easily handled in a standard 50-ml syringe equipped with a 9-in. needle.

Insert the 9-in. needle through the liquid sample inlet tube and introduce below the surface of the

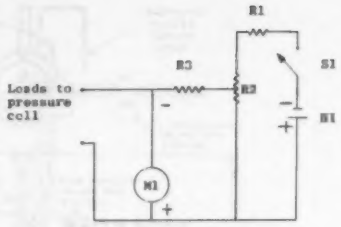

Circuit Diagram
Voltage Source

B1 - 1.3V Mallory Cell RM-42-R
S1 - Single pole, single throw switch
R1 - 2,500 ohm Resistor
R2 - 5,000 ohm, 10 Turn Helipot
R3 - 100,000 ohm Resistor
M1 - RCA Senior VoltOhmist
VTVM No. WV-98A or equivalent
Circuit housed in suitable cabinet

Fig. 3 Leads from electrodes of the flask are attached to the voltage source and voltohmmeter

TABLE I

REPRODUCIBILITY OF THE STANDARDIZATION PROCEDURE

Methanol Added, grams	Water Added, micrograms	Standardization Factor, micrograms per ml
0.181	115	14.0
0.295	187	15.0
0.311	197	14.6
0.7988	206	25.1
1.1225	317	26.4
0.944	274	30.5
0.804	234	32.3
1.1556	454	31.2
1.4472	422	32.1
1.1842	386	37.0
1.1782	384	36.0
	Standard deviation	0.73

liquid in the cell approximately 30 gm of the sample taken from the liquid phase. Reweigh the sample container to obtain the weight of sample used. Allow the contents of the flask to mix one minute and titrate with Karl Fischer reagent until the voltage remains at 0.1 volt or less for 60 ± 5 seconds. Record the volume of reagent and sample size. Make three additional determinations using the same cell and procedure. When necessary, the cell can be drained through the inlet tube at the bottom of the cell.

Procedure for Refrigerants 12, 22 and 114 – Prepare the pressure cell as previously described. The use of a safety shield in front of the cell is required to prevent injuries in case of breakage of the cell. Circulate coolant at 0 C through the jacket around the cell for Refrigerants 12 and 22; no coolant is required for Refrigerant 114.

Weigh a conveniently sized cylinder of the sample to the nearest 0.1 gm, and connect the cylinder to the glass inlet tube at the bottom of the pressure cell so that the liquid phase of the sample will be used. Protect the cylinder outlet and the cell inlet with Drierite-filled drying tubes when they are not connected. Titrate the contents of the cell with dilute reagent until the voltage remains at 0.1 volt or less for 60 ± 5 seconds. Add 5 ml, measured to the nearest 0.02 ml, of the reagent in excess.

Open the stopcock at the bottom of the cell and carefully open the valve on the sample cylinder to permit the liquid sample to vaporize into the inlet tube and bubble up through the solution in the cell. The use of a heat lamp on the inlet tube is necessary to keep samples of Refrigerant 114 in the gaseous state. Continue the slow bubbling until the voltage just begins to rise above the 0.1 volt mark.

Immediately close the sample cylinder valve and the inlet stopcock. Disconnect the sample cylinder and reweigh to determine the size of sample used. Protect the cylinder outlet and cell inlet with drying tubes. If the sample size is under 15 gm, repeat the determination using 10 ml excess of reagent measured to the nearest 0.02 ml. Make three additional determinations by repeating the procedure.

Relieve the pressure in the cell immediately after each determination by venting through a piece of rubber tubing attached to the vent stopcock. Thus, the same cell may be used for several determinations. The level of the solution in the cell may be lowered by draining under pressure through the bottom inlet tube. When the solution in the cell becomes cloudy, it must be drained, cleaned, and re-conditioned as previously described.

CALCULATIONS

Factor for Standard Reagent

$$\frac{A \times 100}{B} = C$$

A = gm of water added
B = ml of standard reagent required for titration
C = factor, gm of water equivalent to 100 ml of standard reagent

Water Content of the Standard Methanol-Water Solution

$$\frac{D \times C \times 10{,}000}{\text{gm sample}} = E$$

C = factor for standard reagent
D = ml of standard reagent required for titrating the methanol-water solution
E = ppm water (micrograms per gm)

Factor for Dilute Reagent

$$\frac{F \times E}{G} = H$$

E = ppm water in standard methanol-water solution
F = gm of standard methanol-water solution added to cell
G = ml of dilute reagent required
H = reagent factor, micrograms water per ml of dilute reagent

Water in Fluorocarbon Sample

$$\frac{I \times H}{\text{gm sample}} = \text{water, ppm}$$

I = ml of dilute reagent required for titration
H = factor for dilute reagent

RESULTS

The standard reagent, which is ordinarily used in the laboratory, has a factor of approximately 2,000 micrograms of water per ml of reagent. Using this reagent, a 2000-g sample containing 1 ppm water would consume only one ml of titrant. Various dilutions were prepared, ranging from ½ to 1/400 of the standard reagent.

The stronger solutions lacked the required sensitivity and ex-

TABLE II

STABILITY OF DILUTE REAGENT

Original Factor, micrograms per ml	Factor After 1 Week, micrograms per ml	Factor After 2 Weeks, micrograms per ml	Factor After 3 Weeks micrograms per ml
14.5	14.8	15.0	14.0
31.0	31.2	30.8	31.5
32.8	31.8	33.4	32.0

tremely dilute solutions would not produce a measurable end point. A dilute reagent having a factor of 30 to 45 micrograms of water per ml was adopted.

In order to standardize the dilute reagent, it was necessary to add accurately not more than 400 micrograms of water to the flask. The usual method of adding hydrates was not used because they cannot be weighed into the titration flask without opening the flask to the atmosphere.

The problem was solved by applying the common technique of using methanol containing a known amount of water as a standard.[6] The water content of methanol containing 300 to 500 ppm water was determined with standard reagent which had been previously standardized against pure water. This methanol was stored in a bottle fitted with a rubber serum bottle cap and a Drierite-protected vent. Aliquots were withdrawn with a hypodermic syringe and weighed into the flask, and the reagent standardized in this manner.

Bottles of this standard methanol-water solution have remained unchanged in water content for three weeks and can probably be stored indefinitely. The data in Table I show the reproducibility of the standardization procedure.

The dilute reagent is remarkably stable if it is well protected

TABLE III

DETERMINATION OF KNOWN AMOUNTS OF WATER IN METHANOL

Water, micrograms contained in methanol	Reagent Factor, micrograms per ml	Water Added (30 gm basis), ppm	Water Found (30 gm basis), ppm	Recovery, %
46	15	1.5	1.5	100
107	15	3.6	3.4	95
119	15	4.0	4.0	100
119	15	4.0	4.1	102
194	15	6.5	6.3	97
204	15	6.8	6.7	99
77	30	2.6	2.8	108
77	30	2.6	3.0	115
157	30	5.2	5.6	107
234	30	7.8	9.0	115
422	30	14.1	13.1	93
453	30	15.1	14.5	96
495	30	16.5	16.0	97
129	36	4.3	4.1	95
131	36	4.4	4.2	95
247	36	8.2	8.6	105
384	36	12.8	12.5	98
387	36	12.9	13.1	101
390	36	13.0	12.7	98
		Average Recovery		101

TABLE IV

DETERMINATION OF WATER IN FLUOROCARBONS

Fluorocarbon	11	12 (a)	12 (b)	22 (a)	22 (b)	113	114
Water in original sample, ppm (c)	0.6	3.3	3.0	6.9	6.7	8.2	14.4
Water added, ppm	17.7	3.2	4.3	9.8	81.6	10.8	13.5
Theoretical water content, ppm	18.3	6.5	7.3	16.7	88.3	19.0	27.9
Water by analysis, ppm (c)	17.3	8.1	6.9	17.7	88.4	18.0	27.5
Recovery, %	94.5	124.6	94.5	106.0	100.1	94.7	98.6

(a) Original analysis
(b) Analysis performed 2 weeks later on same sample
(c) Average of 2 to 4 determinations

against atmospheric moisture. Any loss in the strength of the solution appears to be due to water contamination rather than the usual side reactions found in the more concentrated reagent. Three bottles of the dilute reagent were standardized after standing for varying periods of time with results shown in Table II.

To provide the accuracy of the method, various portions of methanol which contained a known amount of water were weighed into the titration flask and analyzed. The water added in this manner was calculated as ppm water assuming a theoretical sample size of 30 g. The data are presented in Table III.

Various fluorocarbons were analyzed by this procedure. The results were found to be reproducible within approximately ± 1 ppm and within the 10 ppm maximum limit set by the fluorocarbon industry. Samples of known composition were prepared from these fluorocarbons by introducing a small known amount of water with

TABLE V

PPM WATER IN FLUOROCARBONS, REPRODUCIBILITY OF METHOD

	1st Day		2nd Day		3rd Day		4th Day	
Analyst	113	22	113	22	113	22	113	22
A	8.6	4.5	9.1	4.9	9.8	5.3	8.3	5.5
	9.6	4.7	8.9	4.7	9.5	5.4	9.4	4.4
Average	9.1	4.6	9.0	4.8	9.7	5.3	8.9	5.0
B	9.6	4.7	8.8	4.9	9.4	4.9	8.8	4.2
	10.0	4.2	9.1	4.9	10.1	5.2	9.4	4.4
Average	9.8	4.5	9.0	4.9	9.8	5.0	9.1	4.3

STANDARD DEVIATION, PPM PER DETERMINATION

Analyst	Refrigerant 113	Refrigerant 22
A	0.53	0.49
B	0.51	0.74

a hypodermic needle through the wall of rubber pressure tubing connecting an evacuated cylinder and a cylinder containing fluorocarbon with a known water content.

After introducing the water into the tubing, the valve of the evacuated cylinder was opened and then the valve of the cylinder containing fluorocarbon was opened slowly so that the fluorocarbon would carry the moisture into the evacuated cylinder. The data obtained by analyzing these known mixtures are shown in Table IV. The average recovery by the method is 101.9%; the average accuracy is ± 1 ppm water.

To obtain reproducibility data for the method, two analysts examined samples of Refrigerants 22 and 113 on four different days. The results of these analyses are shown in Table V. The average standard deviation for one determination is 0.6 ppm water for both liquid and gas samples. Because a reproducibility of ± 1 ppm is desired, we recommend taking the average of two determinations which has a standard deviation of 0.4 ppm.

Thus, 95% of the time the average of two determinations will be within a ±0.8 ppm probability range.

Samples of fluorocarbons were analyzed by the method and the phosphorus pentoxide procedure. The data obtained are compared in Table VI.

CONCLUSION

This method of analysis, after preliminary standardization and preparation of equipment, can be performed in a routine analytical laboratory in approximately fifteen minutes per determination. It has been found suitable for analyzing Refrigerants 11, 12, 22, 113 and 114 and should be applicable to other fluorocarbons and related compounds. The average standard deviation of the procedure is 0.6 ppm, and the accuracy is ± 1 ppm water in the 1 to 20 ppm range.

On the basis of the results obtained, the procedure is recommended for routine analysis of

TABLE VI

COMPARISON OF METHODS

Refrigerant	Water by P_2O_5 method, ppm (a)	Water by Karl Fischer method, ppm (b)
11	6.0	6.8
12	1.9	2.7
12	3.0	2.8
12	2.7	2.8
12	6.7	5.6
12	4.2	4.2
12	3.5	3.0
22	3.0	4.9
114	2.9	2.9

(a) Results of analysis by independent laboratory
(b) Results of analysis by a Union Carbide Chemicals Company routine analytical laboratory

fluorocarbons for water. It is believed that the use of the method is advantageous from the standpoint of accuracy, precision, ease of performance and analytical time saved.

ACKNOWLEDGMENT

Acknowledgment is made of contributions by R. L. Anderson and L. J. Stanley of this department and D. E. Peterson of the Institute Works Laboratory of Union Carbide Chemicals Company.

REFERENCES

(1) Reed, F. T., Refrigerating Engineering *62*, No. 7, p. 65 (July 1954).
(2) Reed, F. T., Downing, R. C., Proceedings, the 38th Annual Meeting, Chemical Specialties Manufacturers Association, Inc., p. 41 (December 1951).
(3) Benning, A. F., Ebert, A. A., and Irwin, C. F., Refrigerating Engineering *55*, p. 166 (February 1948).
(4) Taylor, E. S., Refrigerating Engineering *64*, No. 7, p. 41 (July 1956).
(5) Weaver, E. R., and Riley, R., National Bureau of Standards, Research Paper RP1865, 40, 1948.
(6) Mitchell, J. Smith, D. M. Aquametry, Interscience Publishers, Inc., New York, 1948.

DISCUSSION

R. C. McHARNESS, Wilmington, Del.: The authors are to be complimented on the development of a very interesting modification of the Karl Fischer method for use in the analysis of refrigerants for moisture. In their discussion of alternate methods, they have made a statement about the electrolytic moisture analyzer which is subject to possible misinterpretation and, accordingly, needs clarification.

It is true that, in the case of the higher boiling compounds such as Refrigerants 11, 113, and 114, precautions must be taken regarding the instrument temperature. However, this is true only to the extent that it is necessary to avoid any condensation in the instrument itself. The sample itself, can be at a wide range of temperatures. In the case of lower boiling compounds such as Refrigerants 12 and 22, no particular precautions are necessary. Thus, the electrolytic analyzer has been used with these refrigerants at temperatures varying from 30 to 85 F without affecting the result within the limitts of accuracy of the method.

CLOSURE BY MR. ENGLE: It was not intended to imply that any of the other methods were not usable. The statement that the analyzer was affected by temperatures certainly could be clarified. It was intended to point out what could happen in the analysis of a wide variety of discrete fluorocarbon samples in which condensation results from the higher boiling refrigerants in the electrolytic cell. Your point is well taken.

H. O. SPAUSCHUS, Louisville, Ky.: What are the upper limits of moisture that can be determined with your dilute Karl Fischer reagent and the equipment used?

MR. ENGLE: When this work was initiated, the primary concern was to develop a procedure for water concentrations of 20 ppm or lower. Therefore, the analysis of materials containing higher concentrations of water was not investigated thoroughly. Analysis was made of at least one or two synthetically-prepared samples containing as high as 80 ppm of water. There is no reason why the procedure wouldn't work for higher concentrations provided sample size is taken into consideration. Another method of determining higher concentrations of water is to increase the concentration of the Karl Fischer reagent. DuPont, I believe, has published a procedure for analyzing aerosol preparations using Karl Fischer which was intended for water concentrations in the range of 200-500 ppm.

R. E. AHLF, Evansville, Indiana: When low boiling fluorocarbons are bubbled through the dilute Karl Fischer reagent, is the water proportionately distributed in the first, second and third samples from the sample bottle?

MR. ENGLE: The first determination may be somewhat higher than subsequent determinations because of moisture that may have entered into the connections between the sample cylinder and the cell. Our experience has been that this is normally flushed out in the first determination, and the subsequent determinations are quite repeatable. All sampling is taken from the liquid phase of the cylinder, not the vapor phase.

R. N. CORK, Chicago, Ill.: It is possible to check moisture for a Refrigerant 12-22 mixture. Have you done so?

MR. ENGLE: This procedure for checking moisture has been used in the analysis of fluorocarbon blends since blends are commonly-used in the aerosol propellant field. This same procedure is used for blends of 11 and 12 and 12 and 114. I see no reason why it couldn't be used for a 12 and 22 mixture.

1728

No. 1728

A Study of the Factors Influencing the Stability of Mixtures of Refrigerant 22 and Refrigerating Oils

W. O. WALKER
Fellow, ASHRAE

S. ROSEN

S. L. LEVY

This is the first of a series of reports on a broad study of the factors influencing the stability of fluorocarbon refrigerants and refrigerating oil mixtures. To date, limited attention has been paid to these mixtures. Philipp and Tiffany[1] proved that sulfur dioxide and refrigerating oils react at elevated temperatures and used the reaction to select suitable oils.

Steinle[2,3] studied this reaction in refrigerators and made use of the Philipp test to investigate the stability of Refrigerant 12 and methyl chloride-oil mixtures. Elsey[4] modified the Philipp test in order to develop a method of evaluating refrigerator oils. This involved the study of the stability of several refrigerants with refrigerator oils at elevated temperatures.

Williamitis[5] showed that a Refrigerant 12-oil mixture deteriorates more rapidly as the temperature is increased and that the type of oil may change the rate of deterioration. He also discussed the mechanism of the refrigerant-oil mixture reaction. Kvalnes and Parmelee[6] investigated the stability of Refrigerants 12 and 22-oil mixtures as it relates to the type and viscosity of oils, oil additives, temperature, metals, moisture, anti-freeze agents, and cellulose.

In this study, Refrigerants 11, 12, 22, 12 and 22, 113, 114, 114A, 500, and three refrigerating oils are being investigated as to the effects of water, air, temperature, time, and various metal combinations on their mixtures. The sealed glass tube method[4,7,8] was used throughout and the techniques are those

W. O. Walker is Dean, Div of Research and Industry; S. Rosen is Research Instructor, University of Miami. S. L. Levy is Research Chemical Engineer, General Chemical Div, Allied Chemical Corporation. This paper was presented at the ASHRAE 67th Annual Meeting in Vancouver, B. C., June 12-15, 1960.

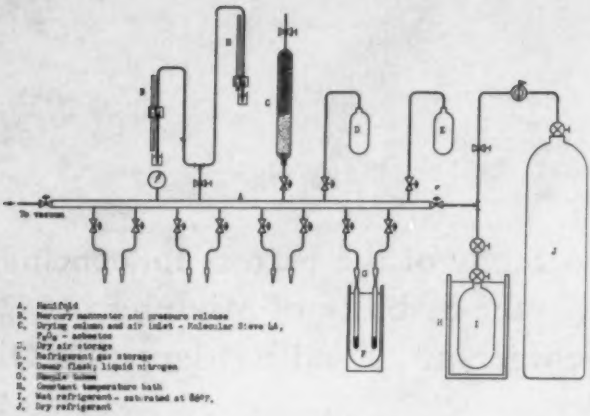
To vacuum
A. Manifold
B. Mercury manometer and pressure release
C. Drying column and air inlet - Molecular Sieve 5A, P2O5 - asbestos
D. Dry air storage
E. Refrigerant gas storage
F. Dewar flask; liquid nitrogen
G. Sample tubes
H. Constant temperature bath
I. Wet refrigerant - saturated at 86°F.
J. Dry refrigerant

Fig. 1 Apparatus for adding refrigerant and air to sample tubes

commonly employed for work of this type.

EXPERIMENTAL

Metal Combinations—Metal sheets were cut into strips (12 by 2 in.) and then treated as follows:

The brass and copper strips were buffed with steel wool. Neither the steel nor aluminum were buffed since the former was free of rust and the latter is damaged by steel wool. All brass, copper, steel, and aluminum strips were washed, first with benzene and finally with isopropyl alcohol. The strips thereafter were handled with gloves, tweezers, or pliers. They were cut into 2 by ⅛ in. pieces. The following combinations were prepared:

Copper – Steel
Copper – Aluminum
Brass – Steel
Copper – Aluminum – Steel

in the quantities required for the tests. The upper part of the brass or copper strips was bent about 45 deg to act as a spring to hold the metal strips in position at the bottom of the tube. After a final benzene-isopropyl alcohol wash, the combination strips were dried in a vacuum at 150 F for a minimum of 4 hr. The vacuum was broken with dry nitrogen and the combinations were stored in a desiccator until used.

Glass Tubes—Standard 8 mm (OD) Pyrex glass tubing was cut into 7¼ in. lengths which were fire polished at one end, washed with chromic acid cleaning solution, rinsed with tap and finally distilled water, and dried. They were numbered with ink 3½ in. from the unpolished end. The unpolished end was sealed to form the bottom

of the tube. Finally, the tube was rinsed with tap and then distilled water, and dried at 230 F.

Water Saturated Refrigerant 22 – Refrigerant 22 was added to a refrigerant supply cylinder containing silica gel which was saturated with water. The cylinder was fitted with a drop tube so that refrigerant came from the bottom where it was in contact with the saturated silica gel. A porous bronze filter was soldered to the lower end of the drop tube to prevent solids from being carried along with the refrigerant. Analysis by the P_2O_5 method showed the moisture content of the refrigerant to be 1500 ppm at 86 F.

Addition of Oil to Glass Tubes – Since oil on the upper part of the glass tubes complicates the sealing operation, a syringe equipped with a special needle was used. After the addition of oil, batches of tubes were placed in a large metal container at 150 F which was evacuated for 8 hr. The tubes were stored under vacuum at room temperature until ready for addition of refrigerant.

Addition of Refrigerant 22 – The tubes, after capillaries had been drawn, were connected to the manifold (Fig. 1) with small pieces of Tygon tubing and cooled by immersing the lower half in liquid nitrogen, after which the system was evacuated. Next, the valves between the tubes and the manifold were closed, and the tubes leak-tested with a high-vac leak detector. The manifold was then filled with refrigerant gas, and 0.5 ml of refrigerant condensed into each tube. This resulted in a 50-50% by volume mixture of oil and refrigerant.

After all 8 tubes were filled and their contents frozen solid, the system was again evacuated. If air was not to be added, the valves to the tubes were opened and the tubes sealed off. However, if air was to be added, the system was flushed and then filled with dry air which was metered into each tube. The valves to the manifold were closed and the tubes sealed off.

Before filling the wet tubes with refrigerant, a drop of water was added, the tube was reduced to capillary size near the top and, while still hot, was connected to the manifold. Thereafter, the wet tubes were filled and sealed in exactly the same way as the dry tubes.

Dry refrigerant was transferred from the supply cylinder to the manifold in the vapor phase. Saturated refrigerant was introduced by vaporizing the moisture saturated liquid directly into the manifold.

Test Variables—Refrigerant 22 (Refrigerant Grade):

Oil*

A—Naphthenic—150 viscosity SSU at 100 F.
B—Paraffinic—90 viscosity SSU at 100 F.
C—Naphthenic—150 viscosity SSU at 100 F. (inhibited)

* Preliminary tests involving fourteen different oils led to the selection of these three as being typical. Other tests proved that viscosity was not important. Oils A and C are pale yellow; B is water white.

Fig. 2 Test tube and shielding tubing

Water
- Dry—(Approximately 10 ppm)
- Saturated—(1500 ppm)
- Wet—(approximately 10,000 ppm—1 small drop of water)

Air
- None
- 1% by weight of refrigerant

Metal Combinations
- None
- Copper (commercially pure sheet—99.9%) and Steel (valve reed stock)
- Copper and Aluminum sheet (2SO—99+%
- Steel and Brass (yellow, half-hard — 65% copper — 35% zinc)
- Copper, Steel and Aluminum

Temperature
- 250 F.
- 375 F.
- The first may be considered to be a normal operating temperature; the second is excessively high.

After sealing, the glass tubes were put in aluminum shields (Fig. 2) which were capped and placed in racks (Fig. 3). One-half of the tubes were tested at 250 F; the other at 375 F.

POSSIBLE COMBINATIONS OF TEST VARIABLES

In order to set up every possible combination of test variables, to avoid duplication, to provide numbers for marking tubes and for use in recording observations, numbering systems were devised. They are based on the variables described herein. The total number of combinations of variables (cases, Fig. 12) is obtained by multiplying the refrigerant (1) × oils (3) × water contents (3) × air (2) × metal combinations (5) × temperature (2) = 180. A total of 630 tubes was prepared, three for each of the 180 combinations and 90 for replacements and room temperature checks.

Observations — Observations were made for color, viscosity change, sediment, wall deposits, corrosion of metals (including a specific observation for formation of varnish on the metals), and copper plating. Since it was felt that varnish was of the same origin as wall deposits, these two were combined in the final analysis of results. Where possible, separate observations were made in liquid and vapor phases. These were not distinguished in the analysis of results.

Color readings ranged from 0

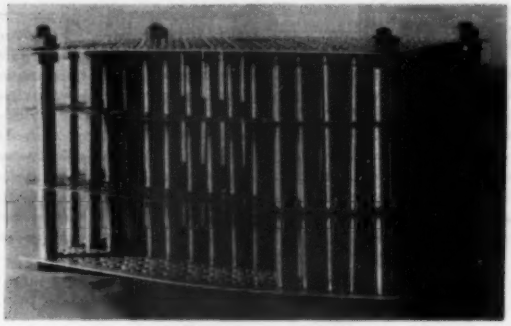

Fig. 3 Rack holding armored tubes

to 9 and were made by comparison with color standards prepared by mixing appropriate quantities of a heat darkened oil with a white oil. Each succeeding sample had twice as much dark oil as the previous one. Viscosity change was noted merely as increase or decrease since there was no convenient method for determining other than gross changes. All other readings were recorded on the basis of none, slight, medium or heavy.

Observations except color were made by examining the inverted tube and its contents in the light of a No. 2 photoflood lamp. The readings were first recorded on a data sheet and then transcribed on IBM cards.

Observations were made according to the time schedule in Table I.

TABLE I
TIME SCHEDULE

Period	Days on Test
0	0
1	1
2	7
3	30
4	90
5	180
6	270
7	360

IBM Data Handling—It is obvious from the number of variables in these tests that a large number of sample tubes was inevitable and their records voluminous. Accordingly, IBM data processing procedures were developed to provide a mechanical means for handling the large volume of experimental data. The exact details of IBM procedure are probably not of general interest, but a brief outline may be helpful to others interested in this approach.

The basic item for recording observations is the IBM Mark-Sense card (Fig. 4). This is the same size as the standard IBM card (3¼ x 7⅜ in.) but contains only 27 columns, each three times the width of the standard column. Special electrically conductive pencil lead is used to produce marks that are

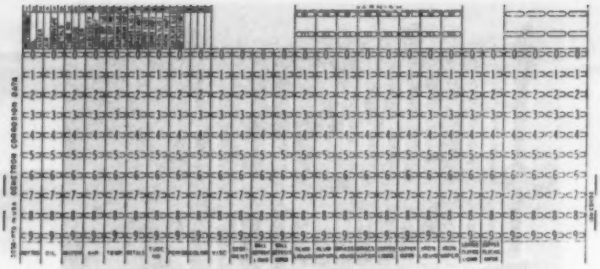

Fig. 4 IBM card

sensed by the brushes on an IBM machine and automatically converted into punched holes on the same card.

For convenience in marking cards, a template was developed (Fig. 5). The original marks are not destroyed by the punched holes thus preserving the original record. Duplicate decks of cards may be prepared in a matter of minutes.

Only 24 columns of the card were needed to identify the sample and record the observations. It should be noted that titles along the bottom margin are the same as those in the top left margin. The bottom listings indicate the Mark-Sensing positions; the top listings are a guide to the punches; i.e., the punches occupy only about one-third of the card.

Each observation produces a card recording results for the individual tube. Excluding breakage and tubes removed from test, 8 sets (for 8 observation times) of 540 cards each (180 combinations in triplicate) result. To reduce the number of cards to be handled, in deriving conclusions from tests, 8 sets of 180 cards each were produced by averaging the results of triplicate observations. The averaging was done on an IBM 650 computer which was programmed

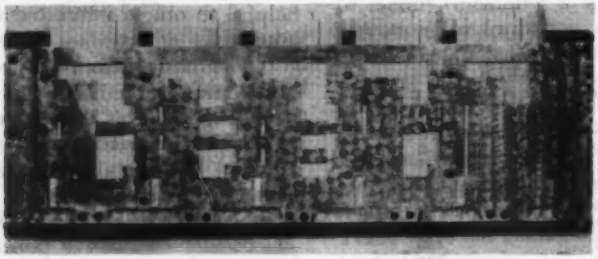

Fig. 5 Template for marking IBM cards

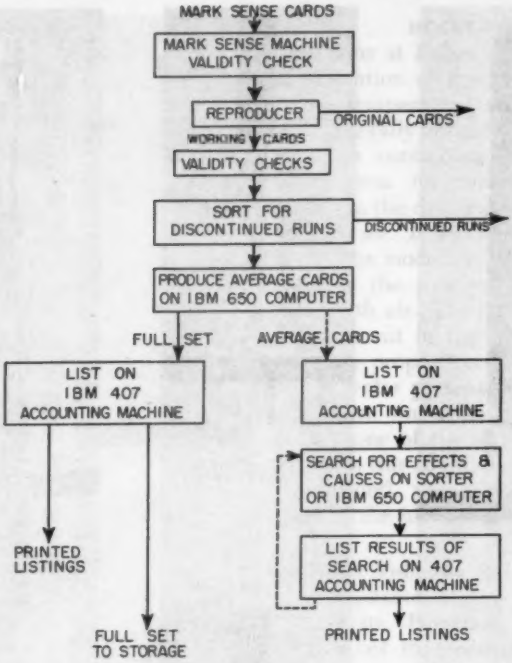

Fig. 6 Data processing procedure

to read each set of triplicate cards, average the results and punch a single card showing the averaged results. The entire data processing procedure is outlined in Fig. 6.

On these average cards an attempt was made to determine effect of variables by sorting in combinations of two variables at a time. The IBM 650 computer was programmed to search a deck of cards and arrange them in sequence according to any two pre-selected columns. The results of this sequencing were punched on cards and listed.

To illustrate the technique, consider the probable influence of air and temperature on copper plating. The complete average deck (including all time periods) was sorted, using an 082 sorter for IBM cards which indicated copper plating in any degree. Obviously, the deck could have been separated into each of three degrees of copper plating but this refinement was decided against for the present. The cards showing copper plating were then sequenced by the 650 computer into four groups as follows:

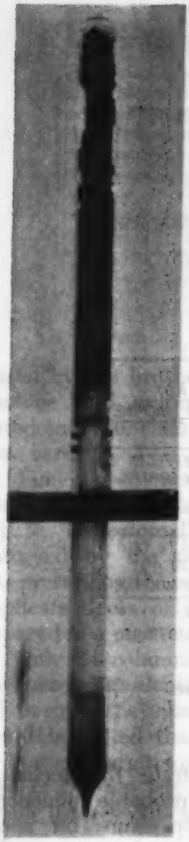

Fig. 7

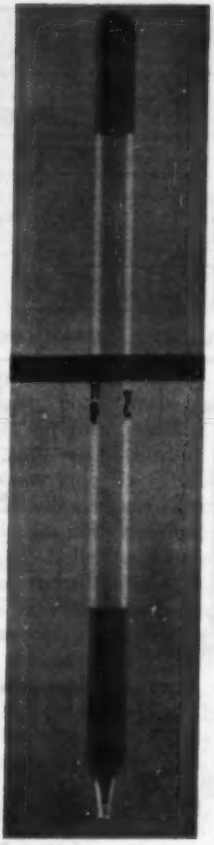

Fig. 8

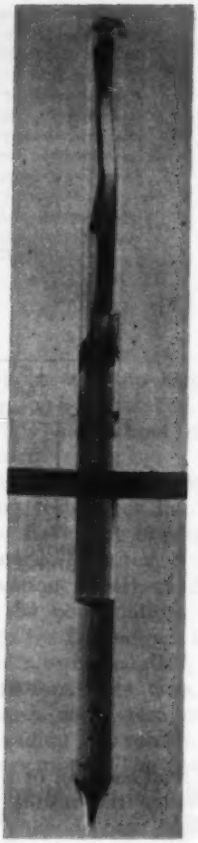

Fig. 9

Fig. 7 Heavy corrosion of metals, partial solidification of liquid glass badly etched. Fig. 8 Wall deposit in liquid phase. Fig. 9 Wall deposit and varnish on aluminum in vapor phase.

(1) Plating in tubes with no air at 250 F.
(2) Plating in tubes with no air at 375 F.
(3) Plating in tubes with 1% air by weight at 250 F.
(4) Plating in tubes with 1% air by weight at 375 F.

Printed listings of each of the above four groups were prepared for visual examination. The 650 computer program can be used in

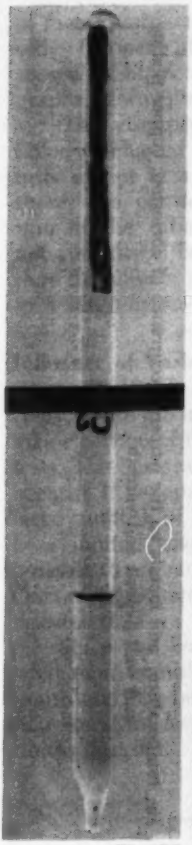

Fig. 10

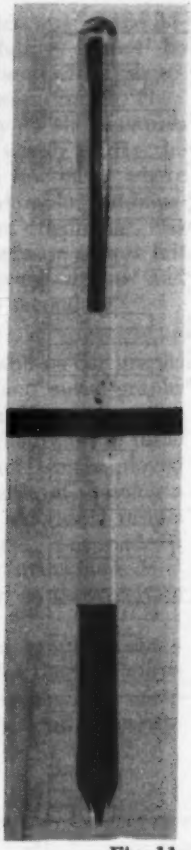

Fig. 11

Fig. 10 Corrosion of aluminum in vapor phase. Fig. 11 Corrosion of aluminum in liquid and vapor phases

conjunction with a sorter to sequence cards with respect to any number of the five variables taken at one time. Tables were prepared from the listings and, from them, bar graphs and curves have been made.

RESULTS

Reactions at Room Temperature – Examination of the spare tubes at room temperature showed there was generally corrosion of the steel in tubes containing liquid water. There was no corrosion of the metals in the dry or saturated tubes without air. It was also found that there was moderate color development in the pale yellow oil mixtures with air. The degree of color development in the air tubes was inversely proportional to the quantity of water present.

There was color development in only one of the water white oil mixtures; this contained brass-steel, water (wet), and air. It was the spare of the tubes which exploded.

Exploded Tubes – Relatively few tubes exploded during the course of the tests. However, 6 of the 9 375 F tubes that contained brass-steel, water, and air exploded; five after approximately 60 days and the other after more than 180 days.

The reaction under these conditions is so severe that it produces enough gases (hydrochloric acid, hydrofluoric acid, and hydrogen) to build up sufficient pressure to cause the explosions. In addition, the tubes may have been weakened by the etching action of the hydrofluoric acid. Fig. 7 is a photograph of a tube similar to those which exploded.

Normal Tubes – Figs. 7-11 show conditions in certain tubes at the end of the test. They were selected to illustrate typical examples of wall deposit and varnish, corrosion

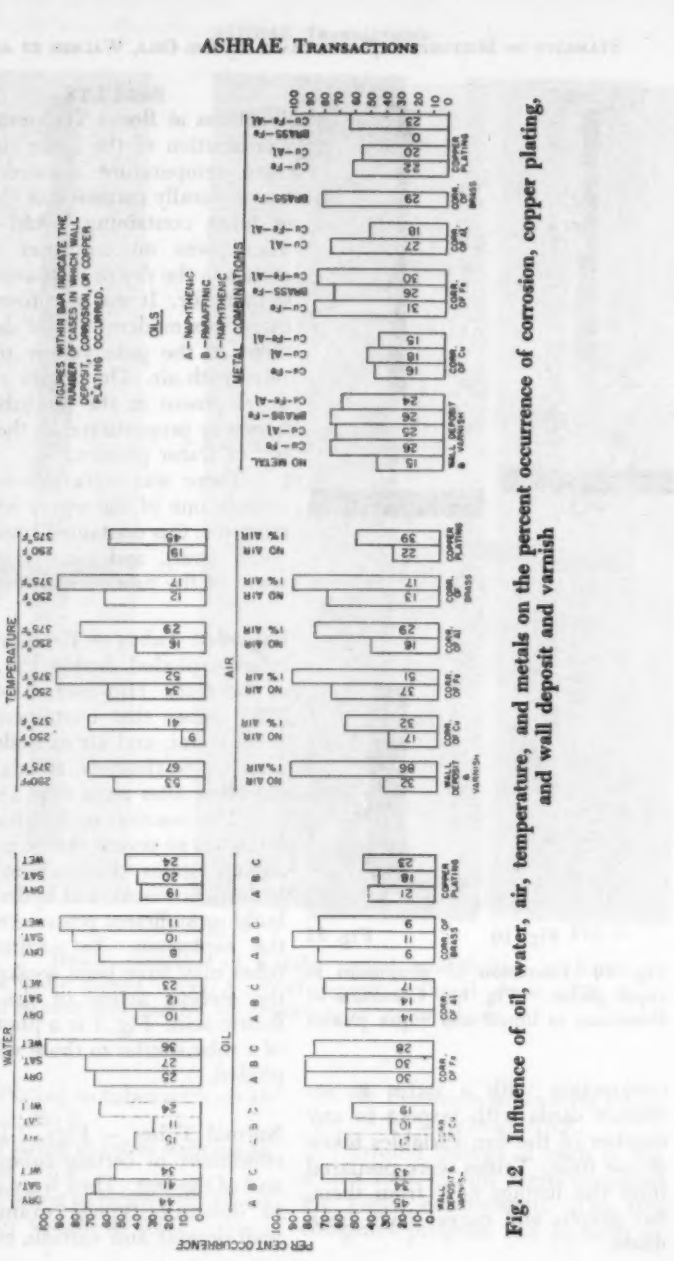

Fig. 12 Influence of oil, water, air, temperature, and metals on the percent occurrence of corrosion, copper plating, and wall deposit and varnish

of metals, and darkening of the liquid. Copper plating cannot be shown in black and white photographs; it was present in Fig. 11.

The viscosity of the mixtures failed to change visibly during the tests except in a few cases where there was considerable solidification in the tubes. Sediment was not considered because it was felt that the effects were obvious and to a large extent secondary.

Influence of Variables—Bar graphs (Figs. 12, 19-23) and curve graphs (Figs. 13-18) are used to present the major portion of the results of these tests. The bar graph was employed because it is capable of showing a large number of individual results in a limited space. This made it possible to present many more data. Curves were used to show certain selected data.

Since the bar graph is somewhat more complex than the curve graph and has been used in scientific literature less, a brief description is in order.

SINGLE VARIABLES

Fig. 12 shows the influence of single variables on the percent occurrence of corrosion, copper plating, and wall deposits and varnish. Variables are listed at the top of each section, the percent occurrence is plotted on the left, and the observed phenomena are shown at the bottom. Variations in the concentration of water are given at the top of the section.

Differences in oil, temperature, air, and metal combinations are also listed at the top of appropriate sections. The percent occurrence was calculated at the end of the tests. Although data are available for each period of time of the schedule (Table I), they were omitted because their inclusion added to the complexity of the bar graph and but little to the total information.

The total number of cases (combinations of variables) is the product of the variables, 180 in all or a total of 540 tubes. Thus, there are 60 cases (180 tubes) described as dry, and an equal number for

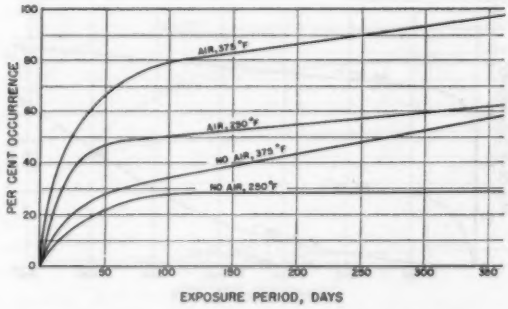

Fig. 13 Effect of air and temperature on corrosion of aluminum

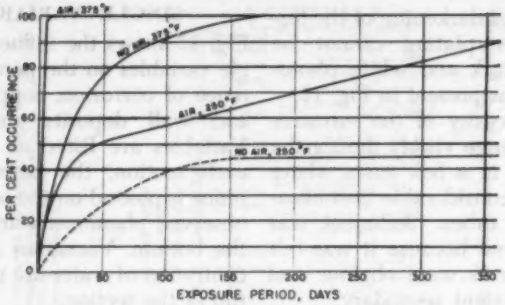

Fig. 14—Effect of air and temperature on corrosion of brass

each of the saturated and wet conditions. A similar distribution holds for the three oils.

Since there are but two temperatures and two air conditions, the total number of cases for each of the two conditions of each of these variables is 90. There are 36 cases (108 tubes) with no metal in tubes and a similar number for each of the four metal combinations. All the cases reported under water are also reported in connection with oil, temperature, air, and metal combinations.

Each bar is similar to a single curve (Figs. 13-18), the top of the bar being the final point on the curve. The bar may be converted into a curve by plotting the percent occurrence at the end of each time period against time. The efficiency of the bar graph becomes apparent since it would require 77 curves to show the data given in Fig. 12. Comparisons of the vari-

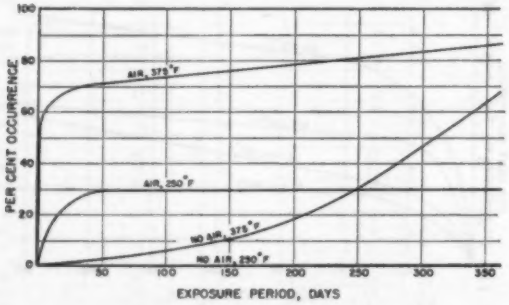

Fig. 15 Effect of air and temperature on corrosion of copper

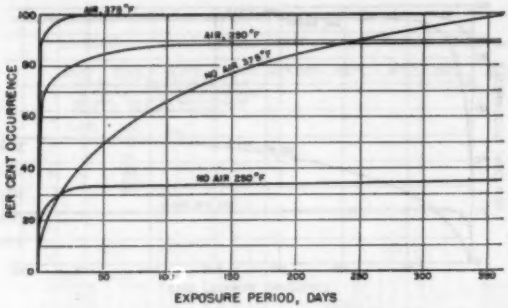

Fig. 16 Effect of air and temperature on corrosion of steel

ous data are more readily made from the compact bar graph.

Specific uses of the bar graph will be illustrated by considering the effect of temperature on the percent occurrence of corrosion of metals, copper plating, and wall deposits and varnish.

Where the heights of the bars in a pair differ markedly, there is a large temperature effect. The degree of difference shows the temuerature effect to be large or small. The relation of the percent occurrence at 250 F is made by comparing these bars. A similar comparison may be made for the 375 F bars. A general conclusion is obvious; the percent occurrence is greater at 375 than 250 F. By a similar examination pertinent conclusions may be derived from all other portions of Fig. 12.

Specific questions may also be asked from the bar graph. Do the oils affect the percent occurrence of

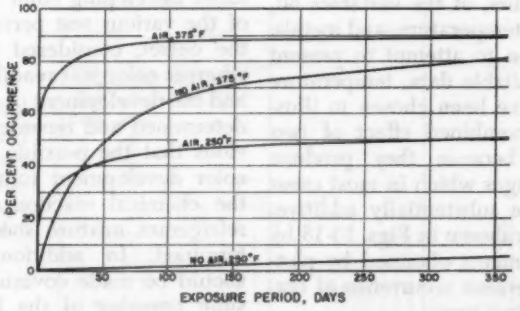

Fig. 17 Effect of air and temperature on copper plating

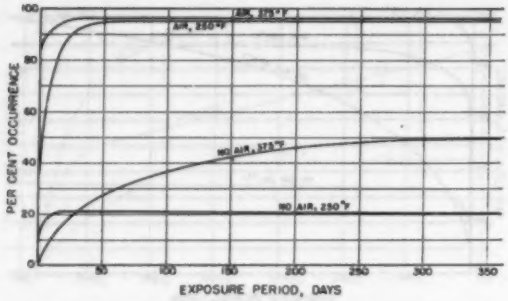

Fig. 18 Effect of air and temperature on wall deposit and varnish

the corrosion of steel? A check under oil shows the three bars to be about equal in height, thus indicating no oil effect. Does air have an effect on the corrosion of steel? Under air (corrosion of Fe), it is apparent that air increases the percent occurrence of corrosion. Is copper plating influenced by air? Under air (copper plating), it may be seen that copper plating is greater when 1% air is present.

Two Variables Acting Together—There are ten possible combinations, in pairs, of the variables oil, water, air, temperature, and metals. Rather than to attempt to present all the available data, temperature and air have been chosen to illustrate the combined effect of two variables, because they produce major changes which in most cases seem to be substantially additive. Results are shown in Figs. 13-18 by means of curves obtained by plotting the percent occurrence of corrosion against time.

Color Development—There is a considerable difference of opinion as to the significance of color development in oil-refrigerant mixtures. Both Steinle[3] and Elsey[4] used color to show the progress of the reaction at higher temperatures. A similar attitude is taken in this study. Kvalnes and Parmelee[6] analyzed the contents of tubes but did not correlate their findings with the colors developed. The present study involved 540 tubes which were kept under test conditions for one year.

Analysis of the contents of tubes developing color at the end of the various test periods was, at the outset, considered impractical whereas color was readily observed and the development of color easily determined and recorded. It is obvious that the possible relation of color development to the rate of the chemical reaction in the oil-refrigerant mixture should be determined. In addition, a study should be made covering the possible lowering of the lubricity of the oil.

Whether color development is

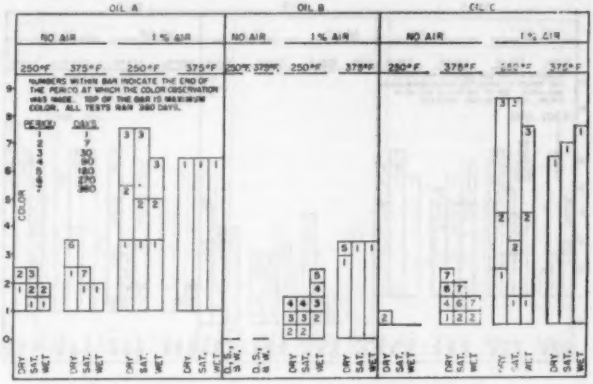

Fig. 19 Color development in Refrigerant 22 — oil mixtures without metals

of primary significance or is merely a convenient method of following reactions in tubes or both or neither remains to be determined by additional work.

Since the intent of this study was to observe color development, among other phenomena, an analysis was made of the results in which it figured. These are presented in bar graphs (Figs. 19-23). They were constructed, and are read, in a manner similar to that used with Fig. 12.

There are, however, some differences in details. The base lines differ for the three oils since two possess color; the third is water white. Each line within the bar shows the color of the mixture at the end of the periods.

Numbers within the bar indicate the end of the period at which the color observation was made.

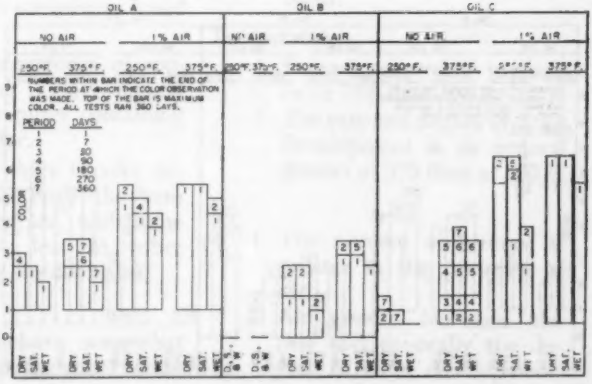

Fig. 20 Color development in Refrigerant 22 — oil mixtures with copper and steel

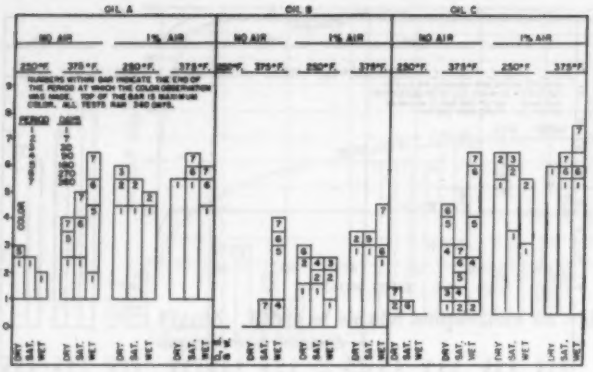

Fig. 21 Color development in Refrigerant 22 — oil mixtures with copper and aluminum

Color is indicated on the left. Few tubes continued to develop color throughout the entire test. The number at the top of each bar represents the period at which maximum color developed and beyond which no further color change occurred.

Thus, in an oil C mixture at 250 F, dry, no air, no metal (Fig. 19), there was no color at the end of one day. At the end of seven days (second period), a color of 1 had developed which did not change during the remainder of the 360 days test period. Similar tubes (sat., wet) failed to change color at all.

The influence of each of the variables is determined by comparing the height of the appropriate bars for degree, and the numbers within the bars for rate, of color development.

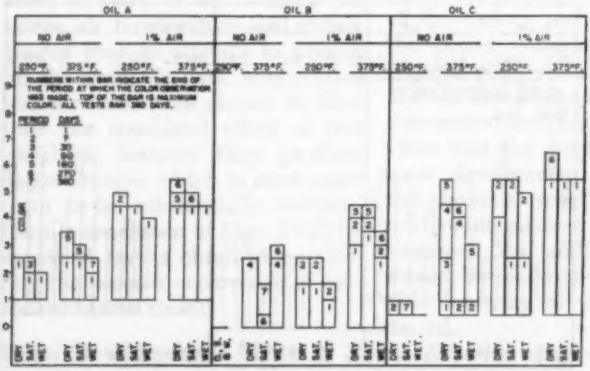

Fig. 22 Color development in Refrigerant 22 — oil mixtures with brass and steel

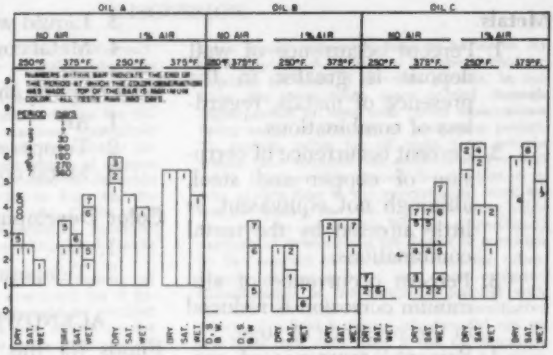

Fig. 23 Color development in Refrigerant 22 — oil mixtures with copper, steel and aluminum

SUMMARY

Influence of Water, Oil, Temperature, Air and Metals on Color Development and the Percent Occurrence of Corrosion, Copper Plating, and Wall Deposit and Varnish

Water

1. Percent occurrence of wall deposit is slightly less in tubes containing liquid water.
2. Percent occurrence of corrosion is considerably greater in tubes containing liquid water.
3. Percent occurrence of copper plating is only slightly greater in tubes containing liquid water.
4. Wherever there is color development, both the rate and degree are, with some exceptions, less in tubes containing liquid water.

Oil

1. All oils behave somewhat alike except the water white oil which shows slightly lower percent occurrence of wall deposit, copper corrosion, and copper plating.
2. Conclusions relative to color development are complicated by the fact that the initial color of the refrigerant-oil mixtures is different. However, it is obvious that there is some difference between the water white and the pale yellow oils with respect to color development.

Temperature

1. Percent occurrence is greater at 375 than 250 F.
2. The rate and degree of color development is in general greater at 375 than at 250 F.

Air

1. The percent occurrence is greater in the presence of air.
2. Air greatly increases the rate and generally the degree of color development.

Metals

1. Percent occurrence of wall deposit is greater in the presence of metals, regardless of combinations.
2. Percent occurrence of corrosion of copper and steel, although not equivalent, is little affected by the metal combinations.
3. Percent occurrence of aluminum corrosion is reduced in the presence of steel.
4. Percent occurrence of corrosion of brass is of the same order as steel.
5. Percent occurrence of copper plating is alike in all cases except with the brass-steel combination, in which case there is none.
6. In general, the copper-aluminum combination produces a greater rate and degree of color development than the other metal combinations.
7. The rate and degree of color development in the pale yellow oils are greatest in the no metal tubes with air.

Variables Showing a Major Influence on Copper Plating, Corrosion, Wall Deposit and Varnish, and Color Development

Copper Plating

1. Air
2. Temperature

Corrosion

1. Air
2. Temperature
3. Liquid water
4. Metal combinations

Wall Deposit and Varnish

1. Air
2. Temperature
3. Metal combinations

Color Development

1. Air
2. Temperature

ACKNOWLEDGMENTS

Funds for this investigation were granted to the University of Miami by General Chemical Div, Allied Chemical Corporation.

The authors wish to thank W. A. Knapp of the General Chemical Research Staff and A. A. Sakhnovsky of the University of Miami for their helpful suggestions and criticisms.

BIBLIOGRAPHY

1. Philipp, L. A., and B. E. Tiffany, Thermodynamics of Sulfur Dioxide Oil Systems, *Refrigerating Engineering*, 27, No. 5, pp. 248-54, 262, 264, May 1934.

2. Steinle, H., Chemischen Reaktionen Zwischen. Schwefeldioxid und Olen. *Kaltetechnik*, Jg. 1, S. 14, 1949.

3. Steinle, H., Chemische Reaktionen Zwischen Kaltemitteln und Olen in Kaltemaschinen. *Ibid.* Band 2, Heft Nr 7, Seite 174, bis 178, 1950.

4. Elsey, H. M., L. C. Flowers and J. B. Kelly, A Method of Evaluating Refrigerator Oils, *Refrigerating Engineering*, 60, No. 7, p. 737, 1952.

5. Williamitis, V. A., How Chemical Stability Assures Long Attention-Free Performance of Sealed Refrigeration Systems, *General Motors Engineering Journal*, 2, No. 1, pp. 22-29, 1955.

6. Kvalnes, D. E., and H. M. Parmelee, Behavior of Refrigerants 12 and 22 in Sealed-Tube Tests *Refrigerating Engineering*, 56, No. 11, pp. 40-42, 82, 84, 86, Nov. 1957.

7. Walker, W. O., and K. S. Willson, Refrigerant Driers, *Ansul News Notes*, 1 (3) 1937, Ansul Chemical Co.

8. Handling "Freon" Fluorinated Hydrocarbon Compounds in the Laboratory. Technical Memorandum 14. Sept. 8, 1953. Revised April 1, 1955. Freon Products Division, E. I. duPont de Nemours & Co., Inc.

DISCUSSION

J. D. BOPP, Marinette, Wisc. (Written): Although a large number of sealed-tube tests were conducted, only visual observations were made. Halide and metal ion determinations could have been carried out to follow the degradation and corrosion reactions throughout the experiment. A report of the relative severity along with the occurrence of copper plating, wall deposit, etc., would be desirable in comparing, for example, in Fig. 12, the difference between oils A and C for wall deposit and varnish. Quantitative measurement of refrigerant decomposition would make a better comparison.

It is stated that the tubes containing oil are stored at 150 F and evacuated for 8 hr. As some of the lighter ends could be distilled off, what kind of vacuum was drawn on the system? Furthermore, was more than one oil stored in the container at the same time?

From the saturation solubility chart in the 10th Design volume of the ASRE DATA BOOK, I derived the following equation:

$$\log_{10} \text{saturation solubility of } H_2O \text{ in } R\,22 = (-2.003676)\left(\frac{1000}{F + 460}\right) + 6.844519$$

If the solubility characteristics hold true, this equation can be used to extrapolate the solubility of water under the test conditions of 250 F and 375 F. Calculations give a saturation solubility of water in Refrigerant 22 of 10,500 ppm at 250 F and 27,800 ppm at 375 F. It is stated that the "wet" system contained about 10,000 ppm of water; therefore it cannot be stated absolutely that liquid water was present.

It would be interesting if some of this work would be continued in the presence of a desiccant to determine its influence.

Further theoretical explanation should be given on the following:

(a) Why is the occurrence of wall deposit slightly less in tubes containing liquid water?
(b) Why is the color development less in tubes containing liquid water?
(c) In what way is the color development different between the water white oils and the pale yellow oils? Why does this happen?
(d) Why is the rate and degree of color development greatest in the non-metal tubes with air?

CLOSURE BY AUTHOR WALKER: The first criticism of why we simplified our method of approach is based upon encompassing a field we could manage. I am quite aware that there are many other things which could have been done, all of which we discussed in deciding upon the limitations to be put on the project. When one is dealing with 640 tubes, the addition of one single variable involving all of them results in the addition of this same number of tubes to the project. This is a qualitative project and in order to make it quantitative by analyzing for halide and metal ions, an extensive addition to the number of tubes would necessarily have to be made. As an example, a complete set of tubes would be required for each of the time periods. In our tests, the same tubes were carried through eight periods of time with visual observations being made at the end of each time period. To provide tubes for all eight time periods would have required the addition of 7 x 640 tubes. I believe this answers the question as to why at this time in the experimental work we did not analyze for ions. The same thing holds true for the application of the conventional methods of determining the degree of corrosion by the removal of the metals from the tubes. Copper plating falls in the same category. Consideration of the foregoing coupled with the fact that this is an overall qualitative survey of a field indicates why we did not go into these tests more fully. It was our intention to spot, by an overall check, areas in which further quantitative work should be done.

The question of whether or not we drew off any non-condensables, or any condensable materials, or high fractions from the oil is a question we also asked ourselves. We are not certain that in our procedure we did not lose some of the more volatile materials from the oil. We plan to check it.

Concerning the solubility of water, we put in one drop of water in order to have a high concentration. Water as a liquid was undoubtedly present throughout the tests although we had no visual proof of it.

The critical temperature of R 22 is 205 F. This is exceeded by both temperatures used in our tests (250, 375 F); consequently, there is no liquid R 22 present. Hence, the solubility limitations referred to by Mr. Bopp do not apply. We therefore have a mixture of very dense R 22, gas and water vapor. The pressures of the individual gases should follow roughly the partial pressure law. Inasmuch as the critical temperature of water is 705 F, we should have liquid water present provided the one drop was sufficient to establish the required equilibrium.

It would be interesting to carry out these tests in the presence of a desiccant but again such a test would complicate the experimental work by the addition of more tubes since it would be necessary to test not one desiccant but all of those being used in the field.

Mr. Bopp's request for theoretical explanation of the items listed under (a), (b), (c), and (d) cannot be acceded to at this time since we do not know why certain results were obtained. We have asked ourselves these same questions and we have debated the reasons for the results but, in the present qualitative state of this investigation, there is no answer available. We are simply reporting observations.

H. O. SPAUSCHUS, Louisville, Ky: Did the computer technicians consider applying a statistical analysis of variance to the results to compare the significance of the variables to your modified bar graph method in order to understand the total data collected?

W. A. KNAPP (answering for W. O. WALKER): This method has been contemplated, but it has not been done as yet. For example, when the tubes were read, degrees of corrosion were read as "none", "slight", "moderate", and "heavy". The data are on cards and if someone had a question as to what happened under certain conditions, some qualitative indication can be obtained from this data.

L. F. ALBRIGHT, Lafayette, Ind.: It was stated that HCl, HF, and H_2 were present in a mixture. Was this mixture analyzed to determine the presence of these gases, or was their presence assumed?

Is there a possibility of applying quantitative measurement to color? Perhaps by a Spectrometer method?

The fact of placing the tubes under a vacuum does not necessarily remove all the air or the water. I assume you are aware of this condition.

AUTHOR WALKER: The hydrofluoric-hydrochloric acids are rather apparent from the knowledge of the reaction obtained with the materials present. The hydrogen would be present in wet tubes. Dr. Spauschus is working on the determination of occurrences in these reactions by using different methods.

We plan to open some of these tubes which have color relationships and analyze their contents. Originally, this was not in the scope of the test. Trying to get a color chart that is usable in this instance is very difficult. H. M. Elsey and H. Steinle had trouble doing it. ASTM color charts do not apply.

Actually, no attempt was made to remove all of the moisture. There is some in all of these systems. However, prior treatment of the glass tubes was such that the amount of water and air was reduced to a minimum value where it should not have any particular effect on the test results.

1729

No. 1729

Time Factors in the Removal of Moisture from Refrigerating Systems with Desiccant Type Driers

W. O. KRAUSE A. B. GUISE E. A. BEACHAM

A primary function of driers in the refrigerating system is to remove moisture from the refrigerant, thus preventing expansion valve or capillary tube freeze-up and minimizing the formation of harmful corrosion products. Because this function is vital to the performance and service life of a refrigerating system, drier installation is standard procedure in field assembly, in many factory built systems or when a sealed system has been opened for servicing.

Accordingly, the desiccants used in various commercially available driers have been the subject of a great deal of study. Recently, for instance, it has become the practice to publish the water capacity of refrigerant driers, defining the water capacity of a desiccant at equilibrium between the refrigerant and the desiccant under given specific conditions.[1,2] This permits the rating of driers by the amount of water they can remove from a system and still assure a satisfactorily low moisture level.

The importance of adequate capacity for water cannot be overemphasized. Not only can "freeze ups" occur but if the moisture level is disproportionately high, formation of corrosion products is a distinct possibility. At evaporator temperatures of air conditioning applications, other than automotive, the freezing point of water is not attained. Therefore, a system may be operating with a moisture content at which corrosion products may form and still not give indication that an aggravated condition exists by means of a freeze up.

Yet, despite the accepted importance of driers and the extensive

W. O. Krause is Refrigeration Research Chemist, Development and Design, A. B. Guise is Director of Development and Design and E. A. Beacham is Manager, Refrigeration Sales Development, Ansul Chemical Company. This paper was presented at the ASHRAE 67th Annual Meeting, Vancouver, B. C., June 12-15, 1960.

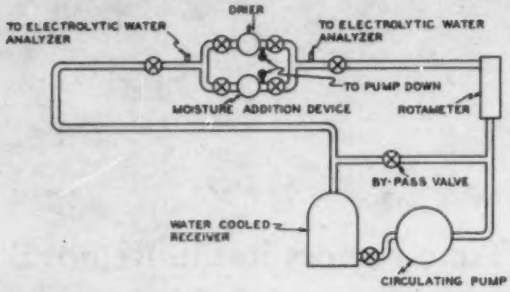

Fig. 1 Circulating system used for rate of drying investigation

study of their absolute water capacity, little work has been done to investigate the factors affecting the time required to reduce the moisture level of a system.[3,4] The drying process is not instantaneous,[3,5] and an understanding of how a given system may be expected to progress from a "wet" to a "dry" state is necessary to help engineers and technicians evaluate drier application.

Presented here are the results of studies of the effects of some of the basic refrigerating system variables on the progress of the drying action. These variables are (1) the rate of flow of the refrigerant, (2) the internal area of the refrigerating system, and (3) the size of the drier or depth of desiccant bed.

It is recognized that other variables exist such as particle size and type of desiccant, temperature, and type of refrigerant, but influences of these variables are not included here.

OPERATION OF SYSTEM

To perform these experiments, a simple system with an internal surface area of A_1 as shown in Fig. 1 was assembled and operated under carefully controlled conditions. Refrigerant 12 was circulated through the system and a parallel arrangement of the drier and moisture addition device permitted stabilization of the system at a given moisture level before beginning observation of drier action.

The moisture addition device used was a saturated drier. It was found that pre-loading a drier containing 420 g desiccant with 128 ml of water in accordance with ASRE standard 35B[1] would "charge" the system to an equilibrium level of 60 ppm of water. This level, representative of an aggravated moisture condition, was maintained as the starting moisture content for the entire series of experiments.

Further, equilibrium of the system at the 60 ppm level was carefully assured before each data run by prolonged operation of the system without the addition or removal of moisture. Taps for elec-

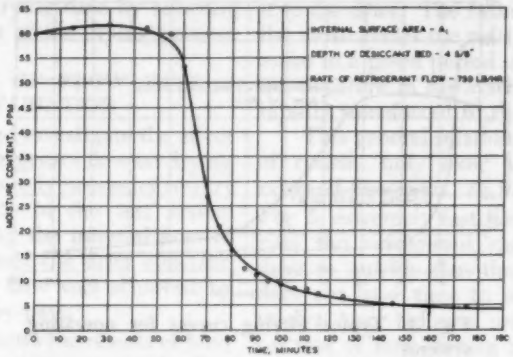

Fig. 2 Typical drying curve obtained with test equipment

trolytic analysis of moisture content of the refrigerant stream were installed immediately upstream and downstream of the drier.

With the system in operation, the progressive effect of drier action on refrigerant moisture content was first observed with the result shown in Fig. 2. Moisture readings were taken at the upstream tap.

Note that the moisture content of the refrigerant is actually seen to rise for a period of time after the drier has been placed in operation. This somewhat surprising effect may be explained when it is remembered that the moisture carried in the refrigerant stream is only a portion of the total moisture in the system. A certain amount of moisture will always be adsorbed by the internal surfaces of the system itself in a proportion determined by the relative tendency of the refrigerant to dissolve moisture balanced against the tendency of the system internal surfaces to adsorb moisture.[6,7]

As the temperature of the refrigerant rises slightly when the drier first begins to act, the heated refrigerant has a greater capacity for moisture and the internal surfaces have a reduced moisture capacity. The net result is a slight, temporary increase in the observed moisture level of the refrigerant.

The temperature rise of the refrigerant as it begins to flow through the drier is due to both heat of adsorption of refrigerant in the desiccant material and the increased energy necessary to maintain the same rate of refrigerant flow with the added resistance of the drier.

Once this initial rise in moisture level has been overcome, the moisture content of the refrigerant falls off rapidly as dry refrigerant emerging from the drier scavenges surface adsorbed moisture from the system. The level at which equilibrium is reached, of course, de-

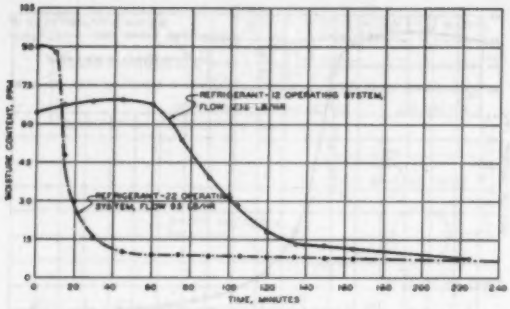

Fig. 3 Typical drying curves for operating systems

pends on the relationship between the absolute moisture content of the drier in use and the absolute moisture content of the system.

To confirm this observation of the progessive effect of drier action, similar tests were run on typical operating open type refrigerating systems. The results of these tests are shown in Fig. 3. Note that the curves display the same general characteristics of drier action as observed in the test system.

More important, perhaps, than the general confirmation of the basic test system, the actual operating unit curves of Fig. 3 point out the detailed differences in the progress of drying action that can occur when rate of refrigerant flow, size of system and size of drier are varied. Each of these variables

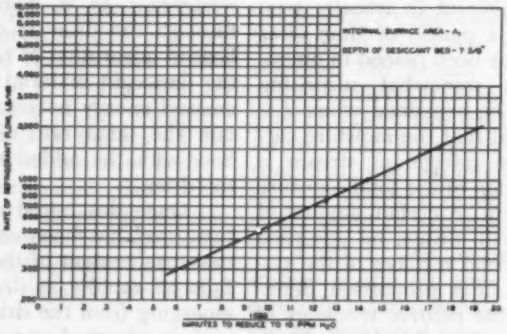

Fig. 4 Effect of rate of flow on drying time with drier and system held constant

influences drying time by affecting the progress of the drying process.

EFFECT OF FLOW RATE VARIATION

To isolate and investigate the effect of rate of refrigerant flow on drying action, it was only necessary to vary the flow rate in the test system while holding the internal area of the system and the drier constant. Variation in flow was achieved by means of a by-pass.

Fig. 5 shows the results of tests conducted in this manner. In Fig. 4, the same data are plotted against a logarithmic ordinate to derive a straight line function between rate of refrigerant flow and the reciprocal of the drying time.

For a given drier size and internal surface area, the rate at which a system is relieved of its moisture is increased with increasing rate of refrigerant flow. The dry refrigerant leaving the drier picks up moisture from the internal surfaces of the system and brings it to the drier. The faster the flow, the more cycles the refrigerant can make in a given period of time and the moisture in the system is more rapidly transferred to the drier.

This general relationship holds, of course, only over a practical range of flow rates. As indicated in Fig. 5, extremely fast flow tends to pass the refrigerant through the drier so quickly that the desiccant does not have time to work effectively. Also, below a certain critical rate of flow, drying time is extended disproportionately by any further decrease in flow rate.

EFFECT OF INTERNAL SURFACE AREA VARIATION

Holding the rate of refrigerant flow and drier size constant in the test system while varying the internal surface area produced the results shown in Fig. 6. The increase of internal area of the system was accomplished by adding 50 ft lengths of ⅜ in. copper tubing to the refrigerant flow circuit. Each length

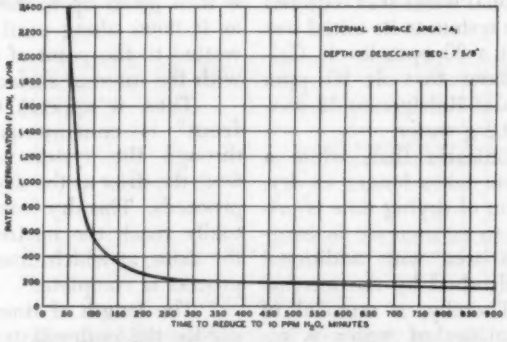

Fig. 5 Effect of rate of flow on drying time with drier and system held constant

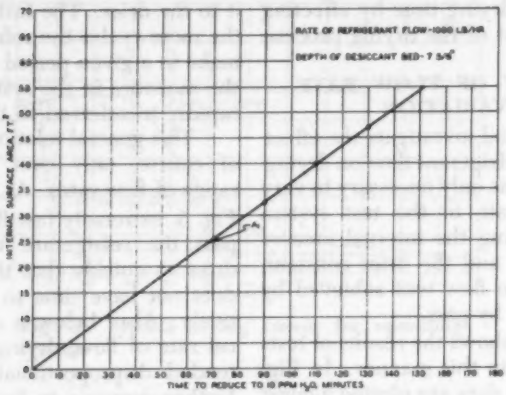
RATE OF REFRIGERANT FLOW-1000 LB/HR
DEPTH OF DESICCANT BED- 7 5/8"
INTERNAL SURFACE AREA, FT²
TIME TO REDUCE TO 10 PPM H₂O, MINUTES

Fig. 6 Effect of increasing surface area on drying time with drier size and flow rate held constant

of this tubing added approximately 7.4 sq ft of internal surface area; 150 ft were added.

For each additional 50 ft of tubing installed in the system, 7.5 lb of Refrigerant 12 had to be added to the total amount of fluid in the system. Despite this increase in the amount of refrigerant circulating, little additional water was required to bring the system to its initial wet condition at a 60 ppm level. Calculations show that at 60 ppm water 7,5 lb of Refrigerant 12 contains only 0.2 g water.

This indicates that, while a larger system takes longer to dry, the extension of drying time is primarily due to an increase in internal surface area with additional moisture adsorbed by the internal surfaces. Thereby, a removal of larger quantities of water is required.

As the refrigerant passes through the desiccant bed, it is dried to a lower moisture level than when it entered the drier. As it leaves the drier, it contacts the internal surfaces of the system which were in a state of moisture equilibrium with the refrigerant at a higher moisture level. Adsorbed moisture from the system surfaces is then given up to the refrigerant as it flows along until it is again wetted to the point of equilibrium with the internal surfaces.

Thus, it appears that a "dry front" is continuously moving through the system downstream from the drier as the drying process proceeds. This dry front will eventually reach the upstream side of the drier, at which time the drying process is complete.

The length of time needed to reduce the entire system to a low moisture level will be greater or smaller in proportion to the varia-

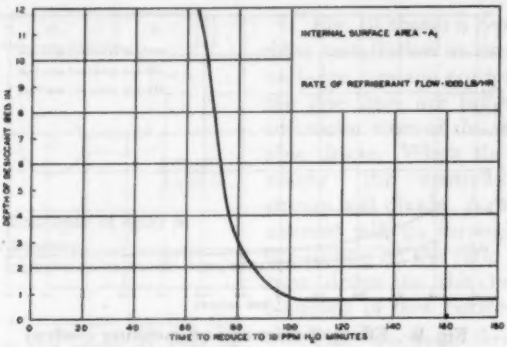
INTERNAL SURFACE AREA - A_i
RATE OF REFRIGERANT FLOW - 1000 LB/HR
DEPTH OF DESICCANT BED, IN.
TIME TO REDUCE TO 10 PPM H_2O MINUTES

Fig. 7 Effect of depth of desiccant bed on drying time with rate of flow, system size and drier diameter held constant

tion in the distance that this dry front must travel, or in proportion to variations in the internal area of the system.

EFFECT OF VARIATION OF DRIER SIZE

Holding the size of the system and the rate of refrigerant flow constant permits isolation and study of the effect of variations in drier size on drying time. Actually, the significant variation here is in the depth of the desiccant bed through which the refrigerant passes.

Fig. 7 shows that the deeper the desiccant bed in a drier, the more rapidly the moisture will be removed at a given flow rate. Fig. 8 shows these data plotted against a logarithmic ordinate to derive a straight line function between the depth of desiccant bed and the

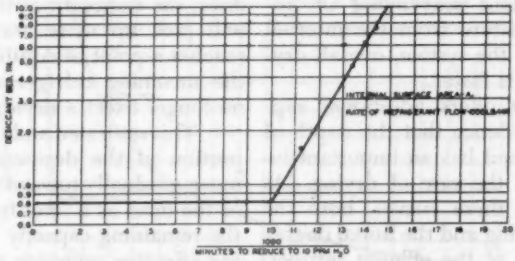

Fig. 8 Effect of depth of desiccant bed on drying time with rate of flow, system size and drier diameter held constant

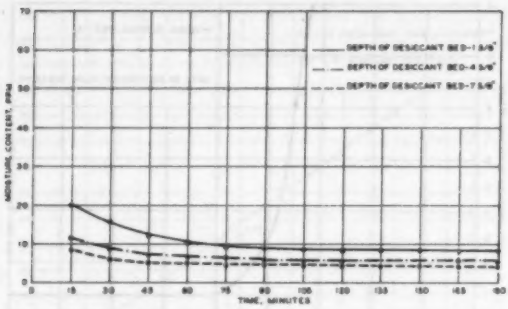

Fig. 9 Effect of drier size on moisture content of effluent Refrigerant 12 with refrigerant flow of 1000 lb/hr and internal surface area of A_1, + 14.8 ft²

reciprocal of the drying time. It was observed further that the slope of the typical drying process curve as shown in Fig. 2 becomes steeper as the depth of the desiccant bed is increased.

This demonstrates the importance of contact time of refrigerant with desiccant bed. The longer the contact time, the more thoroughly the refrigerant will be dried during its passage through the drier. Since a lower moisture content in the refrigerant leaving the drier means more efficient scavenging of adsorbed moisture from the internal surfaces of the system, overall drying action is faster.

Fig. 9 offers additional supporting evidence that the depth of desiccant bed has an important influence on the rate of drying. As seen from these curves, both the rate of drying and the initial degree of dryness of the effluent refrigerant is related to the desiccant bed depth.

Field experience has consistently shown that over-sizing of driers on wet systems is more effective in preventing freeze ups at the flow control during the early phases of the drying process than the use of a smaller correctly sized drier.

As refrigerant at a certain moisture level enters the drier, it contacts the desiccant bed and begins to give up moisture, becoming progressively drier until it leaves the desiccant bed. As the flow of wet refrigerant continues to enter the drier, the desiccant at the entrance will pick up more water until it reaches a point of equilibrium with the incoming refrigerant and can no longer exert a drying effect.

This saturated and equilibrated portion of the desiccant bed will move gradually toward the exit end of the drier as a "wet front" so that the remaining capacity of the drier for effective moisture removal becomes progressively smaller. Finally, as the wet front reaches the exit end of the drier, the moisture

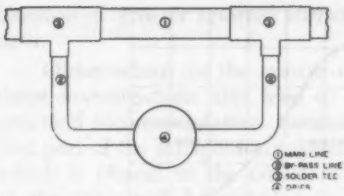

Fig. 10 Example of drier installed in by-pass

level of the refrigerant leaving the drier will be the same as that of the refrigerant entering the drier and a condition of moisture equilibrium will exist between the desiccant and the refrigerant.

ADDITIONAL DATA

To complete this study, two additional experiments concerning drier action under frequently encountered field situations were performed, one where the drier is installed in a bv-pass and the other where liquid water is present in the system.

Fig. 10 shows a typical by-pass drier installation as used generally on large tonnage equipment where the line sizes are bigger than the connector sizes of the readily available driers. When the refrigerant reaches the upstream tee, the stream will divide. A proportionate amount will go through the drier, depending on the ratio of the pressure drops in the two possible channels of flow between the tees.

This "fractional flow" of refrigerant through the drier naturally has the same effect as reducing the rate of flow in the system and increases drying time. However, assuming a drier of adequate capacity, this is the only effect on the progress of drying action which proceeds normally as shown in Fig. 11. The size of the main line between the by-pass tees can be reduced to improve drying time.

When improper dehydration procedures are used before equipment start up, liquid water may be

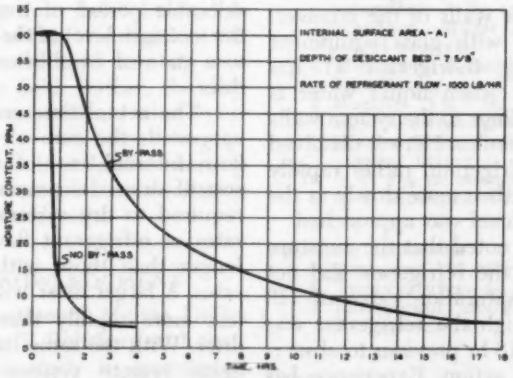
INTERNAL SURFACE AREA - A₁
DEPTH OF DESICCANT BED - 7 5/8"
RATE OF REFRIGERANT FLOW - 1000 LB/HR
5" BY-PASS
5" NO BY-PASS
MOISTURE CONTENT, PPM
TIME, HRS

Fig. 11 Effect of installing drier in a by-pass

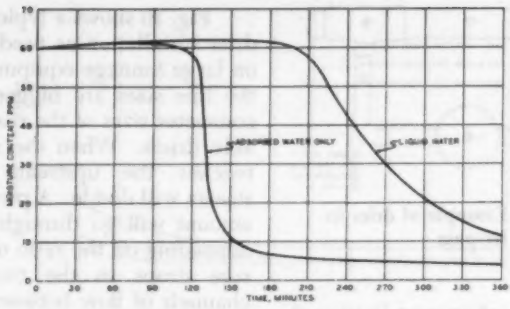

Fig. 12 Effect of liquid water in the system on drying time using a drier with 7⅝ in. depth desiccant bed, internal surface area of A_1, + 22.2 ft² and a rate of flow of 500 lb/hr

present in the system. Fig. 12 presents the drying curve for a system containing liquid water. Approximately one fluid ounce of water was added to the test system for this study and the largest size drier available was used to assure ample capacity.

It is assumed that the liquid water in the system found its way to the receiver where it floated on the surface of the refrigerant or adhered to the walls of the receiver. Experience with glass equipment recirculating Refrigerant 11 has shown that when liquid water is present it clings to the system walls in small globules. Here it dissolved into the refrigerant, rather rapidly at first and then more slowly as the saturation level was approached.

It was noted that the moisture content of the refrigerant did not reach the saturation value of 110 ppm although the refrigerant was cycled for 18 hr previous to observing drying action. Experience has shown that when less than saturation values are desired, thorough agitation for 72 hr is needed to assure complete solution of the liquid water added to the refrigerant.

Except as noted, liquid water in the system showed no marked effect on drier action.

CONCLUSION

The action of a drier in a given refrigerating system requires a considerable period of time to bring the moisture level of the refrigerant to a state of equilibrium with the drier.

The actual time required will vary with the rate of refrigerant flow, internal area of system and size of drier. In general, the time required to dry systems with low rates of refrigerant flow will take longer than those with high flow rates. A larger drier will dry a system more rapidly than a smaller drier. With the same basic components remote systems will take longer to dry than packaged units

because of greater internal surface area.

Observations in the course of these investigations also lead to a practical recommendation. Because that part of the refrigerating system which is closest to the outlet end of the drier will be reduced to a low moisture level almost as soon as the drying process begins, the drier should be installed as close upstream to the expansion valve or capillary tube as possible. Thus, one of the sensitive parts of the system as far as moisture is concerned will be in the "dry zone" well before the entire system is dry. This assures immediate and continuing protection against freeze-ups, regardless of drying time required, as long as drier capacity is adequate.

In a system a large drier will reduce the moisture content to a lower degree and in a shorter period of time than a small drier. Accordingly, the possibility of freeze ups and formation of corrosion products due to moisture are minimized.

Drying time data obtained in the course of this investigation will not necessarily hold true for systems in the field. Rather, the data presented here indicate what to expect when the care taken in equipment dehydration before start-up and the nature of the installation itself are considered.

ACKNOWLEDGMENT

The cooperation of Melvin DePas and William T. Rohrberg with their help in this study is appreciated greatly. The authors are particularly grateful to Walter O. Walker, Dean of the Division of Research and Industry, University of Miami and Lyle F. Albright, Professor, Chemical Engineering, Purdue University, for their comments and criticisms of this paper.

REFERENCES

1. "Methods of Rating and Testing High Side Liquid Line Driers", Standard 35, part B, (American Society of Refrigerating Engineers).
2. "1958 ARI Standard for Liquid Line Driers", Standard 710, Air-Conditioning and Refrigeration Institute.
3. Sterk, B. J. "Certain Test Results for Three Desiccants in a Freon-12 System", Refrigerating Engineering, 57 No. 8, 782 (1949).
4. Pennington, W. A. "Role of Adsorption—Type Desiccant in Refrigeration Units", Refrigerating Engineering, 59 No. 3, 272 (1951).
5. Walker, W. O. and Wilson, K. "Refrigerant Driers", Ansul News Notes, 1 No. 3, pp. 1-7 (1937).
6. Brisken, W. R. "Moisture Migration in Hermetic Refrigeration Systems as Measured under Various Operating Conditions", Refrigerating Engineering 63 No. 7, 42-48 (1955).
7. Krause, W. O. "Adsorption of Moisture by Cylinder Walls", Ansul News Notes, pp. 8-9 (June 1953).

APPENDIX

Experimental System—A_1 (Fig. 1)

1 Roth Model 1133 AT turbine pump
1 S&K Model 18210 Safeguard rotameter—1 in. tube
1 Standard Model V-5 water cooled receiver
4 Mueller ⅝ in. diaphragm valves flare fitting
3 Mueller 1⅛ in. diaphragm valves—sweat fitting
1 Mueller ¾ in. diaphragm valve —sweat fitting
16 ½ ft 1⅛ in. copper tubing
3 ft ¾ in. copper tubing

Operating conditions

1. Pressures—90-96 psig
2. Temperatures—84-88 F
3. Refrigerant charge—25-40 lb Refrigerant 12

Driers

1. Used in wetting system—Ansul

T-30 driers containing 420 and 510 g processed H-151 activated alumina preloaded with 128 cc water in accordance to procedure outlined in ASRE Standard 35B.

2. Used in drying system—Ansul TR-42 receiver drier shell containing 110, 310, 420, and 510 g H-151 activated alumina having a bed depth of 1⅝, 4⅝, 6¼ and 7⅝ in. respectively. Desiccant bed diameter was held to 2.4 in.

Procedure—Experimental results were obtained using equipment shown in Fig. 1. Moisture analyses were made with an electrolytic water analyzer equipped with an oil separator. When not in use, the water analyzer was continuously swept with Refrigerant 12 having a moisture content of 4 ppm. Calibration of the instrument was continuously checked by this means.

In establishing the drying curves one leg of the parallel arrangement contained the drier preloaded with water. The other leg, at this time, did not contain any test drier. Refrigerant 12 was flowed through the drier preloaded with water for 24 hr at the rate of 500 lb/hr. At the end of this time the refrigerant stream was analyzed for moisture content. The refrigerant was diverted to flow through the other leg of the parallel arrangement for an additional 24 hr and another moisture analysis was made.

If analyses agreed within 1 ppm the system was considered in equilibrium. With continuous moisture analysis the refrigerant stream was again diverted through the preloaded drier. The refrigerant in the other leg was pumped into the receiver and the test drier was installed. The refrigerant was diverted through the test drier after one hour in continuous moisture analysis showed no change in moisture content.

Rate of refrigerant flow was adjusted to the desired flow. During the drying period moisture readings were taken every five minutes. When no further change in moisture content was noted over a one hour period the system was stopped. The refrigerant in the test drier was pumped into the receiver and the test drier removed.

The system was again started up and refrigerant was recirculated for an additional 24 hr period after which another moisture analysis was made to determine whether equilibrium had been established.

Calculations based on final equilibrium moisture content indicate that the driers removed 4.0-8.0 g water depending upon the internal surface area.

DISCUSSION

W. B. LEIGHTON, Tarrytown, N. Y. (Written): This paper should prove helpful to the refrigerant industry in establishing minimum desiccant charges and dehydrating times required to insure optimum refrigeration machine performance. What is the approximate ratio of refrigerant flow through the by-pass to the refrigerant flow in the main line establishing the moisture removal times shown in Fig. 11?

CLOSURE BY AUTHOR BEACHAM: The ratios of refrigerant flow are: 1:7, 1:5, 1:3, and 1:2.

H. O. SPAUSCHUS, Louisville, Ky.: In my opinion, the paper should include the type of drier and the temperature at which the experiments were made, not because it is important to have proprietary information but in order for the results to be generally useful. Could not the characteristics of these curves be greatly changed with the use of a different drier?

L. F. ALBRIGHT, Lafayette, Ind.: It was stated that surface absorption phenomena occurred. What was the surface material? In one case, the surface was increased by adding copper tubing. Was copper the surface used in all procedures?

Wouldn't it also be important to know the surface-to-volume ratio?

AUTHOR BEACHAM: Copper was the only surface material used. Work is being carried on at the present time to determine the effect if surfaces were aluminum, iron or steel.

1730

No. 1730

Production Control Testing of Thermoelectric Materials

G. V. DOWNING, JR.

Because the usefulness of thermoelectric materials, such as bismuth telluride and lead telluride is a result of their unusual electrical and thermal properties, rapid and precise control procedures are essential to insure the quality of material being produced.

In our laboratories the ratio Z is used as the figure of merit on which our evaluation is based. This is defined as:

$$Z = \frac{S^2}{\rho K} C^{-1}$$

where

S = Seebeck coefficient uv/C
ρ = Resistivity ohm-cm
K = Thermal conductivity watts/deg cm

While it is possible to measure Z directly by either the Harmon method or in the so-called "Δ T max" apparatus, both of these require cutting the material and consequently result in loss of saleable material. In addition, they are time-consuming and not suitable for routine control purposes.

Non-destructive total testing is used which enables us to measure the actual material sold rather than a sample which may or may not be representative of the material made.

As a materials supplier we evaluate a number of different supply shapes. Normally, the material is prepared in cylindrical ingots of varying length and diameter so that apparatus must be flexible. We measure a resistivity profile and the Seebeck coefficient on every ingot. Thermal conductivity is measured only occasionally.

RESISTIVITY

Resistivity is the most sensitive quality control and is the most easily measured. We use an ac method; since these are thermoelectric materials, the use of any appreciable dc current would create

G. V. Downing, Jr., is active in Physical and Inorganic Chemical Research with the Merck Sharp & Dohme Research Laboratories, Div. of Merck & Company, Inc. This paper was presented at the ASHRAE 67th Annual Meeting, Vancouver, B. C., June 13-15, 1960.

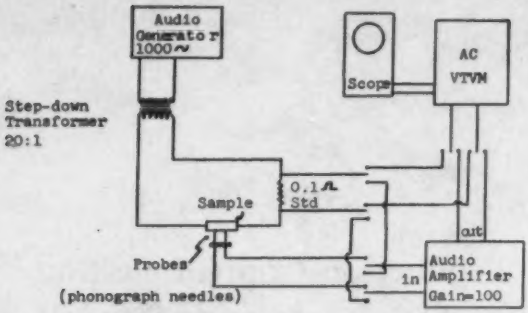

Fig. 1 Apparatus for measuring resistivity

both temperature and potential differences between the ends of the ingot which interfere with the measurement. The use of small dc currents is satisfactory but there are problems in amplifying small dc voltages.

A block diagram of the apparatus is shown in Fig. 1. It consists of an audio generator, the output of which is stepped down through a filament transformer in order to get sufficient current through the sample. A standard 0.1-1.0 ohm resistance decade is placed in series with the sample. The voltage across this can be switched to the vacuum tube voltmeter, and hence the current through the sample can be determined and the output of the generator adjusted to give a "known" current, usually 100 or 200 milliamp.

The voltage across a 1 cm interval on the ingot is measured by a two-point probe; this voltage is amplified and read on the meter. The amplifier is adjusted to a gain of 100 by switching the input across the standard resistor and adjusting the volume control. The amplifier has been tested and found to be linear and stable under these conditions.

In addition, the bass control acts as a filter and by "cutting" the bass, all 60 cycle hum is rejected. The oscilliscope is used as a monitor of the wave form of the input to the meter to insure that proper contact has been made and that no interfering frequencies are present. The meter has an accuracy of 1 per cent.

The sample holder is adjustable and spring loaded so that contact to any length ingot is readily made. The resistivity is then calculated:

$$\rho = \frac{E_p}{E_r} \times \frac{R_r \times A}{G} \text{ ohm/cm}$$

E_p = Voltage drop across 1 cm probes
E_r = Voltage drop across standard resistor
R_r = Resistance of standard resistor (usually 0.1 ω)
G = Gain of amplifier (usually 100)
A = Cross sectional area of the ingot

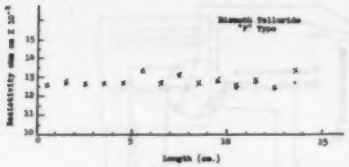

Fig. 2 Bismuth telluride "P" type

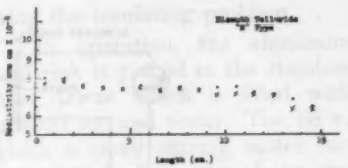

Fig. 3 Bismuth telluride "N" type

Resistivity is measured at 1 cm intervals along the ingot at two points on the circumference and the resulting profiles must fall within certain limits. A range of $\pm 1.5 \times 10^{-4}$ ohm-cm is allowed in the case of bismuth telluride. Usually, there are regions at the extreme ends of the ingot which fall outside the range and these are then cut off. Typical profiles are shown in Figs. 2 and 3.

The time required to obtain a profile by construction of a multipoint probe shown in Fig. 4 has been considerably decreased. The points are spaced 1.00 cm apart along the probe. By means of a switch the voltage across each pair of points is measured in turn. By adjusting the current in proportion to the area, the resistivity is read directly off the meter and may be plotted directly.

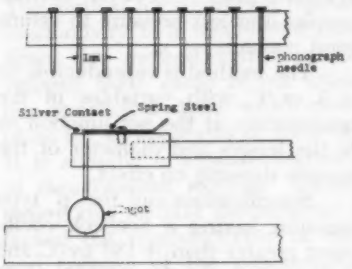

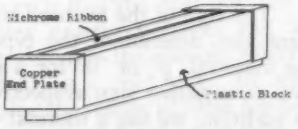

Fig. 4 Multipoint probe

Time required to obtain a profile is of the order of five minutes. Under development is an automatic unit operated by a stepping switch with the read-out either plotted on a graphic recorder or printed on a tape.

We have found that a strip of nichrome ribbon mounted on a plastics block is a convenient standard for checking the probe spacing and the general proper functioning of the apparatus.

SEEBECK COEFFICIENT

The ingot which now has a uniform resistivity profile is next measured for Seebeck coefficient. The ends of the sample are coated with a thin layer of In-Sn amalgam. It has been found that this wets the materials readily and is easily applied. It affords good thermal and

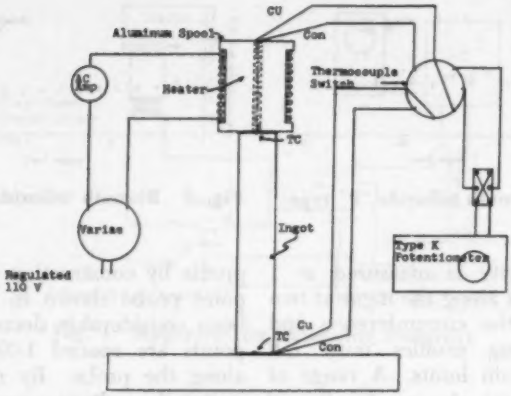

Fig. 5 Seebeck coefficient apparatus

electrical contact to the end of the ingot.

The ingot is now placed in the apparatus as shown in Fig. 5 with a copper constantan thermocouple at the base, and the heater with the thermocouple through the center is clamped firmly onto the top. Cotton is placed around the ingot to cut down convection. The heater is run at a voltage which gives a temperature differential of about 10 C, and the system is allowed to equilibrate for 15 to 20 min. The thermocouple emf's and the emf between the copper leads at each end of the ingot are measured with a Type K potentiometer and the Seebeck coefficient calculated according to the formula:

$$S = \frac{E_1}{[E'_1 - E'_2] \times f} \times 10^3 \text{ uv/C}$$

E_1 = emf between copper leads expressed in mv.
E'_1 = emf of hot thermocouple in mv.
E'_2 = emf of cold thermocouple in mv.
f = conversion factor C/mv.

Values obtained with and without the amalgam agree; the use of the amalgam requires less attention to careful placement of the thermocouples and less pressure to assure good contact.

The method is reproducible to ± 3 uv/C with variables in the temperature at the hot junction or in the length and diameter of the sample showing no effect.

Specifications call for "p" type material having a Seebeck coefficient greater than $+180$ uv/C and "n" type greater than -160 uv/C. Normal values are $+200$ to 220 uv/C for "p" type and -180 to 190 uv/C for "n" type.

The sign of the Seebeck coefficient also determines the type of the material "p" or "n" for a positive or negative sign respectively. In addition, we use a thermal voltage probe with a heated copper

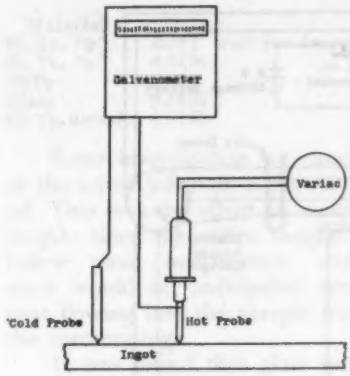

Fig. 6 Type probe

tip and a copper reference probe as shown in Fig. 6 to examine the ingot for any evidences of segregation resulting in change of type.

THERMAL CONDUCTIVITY

The method for measuring thermal conductivity is a steady-state one. After this method had been developed there came to our attention an article by Ioffe[1] which stated plans for an apparatus of this type. It is actually a logical outgrowth of the transient method. Investigating this method showed that it lacked the reproducibility of ours and because of the computation, time involved was no more rapid.

The apparatus is extremely simple and is shown in Fig. 7. The theory is that the heat put into the heater exactly balances the heat lost through the sample which is placed on a cold sink. By maintaining the heater at room temperature no heat flows to or from the surroundings, thus greatly simplifying the insulating problem.

In operation, the aluminum cold sink is placed in the stainless steel dewar which is filled with crushed ice and water. The lid to which a small stirring motor has been attached is placed on the dewar. An aluminum plug, the upper half of which is machined to the same diameter as the sample, is placed in the sink. This plug has a small hole for a thermocouple drilled quite close to its upper surface.

The sample which is about 1 cm long is prepared by machining a smooth surface on each end. It is then attached to the sink with a thin film of stopcock grease such as "cellogrease." The heater is made from a copper cylinder of the same diameter as the sample. A small hole for a thermocouple is drilled close to one face. A coating of nail polish is applied and the heating wire is wrapped around the cylinder.

A length of about 12 in. is used which gives a resistance of about 35 to 40 ohm. Flexible copper leads of No. 30 wire are attached to the ends of the heater wire, and the assembly is wrapped with tape. The resistance of the heater is measured accurately with a Wheatstone bridge.

The heater is attached to the top of the sample with the same grease. No. 30 copper-constantan thermocouples are inserted in the holes in the heater and sink. Blocks of styrofoam insulation with holes cut out are used for insulation.

The current through the heater is adjusted by means of the rheo-

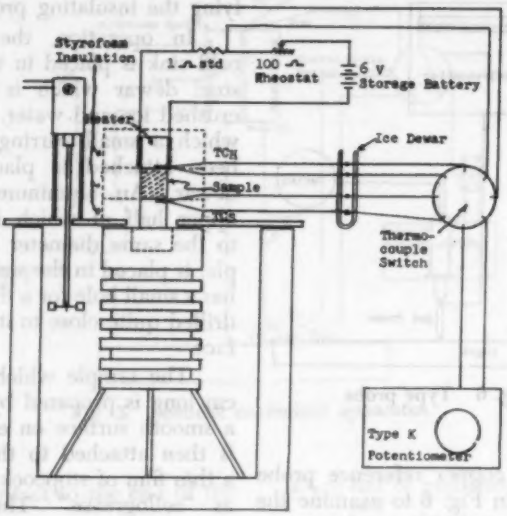

Fig. 7 Thermal conductivity apparatus

stat until the heater thermocouple is at the same temperature as the ambient. Because of the relatively small mass of the heater and the relatively poor thermal conductivity of thermoelectric materials, the heater responds quickly to changes in current.

Only 10 to 15 min are required to bring the system to equilibrium. The current is then measured by measuring the voltage across the standard resistor, and the temperature of the cold sink is measured. The thermal conductivity is then caluclated.

$$K = \frac{I^2 R \times l}{A \times (T_H - T_S)}$$

I = current through heater
R = resistance of heater
l = length of sample
A = area of sample
T_H = temperature of heater
T_S = temperature of sink

A typical calculation is given below:

$R = 26.7\ \omega$
$T_H = 1.114$ mv $\equiv 21.9$ C
$T_S = .039$ mv $\equiv 0.8$ C
$\Delta = 21.1$ C
$L = 1.15$ cm
$D = 0.64$ $A = .322$ cm^2
Room temp. $= 21.7$
$I = 0.0625$ amp

$$K = \frac{(0.0625)^2\ (26.7)\ (1.15)}{(0.322)\ (21.1)} =$$

.0176 watt/deg/cm

The apparatus was checked by using borosilicate glass, and the value obtained was 0.0105 watt per deg/cm which is the value given by the National Bureau of Standards for this material. Reproducibility is $\pm$ 2%. Typical values are given:

Material	
Bi_2Te_3 "p"	0.017 watt per deg/cm
Bi_2Te_3 "n"	0.0190
PbTe	0.040
Glass	0.0105
Bi_2Te_3 doped	0.0153

Some investigation was made of the errors inherent in the method. One was the effect of sample length; since the entire sample is below room temperature, some error would be anticipated from heat flowing into the sample from the surroundings.

It was found that glass samples up to two cm in length showed no error, but longer ones gave the lower values one would expect. Thermocouples placed in the sample showed a linear temperature drop for the two-centimeter sample but a non-linear profile for a 4-cm piece.

A possible explanation is that the heater actually loses some heat to the surroundings since the temperature of the heating wire is probably higher than the block, and this loss is balanced by the flow of heat into the sample.

Error due to not balancing the heater exactly at room temperature turned out to be on the order of 1% for temperatures as much as ± 5 C from the ambient for glass but of the order of 2 to 3% for a material with a thermal conductivity of ≈ 0.03.

As Ioffe points out, materials with a thermal conductivity of approximately 0.01 are the easiest to measure accurately. If one approaches 0.1, the thermal resistance of the contacts becomes a problem; in fact, for lead we obtained a value of ≈ 0.15, about half the correct value. For materials with a K of the order of 0.001, heat leakage would be a significant error. Fortunately, most materials of interest as thermoelectrics fall in the range of 0.005 to 0.050.

This method has reduced the time and uncertainty in measuring thermal conductivity and made the measurement a practical one for routine purposes. Fifteen samples can be run in a day with no great difficulty.

SUMMARY

The methods described for the measurement of resistivity, Seebeck coefficient, and thermal conductivity are all suitable for use in routine quality control of thermoelectric materials. The accuracy of each measurement is of the order of $\pm 3\%$ and the precision is $\pm 2\%$ in the case of thermal conductivity and probably somewhat better for resistivity and Seebeck coefficient.

REFERENCE

1. Ioffe, A. V. and Ioffe, A. F., Zhur. Tekh. Fiz. 28, 2357 (1958). [Translation in Infosearch Publication SEM-7-59, Paper #9, January 1959.]

DISCUSSION

P. F. TAYLOR, Philadelphia, Pa. (Written): This is a very good summary of measuring techniques which are useful for basic studies in thermoelectricity.

There are two minor criticisms of the techniques:

I question the advisability of the measurement of Seebeck coefficient on whole ingots which have a non-constant resistivity, as shown in Figs. 2 and 3.

The temperature difference across the sample for thermal conductivity (21.1 C) is

rather larger than is usually accepted on account of radiation losses from the side of the sample.

CLOSURE BY AUTHOR DOWNING: The ends of the ingots which have non-uniform resistivities are cut off before measuring the Seebeck coefficient. The Seebeck coefficient is measured at each end of the rod. If marked deviations in resistivity are found within the rod, the rod is discarded. If one or two centimeters is removed from the samples, such as shown in Figs. 2 and 3, then the Seebeck coefficient is found to be uniform. This was determined by sectioning such rods and measuring the value of S for each section.

Heat flows into the sample since the surroundings are at a higher temperature than the sample. This was a problem, but, in checking, it was found that with short samples of less than 2 cm, the values obtained for glass agreed with the published data. No difference was observed when smaller temperature differences were used. If a large ΔT were used, the results would be erroneous.

1731

No. 1731

A Simplified Engineering Approach to Thermoelectric Heat Pumping

WILLIAM HUCK

During the past several years a great deal of interest has been shown in the field of thermoelectricity, both in the thermoelectric conversion of heat into electricity and in the pumping of heat by thermoelectric means. Fig. 1 is a schematic description of these two phenomena.

BACKGROUND

The basic concepts of thermoelectric (TE) conversion and heat pumping were discovered early in the last century by Seebeck and Peltier. Until recently a surprisingly small amount of research had been conducted in the field. This is rather startling when we realize that at one time TE conversion was equal in efficiency to the best rotary machinery and at one time TE cooling would have been the only practical form of refrigeration below the freezing point of water.

W. Huck is Applied Research Supervisor, Thermoelectric Products, Minnesota Mining and Mfg. Company. This paper was presented at the ASHRAE 67th Annual Meeting, Vancouver, B. C., June 13-15, 1960.

For years these two effects were merely laboratory curiosities, the first application was the use of metallic thermocouples in thermometry. The first commercial use, in the early 1930's, was in gas appliance burner controls. It was not until the 1940's, when TE semiconducting materials were first formulated and measured, that researchers could see TE products over the horizon.

In 1948 a research group, headed by Dr. S. Karrer, at Baso Inc., initiated a search for TE materials having exploitable properties. This group found that by suitably doping lead telluride, a binary compound, highly efficient TE materials could be obtained. Lead telluride was then incorporated into a thermocouple, powering a gas furnace control system; and this is still the only mass-produced commercial thermoelectric device using semiconducting materials, Fig. 2.

This research work, dating

back to 1948, is being expanded at Minnesota Mining & Manufacturing Company and has resulted in the development and sale of new semiconducting materials for use in heat pumps as well as generators; the SNAP III generator, a line of similar generators for sale (Fig. 3), commercial elements for prototype studies, a heat pump test kit for educational use, and several heat pump devices which will be described later.

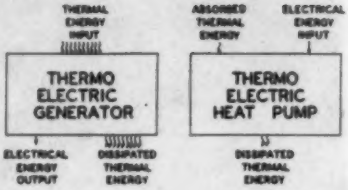

Fig. 1 Energy flow for thermoelectric conversion and heat pumping

TE semiconductor materials are developed for a given temperature range of use; thus PbTe appears to be one of the better materials for use below 1200 F, whereas Bi_2Te_3 type materials are more suitable for use below 500 F and since most heat pump applications fall in the low temperature range, the latter compounds are more commonly used. It would be unreasonable to presume that PbTe and Bi_2Te_3 are the ultimate TE materials; we should expect superior materials to be developed in the future.

The interest in thermoelectricity today is divided between those wishing to pump heat and those wishing to generate electricity. There are many similarities in these two fields; the same general types of materials are used, the same physical parameters are of interest, and the same physical theory encompasses both. The major differ-

Fig. 2 PbTe thermoelectric generator used in gas furnace control system

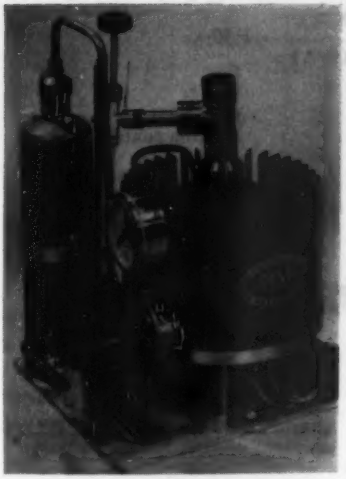

Fig. 3 5 watt propane fired thermoelectric generator

ence is in goal. A thermoelectric generator is a conversion device, one that converts thermal energy directly into electrical energy, while a thermoelectric heat pump is an energy transfer device, using electrical energy to transport thermal energy from one point to another.

THEORY

The three physical properties which are of importance when discussing heat pump materials are: the Seebeck coefficient (S), the electrical resistivity (ρ), and the thermal conductivity (k). All three properties can be and generally are functions of temperature which explains why a material with good performance in one temperature range may be poor in another. The performance

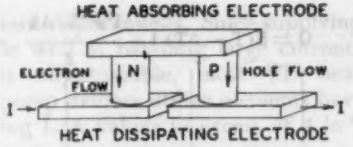

Fig. 4 Schematic heat pump where the absorbing junction is the cold junction electrode. Electrical carriers are holes in the P-type material and electrons in the N-type. In both legs of the heat pump the carriers transport thermal energy away from the absorbing electrode

of TE materials is related to $S^2/k\rho$; a quantity commonly referred to as the figure of merit.

Physical, chemical, and metallurgical studies are being conducted in an effort to increase the figure of merit and although S, ρ, and k are not completely independent of one another, some progress is being made in lowering k for a given S and ρ.

TE heat pumps are assemblages of "N" and "P" type materials (Fig. 4) which are connected in series electrically. Each conduction electron in the "N" type material carries a small amount of energy away from the absorbing electrode and each hole in the "P" type material does the same; the net result is the lowering of the absorbing junction temperature.

The following energy flow equation describes the steady state conditions at the absorbing junction and applies to either the "N" or "P" leg of the heat pump:

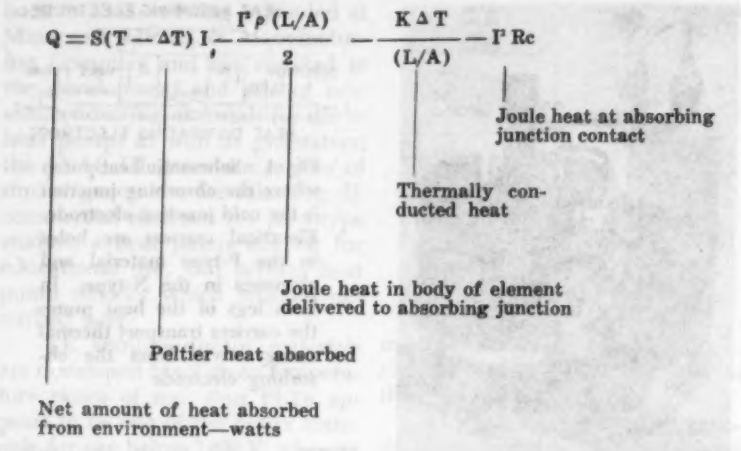
$Q = S(T - \Delta T) I - \frac{I^2 \rho (L/A)}{2} - \frac{K \Delta T}{(L/A)} - I^2 Rc$
Joule heat at absorbing junction contact
Thermally conducted heat
Joule heat in body of element delivered to absorbing junction
Peltier heat absorbed
Net amount of heat absorbed from environment—watts

S — Seebeck coefficient—90 to 130 μV/F.
T — Dissipating junction temperature—R
ΔT — Temperature difference across element—F
I — Direct current through element—amp
ρ — Electrical resistivity—300 to 600 $\mu\ \Omega$ in.
(L/A) — Ratio of element length to area—in.$^{-1}$
k — Thermal conductivity — 0.012 to 0.02 watts/in. F
Rc — Contact resistance — 10^{-1} to 10^{-6} ohm

Academically detailed discussions of the heat pump equation may be obtained from many sources (see reference list). Although S, ρ, and k are functions of temperature, one may assume that for the ΔT's involved in heat pumping, use of average values will not seriously affect the accuracy of the above equation.

From the equation it is apparent that we would like S to be large and ρ, k, and Rc to be small. The functional dependence of Q on I, (L/A) and ΔT, is not easily seen but will become obvious when the experimental data are viewed.

If the contact resistance were zero, the only way in which the thermoelectric element geometry enters is in the form of a ratio, length/area (L/A), thus implying that for constant L/A a small element will perform as well as a large element, i.e., pump the same quantity of heat at the same ΔT for the same current. Therefore, the heat pumped per unit area from the cold junction increases as the element decreases in size.

Carrying this reasoning to its logical conclusion, it would seem possible to pump an ever increasing amount of heat per unit area by decreasing the element size. The practical limitation to miniaturization is the existence of a finite contact resistance Rc which increases as the cross-sectional area of the element decreases. Since the choice

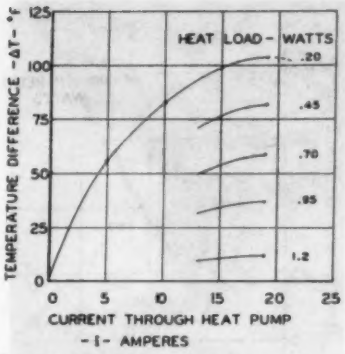

Fig. 5 Temperature difference across heat pump at various heat loads as a function of supply current

of physical size can be quite arbitrary, workers in the field have used 1/16 to ½ in. diam elements. 3M Company has thus far standardized on two diameters: 3/16 and 9/32 in.

To the first approximation, curves of ΔT vs. I at constant values of Q will be quadratic as in Fig. 5. That portion of the curve beyond the maximum ΔT is of no interest since performance suffers when the current is raised above the optimum value. Note that to the expression "optimum current" must be added one of the qualifying expressions, at maximum ΔT, at maximum Q, etc., since the optimum current may differ in each case.

Experimentally optimizing the heat pump geometry results in the discovery that better performance, i.e., higher Q for a given ΔT, is obtained for low values of L/A with correspondingly higher current requirements. Since supplying as well as handling large currents is objectionable, most TE heat pump devices utilize elements having L/A values in excess of 4 in^{-1}.

ENGINEERING DATA

The experimentally determined relationship of temperature difference ΔT, heat load Q, and current I, is shown in Fig. 5. A brief description of the method used to obtain this data follows:

A small copper cylinder containing a heater coil is mounted at the heat absorbing (cold) junction of the heat pump couple which is to be tested. The heat dissipating (hot) junctions of the elements are fastened to a heat sink held at 81 F (81 F = 300 K, which has become the accepted reference temperature). Material properties vary with temperature in such a way that performance falls off at lower temperatures and picks up at higher ones. For example, with a given heat load (Q) a ΔT approximately 25% greater can be obtained when the dissipating junction is held at 212 F or 373 K.

The temperature difference or ΔT is a function of both the heat input or heat load to the copper cylinder and the pumping current. In Fig. 5, the ΔT falls off with increasing heat load. A family of curves cross-plotted from Fig. 5 type data is shown in Fig. 6; each line corresponding to a particular element geometry.

These data, being actual experimental data, include contact resistance, the effects of the material constants, and all temperature dependencies.

In Fig. 6, each curve is a straight line and can be easily fit with a simple empirical equation:

$$\Delta T = 110\ F - \beta Q$$

Where β is the slope of a given curve and is primarily a function of the geometry, i.e., a function of (L/A). The maximum ΔT under no load conditions can be raised higher than 110 F by using better thermoelectric materials or by using larger elements, thereby lessening the effect of contact resistance.

Before trying to solve a typical heat pump problem, some of the design limitations not apparent in Fig. 6 should be mentioned.

All the heat that is pumped from the cold junction plus all the loss in the body of the element must be removed from the hot junction; this can be a problem, especially if small elements are placed close together in order to pump a great deal of heat from a given area. Sufficient heat sink and dissipation means must be provided.

An illustration may be looked upon as being a black box which transfers energy from one side to the other, and which costs ($I^2R + S\Delta TI$) units of energy to run (power required in watts – Fig. 1). The cold side of the box absorbs Q units of thermal energy while $Q + I^2R + S\Delta TI$ units of thermal energy are emitted from the dissipating side of the box.

The coefficient of performance for cooling systems can now be defined as

$$\frac{Q}{I^2R + S\Delta TI}$$

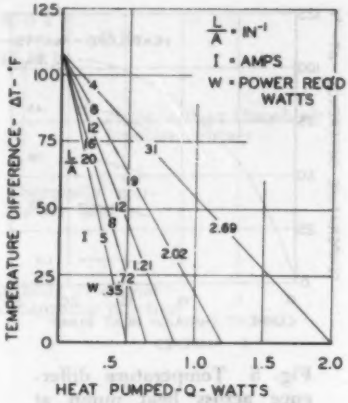

Fig. 6 Experimentally determined heat pump load line graph. Each line corresponds to a different element geometry distinguished by the ratio length/area. 1 watt = 3.42 Btu/hr = .239 cal/sec

The COP for practical thermoelectric cooling systems will generally lie between 0.1 and 2, depending primarily on the temperature difference. Under similar conditions of heat load and ΔT this will be equal to or greater than the COP for an absorption refrigeration system.

Supplying power to drive heat pumps is somewhat of a problem since they are inherently low voltage and high current devices. In addition, reasonably flat dc is desirable; the performance would suffer if the ac ripple were in excess of 20% of peak value.

PROBLEM

Operation of an electronic component at 60 F when the best heat

Fig. 7 Spot cooler used on fluorescent lamps to adjust internal mercury pressure and thus maximize light output

sink in the vicinity is at 70 F. The internal load of the component is 25 watt. A 31-amp power supply can be made available.

SOLUTION

The 25-watt load must be pumped up a 10 F temperature gradient; this of course cannot be done with one heat pump couple, however, many couples can be assembled in series electrically, each sharing a portion of the thermal load. The electrodes will have to be electrically insulated from one another and from the heat sink. When 25 watt are transferred through thin electrical insulating films, the additional temperature drop may easily be 5 F. This means we need a total ΔT of 15 F across the elements.

A 31 amp power supply is best suited to elements having a length/area ratio of 4 in.$^{-1}$ (Fig. 6), and couples having this geometry will pump 1.72 watt with a ΔT of 15 F. Thus, in order to pump 25 watt at least 15 couples are needed. The operating cost of the cooler will be 15×2.69 (Fig. 6) or approximately 40 watt. The heat sink must be capable of absorbing $40 + 25$ or 65 watt.

PRESENT HEAT PUMP DEVICES

Several American companies have built heat pump devices ranging from bottle coolers and warmers to room air conditioners. Although appliances such as these are not merely scientific curiosities, they are still not economically feasible. It should not be long before small refrigerators and dehumidifiers are seen on the market, but at the present time it appears that the field will be limited to smaller industrial applications.

As an example, high power outdoor fluorescent lamps run so hot during most of the year that the contained mercury pressure goes above the optimum level with an accompanying drop in light output. A properly designed heat pump can be used to cool a small spot on the surface of the lamp, condensing mercury vapor and raising the light output to its rated value.

In this way a few watts supplied to the heat pump result in a considerable increase in light output from the lamp. A lamp cooler developed in conjunction with the Line Material Industries is shown in Fig. 7; it cools an area of ½ in.^{2} The light output of a standard Line Material Industries 4 lamp street

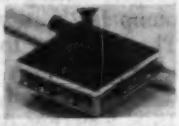

Fig. 8 A 2 in. square flat plate cooling module which may be mounted between the component to be cooled and any suitable heat sink

lighting luminaire was increased 72% under standard rating conditions.

A flat plate cooler shown in Fig. 8 is designed to be fastened to a chassis or any other heat sink. Small electrical components attached to the upper surface may then be cooled. Operational data are shown in Fig. 9.

Another device shown in Fig. 10 is designed to cool or heat a cylindrical cavity. The cavity may contain passive items such as crystals or active electrical loads up to 10 watt.

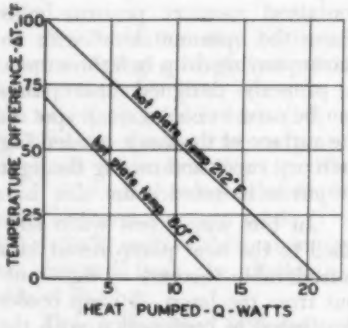

Fig. 9 Operational data on the flat plate cooler. The temperature difference is that between the top and bottom plate

Of the many commercially available refrigerated appliances, none at the present time utilizes the TE phenomenon. There can be only two reasons for this: lack of either technical or economic feasibility. With the latest materials, temperature differences up to 125 F have been obtained in our laboratory from a single stage dissipating to an 81 F (300 K) environment.

Thus, it might appear that TE devices are not widely used because of economic reasons. This is largely true, present material and assembly costs place this new system out of many markets. In most cases assembly and handling costs outweigh materials costs. Improved materials can and will mean simpler and cheaper assemblies. The reasons for high costs are that labo-

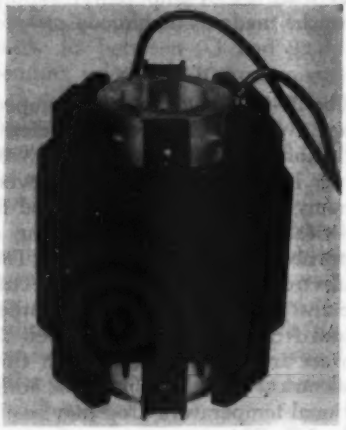

Fig. 10 Cylindrical cavity cooler with capacity in excess of 10 watt. Cavity 1½ in. diam and 3 in. long

ratory rather than production methods have been used to date and only small quantities are being produced. It is possible, however, that automated production could break this economic barrier.

Approaching the problem from the opposite direction, presently used semi-conducting materials are not overly expensive in the raw form and therefore are not the largest contribution to ultimate cost and do not in themselves stand in the way of commercial developments.

Thermoelectric heat pumps may not prove to be a panacea for those with excess heat or temperature control problems, however, this relatively simple new system may fill in some of the gaps in present heat transfer problems.

REFERENCES

1. Thermoelectric Effects, Frank E. Jaumot, Jr., Proceedings of the IRE, March, 1958, pp. 538-544.
2. Thermoelectric Refrigeration, R. L. Eichhorn, REFRIGERATING ENGINEERING, June 1958, pp. 31-35.
3. Thermoelectric Refrigeration, L. A. Staebler, ASHRAE JOURNAL, August, 1959, pp. 60-65.
4. Semiconductor Thermoelements and Thermoelectric Cooling, A. F. Ioffe, 1957, Infosearch Limited, London.

DISCUSSION

A. P. BOEHMER, Des Plaines, Ill.: What is the dc power supply for the fluorescent light cooler which is shown and what are some of its characteristics?

CLOSURE BY AUTHOR HUCK: Voltage across the four modules in the lighting fixture is approximately 1.6 volts and the required current is 7 to 10 amperes. A full wave silicon diode rectifier with choke filter is used. The cost of the power supply is approximately $20.

E. J. OVERMYER, Seattle, Wash.: What would be the weight vs. capacity of these units in the larger size?

AUTHOR HUCK: There isn't too much data available on this, but it would appear variable. This will be a matter for manufacturers to work on.

1732

No. 1732

A Comparative Study of the Manufacturing Costs of Thermoelectric and Mechanical Refrigerating Systems

D. W. SCOFIELD P. F. TAYLOR L. A. STAEBLER
Member ASHRAE

The thermoelectric effects discovered by Seebeck, Peltier and Thomson during the 19th century are well known to engineers and scientists. However, until approximately five years ago the practical application of these effects was restricted almost exclusively to the use of thermocouples for temperature measurement. Over the years a small devoted band of scientists, Telkes, Justi, Wall, Altenkirch, Euchen, Forsborg, to name a few, applied themselves to investigations of these phenomena in the hope of discovering new materials in which the thermoelectric effects were of sufficient magnitude to extend their application beyond that of the measurement of temperature. This eventually led to the consideration of semiconductors, culminating in the work of A. F. Ioffe.[1]

During the past five years progress in this field has accelerated. The discovery and development of the transistor and other solid state devices has stimulated the need for a deeper understanding of the electrical and thermal processes in semiconductors. This has led to the detailed study of Bi_2Te_3, a material first suggested by Goldsmid[2] for thermoelectric applications. The study of this material[3,4,5,6] and associated alloys[7,8,9] has led to the development of practical devices for thermoelectric cooling. The present state of the art has received wide attention[10,11,12,13] and is fairly well known today.

D. W. Scofield is Project Engineer, P. F. Taylor is Project Scientist, and L. A. Staebler is Manager, Advanced Development Department of the Appliance Div, Philco Corp. This paper was presented at the 67th ASHRAE Annual Meeting, Vancouver, B. C., June 13-15, 1960.

Thermoelectricity as applied to heat pumping has certain advantages over the mechanical system. These advantages include, (a), the elimination of moving parts except perhaps for a small fan to assist the heat transfer processes; (b), a reduction in noise; (c), the substitution of simple electrical wiring for the hermetically sealed system required to contain the refrigerant; (d), modulation of heat pumping capacity accomplished readily through a corresponding modulation of the operating current; (e), reverse cycling easily achieved by current reversal; and (f), the ease with which the thermoelectric system can be used for small capacity cooling applications.

Despite these advantages it is obvious that thermoelectric heat pumping must be competitive in manufacturing cost in order to replace the conventional mechanical system to any significant degree in the Consumer Appliance Market.

The purpose of this study was to compare the manufacturing costs of thermoelectric heat pumps with those of conventional mechanical systems for various design capacities. In order to achieve this we have developed a relationship between cost and heat pumping capacity for a thermoelectric system. The cost of the basic semiconductor materials used in establishing this relationship has been that which present manufacturers of these materials consider to be attainable within the next few years. The data obtained from this study were then used to relate manufacturing cost to system performance.

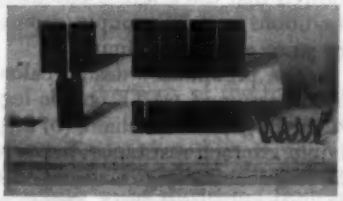

Fig. 1 Section of thermoelectric cooling unit and its components

The cost figures for mechanical refrigeration systems are well established and will probably remain relatively stable during the next few years. Comparable information concerning costs and future trends for the thermoelectric system is not generally available. This study is an attempt to develop such data.

PRELIMINARY DESIGN FOR COSTING

In order to derive detailed thermoelectric costs a working system first had to be designed and built. An illustration of the make-up of a section of the cooling unit is shown in Fig. 1. The system selected was designed for 100 Btu per hr for hot and cold junction operating temperatures of 90 and 40 F, respectively. The design equations[1] used were:

$$Qi = I\,T_c\alpha - \tfrac{1}{2}\,I^2R - C\,\Delta\,T$$
$$W = I^2R + I\,\alpha\,\Delta\,T$$
$$\phi = Qi/W$$
$$N = Q/Qi$$

The symbols are defined in the Nomenclature.

Preliminary design of the TE couple geometry and selection of operating current quickly revealed

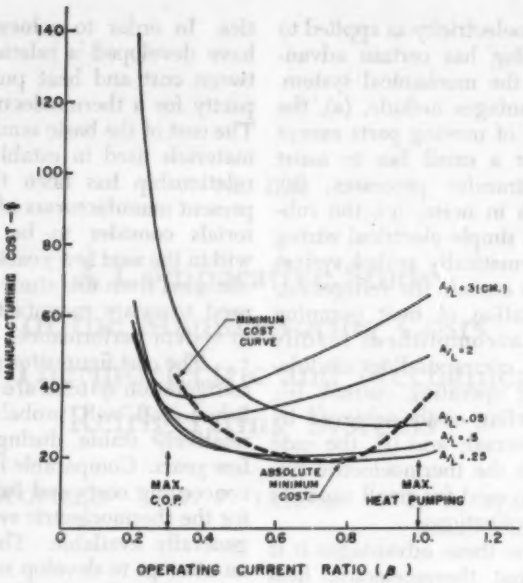

Fig. 2 Effect of design parameters on manufacturing cost (100 Btu per/hr TE system. $T_h = 90$ F, $T_c = 40$ F) $Z = 3 \times 10^{-3}$ C^{-1}

that these design parameters could have a profound effect on the total manufacturing cost of the refrigerating system. To illustrate this point the cost data derived later in this study have been used to plot the curves shown in Fig. 2.

A minimum manufacturing cost can be obtained by designing the system to operate at some appropriate condition between that of maximum C.O.P. and maximum heat pumping capacity. Because the C.O.P. may also be an important consideration a compromise can then be made between minimum manufacturing cost and maximum C.O.P. This matter is covered in detail later, and is illustrated in Fig. 3.

The unit under consideration was designed with this compromise in mind and subsequent calculations based upon the cost data provided from the above approach showed that the selected operating conditions and TE couple geometry were close to optimum.

The preliminary design calculations assumed, (a) TE couple legs ¼ in. long by ¼ in. diam, (b) negligible contact resistance between the semiconducting material and the copper connecting strips in the couples, and (c) a TE material with a Figure of Merit (Z) of 3 x

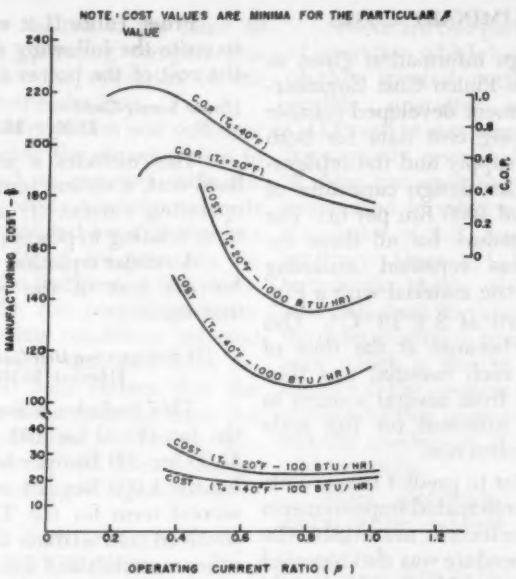
NOTE: COST VALUES ARE MINIMA FOR THE PARTICULAR β VALUE
MANUFACTURING COST - $
C.O.P.
C.O.P. (T_c = 40°F)
C.O.P. (T_c = 20°F)
COST (T_c = 20°F - 1000 BTU/HR)
COST (T_c = 40°F - 1000 BTU/HR)
COST (T_c = 20°F - 100 BTU/HR)
COST (T_c = 40°F - 100 BTU/HR)
OPERATING CURRENT RATIO (β)

Fig. 3 Effect of the operating current ratio (β) on manufacturing cost and C.O.P. for 100 and 1000 Btu per/hr TE systems. (T_h = 90 F, T_c = 40 F, and 20 F) $Z = 3 \times 10^{-3}\ C^{-1}$)

$10^{-3}\ C^{-1}$. The various parameters contributing to the Z of this material are shown below. They are representative of the best TE materials presently available.

Seebeck coefficient = $\pm$ 200 μ v/C
Electrical resistivity = $0.83 \times 10^{-4}\ \Omega$ cm
Thermal conductivity
= 1.6×10^{-2} W $Cm^{-1}\ C^{-1}$

On the basis of the foregoing, the number of couples required and the characteristics of the power supply were determined. In addition, the heat to be dissipated from the hot junctions was calculated and from this information an actual system was designed consisting of an array of thermoelectric couples with heat exchange fins on both the hot and cold junctions.

An air moving system was incorporated which employed a small motor with double ended shaft and two fans, one to circulate the air over the cold fins in the refrigerated enclosure and the other to pass ambient air over the hot fins. The same design considerations were then extended to 300 and 1000 Btu per hr capacity systems.

Representative design information developed for costing purposes is shown in Table I.

PRELIMINARY COSTS

From design information given in Table I the Philco Cost Engineering Department developed reliable manufacturing cost data for both the power supply and the refrigerating unit for design capacities of 100, 300 and 1000 Btu per hr. The entire procedure for all three capacities was repeated assuming thermoelectric material with a Figure of Merit of $2 \times 10^{-3}\ C^{-1}$. This was done because at the time of the study such material was then obtainable from several sources in quantities sufficient for full scale device construction.

In order to predict future costs based on anticipated improvements in thermoelectric materials, the costing procedure was also repeated with Figures of Merit of $5 \times 10^{-3}\ C^{-1}$ and $10 \times 10^{-3}\ C^{-1}$, with each of the basic parameters improved in approximately equal proportions. This appeared to be the best procedure since it is difficult to predict in which of the parameters the major improvement may come.

The cost information developed for the refrigerating system using a TE material with a Figure of Merit of $3 \times 10^{-3}\ C^{-1}$ is shown in Table II.

From Table II it was possible to write the following equation for the cost of the power supply:

$$\text{(Power Supply Cost)} = \$2.00 + \$0.25I + \$0.03W$$

This includes a term for the fixed cost, a second term related to operating current (I) and a third term relating to power (W).

A similar equation was written for the cost of the refrigerating unit itself:

$$\text{(TE Refrigerating Unit Cost)} = \$(\text{fan}) + \$0.3N + \$0.07N$$

This includes a fixed term for the fan ($3.00 for 100 Btu per hr, $5.00 for 300 Btu per hr, and $7.00 for the 1,000 Btu per hr system), a second term for the TE materials involved and a third term for the other materials and assembly. Both the second and third terms are related to the number (N) of TE couples involved.

The cost curve for conventional mechanical systems was determined by plotting the established costs of 1/12 hp, ⅛ hp, ¼ hp and ⅜ hp units. Since the 1/12 hp unit is the smallest commercially available its cost was assumed to be the minimum now attainable for mechanical refrigerating systems. The capacity ratings for these sys-

TABLE I

PRELIMINARY DESIGN INFORMATION

Design Capacity—Btu per/hr	100	300	1000
Number of TE Couples	25	66	215
Current (Amp), dc	21.4	25.6	27.2
Voltage (Volt)	2.1	6.4	22.0
Power Input (Watts)	44	163	598
C.O.P.	0.67	0.54	0.49
Heat to be Dissipated—Btu per/hr	250	857	3040

tems were related to the same 40 and 90 F operating temperatures selected for the operation of the thermoelectric devices.

This information was sufficient for producing the curves shown in Fig. 4 and to proceed with the study of cost minimization. It should be pointed out that the data shown in Fig. 4 are primarily the result of the first part of the study. Fortunately, the couple geometry and operating conditions selected for calculating this data were intuitively so well chosen that the use of the data deduced from the cost minimization procedures subsequently described do not change the curves of Fig. 4 significantly.

COST MINIMIZATION PROCEDURE

When considering the design of a thermoelectric heat pump of any specific capacity, once the couple leg length L has been decided upon, there are two basic variables which ultimately determine the cost. As indicated previously, these are current (I) and the ratio of the cross-sectional area to length of the couple legs (A/L). There are an infinite number of combinations of these two variables which yield the same heat pumping capacity.

There are two particular modes of operation which have been thoroughly treated mathematically, namely, operation at maximum C.O.P. and at maximum heat pumping capacity per couple. For each of these two operating conditions I is specified in relation to A/L but the choice of A/L can still remain arbitrary. Once A/L has been selected, the choice of L is not so arbitrary since its value determines the deterioration in couple performance which is due to a finite resistance at the contacts between the semiconducting material and the metallic conductors at the hot and cold junctions.

More specifically, Z can be shown to be reduced by a factor $\left(1 + \frac{2\rho_c}{\rho L}\right)$ due to this contact resistance in a couple, where ρ and ρ_c are respectively the semiconductor resistivity and the contact resistance for 1 cm². Thus the designer must resign himself to a certain deterioration in Z based on the known values of ρ and ρ_c and then select L accordingly. The importance of reducing ρ_c is readily apparent when one bears in mind the fact that the volume of material used for a specific operating con-

TABLE II

PRELIMINARY COST INFORMATION

Design Capacity—Btu per/hr ..	100	300	1000
Power Supply Costs	$ 8.67	$13.29	$ 26.77
TE Material Costs	7.50	19.77	64.60
Other Material and Labor Costs	1.75	4.63	15.00
Fixed Costs	3.00	5.00	7.00
Total Costs	$20.92	$42.69	$113.37

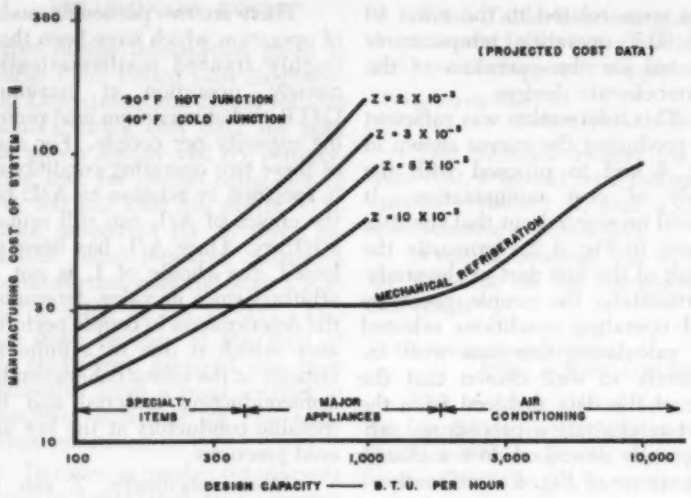

Fig. 4 Comparative manufacturing costs of thermoelectric vs mechanical refrigeration systems

dition is proportional to L^2.

In selecting couple geometry there are other important and practical considerations which must also be taken into account. As improvements in contact resistance come about it will be desirable to reduce L in order to conserve material but there is a practical limit to this which will be set by the heat leakage through the insulating medium in which the couples are imbedded. This can be minimized by packing the couples quite close together but in so doing one reduces the basic area available for heat transfer on the two sides and this may present an additional practical problem.

It is readily apparent that as I and A/L are increased, the number of couples (N) required for a given total capacity unit decreases, and vice versa. It should be therefore possible to determine a combination of I, A/L and N which yields a minimum cost figure.

This section covers such a procedure and also shows the relationship between cost and C.O.P. This is valuable information since both are important factors to be considered in the final design.

THEORY AND CALCULATIONS

For these calculations certain cost figures determined from the first part of this study have been used. They are given below, together with the nomenclature employed to develop the cost data.

NOMENCLATURE

α = Net Seebeck Coefficient, V/C = $|\alpha_N| + |\alpha_P|$

TABLE III

COST OF 100 BTU PER/HR SYSTEM AS A FUNCTION OF β (T_H = 90 F, T_c = 20 F)

β	Power Supply Cost	Fixed Cost	Assembly Cost	T.E. Material Cost	C.O.P.	A/L	Total Cost
1.0	$9.08	$3.00	$3.91	$7.49	0.28	0.244	$23.48
0.8	7.86	3.00	3.62	8.00	0.39	0.282	22.48
0.6	7.18	3.00	3.51	10.00	0.53	0.365	23.69
0.4	7.21	3.00	3.78	17.52	0.62	0.587	31.51

It thus appears that the absolute minimum cost is about $22.48 with $\beta = 0.8$ and A/L = 0.282.

ρ = Resistivity (Ω cm)
K = Thermal Conductivity (W Cm^{-1} C^{-1})
Z = Figure of merit
A = Couple leg cross-section area (cm^2)
L = Couple leg length (cm)
G = A/L (cm)
ϕ = Coefficient of performance C.O.P.
Qi = Heat pumping capacity of a couple (Watts)
Q = Heat pumping capacity of a unit (Watts)
W = Total power to operate a unit (Watts)
N = Number of junctions in a unit
I = Current (amps)
β = Operating current ratio = Operating current / Current for maximum heat pumping
T_H = Hot junction temperature (K)
T_c = Cold junction temperature (K)
ΔT = Th — Tc (K)
R = Couple resistance (ohms)
C = Couple thermal conductance (WC^{-1})
F = Fixed cost of a unit ($)
P = Power supply cost = $f + aI + bW$ where f is a fixed cost and a and b are costs related to the current and power requirements of the supply
E = Assembly cost per couple
M = Semiconductor material cost per cm^2
S = Total cost

The numerical values of the cost constants were taken as follows (see Table II):

F = $3.00 for 100 Btu/hr unit
= $5.00 for 300 Btu/hr unit
= $7.00 for 1,000 Btu/hr unit
f = $2.00
a = $0.25
b = $0.03
E = $0.07
M = $0.68

Now S = Fixed cost + power supply cost + assembly cost + material cost

$$= F + f + aI + bW + NE + 2NALM \quad (1)$$

$$\text{and } Qi = I\,T_c\alpha - \tfrac{1}{2} I^2 R - C\,\Delta T = I\,T_c\alpha - I^2\rho \frac{L}{A} - 2K\frac{A}{L}\Delta T \quad (2)$$

$$\text{Thus } N = \frac{Q}{I\,T_c\alpha - I^2\rho\,L/A - 2K\,A/L \cdot \Delta T} \quad (3)$$

$$\text{and } W = N(I^2R + I\alpha\Delta T) = \frac{Q(I^2R + I\alpha\Delta T)}{I\,T_c\alpha - I^2\rho\,L/A - 2K\,A/L \cdot \Delta T} \quad (4)$$

$$\text{Hence } S = F + f + aI + \frac{Qb(2I^2\rho\,L/A + I\alpha\Delta T)}{(I\,T_c\alpha - I^2\rho\,L/A - 2K\,A/L \cdot \Delta T)} + \frac{QE}{(I\,T_c\alpha - I^2\rho\,L/A - 2K\,A/L \cdot \Delta T)} + \frac{2QALM}{(I\,T_c\alpha - I^2\rho\,L/A - 2K\,A/L \cdot \Delta T)}$$

$$= F + f + aI + \frac{Q[b(I^2 2\rho/G + I\alpha\Delta T) + E + 2L^2GM]}{(I\,T_c\alpha - I^2\rho/G - 2KG\Delta T)} \quad (5)$$

Current required for maximum heat pumping is $\frac{T_c \alpha}{R}$

We can introduce another variable, β, putting I in equation 5 equal to $\frac{\beta T_c \alpha}{R}$, and a relationship between β and G at minimum cost can be obtained.

This substitution yields:

$$S = F + f + \frac{a \beta T_c \alpha G}{2 \rho} + \frac{Q\,[b\,(2\beta^2 T_c^2 Z + 2\beta T_c \Delta TZ) + E/GK + 2L^2 M/K]}{(2\beta T_c^2 Z - \beta^2 T_c^2 Z - 2\Delta T} \quad (6)$$

Differentiating equation with respect to G and equating it to zero gives the value of G yielding minimum cost for a particular mode of operation, i.e., a given β. Variation of β then leads to a value of the absolute minimum cost.

In (6) putting $\frac{\delta S}{\delta G} = 0$ yields $G = \sqrt{\frac{Q E \rho}{K_a \beta T_c \alpha(\beta T_c^2 Z - \frac{1}{2}\beta^2 T_c Z - \Delta T)}}$ (7)

For example, putting $\beta = 1$, equation 7 reductes to $G =$

$$\sqrt{\frac{Q E \rho}{K_a T_c \alpha (\Delta T_{max} - \Delta T)}} \quad (8)$$

This means that a heat pump of capacity Q employing the full heat pumping capacity for a given ΔT will be most economically constructed if A/L obeys the relationship shown in equation 8.

Substitution of G as given in equation 7 into equation 6 gives the following terms in the cost equation:

Fixed cost of cooling unit = F
Fixed cost of power supply = f

TABLE IV

COST OF 100 BTU PER/HR SYSTEM AS A FUNCTION OF β (T_H = 90 F, T_c = 40 F)

β	Power Supply Cost	Fixed Cost	Assembly Cost	T.E. Material Cost	C.O.P.	A/L	Total Cost
1.0	$8.03	$3.00	$3.49	$5.72	0.34	0.209	$20.24
0.8	6.96	3.00	3.21	6.01	0.50	0.240	19.18
0.6	6.28	3.00	3.02	7.14	0.71	0.301	19.57
0.4	5.92	3.00	2.76	8.91	.99	0.412	22.80

In this case the minimum cost is about $19.18 with β = 0.8 and A/L = 0.240.

$$\text{Current dependent power supply cost} = \sqrt{\frac{Q\,Ea\,\beta\,T_c\,\alpha}{2K\rho\,(2\beta T_c^2 Z - \beta^2 T_c^2 Z - 2\Delta T)}}$$

$$\text{Power dependent power supply cost} = \frac{Qb\,(2\beta^2 T_c^2 Z + 2\beta T_c \Delta T Z)}{(2\beta T_c^2 Z - \beta^2 T_c^2 Z - 2\Delta T)}$$

$$\text{Assembly cost} = \sqrt{\frac{Q\,Ea\,\beta\,T_c\,\alpha}{2K\rho\,(2\beta T_c^2 Z - \beta^2 T_c^2 Z - 2\Delta T)}}$$

$$\text{Semiconductor material cost} = \frac{2\,Q\,L^2\,M}{K\,(2\beta T_c^2 Z - \beta^2 T_c^2 Z - 2\Delta T)}$$

The final expression shows that the material cost is proportional to L^2 as previously mentioned.

These equations are now applied to specific capacities and the results are shown in Tables III, IV, V and VI and Fig. 3.

Example 1. (relates to Table III)
100 Btu per/hr capacity
$T_H = 90$ F $T_c = 20$ F

$Z = 3 \times 10^{-3}\ C^{-1}$
$\alpha = (|\alpha_N| + |\alpha_P|) = 400\ \mu V/C$
$\rho = 8.3 \times 10^{-4}\ \Omega$ cm
$K = 1.6 \times 10^{-3}$ W $Cm^{-1}\ C^{-1}$

Example 2. (relates to Table IV)
100 Btu per/hr capacity
$T_H = 90$ F $T_c = 40$ F
Z and individual parameters as in Example 1.

Example 3. (relates to Table V)
1000 Btu per/hr capacity
$T_H = 90$ F $T_c = 20$ F
Z and individual parameters as in Examples 1 and 2.

Example 4. (relates to Table VI)
1000 Btu per/hr capacity
$T_H = 90$ F $T_c = 40$ F
Z and individual parameters as in Examples 1, 2 and 3.

Some general observations can be drawn from Fig. 3. They are as follows:

1. For large values of β the cost changes slowly, whereas, for small values of β the cost changes rapidly.

2. The range over which the cost remains fairly constant decreases as:
   a. The operating temperature difference increases.
   b. The design capacity of the device increases.

3. Considerably enhanced C.O.P. can be achieved with little increase in cost by operating cou-

TABLE V

COST OF A 1000 BTU PER/HR SYSTEM AS A FUNCTION OF β ($T_H = 90$ F, $T_c = 20$ F)

β	Power Supply Cost	Fixed Cost	Assembly Cost	T.E. Material Cost	C.O.P.	A/L	Total Cost
1.0	$46.15	$7.00	$12.35	$74.90	0.28	0.772	$140.40
0.8	35.92	7.00	11.42	80.00	0.39	0.893	134.34
0.6	29.95	7.00	11.15	100.00	0.53	1.157	148.10
0.4	28.28	7.00	11.98	172.52	0.62	1.86	222.78

ples at somewhat less than their maximum heat pumping capacity.

4. The design to achieve minimum costs becomes more critical at higher capacities. For example, if one can extrapolate to a 10,000 Btu per hr capacity a change in β from 1.00 to 0.8 represents a saving of $48.00 or 4.4%.

5. The arbitrary choice of A/L = 0.5 Cm selected for the preliminary analyses is probably close to optimum design.

6. By consideration of the contribution to the total cost of a system by the basic material used and the power supply it can readily be seen where cost reduction must be sought. For example, by referring to the minimum cost figures we see that for the 1,000 Btu per hr unit the power supply and TE material comprise 86.7% of the total cost (26.7% and 60% respectively). For the 100 Btu per hr unit the corresponding figures are 67% (36% and 31%). By merely reducing the quantity of material employed in a device by a factor of 2 (L reduced by $\sqrt{2}$) the manufacturing cost curve for $Z = 3.0 \times 10^{-3} C^{-1}$ becomes almost identical with the curve shown for $Z = 5 \times 10^{-3} C^{-1}$. This is indicative of the possibilities for future cost reduction.

Contact resistance has been considered to be negligible in this study. Although this may be somewhat optimistic its omission does not seriously affect the general conclusions. The method employed here is a general one applicable for any cost figures and any capacity device operating at any desired condition. It consequently provides helpful guide lines for design of future devices.

Effect of Changes in the Individual Parameters Comprising Z — The Figure of Merit, Z, has been considered the all important parameter of a thermoelectric material. This is true from considerations of performance since it determines the coefficient of performance under any operating conditions. However, when one re-examines the cost equations the individual parameters α, ρ and K become important, since they influence the cost independently of Z.

The complete cost equation can be rewritten as follows:

$$S = F + f + \sqrt{\frac{Z}{\alpha}} \times \sqrt{\frac{Q E a \beta T_c}{(\beta T_c^2 Z - \tfrac{1}{2} \beta^2 T_c^2 Z - \Delta T)}} +$$

TABLE VI

COST OF A 1000 BTU PER/HR SYSTEM AS A FUNCTION OF β (T_H = 90 F, T_c = 40 F)

β	Power Supply Cost	Fixed Cost	Assembly Cost	T.E. Material Cost	C.O.P.	A/L	Total Cost
1.0	$38.47	$7.00	$11.07	$52.70	.34	.661	$113.74
0.8	29.67	7.00	10.17	60.10	.50	.760	106.94
0.6	23.96	7.00	9.66	72.40	.71	.953	113.02
0.4	20.43	7.00	9.63	108.40	.99	1.304	145.46

$$\frac{Qb\,(2\beta^2 Z T_c^2 + 2\beta T_c \Delta T Z)}{(2\beta T_c^2 Z - \beta^2 T_c^2 Z - \Delta T)} + \frac{2 Q L^2 M}{K\,(2\beta T_c^2 Z - \beta^2 T_c^2 Z - 2\Delta T)} + \sqrt{\frac{Z}{\alpha}} \times \sqrt{\frac{Q E a \beta T_c}{(\beta T_c^2 Z - \tfrac{1}{2}\beta^2 T_c^2 Z - \Delta T)}}$$

The 3rd, 5th and 6th terms contain individual parameters and consequently their values have a direct bearing on the cost of the device. It is readily apparent that materials having high values for α and K are desirable. For example, if α changed from 400 to 800 μV/C and K from 1.6 x 10^{-2} to 6.4 x 10^{-2} $Wcm^{-1}\,C^{-1}$, with Z remaining at 3 x 10^{-3} C^{-1} in going from one material to another having the same basic cost, the cost of a 1000 Btu per hr system could be reduced by almost 50%. Although this may be a grossly exaggerated example, consideration of the effects of individual parameters does bring out the following important points:

(1) Although Z is important in determining performance it does not necessarily determine the total cost of the TE materials used. This is because the amount of the TE materials required is influenced more by the parameters making up the Z than by the Z itself.

(2) A moderate Z might well be more acceptable than a high Z if the former has a better blend of parameters.

(3) Work on compounds made from expensive elements should not be discouraged on the grounds of cost, since the possibility exists of such a material not only having an improved Z, but also of having a blend of parameters which would reduce the cost of a device in such a way as to more than offset the increase in basic material cost.

(4) If sufficiently high Z values are obtained in the future, then the opportunity of doping such a material in a way such as not to realize its full potential but to obtain more favorable individual parameters from the cost viewpoint might present itself.

CONCLUSIONS

The purpose of this study was to compare the manufacturing costs of thermoelectric and mechanical refrigerating systems for various design capacities. These comparative costs are shown in Fig. 4. In order to permit this comparison a relationship between cost and heat pumping capacity was developed for the thermoelectric system. This relationship was developed by writing a cost equation for the complete TE system, including power supply, thermoelectric couples and heat exchange surfaces. The variables involved include total Btu per hr design capacity, TE material parameters, operating current and the geometry of the thermoelectric couple. From this equation a relationship between couple geometry and the operating current for minimum cost was obtained. Then, by selection of various operating currents an absolute minimum cost was deduced. This allowed us to relate manufacturing cost with C.O.P.

and arrive at a design compromise between absolute minimum cost and maximum C.O.P.

The cost of the TE materials used in establishing the relationship is somewhat below the present market price. However, it is one which companies presently engaged in the fabrication of such materials consider to be attainable within the next few years. At present, materials with $Z = 3 \times 10^{-3}\ C^{-1}$ are commercially available at approximately \$0.22 g in production quantities, as compared with the \$0.085 g assumed in these calculations.

Since the high purity elements used in the fabrication of Bismuth ternary material cost only about \$0.05 g before processing, a final cost somewhat less than \$0.10 g may well be realized in the near future. Other costs are based upon present day technology of TE couple fabrication and upon conventional design of the dc supply.

If significant improvements are made in the Figure of Merit of the TE materials or in couple fabrication, either of which will permit the use of less TE material for the same performance, then thermoelectricity will become more competitive than this study indicates. Further cost reduction may likewise be possible in dc power supplies.

Already the use of thermoelectricity for military and other special applications is increasing rapidly. This is evidenced by the government support enjoyed by many companies working in this field. In the consumer appliance industry economic factors become of prime importance. However, despite the competition of the low cost mechanical refrigerating system, thermoelectricity may have applications in the near future for devices of capacities up to 200 Btu per hr, and within just a few years thermoelectric refrigerators of up to 4 cu ft may be available to the public.

Although it does not appear that thermoelectricity will in the foreseeable future completely replace or obsolete the mechanical system, there are good reasons to expect that continued research will eventually provide a combination of improved thermoelectric materials, simplified manufacturing techniques, and low cost power supplies which will make thermoelectric refrigeration economically competitive with mechanical refrigeration for the larger major appliances.

REFERENCES

1. Ioffe, A. F., Semiconductor Thermoelements and Thermoelectric Cooling, Infosearch Ltd., London 1957.
2. Goldsmid, H. J., Journal of Electronics, *1*, 218, 1955.
3. Ainsworth, L., Proceedings of the Physical Society B *69*, 606, 1956.
4. Goldsmid, H., Ibid *72*, 17, 1958.
5. Goldsmid, H., Ibid *71*, 633, 1958.
6. Vlasova, M., Stilbans, L. Zhurnal Tekhnicheskoi Fiziki, *25*, 569, 1955.
7. Sinani, S. S., Gordyakova, G. N., Ibid *26*, 2398, 1956.
8. Airapetyants, S., Efimova, B., Russian Journal of Technical Physics, Aug. 1958.
9. Rosi, F., Abeles, R., Jensen, R., Journal of Physics and Chemistry of Solids, *10*, 191, 1959.
10. Staebler, L. A., A Primer of Thermoelectric Refrigeration, ASHRAE JOURNAL, August 1959.
11. Celent, C., Thermoelectricity—State of the Art, Electronic Industries, July 1959.
12. Goldsmid, H., Thermoelectric Cooling, Electronics, Feb. 13, 1959.
13. Gettings, H., Prospects for Thermoelectricity, *Missiles and Rockets*, June 22, 1959.

DISCUSSION

A. F. PHILLIPS, Washington, D. C. (Written): I think it should be emphasized that Fig. 4 represents a particular set of circumstances as described in the paper and cannot be interpolated beyond the specific example for which it was plotted, that is to show that specialty items are becoming practicable. For example, it cannot be inferred from Fig. 4 that, even with high Z values, large capacity thermoelectric devices will virtually never be able to compete satisfactorily with mechanical refrigeration. This may not be the case and the authors probably had no intention of implying any future possibilities other than those mentioned briefly in the text. To make long range predictions, Fig. 4 would have to be replotted to reflect improved values which might come out of mass production.

It is possible to receive an erroneous impression that Fig. 4 is the result of the "Cost Minimization Procedure" and, therefore, represents a minimum cost varying only with Z.

I think it would have been a good idea to have given with Fig. 4 the cost values used, in the same manner as the junction temperatures are given. Although these data are given in Table II, it is too far from Fig. 4. This is a small point, but I think there will be a number of people who will find it easy to reach unintended conclusions by grasping Fig. 4 without having fully absorbed the text.

The method and formulas given should make it possible to predict just how much cost reduction in the various cost areas will be necessary for TE to compete with mechanical refrigeration. Since the authors look ahead to a Z of $1^{0} \times 10^{-3}$, it would have been interesting also to see what the same curve would look like using expected future minimum cost values for the various cost factors, particularly material costs.

CLOSURE BY AUTHOR STAEBLER: It is evident from Mr. Phillip's helpful remarks that some amplification of Fig. 4 would be in order. The cost figures used for mechanical refrigeration are well established and no further clarification is required. For the thermoelectric system it should immediately be pointed out that the cost figures shown certainly do not represent the ultimate that is attainable. The curve for $Z = 3 \times 10^{-3}\ C^{-1}$ represents what can be achieved with presently available materials, fabrication techniques and power supplies, providing TE materials were available at $0.085 per gm. Since the original submission of this paper it has come to the attention of the authors that fabricated TE couples are now commercially available in production quantities at prices in the region of $0.37 per couple and hence it can be stated that the curve for $Z = 3 \times 10^{-3}\ C^{-1}$ shown in Fig. 4 represents the present competitive position of TE refrigeration. The rate of progress appears

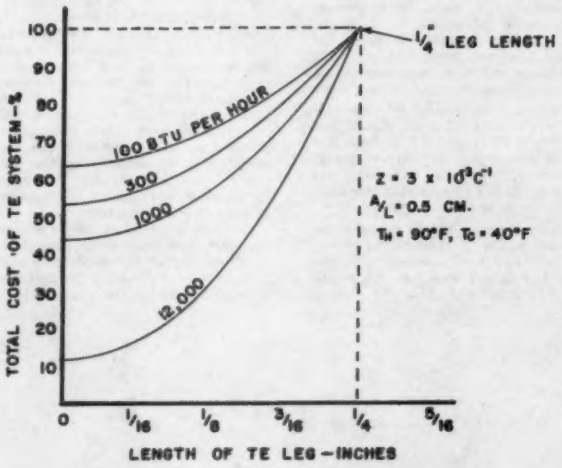

Fig. 5 Effect of thermoelectric couple miniaturization on manufacturing costs

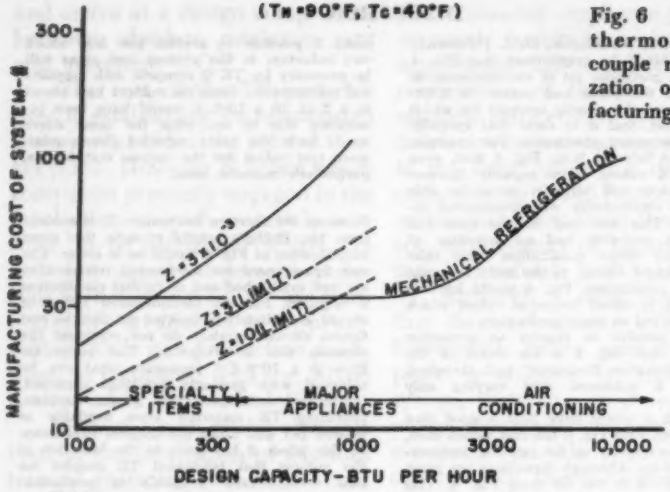

Fig. 6 Effect of thermoelectric couple miniaturization on manufacturing costs

to be much more rapid than the initial estimates made by the authors.

With regard to future prospects, the authors wish to submit two additional figures. Fig. 5 shows the effect of TE couple miniaturization on manufacturing costs. With present techniques of couple fabrication L = ¼ in. is considered to be a realistic minimum couple length. However, with improvements in junction contact resistance and assembling techniques the authors see no reason why shorter leg lengths, accompanied by considerable savings in TE material costs, should not come about. Fig. 5 illustrates the savings that can be made in this respect for various design capacities. Naturally, the cost reductions are much more evident for the larger capacity devices employing more TE couples.

The ultimate effect of couple miniaturization is illustrated in Fig. 6. The curves shown are for $Z = 3 \times 10^{-3}$ C^{-1}, identical with the curve of Fig. 4, together with two additional curves Z = 3 (limit) and Z = 10 (limit) which are manufacturing cost curves with TE material costs reduced to the vanishing point. These curves could be said to represent the ultimate attainable for these respective Z values, but once again certain reservations should be stressed. In particular, it should be emphasized that these curves do not consider possible power supply cost reductions. Some cost reductions are undoubtedly possible within the framework of conventional design. However, radically new concepts may also have an important effect on costs. For example, the introduction of the fuel cell, essentially of a low voltage, high current dc generator, as a primary source of power in the home (which might well be feasible within the next five years) would considerably further enhance the competitive position of thermoelectricity for refrigeration and heating.

Thus, in view of recent economic developments and foreseeable technical advances, it would appear inevitable that thermoelectric refrigeration will move beyond the range of specialty items in the near future.

In Memoriam 1960

Name	Joined
C. B. Acker, Mary Esther, Fla.	1946
Joseph A. Aguado, Cincinnati, Ohio	1953
Guy J. Amorosa, Narberth, Pa.	1958
W. M. Andrews, Houston, Tex.	1941
Ernest R. Arvidson, St. Albans, W. Va.	1945
A. H. Bearse, Jr., Old Saybrook, Conn.	1954
A. G. Belden, Terre Haute, Ind.	1944
Everett R. Benedict, Dunedin, Fla.	1954
Frank M. Bennett, *(Life Member),* Canton, Ohio	1914
Clyde D. Berger, Merion Station, Pa.	1947
Louis K. Berman, *(Life Member),* New York, N. Y.	1908
John H. Blake, Providence, R. I.	1959
Walter A. Bornemann, *(Life Member),* Glenside, Pa.	1923
Leo A. Brissette, *(Life Member),* Melrose, Mass.	1930
William Bronlow, Sr., Philadelphia, Pa.	1944
John H. Bryce, Buffalo, N. Y.	1944
Leo L. Burns, Los Angeles, Calif.	1957
Charles G. Burritt, *(Life Member),* Minneapolis, Minn.	1916
Lawrence D. Chellis, Weymouth, Mass.	1947
Thomas Chester, *(Life Member),* Birmingham, Mich.	1917
Erik D. Coachman, Rio de Janeiro, Brazil	1949
Martin Corbman, Cleveland, Ohio	1950
L. E. Cover, Lancaster, Pa.	1941
E. E. Crowley, Wilmington, Del.	1953
E. L. Crosby, *(Fellow),* Baltimore, Md.	1936
Irving S. Dane, Medford, Mass.	1947
A. B. Darling, Montreal, Que.	1929
John A. Darts, *(Life Member),* New York, N. Y.	1919
Theodore E. DeVries, Bristol, England	1950
M. L. Diver, *(Life Member),* San Antonio, Tex.	1924
E. M. Dodds, *(Life Member),* Kansas City, Mo.	1923
William Feldern ann, S. Orange, N. J.	1937
B. D. Fjeseth, La Crosse, Wis.	1955
George E. Ford, Jr., Maplewood, N. J.	1954
F. M. Friscoe, N. Bellmore, N. Y.	1953
E. J. Gardiner, *(Life Member),* Sydney, Australia	1906
Gerald Gearon, Chicago, Ill.	1937
Oscar German, Trois Rivieres, Que.	1935
Charles M. Gilbert, *(Life Member),* Mt. Vernon, Ohio	1940
Herman W. Goldner, Philadelphia, Pa.	1944
George V. K. Greene, Baltimore, Md.	1906

In Memoriam 1960 *(Continued)*

NAME	JOINED
G. Nelson Haden, *(Life Member)*, London, W.C.1, England	1922
Carl W. Harnish, Fort Worth, Tex.	1952
Harold M. Hendrickson, *(Fellow)*, Seattle, Wash.	1935
William S. Hobbs, Swarthmore, Pa.	1936
Harold Holmberg, Battle Creek, Mich.	1949
G. Baillie Houliston, Cincinnati, Ohio	1928
Frank P. Isaac, Warrensburg, Mo.	1949
N. E. Jennison, Burlington, Vt.	1955
Alfred Jones, *(Life Member)*, Haverford, Pa.	1951
Frederick B. Jones, New York, N. Y.	1943
William J. Kennedy, Chicao, Calif.	1945
D. C. Kieffer, Dallas, Tex.	1949
B. F. Kubaugh, Louisville, Ky.	1953
Martin Langberg, New York, N. Y.	1941
M. G. Lehman, Lincoln, Nebr.	1937
Charles S. Leopold, *(Presidential Member and Fellow)* Philadelphia, Pa.	1934
C. A. L. Loney, *(Life Member)*, Sydney, Australia	1906
A. E. Magher, *(Life Member)*, New York, N. Y.	1919
James C. Matchett, *(Life Member)*, Chicago, Ill.	1923
Bert C. McKenna, Chicago, Ill.	1953
William W. Medlin, Houston, Tex.	1956
Karl A. Meyer, Cincinnati, Ohio	1938
Myron D. Miller, New York, N. Y.	1952
Milton M. Mister, Hyattsville, Md.	1959
C. Raymond Morris, *(Life Member)*, Paterson, N. J.	1938
C. E. Morrow, *(Life Member)*, Boston, Mass.	1930
Wesley A. Mullett, Vancouver, B. C.	1954
Morris E. Naftzger, Hammond, Ind.	1948
W. H. Ness, Los Angeles, Calif.	1931
Andre Nessi, Paris, France	1948
Aldo E. Nessler, Evanston, Ill.	1942
John M. Nicholls, Pittsfield, Mass.	1939
Lee Nusbaum, *(Life Member)*, Philadelphia, Pa.	1915
Orion Oaks, *(Life Member)*, Summit, N. J.	1917
George W. Ott, Los Angeles, Calif.	1946
J. J. Philippi, Chicago, Ill.	1939
Louis C. Plaehn, Milwaukee, Wis.	1949
C. E. Ploeger, Evansville, Ind.	1929
C. G. Quermann, Evanston, Ill.	1941
Clinton H. Quirk, *(Life Member)*, Hempstead, N. Y.	1915
J. F. Raether, Ft. Lauderdale, Fla.	1919

In Memoriam 1960 *(Continued)*

Name	Joined
David F. Robertson, Detroit, Mich.	1950
W. R. Ronemous, Charleston, S. C.	1926
Lowell H. Rood, Palo Alto, Calif.	1944
Austin L. Roth, Hyattsville, Md.	1944
Ernest W. Roy, Knoxville, Tenn.	1945
Harry K. Ruyle, Peoria, Ill.	1947
William F. Ryan, Salina, Kansas	1940
Ernest J. Sandland, Rexdale, Ont.	1949
Frank E. Saracino, Wilmette, Ill.	1945
Leonard C. Savage, Baltimore, Md.	1952
I. Ernest Shaer, Chestnut Hill, Mass.	1934
T. F. Shelldrop, E. Williston, N. Y.	1942
Edward C. Shepard, Millburn, N. J.	1943
Oliver R. Simmers, Malvern, Pa.	1946
F. R. Slessar, Melbourne, Australia	1945
Jasper A. Smith, Dayton, Ohio	1945
Kenneth T. Sprague, Syracuse, N. Y.	1948
Louis J. Steilen, Hatboro, Pa.	1946
James T. Sullivan, Boston, Mass.	1944
Harvey G. Swart, Chicago, Ill.	1944
Ralph C. Taggart, *(Life Member),* Lanesville, Mass.	1912
Walter C. Thatcher, Chicago, Ill.	1959
Barney M. Thornburg, Portland, Ore.	1947
Homer A. Thrush, *(Life Member),* Peru, Ind.	1918
W. Walter Timmis, W. Lafayette, Ind.	1925
John I. Trimble, Columbus, Ohio	1945
P. J. Vanderlip, Sunland, Calif.	1946
E. G. Waters, Park Ridge, Ill.	1942
Irving E. Weber, Dallas, Tex.	1955
Howard J. Wenzell, Ocean Park, Calif.	1957
Charles W. Wheeler, *(Life Member),* Fort Myers, Fla.	1942
K. E. Whitman, Evanston, Ill.	1954
John H. Wickersham, *(Life Member),* Lancaster, Pa.	1937
Arthur C. Willard, *(Honorary, Presidential and Life Member),* Urbana, Ill.	1914
Charles S. Wilmot, *(Life Member),* Narberth, Pa.	1919
H. Gordon Winters, Ste. Therese de Blainville, Que.	1946
William H. Worth, Lombard, Ill.	1957
C. P. Yaglou, Boston, Mass.	1923
John A. Youtz, Philadelphia, Pa.	1957

A.V. Hutchinson

1896-1960

Aubry Vaughan Hutchinson, Secretary Emeritus of ASHRAE, died in Lafayette, Ind., June 6, 1960. Associated with the former ASHAE for 37 years, he became the first Executive Secretary of ASHRAE when the merger was effected and served in that capacity until his retirement in 1959.

Mr. Hutchinson joined ASHVE in 1922 as Manager of Publications; he was appointed Secretary in 1926 and Executive Secretary in 1950. When ASHVE became ASHAE he continued as Executive Secretary and Manager of Publications.

Born in Brooklyn, Mr. Hutchinson attended schools in Ridgewood, N. J., taking special courses in journalism and engineering. Until his retirement, he made his home for many years in Wyckoff, N. J. He was a member of the Society of American Military Engineers and the American Legion.

Prior to his association with the Society, he entered the publishing field with the David Williams Company, New York, N. Y., in 1914-15. He then served from 1916-17 as assistant and later associate editor of Metal Worker, Plumber and Steam Fitter in New York and as western editor for Sheet Metal Worker and Heating Engineer in Chicago from 1920-21. He served with the U.S. Army in 1918-19.

Mr. Hutchinson's interests and activities were broadly allied with the engineering, publishing and industry functions of the Society with which he was so long associated. In his 37 years of service, Mr. Hutchinson witnessed the growth of the Society from a small group to that of one of the five largest professional engineering societies. At the time of his retirement then President Arthur J. Hess paid high tribute to his work stating, "Probably the most important contribution, among the many he made, was his work on the GUIDE which he built up into the 'Bible' of the industry and one of the most respected publications of any technical society. To Mr. Hutchinson we owe much more than we can say in words, or do in deeds".

Mr. Hutchinson is survived by his widow, the former Janis Louise Barr.

Constantin P. Yaglou

1896-1960

Constantin P. Yaglou, Professor of Industrial Hygiene at Harvard University School of Public Health for many years, died June 3, 1960. He was the 1959 recipient of the F. Paul Anderson Medal, given in recognition of outstanding work in his field. Long engaged in teaching and research on hygienic aspects of air conditioning, he contributed numerous papers on various phases of this subject for publication in engineering, medical and public health journals.

Born in Constantinople, Turkey, he attended the French-Greek College of Arts and Sciences, later graduating from the Engineering School of Robert College with a degree of B.S.M.E. His formal education was completed at Cornell University, where he received his M.M.E. degree.

From 1921-25 he served on the staff of the former ASHVE Research Laboratory. During these years he was associated closely with most of the pioneering studies in development of the original effective temperature scales, determination of the comfort zone and physiological effect of heat and cold. With the School of Public Health since 1925, he had conducted further studies in the comfort, health and therapeutic aspects of air conditioning and on working efficiencies in climatic extremes.

A member of ASHAE since 1923, Professor Yaglou served on the GUIDE Publication Committee in 1926, 1946 and 1947, and on the Nominating Committee as a delegate from the Massachusetts Chapter in 1932 and 1938. Active on numerous Research Technical Advisory Committees, he was Chairman of the committees on Comfort Air Conditioning, Re-study of Comfort Chart and Comfort Line and Sensations of Comfort and a member of Comfort Standards for Summer Cooling, Instruments, Navy Studies, Human Calorimetry and Physiological Research.

. Local Chapter activities included serving on the Board of Governors of the Massachusetts Chapter in 1936 and 1941, as Vice President in 1937 and 1939 and President in 1940.

Arthur Cutts Willard

1878-1960

Arthur Cutts Willard, past-president of ASHAE (1928) and Honorary Member of ASHRAE, died in Urbana, Ill. on September 11, 1960 following a heart attack. Dr. Willard, recipient in 1936 of the F. Paul Anderson Award, was President Emeritus of the University of Illinois and one of the nation's leading heating, ventilating and air conditioning engineers.

Born in Washington, D. C., he received a B.S. degree in chemical engineering from Massachusetts Institute of Technology in 1904. He then entered the teaching profession as an instructor in industrial chemistry at California School of Mechanical Arts and in 1906 was appointed Assistant Professor of Mechanical Engineering at George Washington University, leaving in 1909 to join the United States Quartermaster Corps, where he served until 1913.

Dr. Willard went to the University of Illinois in 1913 as Assistant Professor of Heating and Ventilation, advanced to a full professorship in 1917 and became Head of the Mechanical Engineering Dept. in 1920. In 1933-34 he was acting Dean of the College of Engineering and Director of the Engineering Experiment Station. It was from this post that he rose to the presidency in 1934. He was President Emeritus since 1946, and during this time he retained his interest in activities of the University, continuing to serve as a valued counsellor.

A member of ASHAE since 1914, he served in many capacities, including the offices of Second (1926) and First (1927) Vice President, President (1928), a member of Council (1925-1929), and was a member of numerous committees. He was made a Life Member in 1944 and an Honorary Member in 1956.

A specialist in the fields of heating, ventilating and air conditioning, Dr. Willard was consulting engineer for New York City's Holland Tunnel, the U.S. Capitol, U.S. Bureau of Mines, U.S. Public Health Service and the Chicago subway system. He was a leader of research teams which developed guiding principles for today's domestic furnaces and air conditioning and a collaborator with medical scientists in pioneering investigation of atmospheric environmental influences on mankind. Through his untiring efforts, a residence for research purposes was constructed at the University of Illinois.

His widow, the former Sarah Lamborn, survives him.

Charles Stein Leopold

1896-1960

Fellow of the American Society of Heating, Refrigerating and Air Conditioning Engineers, past-President of precedent American Society of Refrigerating Engineers and 1954 recipient of the F. Paul Anderson Award, Consulting Engineer Charles Stein Leopold died in Philadelphia, Pa., on November 24, 1960, following a heart attack.

As founder (in 1923) and head of the firm which bears his name, Mr. Leopold was noted for his achievements in the fields of heating, air conditioning and ventilating, and was the designer of systems for such projects as the Pentagon Building, U.S. Capitol, New York Stock Exchange, Philadelphia's Convention Hall, Madison Square Garden and research laboratories for the U.S. Atomic Energy Commission at Los Alamos, N. M., and Ames, Iowa. In addition, he developed a method of controlled air supply for testing carburetors of airplanes during World War II.

Co-author of a study on air filtration for relief of asthma and hay fever patients, his technical papers delivered at Annual and Semiannual Meetings of the Society included discussions of smoke measurement, importance of radiation in air conditioning design, comfort conditions, panel cooling and problems of thermal storage, radiation, convection and conduction.

Born May 8, 1896, in Philadelphia, he was the son of Isaac and Sarah (Stein) Leopold. Educated at local Philadelphia schools, he later attended the University of Pennsylvania, where he received the degrees of B.S. in electrical engineering in 1917 and E.E. in 1947. During the first World War, Mr. Leopold served as an Ensign in the U.S. Naval Reserve. In 1920 he married Marian Rose Bettmann, who survives him.

Active in the former ASHAE and precedent ASHVE since his election to membership in 1934, he served as a member of Council and on numerous committees.

He was also prominent in the former ASRE activities.

INDEX

A

Absorption Cycle, Air-Cooled, by R. H. Merrick and R. A. English 339
Accountant's Report 49
Activated Charcoal to Decrease Odor and Odor Transfer in Domestic Refrigerators, Use of, by Aaron L. Brody, Jess W. Thomas and Lois Lafeber 217
Air Conditioner, Gas-Fired Open Cycle, by B. E. Eakin and R. T. Ellington 319
Air-Cooled Absorption Cycle, by R. H. Merrick and R.A. English 339
Discussion 346
Alaska Summer Weather Data, by Robert Burggraaf 240
Discussion 247
Albright, L. F., T. C. Doody, P. C. Buclez and C. R. Pluche, Solubility of Refrigerants 11, 21 and 22 in Organic Solvents Containing an Oxygen Atom 423
Analysis of the Necessity to Insulate Floors of Cold Storage Rooms at 35 F, by J. D. Hovanesian, H. F. Prost and C. W. Hall 69
Discussion 78
Apple Cooling Rates, Packed in Different Bushel Containers and Stacked at Different Spacings in Cold Storage, D. V. Fisher 414
ASHRAE By-laws 39
ASHRAE Membership 60
ASHRAE Semiannual Meeting, 1960 (Dallas, Texas) 61
ASHRAE Sixty-seventh Annual Meeting, 1960 (Vancouver, B. C.) 309
Attenuation and Generation of Sound in Elbows with Turning Vanes, by W. F. Kerka 129
Discussion 152

B

Baker, J. T., C. M. Humphreys and B. H. Jennings, Saturated Steam Flow in Copper Tubing 167
Baker, Merl and J. M. Elliott, Heat Loss from a Heated Basement 400
Basement, Heat Loss from a Heated, by J. M. Elliott and Merl Baker 400
Beacham, E. A., W. O. Krause and A. B. Guise, Time Factors in the Removal of Moisture from Refrigerating Systems with Desiccant Type Driers 465
Brody, Aaron L., Jess W. Thomas and Lois Lafeber, Use of Activated Charcoal to Decrease Odor and Odor Transfer in Domestic Refrigerators 217
Brown, W. G. and C. Wachmann, Draft Performance of Chimneys 154
Buclez, P. C., L. F. Albright, T. C. Doody and C. R. Pluche, Solubility of Refrigerants 11, 21 and 22 in Organic Solvents Containing an Oxygen Atom 423
Burggraaf, Robert Alaska Summer Weather Data 240
By-laws 39

C

Chimneys, Draft Performance of, by W. G. Brown and C. Wachmann 154
Cold Storage Rooms, An Analysis of the Necessity to Insulate Floors of at 35 F, by J. D. Hovanesian, H. F. Prost and C. W. Hall 69
Comfort Range, Sensation Responses to Temperature and Humidity under Still Air Conditions in, Environmental Study II, by Walter Koch, B. H. Jennings and C. M. Humphreys 264

Comparative Study of the Manufacturing Costs of Thermoelectric and Mechanical Refrigerating Systems, by D. W. SCOFIELD, P. F. TAYLOR and L. A. STAEBLER 494
Discussion 507
Compressor Characteristics, Effect of, on Motor Performance, by ERIK H. JENSEN 194
Cooling Rates of Apples Packed in Different Bushel Containers and Stacked at Different Spacings in Cold Storage, by D. V. FISHER 414
Discussion 422
Copper Tubing, Saturated Steam Flow in, C. M. HUMPHREYS, J. T. BAKER and B. H. JENNINGS 167

D

Determination of Moisture in Fluorocarbons, by JOSEPH D. MORTON and LAURA K. FUCHS 434
Discussion 444
Digital Computer, Muffler Analysis, by D. F. MILLER and B. W. HATTEN 202
DOELLING, NORMAN, Noise Reduction Characteristics of Package Attenuators for Air-Conditioning Systems 114
DOODY, T. C., L. F. ALBRIGHT, P. C. BUCLEZ and C. R. PLUCHE, Solubility of Refrigerants 11, 21 and 22 in Organic Solvents Containing an Oxygen Atom 423
DOWNING, G. V., JR., Production Control Testing of Thermoelectric Materials 477
Draft Performance of Chimneys, by W. G. BROWN and C. WACHMANN 154
Driers, Desiccant-Type, Time Factors in the Removal of Moisture from Refrigerating Systems, by W. O. KRAUSE, A. B. GUISE and E. A. BEACHAM 465
Dual Solution System—A Different Approach to Some of the Problems of Air Conditioning, by F. H. HIBBERD 348
Discussion 358

E

EAKIN, B. E. and R. T. ELLINGTON, Gas-Fired Open Cycle Air Conditioner 319
Effect of Compressor Characteristics on Motor Performance, by ERIK H. JENSEN 194
Discussion 201
Electronic Computer Aids Calculation of Reaction Forces in a Scotch Yoke, by V. G. FORIS and B. W. HATTEN 391
ELLINGTON, R. T. and B. E. EAKIN, Gas-Fired Open Cycle Air Conditioner 319
ELLIOTT, J. M. and MERL BAKER, Heat Loss from a Heated Basement 400
ENGLISH, R. A. and R. H. MERRICK, Air-Cooled Absorption Cycle 339
Environmental Study II—Sensation Responses to Temperature and Humidity under Still Air Conditions in the Comfort Range, by WALTER KOCH, B. H. JENNINGS and C. M. HUMPHREYS 264
Discussion 282

F

FISHER, D. V., Cooling Rates of Apples Packed in Different Bushel Containers and Stacked at Different Spacings in Cold Storage 414
Fluorocarbons, Determination of Moisture in, by JOSEPH D. MORTON and LAURA K. FUCHS 434
FORIS, V. G. and B. W. HATTEN, Electronic Computer Aids Calculation of Reaction Forces in a Scotch Yoke 391
Frost Formation on Refrigeration Coils, by W. F. STOECKER 91
Discussion 102

Frost Formation upon a Thin Aluminum Tank Containing Liquid Oxygen, by J. L. LOPER ... 104
Discussion ... 113
FUCHS, LAURA K. and JOSEPH D. MORTON, Determination of Moisture in Fluorocarbons ... 434

G

Gas-Fired Open Cycle Air Conditioner, by B. E. EAKIN and R. T. ELLINGTON ... 319
Discussion ... 338
GUISE, A. B., W. O. KRAUSE and E. A. BEACHAM, Time Factors in the Removal of Moisture from Refrigerating Systems with Desiccant Type Driers ... 465

H

HALL, C. W., J. D. HOVANESIAN and H. F. PFOST, Analysis of the Necessity to Insulate Floors of Cold Storage Rooms at 35 F ... 69
HANDEGORD, G. O. and C. E. TILL, Proposed Humidity Standard ... 288
HATTEN, B. W. and D. F. MILLER, Muffler Analysis by Digital Computer ... 202
HATTEN, B. W. and V. G. FORIS, Electronic Computer Aids Calculation of Reaction Forces in a Scotch Yoke ... 391
Heat Exchangers, A Method of Comparing, by DONALD G. RICH ... 80
Heat Loss from a Heated Basement, by J. M. ELLIOTT and MERL BAKER ... 400
Discussion ... 412
HIBBERD, F. H., Dual Solution System—A Different Approach to Some of the Problems of Air Conditioning ... 348
High-Temperature Water Systems, Proposed Pipe Friction Chart for, by T. C. MIN and P. J. POTTER ... 374
HOVANESIAN, J. D., H. F. PFOST and C. W. HALL, Analysis of the Necessity to Insulate Floors of Cold Storage Rooms at 35 F ... 69
HUCK, WILLIAM, Simplified Engineering Approach to Thermoelectric Heat Pumping ... 485
Humidity Standard, Proposed, by C. E. TILL and G. O. HANDEGORD ... 288
HUMPHREYS, C. M., J. T. BAKER and B. H. JENNINGS, Saturated Steam Flow in Copper Tubing ... 167
HUMPHREYS, C. M., WALTER KOCH and B. H. JENNINGS, Environmental Study II—Sensation Responses to Temperature and Humidity under Still Air Conditions in the Comfort Range ... 264
HUTCHINSON, A. V. In Memoriam ... 512

I

In Memoriam ... 509
Insulating Floors of Cold Storage Rooms at 35 F, Analysis of the Necessity to, by J. D. HOVANESIAN, H. F. PFOST and C. W. HALL ... 69

J

JENNINGS, B. H., C. M. HUMPHREYS and J. T. BAKER, Saturated Steam Flow in Copper Tubing ... 167
JENNINGS, B. H., WALTER KOCH and C. M. HUMPHREYS, Environmental Study II—Sensation Responses to Temperature and Humidity under Still Air Conditions in the Comfort Range ... 264
JENSEN, ERIK H., Effect of Compressor Characteristics on Motor Performance 194

K

KERKA, W. F., Attenuation and Generation of Sound in Elbows with Turning Vanes 129
KERKA, W. F., Re-Evaluation of the Steam-Pipe Size Tables for the ASHRAE GUIDE 183
KOCH, WALTER, B. H. JENNINGS and C. M. HUMPHREYS, Environmental Study II—Sensation Responses to Temperature and Humidity under Still Air Conditions in the Comfort Range 264
KRAUSE, W. O., A. B. GUISE and E. A. BEACHAM, Time Factors in the Removal of Moisture from Refrigerating Systems with Desiccant Type Driers 465

L

LAFEBER, LOIS, AARON L. BRODY and JESS W. THOMAS, Use of Activated Charcoal to Decrease Odor and Odor Transfer in Domestic Refrigerators .. 217
LEOPOLD, C. S., In Memoriam 515
LEVY, S. L., W. O. WALKER and S. ROSEN, Study of the Factors Influencing the Stability of Mixtures of Refrigerant 22 and Refrigerating Oils 445
Liquid Oxygen, Frost Formation upon a Thin Aluminum Tank Containing, by J. L. LOPER 104
LOPER, J. L., Frost Formation upon a Thin Aluminum Tank Containing Liquid Oxygen 104

M

Mechanical and Thermoelectric Refrigerating Systems, A Comparative Study of the Manufacturing Costs of, by D. W. SCOFIELD, P. F. TAYLOR and L. A. STAEBLER 494
MERRICK, R. H. and R. A. ENGLISH, Air-Cooled Absorption Cycle 339
Method of Comparing Heat Exchangers, by DONALD G. RICH 80
Discussion 89
MILLER, D. F. and B. W. HATTEN, Muffler Analysis by Digital Computer 202
MIN, T. C. and P. J. POTTER, Proposed Pipe Friction Chart for High-Temperature Water Systems 374
Moisture, Determination of in Fluorocarbons, by JOSEPH D. MORTON and LAURA K. FUCHS 434
Moisture, Time Factors in the Removal of from Refrigerating Systems with Desiccant Type Driers, by W. O. KRAUSE, A. B. GUISE and E. A. BEACHAM 465
MORTON, JOSEPH D., and LAURA K. FUCHS, Determination of Moisture in Fluorocarbons 434
Motor Performance, Effect of Compressor Characteristics on, by ERIK H. JENSEN 194
Muffler Analysis by Digital Computer, by D. F. MILLER and B. W. HATTEN .. 202
Discussion 216

N

Noise Reduction Characteristics of Package Attenuators for Air-Conditioning Systems, by NORMAN DOELLING 114
Discussion 126

O

Odor and Odor Transfer in Domestic Refrigerators, Use of Activated Charcoal to Decrease, by AARON L. BRODY, JESS W. THOMAS and LOIS LAFEBER .. 217
Officers and Board of Directors (February—June 1960) 5

Officers and Board of Directors (June 1960—February 1961) 19
OZISIK, N. and L. F. SCHUTRUM, Solar Heat Gain Factors for Windows with Drapes 228
OZISIK, N. and L. F. SCHUTRUM, Solar Heat Gains through Slat-Type Between-Glass Shading Devices 359

P

Package Attenuators for Air Conditioning Systems, Noise Reduction Characteristics of, by NORMAN DOELLING 114
PFOST, H. F., J. D. HOVANESIAN and C. W. HALL, Analysis of the Necessity to Insulate Floors of Cold Storage Rooms at 35 F 69
Pipe Friction Chart, Proposed, for High-Temperature Water Systems, by T. C. MIN and P. J. POTTER 374
PLUCHE, C. R., L. F. ALBRIGHT, T. C. DOODY and P. C. BUCLEZ, Solubility of Refrigerants 11, 21 and 22 in Organic Solvents Containing an Oxygen Atom 423
POTTER, P. J. and T. C. MIN, Proposed Pipe Friction Chart for High-Temperature Water Systems 374
Production Control Testing of Thermoelectric Materials, by G. V. DOWNING, JR. 477
Discussion 483
Proposed Humidity Standard, by C. E. TILL and G. O. HANDEGORD 288
Discussion 305
Proposed Pipe Friction Chart for High-Temperature Water Systems, by T. C. MIN and P. J. POTTER 374
Discussion 387

R

Rational Method of Determining Summer Weather Design Data, by H. C. S. THOM 248
Discussion 261
Re-Evaluation of the Steam-Pipe Size Tables for the ASHRAE GUIDE, by W. F. KERKA 183
Refrigerant 22 and Refrigerating Oils, A Study of the Factors Influencing the Stability of Mixtures of, by W. O. WALKER, S. ROSEN and S. L. LEVY 445
Refrigerants 11, 21 and 22, Solubility of in Organic Solvents Containing an Oxygen Atom, by L. F. ALBRIGHT, T. C. DOODY, P. C. BUCLEZ and C. R. PLUCHE 423
Refrigeration Coils, Frost Formation on, by W. F. STOECKER 91
Report of the Research and Technical Committee 55
Research and Technical Committee, Report of 55
RICH, DONALD G., Method of Comparing Heat Exchangers 80
ROSEN, S., W. O. WALKER and S. L. LEVY, Study of the Factors Influencing the Stability of Mixtures of Refrigerant 22 and Refrigerating Oils 445

S

Saturated Steam Flow in Copper Tubing, by C. M. HUMPHREYS, J. T. BAKER and B. H. JENNINGS 167
Discussion 182
SCHUTRUM, L. F. and N. OZISIK, Solar Heat Gain Factors for Windows with Drapes 228
SCHUTRUM, L. F. and N. OZISIK, Solar Heat Gains through Slat-Type Between-Glass Shading Devices 359

SCOFIELD, D. W., P. F. TAYLOR and L. A. STAEBLER, Comparative Study of the Manufacturing Costs of Thermoelectric and Mechanical Refrigerating Systems 494
Scotch Yoke, Electronic Computer Aids Calculation of Reaction Forces in, by V. G. FORIS and B. W. HATTEN 391
Sensation Responses to Temperature and Humidity under Still Air Conditions in the Comfort Range—Environmental Study II, by WALTER KOCH, B. H. JENNINGS and C. M. HUMPHREYS 264
Shading Devices, Solar Heat Gains through Slat-Type Between-Glass, by N. OZISIK and L. F. SCHUTRUM 359
Simplified Engineering Approach to Thermoelectric Heat Pumping, by WILLIAM HUCK 485
Discussion 493
Solar Heat Gain Factors for Windows with Drapes, by N. OZISIK and L. F. SCHUTRUM 228
Discussion 239
Solar Heat Gains through Slat-Type Between-Glass Shading Devices, by N. OZISIK and L. F. SCHUTRUM 359
Discussion 372
Solubility of Refrigerants 11, 21 and 22 in Organic Solvents Containing an Oxygen Atom, by L. F. ALBRIGHT, T. C. DOODY, P. C. BUCLEZ and C. R. PLUCHE 423
Discussion 432
Sound, Attenuation and Generation of in Elbows with Turning Vanes, by W. F. KERKA 129
STAEBLER, L. A., D. W. SCOFIELD and P. F. TAYLOR, Comparative Study of the Manufacturing Costs of Thermoelectric and Mechanical Refrigerating Systems 494
Steam-Pipe Size Tables for the ASHRAE GUIDE, Re-Evaluation of, by W. F. KERKA 183
Steam, Saturated, Flow in Copper Tubing, by C. M. HUMPHREYS, J. T. BAKER and B. H. JENNINGS 167
STOECKER, W. F., FROST Formation on Refrigeration Coils 91
Study of the Factors Influencing the Stability of Mixtures of Refrigerant 22 and Refrigerating Oils, by W. O. WALKER, S. ROSEN and S. L. LEVY 445
Discussion 463

T

TAYLOR, P. F., D. W. SCOFIELD and L. A. STAEBLER, Comparative Study of the Manufacturing Costs of Thermoelectric and Mechanical Refrigerating Systems 494
Thermoelectric and Mechanical Refrigerating Systems, a Comparative Study of the Manufacturing Costs of, by D. W. SCOFIELD, P. F. TAYLOR and L. A. STAEBLER 494
Thermoelectric Heat Pumping, a Simplified Engineering Approach to, by WILLIAM HUCK 485
Thermoelectric Materials, Production Control Testing of, by G. V. DOWNING, JR. 477
THOM, H. C. S., Rational Method of Determining Summer Weather Design Data 248
THOMAS, JESS W., AARON L. BRODY and LOIS LAFEBER, Use of Activated Charcoal to Decrease Odor and Odor Transfer in Domestic Refrigerators 217
TILL, C. E. and G.O. HANDEGORD, Proposed Humidity Standard 288
Time Factors in the Removal of Moisture from Refrigerating Systems with Desiccant Type Driers, by W. O. KRAUSE, A. B. GUISE and E. A. BEACHAM 465
Discussion 476

U

Use of Activated Charcoal to Decrease Odor and Odor Transfer in Domestic Refrigerators, by AARON L. BRODY, JESS W. THOMAS and LOIS LAFEBER.. 217
Discussion 227

W

WACHMANN, C. and W. G. BROWN, Draft Performance of Chimneys..... 154
WALKER, W. O., S. ROSEN and S. L. LEVY, Study of the Factors Influencing the Stability of Mixtures of Refrigerant 22 and Refrigerating Oils..... 445
Weather Data, Alaska Summer, by ROBERT BURGGRAAF..... 240
Weather Design Data, Summer, A Rational Method of Determining, by H. C. S. THOM 248
WILLARD, A. C., In Memoriam..... 514
Windows, with Drapes, Solar Heat Gain Factors for, by N. OZISIK and L. F. SCHUTRUM 228

Y

YAGLOU, C. P., In Memoriam 513